



Durham E-Theses

Novel Applications of Polyfunctionalised Organoboron and Nitroso Compounds

EBERLIN, LUDOVIC,JEAN,ADOLPHE

How to cite:

EBERLIN, LUDOVIC,JEAN,ADOLPHE (2016) *Novel Applications of Polyfunctionalised Organoboron and Nitroso Compounds* , Durham theses, Durham University. Available at Durham E-Theses Online:
<http://etheses.dur.ac.uk/11447/>

Use policy

The full-text may be used and/or reproduced, and given to third parties in any format or medium, without prior permission or charge, for personal research or study, educational, or not-for-profit purposes provided that:

- a full bibliographic reference is made to the original source
- a [link](#) is made to the metadata record in Durham E-Theses
- the full-text is not changed in any way

The full-text must not be sold in any format or medium without the formal permission of the copyright holders.

Please consult the [full Durham E-Theses policy](#) for further details.

Academic Support Office, Durham University, University Office, Old Elvet, Durham DH1 3HP
e-mail: e-theses.admin@dur.ac.uk Tel: +44 0191 334 6107
<http://etheses.dur.ac.uk>



Novel Applications of Polyfunctionalised Organoboron and Nitroso Compounds

Thèse / Université de Rennes 1 (F)

*sous le sceau de l'Université Européenne
de Bretagne pour le grade de*

**DOCTEUR DE L'UNIVERSITÉ
DE RENNES 1**

Mention: Chimie

**Ecole doctorale Sciences de la
Matière**

Thesis / Durham University (UK)

*A thesis submitted in partial fulfilment of
the requirements for the degree of*

DOCTOR OF PHILOSOPHY

Department of Chemistry

Ludovic EBERLIN

Supported by

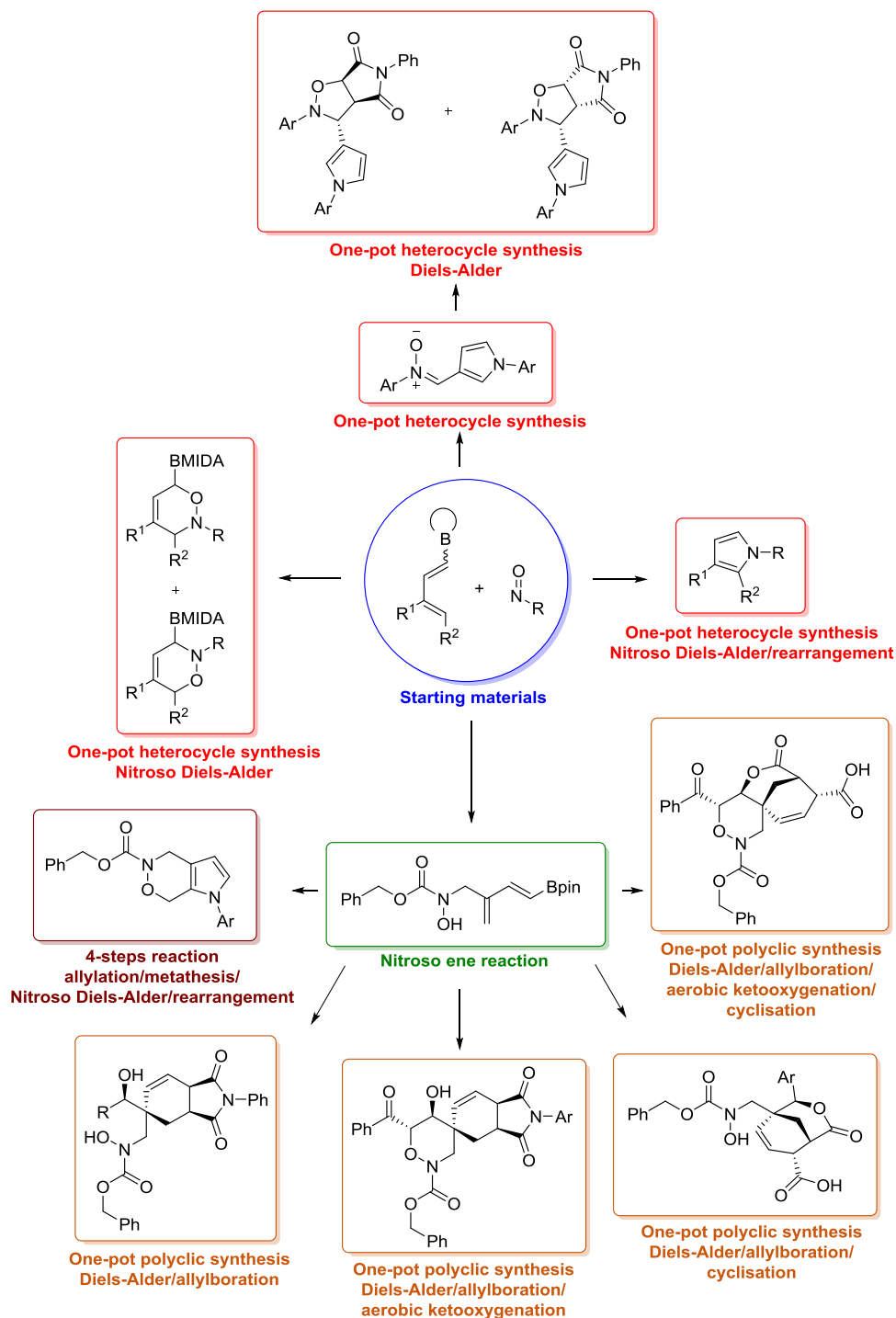
The Department of Chemistry of Durham University

and

La Région Bretagne

Abstract

This thesis presents the reactivity of dienylboronated compounds towards aryl nitroso and carbonyl nitroso derivatives and its use in the synthesis of heterocyclic and polycyclic compounds (see graphical abstract).



The first study focused on the reactivity of dienylboronate compounds with aryl nitroso derivatives resulting in pyrrole or furan products. The outcome and efficiency of the reaction is related to the boron on the dienyl moiety and the solvent used. Depending on the conditions, pyrroles, boronated MIDA ester oxazines or nitrones could be obtained. A one-pot strategy was then applied to synthesise oxazoline derivatives using nitrones as an intermediate.

Theoretical, as well as experimental, work has supported that the formation of the pyrrole was obtained by a regioselective nitroso Diels-Alder reaction/rearrangement/borate elimination cascade process. Details on the nitrone formation have not been clarified, but further investigations are on-going.

Secondly, attention was focused on the reactivity of dienylboronate compounds with carbonylnitroso derivatives. Contrary to the aryl nitroso species, the nature of the carbonylnitroso had a dramatic impact on reactivity. On the one hand, similar reactivity towards the formation of pyrroles and boronated MIDA ester oxazines was observed, however, by employing a higher electron-deficient carbonylnitroso species, the product resulting from a nitroso-ene reaction was obtained.

Ene-product was used as the key intermediate for the synthesis of different polycyclic compounds. A multicomponent, one-pot, Diels-Alder/allylboration procedure was optimised to yield various structures depending on the nature of the dienophile and the aldehyde.

To diversify the chemistry of the ene-product another sequence was designed using the pyrrole synthesis. A multi-step pathway was optimised to afford novel fused bicyclic oxazine-pyrrole products.

Contents

Abstract	1
Contents.....	3
Publication list.....	7
Acknowledgements	8
Abbreviations	11
Literature Review	14
I. Introduction.....	15
II. Boron-substituted 1,3-(hetero)dienes in multicomponent processes	16
II.1 1-Boron-substituted 1,3-dienes	16
II.2. 2-Boron-substituted 1,3-dienes	23
II.3. 1-Boron-substituted 1,3-heterodienes	29
II.3.a. 1-Oxo-4-borono-1,3-dienes	29
II.3.b. 1-Aza-4-borono-1,3-dienes.....	33
II.4. Boron-substituted heterodendralene	36
III. Nitroso derivatives as dienophile.....	39
III.1. Generation of the reactive nitroso species	39
III.2. Nitroso compounds in Diels-Alder reactions.....	41
III.2.a. Reactivity of nitroso compounds towards dienes	41
III.2.b. Regioselectivity of the nitroso Diels-Alder reactions.....	42
III.3. Some applications of nitroso Diels-Alder reactions.....	44
III.3.a. Arylnitroso derivatives as dienophiles.....	44
III.3.b. Carbonylnitroso derivative as dienophile	48
Results & Discussions	56

I.	Research Plan.....	57
II.	Diene syntheses.....	58
II.1.	Enyne hydroboration.....	58
II.2.	Dehydrobromination	62
II.3.	Alkyne bromoboration and Negishi coupling	63
II.4.	Halosulphonylation of 1,3-dienylboronic ester 241c	63
II.5.	Coupling reaction of vinylboronic acid MIDA ester derivatives.....	64
II.5.a.	From (E)-2-bromovinylboronic acid MIDA ester	64
II.5.b.	From 1-bromovinylboronic acid MIDA ester.....	65
II.6.	Modification of the boron substituents	66
III.	Boronated dienes and arylnitroso compounds	67
III.1.	Reaction of 1-dienylboronate pinacolate esters with arylnitroso compounds	67
III.2.	Reaction of tetracoordinated 1-borodienes with arylnitroso compounds	72
III.3.	Impact of the boron substituent on the kinetics of the reaction	79
III.4.	Mechanistic aspects of the reaction 1-borodienes with arylnitroso compounds.....	83
III.4.a.	Computational study.....	83
III.4.b.	Additional experimental study.....	86
III.4.c.	The Nitroso Diels-Alder with boronated diene; a reversible process?.....	94
III.5.	Transformations of borono-1,6-dihydro-1,2-oxazine derivatives.....	95
III.6.	The one-pot nitron formation/1,3-dipolar cycloaddition sequence	97
III.6.a.	Nitron synthesis from 1-dienylboronate pinacolate esters.....	98
III.6.b.	The one-pot procedure nitron formation/1,3-dipolar cycloaddition	101
III.6.c.	Mechanistic aspects	107
III.7.	Summary	112
IV.	Boronated dienes and carbonylnitroso compounds	114
IV.1.	Reaction of 1-dienylboronate pinacolate esters with carbonylnitroso compounds..	114

IV.2. Reaction of tetracoordinated 1-borodienes with carbonylnitroso compounds.....	120
IV.3. Mechanistic aspects.....	122
IV.3.a. The aerobic copper oxidation step.....	122
IV.3.b. The Diels-Alder/ring contraction sequence	123
IV.3.c. The ene reaction: Impact of the boron substituents	124
V. The ene-adduct as key intermediate in cascade reactions.....	128
V.1. The Diels-Alder/allylboration sequence.....	128
V.1.a. The Diels-Alder step.....	129
V.1.b. The Diels-Alder/allylboration one-pot process.....	134
V.1.c. Mechanistic aspects	147
V.2. Modification of the boron substituent	149
V.3. The metathesis/arylnitroso Diels-Alder/ring contraction sequence	150
V.3.a. Synthesis of the O-substituted hydroxycarbamates	151
V.3.b. The ring closing metathesis (RCM) of hydroxamates 358a-c	153
V.3.c. The arylnitroso Diels-Alder/ring contraction sequence.....	162
V.3.d. The Diels-Alder/allylboration sequence.	166
VI. Summary.....	167
Conclusions & Perspectives	169
I. Conclusions.....	170
II. Perspectives	173
Experimental Section	175
General experimental	176
Diene syntheses	178
A. Enyne hydroboration.....	178
B. Halosulphonylation of 1,3-dienylboronic ester 241c	186

C.	Coupling reaction of vinylboronic acid MIDA ester derivatives.....	187
	Boronated dienes and arylnitroso compounds	193
A.	Reaction of 1-dienylboronate pinacolate esters with arylnitroso compounds	193
B.	Reaction of tetracoordinated 1-borodienes with arylnitroso compounds	200
C.	Mechanistic aspects of the reaction 1-borodienes with arylnitroso compounds.....	216
D.	Transformations of borono-1,6-dihydro-1,2-oxazine derivatives	219
E.	The one-pot nitrene formation/1,3-dipolar cycloaddition sequence	221
	Boronated dienes and carbonylnitroso compounds.....	255
A.	Reaction of 1-dienylboronate pinacolate esters with carbonylnitroso compounds..	255
B.	Reaction of tetracoordinated 1-borodienes with carbonylnitroso compounds.....	258
	The ene-adduct as key intermediate in cascade reactions	263
A.	The Diels-Alder/allylboration sequence.....	263
B.	Modification of the boron substituent	280
C.	The metathesis/aryl nitroso Diels-Alder/ring contraction sequence	282
D.	The Diels-Alder/allylboration sequence	299
	References	300

Publication list

Peer-reviewed publications produced from this thesis:

1) Tripoteau, F.; Eberlin, L.; Fox, M. A.; Carboni, B.; Whiting, A. *Chem. Commun.*, **2013**, 49, 5414-5416.

2) Eberlin, L.; Tripoteau, F.; Carreaux, F.; Whiting, A.; Carboni, B. *Beilstein J. Org. Chem.* **2014**, 10, 237–250.

3) Eberlin, L.; Carboni, B.; Whiting, A. *J. Org. Chem.*, **2015**, 80, 6574-6583.

Acknowledgements

Firstly, I would like to thank my supervisors Dr Bertrand Carboni and Prof. Andrew Whiting for giving me the opportunity to work on this project. Thanks to their advice, assistance and support through these years, my journey as a PhD student has been very enriching. I know that boron chemistry is one of their areas of preference, but I have to say that even though it was highly stimulating, boron chemistry can be very frustrating as well. I must confess that since I started this project, I now have nightmares every time I'm travelling and staying in a B&B. For 99.99% of the people around the world, B&B means Bed & Breakfast; whereas to me it now means Boron & Boron. Anyway, it's too late for me now; every hero has his curse, and this will be mine.

Like a brave character in an adventure fiction, I travelled miles and miles, through all of France, from my native cosy Alsace to rainy Brittany, in Rennes, where my life as "only" a PhD student started. I met and worked there, with different friendly and helpful people who made my adaptation in this new environment easier. I would like to thank the two lab-partners Dr. Rémy Hemealaere and Dr. Aurelie Macé who allowed me to work in a relaxed and pleasant atmosphere, and our lab neighbour, my favourite Peruvian, Johal Ruiz, with whom I had some really good moments. I'm also grateful to Dr. Francois Carreaux and Dr. Fabienne Berrée who were there for me when I needed them, and to Dr. Fabien Tripoteau, who did substantial preliminary work on the subject and was always available when I contacted him.

After finishing the first half of the journey, I arrived at a turning point, when prompted by my increased audacity, I started to see everything around me bigger; it was time for me to move from Brittany to GREAT Britain. Thus, I crossed the sea to reach a very beautiful city in the North East of England; Durham. Before going, I had only heard rumours and legends about

this place, like people there do not speak English, but Geordie English, for example. It's totally true. So, after some time of adaptation, I succeeded to fit in and really had a nice time with all my colleagues, Dr. Farhana Ferdousi, Dr. Alexander Gehre, Dr. Wade Leu, Dr. Adam Calow, Hesham Raffat Shawky Haffez, Enrico La Cascia, Katrina Madden, David Chisholm, Sergey Arkhipenko, Alba Pujol, John Purdie, and all the students who came to work with us. As I promise, I would like to give a special mention to Dave, *ma biche*, who helped me to crystallise some of my compounds, and to Enrico and Wade for their support, especially every time we went to The Swan and Three Cygnets and to Fabio's. By working on this interesting project, I also had the opportunity to work in collaboration with Dr. Mark Fox who provided the theoretical DFT calculations within this thesis, and I'm thankful for all these results.

For a journey as a PhD thesis in chemistry to be successful, you need to rely on some other partners. Thus, I would like to thank all the staff involved in the following services; the CRMPO (Centre Régional de Mesures Physiques de l'Ouest), and the NMR department from Rennes University, and also the NMR, the mass and the crystallographic department from Durham University for all their help and expertise.

I'm also grateful to la Région Bretagne and to the Department of Chemistry of Durham University for the funding which allowed me to work on this project.

Cependant je n'oublie pas les personnes qui sont toujours en France, et pour un expatrié, il est toujours bon de rentrer chez soi. Ce prochain paragraphe est dédié aux personnes que malheureusement je n'ai que peu vues durant ces années que ce soit à Orléans ou en Alsace. Petite dédicace à mes deux familles qui m'attendent à bras ouverts à chaque fois que je retrouve mes terres d'origine. Je voudrais premièrement remercier ma famille; mes parents, frère et sœur pour leur soutien durant ce périple. Je voudrais ensuite glisser un mot pour ma famille de substitution, au sein de laquelle je partage de nombreuses amitiés de longues dates.

Merci pour les mémorables moments que l'on passe ensemble à chacun de mes retours. Dans de nombreuses années certains murs s'en souviendront encore.

I would like to thank all the other friendly people I was involved with during these three years; my flatmates, basketball mates, and many others I met during social events.

Finally, because nice stories always finish with a happy ending, the last words are for a very special person to me. I'm so glad that we succeeded to cross the polystyrene boarder between our two benches. I came to know you through the months, and I discovered a wonderful and funny person. Mona, thank you for everything, sooooo much.

Now it's time, for the most brave of you, to see what I've done the past years. Good luck and see you for other adventures!!!!

Abbreviations

Å: Angstrom	dd: Doublet doublet
Ac: Acetyl	DDQ: 2,3-Dichloro-5,6-dicyano-1,4-benzoquinone
AM1: Austin model	de: Diastereomeric excess
aq.: Aqueous	DEA: Diethanolamine
Ar: Aryl	DFT: Density functional theory
ASAP: Atmospheric pressure solids analysis probe	DIBAL: <i>Di</i> sobutylaluminium
atm: Atmosphere	DMAP: 4-Dimethylaminopyridine
B ₂ pin ₂ : Bis(pinacolato)diboron	DMF: Dimethylformamide
BHT: Butylated hydroxytoluene	DMSO: Dimethylsulfoxide
Bn: Benzyl	dppe: 1,2-Bis(diphenylphosphino)ethane
Boc: <i>tert</i> -Butyloxycarbonyl	dpph: 1,2-Bis(diphenylphosphino)hexane
Bu, ⁿ Bu: <i>n</i> -Butyl	dr: Diastereomeric ratio
^t Bu: <i>tert</i> -Butyl	EDC: 1-Ethyl-3-(3-dimethylaminopropyl)carbodiimide
Bz: Benzoyl	ee: Enantiomeric excess
COD: 1,5-Cyclooctadiene	EI: Electron impact
Δ: heat	<i>endo</i> : Endocyclic
d: Doublet	eq.: Equivalent
DA: Diels-Alder	Eq.: Equation
dba: Dibenzylideneacetone	ESI: Electrospray ionisation
DBU: 1,8-Diazabicycloundec-7-ene	ESR: Electron spin resonance
DCM: Dichloromethane	

Et: Ethyl	MeCN: Acetonitrile
EWG: Electron withdrawing group	MIDA: methyliminodiacetic acid
<i>exo</i> : Exocyclic	MOM: Methoxymethyl ether
fod: 6,6,7,7,8,8,8-Heptafluoro-2,2-dimethyl-3,5-octanedione	M.p.: Melting point
Fur: Furyl	m. s.: Molecular sieves
HDA: Hetero Diels-Alder	MW: Molecular weight
hex: Hexyl	N: Normality
HOMO: Highest occupied molecular orbital	NMO: <i>N</i> -oxide 4-methylmorpholine
HPLC: High pressure liquid chromatography	NMR: Nuclear magnetic resonance
Hz, MHz: hertz, megahertz	NOE(SY): Nuclear Overhauser effect (spectroscopy)
Ip ₂ : Diisopinocampheyl	Norphos: 2,3-bis(diphenylphosphino)bicyclo[2.2.1]hept-5-ene
IR: Infrared	[O]: Oxidation
IRC: Internal reaction coordinate	OPT: Option
<i>J</i> : Coupling constant	Pd/C: Palladium on charcoal
K: Kelvin	PG: Protecting group
LCT: Liquid chromatography time of flight	Ph: Phenyl
LDA: Lithium diisopropylamide	pin: Pinacol
LUMO: Lowest unoccupied molecular orbital	PM3: Parameterised model
M: Molar	PMB: 4-Methoxybenzylether
Me: Methyl	ⁿ Pn: <i>n</i> -Pentyl
	ppm: Parts-per million

ⁱPr: *iso*-Propyl

psi: pound force per square inch

QTOF: Quadrupole time of flight

Ra-Ni: Nickel de Raney

R_f: Retention factor

r.t.: Room temperature

s: Singlet

SPhos: 2-Dicyclohexylphosphino-2',6'-
dimethoxybiphenyl

TBDMS: *tert*-Butyldimethylsilyl

TBDPS: *tert*-Butyldiphenylsilyl

TBS: Tributylsilyl

TEMPO: (2,2,6,6-Tetramethylpiperidin-1-
yl)oxyl

TES: Triethylsilyl

Tf: Triflate

THF: Tetrahydrofuran

TLC: Thin layer chromatography

TMS: Trimethylsilyl

TOS/Ts: Tosyl

TQD: Tandem quadrupole detector

TS: Transition state

Literature

Review

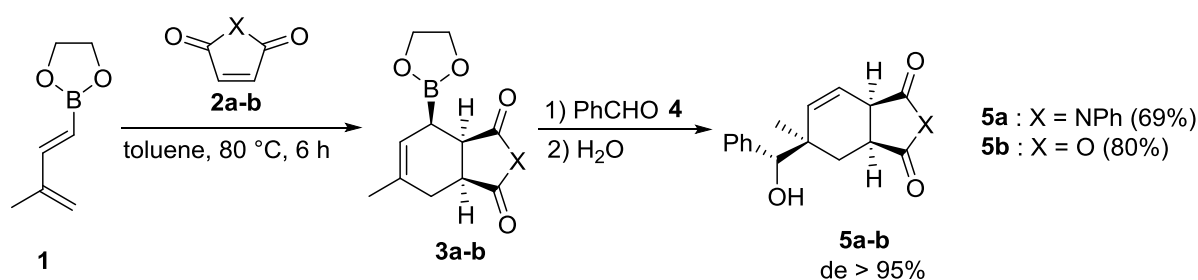
I. Introduction

Multicomponent reactions involving catalytic or non-catalytic step(s) have become essential tools in the field of synthetic organic chemistry.^{1,2,3,4,5,6,7,8,9} Several of these, which now bear the name of their inventors: Strecker; Hantzsch; Biginelli; Mannich; Passerini or Ugi; have been known and widely used for many years, and the development of new multicomponent processes still receives considerable attention. Indeed, these reactions offer a number of attractive advantages including simple experimental procedures, high convergence, and access to diverse structural and functional systems, often with high levels of atom economy. Boron compounds have long been ignored in this attractive area of research despite their wide range of reactivity.^{10,11} In 1993, however, Petasis and co-workers reported a new synthesis of allylamines *via* stepwise condensation of a secondary amine, *para*-formaldehyde and (*E*)-styryl boronic acid.¹² This was the first report of this type of transformation, which is now referred as the Petasis borono-Mannich reaction, and was later extended to a wide variety of other aldehydes, such as glyoxylic acid (for example), boronic acids, esters or trifluoroborates and other amine partners.^{13,14,15} Subsequently, other multicomponent reactions involving trialkylborane,^{16,17} alkenyl-,^{18,19} aryl-,^{20,21} allyl-,²² allenyl-,²³ and alkynyl boronic acids or esters^{24,25,26} have been reported in the literature. Boron substituted 1,3-dienes and heterodienes have also been successfully used as key elements in such strategies.^{27,28}

II. Boron-substituted 1,3-(hetero)dienes in multicomponent processes

II.1 1-Boron-substituted 1,3-dienes

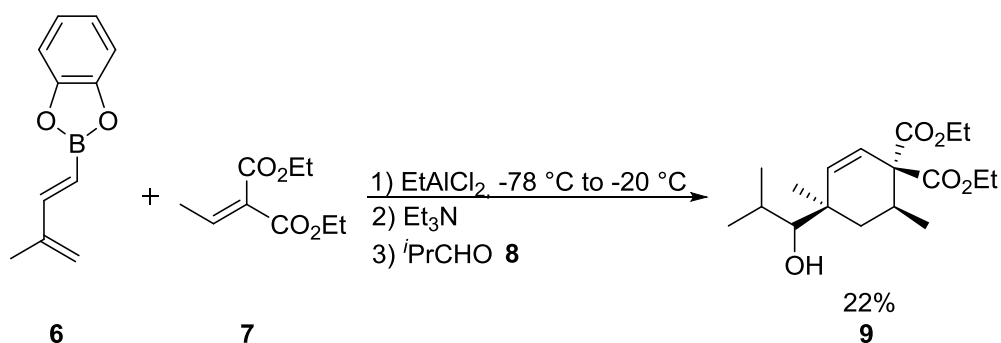
The first Diels-Alder reaction involving a 1-boron-substituted 1,3-diene was described in 1972 by Mikhailov and co-workers,²⁹ and it was only fifteen years later that the groups of Vaultier and Hoffmann highlighted the real potential of these compounds in tandem cycloaddition [4+2]/allylboration processes.³⁰ These dienes reacted with activated dienophiles, such as maleic anhydride **2b** or *N*-phenyl maleimide **2a**, at relatively high temperatures (80 °C in toluene) to afford exclusively the *endo*-isomers **3a-b** (Scheme 1). The resulting cycloadducts, which contain an allylboronate functionality, then reacted with aldehydes to afford the corresponding homoallylic alcohols **5a-b** with high diastereoselectivity (de > 95%).



Scheme 1. 1-Boron-substituted 1,3-diene in a tandem cycloaddition [4+2]/allylboration sequence.

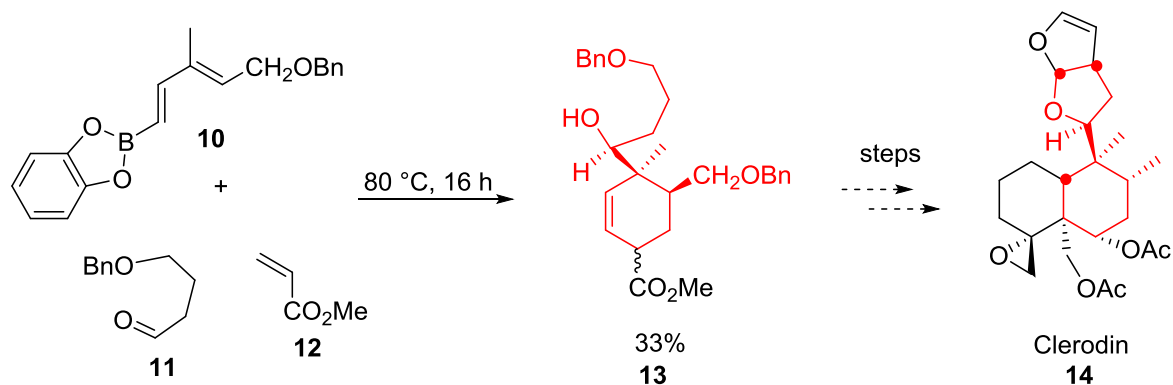
In the case of methyl acrylate or acrylonitrile, a mixture of *endo* and *exo* diastereomers was obtained regioselectively at higher temperature, in a 1:1.6 to 1:1.8 ratio. By contrast, the [4+2] cycloaddition proved to be completely regioselective when performed on the catechol derivative **6** in the absence of solvent.³¹ The use of a stoichiometric amount of EtAlCl₂ as

Lewis-acid catalyst provided a lowering of the reaction temperature, a shortening of the reaction time and good stereocontrol (Scheme 2).³²



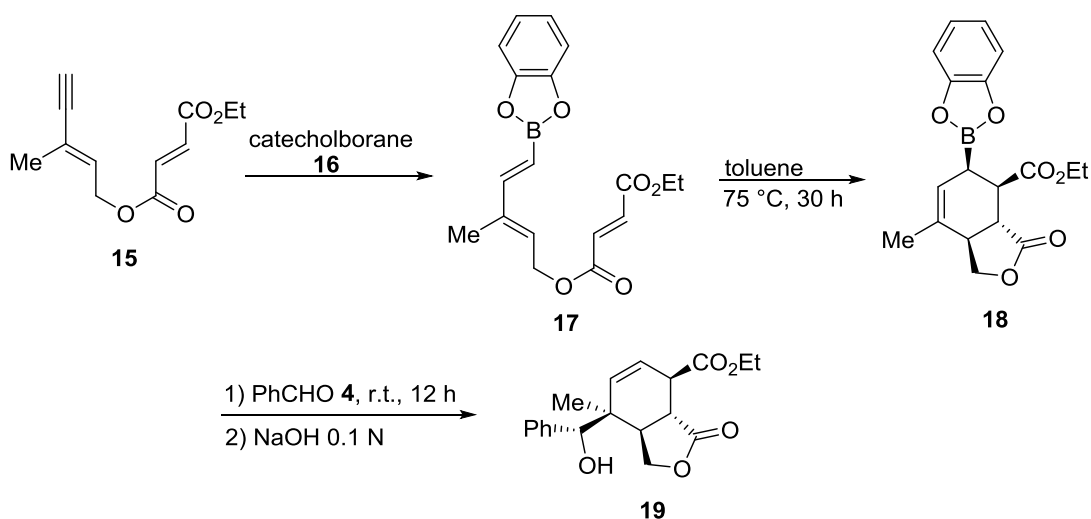
Scheme 2. Lewis-acid catalyst in the tandem cycloaddition [4+2]/allylboration sequence.

Alternatively, simple heating of a mixture of a 1-bora-1,3-diene **10**, a dienophile **12** and an aldehyde **11** gave direct access to polysubstituted cyclohexenes **13** that were difficult to prepare using the previously reported two steps methodology.³³ A concise and efficient synthesis of an advanced precursor of Clerodin **14**, a powerful antifeedant natural product, has been reported using a strategy based on this three-component process (Scheme 3).³⁴



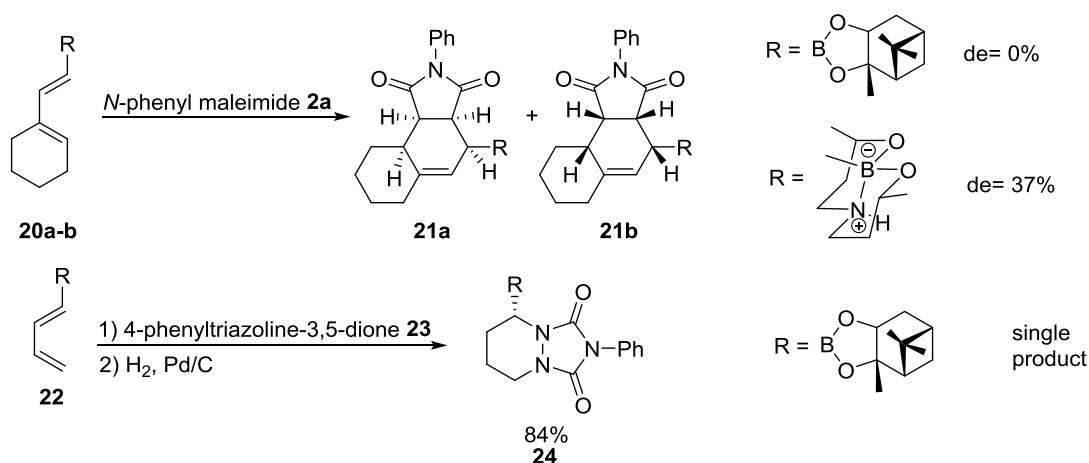
Scheme 3. Synthesis of an advanced precursor of Clerodin **14**.

Extension of this work to the intramolecular version is depicted in Scheme 4. The bicyclic lactone **19** was obtained stereoselectively from a diene-yne **15** in a one-pot process with control of the relative stereochemistry of the five stereogenic centers.³⁵



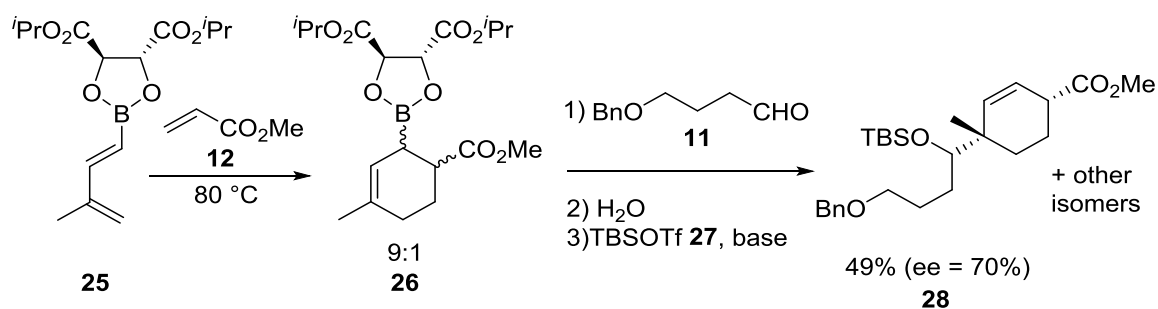
Scheme 4. Intramolecular DA/allylboration sequence.

Concerning the access to enantioenriched compounds by using chiral boron substituents, no diastereoselectivity was observed with the (+)-pinanediol ester **20a** and *N*-phenyl maleimide **2a**.³⁶ 1,3-Dienyldioazaborecane **20b**, derived from a chiral aminodiols of C_2 symmetry, underwent a faster cycloaddition, as already observed for similar tetra-coordinated boron species,^{37,38} but giving only a modest 2.2:1 ratio of diastereoisomers. By contrast, the cycloadduct **24** was obtained as a single product with excellent stereoselectivity in 84% yield, however, this could probably be attributed to the special structure of the dienophile **23** used (Scheme 5).³⁹



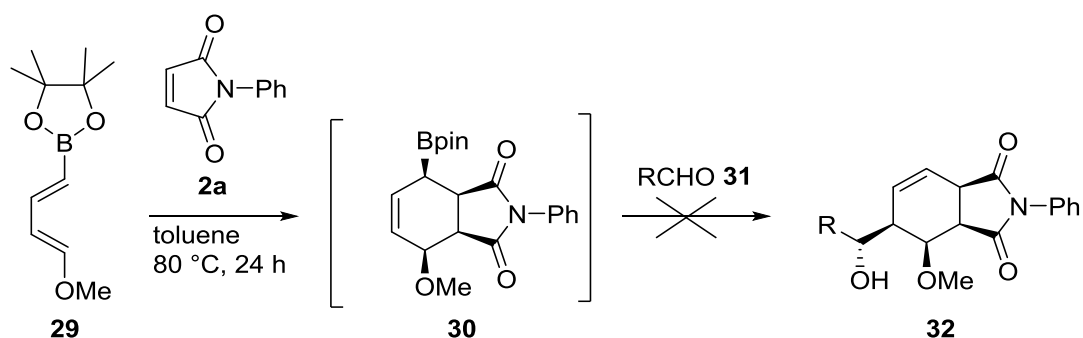
Scheme 5. Diastereoselective DA reaction with *N*-phenyl maleimide **2a** and 4-phenyltriazoline-3,5-dione **23**.

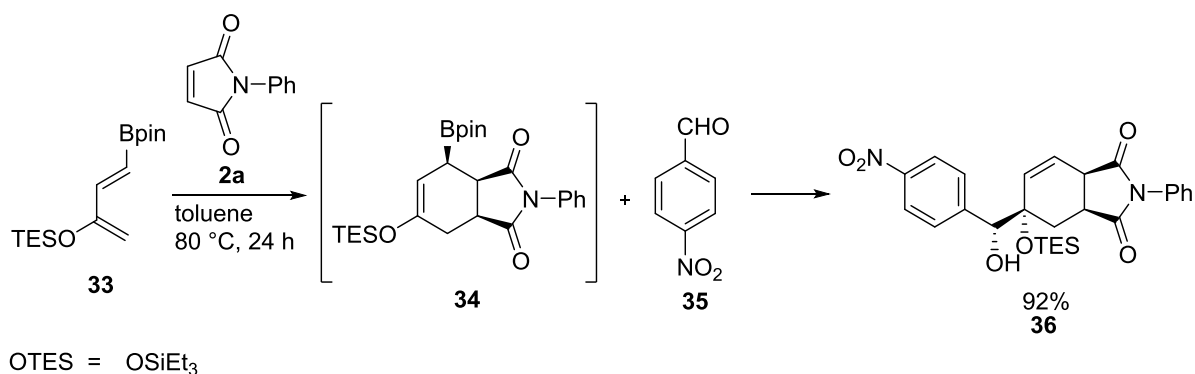
Finally, interesting results were reported with methyl acrylate **12** and dienes derived from tartrate esters **25** (9/1 de, 70% ee for the major isomer) (Scheme 6).⁴⁰



Scheme 6. Asymmetric synthesis of a α -hydroxyalkyl cyclohexane.

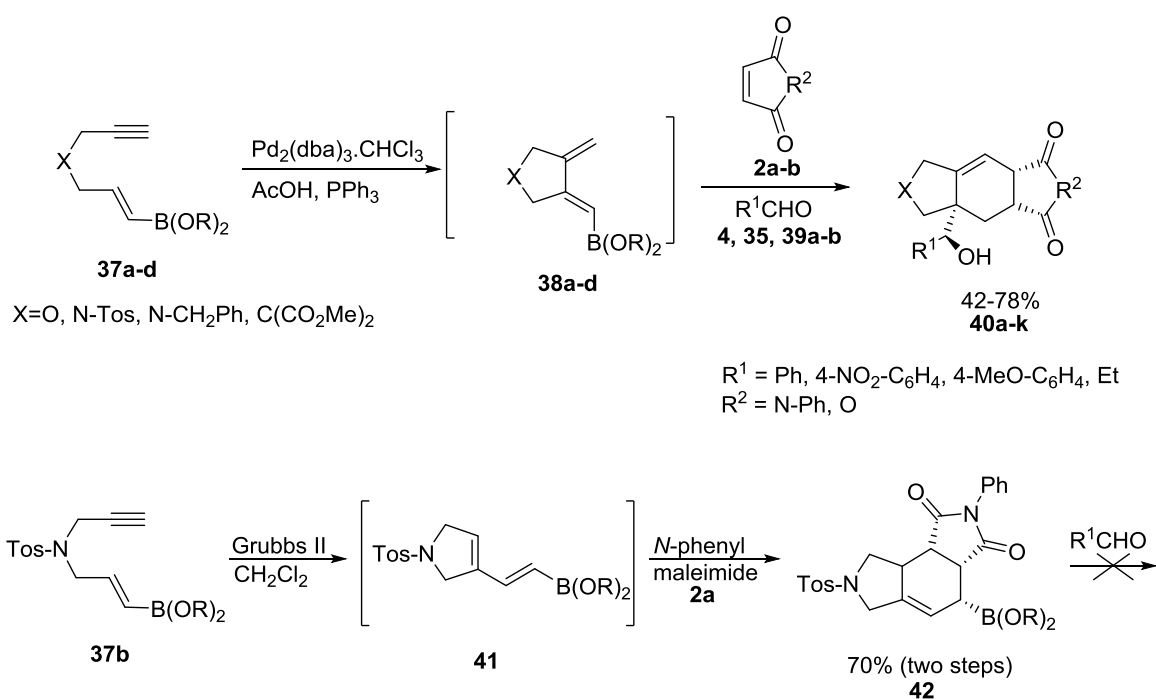
In 2003, Hall and co-workers reported the application of electron-rich alkoxy-functionalised dienyl boronates **29** in one-pot tandem Diels-Alder/allylboration reactions.⁴¹ In the case of the 4-methoxy-substituted diene **29**, if the first step occurred at 80 °C in toluene, it was impossible to obtain the allylation products **32**, even by heating at higher temperature or by activation with EtAlCl_2 . By contrast, with the 3-OTES derivative **33**, bicyclic, three-component adducts **36** were isolated in good yields up to 92%. A single diastereomer was detected with maleimide **2a**, the diastereoselectivity being lower with methyl acrylate and vinyl oxazolidinone (Scheme 7).





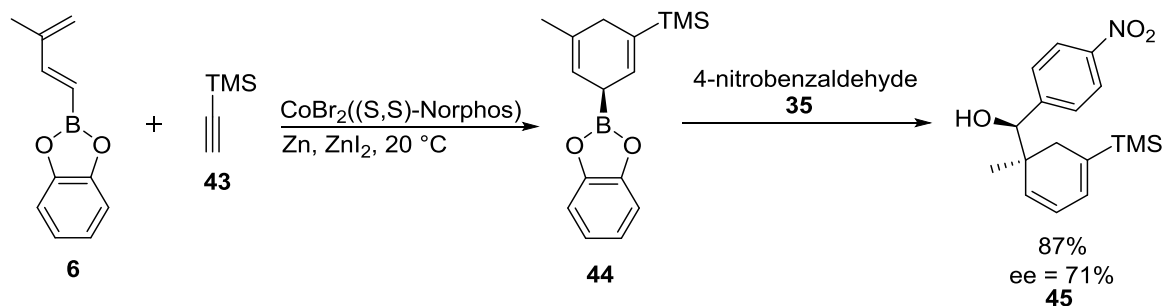
Scheme 7. Tandem [4+2]-cycloaddition/allylboration of 3- and 4-alkoxy-dienyl boronates.

A one-pot, palladium-mediated cycloisomerisation of ene-yne **37a-d** was applied to the synthesis of the boronated diene **38a-d**, which was not isolated, but directly used in a one-pot, Diels-Alder reaction/allylboration sequence. This efficiently generated, in high yields, tricyclic structures **40a-k** with control of the four stereogenic centers created (Scheme 8). In the presence of Grubbs II catalyst, a skeletal isomer **41** was produced from **37b**. If the [4+2]-cycloadduct **42** was obtained with *N*-phenyl maleimide **2a**, it failed to give homoallylic alcohols, probably due to steric hindrance.⁴²



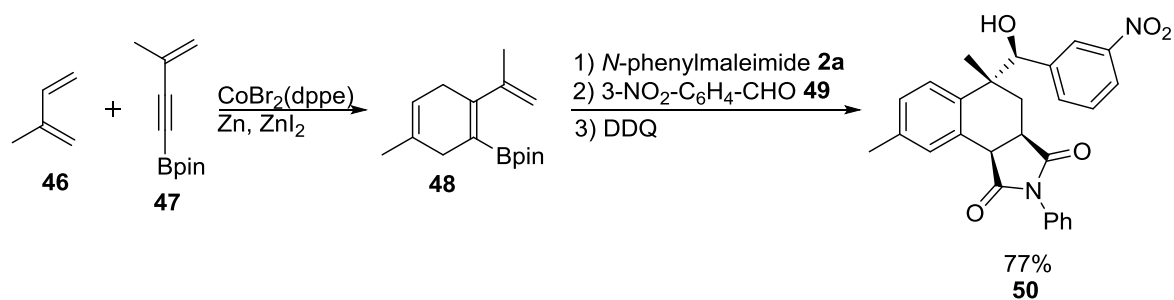
Scheme 8. Metal-mediated cycloisomerisation/Diels-Alder reaction/allylboration sequence.

An elegant, three-component process was developed by Hilt and co-workers using a cobalt-catalysed Diels-Alder reaction as the key step in a one-pot, cycloaddition/allylboration sequence.^{43,44} With (*S,S*)-Norphos as chiral ligand, the desired alcohol **45** was isolated in 87% yield and 71% ee (Scheme 9).



Scheme 9. Cobalt-catalyzed Diels-Alder/allylboration sequence.

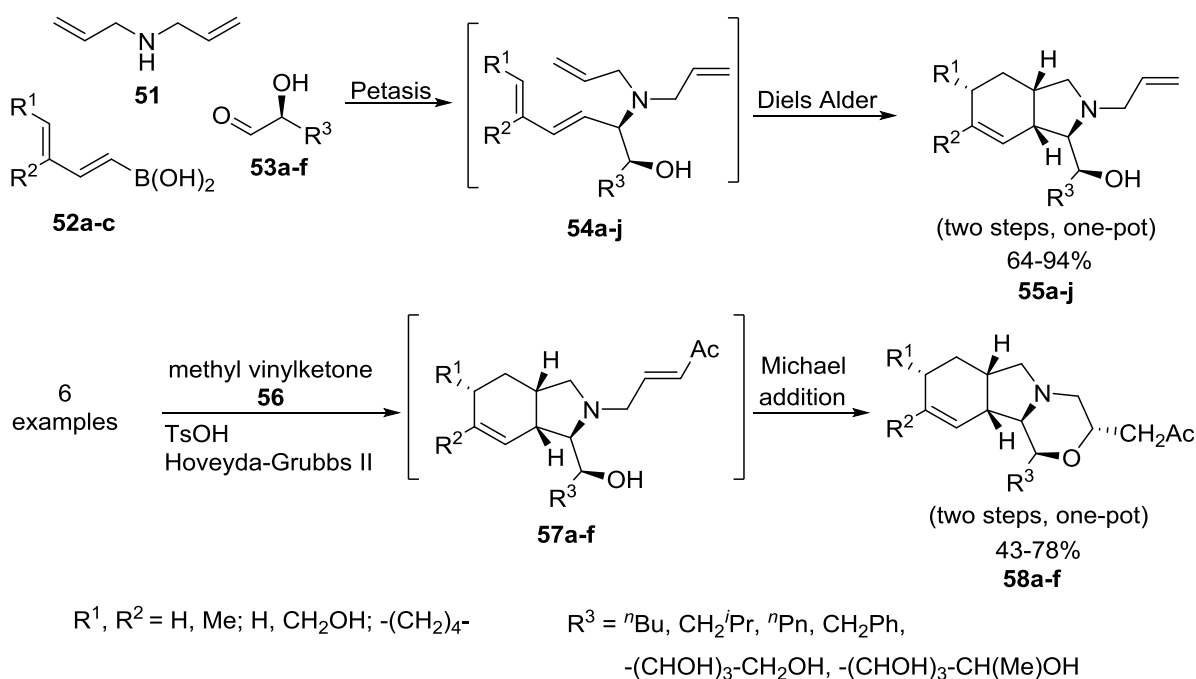
In a related process, the same group reported a two-steps cascade reaction interconnecting four components to afford dihydroaromatic compounds **48** with a high degree of diastereoselectivity and good yields. After cycloaddition and allylboration, the resulting product was oxidized to afford the corresponding tetrahydronaphthalenes **50** (Scheme 10).⁴⁵



Scheme 10. A two step reaction sequence for the synthesis of tetrahydronaphthalenes **50**.

Most of the tandem sequences, in which boron substituted 1,3-dienes were involved, were based on the first Diels-Alder cycloaddition, as shown above. However, a recent report of Norsikian, Beau and co-workers described a novel sequence of tandem transformations which combined the Petasis reaction, intramolecular [4+2]-cycloaddition, cross metathesis and

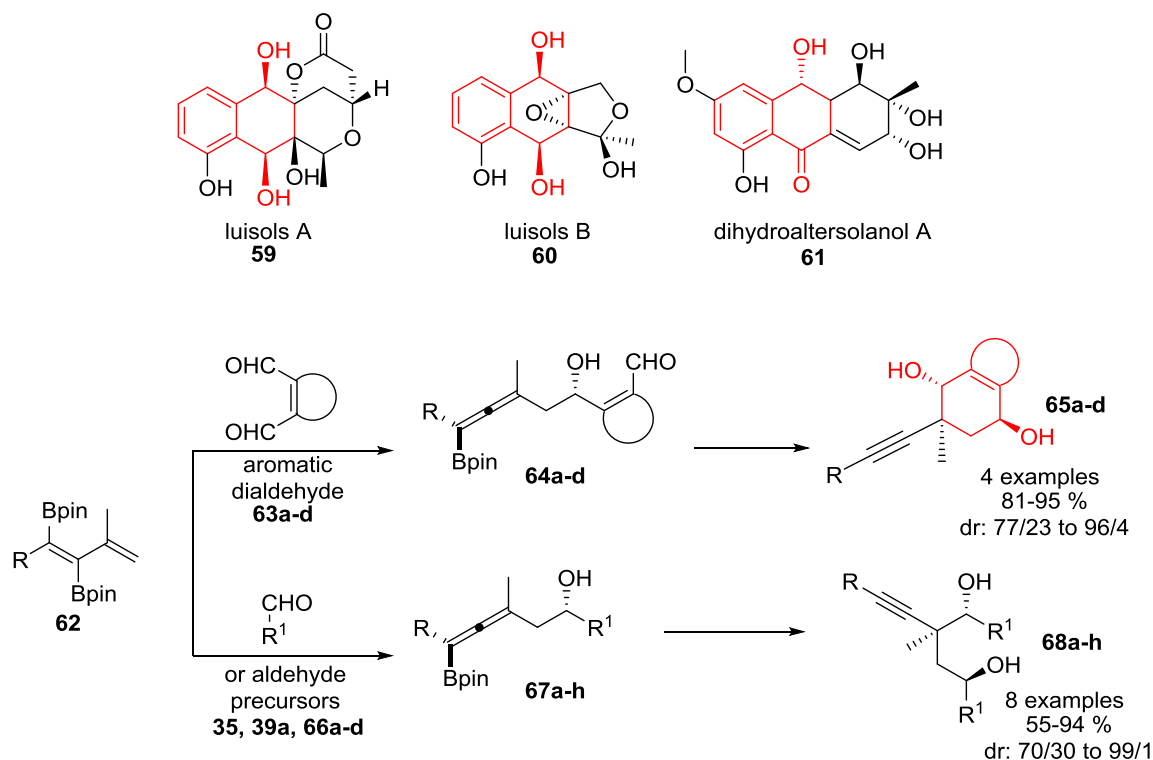
Michael reaction. This process gave access to new polycyclic heterocyclic scaffolds **58a-f** with good yields and complete stereocontrol (Scheme 11).⁴⁶ One year later, the same research team synthesised, based on the same chemistry, more than 30 examples of products with the scaffold as **55**, and proposed a mechanism based on theoretical calculations which supported the involvement of a Diels-Alder reaction occurring through an *endo* approach, with formation of the product with a *cis*-ring junction.⁴⁷



Scheme 11. Tandem sequence based on the Petasis, borono-Mannich reaction as first key step.

Recently, a new sequence using bis-borobutadiene **62** was developed to provide 1,4-diaromatic-diol as well as skeleton like **59**, **60** and **61**. The sequence started with an allylboration to provide the allenylboronate species **64** or **67** with high diastereoselectivity. The allenyl boronate intermediate formed during the first step exerted axial chirality with the substituted allenyl moiety and also a stereogenic carbon center. Depending on the nature of the partner used in the sequence, the outcome of the reaction differed. In the case of a monoaldehyde, a second equivalent of aldehyde did react with moderate to excellent enantioselectivity to afford skeleton **68**, whereas the dialdehyde reacted in an intramolecular

manner to provide 1,4-diaromatic-diol structure **65** (Scheme 12). In every case, the formation of the major diastereoisomer was explained by steric or π -electron conjugation effects in the Zimmerman-Traxler transition state.⁴⁸

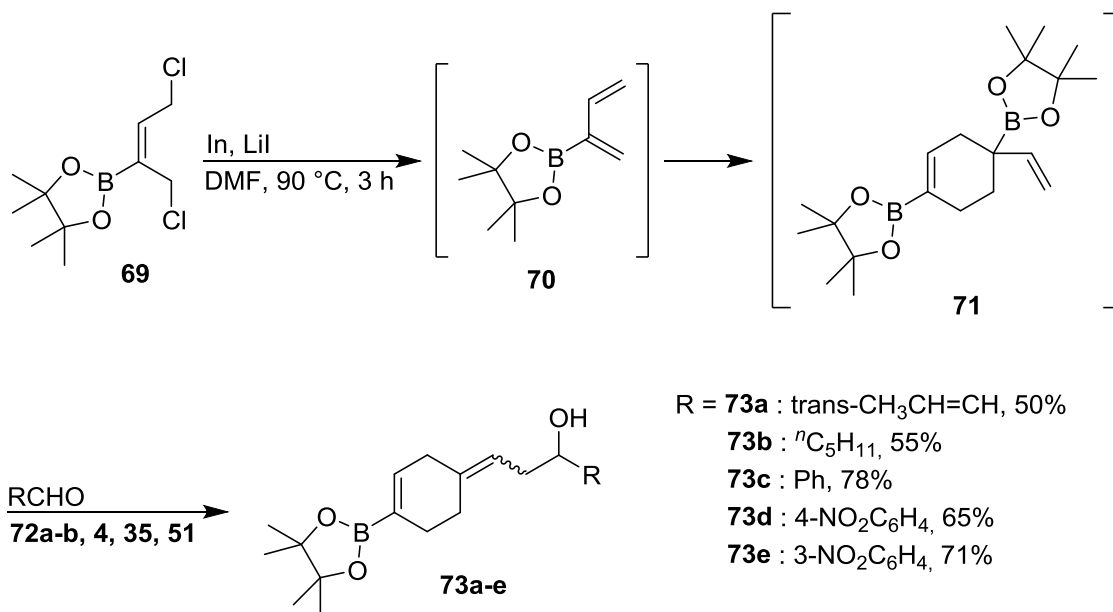


Scheme 12. Reaction of bis-borobutadiene **62** with different aldehydes and dialdehydes.

II.2. 2-Boron-substituted 1,3-dienes

In contrast to 1,3-dienes functionalised with a boron atom in position 1, only a few studies have been reported on the related dienes substituted in position 2. These compounds are often difficult to synthesise and have, at least for the less substituted derivatives, a strong tendency to undergo Diels-Alder dimerisation even at r.t.^{49,50} This process was carefully investigated by Carreaux, Cossio and co-workers with regard to theoretical and experimental aspects.⁵¹ When the dechlorination was carried out in the presence of an aldehyde, the dimer **71** was

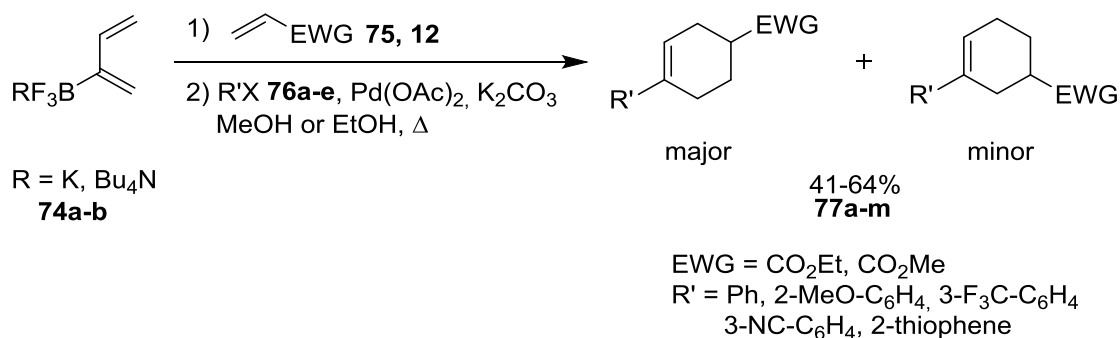
immediately converted to the expected homoallylic alcohols **73a-e** in moderate to good yields as mixtures of *E/Z*-isomers (Scheme 13).



Scheme 13. One-pot tandem dimerization/allylboration reaction of 1,3-diene-2-boronate **69**.

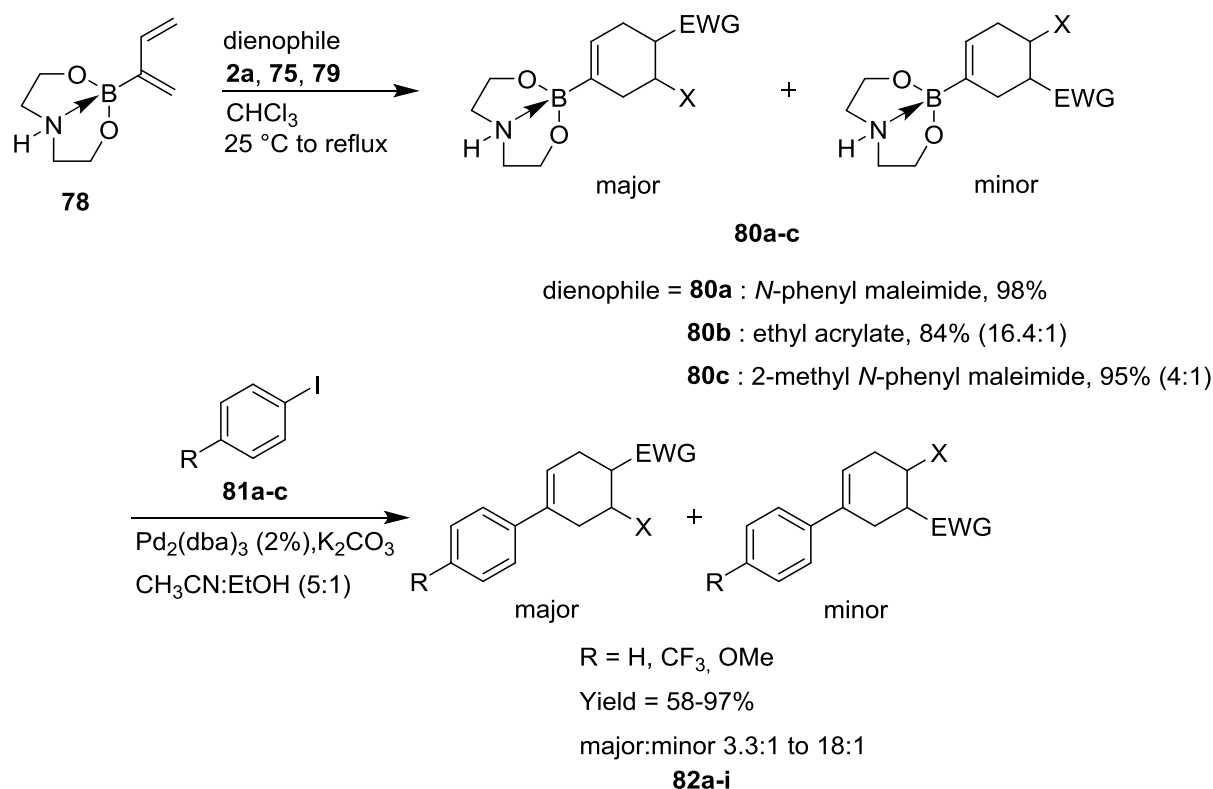
In 2005, Welker and co-workers started a series of studies on the synthesis of 2-boron-substituted 1,3-dienes and their reactivity in tandem reactions, concentrating mainly upon [4+2]-cycloadditions followed by cross-coupling reactions. Potassium and tetra-*n*-butylammonium buta-1,3-dienyl-2-trifluoroborates **74a-b** were synthesised in good yields from chloroprene and showed no propensity to dimerise.^{52,53} Exploration of the reactivity of these dienyl trifluoroborates began with Diels-Alder reactions with ethyl acrylate **75**, methyl vinyl ketone **12** and *N*-phenyl maleimide **2a**. The boron-containing cycloadducts, isolated with high yields, were subsequently cross-coupled using palladium catalysis. A one-pot sequence was also developed, first heating the boron diene with the dienophile, then adding an aryl halide **76**, Pd(OAc)₂ (5 mol%), K₂CO₃ (3 eq.) and finally refluxing the mixture in EtOH or MeOH for 5 h (Scheme 14). Reactions with various aryl halides **76**, substituted by electron-donating or -withdrawing groups and heteroaromatic halides occurred in moderate to

good yields (41% to 64% over two steps) with a preference for the *para*- over *meta*-regioisomers (2.3:1 to 5.7:1 ratio).



Scheme 14. Tandem Diels-Alder/Cross-Coupling reactions of trifluoroborates **74a-b**.

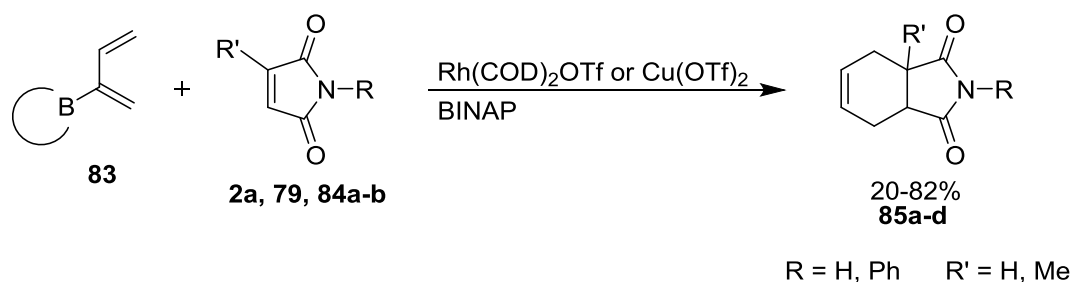
Using the same methodology, the preparation and reactivity in tandem Diels-Alder/palladium cross-coupling sequences of a 2-diethanolaminoboron-substituted 1,3-diene **78** were investigated.⁵⁴ This diene has proved to be significantly more reactive and more regioselective in [4+2]-cycloadditions compared to the corresponding trifluoroborate. The cycloadducts were then efficiently cross-coupled to iodobenzene **81a**, 4-trifluoromethyl-1-iodobenzene **81b** and 4-iodoanisole **81c**. The regioselectivity observed in the initial Diels-Alder reactions were maintained after cross-coupling (Scheme 15).



Scheme 15. Diels-Alder/cross-coupling reactions of **78**.

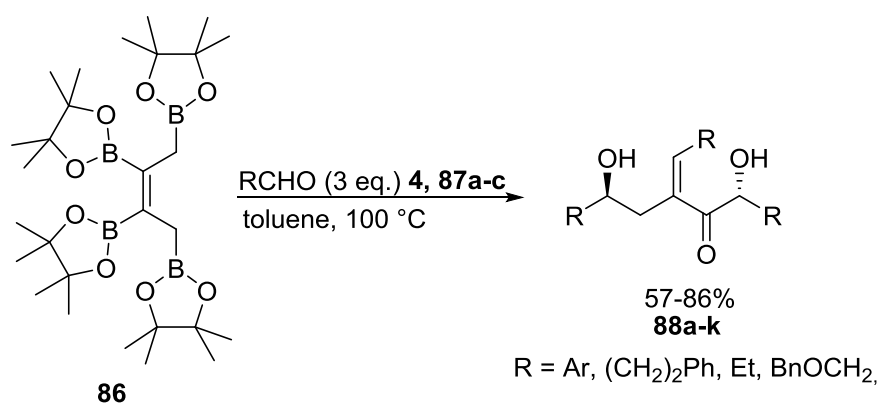
More recently, new 2-boron substituted 1,3-dienes containing diol and triol ligands were prepared under basic conditions that prevent the dimerisation by-product formation. These four-coordinate boron complexes participated in the same tandem Diels-Alder/Suzuki cross-coupling sequence, which appeared to be palladium-catalysed. The final cycloadducts were obtained in good yields (63% to 83%).⁵⁵

Finally, Welker and co-workers described metal catalysed tandem Diels-Alder/hydrolysis reactions of 2-boron substituted 1,3-dienes.^{56,57} Boron-dienes containing various ligands reacted with maleimides in the presence of rhodium and copper catalysts using BINAP as ligand (Scheme 16). NMR analysis of the crude product showed traces of the boron cycloadduct, highlighting that mechanism proceeded, first with a Lewis-acid catalysed [4+2]-cycloaddition, and then by Lewis-acid assisted C-B bond protonation.



Scheme 16. Metal catalyzed tandem Diels-Alder/hydrolysis reactions.

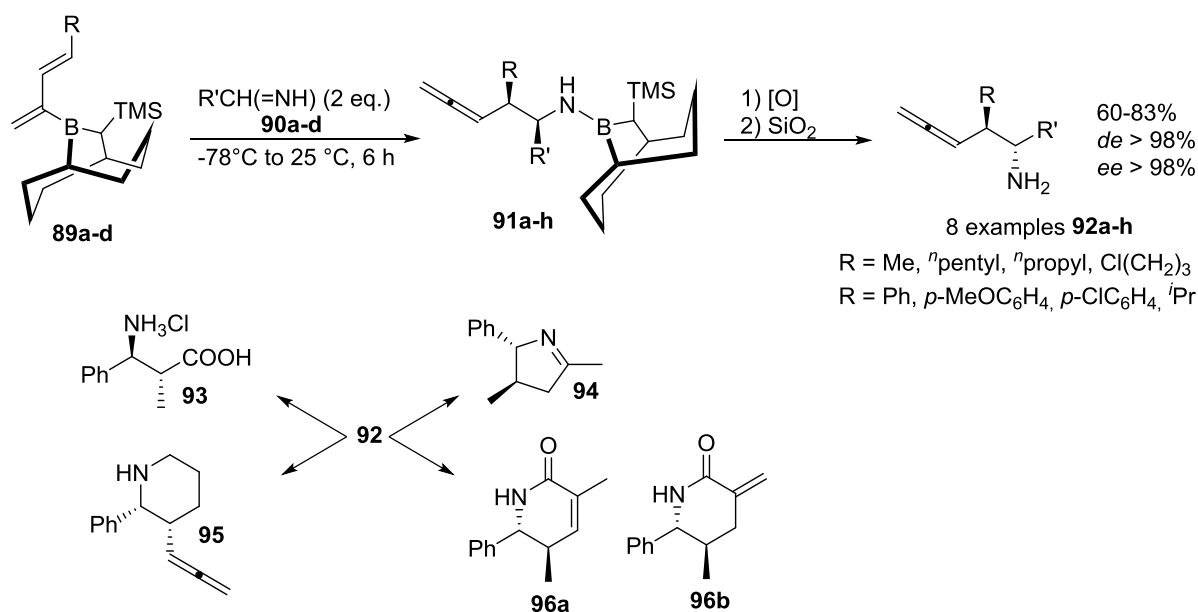
In a different approach which exploited another aspect of the reactivity of boron-substituted diene, 2,3-bis[(pinacolato)boryl]-1,3-dienes **86**, synthesised by treatment of 1,1-[bis(pinacolato)boryl]alkenes with excess of 1-bromo-1-lithioethene, was engaged in a triple cascade aldehyde addition.^{58,59} 1,5-*Anti*-diols **88a-k** were produced *via* successive diboration, allylboration reactions and finally elimination of boryl and boroxo groups. Four C-B bonds were converted into two C-C and one C=C bonds with total stereocontrol in each step (Scheme 17).⁶⁰



Scheme 17. Synthesis of *anti*-1,5-diols **88** by triple aldehyde addition.

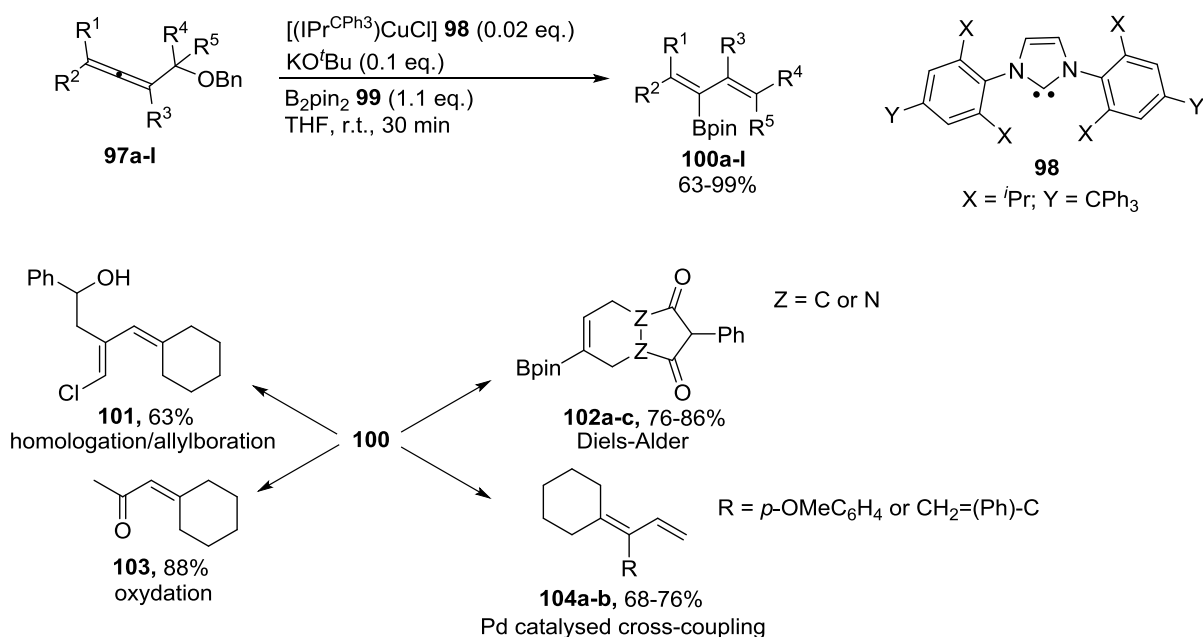
Dienes **89a-d** were synthesised through a hydroboration/vinylidene insertion sequence. The resulting dienes were then used to synthesise the boronic amide derivatives **91a-h**, by addition of *N*-DIBAL aldimine **90a-d**. Oxidative workup followed by hydrolysis led to the formation of β -allenylamines **92a-h** with high stereoselectivities in moderate to excellent yields. Products

92 were employed as precursors for the synthesis of enantiomerically pure *N*-heterocyclic products **94**, **95** and **96** and β -amino acids **93**.⁶¹



Scheme 18. Preparation of β -allenylamines **92** and their use in the synthesis of enantiopure products.

Another approach based on allenylborane chemistry, using copper(II) catalysed reaction and B_2pin_2 **99** as boron donor, was developed recently to synthesise 2-boron-substituted 1,3-dienes **100a-l**. The resulting dienes **100a-l** were then engaged: 1) in Diels-Alder cycloadditions to provide **102a-c**; 2) in Pd catalysed cross-coupling to give **104a-b**; 3) in an oxidation to yield α,β -unsaturated ketone **103**; and 4) in a homologation/allylboration sequence to afford the diene **101** (Scheme 19).⁶²

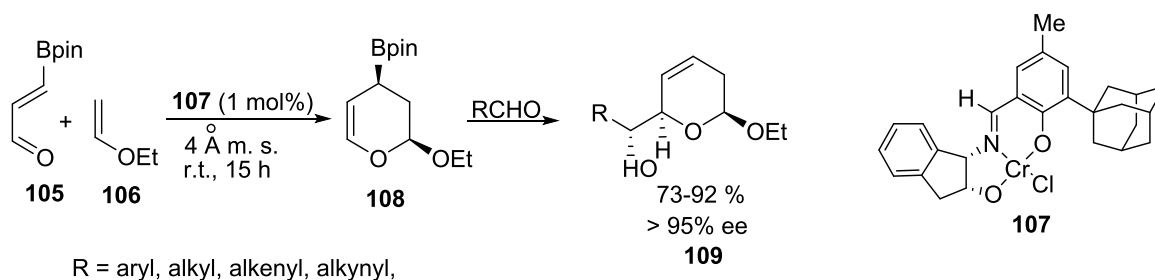


Scheme 19. Preparation of polysubstituted 2-boron-1,3-dienes and their use in different reactions.

II.3. 1-Boron-substituted 1,3-heterodienes

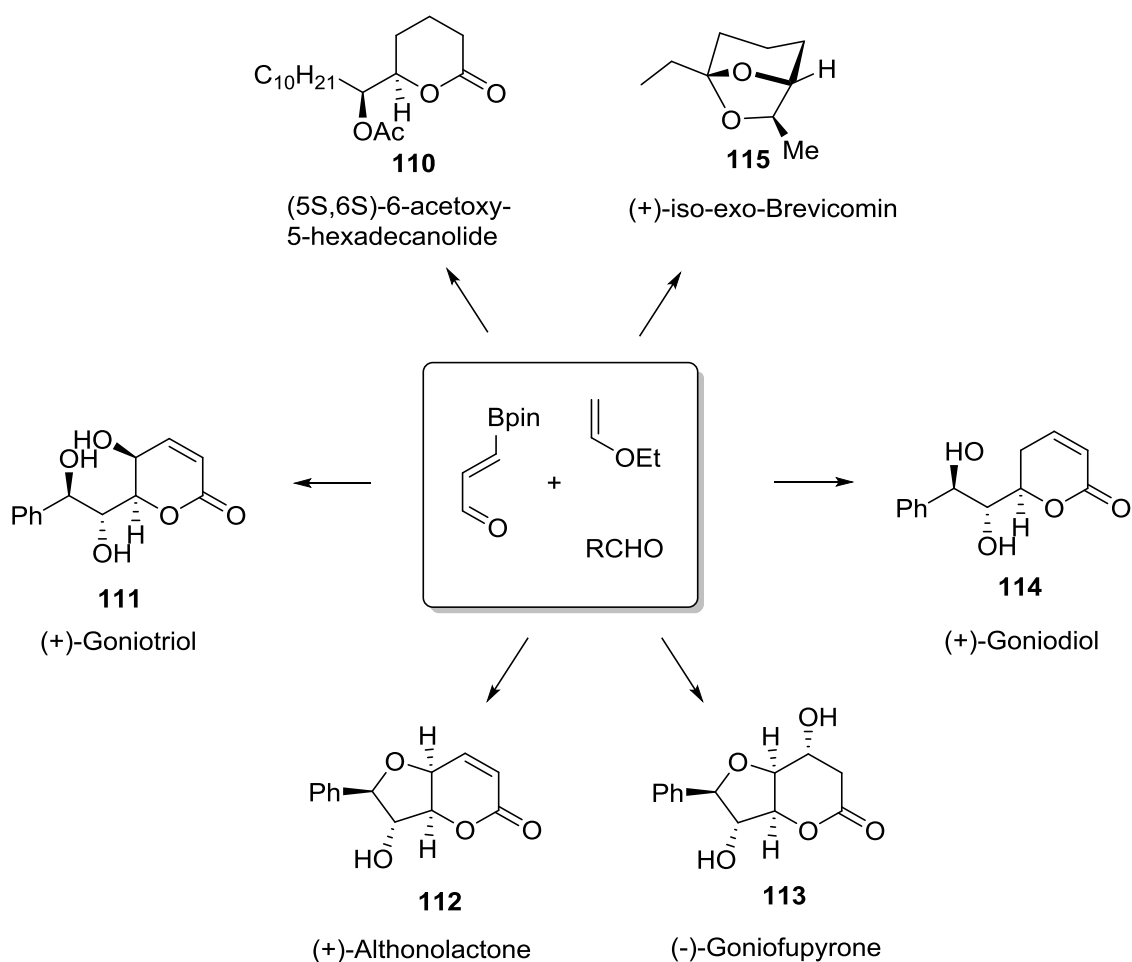
II.3.a. 1-Oxo-4-borono-1,3-dienes

In 2003, first examples of a novel diastereoselective routes to α -hydroxyalkyl dihydropyrans were reported; a sub-structure frequently encountered in the core of a wide-range of natural products.^{63,64,65} As in the carbocyclic variant, the intermediate cyclic allylboronate **108**, prepared from 3-boronoacrolein **105**, was the key element of a sequential Diels-Alder/allylation. In this case, the catalytic asymmetric version was carried out efficiently in the presence of the Jacobsen's tridentate chromium(III) complex **107** with high diastereo- and enantio-selectivity (Scheme 20).



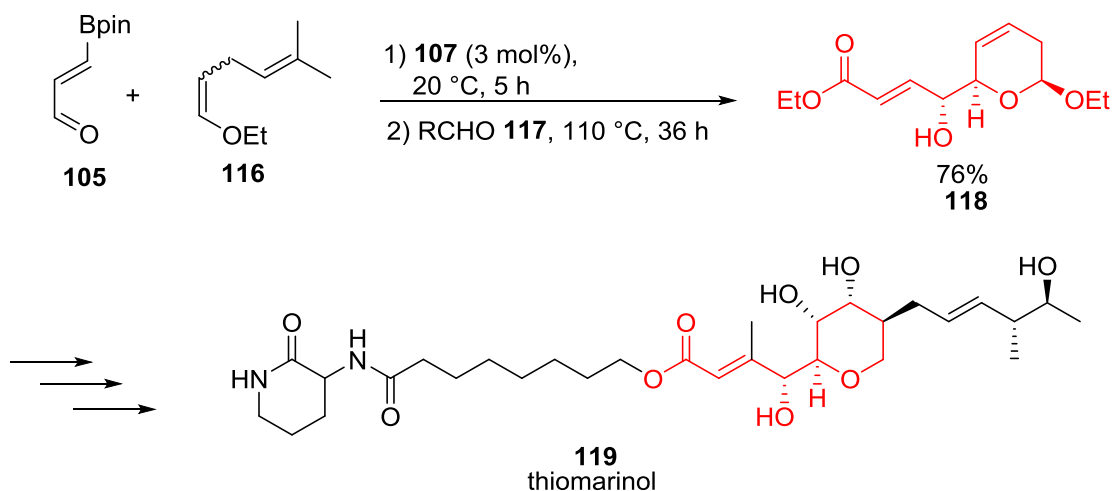
Scheme 20. Catalytic enantioselective three-component hetero-[4+2] cycloaddition/allylboration sequence.

The first application of this strategy in the synthesis of natural products and analogues concerned (5*S*,6*S*)-6-acetoxy-5-hexadecanolide **110**, the oviposition attractant pheromone of a mosquito capable of transmitting the West Nile Virus.⁶³ Thereafter, several members of the natural styryllactone family **111-114**, displaying cytotoxic and antitumor activities, have been also prepared according to this methodology.^{66,67,68} The combination of the catalytic hetero-Diels-Alder/allylboration sequence with a ruthenium-catalysed isomerisation gave access to the 6,8-dioxabicyclo[3.2.1]octane skeleton of (+)-*iso-exo*-brevicommin **115** (Scheme 21).⁶⁹



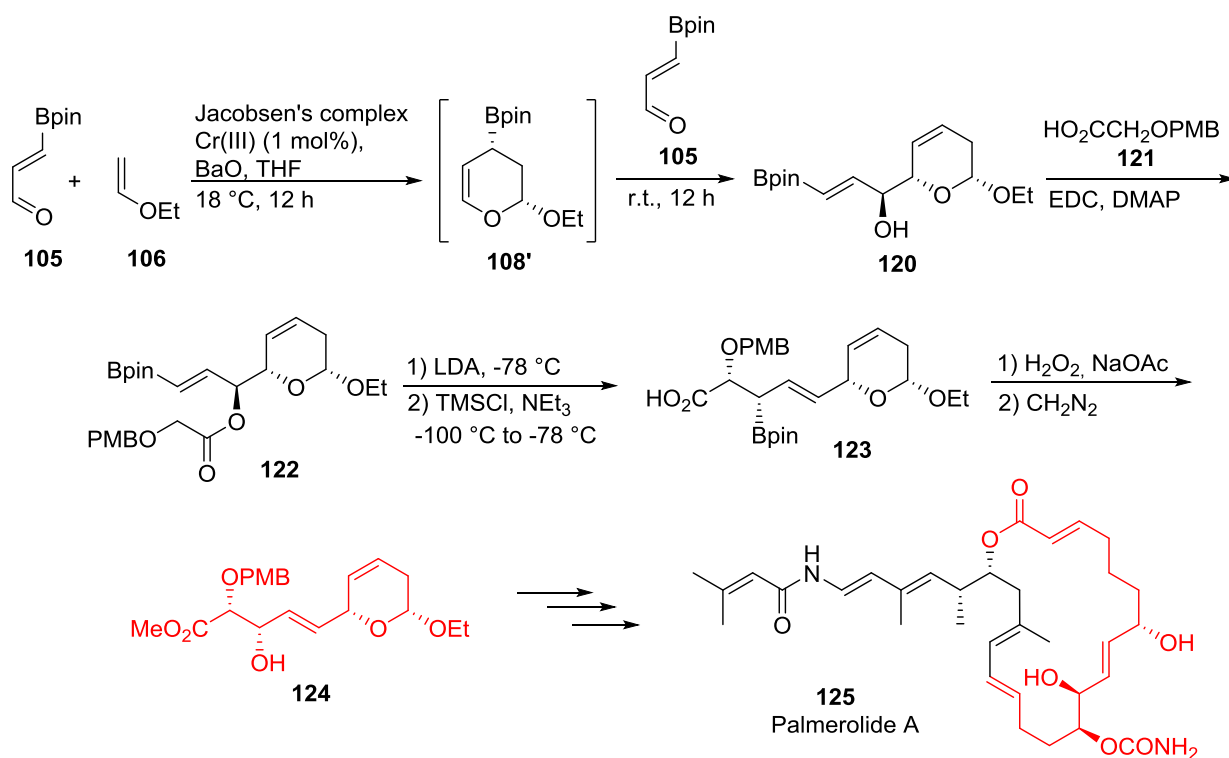
Scheme 21. Synthesis of natural products using the catalytic enantioselective HDA/allylboration sequence.

When a *Z:E*-mixture of 2-substituted enol ethers **116** was used as dienophile, only cycloadducts resulting from a selective reaction of the *Z*-isomer were present in the final product, that prevented the tedious preparation of an isomerically pure starting material. While the second allylboration step required conditions more severe than those employed in the case of ethyl vinyl ether, this approach was successfully applied in the key steps of the total synthesis of a member of the thiomarinol class of marine antibiotics **119** (Scheme 22).^{70,71}



Scheme 22. Total synthesis of a thiomarinol derivative **119**.

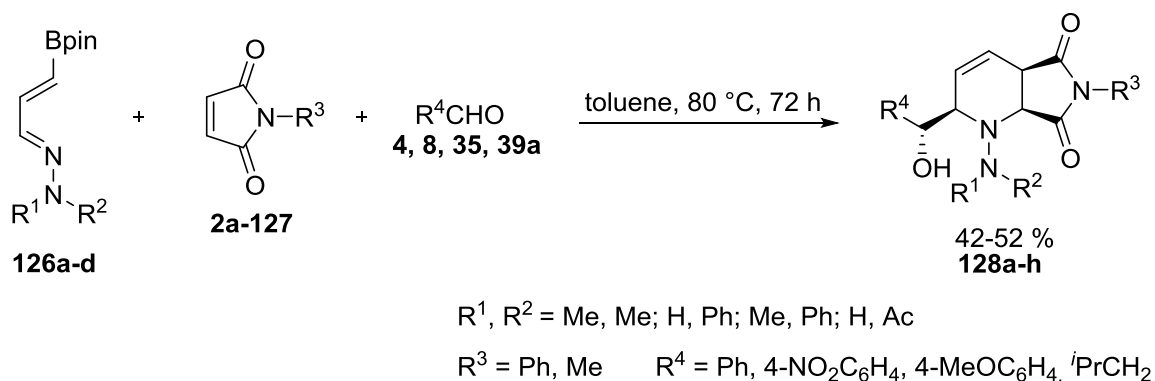
More recently, Hall and co-workers described the total synthesis of a complex 20-membered marine macrolide, palmerolide A **125**, a potent and unusually selective antitumor agent.⁷² In this case, the cyclic allylboronate **108'** prepared from the [4+2]-cycloaddition reacted with the starting 3-bromoacrolein **105** which then played the role of the aldehyde partner. The hydroxyl group of the resulting homoallylic alcohol was then engaged in a Claisen-Ireland rearrangement to afford an advanced intermediate **124** for the completion of the total synthesis (Scheme 23).



Scheme 23. Synthesis of an advanced intermediate **124** for the east fragment of palmerolide A **125**.

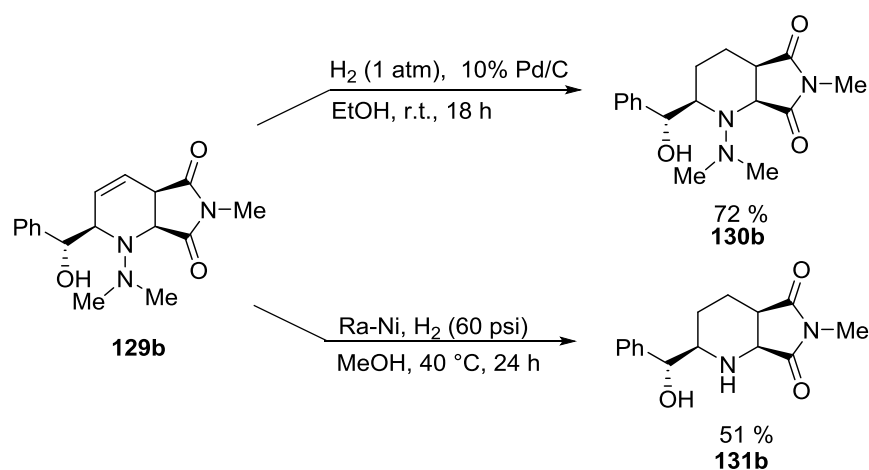
II.3.b. 1-Aza-4-borono-1,3-dienes

A few years before the description of the tandem process concerning the 3-boronoacrolein **105**, Hall and co-workers performed a multicomponent reaction involving 1-aza-4-borono-1,3-dienes **126** as key starting materials for the preparation of α -hydroxylalkyl piperidines **128a-h**. These scaffolds are present in several natural products, particularly in the alkaloid family of palustrine. The tandem process started with the hetero-[4+2]-cycloaddition of an hydrazone diene with maleimides, as electron-poor dienophiles, followed by an allylboration (Scheme 24).⁷³ This sequence proceeded with high stereocontrol, as already observed with the carbon and oxygen analogues. In addition, the absolute stereochemistry of the four newly created stereogenic centers were controlled by using a chiral auxiliary (>95% *de* in the case of an *L*-proline derived diene).



Scheme 24. Bicyclic piperidines from tandem aza-[4+2]-cycloaddition/allylboration.

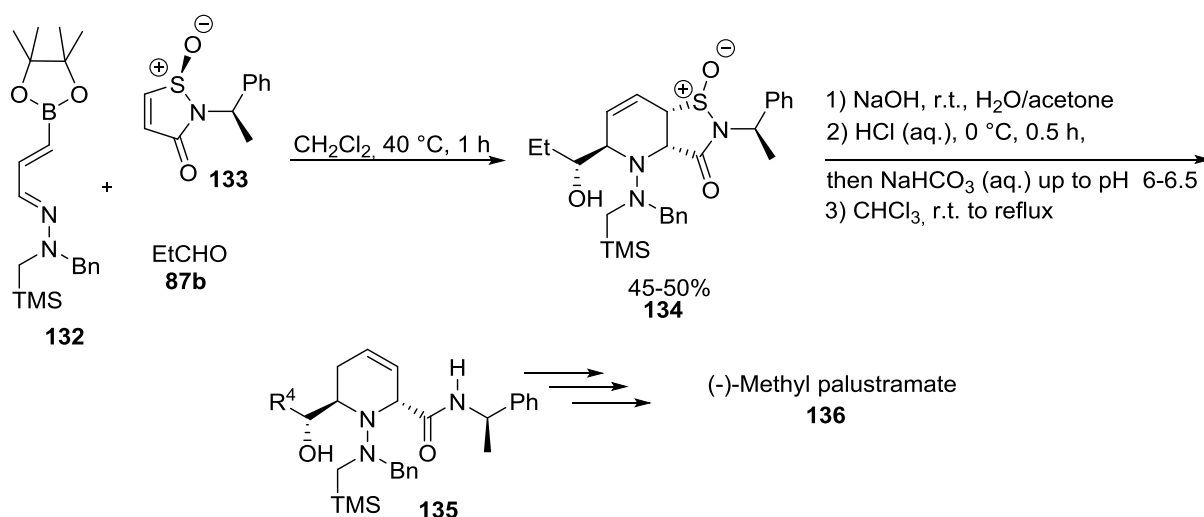
Diversification on the different units, diene, dienophile and aldehyde, has been described. Concerning the maleimide material, substituent R^3 did not exert any significant effect on the process. Other dienophiles have also been tested (acrylates, maleic anhydride), giving no products or unsatisfactory results. A large range of aldehydes, as aliphatic, electron-rich or electron poor benzaldehyde, could be used. Only very hindered aldehydes did not afford any product and both mono- and di-substituted arylhydrazines have proven to give the best yields, probably due to the higher reactivity of the corresponding hydrazones. Furthermore, the double bond of **129b** was selectively hydrogenated under palladium on charcoal, while hydrogenolysis of the hydrazone moiety occurred in the presence of Raney nickel (Scheme 25).



Scheme 25. Hydrogenolysis reactions of hydrazinopiperidines.

Following these results obtained in the liquid phase, Hall and co-workers also examined the suitability of a solid-phase strategy. Finally, due to problems of purity encountered with an *N*-arylmaleidobenzoic acid functionalised resin,⁷⁴ or availability of the supported aldehyde partner, a four-component variant of this chemistry was developed in solution phase. The pre-formation of the aza-butadiene component was not necessary and this gave access to a library of 944 polysubstituted piperidines with sufficient purity suitable for biological screening after purification by HPLC with mass-based fraction collection.⁷⁵

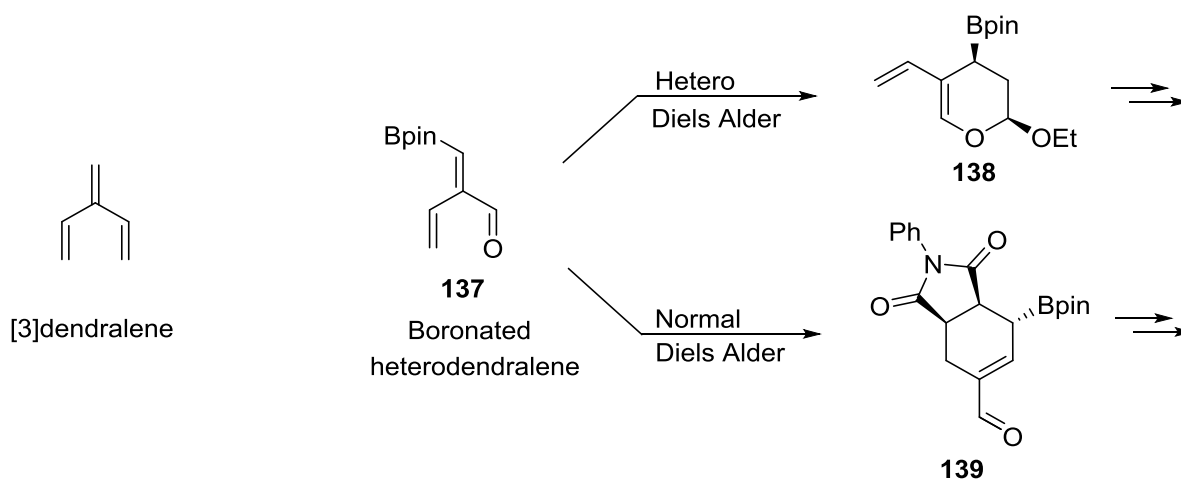
The flexibility and usefulness of this chemistry was also demonstrated in target-oriented synthesis with the synthesis of (-)-methyl palustramate and other 2,6-disubstituted piperidines.^{76,77} A chiral sulfinamide **133** was used as dienophile and a sequential three component aza-[4+2]-cycloaddition/allylboration/retro-sulfinyl-ene sequence was performed to afford 1,2,5,6-tetrahydropyridine **134** with high regio- and diastereo-selectivity (Scheme 26).



Scheme 26. Tandem aza[4+2]-cycloaddition/allylboration/retrosulfinyl-ene sequence.

II.4. Boron-substituted heterodendralene

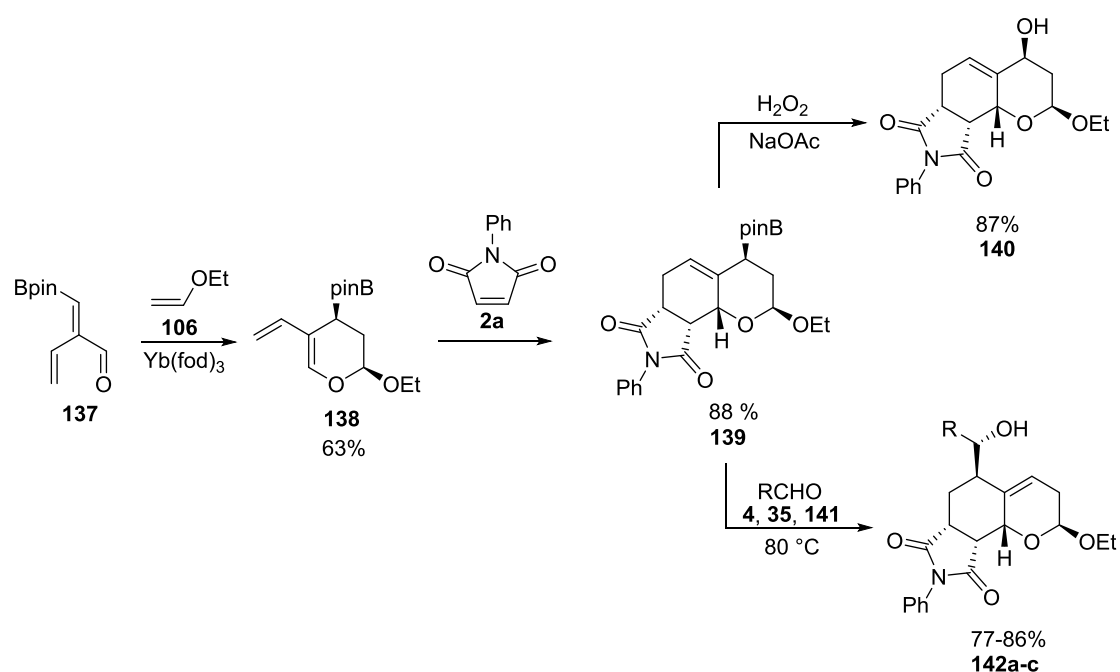
On the basis of these precedents, boronated 2-vinyl- α,β -unsaturated aldehydes **137** were designed to fully exploit the synthetic potential of these classes of organoboranes. These compounds, that can be named boronated [3]-1-heterodendralenes by analogy with the corresponding carbotrienes,⁷⁸ allow rapid access to polycyclic heterocycles with control of multiple stereocenters.⁷⁹ Thus, sequential Diels–Alder/hetero Diels–Alder reactions (or *vice versa*) can be carried out chemoselectively depending upon the intrinsic reactivity of each 1,3-dienyl system or the order of introduction of the reagents. Furthermore, the allylboronic ester moiety, created in the first cycloaddition step or in the combination of two Diels–Alder reactions, can be engaged in an allylation reaction, which constitutes an additional asset for creating structural diversity (Scheme 27).



Scheme 27. Boronated heterodendralenes **137** in [4+2]-cycloadditions.

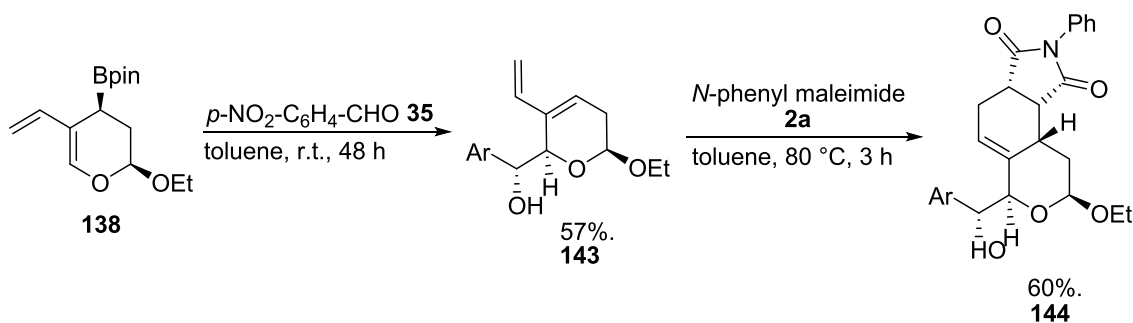
As 3-boronoacrolein **105** esters which have been used in metal-catalysed inverse electron demand [4+2]-cycloadditions with enol ethers, **137** reacted with ethyl vinyl ether **106** in the presence of $\text{Yb}(\text{fod})_3$ to afford the corresponding 2-alkoxy-3,4-dihydro-5-vinyl-2H-pyran **138**. In the presence of electron-poor alkenes, as *N*-phenyl maleimide **2a**, maleic anhydride **2b**,

activated azo compounds or naphthoquinone, **138** underwent normal Diels–Alder reactions to afford the corresponding cycloadducts **139** as single diastereomers (Scheme 28). These reactions can also be advantageous when conducted in a one-pot process without formation of any product resulting from a first cycloaddition of the 1,3-butadienyl moiety. Various further transformations were then carried out taking advantage of the presence of an allylboronate moiety, for example, oxidation and, more interestingly (in terms of additional diversity), addition to aldehydes, which provided access to the corresponding homoallylic alcohols **142a-c** in 77-86% yields.



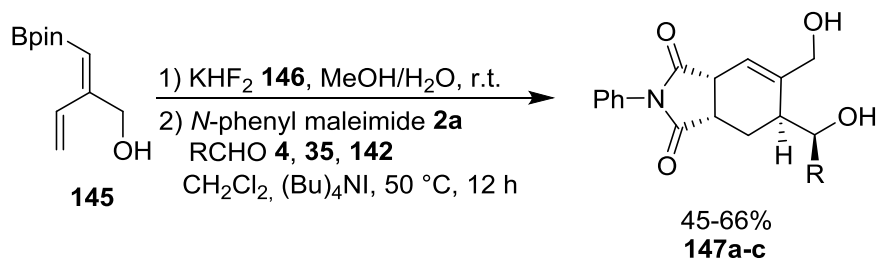
Scheme 28. Synthesis of tricyclic imides derivatives.

Alternatively, as the cycloadduct **138** bears a boronic ester group in an allylic position, the allylation and the normal-electron demand [4+2]-cycloaddition steps can be reversed, thus generating supplementary skeletal diversity from the same starting heterodendralene. As an illustration, **138** and 4-nitrobenzaldehyde **35** were allowed to react at r.t. to afford **143**, which underwent a further cycloaddition with *N*-phenyl maleimide **2a** to furnish the single tricyclic compound **144** (Scheme 29).



Scheme 29. Synthesis of **144** via a HDA/allylboration/DA sequence.

The initial boronic ester group of **145**, the direct precursor of **137**, can be also converted into a trifluoroborate substituent by treatment with KHF_2 in $\text{MeOH}/\text{H}_2\text{O}$ to increase the reactivity of the dienyl moiety towards electron-poor dienophiles. It was directly engaged in a Diels-Alder cycloaddition with *N*-phenyl maleimide **2a** at 50°C in acetone for 12 h in the presence of various aldehydes to afford diols **147** as major diastereoisomers (>95%) and in good overall yields (Scheme 30).



Scheme 30. Diels-Alder/allylboration sequence.

III. Nitroso derivatives as dienophile

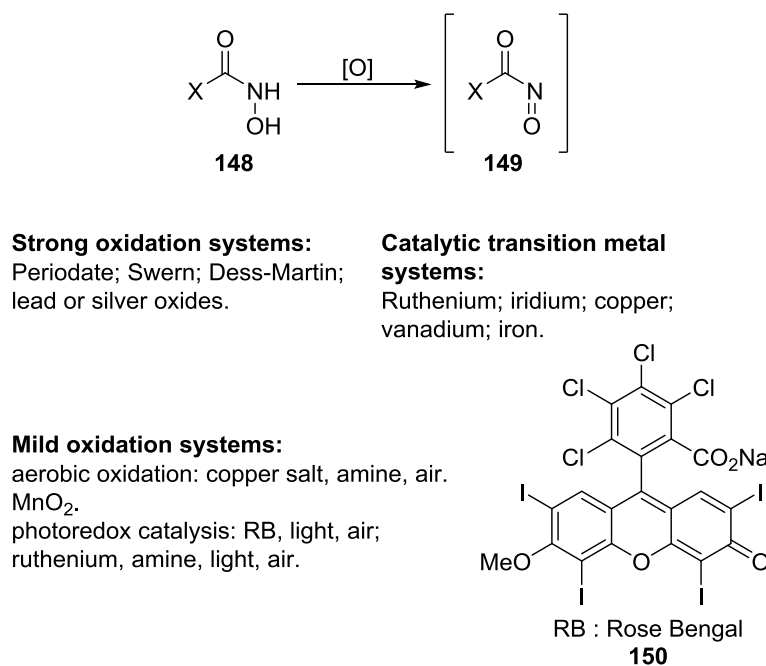
The nitroso hetero-Diels–Alder (HDA) reaction was first described six decades ago by Wichterle⁸⁰ and Arbuzov⁸¹ and since then, it has been demonstrated to be a useful chemical tool for the creation of unique structural and functional diversity.⁸²

First investigations on this strategy were carried out on aryl nitroso derivatives which show higher stability compared to the carbonyl nitroso derivatives. In fact, most aryl nitroso compounds are stable solids whereas carbonyl nitroso does not exist in this form, and need to be prepared *in situ* because of their 1 ms lifetime at infinite dilution.⁸³ Despite this drawback, carbonyl nitroso compounds have been predominantly studied for the last few decades because of their higher versatility as nitroso donor reagents. In the next sections, the preparation of the nitroso species will be discussed, and a brief overview of their reactivity and applications in synthesis.

III.1. Generation of the reactive nitroso species

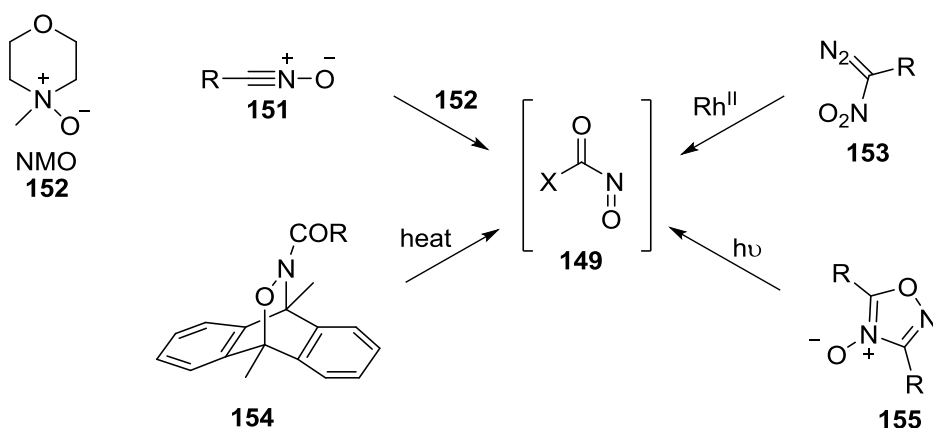
Aryl nitroso species do not require *in situ* preparation and can be directly purchased or easily prepared.⁸⁴ Concerning the carbonyl nitroso species, numerous approaches were developed in order to further expand the synthetic applications of nitrosocarbonyl Diels–Alder reactions. The most common way to obtain carbonyl nitroso derivatives is by oxidation of the corresponding hydroxamic acid derivative. Different oxidation protocols were successfully used such as, periodate,⁸⁵ Swern,⁸⁶ Dess–Martin,⁸⁷ and silver or lead oxide.⁸⁸ Later, transition metal catalysed systems based on ruthenium, iridium, vanadium and iron catalysts⁸⁹ in

association with peroxides as oxidant, have been used. Recently, milder useful conditions emerged, based on copper salt, and aerobic oxidation in the presence of amine co-catalysts,⁹⁰ manganese oxide⁹¹ and photoredox catalysis using either rose bengal or ruthenium catalysts (Scheme 31).⁹²



Scheme 31. In situ generation of nitrosocarbonyl compounds.

Other pathways starting from diverse reagents can be also used to generate the carbonylnitroso species **149**, as oxidation of nitrile oxides **151** using NMO,⁹³ nitrocarbene rearrangement of **153** using rhodium catalyst,⁹⁴ retro-Diels-Alder reactions of 9,10-dimethylantracene cycloadducts **154** under high temperature conditions⁹⁵ and photochemical cleavage of 1,2,4-oxadiazole 4-oxides **155** (Scheme 32).⁹⁶

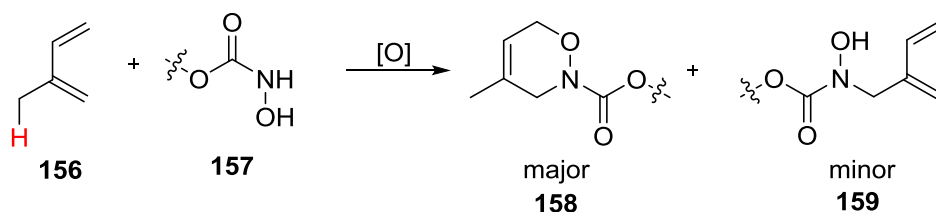


Scheme 32. *In situ* generation of nitrosocarbonyl compounds using various reagents.

III.2. Nitroso compounds in Diels-Alder reactions

III.2.a. Reactivity of nitroso compounds towards dienes

Nitroso compounds are valuable partners in Diels-Alder reactions. However, when the diene **156** possesses an allylic hydrogen (in red on scheme 33), a possible competition could take place between the nitroso Diels-Alder and nitroso ene reactions (Scheme 33). This competition has been pointed out by both Whiting *et al.*^{90a} and Alaniz and *et al.*^{90b} using carbonyl nitroso derivatives.



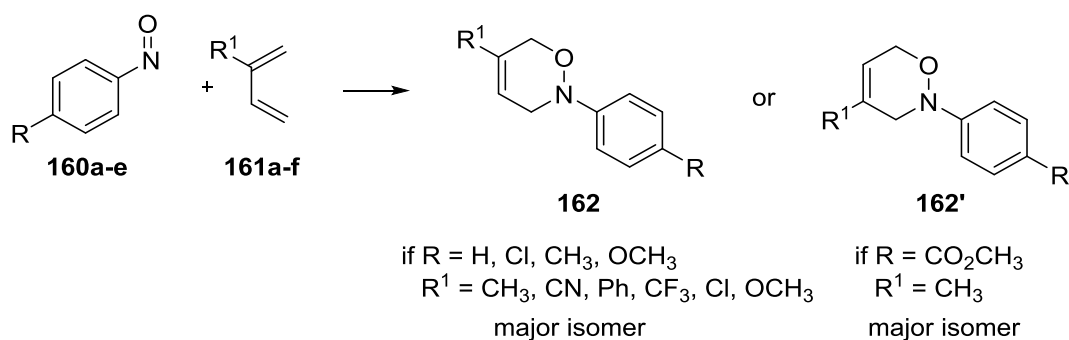
Scheme 33. Competition between [4+2]-cycloaddition and nitroso-ene reaction

Even if the nitroso Diels-Alder reaction has been generally accepted as the more rapid reaction compared to the nitroso-ene reaction, three parameters play a major role in the ratio between the cycloadduct and the ene-product. Firstly, the solvent has a dramatic impact on the

ratio between cycloadduct/ene-product, which varies from a 25:1 to a 4:1 mixture. However the origin of this solvent effect remains unclear.^{90a} Secondly, the conformations of the diene need to be considered. For the Diels-Alder reaction to take place a *s-cis* conformation for diene is required. A competition study was performed using 1,3-cyclohexadiene and 2,3-dimethyl-1,3-butadiene in the presence of a substrate susceptible to undergo an intramolecular nitroso ene-reaction. The study showed that the Diels-Alder cycloadduct was exclusively formed with 1,3-cyclohexadiene (*s-cis* conformation), whereas if 2,3-dimethyl-1,3-butadiene (a mixture of *s-cis* and *s-trans* conformations in solution) was used, the intramolecular nitroso ene-product was predominantly formed (77%). Thus, the conformation of the diene has an important impact as well, and nitroso ene-reaction can be favoured if the reactivity of the diene towards the Diels-Alder was decreased.^{90b} Lastly the influence of a possible metal-nitroso complex can be considered, especially when aryl nitroso derivatives are used. Predominant formation of the nitroso ene-adduct, in the presence of a Diels-Alder trapping agent can take place.⁹⁷

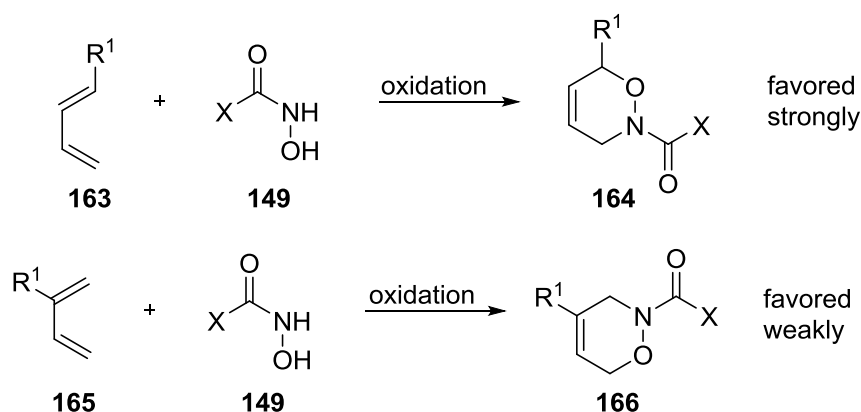
III.2.b. Regioselectivity of the nitroso Diels-Alder reactions

Kresze *et al.*⁹⁸ performed several studies, which indicated that substituted aryl nitroso compounds **160a-e** react regioselectively with unymmetric dienes **161a-f**. The regiochemistry of the reaction depends upon the electronic properties of the substituent on the aromatic ring (Scheme 34).



Scheme 34. Regioselective outcome of the reaction between 4-substituted aryl nitroso compounds and unsymmetric dienes.

As for the aryl nitroso derivatives, some studies⁹⁹ have been performed to analyse the behaviour of unsymmetric dienes towards carbonylnitroso compounds in intermolecular nitroso Diels-Alder reactions. The results can be rationalised and features of the carbonylnitroso Diels-Alder reactions can be summarised; Firstly, 1-substituted 1,3-dienes **163** exert better regioselectivity than 2-substituted 1,3-dienes **165**; Secondly, electronic properties of the diene have a major impact; Thirdly for higher selectivity, stronger electronic properties (electron withdrawing or electron donating groups) were required; Lastly, in the case of intermolecular reactions, solvents do not have an important impact on the regioselectivity (Scheme 35).

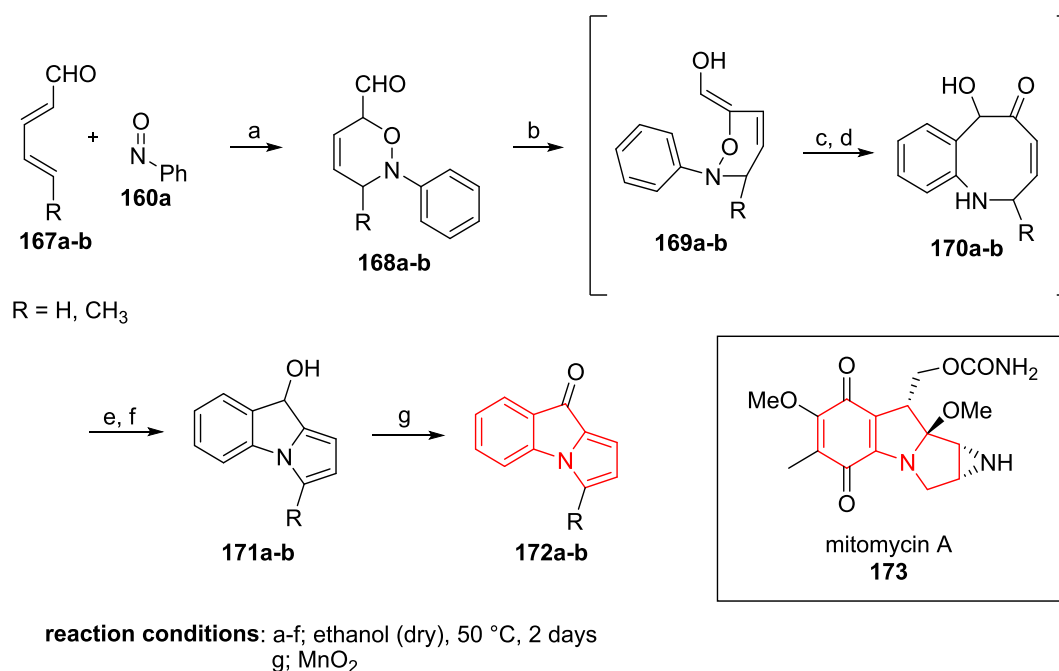


Scheme 35. Regioselectivity of intermolecular carbonylnitroso Diels-Alder reaction.

III.3. Some applications of nitroso Diels-Alder reactions

III.3.a. Arylnitroso derivatives as dienophiles

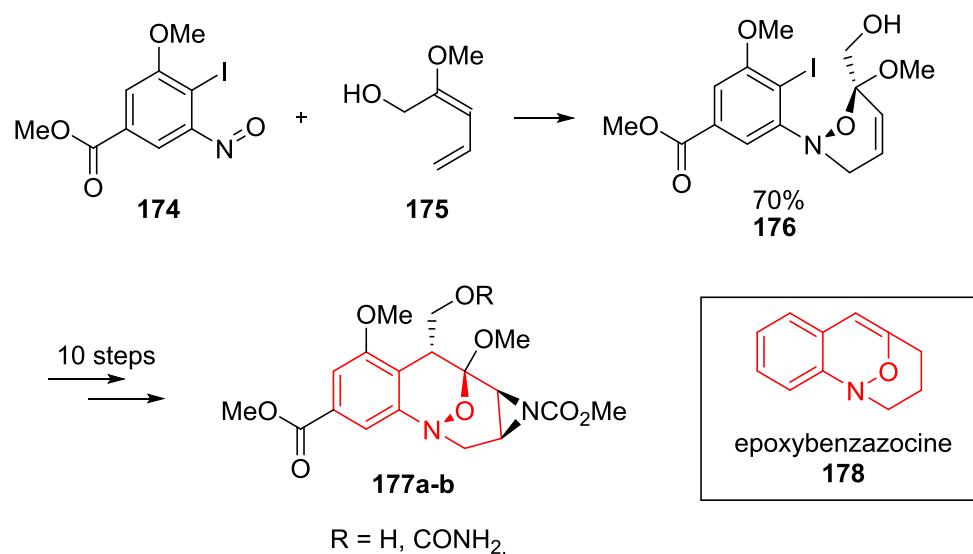
A couple of examples using aryl nitroso compounds for the synthesis of molecules with biological interests were published. Streith and co-workers¹⁰⁰ prepared the mitomycin skeleton using a sequence starting with a nitroso Diels-Alder reaction between diene compounds **167a-b** and nitrosobenzene **160a**, to afford compound **168a-b**. A cascade process beginning with an enolisation (b), followed by hetero-Cope rearrangement (c), prototropy and rearomatisation (d), to finish an intramolecular nucleophilic addition and dehydration (e, f) was described to provide **171a-b**. Oxidation (g) using MnO_2 led to the formation of the final compounds **172a-b** (Scheme 36).



Scheme 36. Preparation of the skeleton of mitomycin A.

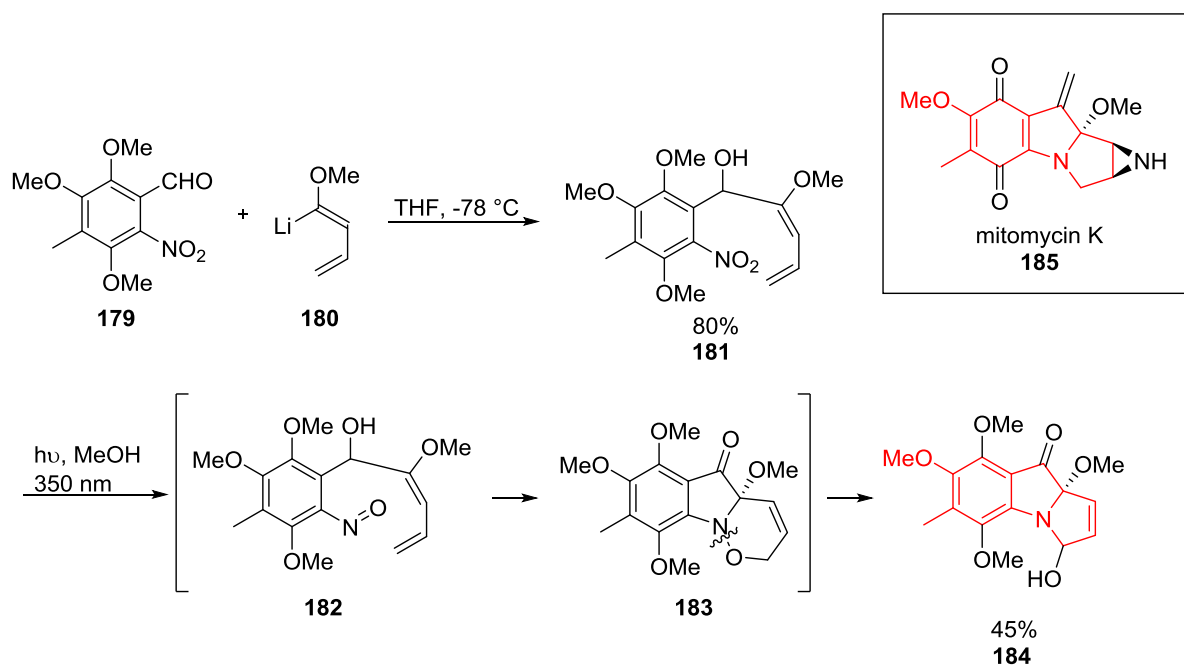
Danishefsky *et al.*,¹⁰¹ presented an efficient approach towards the synthesis of the epoxybenzazocine core present in some natural products. For this purpose, a nitroso Diels-Alder reaction using **174** and **175** was used to afford the key intermediate **176** in 70% yield.

Multiple steps including aziridination and Heck arylation, led to the formation of the structure **177** bearing the epoxybenzazocine skeleton **178** (Scheme 37).



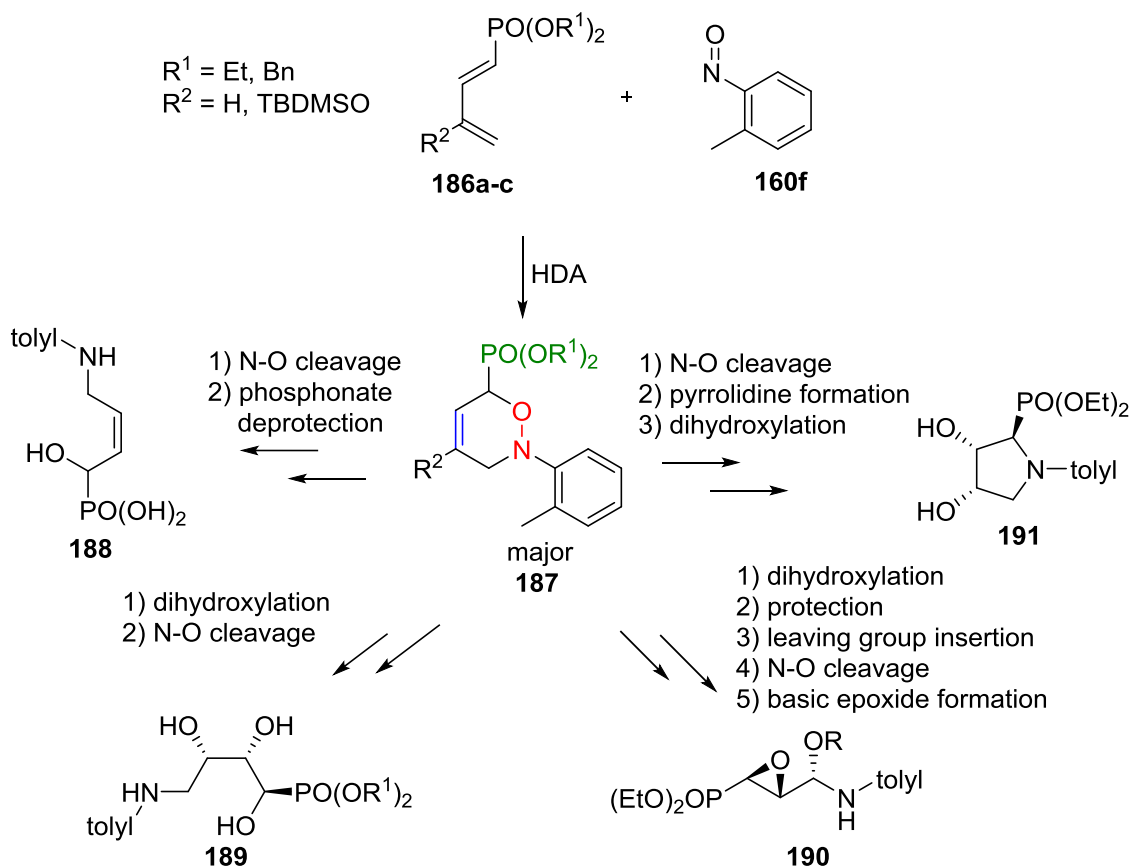
Scheme 37. Synthesis of analogues of FR 900482 based on a 2*H*-1,5-epoxy-benzazocine core.

During the same year, the same group published the total synthesis of mitomycin K **185**.¹⁰² The nitrobenzyl derivative **179** was used as a precursor of the corresponding nitroso compound. First, the (1-methoxy-1,3-butadienyl)lithium **180** was used to prepare the carbinol intermediate **181**. Then, using photochemical redox conditions, nitroso intermediate **182** was formed providing the fused core oxazine **183** by intramolecular nitroso Diels-Alder reaction, which, under these photoredox conditions, was transformed into compound **184** forming the tricyclic scaffold of mitomycin (Scheme 38). No additional explanation has been given to explain the oxidation of the alcohol **182** group into the ketone **183** during the photoredox reaction.



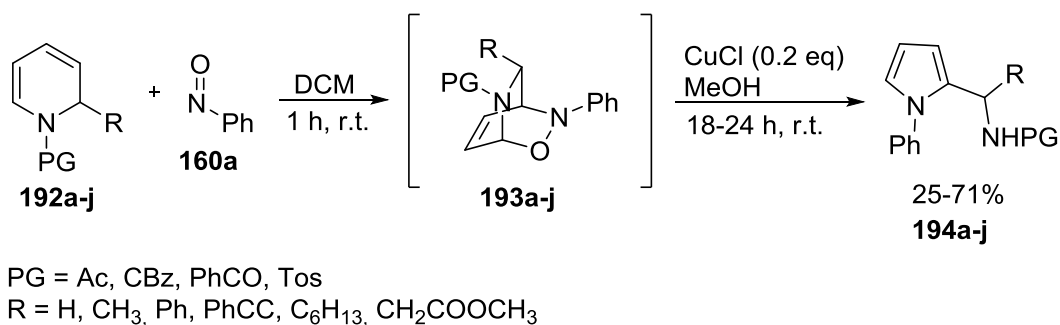
Scheme 38. Synthesis of the precursor **184** for the total synthesis of mitomycin K **185**.

The discovery of aminophosphonic derivatives as biologically active molecules led Marchand and co-workers to study the reactivity of 1-phosphono-1,3-butadienes with nitroso derivatives, and especially *o*-nitrosotoluene **160f**.¹⁰³ Concise experimental and theoretical studies of the cycloaddition between diene **186a-c** with *o*-nitrosotoluene **160f**, showed that the isomer **187** was predominantly formed. The resulting oxazine **187** possesses multiple sites for functionalisation, namely the N-O bond, the C=C double and the phosphonate moiety. Depending on the sequence used, multiple interesting scaffolds **188**, **189**, **190** and **191** were synthesised (Scheme 39).



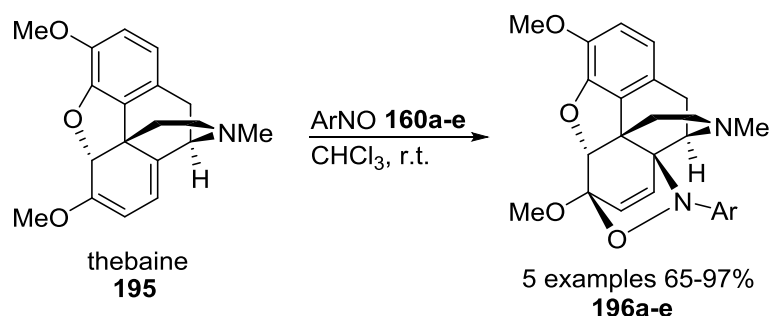
Scheme 39. Synthesis of aminophosphonic derivatives.

Recently, a synthesis of protected (α -branched)-2-pyrrolylamines was described using 1,2-dihydropyridine derivatives **192a-j** and nitrosobenzene **160a**.¹⁰⁴ After formation of the Diels-Alder adduct, addition of CuCl (0.2 eq.) in MeOH caused the formation of the pyrrole derivative **194a-j**, by radical N-O cleavage, rearrangement process and final copper mediated oxidation (Scheme 40).



Scheme 40. Protected (α -branched)-2-pyrrolylamines synthesis.

Kirby and co-workers¹⁰⁵ studied the reaction of thebaine, a natural product, with aryl nitroso derivatives. All aryl nitroso compounds **160** used in these reactions underwent the cycloaddition in good to excellent yields (65-99%). Further modifications of derivative **196a-e** emphasised the possibility to handle natural products containing dienes as well as their homologues for further functionalisation (Scheme 41).



Scheme 41. Arylnitroso Diels-Alder reaction on thebaine **157**.

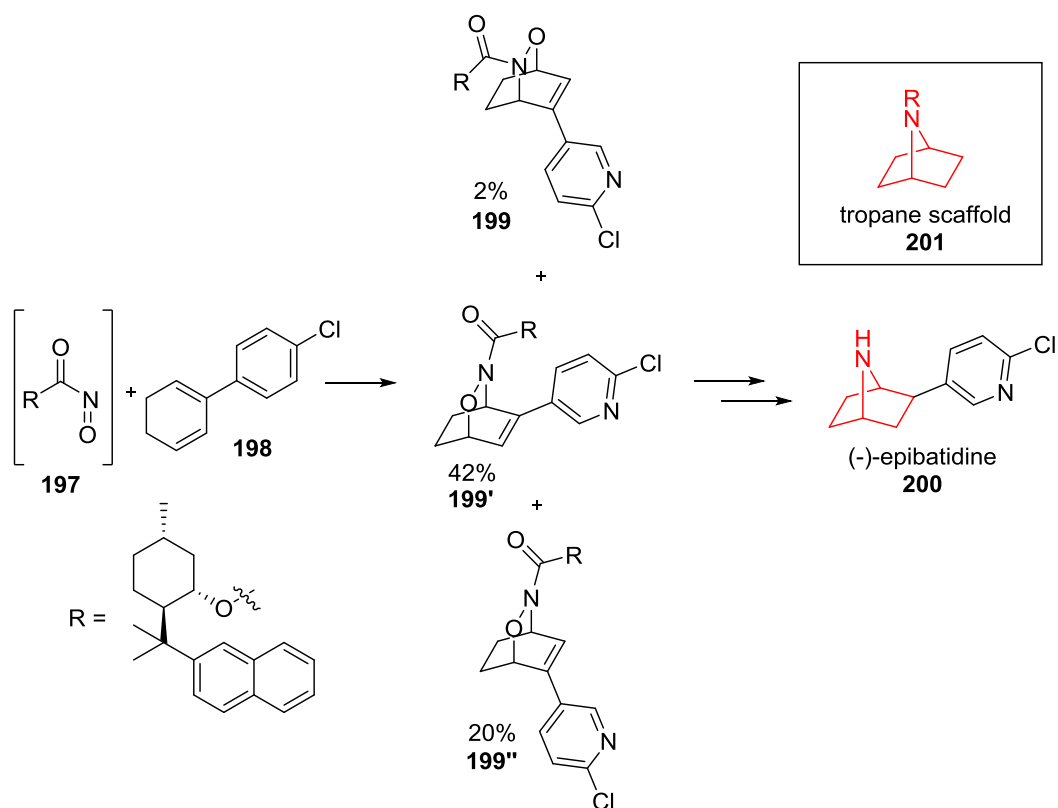
III.3.b. Carbonylnitroso derivative as dienophile

Diels-Alder cycloadditions of carbonylnitroso derivatives have been widely studied and numerous synthetic applications have been presented over the years. A few examples from the literature are presented in the next section.

Alkaloid derivatives are interesting targets due to their wide-range of biological activities, and new methodologies are constantly being developed to enlarge the synthesis of these scaffolds. Among the numerous alkaloids known, tropane derivatives **201**, as well as alkaloids from the *Amaryllidaceae* family, like narciclasine **207**, can be prepared *via* intermolecular carbonylnitroso Diels-Alder reactions.

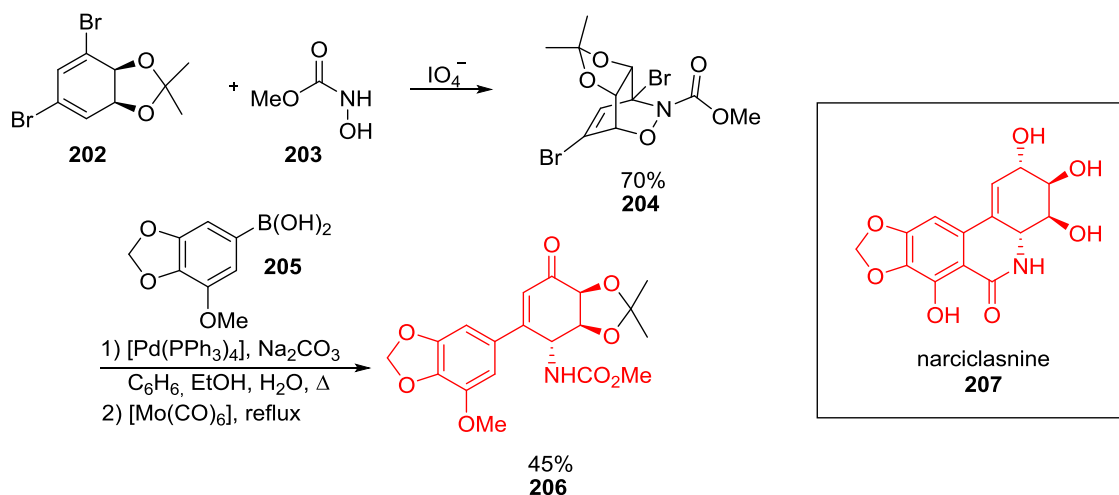
Thus, the total synthesis of (-)-epibatidine has been achieved by Kobayashi and co-workers¹⁰⁶ using chiral carbonylnitroso compound **197** in the presence of the diene **198**. A mixture of

three cycloadducts **199**, **199'** and **199''** was obtained with moderate selectivity. Further modifications of cycloadduct **199'** provided (-)-epibatidine **200** (Scheme 42).



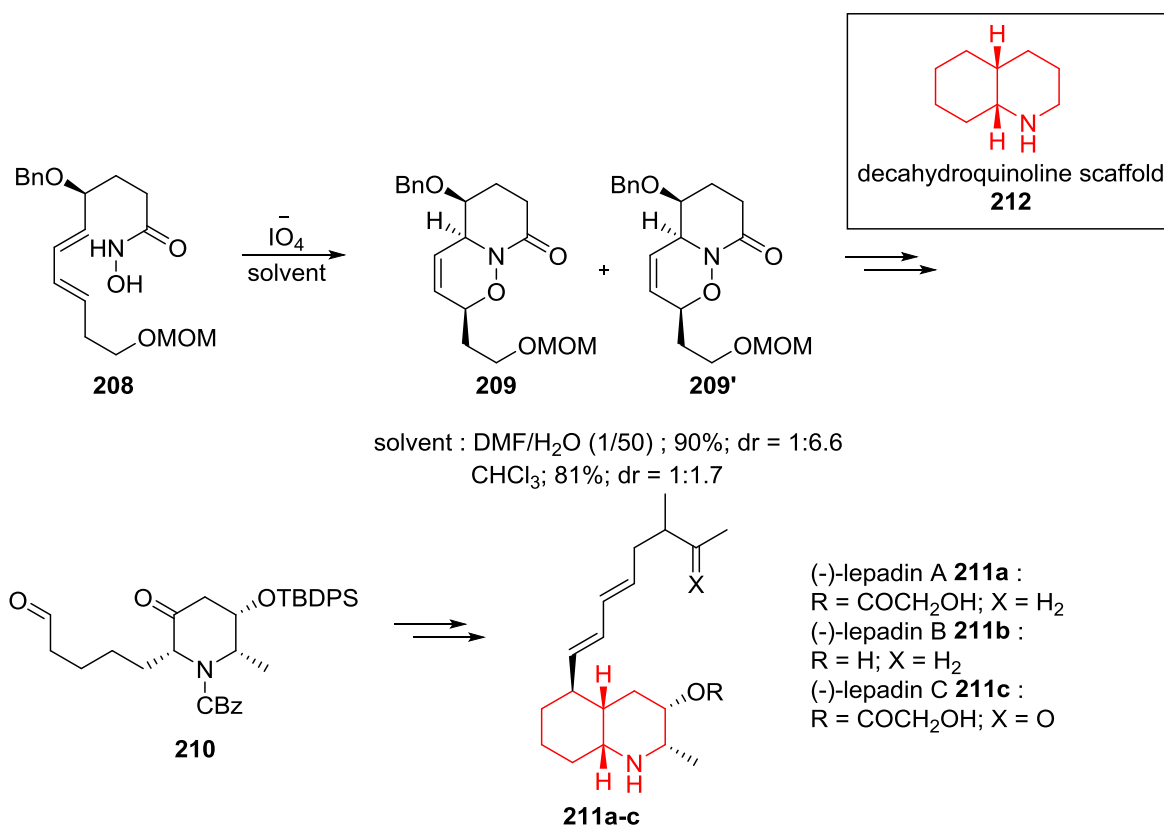
Scheme 42. Total synthesis of (-)-epibatidine **173**.

Hudlicky *et al.* presented a synthetic pathway for the total synthesis of narciclasnine **207**.¹⁰⁷ Oxidation of nitroso precursor **203** in the presence of the diene **202** afforded the cycloadduct **204** in 70% yield. A Suzuki-Miyaura cross-coupling using the boronic acid **205** followed by cleavage of the N-O bond provided molecule **206** as a potential intermediate towards the synthesis of narciclasnine **207** (Scheme 43).



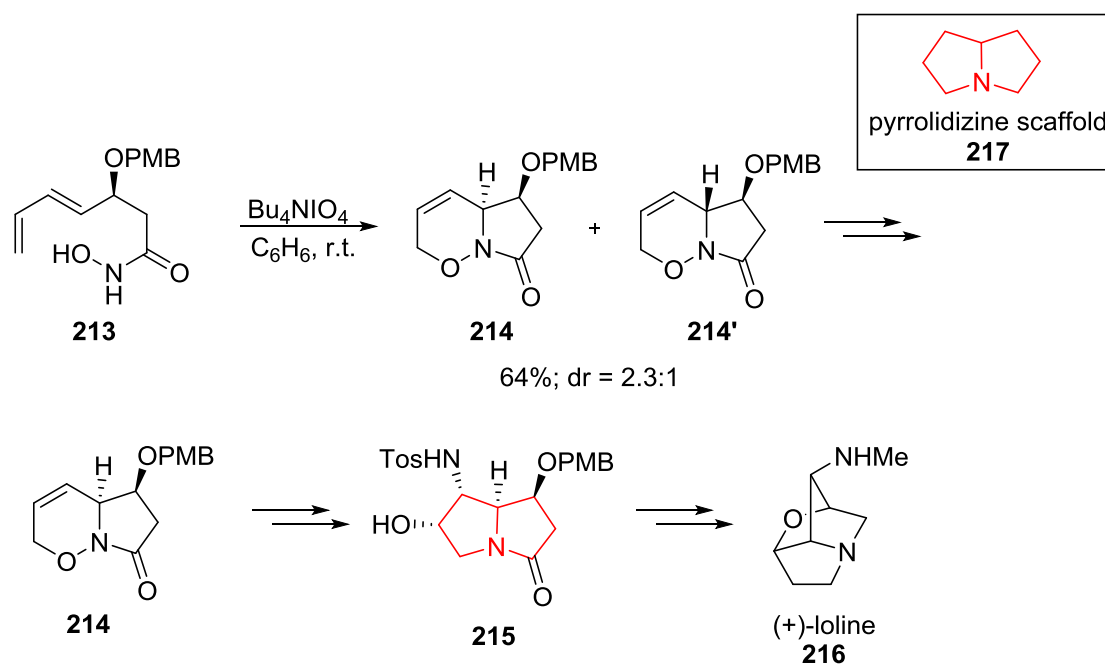
Scheme 43. Synthesis of an intermediate for the total synthesis of narciclasine **207**.

The total synthesis of marine alkaloids (-)-lepadin A, B and C from the family decahydroquinoline has been performed starting from **208**.¹⁰⁸ Intramolecular nitroso Diels-Alder reactions led to the formation of a mixture of two diastereoisomers, **209** and **209'**. The ratio between the diastereoisomers was proved to be solvent dependent. By using an aqueous medium, the diastereoselectivity increased towards the formation of isomer **209'**. Subsequent modifications led to the formation of the desired natural alkaloids **211a-c** (Scheme 44).



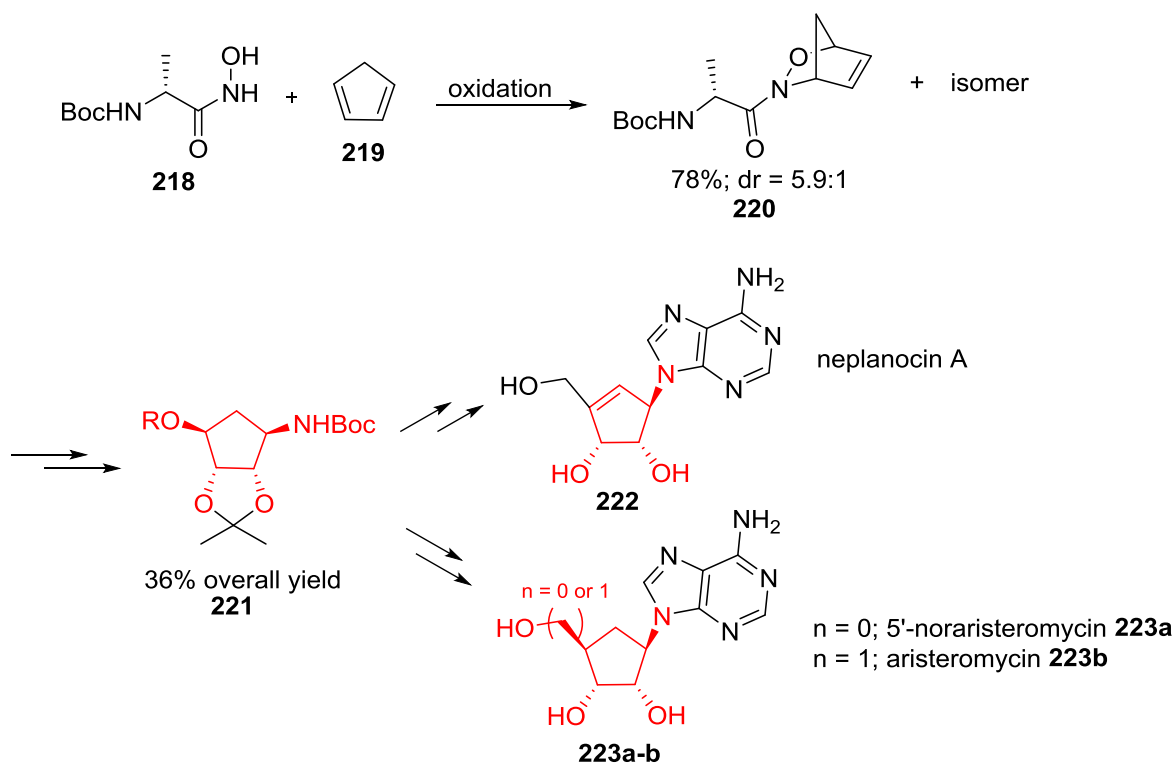
Scheme 44. Total synthesis of (-)-lepadin A, B and C **211a-c**.

Other classes of alkaloids, like molecules bearing a pyrrolidizine core **217** have been synthesised based on such an intramolecular strategy. Yokochi *et al.* were able to achieve the total synthesis of (+)-loline **216** using compound **213** as starting material.¹⁰⁹ A carbonylnitroso Diels-Alder reaction provided bicyclooxazine **214** and **214'** as a mixture of two diastereoisomers. Screening conditions showed that higher temperature gave better yields but lower selectivity. Changing the solvent system from an apolar solvent to an aqueous medium reversed the selectivity of the reaction. The synthesis of (+)-loline was completed after further functionalisations (Scheme 41).



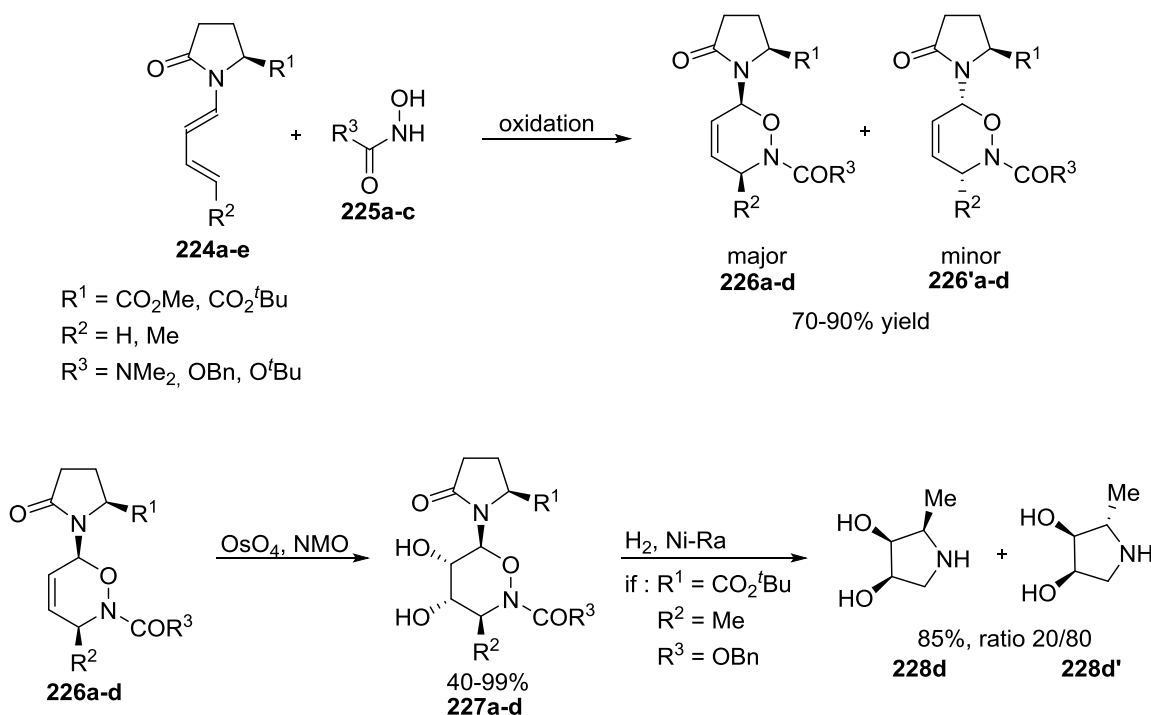
Scheme 45. Total synthesis of (+)-loline **216**.

In addition to alkaloid synthesis, different research groups have focused their attention on the synthesis of azasugar and nucleoside derivatives. Miller and co-workers¹¹⁰ have contributed to this field by developing the preparation of the key intermediate **221**. The synthesis started with the carbonylnitroso Diels-Alder reaction between the chiral nitroso species **218** and cyclopentadiene **219**, providing **220** as the major isomer. A five step pathway using **220** afforded key intermediate **221** in a 36% overall yield. This carbocyclic nucleoside core **221** is present in neplanocin A **222**, aristeromycin **223b** or 5'-noraristeromycin **223a** (Scheme 46).



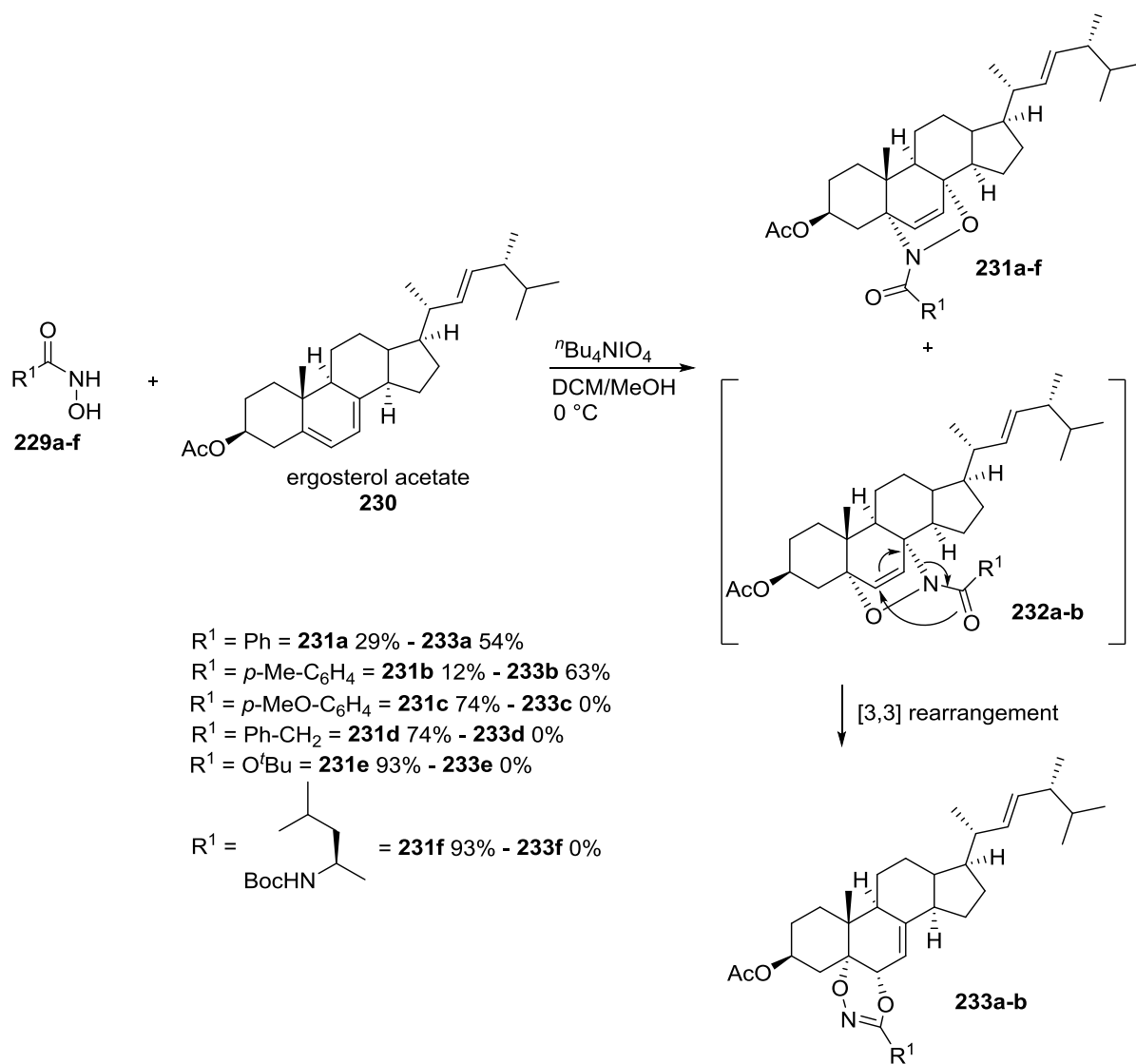
Scheme 46. Synthesis of key intermediate **221**, a precursor to neplanocin A **222**, aristeromycin **223b** and 5'-noraristeromycin **223a**.

Azasugar synthesis can be achieved using nitroso Diels-Alder methodology using asymmetric diene **224a-e** providing oxazine cycloadducts **226a-d** and **226'a-d** in good yields (70-90%) and diastereoisomeric excesses. Dihydroxylation of the major isomers **226a-d** afforded intermediate **227a-d** in moderate to excellent yields. Results of the N-O cleavage reaction are substrate-dependent, and only the compound bearing the following substituents; ($R^1 = \text{CO}_2^t\text{Bu}$, $R^2 = \text{Me}$, $R^3 = \text{OBn}$ **227d**), led to the formation of the desired pyrrolidine ring in a 85% yield as a mixture of two diastereoisomers **228d** and **228d'** (80/20) (Scheme 47).¹¹¹



Scheme 47. Synthesis of pyrrolidine azasugar derivatives.

Among natural products containing a diene moiety in their skeleton, steroidal dienes, and more precisely ergosterol, have shown interesting behaviour towards Diels-Alder reactions. This molecule, and other related structures, have been used for years for the design of new biologically active compounds. Thus, Miller and co-workers in 2009 described the reactivity of carbonylnitroso derivative **229a-f** in the presence of ergosterol acetate **230**.¹¹² By this method, the synthesis of novel C₅ and C₈ disubstituted sterol analogues was achieved. Oxazine **231a-f** was obtained in low to good yields. In fact, the regioselectivity was impacted by the R¹ substituent on the nitroso species **229a-f**. If R¹ was a phenyl or a *p*-Me-phenyl moiety **229a** and **229b** respectively, oxazines **232a-b** were predominantly formed. These compound were never isolated due to a [3,3]-sigmatropic rearrangement which afforded **233a-b** as the major products. In all other cases, regioisomers **231c-f** were obtained as single compounds.



Scheme 49. Functionalisation of ergosterol acetate **230** by carbonylnitroso Diels-Alder reaction.

Results

&

Discussions

I. Research Plan

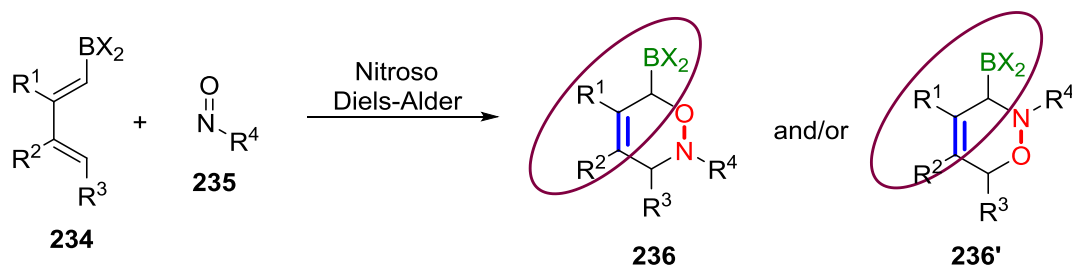
The initial research plan was to combine 1-boron-substituted 1,3-dienes and nitroso compounds in pericyclic reactions and to explore the scope and limitations of this chemistry (Scheme 50). In particular, the study of the influence of different parameters towards the nitroso Diels-Alder reaction was envisaged *i.e.*:

- The nature of the boron substituent (hybridisation sp^2 versus sp^3)
- The electronic properties and the position of the substituents on the diene (R^1 , R^2 and R^3)
- The nature of the nitroso partner (arylnitroso and carbonylnitroso derivatives).

The second part of the project was to functionalise [4+2]-oxazine cycloadducts. Indeed, oxazines **236** and **236'** are interesting building blocks giving access to numerous functionalised compounds. Hence, it was envisaged to explore the reactivity of:

- The C=C double bond
- The N-O bond
- The allylborane moiety

By taking advantage of this chemistry, novel synthetic sequences could be considered.



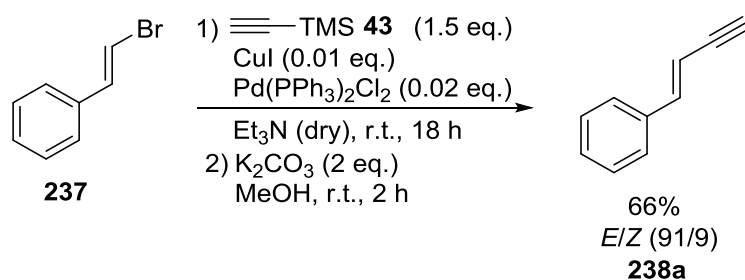
Scheme 50. General preliminary thesis research plan.

II. Diene syntheses

The syntheses of the dienes used for this study were performed according to different procedures. The choice of one method or the other was mainly driven by the nature of the boron substituent on the final diene and the availability of the starting materials.

II.1. Enyne hydroboration

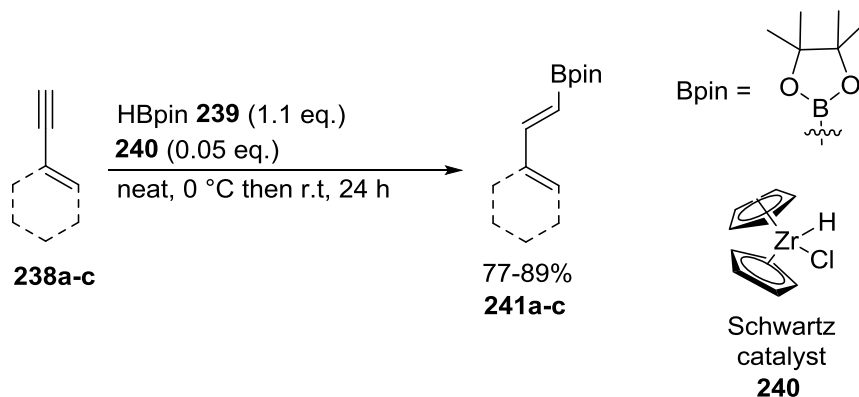
Catalytic hydroboration using Schwartz reagent **240** was first used.¹¹³ Starting enynes **238b** and **238c** were commercially available, whereas enyne **238a** had to be prepared starting from β -bromo styrene **237**. Sonogashira cross-coupling using trimethylsilylacetylene **43**, followed by a basic proto-desilylation,¹¹⁴ led to the desired enyne with a 66% yield as a mixture of two *E/Z*-isomers (91/9) (Scheme 51). The ratio *E/Z* of the starting **237** has not been checked prior to use, which can explain the formation of **238a** as a mixture of two *E/Z*-isomers (91/9).



Scheme 51. Synthesis of enyne **238a**.

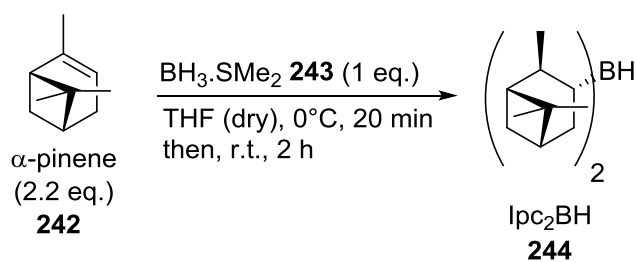
Hydroboration using pinacolborane **239** of the enynes **238a-c** afforded the desired (*E*)-1,3-dienylboronic pinacol ester **241a-c** in good to excellent yields (Table 1).

Table 1. Synthesis of 1,3-dienylboronic ester **241a-c** by hydroboration.



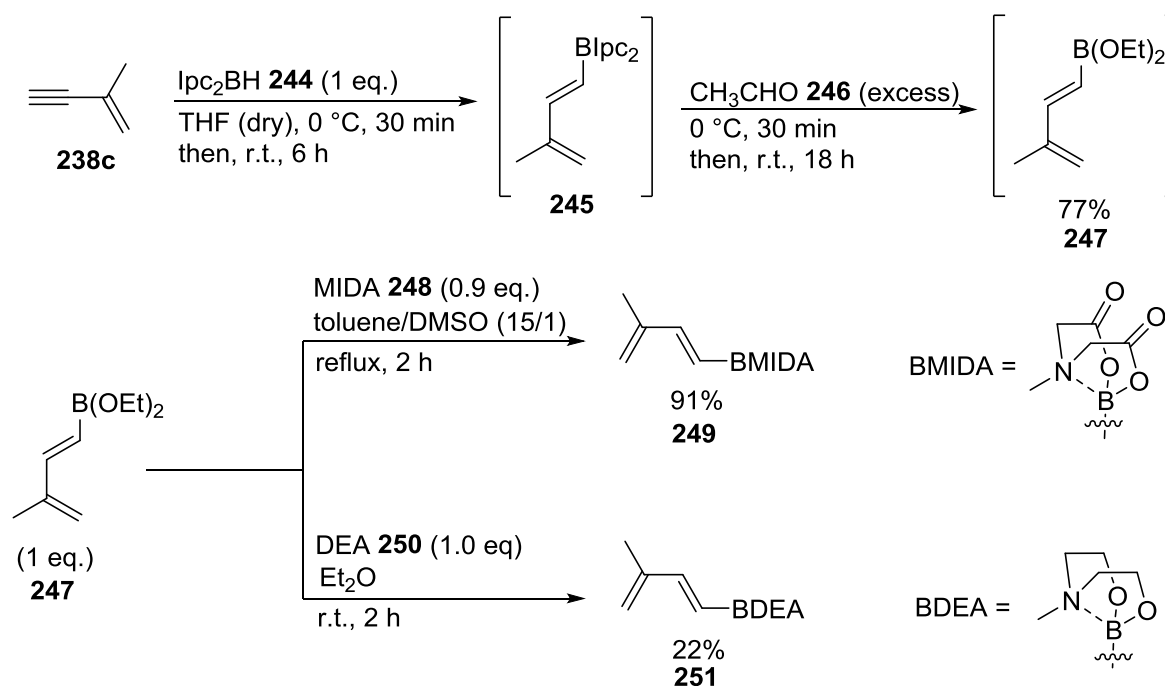
Entry	Starting enyne	Diene	Isolated yield (%)
1			85
2			77
3			89

The second method used for the hydroboration was based on the *in situ* preparation of the diisopinocampheylborane reagent **244** by mixing α -pinene **242** with borane dimethyl sulfide complex **243** (Scheme 52).¹¹⁵



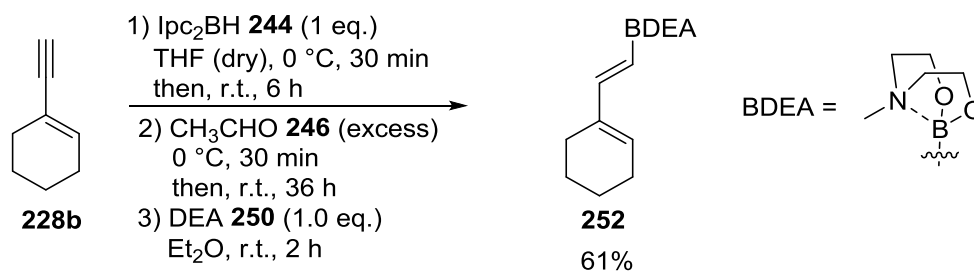
Scheme 52. Preparation of $\text{Ipc}_2\text{BH } \mathbf{244}$.

Enyne **238c** was then directly added to Ipc_2BH **244**, providing exclusively the *E*-vinylborane intermediate **245**.¹¹⁶ The 1,3-dienylborane **245** was converted into the corresponding diethyl 1,3-dienylboronic ester **247** in the presence of a large excess of acetaldehyde **246**. This intermediate was used for modification of the boron substituent. In the case of boronic acid MIDA ester derivative **249**, a mixture of toluene/DMSO (15/1) was required to obtain a better solubility of the MIDA reagent **248** in reflux conditions.¹¹⁷ Diene **249** was isolated with an excellent yield of 91%. For the preparation of diene **251**, milder conditions were used to observe the total conversion of the compound **247**.¹¹⁸ Despite the fact that diene precipitates out from the reaction, several precipitations and finally a slow crystallisation in a mixture of DCM/ Et_2O were necessary to isolate diene **251** without observing any contamination by remaining diethanolamine. These purification steps explained the low 22% yield (Scheme 53).



Scheme 53. Synthesis of the 1,3-dienylboronic ester **249** and **251**.

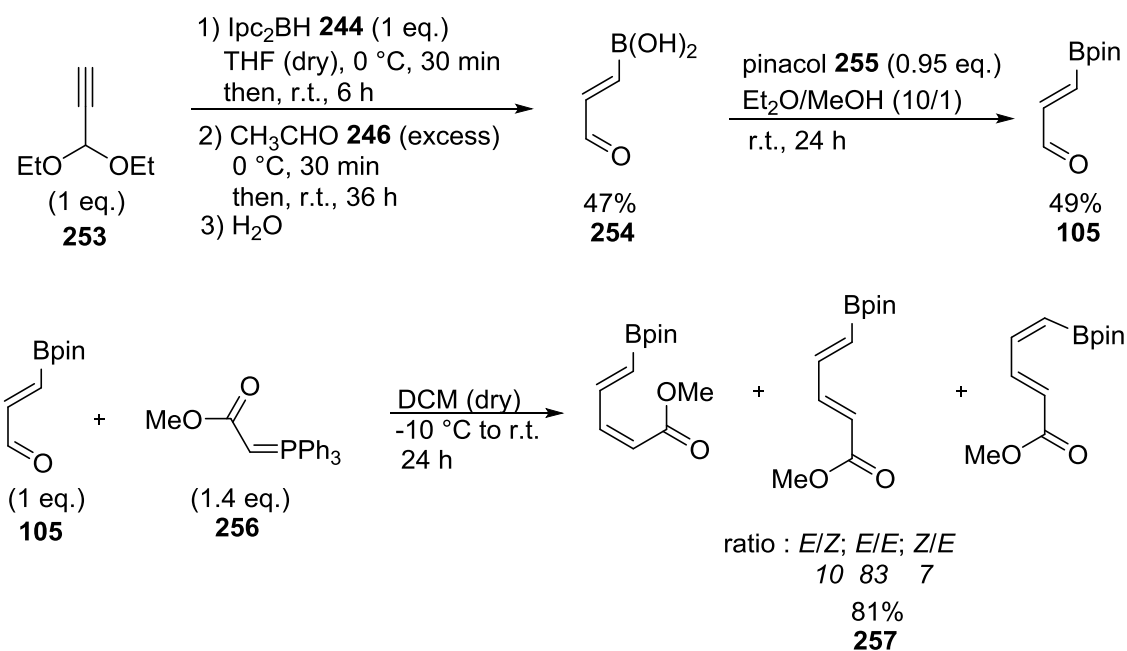
For the 1,3-diene **252**, the same methodology with Ipc_2BH was used to afford **252** in an isolated 61% overall yield (Scheme 54).*



Scheme 54. Preparation of diene **252**.

The synthesis of the diene **257** bearing a methyl carboxylate function in position 4 was achieved from β -borylacrolein pinacol ester **105**. Hydroboration of propionaldehyde diethyl acetal **253** using the same procedure as described above for **247** was used, giving after hydrolysis, the boronic acid **254** in a moderate 47% yield. The corresponding β -borylacrolein pinacol ester **105** was obtained by esterification with pinacol in 49% yield. Diene **257** was then synthesised by a Wittig route from an ester-stabilised ylide in a mixture of three stereoisomers ($E,E,E,Z,Z,E = 83:10:7$, determined by ^1H NMR) in a 81% yield (Scheme 50).¹¹⁹

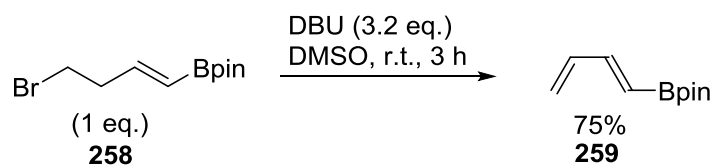
* Reaction performed by previous PhD student (Fabien Tripoteau) and has not been repeated.



Scheme 55. Synthesis of diene **257**.

II.2. Dehydrobromination*

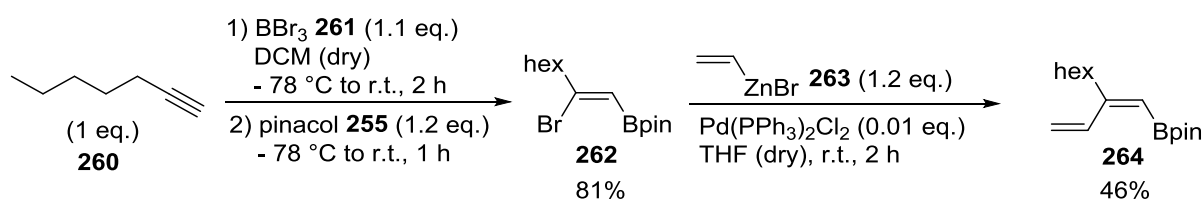
The synthesis of the parent diene was achieved by dehydrobromination of 4-bromobut-1-en-1-boronic acid pinacol ester **258**, itself prepared by hydroboration of 4-bromo-1-butene and pinacolborane, with DBU in a 75% yield (Scheme 56).



Scheme 56. Synthesis of the unsubstituted boronated diene **259**.

II.3. Alkyne bromoboration and Negishi coupling*

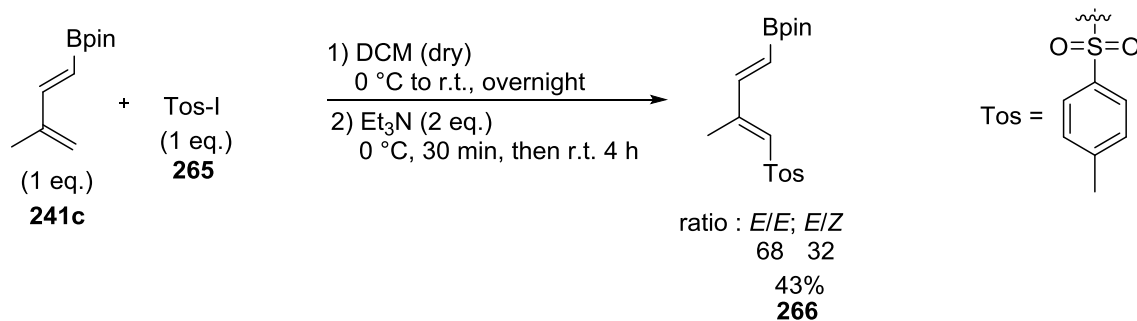
The preparation of diene **264** was based on a bromoboration/Negishi coupling sequence.¹²⁰ Bromoboration of 1-octyne **260** occurred in a *syn* fashion to afford *Z*-2-bromo-1-hexenyldibromoborane, which, in the presence of pinacol **255**, was converted into the corresponding boronate **262** in 81% yield. Negishi cross-coupling with organozinc **263** provided the diene **264** in 46% yield (Scheme 57).



Scheme 57. Bromoboration and Negishi coupling for the preparation of diene **264**.

II.4. Halosulfonylation of 1,3-dienylboronic ester **241c**

A halosulfonylation/dehydrohalogenation sequence was used to prepare diene **266**. Sulfonyl halide **265** was added *via* a free radical pathway onto the terminal alkene moiety of the diene **238c**, thus providing the corresponding δ -iodobutenyl sulfone. This intermediate was treated *in situ* with triethylamine and the dehydroiodinated compound **266** was obtained as a mixture of two isomers (*E/E;E/Z* = 68:32, determined by ^1H NMR) in a 43% yield (Scheme 58).¹²¹

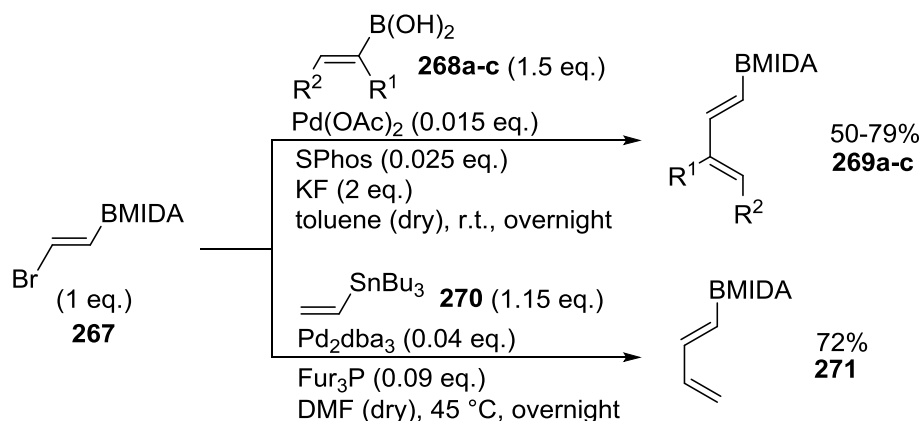


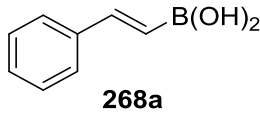
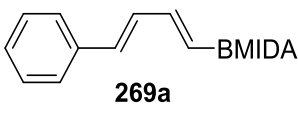
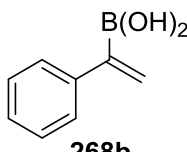
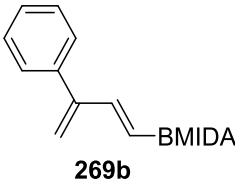
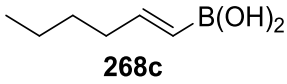
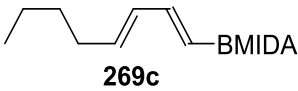
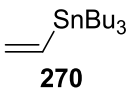
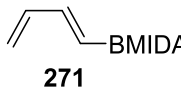
Scheme 58. Halosulfonylation of diene **241c**.

II.5. Coupling reaction of vinylboronic acid MIDA ester derivatives

II.5.a. From (*E*)-2-bromovinylboronic acid MIDA ester

The synthesis of 1,3-dienylboronic MIDA ester was achieved following the Burke *et al.* procedure, involving Suzuki-Miyaura or Stille cross-couplings.¹²² *E*-2-Bromovinylboronic acid MIDA ester **267** was subjected to Suzuki-Miyaura cross-coupling with (*E*)-styrylboronic acid **268a**, 1-phenylvinylboronic acid **268b** and *E*-hex-1-ene boronic acid **268c** to yield the desired dienes **269a-c** in 76%, 68% and 50% yields respectively. The aryl substituted boronic acid reagents showed better reactivity compared to the alkyl derivatives. Indeed, a full conversion of starting material was observed using **268a** and **268b**, whereas, **268c** only showed a 63% conversion even with extended reaction times. No optimisation or screening of other catalyst/ligand systems has been undertaken to increase conversion. Non-substituted 1,3-dienylboronic MIDA ester **271** was prepared by Stille coupling using vinyltributyltin **270**, thus affording diene **271** with a satisfactory 72% yield (Table 2).

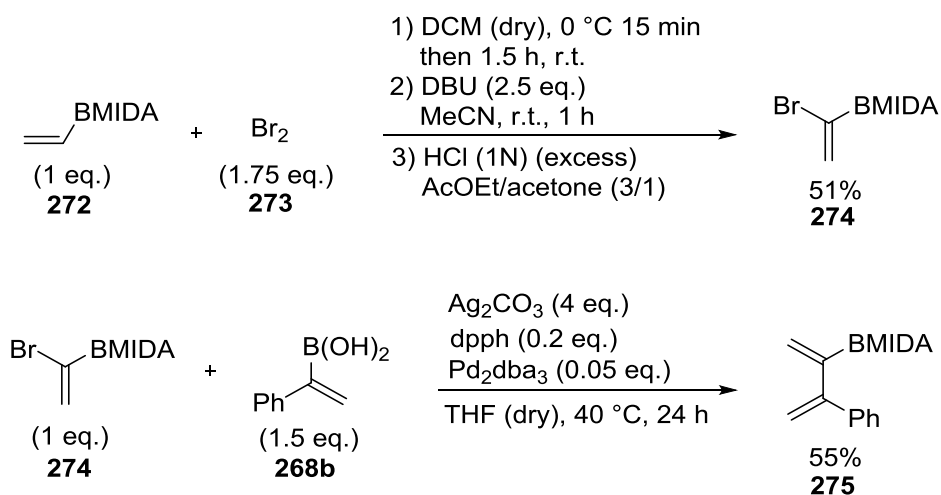
Table 2. 1,3-dienylboronic MIDA ester synthesis by coupling reaction.

Entry	Coupling partner	Diene	Conversion	Yield (%)
1	 268a	 269a	100	76
2	 268b	 269b	100	68
3	 268c	 269c	63	50
4	 270	 271	100	72

II.5.b. From 1-bromovinylboronic acid MIDA ester

The preparation of the 1,3-dienyl-2-boronic MIDA ester **275** started by the preparation of 1-bromovinylboronic acid MIDA ester **274** by bromination of vinylboronic MIDA ester **272** followed by a treatment with DBU (51% yield).¹²³ Suzuki-Miyaura cross-coupling with 1-phenylvinylboronic acid **268b** showed a conversion of 79%, which is in accordance with the results presented by Burke and co-workers.¹²³ Purification by silica gel chromatography did

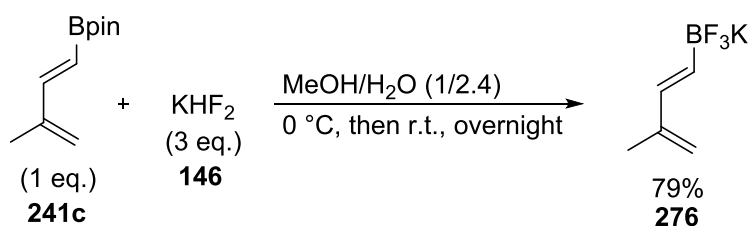
not permit separation of the starting material **274** from the diene **275**. The 30/70 mixture was used in the next step (Scheme 59).



Scheme 59. Preparation of 1,3-dienyl-2-boronic MIDA ester **275**.

II.6. Modification of the boron substituents

The preparation of the trifluoroborylated salt **276** was carried out by treatment with potassium hydrogenfluoride **146**, which yielded **276** in 79% yield (Scheme 60).¹²⁴

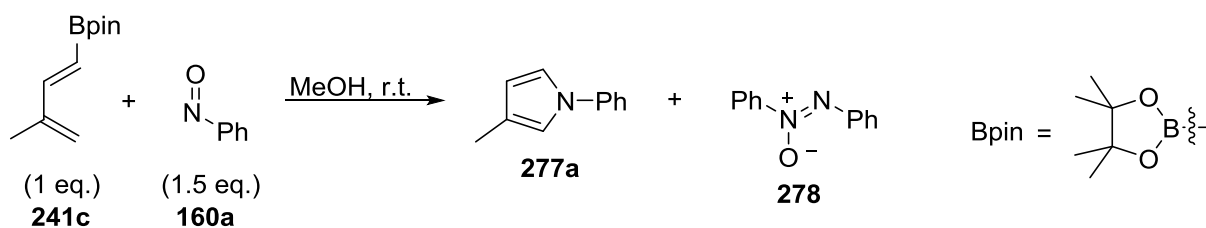


Scheme 60. Synthesis of the trifluoroboronated diene **276**.

III. Boronated dienes and arylnitroso compounds

III.1. Reaction of 1-dienylboronate pinacolate esters with arylnitroso compounds

Initial investigations into the nitroso Diels-Alder reaction using the dienyl boronate **241c** and nitrosobenzene **160a** as model substrates resulted in the formation of the unexpected *N*-phenylpyrrole **277a**, instead of oxazine cycloadducts (Scheme 61). Although it is known that 3,6-dihydro-1,2-oxazines can be converted to pyrroles, the conditions employed here (room temperature, no additional reagent, one pot reaction) are clearly different than those already reported: requiring several steps,¹²⁵ specific substituents,^{100,126} photolysis,¹²⁷ high temperature,¹²⁸ samarium diiodide,¹²⁹ oxidants,¹³⁰ basic or acid reagents.¹³¹ Furthermore, even when the reaction was followed by ¹H NMR, only 3-methyl-1-phenyl-pyrrole **277a**, together with some azoxybenzene **278**, was identified. There was a notable absence of any oxazine cycloadducts and the reaction was complete after 5 hours to afford **277a** in 82% isolated yield (Entry 3, Table 3).

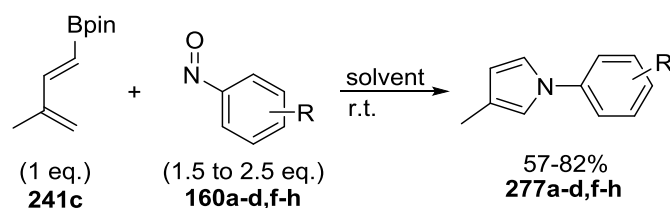


Scheme 61. *N*-Phenylpyrrole **277a** formation from the reaction of boronated diene **241c** and nitrosobenzene **160a**.

As shown in Table 3, different arylnitroso compounds **160** do undergo this conversion with boronated diene **241c** to provide the corresponding *N*-arylpyrroles **277**. Yields were moderate to good and the reaction could be conducted either in a protic solvent (MeOH) or an aprotic

solvent (DCM) (Entries 1 and 2, Table 3). A slightly higher yield resulted from an excess of the arylnitroso compound **160** (Entries 1 and 3, Table 3), hence, 2.5 equivalents of arylnitroso compounds **160** were used for most of the reactions. Surprisingly, no significant influence was observed on either the nature or location of the aromatic ring substituent and yields for pyrroles **277a-d, f-h** varied from 57 to 82% (Entries 4-9, Table 3).

Table 3. Pyrrole formation from the reaction of arylnitroso compounds **160** with diene **241c**.



Entry	Nitroso compound	Product	Yield (%)
1 ^[a]	160a	277a	67
2 ^[b]	160a	277a	61
3 ^[c]	160a	277a	82
4 ^[c]	160b	277b	60
5 ^[c]	160c	277c	68
6 ^[c]	160d	277d	65
7 ^[c]	160f	277f	69
8 ^[c]	160g	277g	57
9 ^[c]	160h	277h	77

[a] Reaction with 1.5 eq of ArNO in MeOH at r.t. for 5 h. [b] Reaction with 1.5 eq of ArNO in DCM at r.t. for 48 h. [c] Reaction with 2.5 eq of ArNO in MeOH at r.t. for 5 h.

The parent diene **259** when reacted with nitrosobenzene **160a** gave the corresponding pyrrole **277j** in 78% yield (Entry 2, Table 4).^{*} However, with a more sterically hindered diene **241b**, there was a significant decrease in yield (16% for the pyrrole **277i**), even after an extended reaction time (Entry 1, Table 4).^{*} Changing the dienyloboronate geometry from *E* to *Z*, as in compound **264**, also had a detrimental effect upon the reaction, with adduct **277k** only being isolated in 34% yield, after 16 h (Entry 3, Table 4).^{*}

Table 4. Reaction of dienes **241b**, **259** and **264** with nitrosobenzene **160a**.

(1 eq.) **241b, 259, 264** + (2.5 eq.) **160a** $\xrightarrow[\text{time}]{\text{MeOH, r.t.}}$ **277i-k**

Entry	Diene	Product	Yield (%)
1 ^[a]	 241b	 277i	16
2 ^[b]	 259	 277j	78
3 ^[b]	 264	 277k	34

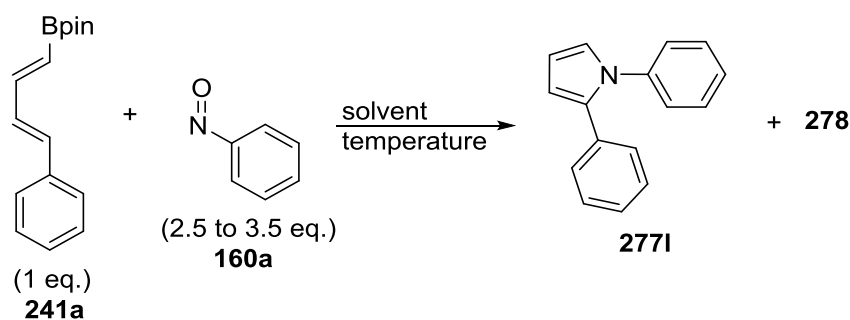
[a] Reaction with 2.5 eq of ArNO at r.t. for 16 h. [b] Reaction with 2.5 eq of ArNO at r.t. for 5 h.

Next, the influence of substituents on the borodiene was examined. Diene **241a**, bearing a phenyl group, **257** with a methyl carboxylate function, and **266** bearing a sulfonyl moiety in position 4, were tested.

In the presence of nitrosobenzene **160a**, no reaction of diene **241a** was observed at r.t. either in toluene or in MeOH (Entries 1 and 2, Table 5). Heating the mixture caused formation of

pyrrole, according to ^1H NMR (Entries 3 and 4, Table 5). The starting nitrosobenzene **160a** was consumed after an extended 22 h reaction time, resulting in 72% conversion of diene **241a** (Entry 5, Table 5). No further improvement was observed if the nitrosobenzene **160a** was added in portions in an attempt to decrease azo-by-product formation **278** (1 eq. at the outset - 1 eq. after 4 h - 0.5 eq. after 4 h), or by slow addition of a MeOH solution by syringe pump (Entries 6 and 7, Table 5). Finally, the use of 3.5 eq. of **160a** (Entry 8, Table 5) was required in order to achieve complete conversion of both stereoisomers of diene **241a**, resulting in the formation of pyrrole **277i** in 36% isolated yield.

Table 5. Study of the reactivity of diene **241a** with nitrosobenzene **160a**.



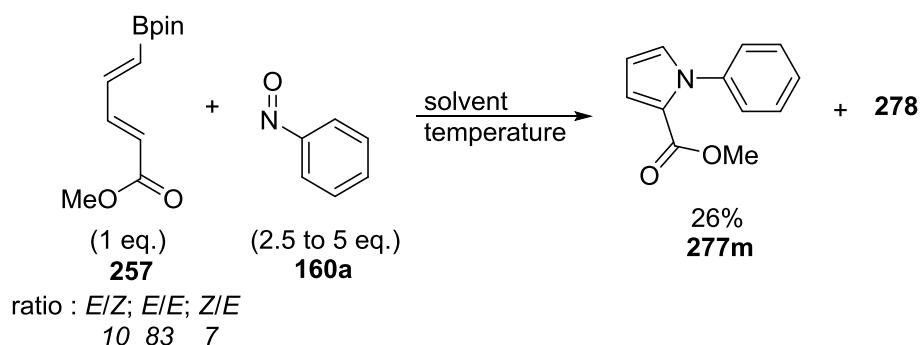
Entry	Solvent	Temperature (°C)	Time (h)	Conversion (Isolated yield) (%)
1 ^[a]	MeOH	rt	16	0
2 ^[a]	Toluene	rt	16	0
3 ^[a]	MeOH	reflux	5	50
4 ^[a]	Toluene	70	16	50 (14)
5 ^[a]	MeOH	reflux	22	72 (19)
6 ^[b]	MeOH	reflux	22	77 (20)
7 ^[c]	MeOH	reflux	22	82 (24)
8 ^[d]	MeOH	reflux	22	100 (36)

[a] Reactions with 2.5 eq of nitrosobenzene. *[b]* Reaction with 2.5 eq of nitrosobenzene added in portions. *[c]* Reaction with 2.5 eq of nitrosobenzene added slowly by syringe pump. *[d]* Reaction with 3.5 eq of nitrosobenzene.

The introduction of an electron withdrawing group (ester function) in position 4 of the borodiene was next examined. Diene **257** proved to be even less reactive than diene **241a**, and

longer reaction times and higher temperatures were required to improve the conversion (Entries 1-5, Table 6). In order to form the pyrrole **277m**, 5 eq. of nitrosobenzene **160a** and a 128 h reaction time was required in toluene at reflux, and only the *E,E*-stereoisomer reacted. Indeed, even with longer reaction times, the other isomers were still observed in the reaction mixture on the crude ^1H NMR. Nevertheless, 26% of the corresponding pyrrole **277m** was isolated after silica gel chromatography (Entry 5, Table 6).

Table 6. Study of the reactivity of diene **257** with nitrosobenzene **160a**.

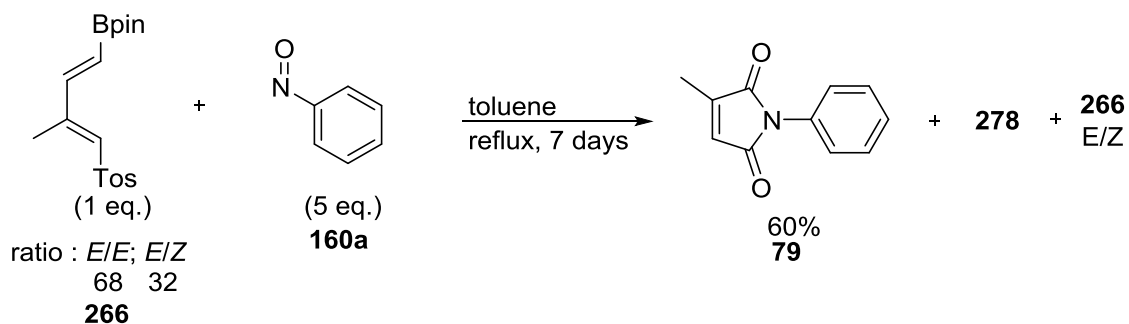


Entry	Solvent	Temperature (°C)	Time (h)	<i>E,E</i> -isomer conversion (Isolated yield) (%)
1 ^[a]	MeOH	rt	16	0
2 ^[a]	MeOH	reflux	16	0
3 ^[a]	Toluene	rt	16	0
4 ^[a]	Toluene	reflux	64	15
5 ^[b]	Toluene	reflux	128	100 (26)

[a] Reactions with 2.5 eq of nitrosobenzene. [b] Reaction with 5 eq of nitrosobenzene.

Diene **266** showed the same low reactivity as for the methyl carboxylate derivative **257**. No reaction occurred at r.t. in either MeOH or in toluene. Reflux conditions in toluene were necessary to observe the conversion of the *E,E*-isomer of **266**. The reaction required 7 days to observe full consumption of this isomer of **266**, whereas the *E,Z*-isomer did not show any reactivity. In this case, no pyrrole was isolated, or even observed in the crude reaction mixture by ^1H NMR analysis. Only, the corresponding maleimide **254** was obtained. If the reaction

was performed under argon, 9 days were required to obtain full conversion of the *E,E*-isomer, which highlighted the possible role of an aerobic oxidation step during the reaction (Scheme 62), but we have hitherto no mechanistic hypothesis to rationalise this result.



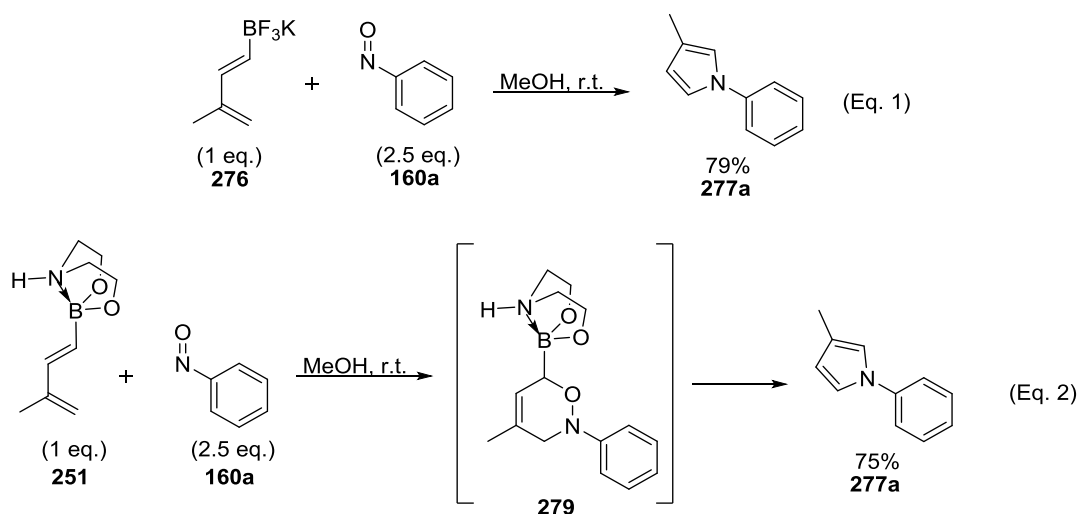
Scheme 62. Unexpected formation of maleimide **79**.

III.2. Reaction of tetracoordinated 1-borodienes with arylnitroso compounds

Since the various 1-borodienes with pinacolate esters all resulted in reactions in which the oxazine was not observed, attention was turned to the study of the influence of boron substituents that might result in the oxazine cycloadducts being isolated.

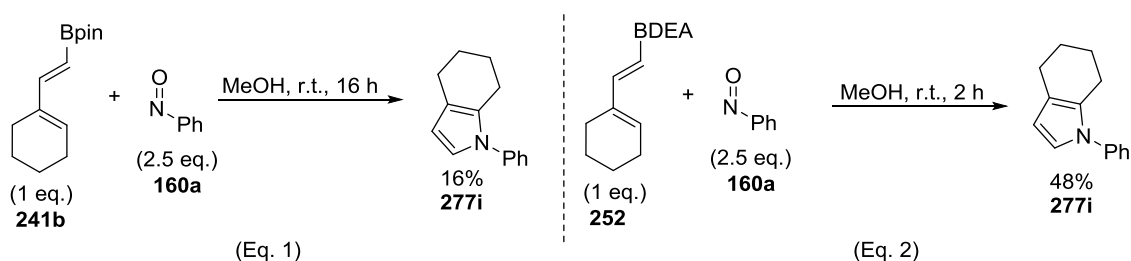
First, attention was devoted to the trifluoroborylated salt **276**. As previously, no oxazine was observed from the reaction of **276** with nitrosobenzene **160a** and the reaction yielded pyrrole **277a** in 79% (Eq. 1, Scheme 63). The replacement of the pinacol ester group **241c** by a diethanolamine moiety was then examined. Reaction of diene **251** with nitrosobenzene **160a** resulted in the identification of the [4+2]-cycloadduct **279** in the ^1H NMR spectrum of the crude mixture. Its structure was confirmed later by comparison of its ^1H spectrum with that of the corresponding MIDA cycloadduct **280a** (Entry 1, Table 7). After 2 h, all the diene **251** was consumed, the intermediate boro-1,2-oxazine **279** had disappeared, and only pyrrole **277a**

formation was observed, together with small amounts of azoxybenzene **278** (Eq. 2, Scheme 63).



Scheme 63. Reactivity of dienes **251** and **276** with nitrosobenzene **160a**.

This increased reactivity of the diethanolamine derivative was confirmed by the reaction of cyclic diene **252** which provided pyrrole **277i** after only 2 h and in a 48% yield as shown in Eq. 2, Scheme 64.



Scheme 64. Comparison of the reactivity between **241b** and **252**.

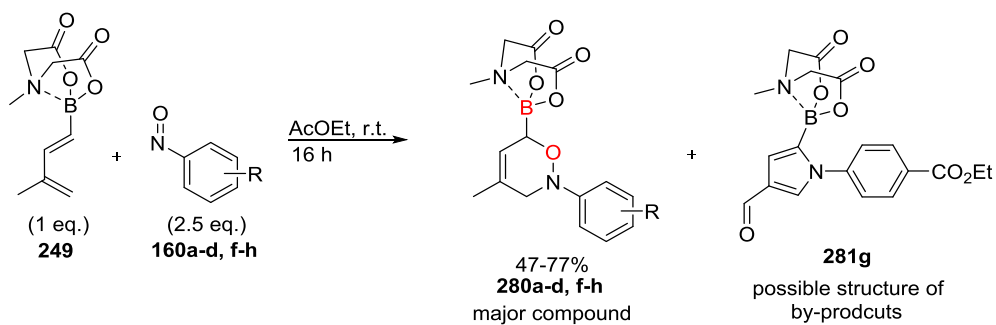
Most interestingly was the observation of the transient [4+2]-hetero-Diels-Alder cycloadduct **279** (Eq. 2, Scheme 63) that confirms the key role of the oxazine cycloadduct in the subsequent formation of the pyrrole. Diethanolamine esters are known for their facile hydrolysis or methanolysis to regenerate the corresponding boronic acid or ester,¹³² however, simply the reversibility of B-N chelation could be responsible of the facile rearrangement to

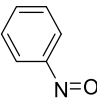
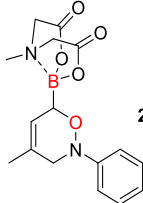
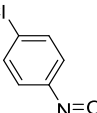
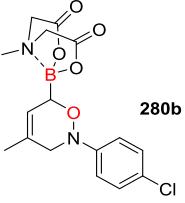
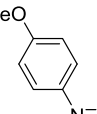
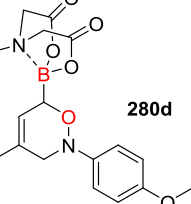
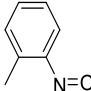
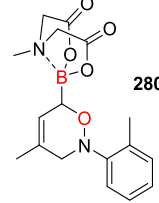
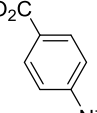
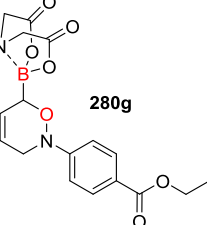
the pyrrole (*vide infra*). We can also notice, the beneficial effect of the tetracoordinated boronate ester, which increased the electron density on the diene moiety, and hence, made it more reactive towards the electron deficient dienophile. It is consistent with a "normal" electron demand Diels-Alder [4+2]-cycloaddition.

Prompted by these results, the behaviour of the corresponding MIDA borodiene derivatives **249** was then examined. Because of their high stability towards air and moisture, these compounds have been used as flexible scaffolds for the synthesis of a wide-range of functionalised small molecules.¹³³ It was our expectation that such dienes would make it possible to isolate and study the intermediate oxazine cycloadducts. The presence of an sp³- versus an sp²-hybridized boron species would also be expected to be a useful tool to examine the regioselectivity of the cycloaddition reaction. Hence, the scope of the reaction of the MIDA diene **249** was examined with various arylnitroso compounds **160**, as outlined in Table 7. Reactions were carried out in AcOEt to give improved solubility of the B-MIDA diene **249**. However, even if the reaction was run in MeOH, the same cycloadduct was observed. The reaction of the MIDA-borodiene **249** provided the corresponding oxazine cycloadducts **280** in moderate to good yields with each of the different arylnitroso compounds **160**, without any obvious electronic effects from the aryl substituent. Single regioisomeric products were obtained, as exemplified by the formation of the stable [4+2]-cycloadduct **280a**, obtained from reaction of diene **249** with nitrosobenzene **160a** and isolated in 64% yield (Entry 1, Table 7). Only the boron-oxygen 1,2-related regioisomer (in red in Table 7) was observed; its structure being assigned by NOESY correlation between the *o*-phenyl Hs and one of the NCHs on the oxazine ring. The introduction of different arylnitroso substituents, *i.e.* electron donating and withdrawing groups in positions 2 and 4, did not change the resulting regiochemical outcome (Entries 2-5, Table 7) and yields ranged between 47 to 77%. It is also noteworthy that little or no dimerisation of the arylnitroso compounds took place during these

reactions, reflecting the short reaction times and more reactive diene, reducing the potential for competitive by-product formation from the nitroso compound. Nevertheless, a second compound was isolated when nitroso **160g** was used. This unknown compound was fully characterised by ^1H , ^{13}C , ^{11}B NMR, IR and mass spectroscopy. The molecule possesses a B-MIDA group (δ ^{11}B NMR = 10.3 ppm) and an aldehyde moiety (δ ^1H NMR = 9.76 ppm, s, 1H; δ ^{13}C NMR = 185.4 ppm; IR (C=O) stretch = 1743 cm^{-1}) and seems to have a pyrrole substructure characterised by small coupling constant (δ ^1H NMR = 7.89, d, $J = 1.7\text{ Hz}$, 1H; 6.83, d, $J = 1.7\text{ Hz}$, 1H). Based on these observations, the structure **281g** was proposed. This observation raises further hitherto unsolved mechanistic questions.

Table 7. Reactivity of MIDA-substituted diene **249** with aryl nitroso compounds **160**.

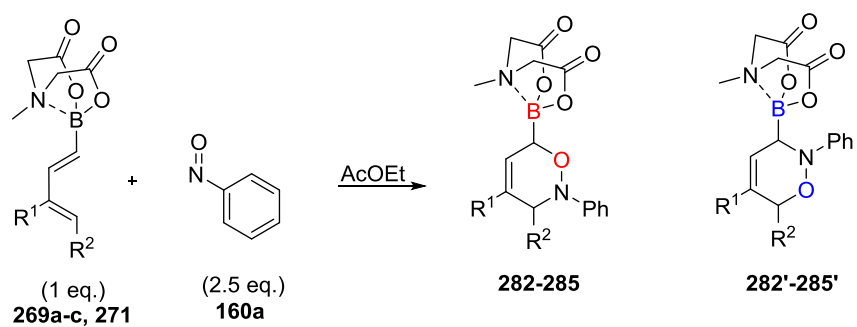


Entry	Nitroso compound	Product	Isolated Yield 280 (%)
1	 160a	 280a	64
2	 160b	 280b	77
3	 160d	 280d	47
4	 160f	 280f	56
5 ^[a]	 160g	 280g	61

[a] Reaction in which the by-product **281g** was isolated in 18% yield.

The impact of the substituents on the dienyl moiety, *i.e.* dienes **269a-c** and **271**, was then examined, nitrosobenzene **160a** being used as a model dienophile. The resulting nitroso-addition reactions are summarised in Table 8. Similar to the results observed with the MIDA derivative **249**, the first three dienes (**269b-c** and **271**) gave the same single regioisomeric boron-oxygen 1,2-related products at r.t. (in red in Table 8), with the boron occupying the α -position relative to the ring oxygen of the oxazine (Entries 1-3, Table 8). The introduction of a phenyl group at C₄ noticeably reduced the reactivity of the borodiene **269a**, with reaction only occurring at reflux in AcOEt over 24 h. In addition, a mixture of regioisomers **285** and **285'** (ratio 40:60) was isolated in an 89% combined yield (Entry 4, Table 8). Both steric and electronic effects of the phenyl ring can explain this observed preferred regiochemistry, as discussed by Houk *et al.* for 1-phenylbutadiene compared with penta-1,3-diene.¹³⁴ The structure of the major boron-oxygen 1,3-related regioisomer **285'** (in blue in Table 8) was secured by single crystal X-ray structure analysis (Figure 1), confirming the *cis*-stereochemistry of the boron and phenyl ring substituents.

Table 8. Reactivity of MIDA-substituted dienes **269a-c** and **271** with nitrosobenzene **160a**.



Entry	Diene	Product	Yield (%) (Isomer ratio)
1 ^[a]	 271	 282	43 (100/0)
2 ^[a]	 269c	 283	68 (100/0)
3 ^[a]	 269b	 284	78 (100/0)
4 ^[b]	 269a	 285 + 285'	89 (40/60)

[a] Reaction with 2.5 eq of nitrosobenzene in AcOEt at rt for 6 h. [b] Reaction with 5 eq of nitrosobenzene AcOEt at reflux for 24 h.

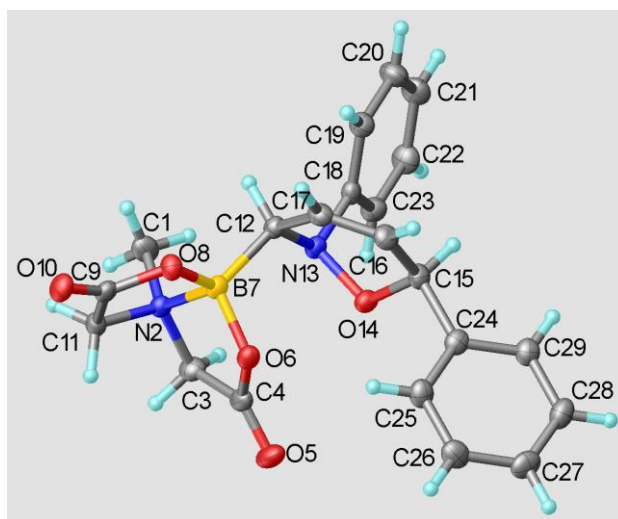
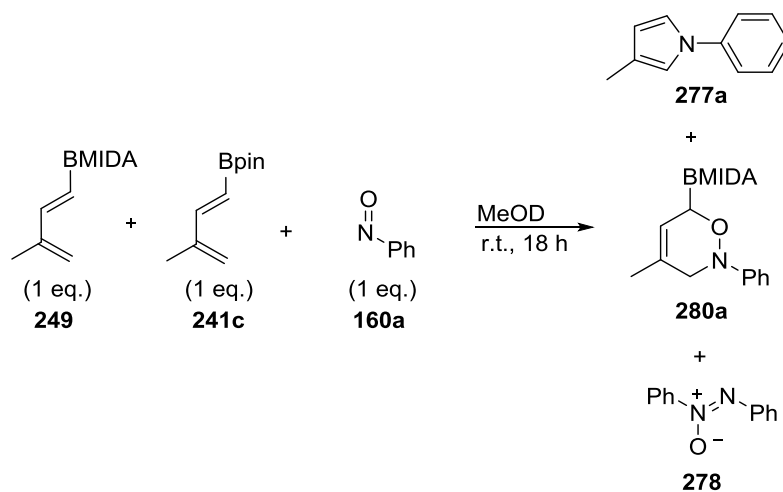


Figure 1. Single crystal X-ray molecular structure of **285'**.

III.3. Impact of the boron substituent on the rate of the reaction

Experimental work has proved that the diethanolamine diene **251** is much more reactive than the pinacol ester **241c**. However, no comparisons between dienes **249**, **241c** and **276** could be drawn based on the experimental outcome of the reaction. Thus, an equimolar mixture of **249** and **241c** was stirred at r.t. in the presence of nitrosobenzene **160a** (1 eq.) in MeOD (Scheme 65).



Scheme 65. Study of the reactivity of the diene **249** and **241c** toward nitrosobenzene **160a**.

After 18 h, the crude mixture was analysed by ^1H NMR (Figure 2). Unfortunately, the sample was not fully soluble in MeOD, so it was impossible to measure accurately the ratio between all the material present in the crude. For a better understanding, the crude reaction mixture was evaporated and diluted with acetone- d^6 showing a better, but not total, solubility towards the B-MIDA derivatives **249** and **280a**. Firstly, it was possible to assume that the diene **241c**, pyrrole **277a** and by-products **278** were fully soluble, whereas the B-MIDA derivatives **249** and **280a** were not. According to the analysis, it is possible to conclude that:

- There is no major difference in reactivity between dienes **249** and **241c**.
- The B-MIDA diene seemed to show a slightly higher reactivity based on this results (diene **249**/diene **241c** 1/2; pyrrole **277a**/oxazine **280a** 1/1.2).

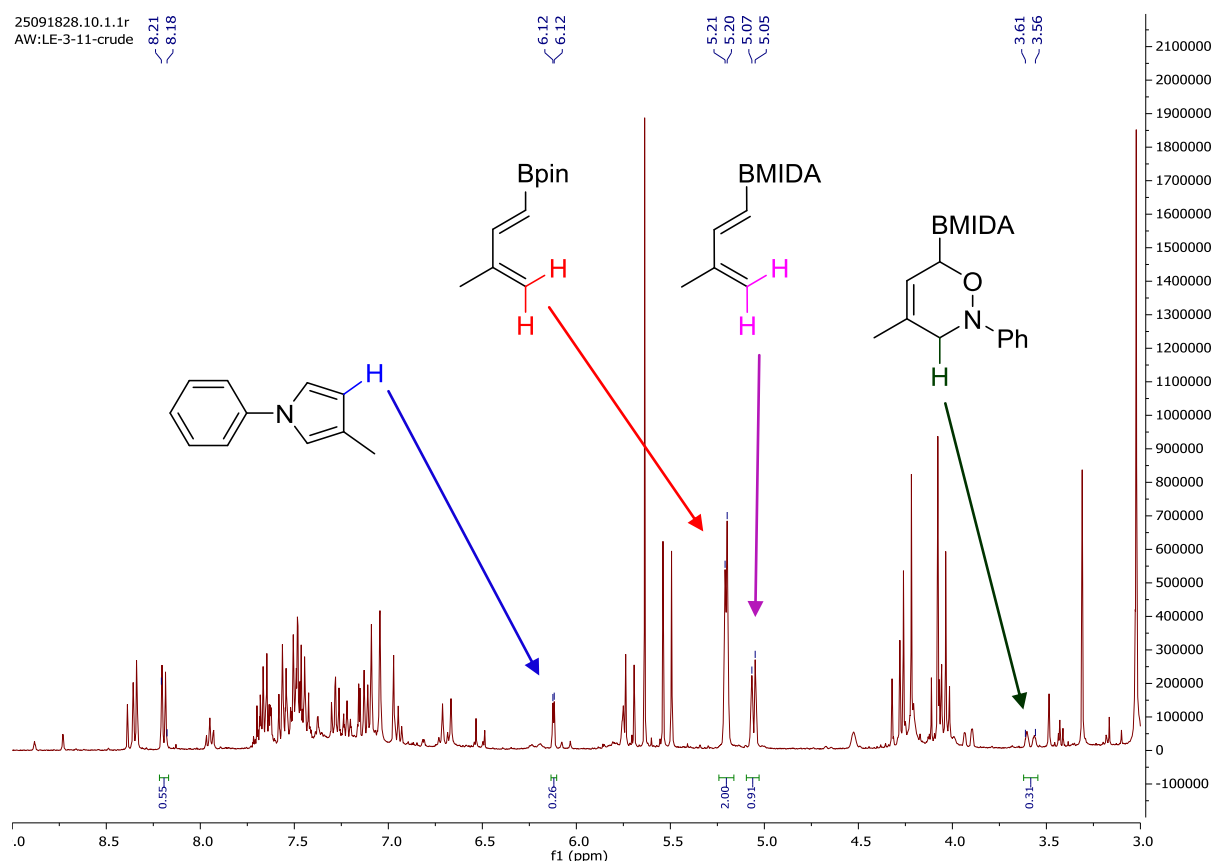
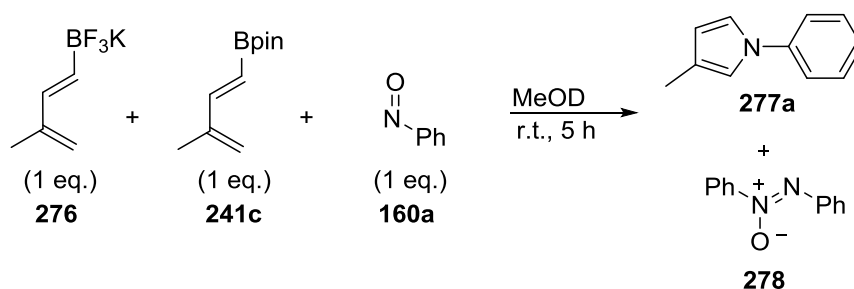


Figure 2. ^1H NMR study of the diene **249** and **241c** toward nitrosobenzene **160a**.

A similar ^1H NMR study was undertaken to evaluate the reactivity of the trifluoroboronated salt (Scheme 66). The reaction was performed using diene Bpin **241c** in competition with the diene **276**. Two ^1H NMR analyses were undertaken, one after 10 min and one after 5 h, when the reaction should be finished according to results shown in Table 3. During the NMR sample preparation, trifluoroboronated salt **276** did not show full solubilisation. After 5 min, the ^1H NMR showed that:

- The ratio between pyrrole diene **241c**/diene **276**/pyrrole **277a** = (63/14/23). Diene **276** and pyrrole **277a** represented only 37% of the crude product. This observation is not consistent with a full mass recovery from the reaction, with a starting ratio of diene **241c**/diene **276** (1/1). It can be explained by the partial solubility of the starting diene **276**. Nevertheless, the reaction showed that diene **276** exerted a dramatic faster reactivity or even reacted exclusively with **160a** compared to the Bpin variant **241c**.
- A small amount of by-products **278** was observed.

After 5 h, only traces of diene **276** were observed, in the presence of pyrrole **277a** and diene **241c**.



Scheme 66. Reactivity of the trifluoroboronated diene **276** toward nitroso Diels-Alder reaction.

During the reaction presented in Scheme 63, a sample from both reaction (Eq. 1 and Eq. 2) was taken after a few minutes to observe the consumption of the starting diene. BDEA diene **251** showed a 50% conversion after 5 min whereas diene **276** gave a 92% conversion after 10

min. Thus, these two tetracoordinated boron species proved to be more reactive than the Bpin **241c** and the BMIDA **249** variant.

As expected, the boron unit has a dramatic effect on the kinetics of the reaction. The more electron rich the diene is, the faster the reaction is, which is consistent with a "normal" electron, frontier-orbital-controlled [4+2]-cycloaddition reaction. The four boron substituents can be divided in two major groups. The first group involves the Bpin and the BMIDA whereas the second one incorporates the BDEA and the BF₃K boron unit. The patterns of these empirical observations are comparable to the results of the nucleophilicity parameters calculated by Mayr and co-workers.¹³⁵ The reactivity towards nitroso Diels-Alder can be summarised as outlined in Figure 3.

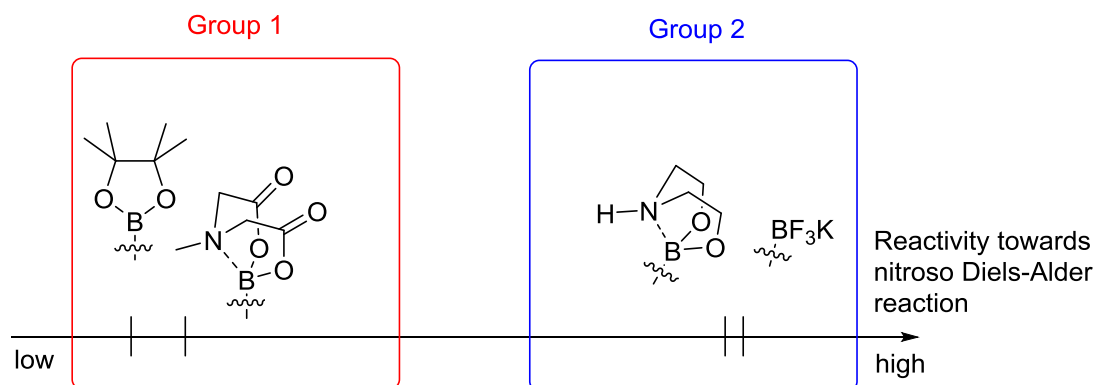


Figure 3. Empirical effects of the boron unit toward the nitroso Diels-Alder reaction.

III.4. Mechanistic aspects of the reaction 1-borodienes with arylnitroso compounds.

III.4.a. Computational study[†]

To probe the possible mechanism responsible of the formation of pyrrole **277** from 1-boronated diene and arylnitroso compounds **160**, a computational study was carried out using Gaussian 09.¹³⁶ The geometries discussed in Schemes 67 and 68 were optimised at the B3LYP/6-31G* level with no symmetry constraints.¹³⁷ The optimised geometries were found to be true minima based on no imaginary frequencies obtained from frequency calculations. The transition-state (TS) geometries were located using the OPT = QST3 method. Frequency calculations on TS geometries revealed one imaginary frequency for each geometry. All intrinsic reaction pathways shown in Schemes 67 and 68 were determined from transition-state geometries using the IRC command.

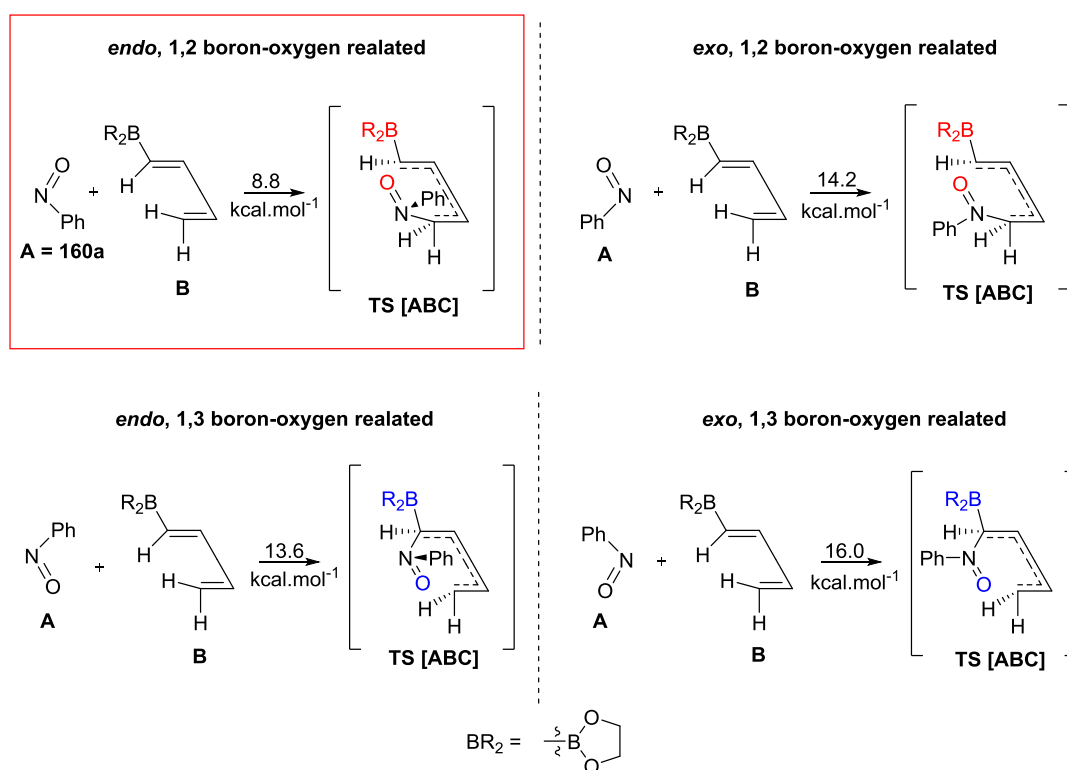
Regioselectivity of the initial cycloaddition

Among the four transition states in Scheme 67, **TS[ABC]** exerted the lower energy (8.8 kcal.mol⁻¹). Calculations showed that the nitrosobenzene **160a** is added through an *endo* pathway with a single regioisomeric boron-oxygen 1,2-related product (in red, Scheme 67).

First the *endo* pathway can be explained by a combination of electrostatic repulsion between the lone pairs of RNO with the electron rich diene and also a repulsive interaction between the *n*-HOMO of the nitroso compound and the π -HOMO of the diene. Secondly, the nitroso

[†] Computational studies were performed by Dr Mark A. Fox in the Chemistry Department at Durham University.

Diels-Alder reaction seems to occur through an asynchronous concerted pathway. This has also been postulated by Houk and co-workers, because of the asymmetry of the dienophile.¹³⁸

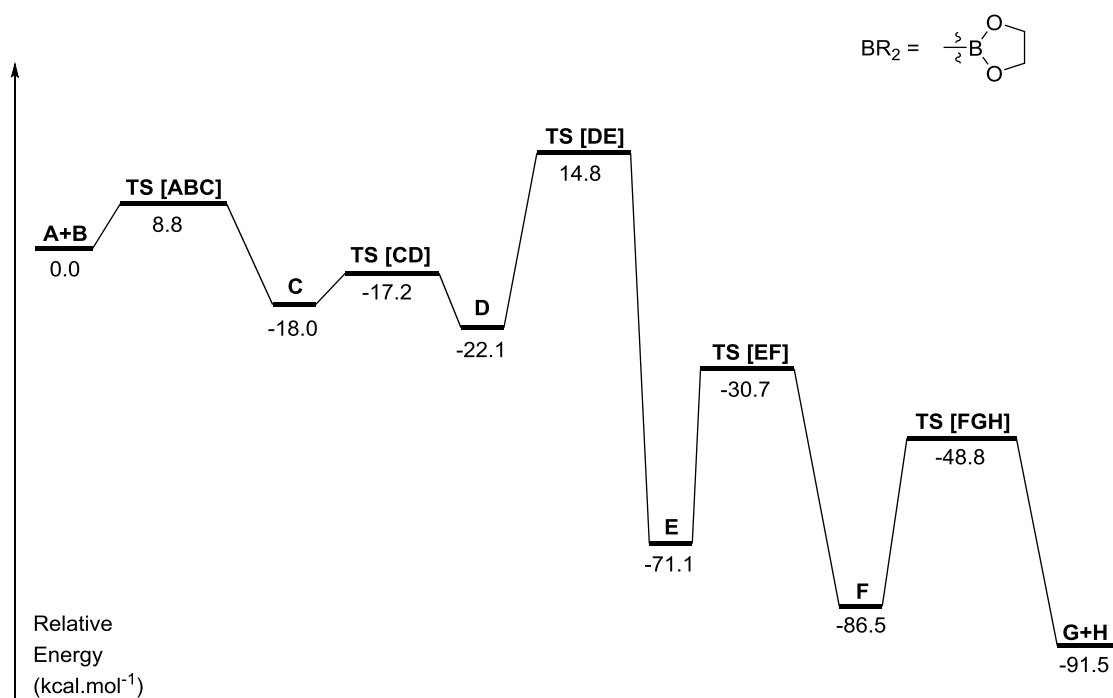
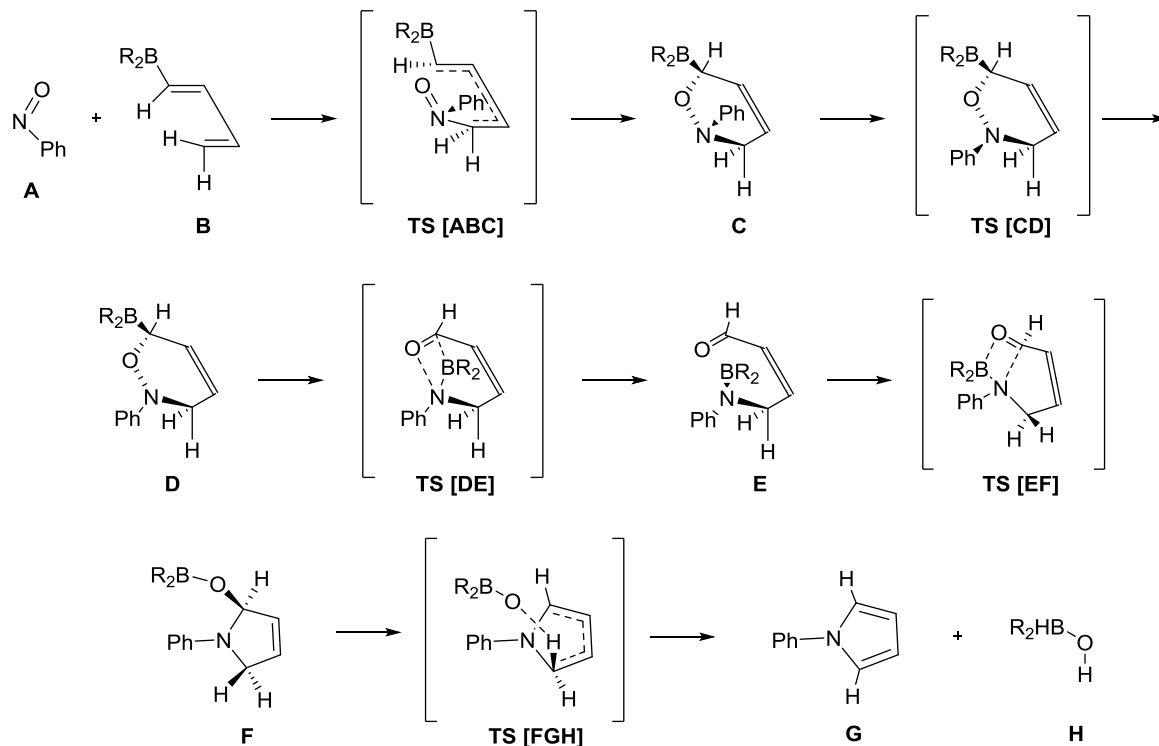


Scheme 67. Four different pathways and their TS energies determined by computations in the Diels-Alder reaction of nitrosobenzene **A** and the 1-boronodiene model molecule **B**.

Mechanism

The proposed mechanism involves pyrrole formation proceeding through a Diels-Alder reaction (to give **C**, Scheme 68), followed by a boryl rearrangement (to give **E**, Scheme 68). Then, intramolecular aza-boryl addition to the aldehyde (to give **F**, Scheme 68) and finally borate elimination gives **G** (Scheme 68). All steps were computed to be exothermic thus supporting the cascade process. Eight possible conformers of the oxazine were formed, where; The boryl group occupies either the axial or equatorial position; The phenyl group is either *endo* or *exo*; The oxazine ring is either in a boat or chair conformation. Among the possible conformers, species **C** and **D** are likely products from the favourable Diels-Alder

pathway *via* **TS[ABC]** with **D** as the most stable conformer of all possible conformers of the oxazine. Theoretical results showed that the rate-limiting step in the reaction pathway is likely to be the hetero-Diels-Alder step or the ring cleavage step *via* boryl group rearrangement.¹³⁹

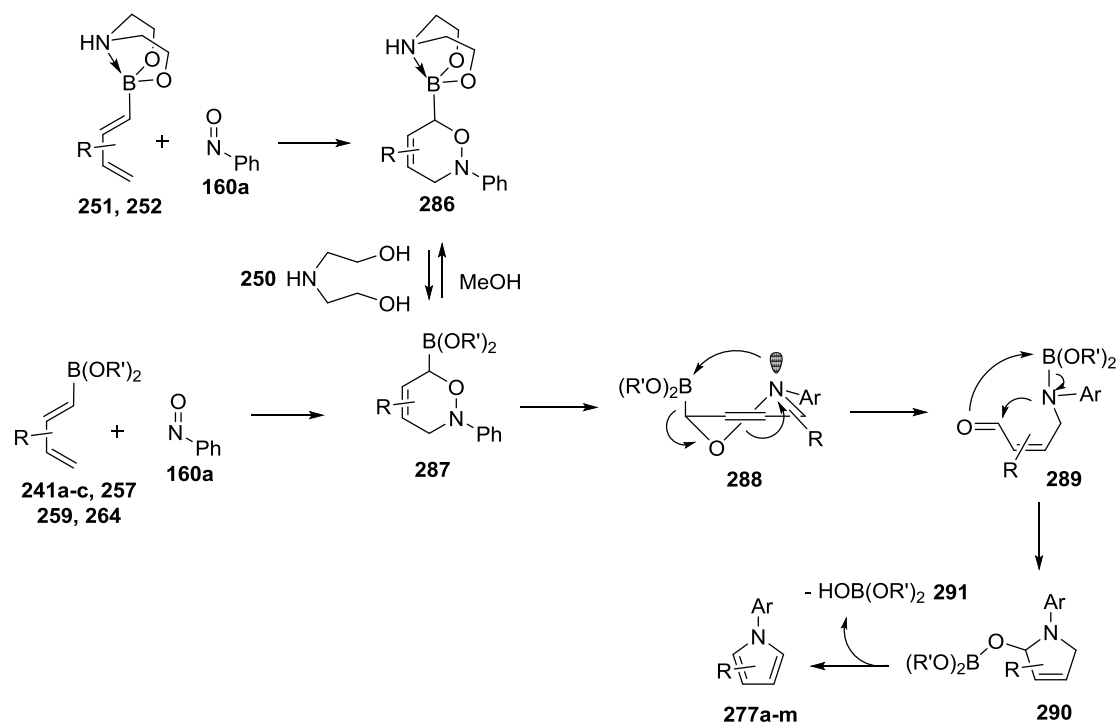


Scheme 68. Possible reaction steps in the formation of 1-phenyl-1H-pyrrole **G** from a 1-boronodiene model **B** and nitrosobenzene **A**.

III.4.b. Additional experimental study

Further experimental investigations were then carried out to support this mechanistic hypothesis and the DFT calculations.

The replacement of the pinacol boronate ester on the diene moiety by diethanolamine (*vide supra*) resulted in the identification of the [4+2]-cycloadduct in the ^1H NMR spectrum of the crude mixture. Reacting diene **251** or **276** with nitrosobenzene **160a** for 2 h, resulted in complete diene consumption and even the boro-1,2-oxazine intermediate **279** totally disappeared to afford only pyrrole **277a** with only small amounts of azoxybenzene **278** produced (Eq. 2, Scheme 63). The pyrrole formation under these conditions can be explained by a facile equilibrium between the dioxazaborocane **286** and the corresponding methyl ester **287** due to solvolysis.¹³² This equilibrium releases the vacant orbital on boron, and hence, a subsequent rearrangement can occur to access the pyrrole (Scheme 69).

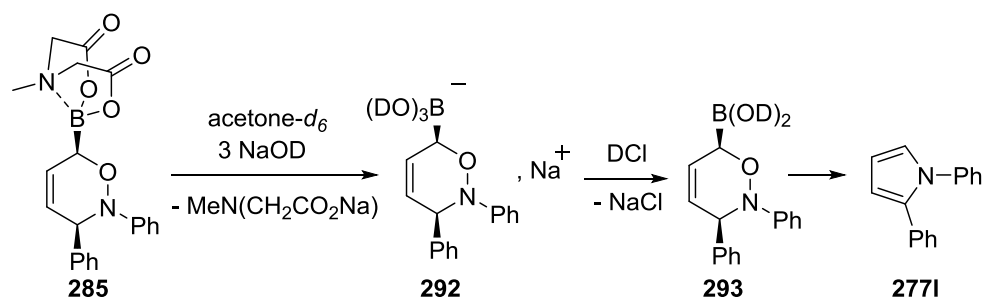


Scheme 69. Proposed mechanism for the formation of pyrroles from the reaction of 1-borodienes with aryl nitroso compounds.

The reaction of nitrosobenzene **160a** with the MIDA boronate **269a** results in the formation of the two regioisomers **285** and **285'** which can be separated (*vide supra*). MIDA derivatives can be easily converted to the boronic esters.¹³³ To confirm the role of the B(OR)₂ in the pyrrole formation, we therefore envisaged to study such transformation with each of the regioisomers by ¹H and ¹¹B NMR, either under basic or acidic conditions.

Under basic conditions

The regioisomer **285** reacted cleanly with (NaOD, 3 eq.) to give the pyrrole **277I**. The proposed reaction sequence for the formation of pyrrole is summarised in Scheme 70.



Scheme 70. Proposed reaction sequence for the formation of pyrrole **277I** from MIDA boronate oxazine derivative **285**.

In ¹H NMR spectrum, the starting oxazine **285** showed the features of a B-MIDA substituent characterised by the two sets of signals (dd) between 4.03 and 4.59 ppm. In the ¹¹B NMR spectrum, there was also the characteristic peak of a tetracoordinated boron species, evidenced by a chemical shift around 10 ppm (10.30 ppm, Figure 4).

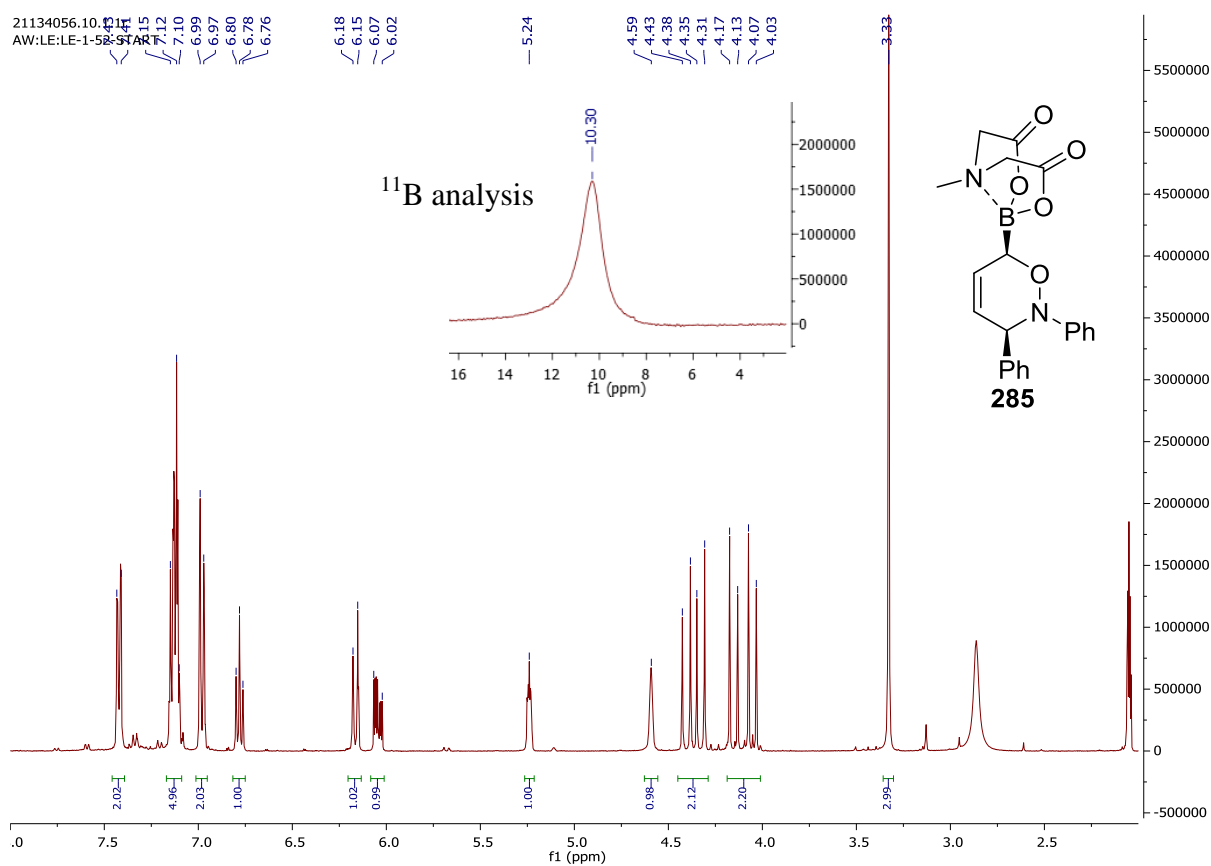


Figure 4. ^1H and ^{11}B NMR of oxazine **285**.

After addition of NaOD (3 eq.), ^1H NMR showed the disappearance of the MIDA signal (no signal between 4 and 5 ppm), while, the oxazine scaffold seemed to remain intact. Interestingly, this intermediate was stable overnight under the reaction conditions. ^{11}B NMR showed a change in boron substituent from a shift at $\delta = 10.30$ to $\delta = 0.64$ ppm, which could be consistent with the formation of compound **292** (Figure 5).

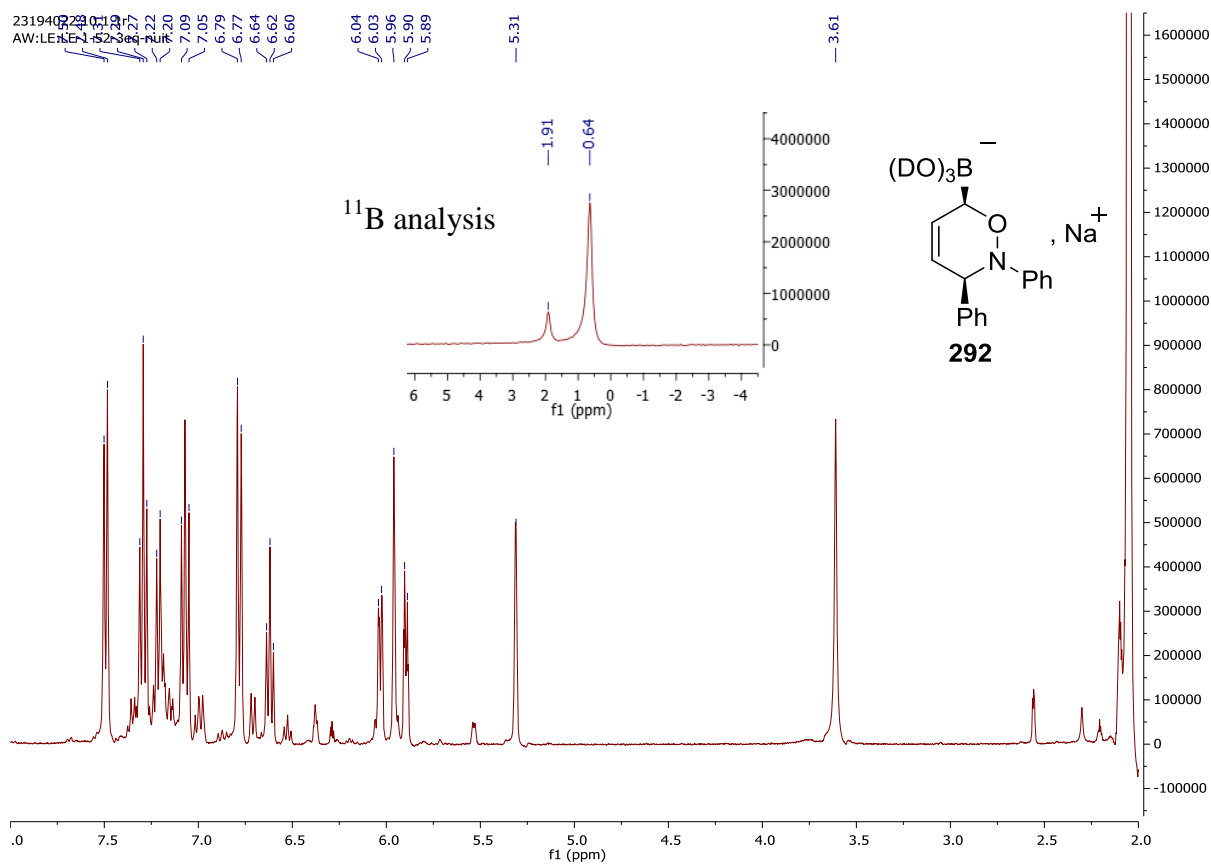


Figure 5. ^1H and ^{11}B NMR of likely intermediate **292** after the addition of NaOD (3 eq.) to oxazine **285**.

Hydrolysis of this postulated borate, using DCl (1 eq.), led instantaneously to a major change in both spectra. In the ^1H NMR, the oxazine scaffold collapsed to provide pyrrole **2771**, while, in the ^{11}B spectrum, the appearance of a signal at 19.9 ppm is consistent with the formation of $(\text{RO})_3\text{B}$ (Figure 6).

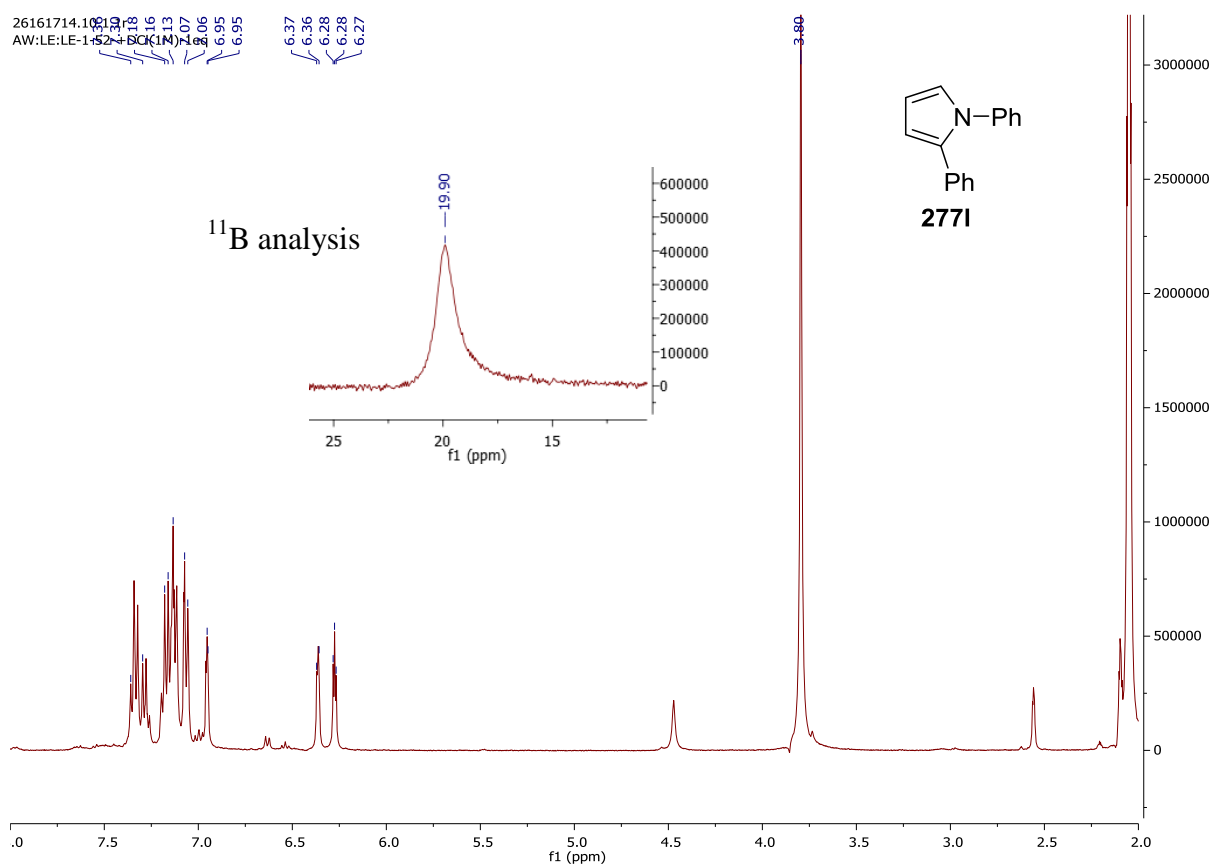
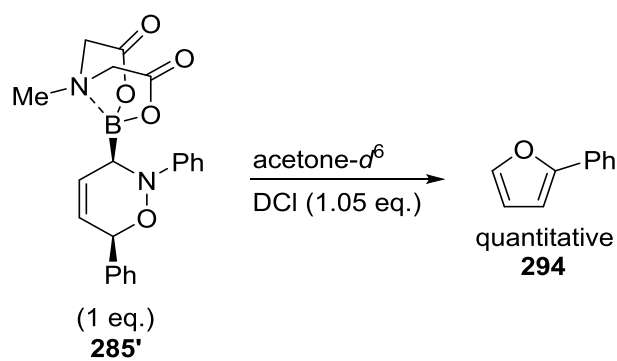


Figure 6. ¹H and ¹¹B NMR of pyrrole **2771** after the addition of NaOD (3 eq.) and DCI (1 eq.) to oxazine **285**.

Under the same basic conditions (NaOD, 3 eq.), regioisomer **285'** gave a mixture of unidentified products.

Under acidic conditions

In contrast, under acidic conditions (DCI 1M, 1 eq), 2-phenylfuran **294** was cleanly and quantitatively produced after 10 min at r.t. in acetone-*d*₆, from regioisomer **285'**, as shown in Scheme 71.



Scheme 71. Furan formation from acidic treatment of oxazine **285'**.

As examined on previous systems, this transformation was also followed by NMR. The starting oxazine **285'** showed similar characteristics in both the ^1H and ^{11}B NMR spectra as for regioisomer **285** (Figure 7).

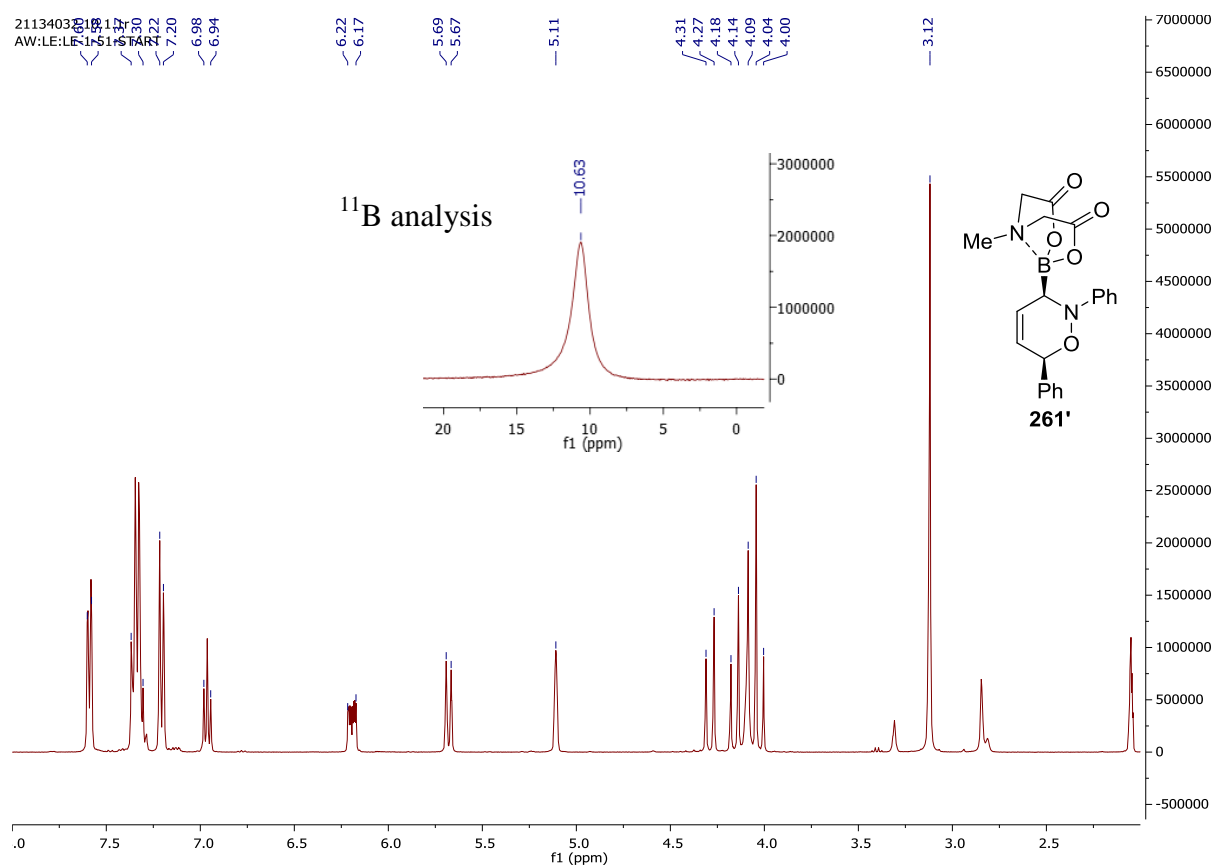


Figure 7. ^1H and ^{11}B NMR of oxazine **285'**.

Addition of DCI (1.05 eq.) provided formation of the furan **294** in 10 min according to ^1H NMR. No intermediate, as under the basic conditions, was observed. ^{11}B analysis provided important information concerning the role of the boron in this process. Indeed, none, or only traces of a salt (chemical shift around 0 ppm) was observed, as any by-product resulting from the hydrolysis (chemical shift around 20 ppm). This could mean that a BMIDA derivative was still present in the reaction mixture (Figure 8).

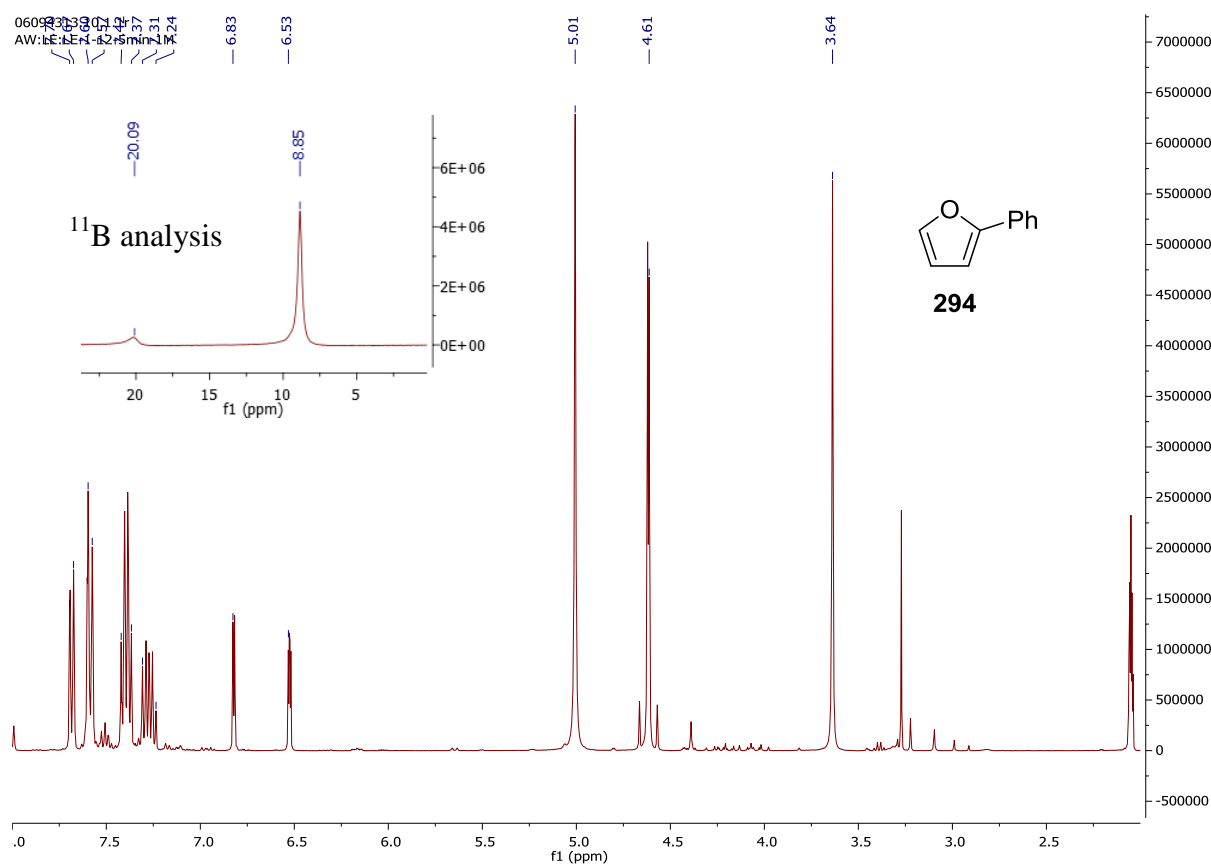
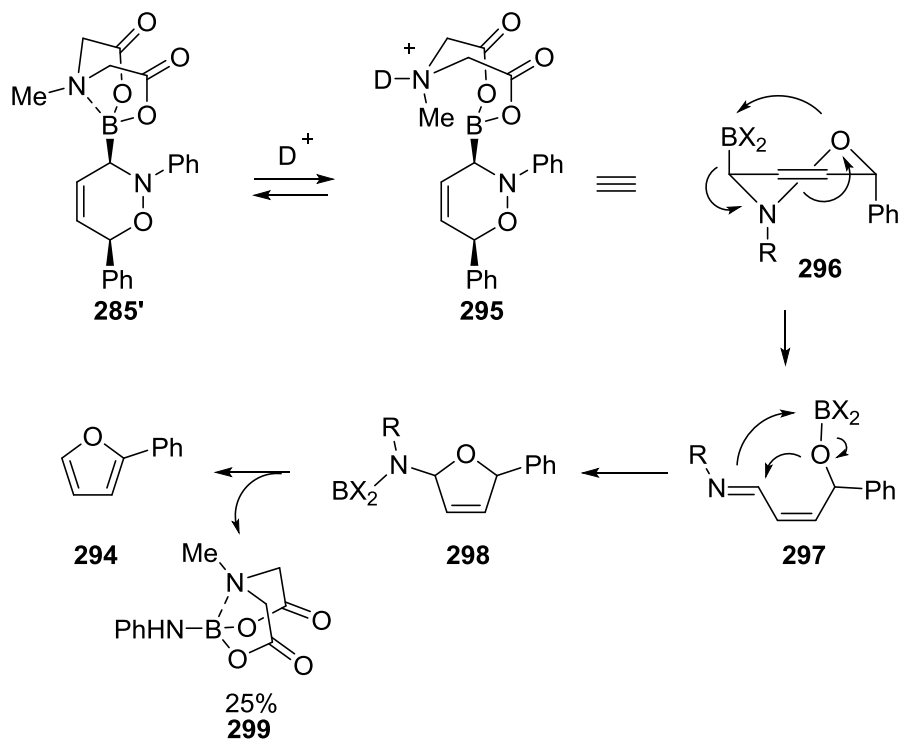


Figure 8. ^1H and ^{11}B NMR of furan **294** after addition of DCI (1.05 eq.) on oxazine **285'**.

To confirm this hypothesis, extraction of the crude mixture with DCM was performed. By-product **299** was isolated in 25% yield (Scheme 72), whose structure was established by ^1H (MIDA signals; 4.25 ppm, d, 2H; 4.09 ppm, d, 2H; 3.01 ppm, s, 3H), ^{13}C (MIDA signals; 167.6 ppm, 2 C=O; 62.1 ppm, 2 CH₂; 45.8 ppm, CH₃) ^{11}B NMR (9.9 ppm), and mass spectroscopy ($[\text{M}+\text{H}]^+ = 249.104$). These experimental observations are in agreement with

that the proposed mechanism outlined in Scheme 69. A preliminary protonation of the nitrogen atom of the MIDA boronate **285'** results in de-coordination of the nitrogen from boron, leading to the intermediate **295**. Formation of this R-BX₂ moiety **295** then enables a facile boryl rearrangement (**296-298**) to take place, and in this case, to form the furan **294** (Scheme 72).



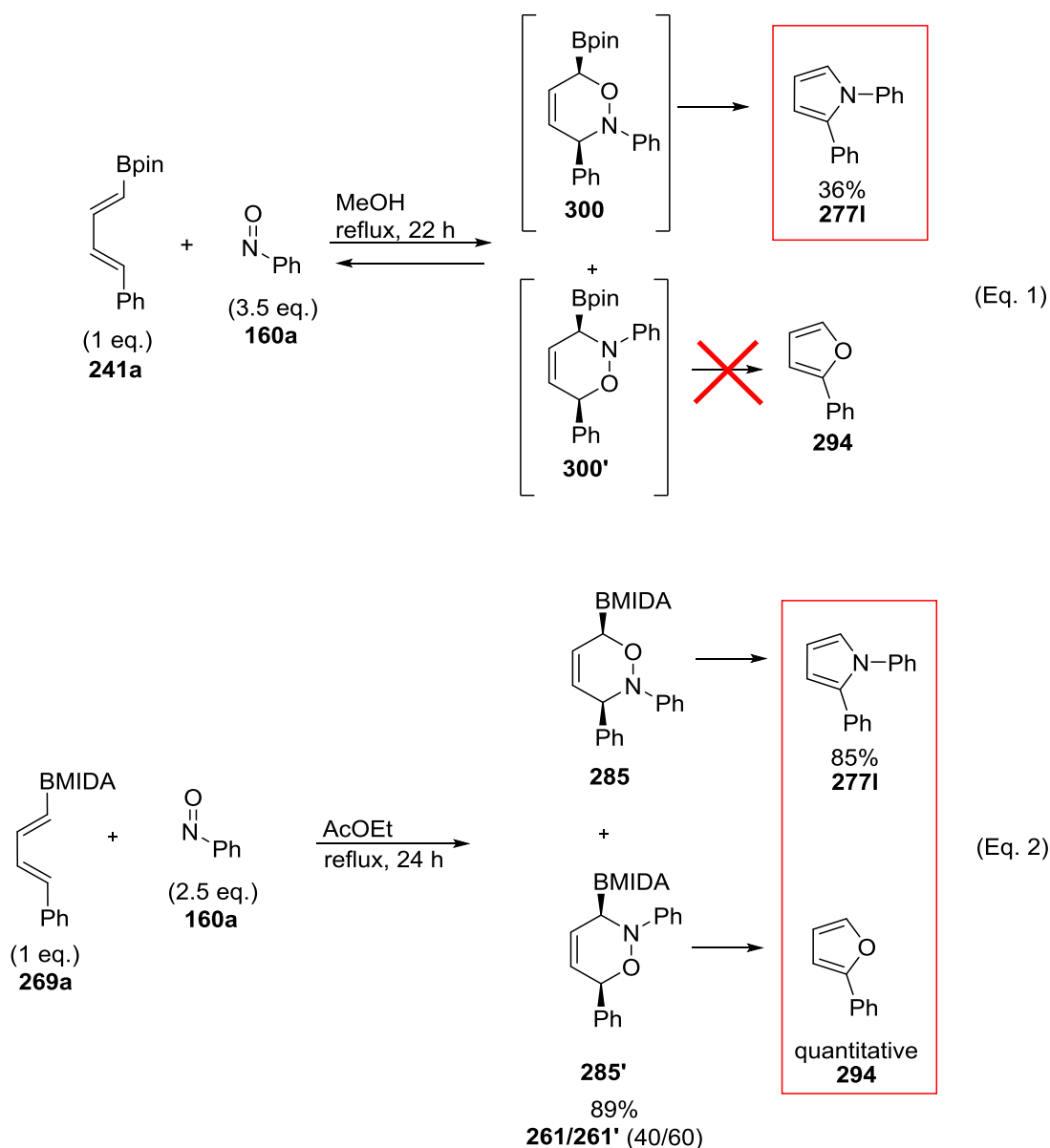
Scheme 72. Proposed mechanism for the formation of furan **294** from **285'**.

It is therefore possible to selectively and cleanly deprotect each regioisomer depending on the reaction conditions. Pyrrole formation was produced from the regioisomer **285** under basic conditions, whereas furan formation occurred from **285'** under acidic conditions.

III.4.c. The Nitroso Diels-Alder with boronated diene; a reversible process?

The formation of the furan **294** from the second regioisomer **285'** highlights another feature of the nitroso Diels-Alder reaction, its reversibility.

By comparison of Eq. 1 and 2 shown in Scheme 73, it is important to note that no furan **294** was formed during the reaction of diene **241a** with nitrosobenzene **160a**. Empirical kinetic studies between diene **249** and **241c** (Scheme 65), as well as previous studies,¹³⁵ showed that Bpin and BMIDA seemed to have quite similar electronic effects. Thus, it is plausible to expect that the regiochemical outcome of the cycloadditions should be comparable. However, no furan **294** was formed using diene **241a**. There are two possible explanations for this observation. Either regioisomer **300'** is highly unstable and decomposed under the reaction conditions, or the nitroso Diels-Alder reaction is reversible. For the first case, decomposition of the regioisomer **300'** could explain the low isolated yield (36%) of pyrrole **2771**. In the case of a reversible process, it might be possible that the retro Diels-Alder reaction of regioisomer **300'** occurred faster than the rearrangement to provide furan **294**, contrary to regioisomer **300**, which was converted instead into pyrrole **2771**. Because of the possible reversibility of the Diels-Alder reaction, all reagents involved in the reaction were subjected to decomposition (oxazine intermediate **300** and **300'**), polymerisation (diene **241a**) or by-products formation (nitrosobenzene **160a**). Unfortunately, no final conclusions could be drawn from this study. Further theoretical calculations relating to this specific case could give important information to support a reversible process.

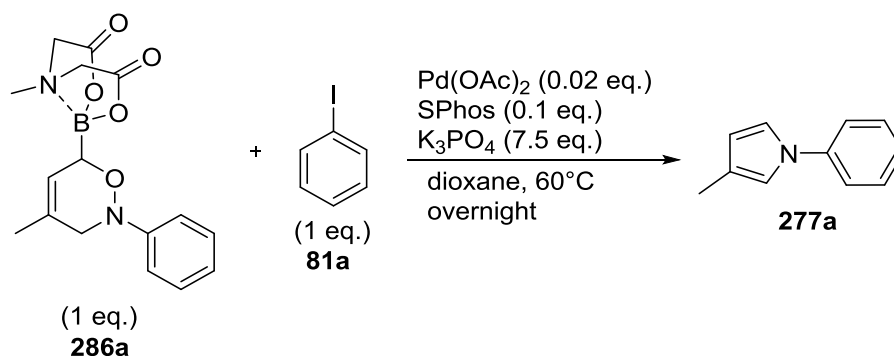


Scheme 73. Comparison of the reaction between dienes **241a** and **269a** with nitrosobenzene **160a**.

III.5. Transformations of borono-1,6-dihydro-1,2-oxazine derivatives

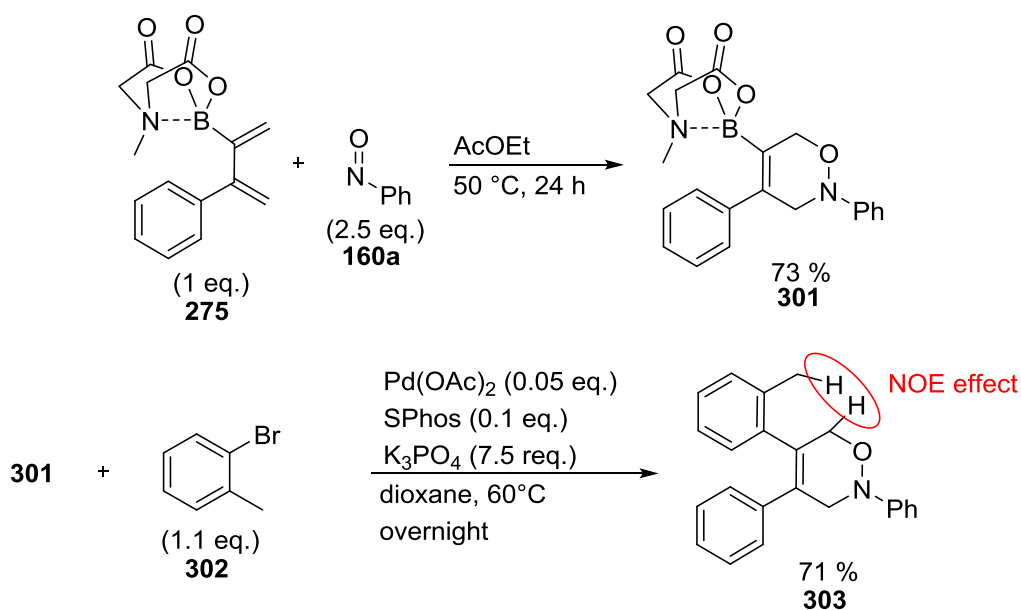
To explore the synthetic potential of BMIDA oxazine derivatives, a Suzuki-Miyaura coupling with the cycloadduct **286a**, chosen as a model substrate, was carried out. Under classical experimental conditions for this class of reaction,^{133b} ¹H NMR of the crude reaction mixture

showed full conversion of the starting material to the pyrrole **277a**, showing that **286a** was not stable enough to survive the Suzuki-Miyaura coupling conditions (Scheme 74).



Scheme 74. Reactivity of oxazine **286a** and iodobenzene **81a** under Suzuki-Miyaura coupling conditions.

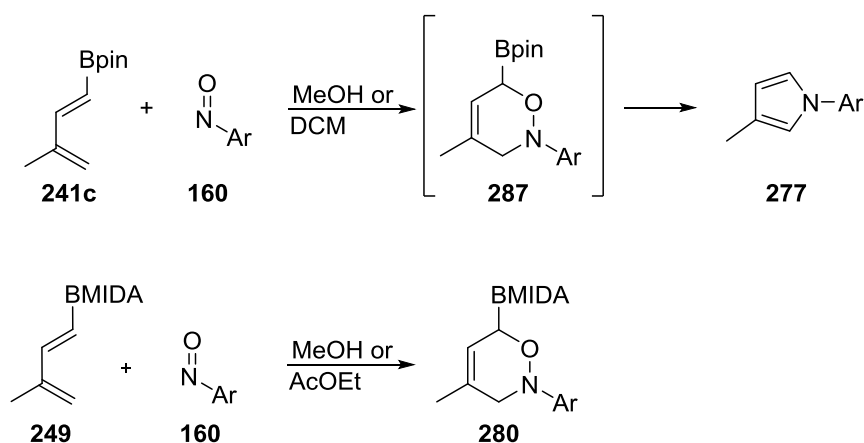
To confirm that this was indeed the location of the boronated group that was responsible for this failure, the cycloadduct **301** was prepared from diene **275** in a 73% isolated yield with only traces of the second regioisomer. It was engaged in a Suzuki-Miyaura cross-coupling with 1-bromotoluene **302** in the presence of palladium(II) acetate and SPhos (Scheme 75). The 2,4,5-trisubstituted dihydrooxazine **303** was isolated in a 71% yield. A NOESY NMR experiment (correlation between Hs of the methyl group of the toluene moiety and Hs on the oxazine ring at C₆) established the relationship of groups in this compound, and consequently the orientation of the first cycloaddition. No ring contraction product was observed in this case, but minor amount of the deborylation product were detected. This confirms that the 1-boryl function is essential for the pyrrole or furan formations, through the boryl addition-elimination sequences previously proposed.



Scheme 75. Synthesis of triarylated oxazine **303** from the nitrosobenzene Diels-Alder/Suzuki-Miyaura cross-coupling reaction sequence.

III.6. The one-pot nitrone formation/1,3-dipolar cycloaddition sequence

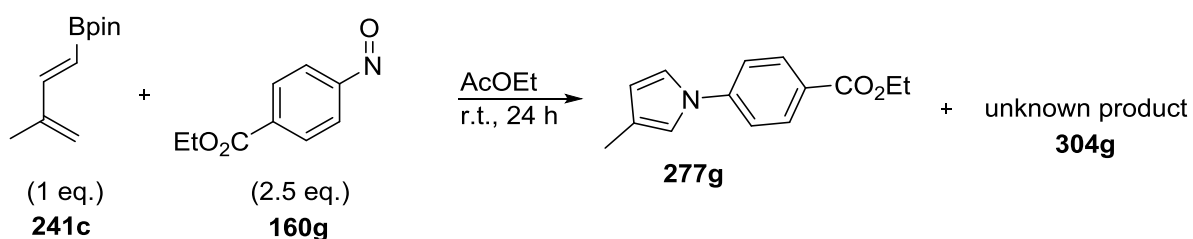
The reaction using the Bpin diene **241c** in presence of arylnitroso **160** was previously performed either in MeOH or in DCM without observing any modifications in the outcome of the reaction. Pyrrole **277** was always observed and isolated in 61 to 82% yield (Entries 2 and 3, Table 3). In the case of the BMIDA diene **249**, if initial experiments were carried out in MeOH, AcOEt was finally preferred because of the improved solubility of the starting diene. In both case, the reaction started with a nitroso Diels-Alder reaction (Scheme 76).



Scheme 76. The nitroso Diels-Alder using diene **241c** and BMIDA **249**.

III.6.a. Nitron synthesis from 1-dienylboronate pinacolate esters

In order to compare the reactivity of the Bpin and BMIDA dienes, we decided to carry out the cycloaddition of **241c** with the aryl nitroso compound **160g** in AcOEt. After 24 h at r.t., analysis of the crude reaction mixture performed by ^1H NMR revealed the presence of an unknown compound **304g** and formation of only a small amount of the expected pyrrole **277g** (**241c/304g/277g** = 47/50/3). No change was observed after 24 h more.



Scheme 77. Reactivity of diene **241c** in AcOEt.

The full consumption of **241c** was achieved by increasing the amount of 4-nitrosobenzoate **160g** (3.2 eq.), the formation of by-products being favoured at higher temperature. Compound **304g** spontaneously precipitated from the reaction mixture and, after addition of hexane, was then isolated in a 54% yield. Its nitron structure was established by crystal X-ray analysis.

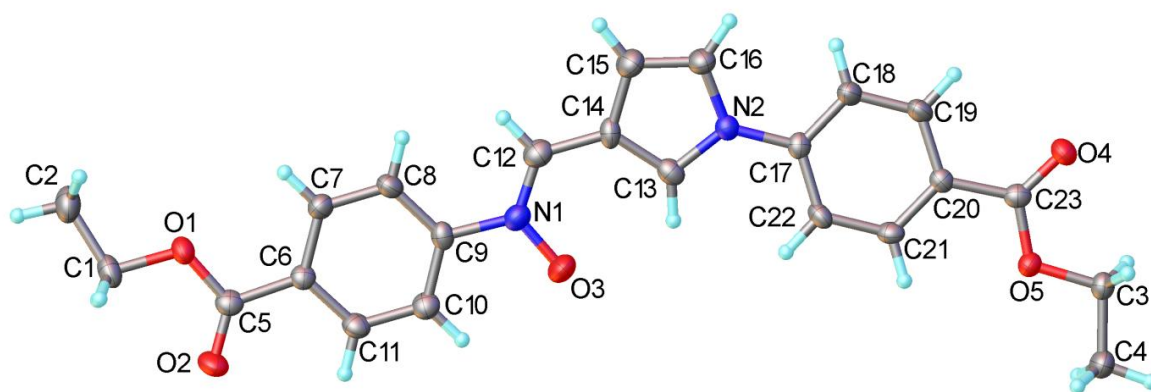


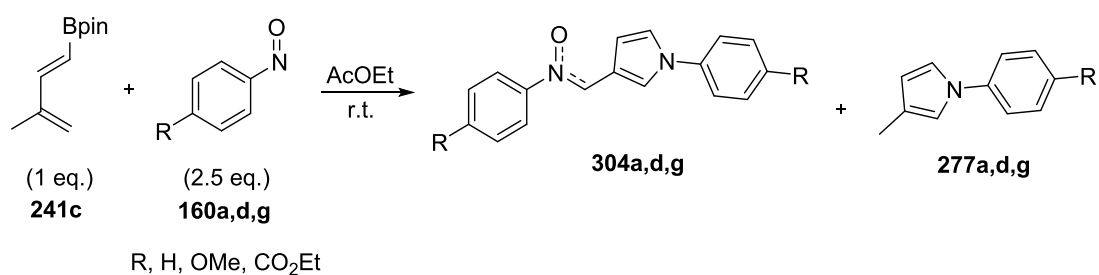
Figure 9. Nitrone crystal structure for **304g**.

Compound **304g** shows the *E*-relationship between the large groups (aromatic ring and the pyrrole substituent). The characteristics of the nitrone functional group are: bond lengths $N_1-C_{12} = 1.301 \text{ \AA}$ and $N_1-O_3 = 1.2991 \text{ \AA}$, and a bond angle $O_3-N_1-C_{12} = 121.81^\circ$ in agreement with other similar nitrones described in the literature.¹⁴⁰ Furthermore, the ^1H NMR data are also in full agreement with this structure ($\delta_{H_{12}} = 8.99 \text{ ppm}$).

With different arylnitroso compounds **160a** and **160d**, formation of the corresponding nitrones was also observed (Table 9). Nitrosobenzene **160a**, and ethyl 4-nitrosobenzoate **160g** formed around the same amount of nitrone (around 50%) after 24 h. The small differences in the conversion of the starting diene was due to the larger amount of pyrrole **277a** obtained as by-products with nitrosobenzene **160a** (17% > 5%, Entries 1 and 3, Table 9). Thus, to observe if the electronic properties of the substitution were responsible for the formation of the pyrrole, a reaction with 4-methoxynitrosobenzene **160d** was performed. A larger amount of pyrrole was observed, and a mixture **304d/277d** (52/48) was obtained after 24 h (Entry 2, Table 9). Thus, the ratio of nitrone **304**/pyrrole **277** was modified by changing the electronic properties of the *para*-substituent. When a more electron rich-nitroso species was used, side-reactions giving pyrroles are more competitive, whereas using an electron-withdrawing group (CO_2Et), **304g** was almost exclusively synthesised (95%). However, with 2.5 eq. of arylnitroso

compounds, the conversion of **241c** ranged only from 53 to 77% after 24 h, and even if the reaction was continued for 24 h, no significant improvement in conversion was observed. In addition to the formation of the pyrrole, standard azoxybenzene by-products **278** were also observed, explaining the moderate conversion. Silica gel chromatography was attempted to purify the nitron species, however due to their high polarity, isolation of pure compounds was not achieved.

Table 9. Electronic arylnitroso effect towards the formation of nitron compounds.



Entry	Nitroso	Diene (%) ^[a]	Nitron (%) ^[a]	Pyrrole (%) ^[a]
1	160a	42	48	10
2	160d	23	40	37
3	160g	47	50	3

^[a] Ratio measured by ¹H NMR analysis on the crude reaction mixture after 24 h with % (Diene + nitron + pyrrole) = 100.

Analysis of the crude reaction mixture was performed using ¹H NMR spectroscopy. Our attention was focused on the identification of suitable peaks for the measurement of the ratio between the diene, the pyrrole and the nitron. For diene **241c** (proton in green), pyrrole **277**

(proton in red) and finally, nitrone **304** (two protons in blue) were used to identify and measure the ratio between the three compounds as shown in Figure 10.

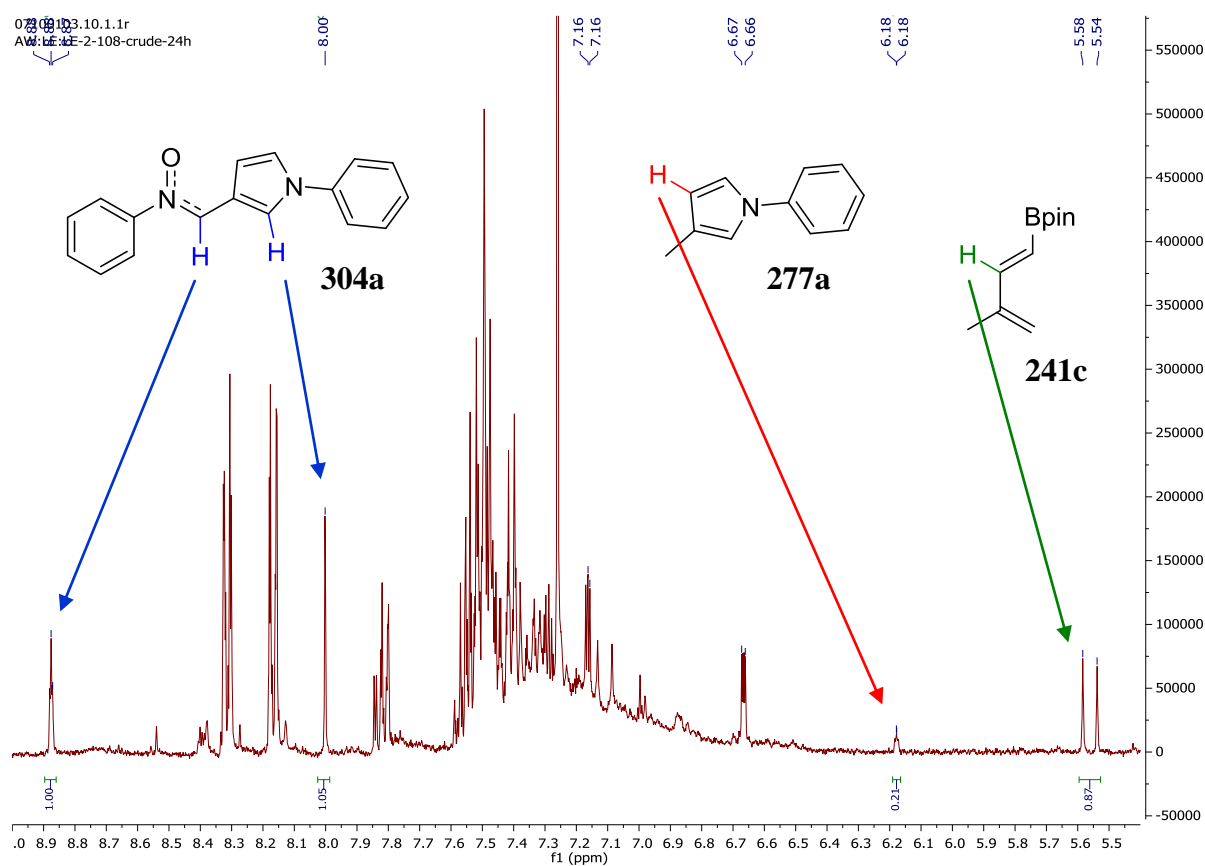


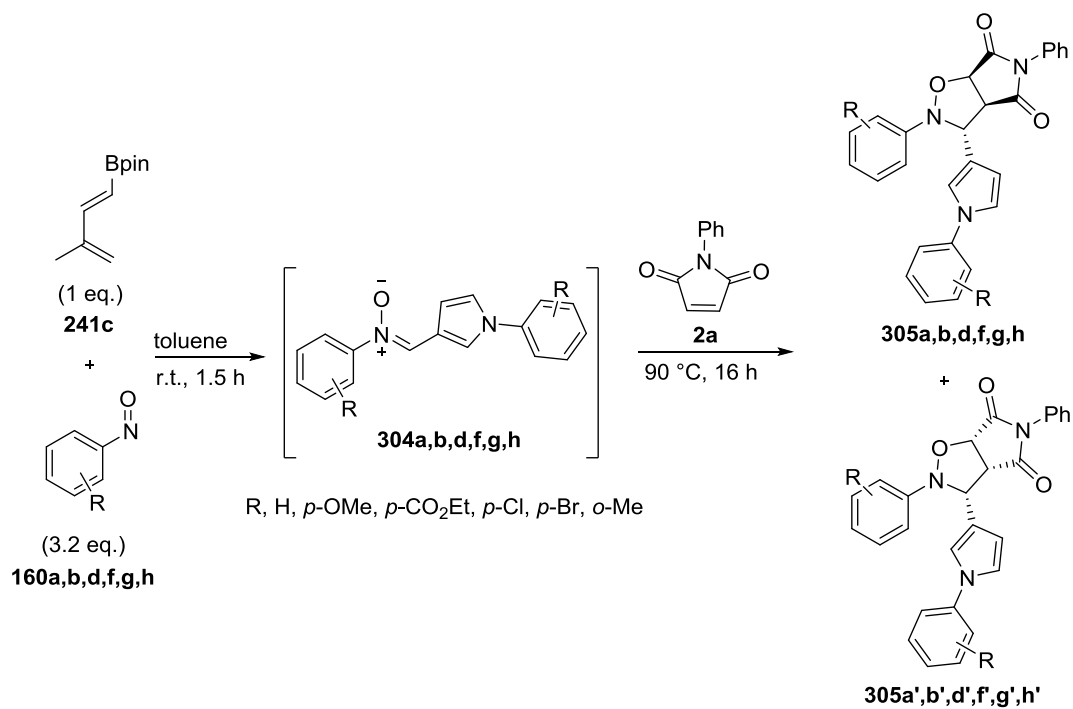
Figure 10. ^1H NMR analysis of the reaction between diene **241c** and nitrosobenzene **160a** after 24 h.

III.6.b. The one-pot procedure nitrone formation/1,3-dipolar cycloaddition

The 1,3-dipolar cycloaddition of nitrones to unsaturated (C-C double or triple bond) compounds is one of the most useful synthetic methods for preparing a variety of heterocycles. It can create as many as three new contiguous stereogenic centres in a single step.¹⁴¹ The interest of the nitrone formation from a boronated diene and a nitroso compound would be significantly increased if this reaction could be coupled with a [3+2]-cycloaddition. Except **304g**, other nitrones **304a** and **304d** were not isolable by precipitation. Therefore, a one-pot process using various dipolarophiles was envisaged.

The scope of the 1,3-dipolar cycloaddition with *N*-phenyl maleimide **2a** was first studied. In order to enlarge the range of the reaction temperature, AcOEt was replaced by toluene, without affecting nitron formation. The crude reaction mixture was checked by ¹H NMR after 1.5 h to ensure full consumption of diene **241c**. The *N*-phenyl maleimide **2a** was then added and the mixture was stirred at 90 °C for 16 h. Nitrosobenzene **160a** and 4-nitrosobenzoate **160g** afforded a mixture of the *endo/exo*-isomers **305/305'** with a ratio around 50/50 (Entries 1 and 2, Table 10). The diastereoisomers were readily separated by silica gel chromatography. When the aryl nitroso was *para*-substituted by a halogen (Cl or Br), the *endo*-isomer **305** was only observed (Entries 3 and 4, Table 10). Nevertheless, the same low yields between 20 and 30% were obtained. In contrast, *para*-methoxy nitrosobenzene **160d** didn't show any formation of the oxazolidine, even if the corresponding nitron was observed by ¹H NMR, before addition of the maleimide (Entry 5, Table 10). Lastly the *ortho*-nitrosotoluene **160f**, showed the formation of an *endo/exo*-ratio **305/305'** of 67/33. However, only the *endo*-isomer was isolated in a very low yield (12%) (Entry 6, Table 10). According to these results, it seemed that the substitution on the aryl moiety of the nitroso had a major impact on the selectivity of the cycloaddition reaction. Further studies are required to rationalise these observations.

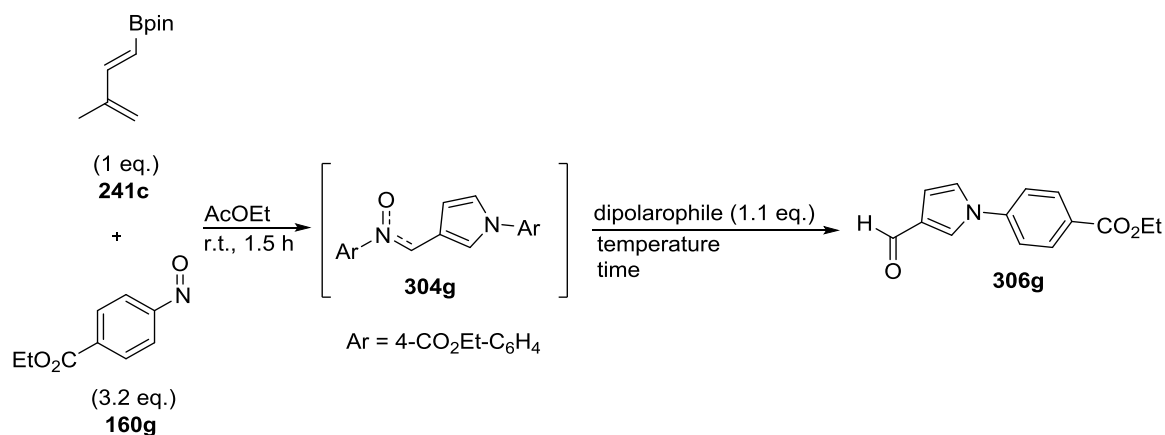
Table 10. Scope of the arylnitroso for the oxazolidine synthesis.



Entry	Nitroso	Isolated yield (%)	<i>endo/exo</i>
1	160a	25%	54/46
2	160g	22%	50/50
3	160b	26%	100/0
4	160h	23%	100/0
5	160d	-	-
6	160f	12%	67/33

Unlike *N*-phenyl maleimide **2a**, diethyl azodicarboxylate **307** (DEAD) and dimethyl acetylenedicarboxylate **308** (DMAD) did not show any formation of the desired product resulting from the [3+2]-cycloaddition, either, at r.t. or under reflux conditions. Only hydrolysis of the nitron intermediate was observed, affording the corresponding aldehyde **306g** in low yield (27 to 43%) (Entries 1-3, Table 11).

Table 11. Screening of the dipolarophile for the [3+2]-cycloaddition.



Entry	Nitroso	Dipolarophile	Temp. (°C)	Time	Isolated yield (%)
1			reflux	18 h	33%
2			r.t.	72 h	43%
3			reflux	22 h	27%

Identification of the endo- and exo-isomers

The *endo*- and the *exo*-isomers **305** and **305'** respectively showed two different ¹H NMR patterns. The protons from the oxazolidine structures were easily identifiable thanks to their chemical shift, but mainly thanks to their different coupling constants. H^A is a doublet of doublets with two close coupling constants of *J* = 8.1 and 8.6 Hz, which was consistent with

the coupling constant measured for the other signals for H^B and H^C of the oxazolidine. When all the protons are on the same face on the structure (*exo*, molecule in red in Figure 11), all coupling constants are in the same range, *i.e.* between 8 and 9 ppm. On the other hand, the second isomer (*endo*, molecule in blue in Figure 11), H^C was on the opposite face from H^A and H^B, leading to a major change in the coupling constants. Indeed, whereas H^A still had a coupling constant $J_{H^A-H^B} = 7.5$ Hz, the second coupling constant was small *i.e.* $J_{H^A-H^C} = 0.9$ Hz.

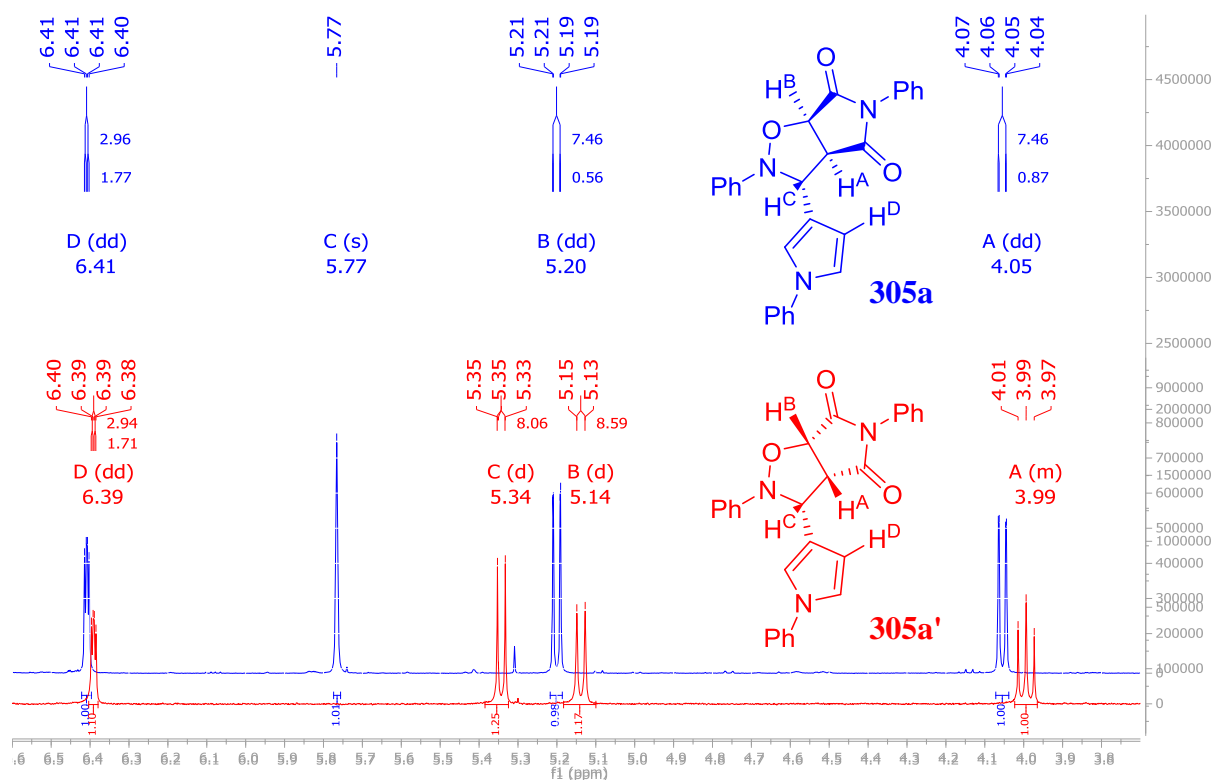


Figure 11. Comparison of the ¹H NMR of the *endo*- and the *exo*-isomer.

The identification of the isomers was confirmed by obtaining crystal structures of **305b** and **305a'** (Figure 12).

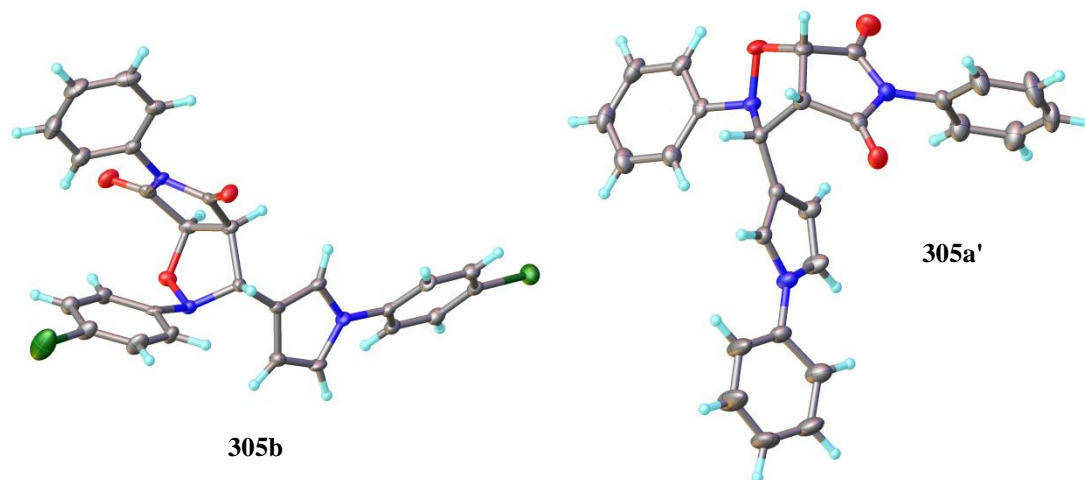
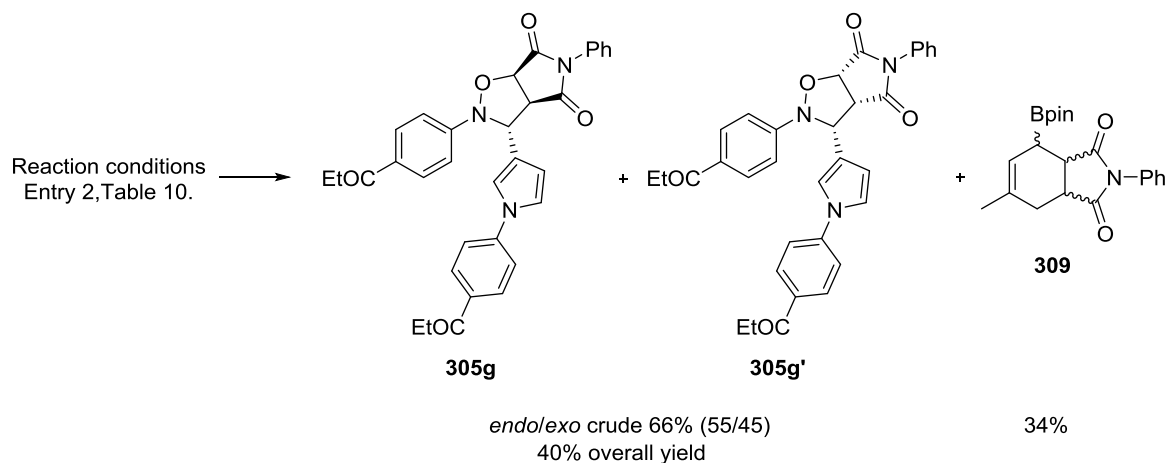


Figure 12. Oxazolidine crystal structures of **305b** and **305a'**.

Preliminary optimisation of the nitron formation/1,3-dipolar cycloaddition

Despite the fact that novel highly functionalised oxazolidine structures were synthesised, the low overall yield remained a handicap for future synthetic applications. Even if the diene **241c** was always consumed entirely during the nitron synthesis, the highest yield observed for the 1,3-dipolar cycloaddition was only 26% yield (Entry 3, Table 10). This can be due to the instability of the nitron under high temperature conditions or to the quality of the diene used for the optimisation of the reaction. Therefore, another batch of freshly prepared diene was subjected to the same reaction conditions. No sample was taken after 1.5 h and the *N*-phenyl maleimide **2a** was directly added. After 16 h at 90 °C, the oxazolidine product were obtained in 66% within a ratio of *endo/exo* (55/45), *i.e.* comparable to the ratio obtained in Entry 2, Table 10. However another compound was observed in the crude ¹H NMR analysis of the reaction mixture, *i.e.* a signal at $\delta = 5.80$ ppm suggested that the unknown product was the result of the Diels-Alder reaction of **2a** with the starting diene **241c** (Scheme 78). This

observation led to reconsideration of the methodology developed for the nitron formation, because this implied an incomplete conversion of the diene. After purification, both isomers were isolated and separated with a combined 40% overall yield.



Scheme 78. One-pot oxazolidine synthesis with new batch of diene **241c**.

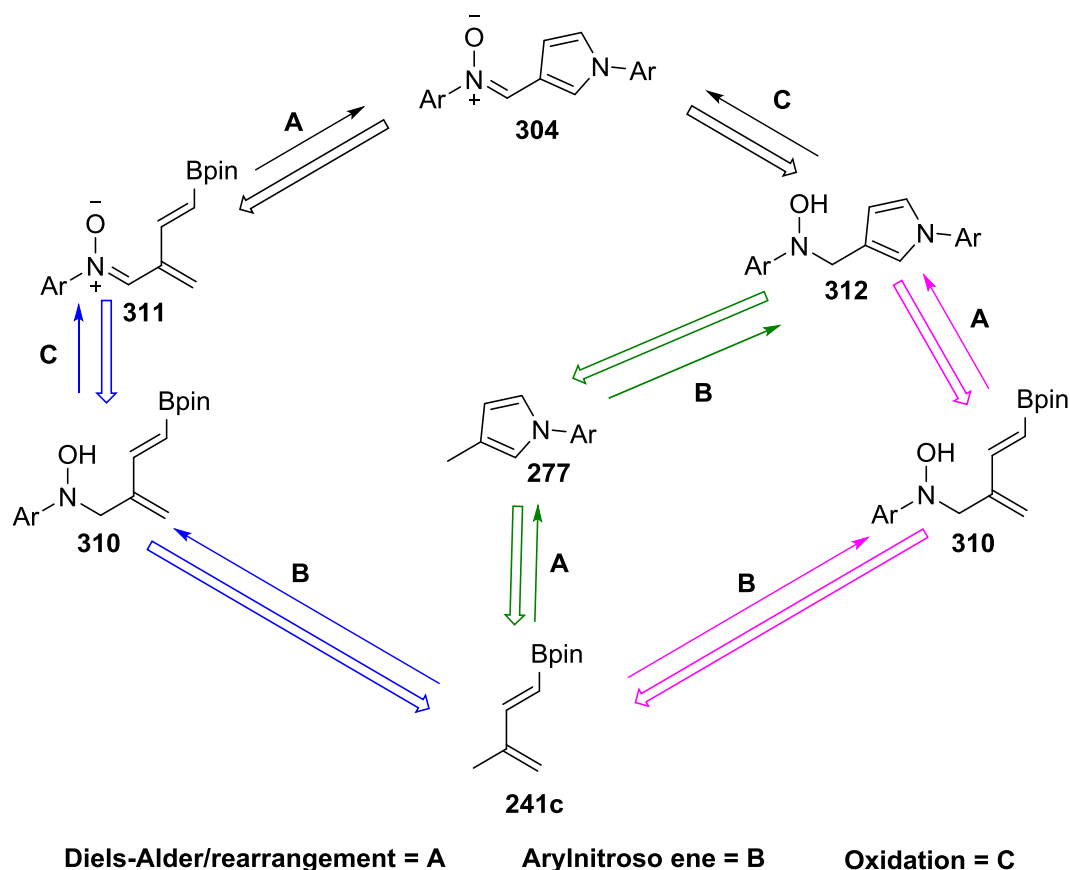
III.6.c. Mechanistic aspects

The nitron formation

The formation of the nitron derivatives using boronated dienes and aryl nitroso compounds obviously raises numerous questions about the reaction mechanism, namely the order of the different steps and the type of mechanism involved in the sequence.

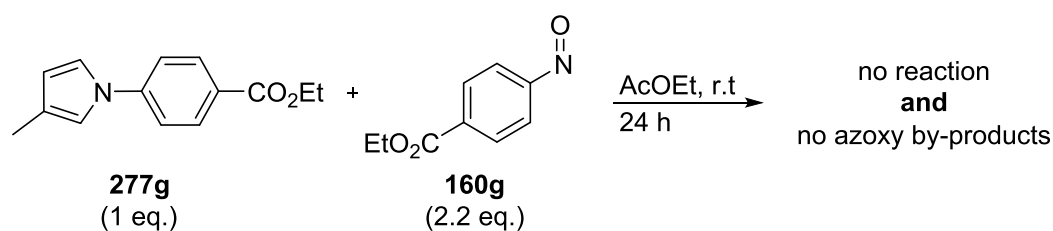
The most common way to synthesise nitron derivatives is by condensation of hydroxylamine with an aldehyde. However, a few examples have been described decades ago, using aryl nitroso derivatives as nitron precursors.¹⁴² The nitron synthesis has not been fully explained, but most of the studies agreed on a nitroso-ene reaction as the first step, followed by an oxidation. An alkenyl aryl nitroxide was detected by ESR spectroscopy,¹⁴³ highlighted the possibility of the nitroso-product as an intermediate. More recently, another work presenting nitron formation using aryl nitroso derivatives as precursors has been published.¹⁴⁴

Three pathways could be envisaged to describe the formation of the nitron, based on three different reactions: a Diels-Alder/rearrangement process; an aryl nitroso-ene reaction; and an oxidation (Scheme 79).



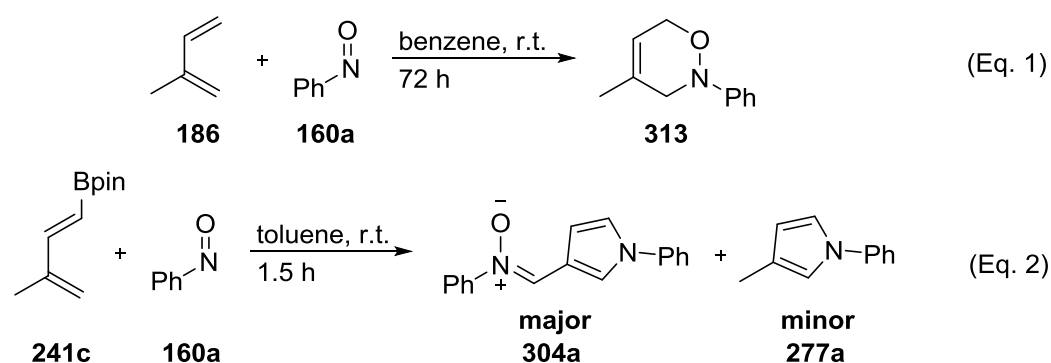
Scheme 79. Pathways envisaged for the nitron formation.

Preliminary studies to ascertain a plausible mechanism started with the pathway shown in green in Scheme 79. If the hypothesis of a first Diels-Alder/rearrangement reaction was in process, reaction of the pyrrole **277g** in the presence of nitroso compound **160g** (2.2 eq.) should provide the nitron in AcOEt at r.t. No reaction occurred after 24 h and no azoxy by-products **278** were observed either (Scheme 80). Thus, the first step of the cascade process is unlikely to be pyrrole formation, and moreover, the absence of by-products, emphasised the influence of the boron moiety on the formation of azoxybenzene and other by-products from the nitroso species, possibly due to Lewis acid activation.



Scheme 80. Reaction of pyrrole **277g** with nitroso **160g**.

Thus, the cascade process had to begin with the formation of the arylnitroso ene adduct **310**. This observation proved that the boron substituent on the 1,3-diene was necessary for the sequence to take place. If the same type of reaction was performed using isoprene **186** in benzene, only the standard [4+2]-cycloaddition occurred to yield the oxazine cycloadduct **313** in 42% (Eq. 1, Scheme 81).¹⁴⁵ In contrast, when the diene **241c** was used, it showed that nitrone **304** was predominantly synthesised (Eq. 2, Scheme 82).

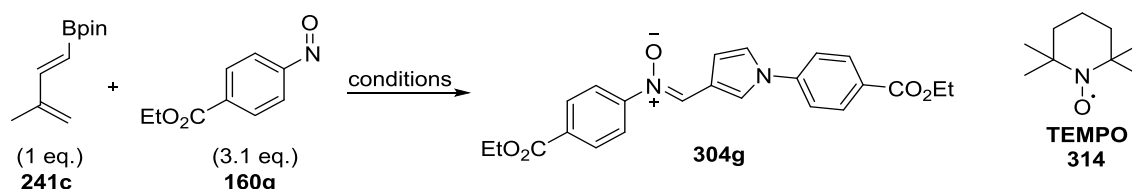


Scheme 81. Comparison of the reaction of nitrosobenzene **160a** with isoprene **186** and diene **241c**.

Another set of reactions was then engaged to improve and determine the most probable oxidation pathway. A standard reaction using normal conditions was performed as a reference, in order to check the conversion after 1.5 h with the one batch of diene used for the later reactions. The conversion obtained after 1.5 h was 77% (Entry 1, Table 12). In order to improve the oxidation step, mild aerobic radical conditions were tried. Thus, a reaction using TEMPO in stoichiometric amounts led to full conversion of the starting diene after 1.5 h

(Entry 2, Table 12), whereas catalytic amounts (0.1 eq.) exerted only a slight improvement of the conversion (85%, Entry 3, Table 12) compared to the reference reaction (77%, Entry 1, Table 12). Hence, full oxidation could be obtained only under those conditions. Further investigations to find a suitable work-up procedure are still in progress. An anaerobic reaction was undertaken to determine whether oxygen was responsible for the partial oxidation, however the nitrone **304g** was also formed in around the same amount (74%), making the aerobic oxidation unlikely.

Table 12. Study of the oxidation step.

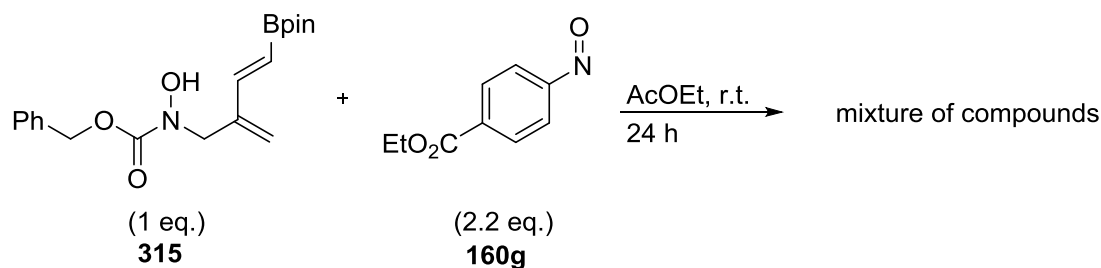


Entry	Reaction conditions	Conversion after 1.5 hours ^[a]
1 ^[b]	AcOEt, r.t.	77%
2 ^[b]	AcOEt, r.t. TEMPO (1 eq.)	100%
3 ^[b]	AcOEt, r.t. TEMPO (0.1 eq.)	85%
4 ^[b]	AcOEt, r.t. inert atmosphere (Ar)	74%

[a] Conversion measured by ¹H NMR. [b] Reaction using the same batch of diene **241c**.

The second possibility envisaged was that one of the aryl nitroso by-products forming during the reaction was responsible for the oxidation step. To support this hypothesis the reaction between **315** and **160g** was undertaken under the nitrone formation conditions (synthesis of **315** will be discussed in the next Chapter). A sample was taken after 1.5 h and analysed by ¹H NMR showing numerous products had been produced, and no final conclusions concerning the formation of the nitrone could be made (Scheme 82). Nevertheless, two signals at $\delta = 8.97$ and 8.95 ppm were observed, which could be consistent with alkenyl protons from the nitrone

moiety. Possible formation of the *trans*- and the *cis*-isomers could explain the two signals. As a comparison, the nitrono alkenyl protons for **304g** showed a $\delta = 8.99$ ppm chemical shift. Furthermore, a large amount of starting material was still remaining in the reaction mixture. If the reaction was continued for 22.5 h, no changes were observed.



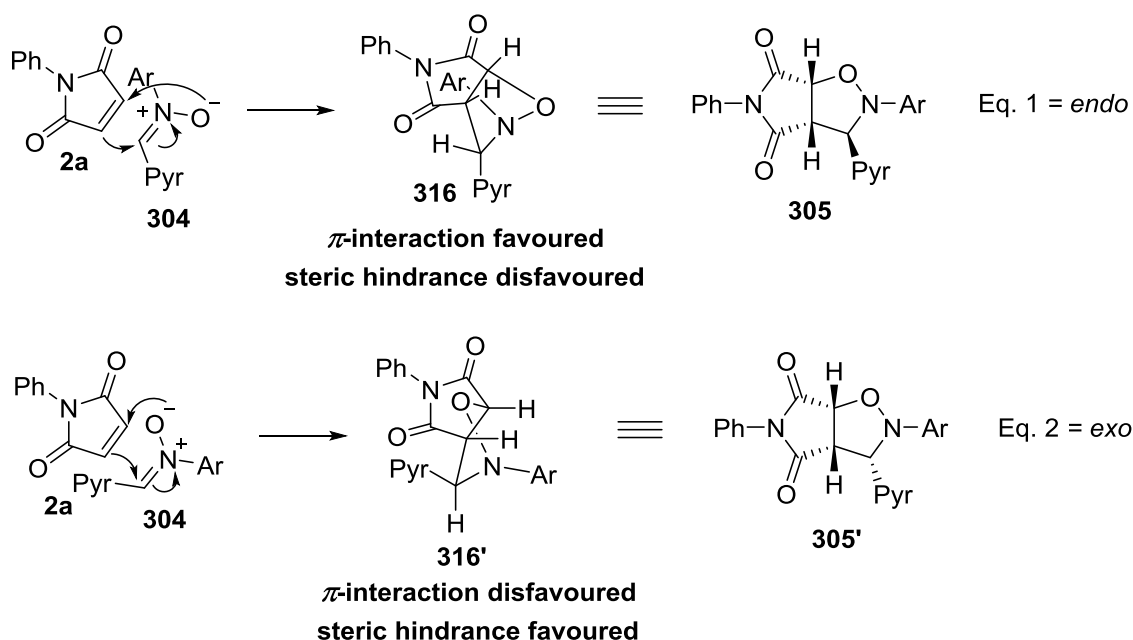
Scheme 82. Oxidation study on the starting material **315**.

The oxidation step seemed to be performed by aryl nitroso by-products, formed during the reaction. AcOEt and toluene had a dramatic influence towards the formation of the nitrono product. However, no reasonable explanation has been found to explain the change in reactivity related to the modification of the solvent. Further reactions need to be performed to ascertain the order of the cascade process.

The 1,3-dipolar-cycloaddition

The 1,3-dipolar cycloaddition has been generally accepted as a concerted asynchronous pericyclic cycloaddition. In the case of nitrono compounds as dipoles, both HOMO-LUMO interactions mode could occur because of the close energy gap in each case. The HOMO (dipole) can pair with the LUMO (dipolarophile), and *vice versa*. The diastereoselectivity of the cycloaddition towards the formation of either the *endo*- or the *exo*-isomer is mainly driven by two factors. The first one is the π -interaction between the aromatic ring of the nitrono

(dipole) and the carbonyl group of the *N*-phenyl maleimide **2a** (dipolarophile), and the second one is the steric hindrance generated by the aromatic ring (Scheme 83). In this case, the diastereoselectivity is dependant on the substituent of the aromatic ring, and the π -interaction seems to be predominant. Indeed, the formation of the *endo*-isomer was always slightly, or exclusively favoured (Table 10). Nevertheless, the difference in diastereoselectivity between each case remained unclear.



Scheme 83. Mechanism and selectivity of the nitron [3+2]-cycloaddition.

III.7 Summary

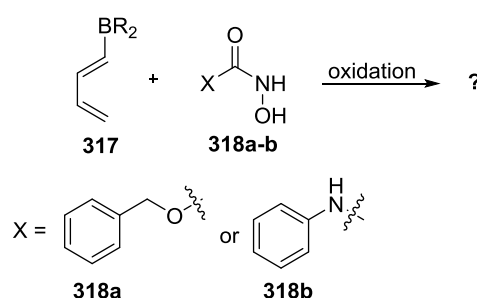
This study revealed that hetero Diels-Alder cycloadditions of aryl nitroso compounds and 1-boronated dienes afford either pyrrole derivatives or oxazine cycloadducts. The most critical parameter to guide these reactions remains the ability of the boron to keep, or not, its sp^3 -hybridization state. The presence of a boronate function α to the oxygen or the nitrogen atom of the oxazine ring is responsible of the ring contraction. Different experimental observations, in addition to theoretical investigations, led to a mechanistic proposal to rationalise these

results. First, the nitroso Diels-Alder reaction took place in a regioselective asynchronous concerted manner. Then, formation of the pyrrole derivative can be explained by a boryl rearrangement, followed by an intramolecular aza-boryl to aldehyde addition and borate elimination. In the case of 2-MIDA boronodienes, the formation of the corresponding [4+2]-cycloadduct is also highly regioselective. No decomposition of the oxazine ring was observed during a Suzuki-Miyaura coupling. A 2,4,5-triaryl-3,6-dihydro-1,2-oxazine was isolated in good yield, thus showing why this approach to prepare these class of heterocycles with complete control of the position of the different substituents could be valuable.

Following these observations, an unexpected and interesting nitrene formation was demonstrated, just by modifying the solvent of the reaction between 1,3-dienylboronate **241c** and arylnitroso derivatives **160**. Taking advantage of this reactivity, a one-pot procedure starting with nitrene formation followed by a "normal" electron demand Diels-Alder reaction was developed to afford functionalised oxazolidines in modest yields. Unfortunately, the scope of the Diels-Alder reaction remained limited to *N*-phenyl maleimide as dipolarophile. The exact mechanism of this process remained unclear and further investigations are necessary both to rationalise these experimental results and to improve the overall yields of this sequence.

IV. Boronated dienes and carbonylnitroso compounds

Following the previous study and as part of the research programme developed by our group on the chemistry of carbonylnitroso compounds,^{90a} we next turned our attention to the reactivity of two compounds (**318a** and **318b**) toward dienylboron substrates (Scheme 84).



Scheme 84. Reactions of boronated dienes with carbonylnitroso compounds.

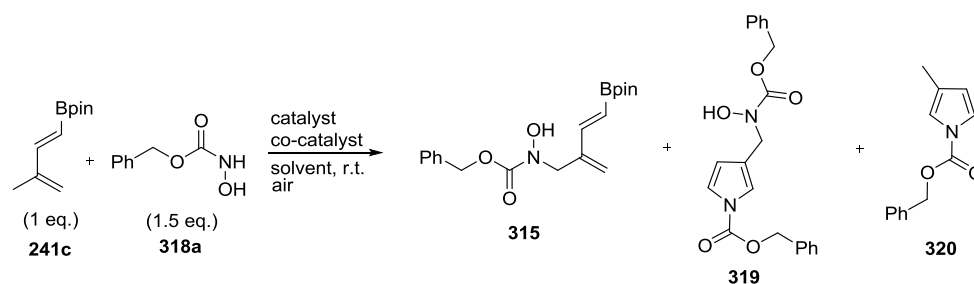
IV.1. Reaction of 1-dienylboronate pinacolate esters with carbonylnitroso compounds

Due to their high instability, the carbonylnitroso species need to be prepared *in situ*. The most common way to generate these carbonylnitroso species is to oxidise the corresponding *N*-hydroxycarbamate **318a** or hydroxyurea **318b**, respectively. The study started by determining a suitable oxidation system which could be used in the presence of the different boronated dienes. Diene **241c** was used as the model substrate because the Bpin variant is presumed to be the most sensitive boron moiety towards oxidation, compared to a BMIDA substituent for example.

The most common oxidation procedure involves periodate as the oxidant.⁸² As expected, these strong oxidation conditions led to the formation of numerous compounds, and more

importantly to the degradation of the boron part of the starting diene. Photoredox conditions, developed by Tan and co-workers,^{92a} using Rose Bengal dye as catalyst, showed formation of a unique compound bearing a new diene unit. No pyrrole formation, from the previously described Diels-Alder-rearrangement process, was observed. However, only a 25% conversion of the starting nitroso precursor **318a** was observed and no improvement was observed if the reaction time was extended or by using a larger amount of Rose Bengal. A major drawback of this method was that an excess of the diene **241c** (3 eq.) was used.

Thus, attention was then focused on aerobic copper-catalysed oxidation. Two different, recently developed systems were tried. The first one used CuCl_2 ^{90a} and the second one CuCl ,^{90b} both conditions being tested with pyridine as co-catalyst. Copper(I) exerted a faster reaction compared to the copper(II) derivative. Indeed, after 16 h at r.t., the reaction using CuCl as a catalyst showed a 71% conversion of the starting diene **215c**, whereas by using CuCl_2 , only a 11% conversion was observed. Three products were observed in the crude reaction mixture (Scheme 85).



Scheme 85. Study of the reaction between diene **241c** and carbonylnitroso precursor **318a**.

The compounds were identified as:

- The ene adduct **315** as the major product which was isolated and fully characterised;

- The pyrrole **319**, resulting from the Diels-Alder/rearrangement process of the ene adduct **315** previously formed. Isolation of pyrrole **319** was not done and the proposed structure was based on the NMR analysis;
- The pyrrole **320** resulting from the the Diels-Alder/rearrangement process of the starting diene **241c**. It was identified by ¹H NMR spectroscopy and comparison with literature data.¹⁴⁶

A screening of the reaction conditions was undertaken in order to optimise the formation of the ene-product. Non-polar or halogenated solvents (toluene, DCM) led to a decrease in reactivity. In both cases, conversion after 16 h was around 10% (Entries 3 and 4, Table 13). The ene-compound was the major compound (> 80%) after 184 h. Polar solvents increased reactivity (THF, MeCN and acetone) with a conversion between 56 and 70% after 16 h (Entries 1, 2 and 5). If acetone was used, the selectivity towards the formation of **315** decreased drastically. If the reaction was not stopped before 30 h, either decomposition or formation of by-products was observed using TLC. A protic solvent (MeOH) favoured formation of numerous by-products, thus, the ratio between **315/319/320** was impossible to determine (Entry 6, Table 13). The use of pyridine as co-catalyst gave cleaner reactions and better yields, while using 2-ethyloxazoline was detrimental (Entry 7). If the reaction is faster with CuCl, better selectivity towards formation of the ene-compound **315** was observed with CuCl₂, compared to the CuCl version (96% > 82%, Entries 1 and 8). Modifying the catalyst loading allowed the optimisation of the selectivity towards the ene-adduct **315**. By decreasing the catalyst loading from 20 to 10 or 5%, a slight improvement in the selectivity was measured (82 to 90 to 94%, Entries 10 and 11). When CuCl (0.05 eq.) was used, the reaction was slower (Entry 11). Conversion after 16 h was decreased by 14% compared to the reaction with 10 and 20%. It is also important to mention that the reaction needed to be carried out between 10 and 20 °C. If the temperature exceeded 25 °C, the ene-compound was never

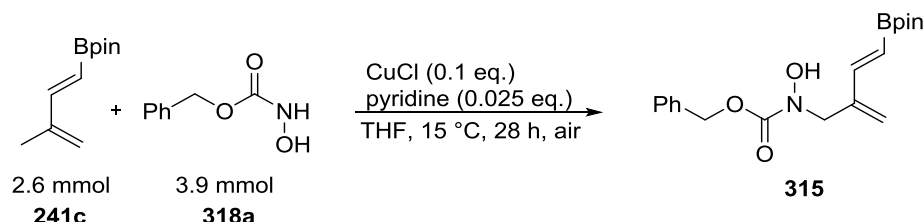
isolated as a white solid and in fact, degradation occurred, ^{11}B NMR analysis showed numerous species.

Tableau 13. Optimisation of the nitroso-ene reaction.

Entry	Solvent	Catalyst	Co-catalyst	Conversion of diene 241c after 16 h ^[d]	Time (h)	Ratio 315/319/320	Yield ene (%)
1 ^[a]	THF	CuCl	Pyridine	71	28	82/12/6	62
2 ^[a]	MeCN	CuCl	Pyridine	70	28	89/3/8	46
3 ^[a]	DCM	CuCl	Pyridine	12	184	83/3/14	55
4 ^[a]	toluene	CuCl	Pyridine	6	184	88/3/9	53
5 ^[a]	acetone	CuCl	Pyridine	56	28	58/27/15	39
6 ^[a]	MeOH	CuCl	Pyridine	63	28	Not determined	31
7 ^[a]	THF	CuCl	2-ethyl oxazoline	41	28	Not determined	13
8 ^[a]	THF	CuCl ₂	Pyridine	11	184	96/0/4	52
9 ^[a]	THF	CuCl/CuCl ₂	Pyridine	Not determined	40	84/10/6	43
10 ^[b]	THF	CuCl	Pyridine	69	28	90/5/5	59
11 ^[c]	THF	CuCl	Pyridine	56	34	94/2/4	60

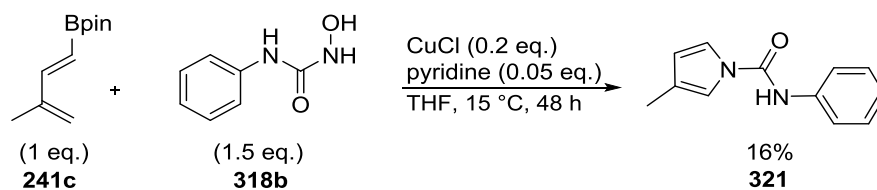
[a] Reaction performed with 0.4 mmol of starting diene, 20 mol% of catalyst and 5 mol% of co-catalyst. [b] Reaction performed with 0.4 mmol of starting diene, 10 mol% of catalyst and 2.5 mol% of co-catalyst. [c] Reaction performed with 0.4 mmol of starting diene, 5 mol% of catalyst and 1.25 mol% of co-catalyst. [d] Conversion measured by ¹H NMR.

Finally, using the best conditions [CuCl (0.1 eq.), pyridine (0.025 eq.) in THF at 15 °C in presence of air], the reaction was scaled up (Scheme 86). The average yield over three runs on a 2.6 mmol scale was 51% with a range of 3%; a small decrease being observed compared to Entry 10 in Table 13.



Scheme 86. Medium scale ene reaction.

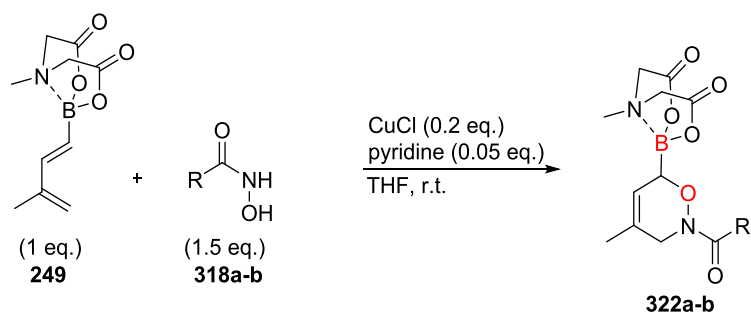
To check whether the synthesis of the ene-compound was substrate dependent, the second nitroso precursor **318b** was used under the aerobic reaction conditions. The reaction was performed with CuCl (0.2 eq.) and pyridine (0.05 eq.), because the first attempt using same optimised conditions as described in Entry 10, Table 13, did not show useful results. By modifying the heteroatom in the α -position of the carbonyl group (O replaced by NH), a total change in reactivity was observed. No ene-adduct was observed in the crude reaction mixture and only pyrrole **321** was identified. After purification by silica gel chromatography, **321** was isolated in a low 16% yield (Scheme 87).



Scheme 87. Synthesis of pyrrole **321** using nitroso precursor **318b**.

IV.2. Reaction of tetracoordinated 1-borodienes with carbonylnitroso compounds

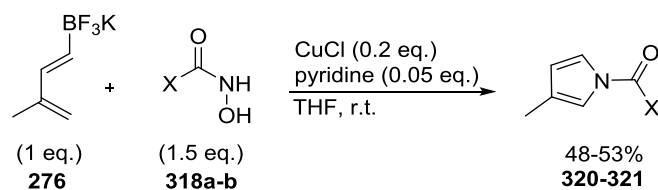
A major impact of boron substituents was previously demonstrated in the case of nitroso Diels-Alder reactions of 1-boronodienes with aryl nitroso compounds. Changing the boron hybridisation from sp^2 to sp^3 enabled the isolation of stable oxazines. A similar behaviour was observed with carbonylnitroso precursors **318a-b** and the BMIDA diene **249**. The nitroso Diels-Alder reaction occurred selectively to provide only the 1,2 related boron-oxygen regioisomer (in red in Table 14), as for aryl nitroso compounds, to provide the oxazines **322a** and **322b** in moderate to good yields 58 and 72%, respectively. The reactions being performed in THF, the BMIDA diene **249** was not fully soluble, that can explain the long reaction times (7 and 9 days). Stronger oxidation conditions (tetrabutylammonium periodate) decreased significantly the reaction time from 9 days to 2 hours when **318a** was used, but also the final isolated yield 37% (Table 14).

Table 14. Regioselective formation of stable oxazines from carbonylnitroso Diels-Alder reactions.

Entry	Nitroso precursor	Product	Time	Isolated Yield (%)
1			9 days ^[a]	72
2	318a	322a	2 hours ^[b]	37
3			7 days ^[a]	58
	318b	322b		

[a] Reaction using the copper aerobic system CuCl (0.2 eq.), pyridine (0.05 eq.) in THF at r.t. [b] Reaction using Bu₄NIO₄ (1.2 eq.) in DCM at -5 °C.

As previously observed, in comparison with the Bpin derivative, the BF₃K diene **276** exerted faster nitroso Diels-Alder reactivity. Pyrroles **320** and **321** were isolated in moderate yields (48 and 53% respectively, Table 15). No competitive ene-adduct was formed.

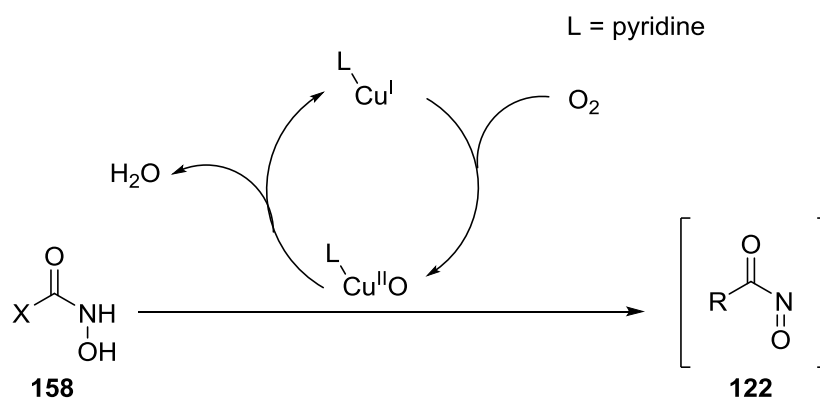
Table 15. Reactivity of trifluoroborylated diene **276** and carbonylnitroso.

Entry	Nitroso precursor	Product	Time (h)	Isolated Yield (%)
1			22	48
2			20	53

IV.3. Mechanistic aspects

IV.3.a. The aerobic copper oxidation step

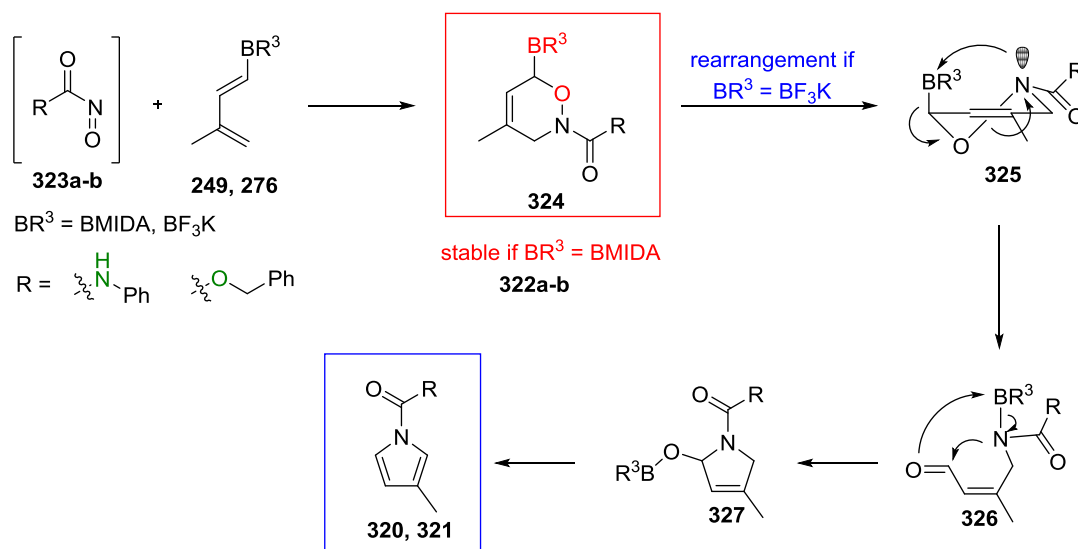
The mechanism of aerobic oxidation of the nitroso precursor is proposed to be based on a $\text{Cu}^{\text{I}}/\text{Cu}^{\text{II}}\text{O}$ catalytic cycle (Scheme 88).¹⁴⁷ Different oxidation pathways can be envisaged related to the Cu/O_2 stoichiometry leading to numerous catalytic species.¹⁴⁸ In most of these reactions, aromatic nitrogens are often used as electron-donating ligands. The nature of the ligand (monodentate or polydentate), as well as the number of ligand attached to the copper center, have been shown to be responsible for the geometry adopted by the Cu-complex.¹⁴⁸ In the system used for the nitroso-ene reaction, pyridine was used as a monodentate ligand. Most of the studies on the topic have proposed the cupric superoxo species ($\text{Cu}^{\text{II}}-\text{O}-\text{O}^{\bullet -}$) as the initiator of the oxydation by hydrogen abstraction.¹⁴⁹ Copper(I) chloride has proved to give the best results, leading to a fast catalytic cycle, which is in accordance with kinetic results obtained by Deng *et al.*¹⁵⁰



Scheme 88. Simplified aerobic oxidation mechanism of the nitroso precursor.

IV.3.b. The Diels-Alder/ring contraction sequence

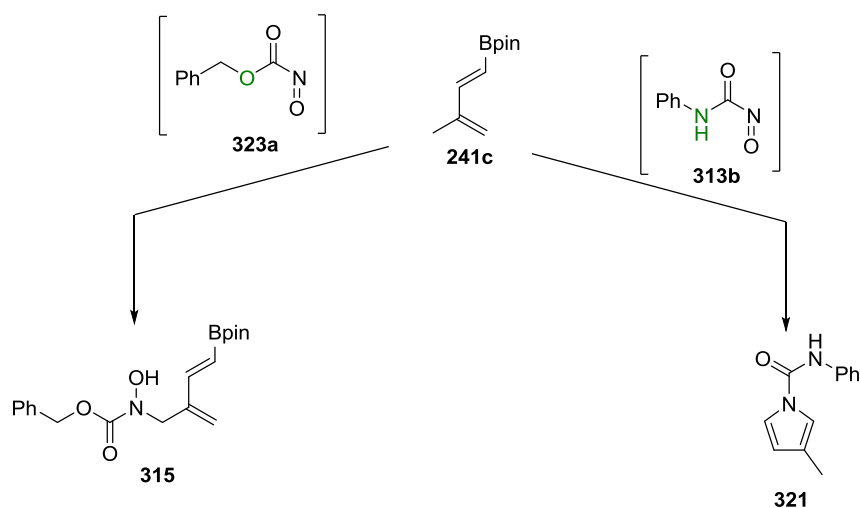
In the presence of the BMIDA dienes **249** and BF_3K **276**, the reactivity of the carbonylnitroso compounds was similar to the aryl nitroso derivatives. Firstly, a regioselective Diels-Alder reaction took place to form the 1,2-related boron-oxygen regioisomer oxazine cycloadduct (in red in Scheme 89). In the case of the diene boronated MIDA ester **249**, the oxazine was stable and could be isolated after chromatography. For the trifluoroboronated salt **276**, the rearrangement (already described in the Chapter 2) slowly provided the pyrroles **320** and **321**. Only a slight difference in rate was measured, especially with diene **249**, nitroso **323b** reacting faster (7 days) than nitroso **323a** (9 days).



Scheme 89. Proposed mechanism for the formation of the oxazine and pyrrole.

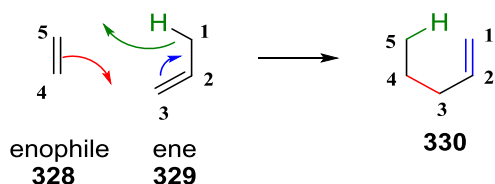
IV.3.c. The ene reaction: Impact of the boron substituents

The results obtained with diene **241c** showed two different reactivities based on the nature of the heteroatom in the α -position of the nitrosocarbonyl group. When the carbonylnitroso was an urea-type (as in compound **323b**), only formation of the pyrrole was observed, presumably *via* the same mechanism as presented in Scheme 89 with diene **276**. On the other hand, the carbonylnitroso bearing an oxygen atom instead of nitrogen, provided predominantly the ene-compound **315**, with only traces of Diels-Alder adduct (Scheme 90). To our knowledge, only transition-metal-catalysed Alder-ene reactions involving boronic esters have hitherto been reported to date.¹⁵¹



Scheme 90. Pyrrole **321** versus ene **315** formation.

The ene reaction is a pericyclic reaction involving an alkene bearing an allylic hydrogen (the ene-partner, *e.g.* **329**) and a molecule containing an electron-deficient multiple bond (the enophile, *e.g.* partner **328**). During the process, a new σ -bond between C₃ and C₄ (in red in Scheme 91), an ene π -bond migration from C₃-C₂ to C₂-C₁ (in blue in Scheme 91) and a hydrogen shift from C₁ to C₅ (in green in Scheme 91) can occur, affording acyclic compound **330**.



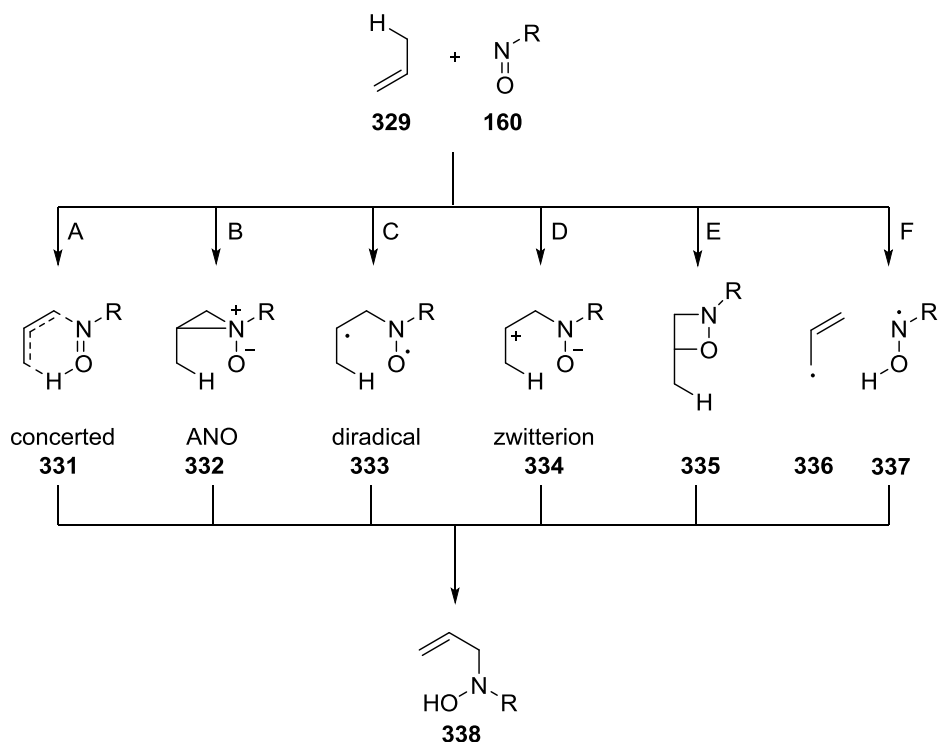
Scheme 91. The ene reaction.

Whereas, the ene-reaction has been described as a concerted, but potentially asynchronous reaction, the exact mechanism of the nitroso-ene still remains unclear. Indeed, the reactivity is directly dependant upon the electronic properties of the reactive partners, and specifically the HOMO-LUMO gap, which is very small for nitroso compounds. The discovery of the nitroso-ene reaction was first reported in 1910 by Alesandri,¹⁵² the first real study was accomplished later by Knight and co-workers.¹⁴² Six different mechanisms have been postulated to

rationalise the course of this reaction (Scheme 92). The first one involves a concerted synchronous or asynchronous pericyclic transition state **331**. This transition state is allowed by the Woodward-Hoffmann selection rules as a $[\pi 2s + \pi 2s + \sigma 2s]$ process (path A).¹⁵³ Other possible pathways involve aziridine *N*-oxides (ANO) **332** (path B)¹⁵⁴ and diradicals **333** (path C).¹⁵⁵ Pathways involving zwitterion **334** (path D) and (pathway E and F) have also been postulated. The last two mechanisms involve a highly strained oxazetidine **335** or two radical species **336** and **337**,¹⁵⁶ which appears the most unlikely.

The first computational work was carried out using PM3 by Davies and Schiesser on propene and nitrosyl hydride.^{154a} They presented two major possible intermediates, and according to the results of the concerted pathway A, it appears that the carbon-nitrogen bond can be almost fully formed before the allylic hydrogen transfer. This observation is consistent with a highly asynchronous mechanism. Nevertheless, they also found that the ANO intermediate **332** described in pathway B provided a lower energy barrier of 8 kcal mol⁻¹ compared to the concerted pathway. Later, another study using the B3LYP/6-31g* basis set for their DFT calculations on the nitroso ene mechanism, supported the assumption that the reaction can go through an aziridine *N*-oxide intermediate as the rate determining step.^{154b,c} Houk and co-workers presented another pathway based on a polarised diradical intermediate **333** (pathway C) using B3LYP/6-31g* DFT calculations.¹⁵⁵ Formation of this polarised diradical intermediate was characterised by high energy rotation barriers of carbon-nitrogen and carbon-carbon bonds (4-5 kcal.mol⁻¹) resulting from an attack of nitrosyl hydride on a propene molecule. The diradical formed during the rate determining step, can then abstract an allylic hydrogen to either form the ene-compound or equilibrate to the aziridine *N*-oxide **332**.

Studies on the regioselectivity of the nitroso ene reaction have also been performed, but in the case of the monosubstituted substrate (olefin bearing the methyl group on **241c** in this study), only the hydrogen from the methyl group can be transferred.¹⁵⁷



Scheme 92. Possible mechanism for the nitroso ene reaction.

With the trifluoroborate **276** the nitroso Diels-Alder/rearrangement process occurred in moderate yields to afford pyrroles regardless the nature of the carbonylnitroso species. By contrast, with a more electron-deficient diene (pinacol ester **241c**), the course of the reaction was governed by the nature of the heteroatom in α -position of the nitrosocarbonyl group. By modifying the HOMO-LUMO gap, the rate of Diels-Alder reaction decreased drastically, and, as a result, with **318b**, only pyrrole **321** was isolated. If the substituent on the nitroso compound has higher electron-withdrawing character, only traces of Diels-Alder cycloadduct was detected, and ene adduct **315** was predominantly isolated.

V. The ene-adduct as key intermediate in cascade reactions

The ene-compound **315** is a polyfunctional molecule with multiple sites for further modifications and therefore can be envisaged as a valuable intermediate for the synthesis of different scaffolds, especially in the field of bioactive compounds. This work focused on:

- the diene (in blue on Figure 13)
- the OH of the hydroxycarbamate (in red on Figure 13)
- the boron unit (in green on Figure 13)

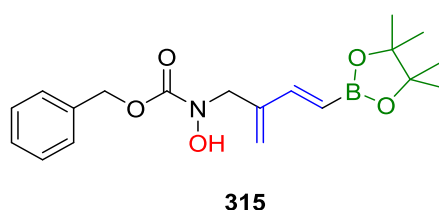


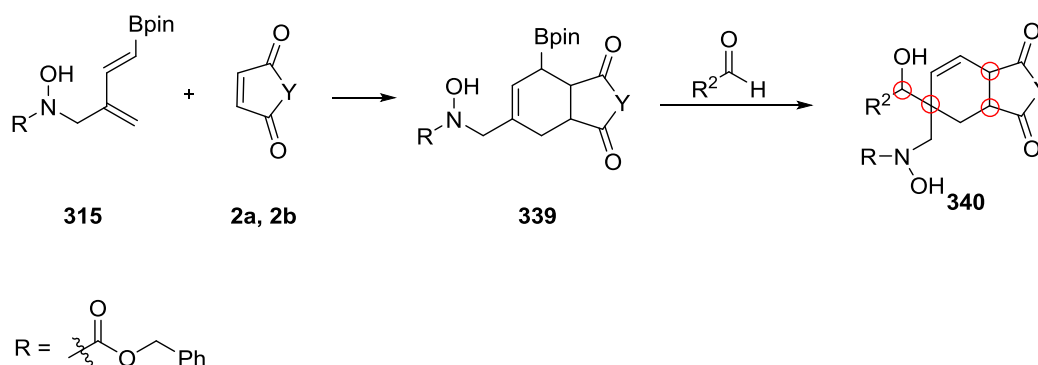
Figure 13. Ene-compound **315**.

V.1. The Diels-Alder/allylboration sequence

The tandem Diels-Alder/allylboration process has been developed to afford numerous scaffolds.¹⁵⁸ It gives access to molecules with a high degree of complexity in a minimum number of steps. Most of the time, the outcome (stereoselectivity and regioselectivity) of the Diels-Alder cycloaddition is directly related to the electronic properties and the steric influences of both the diene and dienophile. In the case of "normal" electron-demand Diels-Alder reactions, electron-poor dienophiles usually react through an *endo* transition state. In the case of organoboron compounds, this reaction has been successfully coupled with an

allylboration, which is also widely used in organic synthesis because of the high stereocontrol.¹⁵⁹

In the case of the diene **315**, such a sequence could provide bicyclic compounds **340**, with control of up to four stereocentres, one of them being quaternary (Scheme 93).



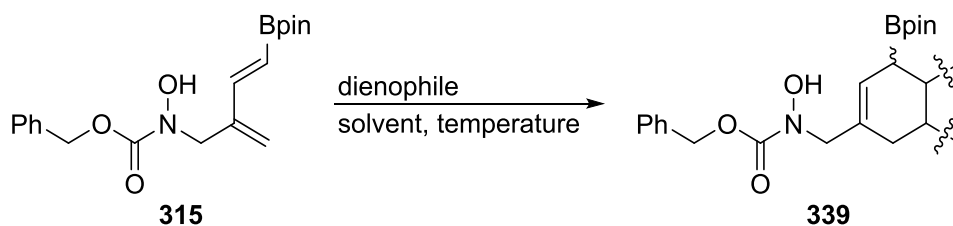
Scheme 93. The Diels-Alder/allylboration sequence on the compound **315**.

V.1.a. The Diels-Alder step

Before envisaging a one-pot procedure, screening of different dienophiles was performed on the ene-adduct **315** to determine its reactivity. In the case of the *N*-phenyl maleimide **2a**, reaction was complete after 24 h in DCM to afford the compound **339a** in 84% isolated yield after silica gel chromatography (Entry 1, Table 16). When maleic anhydride **2b** was used, the reactivity decreased, giving 77% conversion after 44 h in DCM at r.t. and 62 h were necessary to obtain full conversion of the starting compound **315**. Unfortunately, compound **339b** was never isolated due to stability issues. Standard silica gel, deactivated silica gel with Et₃N (2%) and florisil chromatographies or precipitation using different solvent mixtures in different ratios were all unsuccessful (Entry 2, Table 16). Concerning methyl acrylate **12** and *p*-benzoquinone **341**, no reaction was observed at r.t. in DCM after 44 h. The solvent was then changed for a higher boiling point solvent, and reactions took place in toluene when heated at

90 °C. In the case of *p*-benzoquinone **341** and methyl acrylate **12**, no starting material **315** was recovered, but no characteristic peaks of cycloadduct were observed either (Entries 4 and 5, Table 16). Lastly, the dienophile 4-phenyl-1,2,4-triazole-3,5-dione **23** was tested. ¹H NMR of the crude reaction mixture showed full consumption of the starting ene **315** in 24 h, but ¹¹B NMR showed formation of another boron species, instead of the Bpin moiety alone. A peak for boroxine ($\delta = 22$ ppm) was observed (Entry 3, Table 16).

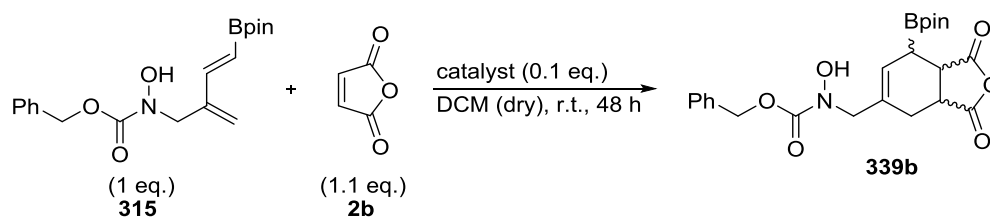
Reactivity of **315** is therefore highly dienophile dependent. For the reaction to take place, a highly electron-deficient dienophile such as maleic anhydride or related structures is required. This preliminary study highlighted the question of stability of the diene **315**, as well as cycloadduct **339**, under high temperature conditions.

Table 16. Diels-Alder reaction of the compound **315**.

Entry	Dienophile	Solvent	Temp (°C)/ Time	Consumption of diene/ Formation of DA adduct	Isolated yield
1		DCM	r.t./24 h	100/yes	339a 84%
2		DCM	r.t./62 h	100/yes	339b /
3		DCM	r.t./24 h	100/yes	339c /
4		DCM	r.t./24 h	0	/
		toluene	90/24 h	100/no	/
5		DCM	r.t./24 h	0	/
		toluene	90/24 h	100/no	/

It has already been reported that Lewis acids can catalyse Diels-Alder reactions.^{32,43,44,56,57}

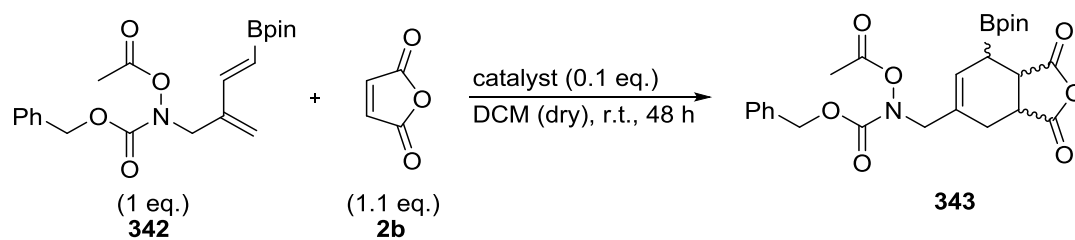
Except for *N*-phenyl maleimide **2a**, all the other dienophiles tested in Table 16 exerted low or no reactivity at all. To counter this problem, various catalysts were tried with no significant improvement. The conversion after 48 h, measured by ¹H NMR, ranged from 68 to 85% (Table 17).

Table 17. Diels-Alder reaction using Lewis acid catalysts.

Entry	Catalyst	Conversion of compound 315 after 48 h (%) ^[a]
1	-	75
2	Yb(OTf) ₃	75
3	Sc(OTf) ₃	78
4	Fe(OTf) ₃	77
5	La(OTf) ₃	68
6	Me ₂ AlCl	85

[a] Conversion measured by ¹H NMR on the crude reaction mixture.

A possible explanation of the inactivity of catalysts, could be the presence of the free alcohol of the hydroxycarbamate on the compound **315**, which might coordinate to the Lewis acid. Hence, a *O*-acetyl protected version **342**, of the ene compound **315**, was synthesised following the reaction conditions described in Table 23. No catalytic effect was observed and only around 50% conversion was only observed after 48 h at r.t. proving that **342** is even less reactive than **315**.

Table 18. Diels-Alder reaction using Lewis acid catalysts on *O*-acetyl compound **342**.

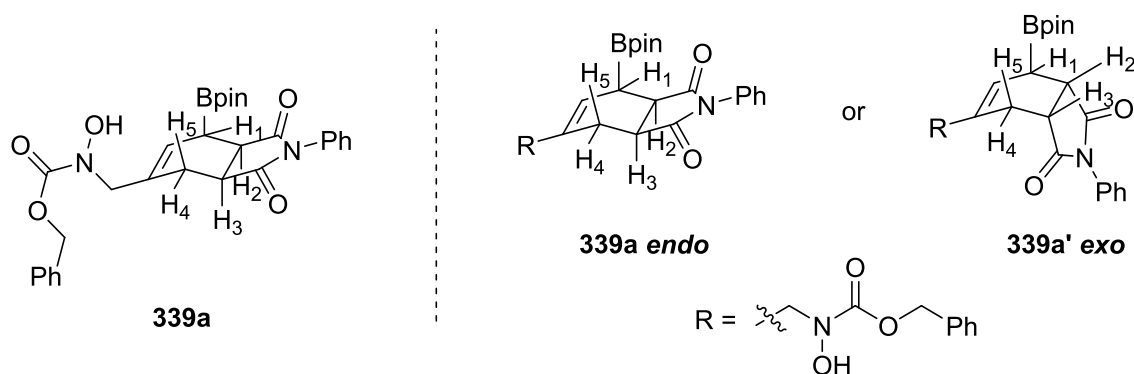
Entry	Catalyst	Conversion of 324 after 48 h (%) ^[a]
1	-	48
2	Yb(OTf) ₃	52
3	Sc(OTf) ₃	50

[a] Conversion measured by ¹H NMR on the crude reaction mixture.

Concerning the stereochemical outcome of this cycloaddition, different attempts at crystallisation were tried on compound **339a** without success. Its structure was determined by analysis of the coupling constants in correlation with calculated values obtained by conformational searches using Spartan '10 (see Experimental section).[‡] Calculated values did not permit assurance of the structure of the cycloadduct. None of the isomers showed all of the coupling constant values within a reasonable margin of error. Nevertheless, comparisons of the coupling constants $J_{\text{H1-H2}}$ (Hz) and $J_{\text{H3-H4}}$ (Hz) led us to the *endo*-structure. In the case of the *endo*-isomer, calculated coupling constants were, $J_{\text{H1-H2}} = 5.4$ Hz and $J_{\text{H3-H4}} = 5.1$ Hz and for the *exo*-isomer $J_{\text{H1-H2}} = 2.2$ Hz and $J_{\text{H3-H4}} = 1.7$ Hz. The comparison with the measured constants ($J_{\text{H1-H2}} = 5.8$ Hz and $J_{\text{H3-H4}} = 4.1$ Hz) is therefore in favor of an *endo*-isomer. Furthermore, comparison with data published on a related cycloadduct,³⁰ suggested also the formation of the *endo*-isomer.

[‡] Calculations performed by Prof. Andrew Whiting.

Table 19. Determination of the stereochemistry of cycloadduct **339a** by coupling constants analysis.

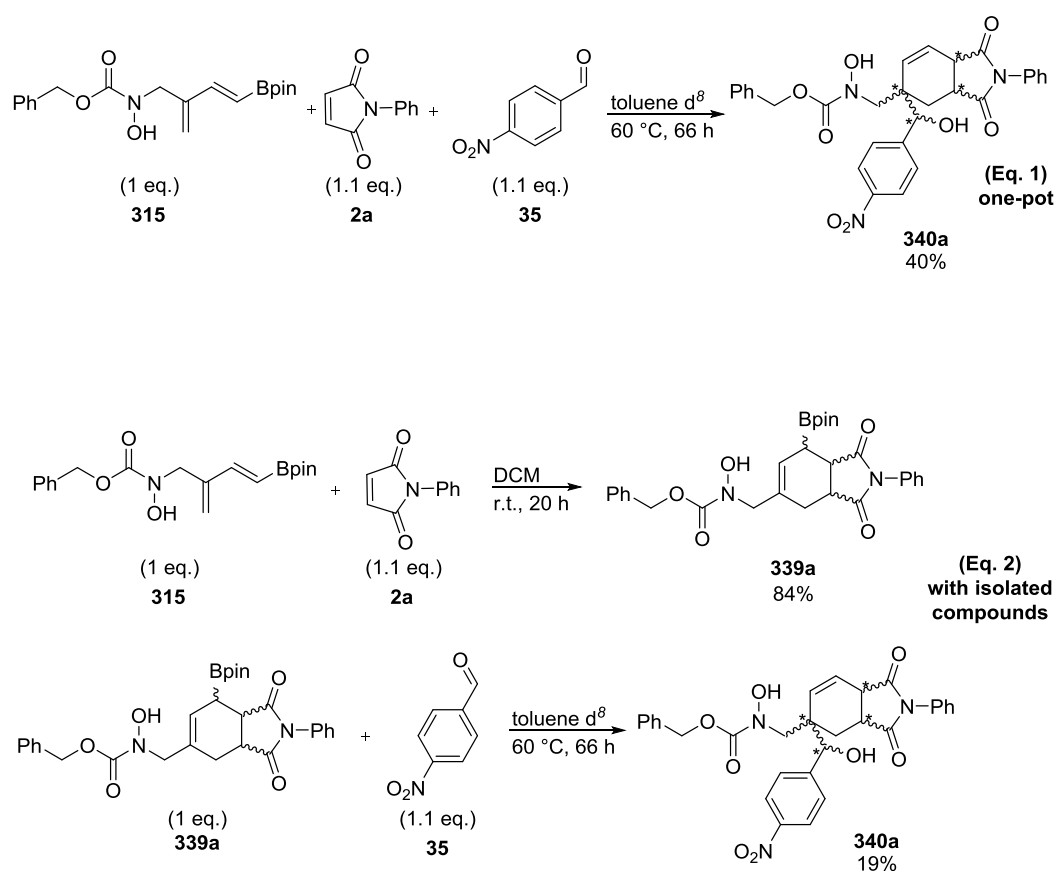


Entry	Molecule	$J_{\text{H1-H2}}$ (Hz)	$J_{\text{H3-H2}}$ (Hz)	$J_{\text{H3-H4}}$ (Hz)	$J_{\text{H3-H5}}$ (Hz)
1	339a	5.8	9.4	4.1	7.7
2	339a endo	5.4	8.1	5.1	9.1
3	339a' exo	2.2	7.2	1.7	7.4

V.1.b. The Diels-Alder/allylboration one-pot process

In order to evaluate the possible advantage of a one-pot sequence, a comparison with a process wherein the two reactions were carried out separately was undertaken. As observed in Table 16, *N*-phenyl maleimide **2a** showed the best reactivity, and thus was used as model dienophile with *p*-nitrobenzaldehyde **35** an electron-deficient aldehyde. For the one-pot procedure (Eq. 1, Scheme 94), the reaction was carried out in toluene at 60 °C for 66 h. The crude reaction mixture showed a mixture of unreacted *N*-phenyl maleimide **2a**, *p*-nitrobenzaldehyde **35**, and pinacol **255**, as well as the desired compound **340a**. It is worthy to note that no compound **315** or cycloadduct intermediate **339a** were observed. The crude product was purified by silica gel chromatography to recover *N*-phenyl maleimide **2a** in 15% yield and *p*-nitrobenzaldehyde **35** in 52%. The desired product **340a** was isolated in 40% yield.

On the other hand, the same sequence was carried out with isolated compounds (Eq. 2, Scheme 94) which afforded only a 16% overall yield. The Diels-Alder step led to the formation of the [4+2]-cycloadduct in 84% yield (Entry 1, Table 16), whereas the allylboration, using the same reaction conditions (toluene, 60 °C, 66 h), provided compound **340a** with a 19% isolated yield, proving that allylboration is the critical step in the sequence. The one-pot procedure is therefore preferred for the following study the most suitable pathway (40% > 16%).



Scheme 94. One-pot procedure *versus* isolated method.

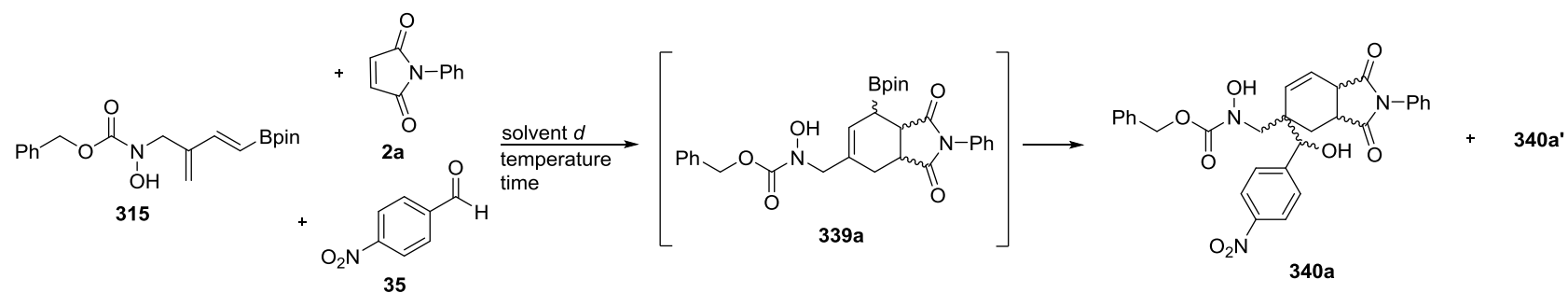
A screening of the reaction conditions was undertaken to define the influence of the solvent, stoichiometry of the reactants, the concentration and the temperature. At r.t., with a concentration of 0.17 mol.L⁻¹ of **315**, the solvent did not show a major impact in either the Diels-Alder or the allylboration step. Toluene showed a slightly better reactivity, with a

higher **315** consumption and allylation compound **340a** formation (Entry 2, Table 20). More importantly, formation of two allylation compounds, **340a** and **340a'**, were observed after 72 h and 1 week. Even if acetone did give the lowest conversion towards the [4+2]-cycloadduct, it seemed that the allylboration step was slightly faster, compared to the reaction using CDCl_3 and MeCN *d*³ (Entries 1, 3 and 4). In order to evaluate the impact of the temperature, toluene and acetone were chosen as solvents. By increasing the temperature to 50 °C and 80 °C, the cycloaddition and the allylboration were faster. However, the ratio between the two allylation compounds **340a** and **340a'** were modified depending on the temperature. At r.t., the reaction in toluene afforded the compounds **340a** and **340a'** in a ratio of (66/34) after one week (Entry 2). At 50 and 80 °C, the ratios were respectively (49/51) and (54/46) (Entries 5 and 6). When acetone was used, and the reaction was heated at 50 °C, the same characteristics were observed. Higher temperature enhanced the reactivity, and modified the ratio of allylation compounds **340a** and **340a'** (100/0 at r.t., 81/19 at 50 °C) (Entries 3 and 9). In addition to the temperature, concentration also had a dramatic impact upon reactivity. If the concentration was increased approximately five-fold from $[\mathbf{315}] = 0.17 \text{ M}$ to $[\mathbf{315}] = 1.00 \text{ M}$, the conversion towards the cycloadduct intermediate and also the allylation were increased (Entries 8 and 10). With acetone, good selectivity was observed after one week with a ratio of (90/10).

Based on these observations, the outcome of the reaction (conversion and ratio) was shown to be highly concentration and temperature dependant. Furthermore, a polar solvent (acetone) gave a faster allylboration reaction. Data showed that the allylboration step was the rate-determining step. Thus, the number of equivalents of the aldehyde partner in the reaction was increased. The impact was not as important as for the concentration and the temperature, but 2.1 eq. of aldehyde provided the best compromise between reactivity and selectivity with 92% conversion, and a 93/7 ratio after 45 h. Because of the lack of reactivity of some dienophiles

(Table 16), a reaction in DMSO at 140 °C was undertaken. Unfortunately, only decomposition of starting materials was observed.

Table 20. Optimisation of the one-pot Diels-Alder/allylboration sequence.



Entry	2a (eq.)	35 (eq.)	Solvent	Temp. (°C)	Conc. 292 (mol.L ⁻¹)	Ratio (22 h) ^[a]	Ratio (45 h) ^[a]	Ratio (72 h) ^[a]	Ratio (week) ^[a]
						315/339a/340a/340a'	315/339a/340a/340a'	315/339a/340a/340a'	315/339a/340a/340a'
1	1.1	1.1	CDCl ₃	r.t.	0.17	36/64/0/0	21/75/4/0	13/78/9/0	7/76/17/0
2	1.1	1.1	Toluene <i>d</i> ⁸	r.t.	0.17	22/70/8/0	10/75/15/0	5/66/21/8	0/61/27/14
3	1.1	1.1	Acetone <i>d</i> ⁶	r.t.	0.17	42/53/5/0	27/65/8/0	17/70/13/0	9/69/22/0
4	1.1	1.1	MeCN <i>d</i> ³	r.t.	0.17	36/64/0/0	21/76/3/0	13/81/6/0	6/83/11/0
5	1.1	1.1	Toluene <i>d</i> ⁸	50	0.17	0/71/17/12	0/58/21/21	0/43/28/29	0/27/36/37
6	1.1	1.1	Toluene <i>d</i> ⁸	80	0.17	0/50/31/19	0/35/37/28	0/23/41/36	0/17/45/38
7	1.1	1.1	Toluene <i>d</i> ⁸	r.t.	0.10	30/67/3/0	17/70/13/0	8/76/16/0	0/69/31/0
8	1.1	1.1	Toluene <i>d</i> ⁸	r.t.	1.00	0/72/24/4	0/53/40/7	0/30/50/20	_ ^[b]
9	1.1	1.1	Acetone <i>d</i> ⁶	50	0.17	10/83/17/0	_ ^[b]	0/53/37/10	0/37/51/12

10	1.1	1.1	Acetone d^6	r.t	1.00	12/75/13/0	_ ^[b]	0/55/45/0	0/33/60/7
11	1.1	1.1	Acetone d^6	50	1.00	0/23/77/0	0/10/78/12	0/0/66/34	_ ^[d]
12	1.1	2.1	Acetone d^6	50	1.00	0/28/61/11	0/8/86/6	_ ^[b]	_ ^[b]
13	1.1	3.1	Acetone d^6	50	1.00	0/19/72/9	0/3/77/20	_ ^[b]	_ ^[b]
14	1.1	1.1	MeCN d^3	80	1.00	0/18/37/45	0/9/42/49	0/0/51/49	_ ^[b]
15	1.1	1.1	DMSO d^6	140	1.00	_ ^[b]	_ ^[b]	_ ^[b]	_ ^[b]

[a] Ratio measured by 1H NMR of the crude reaction mixture. [b] 1H NMR not determined.

The results presented in Table 20 were all calculated using ^1H NMR on the crude reaction mixture. Below are presented two NMR analyses (Figure 14 and 15); one containing only one allylation compound **340a** and a second with a mixture of both compounds **340a** and **340a'**. In acetone, when the NMR was clean enough, attention was focused between the 5.5 and 6.5 ppm region. The remaining **315** compound was characterised by a doublet ($\delta = 5.68$ ppm, $J = 18.6$ Hz), the cycloadduct **339a** by a multiplet ($\delta = 6.02$ ppm), and compound **340a** by a doublet of doublet ($\delta = 6.30$ ppm, $J = 10.2, 2.8$ Hz).

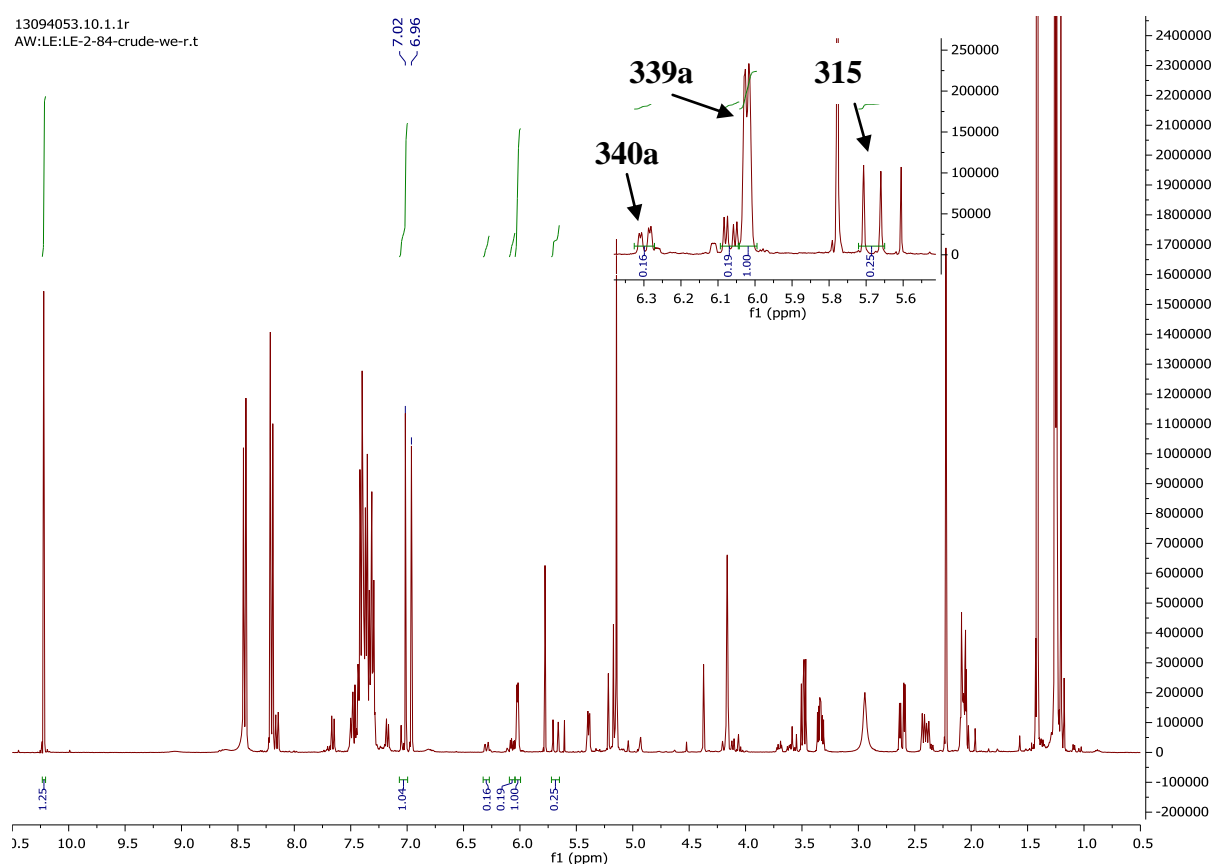


Figure 14. ^1H NMR analysis of the crude reaction mixture in acetone after 72 h.

In toluene, due to the formation of a second isomer, identification of the different compounds involved in the reaction was more tedious. In addition to the area between 6.5 and 5.5 ppm, it was necessary to study a second set of signals between 3.5 and 2.4 ppm. Remaining **315** compound was characterised by a doublet ($\delta = 5.79$ ppm, $J = 18.6$ Hz, not visible on Figure

15), the cycloadduct **339a** by a multiplet ($\delta = 6.11$ ppm), compound **340a** by a multiplet ($\delta = 2.88$ ppm) and compound **340a'** by a doublet ($\delta = 3.36$ ppm, $J = 15.0$ Hz).

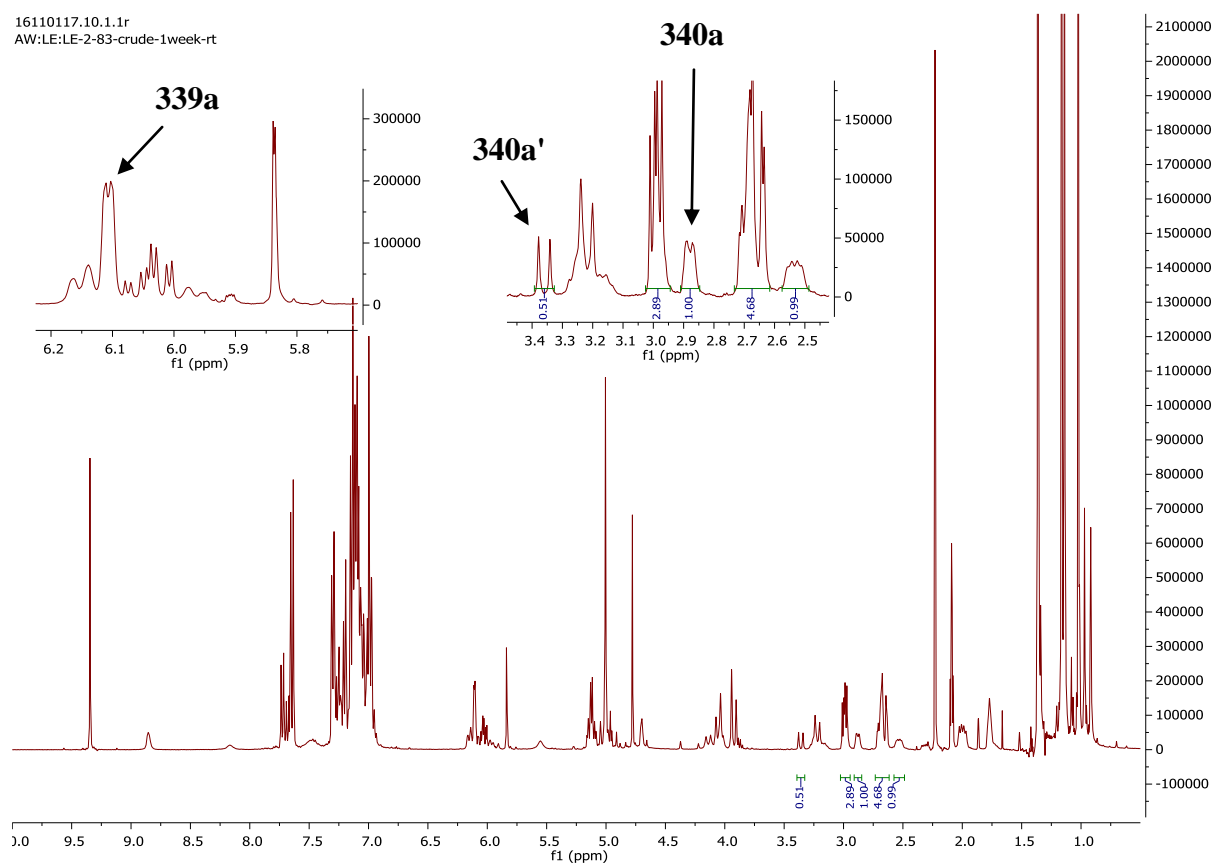
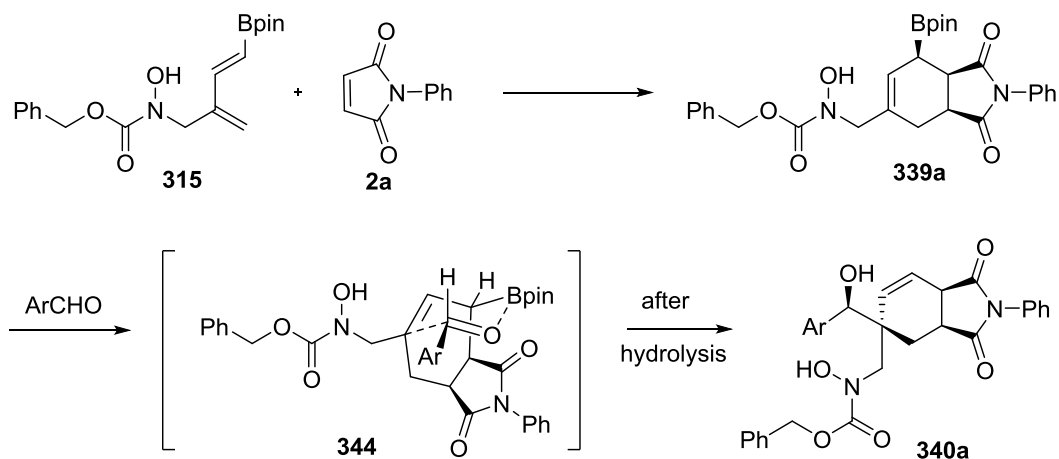


Figure 15. ^1H NMR analysis of the crude reaction mixture in toluene after 7 days.

Depending on the conditions, formation of a single allylboration compound **340a**, or a mixture of **340a** and **340a'**, were observed. The structure of the major isomer was established according to spectroscopic data (NMR and mass), the determination of the X-ray structure of the related compound **350** (page 131) and by comparison with literature data.³⁰ This stereochemistry can be explained by the formation of an *endo* cycloadduct during the Diels-Alder step and an allylboration transition state where the aryl substituent of the aldehyde occupied the equatorial position of a chair-like conformation (Scheme 95).



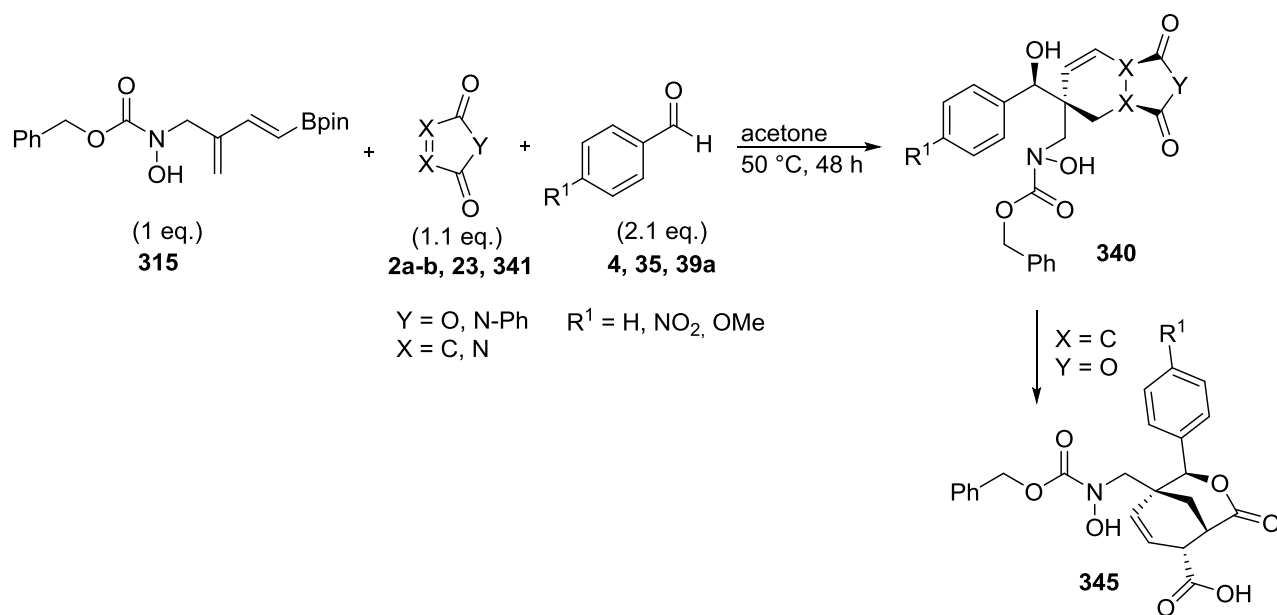
Scheme 95. Stereochemical outcome of the cascade reaction.

A screening of the dienophile and aryl aldehyde was then carried out. *N*-phenyl maleimide **2a** was first used as the dienophile in the presence of different arylaldehydes. Isolated yields after silica gel chromatography were low to moderate (16 - 48%). This was directly related to the electronic properties of the aldehyde, *i.e.* if R¹ was an electron withdrawing group, the allylboration step was accelerated, by increasing the relative positive charge on the carbonyl group. On the other hand, the opposite behaviour was observed with R¹ as an electron donating group.

The same pattern was obtained using maleic anhydride **2b** as dienophile. Better yields were obtained using maleic anhydride **2b**, because no silica gel chromatography was required for purification, since the precipitation of the major compound was observed in CHCl₃ overnight at + 4 °C. Concerning the structures of these products, as it was already reported in the literature,³⁰ intramolecular cyclisation can occur to afford lactone derivatives. To determine whether the cyclisation occurred, a ¹H NMR comparison between **340a** and **345b** in DMSO-*d*⁶ was performed. For **340a**, the hydroxycarbamate signal ($\delta = 9.69$ ppm, s) and alcohol signal ($\delta = 5.92$ ppm, d) were identified, by D₂O exchange. In the case of **345b**, only one signal, corresponding to the hydroxycarbamate signal ($\delta = 9.53$ ppm, s) was detected. Concerning IR analysis, attention was focused on the region between 1600 and 1800 cm⁻¹. Compound **345b**

showed the peak with the highest intensity at 1730 cm^{-1} . δ -Valerolactone (a 6-membered lactone) showed a peak with the maximum of intensity at 1722 cm^{-1} . Furthermore, IR data resulting from the cycloaddition using maleic anhydride has been described, and the C=O bond was measured at 1770 cm^{-1} .¹⁶⁰ Thus according to these data, it was most probable that the product resulting from the reaction using maleic anhydride **2b**, was the lactone **345** resulting from the intramolecular cyclisation. Also, two azo compounds were tested 4-phenyl-1,2,4-triazole-3,5-dione **23** and DEAD **307** leading to a decomposition of the starting **315**.

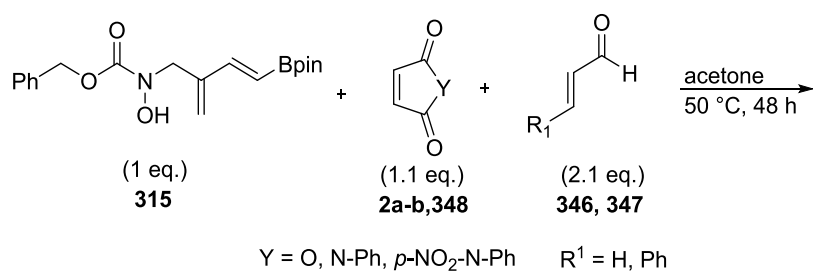
Table 21. One-pot Diels-Alder/allylboration sequence using arylaldehydes.

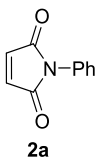
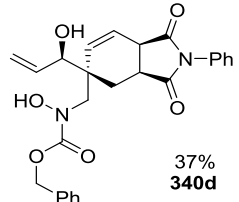
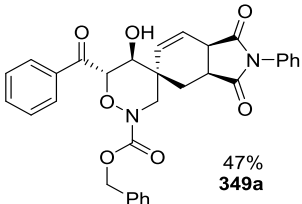
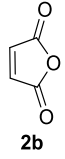
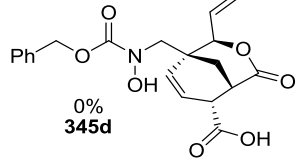
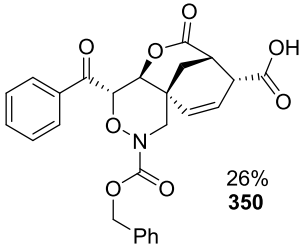
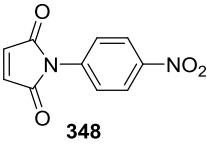
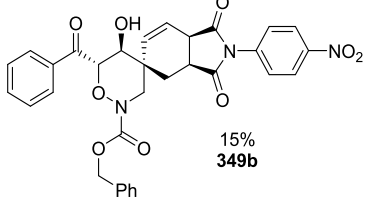


Entry	Dienophile	Aldehyde	Isolated Yield (%)
1		4-nitrobenzaldehyde 35	340a 48
2		Benzaldehyde 4	340b 39
3	2a	4-anisaldehyde 39a	340c 16
4		4-nitrobenzaldehyde 35	345a 75
5	2b	Benzaldehyde 4	345b 64
6		4-anisaldehyde 39a	345c -
7		4-nitrobenzaldehyde 35	-
8		4-nitrobenzaldehyde 35	-

Attention was then turned to α,β -unsaturated aldehyde as partner of this three component reaction. When acrolein **346** was used, the expected polycyclic products **340d** and **345d** were synthesised according to crude ^1H NMR (Entries 1 and 3, Table 22). Nevertheless, only **340d** was isolated in 37% yield (Entry 1). Interestingly, if *trans*-cinnamaldehyde **347** was employed, the reaction afforded the spirocyclic oxazine compounds **349a** and **349b**, using *N*-phenyl maleimide derivatives (Entries 2 and 5). With maleic anhydride **2b**, the spirocyclic oxazine scaffold evolved to form compound **350** as already postulated in Table 21. When a D_2O exchange was performed on molecule **349a**, the signal corresponding to the alcohol disappeared proving that no cyclisation had occurred.

Table 22. One-pot Diels-Alder/allylboration sequence using α,β -unsaturated aldehydes.



Entry	Dienophile	Aldehyde	Product / isolated yield (%)
1	 2a	Acrolein 346	 37% 349d
2		<i>trans</i> -cinnamaldehyde 347	 47% 349a
3	 2b	Acrolein 346	 0% 349d
4		<i>trans</i> -cinnamaldehyde 347	 26% 349e
5	 348	<i>trans</i> -cinnamaldehyde 347	 15% 349b

The preparation of a suitable crystal in the case of compound **350** allowed determination of the exact structure of this polycyclic heterocycle by X-Ray analysis, which is confirmed by ^1H and ^{13}C NMR spectra. By analogy, we were able to deduce the structures of the related products **349a-b**.

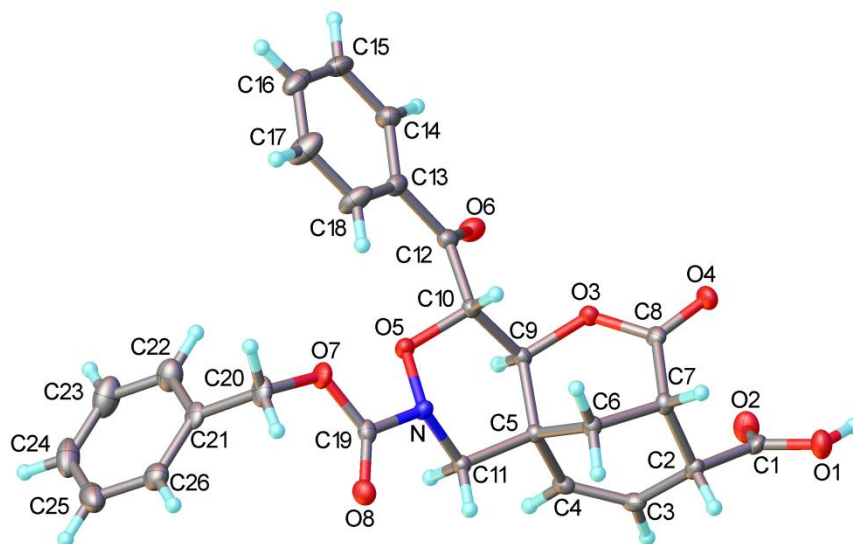
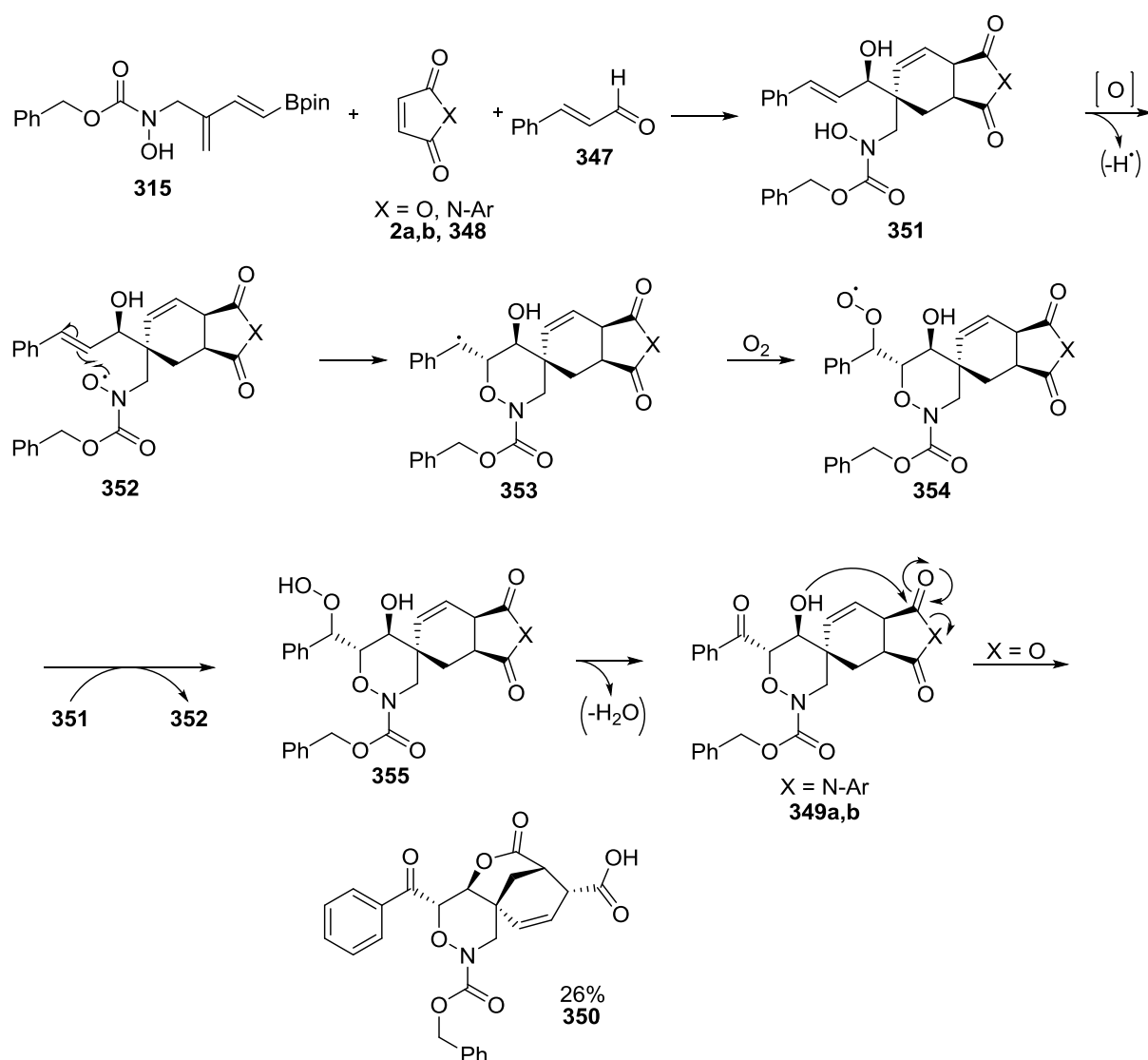


Figure 16. Crystal structure of compound **350**.

V.1.c. Mechanistic aspects

The proposed mechanism starts with a Diels-Alder/allylboration sequence described in Scheme 95. On the basis of Alexanian and co-workers study,¹⁶¹ a mechanism based on an aerobic ketoxygenation was proposed. As an initiation step for the radical reaction to take place, they hypothesised that a small amount of the amidoxyl radical **352** was formed by an autooxidation process. A second alternative could be a boron-catalysed initiation process. The oxygen radical then cyclised to give the oxazine ring **353** by a 6-*exo*-cyclisation process with creation of a carbon-centered radical as a single diastereoisomer. Formation of a stabilised benzylic radical can explain the formation of the 6-membered ring. Radical oxidation with O_2 afforded the radical intermediate **354** which initiate the propagation by a hydrogen abstraction

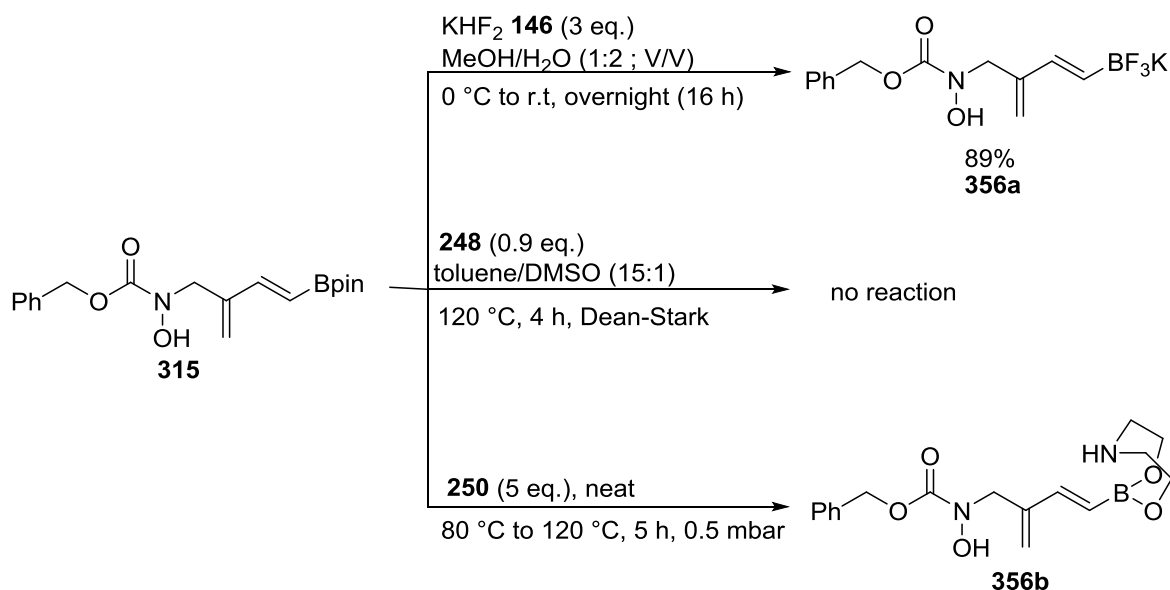
from the substrate **351** yielding radical **352** and producing intermediate **354**.¹⁶¹ Whereas the conditions described in the paper used Ac₂O (1 eq.) and DMAP (0.1 eq.) for the elimination step, in our case no external reagent was necessary to observe the same reactivity. A homolysis of the peroxide intermediate **355** could occur and by abstraction of the benzylic hydrogen, could provide the compounds **349a,b**, releasing water. When maleic anhydride was used as dienophile, an intramolecular lactonisation ended the sequence.



Scheme 98. Ketoxygenation mechanism for the formation of compound **349a,b** and **350**.

V.2. Modification of the boron substituent

The boron substituent has an impact on the rate of the Diels-Alder reaction. No catalytic effect had been observed with compound **315** bearing a Bpin substituent, thus, it was envisaged that modification of the substituent on the boron would impact the reaction. The trifluoroboronated salt **356a** was synthesised using the procedure with potassium hydrogenbifluoride **146**. The desired compound **356a** was obtained with 89% yield. An attempt to synthesise the MIDA derivative using the standard procedure used for the preparation of the diene **249** was unsuccessful. Compounds **315** and **248** were recovered from the reaction. Lastly, the diethanolamine derivative was synthesised. Mixing compound **315** with diethanolamine **250** in Et₂O did not lead to precipitation of the desired compound **356b**. Therefore, the reaction was carried out at high temperature under neat conditions in a distillation apparatus. Pinacol **255** was directly distilled during the process at 80 °C. Then, excess of diethanolamine was removed by increasing the temperature from 80 °C to 120 °C. ¹H NMR and ¹¹B analyses of the crude reaction mixture showed formation of the desired compound. Different methods, including precipitation or washing did not permit the isolation of **356b** as a pure compound.



Scheme 99. Effects of modification of the boron substituent on **315**.

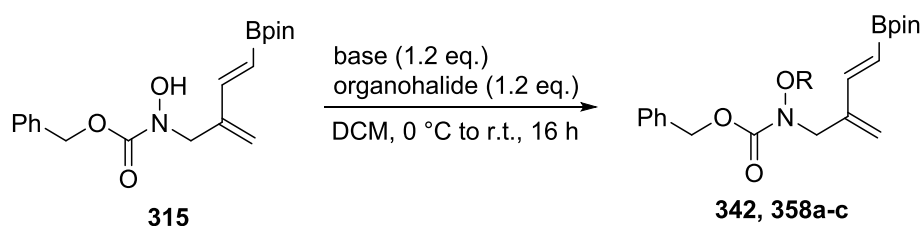
No advanced research on the Diels-Alder reaction was performed, but thanks to a probable higher reactivity towards the Diels-Alder reaction, cycloaddition using **356a-b** with other dienophile could provide a wider range of cycloadducts. Moreover, purification could be facilitated, because most of the products bearing a trifluoroborate moiety could be easily precipitated out from the crude reaction mixture.

V.3. The metathesis/arylnitroso Diels-Alder/ring contraction sequence

Attention to diversify the chemistry of **315** was then turned to the hydroxycarbamate part of the molecule. The presence of this easily derivatisable group should allow a supplementary functionalisation and, therefore, greatly increase the structural diversity accessible from this ene product.

V.3.a. Synthesis of the *O*-substituted hydroxycarbamates

Two different derivatisations were performed, both of them resulting in the introduction of an additional unsaturation to the dienyl moiety, as summarised in Table 23. In the case of allyl bromide, in the presence of DBU, the reaction yielded **362a** in a 49% yield after silica gel chromatography (Entry 1, Table 23), whereas, after classical workup, only polymerised compound was recovered with acryloyl chloride (Entry 4). The same problem was encountered by scaling up the reaction from 0.15 mmol to 0.5 mmol using allylbromide since only 9% of the desired compound **362a** was isolated (Entry 2). It is known that boronated dienes have strong tendency to polymerise. This drastic decrease in yield was suppressed by using 2,6-di-*t*-butyl-*p*-cresol (BHT) as a stabiliser to inhibit the auto-polymerisation of the polyene and rapid filtration over a pad of silica. With these experimental conditions, the isolated yield of **362a** increased from 9 to 85% (Entry 3), and, similarly, the acryloyl derivative **362c** was isolated in 70% yield (Entry 5). Propargyl derivative **362d** was prepared *via* the same method in an isolated 60% yield (Entry 6). **361c-d** could be stored in dark in the fridge (4 °C) under an inert atmosphere, without observing any polymerisation.

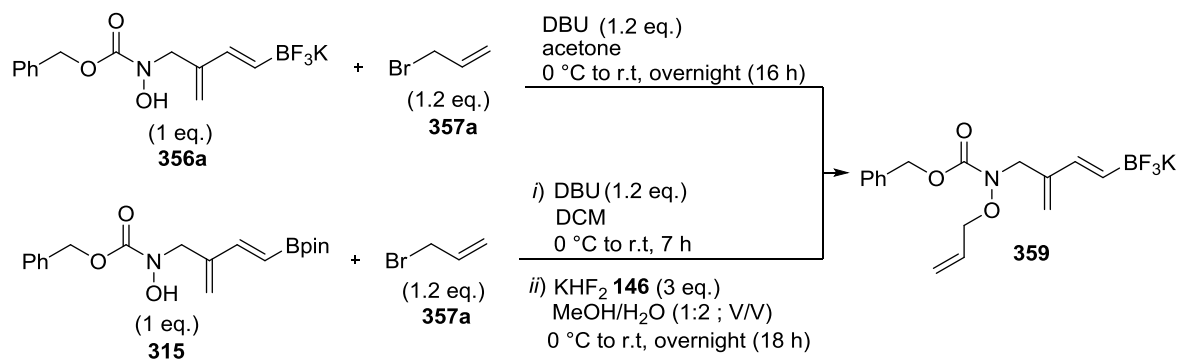
Table 23. Synthesis of protected hydroxy carbamate adducts.

Entry	Base	organohalide	Product	Isolated yield (%)
1 ^[a]	DBU			49
2 ^[b]	DBU			9
3 ^[c]	DBU			85
3 ^[a]	Et ₃ N			56
4 ^[b]	Et ₃ N			54
5 ^[b]	DBU			55
6 ^[a]	Et ₃ N			0
7 ^[d]	DBU			70
8 ^[d]	DBU			60

[a] Reaction performed with 0.15 mmol of compound **315** without optimised purification conditions. [b] Reaction performed with 0.5 mmol of compound **315** without optimised purification conditions. [c] Reaction performed with 2.00 mmol of compound **315** with optimised purification conditions. [d] Reaction performed with 0.5 mmol of compound **315** with optimised purification conditions.

We also tested the same functionalisation with the trifluoroborate **356a**, dichloromethane being replaced as solvent by acetone to increase the solubility. The ¹H and ¹¹B NMR analysis of the crude product indicated that the reaction took place, however several attempts at precipitation using different solvent mixtures (DCM/Et₂O, DCM/hexane, acetone/Et₂O, acetone/hexane) in various ratios failed. Therefore, a second pathway was envisaged starting from the Bpin derivative **315**. First, the allylation was performed, and after full conversion of

the starting material, the modification of the boron substituent was tested based on the same procedure used for the synthesis of **276** (Scheme 60). Analysis of the crude product showed the same results and same purification issues as the first method (Scheme 100).



Scheme 100. Synthesis of the trifluoroborylated allylated compound **359**.

V.3.b. The ring closing metathesis (RCM) of hydroxamates **358a-c**

Metathesis is a reaction which allows the formation of new carbon-carbon double bonds by the reaction of two alkenes. This reaction has been widely developed, and nowadays, numerous catalysts have been developed to enhance the reactivity and the scope of the reaction.¹⁶² Among them, the most well-known catalysts are summarised in Figure 18.

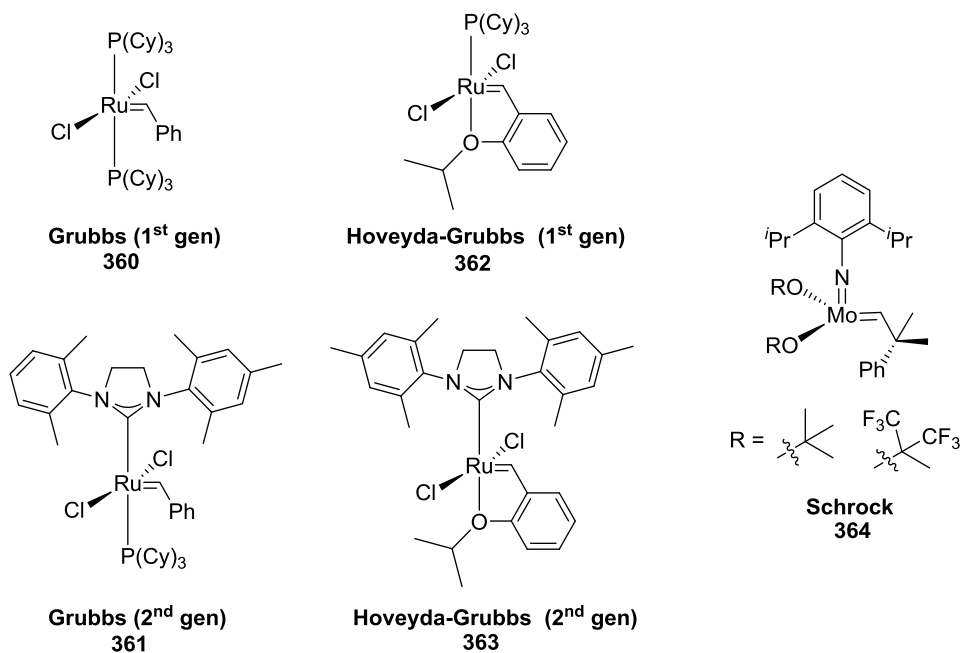
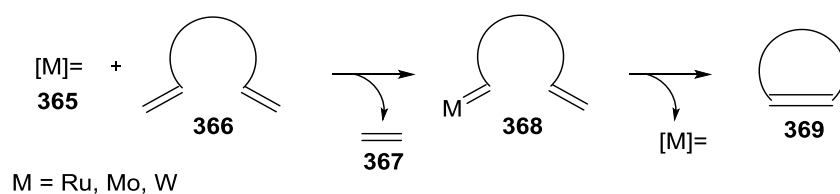


Figure 18. Most used metathesis catalysts.

The ring closure metathesis (RCM), one of the olefin metathesis processes, is one of the most efficient strategies used for the synthesis of cycle, heterocycle and macrocycle compounds.^{162j}

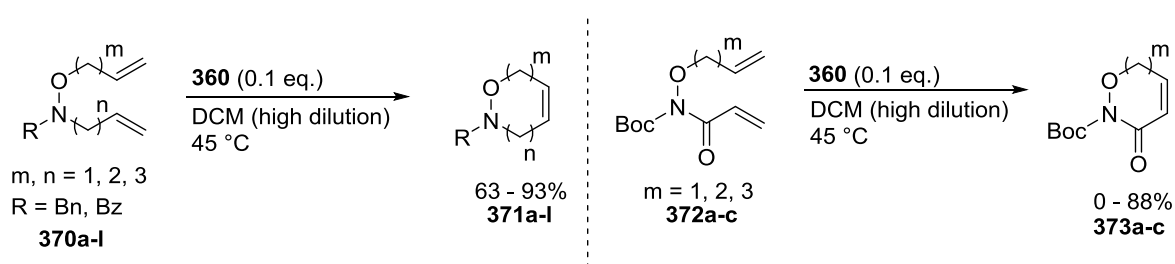


Scheme 101. General formation of cyclic compounds by RCM.

The ring closure metathesis (RCM) for oxazine ring formation: bibliographic data

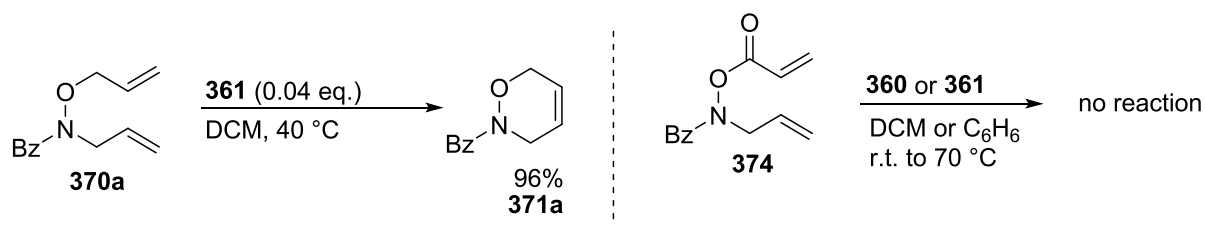
Several examples have already been reported in the field of oxazine derivatives. Tae and co-workers¹⁶³ showed that the RCM can be performed on both Boc and Bz-protected substrates **370** yielding the desired oxazines compound **371** in moderate to excellent yield (63 - 93%). The Boc-protected acryloylamide derivative was subjected to the same reaction conditions,

and 6- and 7-oxazine ring **373a-b** were obtained with high yields (> 80%), whereas the formation of the 8-membered **373c** ring did not take place (Scheme 102).



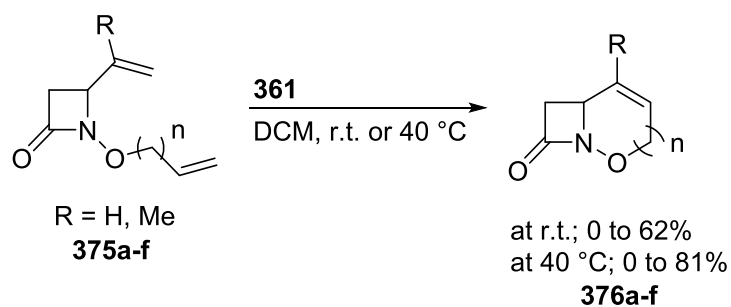
Scheme 102. Synthesis of oxazine using catalysed Grubbs I **360** RCM.

An interesting outcome was pointed out experimentally by Le Flohic *et al.*, with the allylic substrate **370a**, *i.e.* the reaction using **361** afforded the oxazine with an excellent 96% yield, whereas the acryloyl derivative **374** did not exert any reactivity with either **360** or **361** in toluene or DCM at r.t. or 70 °C (Scheme 103). Moreover, according to literature work, the nitrogen needed to be substituted by an electron withdrawing group to enable reactivity.¹⁶⁴



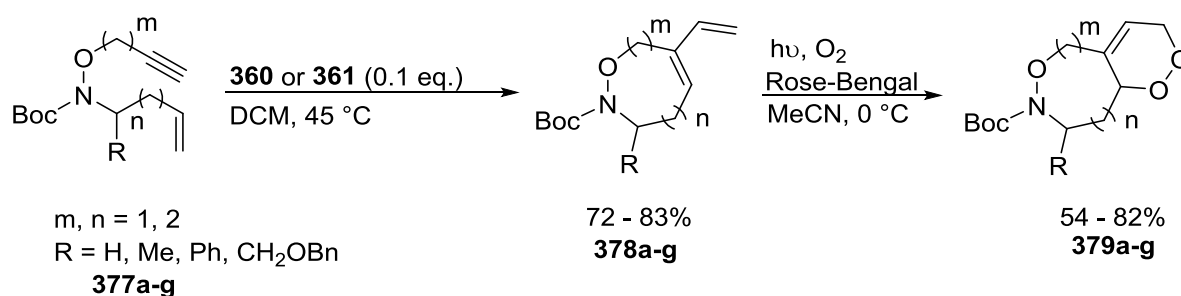
Scheme 103. Differences in reactivity between **370a** and **374** towards the RCM.

The formation of the bicyclic β -lactams **376** using Grubbs' second generation catalyst **361** for ring-closing metathesis was found to depend on ring size (Scheme 104). It is worthy to note that the metathesis reactions involving Grubbs' first generation catalyst **360** gave no product formation.¹⁶⁵ A few other examples were presented in the literature for the synthesis of a library of cell-permeable molecules, or aminoalcohol derivatives.¹⁶⁶



Scheme 104. RCM on derivatives **375**.

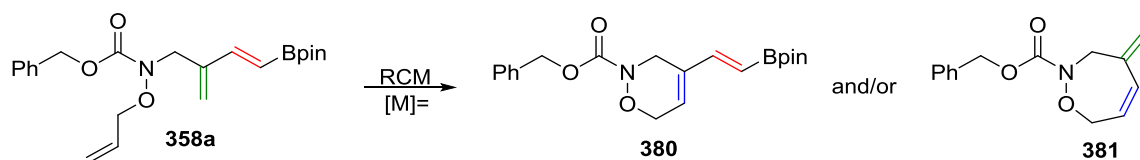
An elegant sequence using this process was presented, starting with the enyne metathesis, followed by a [4+2]-cycloaddition with singlet oxygen to afford cyclic peroxides fused with an oxazine ring **379** (Scheme 105).¹⁶⁷



Scheme 105. Sequence enyne metathesis/Diels-Alder cycloaddition.

The ring closure metathesis (RCM) of hydroxamates **358a-c**

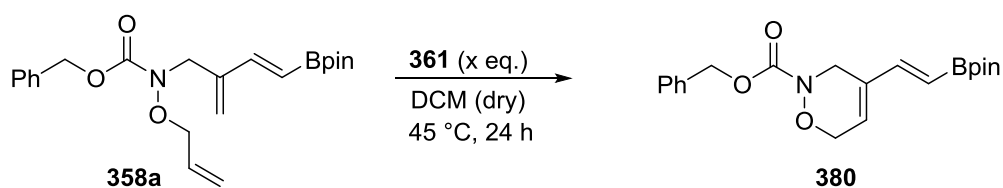
The last example has shown the potential of a sequence metathesis/Diels-Alder sequence for oxazine synthesis. The diene **351** could be an interesting substrate for a ring closure metathesis reaction (RCM) between one of the carbon-carbon double bond of the diene and the allyl moiety making possible a further Diels-Alder step. Two products could be obtained depending on the selectivity on this ring closure process: the 6-membered oxazine ring **374**, thus forming a 1,3-boronated diene or a 7-membered ring **375** with an exocyclic alkene (Scheme 106).



Scheme 106. Possible outcome of the RCM on compounds **358a**.

Grubbs catalyst (2nd generation, **361**) was selected to study the reactivity of **358a**. Previous works on the RCM has proved that reflux conditions in DCM and high dilution favoured the cyclisation over the polymerisation. Thus, concentrations used for the reactions were varying between $[358a] = 0.05$ and 0.07 mol.L^{-1} . A reaction did take place with non-stabilised **358a** and 10 mol% of the catalyst over 24 h, forming a single compound according to crude ¹H NMR analysis (Entry 1, Table 24). After silica gel chromatography, compound **380** including a 1,3-boronated diene moiety was isolated in 61% yield. However, the methodology developed for the synthesis of protected hydroxycarbamate involved BHT as inhibitor to circumvent stability issue. Therefore, the metathesis was tested using derivative **358a** incorporating 14% of BHT. To our satisfaction, no impact was observed between the reaction with stabilised and non-stabilised **358a** (Entries 1 and 2) and both reaction yielded the same compound in around 60% yield. The catalyst loading was then reduced and a slight improvement of the yield was observed with 5 mol% of the catalyst providing **380** with 70% yield. If the loading was decreased to 3 mol%, isolated yield decreased by 4% to reach 66% (Entries 3 and 4). When the reaction was scaled-up with 3 mol%, a small, but measurable, decrease of the isolated yield was observed (Entry 5). It was also noteworthy that **380** is stable on silica gel chromatography. As a result, BHT and presence of by-products from the previous step can be removed at this stage.

Table 24. Metathesis reaction on compound **358a**.



Entry	Catalyst loading	Isolated yield (%)
1 ^[a]	10 mol%	61
2 ^[b]	10 mol%	60
3 ^[b]	5 mol%	70
4 ^[b]	3 mol%	66
5 ^[c]	3 mol%	59

[a] Reaction performed on pure starting material **358a**. *[b]* Reaction performed with starting material containing BHT (10 to 20%) with 0.5 mmol of **358a**. *[c]* Reaction performed with starting material containing BHT (10 to 20%) with 1.7 mmol of **358a**.

The molecular structure of **380** was ascertained by single-crystal X-ray diffraction. Spectroscopic data (¹H and ¹³C NMR, mass) were in full agreement with this structure.

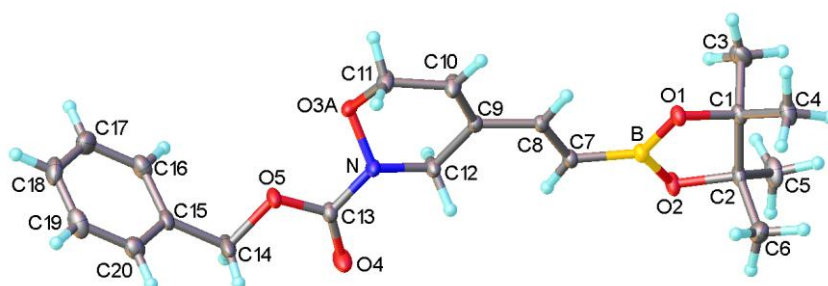
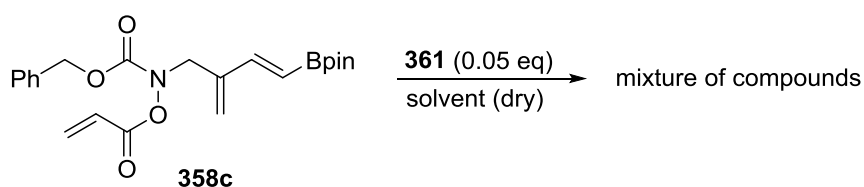


Figure 19. Single crystal X-ray structure of **380**.

The derivative **358c** was subjected to the same reaction conditions as described in Entry 3, Table 24. After 24 h, the reaction was stopped and analysed by ¹H NMR. Starting material **358c** represented more than 80% of the crude mixture (Entry 1, Table 25). Formation of at least two compounds was observed, but we were unable to determine the accurate ratio and to identify these products. Despite the low reactivity, an overview of the stability of the

compound **358c** was obtained. At a moderate temperature range (45-50 °C) under an inert atmosphere in presence of BHT, **358c** was stable and recovered. Thus, a reaction was performed in toluene at 100 °C for 66 h (Entry 2, Table 25). No starting material or identifiable products were found by crude analysis, *i.e.* NMR and TLC. ¹¹B NMR analysis showed that the major product was the formation of a boroxine-type compound with a chemical shift of $\delta = 22.4$ ppm. This low reactivity is in agreement with previous observations.¹⁶⁴

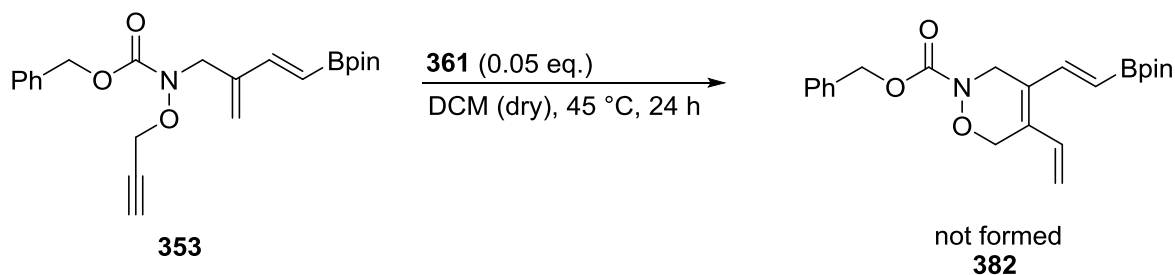
Table 25. Metathesis reaction on compound **358c**.



Entry	Reaction conditions	358c Consumption
1 ^[a]	DCM, 45 °C, 24 h	< 20%
2 ^[a]	Toluene, 100 °C, 66 h	100 %

[a] Reaction performed with a starting material containing 16% of BHT.

The enyne metathesis of **358d** was also tried based on the same reaction conditions in Entry 3, Table 24 in order to prepare the polyene **382**. No reaction occurred and the starting material was recovered after 24 h with 86% yield.

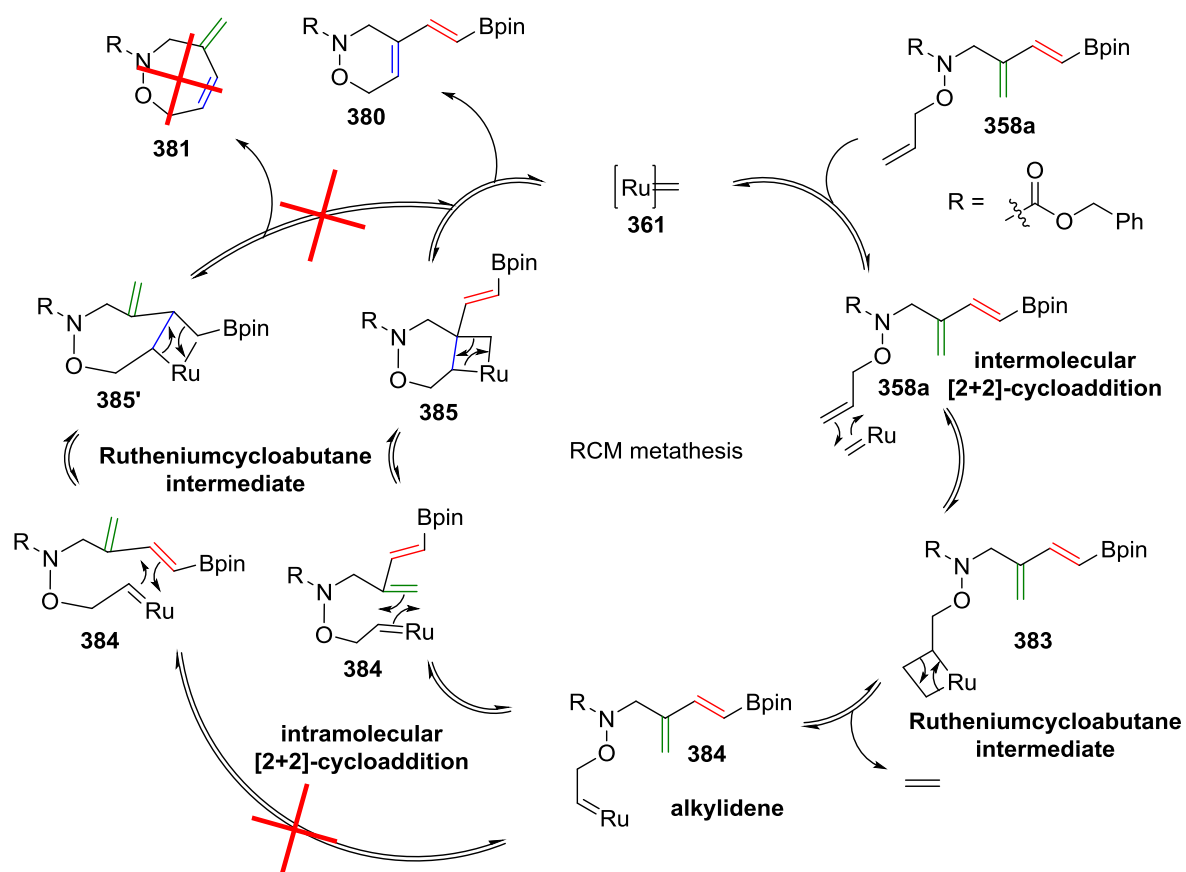
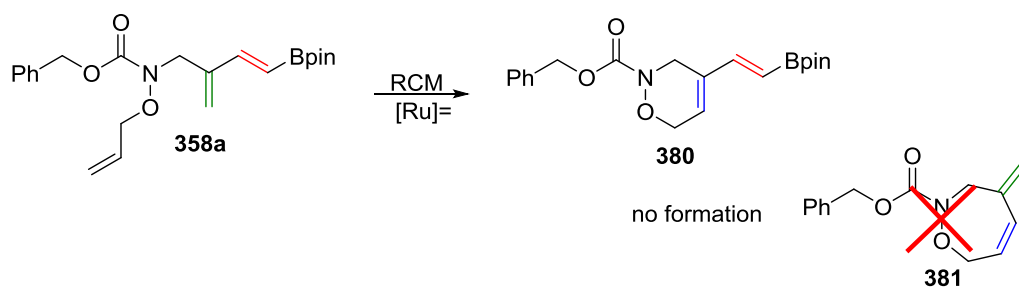


Scheme 107. Enyne metathesis on **358d**.

A study still has to be conducted on substrates **358c** and **358d**, involving a screening of catalysts, and examination of the effect of concentration and temperature.

Mechanistic aspects

The ring closing metathesis on compound **358a** led to the selective formation of the 1,3-boronated diene **380**, without traces of the 7-membered ring **381**. Mechanistically, an intermolecular [2+2]-cycloaddition between the ruthenium complex and the allylic double bond took place to form the rutheniumcyclobutane intermediate **383** that can be likely due to steric hindrance. Retro-cycloaddition provided the active alkylidene specie **384** for the intramolecular [2+2]-cycloaddition. At this stage the ring formation may go through two different pathways: 1) The cycloaddition on the alkene in green on Scheme 108, to afford the intermediate **385** creating the oxazine 6-membered ring. Release of the alkylidene species would have allowed catalytic cycle to proceed and a new 1,3-boronated diene **380** to be formed; 2) The cycloaddition could have occurred on the boron substituted alkene. In this pathway, the intermediate would afford the formation of a 7-membered ring skeleton with an exocyclic double bond in green on **385'**. The metathesis reaction is a catalytic cycle based on reversible steps. Therefore, some parameters have a major impact to drive the reaction towards the formation of the final product, in our case, the formation of volatile ethylene compared with a vinyl boronate. Secondly, the selectivity observed for this reaction can be explained by thermodynamically favoured formation of 6-membered rings compared to higher homologues. Lastly, skeleton **381** is a more constricted structure with a diene including an exocyclic alkene which may result from a higher energy barrier.



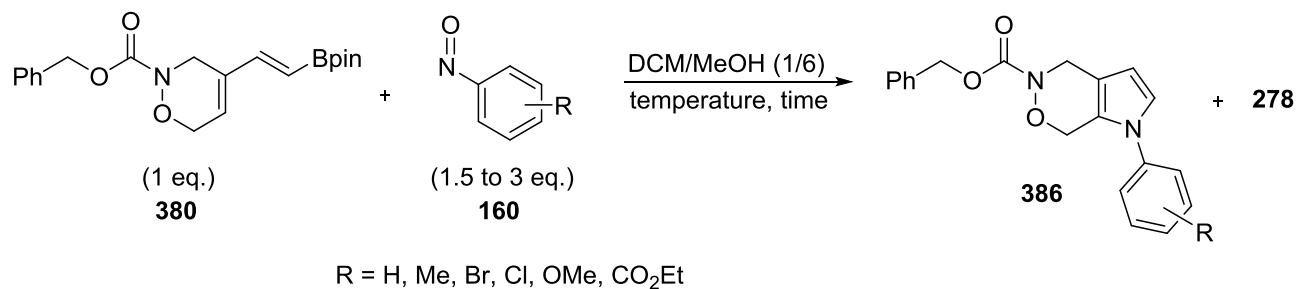
Scheme 108. Mechanism of the RCM to synthesise 380.

V.3.c. *The arylnitroso Diels-Alder/ring contraction sequence*

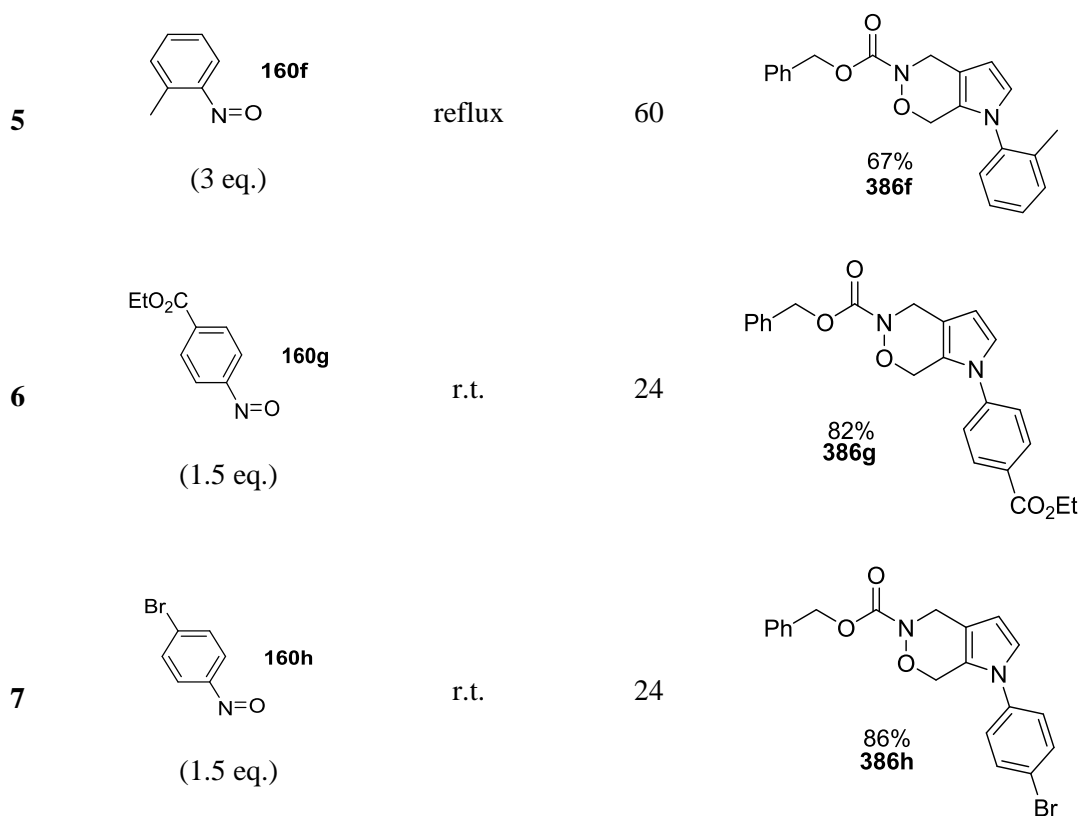
1,3-Boronated dienes have proved to provide pyrroles through a mechanism described in Chapter 2. Despite the fact that compound **380** showed higher strain due to the oxazine ring, it seemed reasonable to expect the same reactivity, even in low yield. Optimisation of the reaction using diene **241c** showed that MeOH was the best solvent for pyrrole formation. However, for better solubility, we chose a mixture of DCM/MeOH (1/6) as solvent. To our delight, the reaction worked smoothly with nitrosobenzene **160a** (2.5 eq.) to provide the desired compound with an excellent 96% yield in 24 h (Entry 1, Table 26). The formation of azoxybenzene **278** was also observed as by-product, but in small amounts. A small decrease in yield was, however, observed with 1.5 eq (89%) (Entry 2). Screening different arylnitroso compounds was performed, and fused, bicyclic oxazine-pyrroles were obtained in good to excellent yields (Entries 3, 6 and 7, Table 26). Electron-deficient arylnitroso derivatives **160b**, **160g** and **160h** showed higher reactivity than the electron-rich arylnitroso **160d**. Whereas reactions with **160b**, **160g** and **160h** showed full conversion of the starting material after 24 h, a 47% conversion of **380** was observed by ¹H NMR analysis of the crude reaction mixture. Furthermore, a larger amount of azoxybenzene **258d** was obtained. By reducing the rate of Diels-Alder/rearrangement process, the competition with the azoxybenzene formation became more problematic. As a result, with electron-donating substituent in the *para*-position of the aromatic ring, 2.5 eq. of arylnitroso **126** and an extended reaction time was necessary to observe full conversion of **380** (Entry 4). Even if the reactivity was decreased, the yield was not affected and product **386d** was isolated in 91%. If an *ortho*-substituted arylnitroso was used, a decrease of the reactivity was also observed. With 1.5 eq. of **160f**, 26% conversion was observed after 72 h at r.t. If another 1.5 eq. was added the conversion reached 58% after 6 days. The reaction was then carried out with 3 eq. of **160f** at reflux conditions and a full

conversion of **380** was observed after 66 h yielded product **386f** in 67% yield (Entry 5). The *ortho*-substitution decreased significantly the rate of the reaction, which can be explained by a steric hindrance effects.

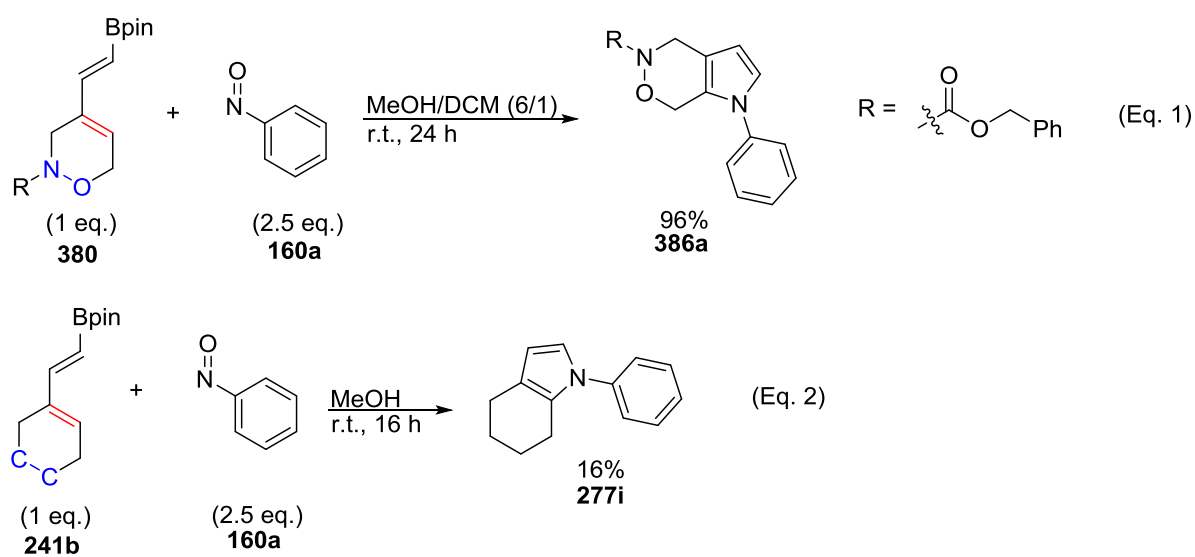
Table 26. Synthesis of fused oxazine-pyrrole bicyclic synthesis.



Entry	Arylnitroso (x eq.)	Temperature (°C)	Time (h)	Product Isolated yield (%)
1	160a (2.5 eq.)	r.t.	24	386a 96%
2	160a (1.5 eq)	r.t.	24	386a 89%
3	160b (1.5 eq)	r.t.	24	386b 77%
4	160d (2.5 eq.)	r.t.	72	386d 91%



The formation of fused oxazine-pyrrole bicyclic synthesis proved to be very efficient (96%), even if one of the olefin was endocyclic (in red in Eq. 1 in Scheme 109), in comparison with the carbocyclic version (Eq. 2).

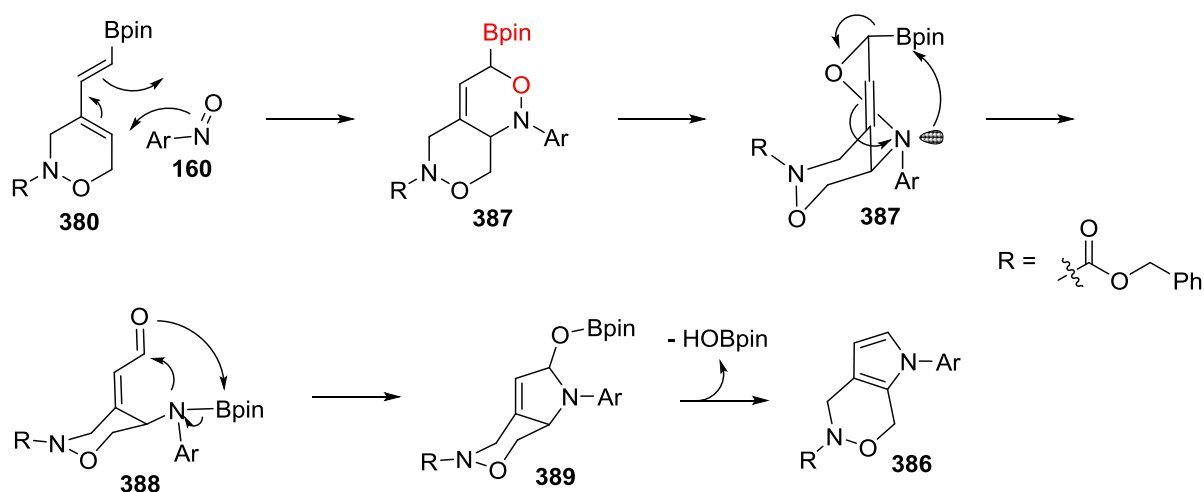


Scheme 109. Comparison on the reactivity between the heterocyclic diene **380** and carbocyclic diene **241b**.

A possible explanation could be found from the difference in the configuration of the cyclohexenyl ring. In some cases, heterocyclic compounds can adopt boat-like conformations which are formed initially through [4+2]-cycloadditions anyway, whereas the cyclohexene ring has a flatter structure.¹⁶⁸

Mechanistic aspects

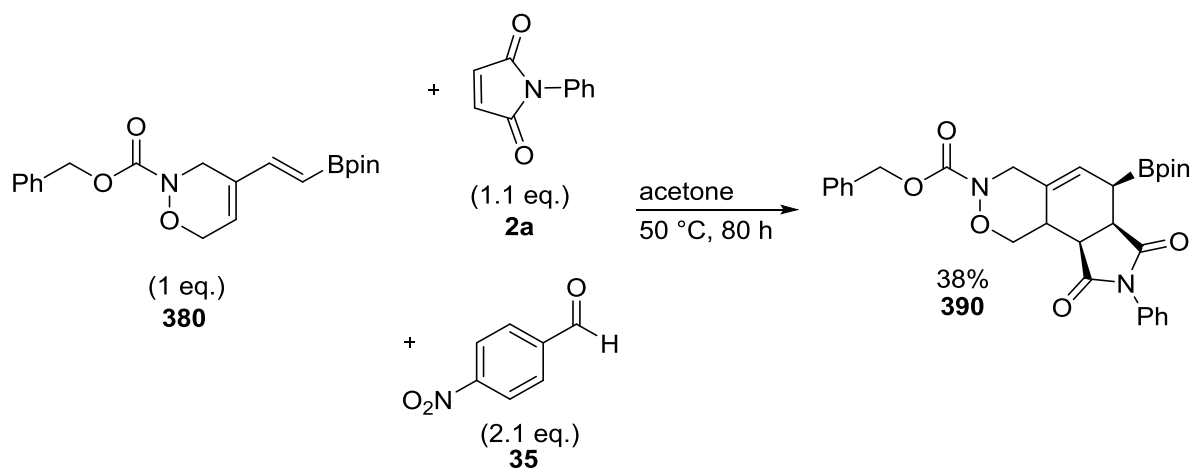
A mechanism explaining the formation of the fused oxazine-pyrrole derivative can be based on the mechanism described in Scheme 69. First, a regioselective aryl nitroso Diels-Alder reaction with a 1,2-oxygen-boron related regioisomer (in red in Scheme 110) reaction could take place to afford the bicyclic oxazine ring system **387**. No theoretical calculations have been made for this particular case, but according to previous results and calculations for the reference rearrangement process using 1,3-dienyl boronate, an *endo*-pathway might be preferred. Then, the consecutive boryl rearrangement leading to **388**, followed by the intramolecular aza-boryl to aldehyde addition to give **389**. Finally, the elimination step would provide the fused oxazine-pyrrole product **386**.



Scheme 110. Mechanism of the formation of the fused bicyclic oxazine-pyrrole product **386**.

V.3.d. The Diels-Alder/allylboration sequence.

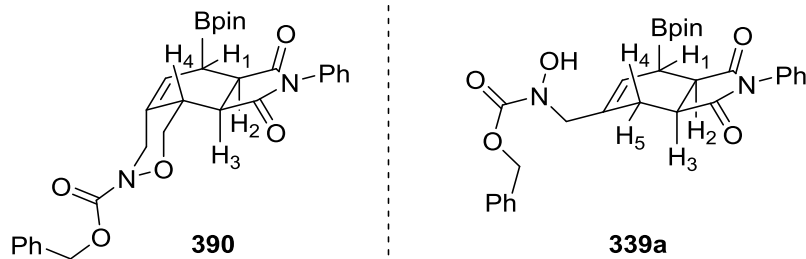
The Diels-Alder/allylboration sequence was also tried on compound **380**, with the optimised reaction conditions described in Entry 12, Table 20, with *N*-phenyl maleimide **2a** as dienophile and *p*-nitrobenzaldehyde **35**. The reaction was stopped after 48 h and checked by ^1H NMR. A 64% conversion of **380** was measured for formation of the cycloadduct **390**. However, no trace of any allylboration compound was observed. No allylation product was observed after 80 h of combined reaction time, and only the [4+2]-cycloadduct **390** was obtained, which was isolated in 38% yield with traces of a second adduct (around 8%) after silica gel chromatography (Scheme 111). Derivative **380** and cycloadduct **390** showed higher ring strain than **315** and **339a**, that could explain the decrease of reactivity, and moreover, avoided the allylboration occurring, as already observed previously.⁴²



Scheme 111. Diels-Alder/allylboration sequence on **380**.

An analysis of the coupling constant is in favor of an *endo* adduct by analogy with compound **339a**. Measured coupling constant for **390**, $J_{\text{H1-H2}} = 5.3$ Hz, was in the same range as $J_{\text{H1-H2}} = 5.8$ Hz for **339a**. In the case of the *exo* isomer **339a'** in Table 22, $J_{\text{H1-H2}} = 2.2$ Hz was calculated.

Table 27. Comparison of coupling constant between **390** and **339a**.



Entry	Molecule	$J_{\text{H1-H2}}$ (Hz)	$J_{\text{H3-H2}}$ (Hz)	$J_{\text{H3-H5}}$ (Hz)	$J_{\text{H3-H4}}$ (Hz)
1	339a	5.8	9.4	4.1	7.7
2	390	5.3	8.9	-	8.9

VI. Summary

Compound **292** has proved to be a key intermediate for the synthesis of different structures, depending on the sequence employed. A one-pot Diels-Alder/allylboration cascade process has been developed to afford polycyclic products. The outcome of the reaction was directly related to the dienophile and the aldehyde used for the sequence. For the Diels-Alder reaction to proceed, a maleic structure was required, yielding stereoselectively the *endo*-isomer. Acetone, a more polar solvent, favoured the allylboration step, with the yield depending on the electronic properties of the arylaldehyde. Electron-poor substituted benzaldehydes exerted better reactivity. This process enabled the synthesis of highly functionalised products with control of four stereocenters. An interesting spirocyclic compound was obtained by using *trans*-cinnamaldehyde. Further tests, using other α,β -unsaturated aldehydes bearing electron-withdrawing groups need to be examined to see if the behaviour of the *trans*-cinnamaldehyde can be generalised. A class of novel oxazine-pyrrole fused bicyclic compounds was also

synthesised based on an allylation/RCM/arylnitroso Diels-Alder/rearrangement process. After solving the problem of polymerisation of the allylation compound by adding a radical inhibitor, the synthesis of the oxazine-pyrrole was straightforward and products were isolated up to 48% overall yield. The same sequence using the acryloyl and the propargyl protected hydroxycarbamate did not show the desired reactivity. A more in depth study of the reaction conditions for the metathesis using these substrates is required. Finally, modification of the boron substituent on compound **292** showed reserved results. Whereas the synthesis trifluoroboronated variant worked perfectly, the synthesis and purification process of the BMIDA and the DEA derivatives still needs to be improved.

Conclusions

&

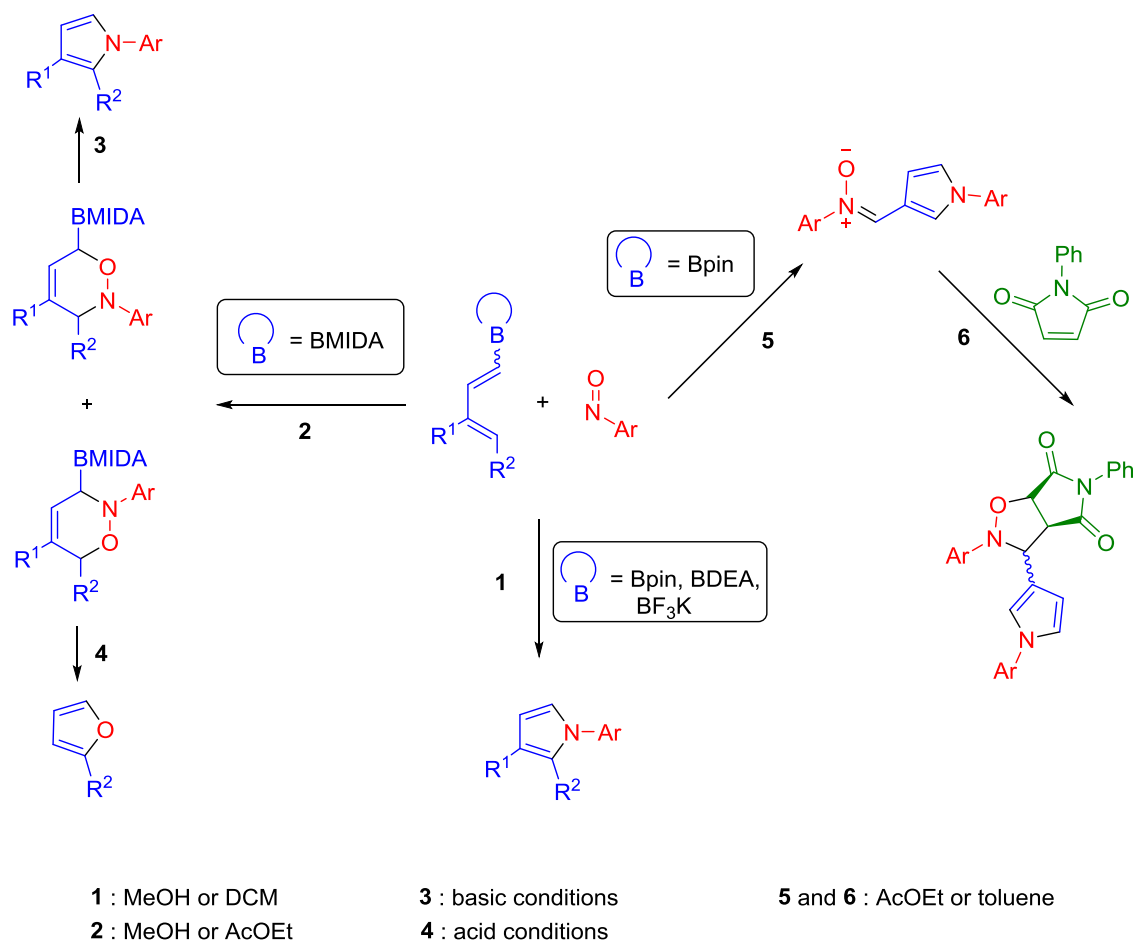
Perspectives

I. Conclusions

The chemistry of 1,3-dienylboronate compounds with aryl nitroso derivatives is driven by three major factors: the hybridisation of the boron unit; the substitution on the diene; and the solvent used for the reaction. The presence of an sp^2 -hybridised (Bpin) or a solvolysable sp^3 -hybridised (BDEA or BF_3K) borodiene led to the formation of the corresponding pyrrole. The yield of the reaction is dependent on the electronic properties and the position of the substituents on the diene. To favour the formation of the pyrrole, less electron-withdrawing boron and R^2 substituents, as well as low steric hindered R^1 and R^2 substituents were required. To isolate the oxazine derivatives resulting from a [4+2]-cycloaddition, stable sp^3 -hybridised boron moiety (BMIDA) is necessary. These cycloadducts were synthesised with a high regiocontrol toward the 1,2-boron-oxygen related adduct. The second isomer 1,3-boron-oxygen related adduct was only observed if R^2 was a phenyl moiety. NMR studies on the two different boronated MIDA ester oxazines highlighted the possibility of selective deprotection of each regioisomer depending on the structure and the media used. Furthermore, it supported the theoretical calculations for the mechanism we proposed, based on an aryl nitroso Diels-Alder/rearrangement/borate elimination cascade process.

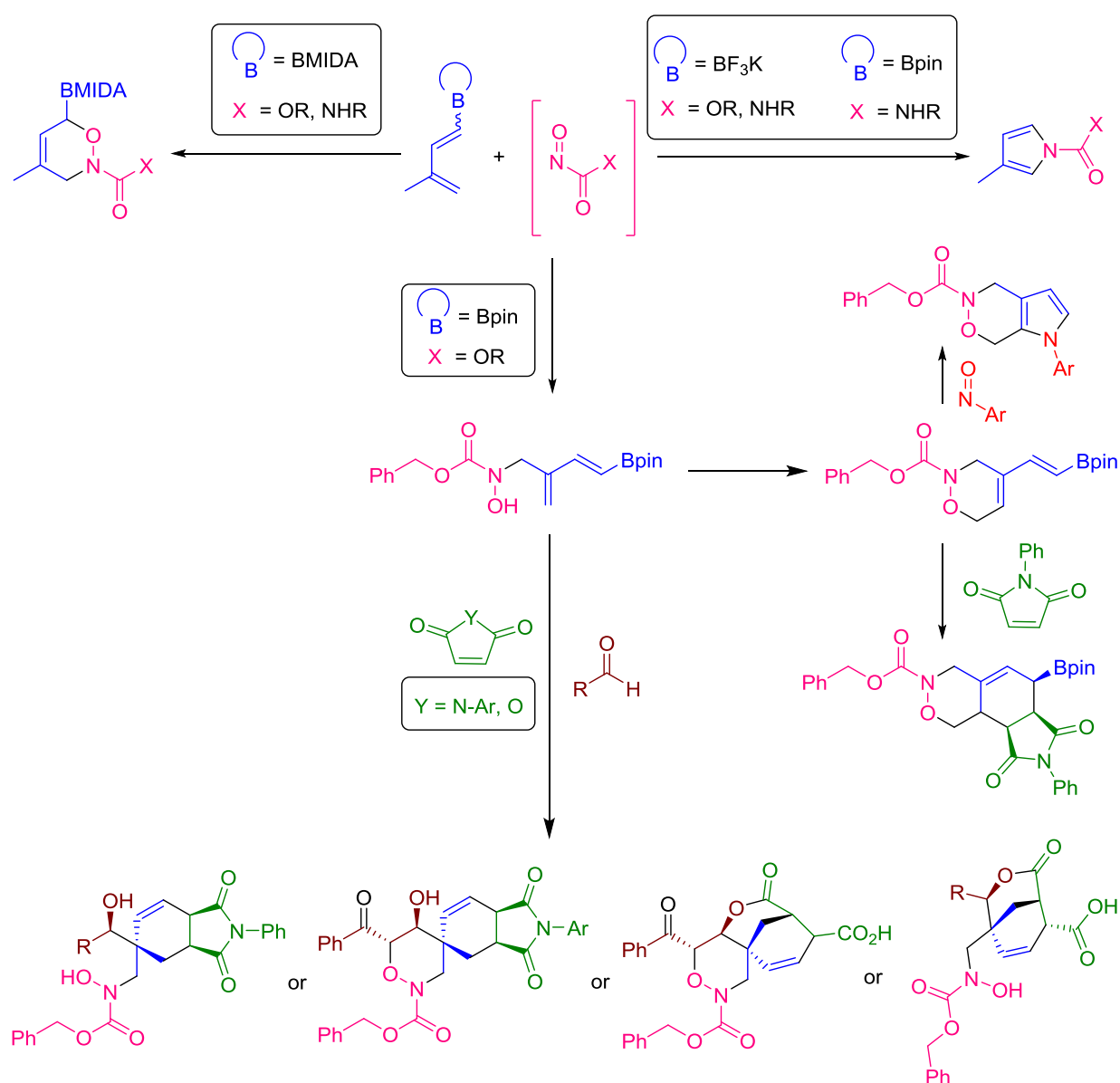
The synthesis of nitrene derivatives bearing a pyrrole unit was also achieved from pinacol 1,3-dienylboronate variant in AcOEt or toluene with excess of aryl nitroso species. First investigations to explain the outcome of the reaction have been performed. Taking advantage of the nitrene formation, a one-pot procedure nitrene/Diels-Alder sequence was used to provide highly functionalised oxazoline derivatives, albeit in modest yield.

These results are summarised in the Scheme below.



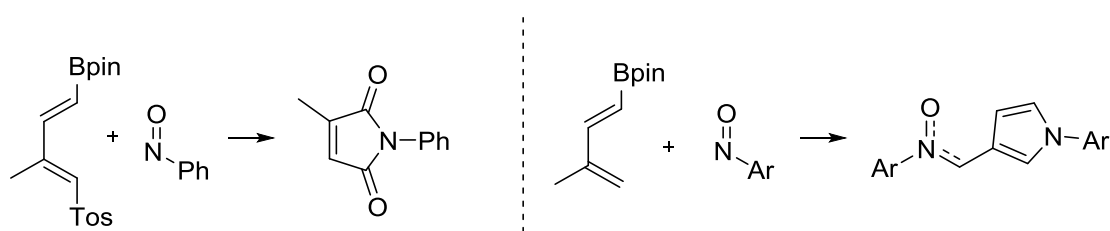
Secondly, we have examined the reactivity of 1,3-dienylboronate compounds towards carbonylnitroso derivatives. Three different scaffolds were formed according to the hybridization of the boron unit and the nature of the X substituent. The MIDA variant exerted the same regioselectivity as for aryl nitroso species. Exclusive formation of the 1,2-boron-oxygen related adduct was observed in moderate yield. When the trifluoroborate was employed, pyrrole was synthesised in moderate yield following the mechanism previously proposed. The outcome of the reaction with the Bpin variant was directly related to the substituent X. With -NHR as substituent, the pyrrole was obtained in very low yield, whereas the -OR substitution led to the formation of the ene-compound in moderate yield. The ene-

intermediate has been further used in different multi-component sequences. First, a one-pot Diels-Alder/allylboration cascade reaction has been optimised to provide polycyclic compounds depending on the nature of both the dienophile and the aldehyde. Novel oxazine-pyrrole fused bicyclic compounds were obtained using metathesis/arylnitroso Diels-Alder/ring contraction sequence. Finally the same Diels-Alder/allylboration was applied on the 1,3-boronated diene oxazine ring. Only Diels-Alder compound was obtained, no allylboration being observed.

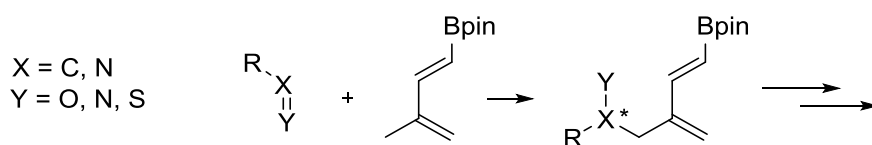


II. Perspectives

This work has shown the synthetic potential of boronated dienes with nitroso derivatives. Concerning the use of arylnitroso derivatives, whereas the pyrrole formation has been rationalised by a mechanism supported by theoretical and experimental studies, the formation of the maleimide, and the nitrono derivatives are not, or have only partially, been explained. Further investigations need to be undertaken to determine the type of mechanism involved, and the influence of each parameter responsible for these differences in reactivity. Despite the synthesis of nitrono with high synthetic potential, only 1,3-dipolar cycloaddition using *N*-phenyl maleimide worked. Yields have to be improved and a diversification of the different partners should be performed to expand the structural diversity.

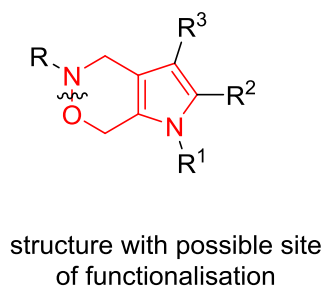
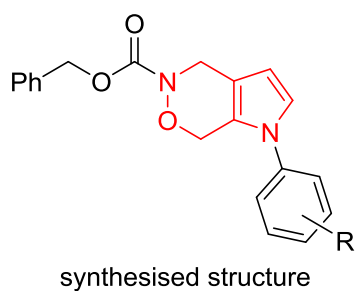


Related to the chemistry of carbonylnitroso derivatives, a highly interesting feature of this chemistry is the possibility to selectively synthesise the ene-adduct by using a strong electron-withdrawing enophile. A screening of possible enophiles has to be carried out to enlarge the range of molecules which can be synthesised. A preliminary study has been done in that sense, and ethyl glyoxylate exerted promising results. An asymmetric version of the ene-reaction could be envisaged. Further functionalisation using methodology developed for the nitroso chemistry could be used to synthesise polycyclic compounds incorporating other heterocycles (piperidine and tetrahydropyran for example).



Among the polycyclic compound synthesised within this work, the fused bicyclic oxazine-pyrrole skeleton exerted an interesting structure for potential biologically active compounds. These compounds have been selected by Eli Lilly and Co. for screening. A library of molecules could be obtained by modifying the substituents:

- R substituent; CBz deprotection, followed by chemistry on the free nitrogen (*N*-alkylation for example)
- R¹ substituent; carbonylnitroso Diels-Alder/rearrangement process to provide carbonyl moiety as R¹
- R² and R³ substituents; electrophilic substitution
- N-O cleavage



Experimental

Section

General experimental

Reagents and solvents were used as received from the supplier, unless specified otherwise. When specified, dried solvents were used; THF and toluene were distilled over sodium, benzophenone and DCM over P₂O₅, or solvents were dried over activated molecular sieves 4 Å overnight.¹⁶⁹ Reactions were monitored by TLC analysis using silica gel 60 F₂₅₄ plates. Purifications on silica gel were carried out using silica gel 0.060–0.200 mm, 60 Å.

NMR spectra were recorded on spectrometer at 300, 400, 500 or 700 MHz for ¹H, 75 or 101 MHz for ¹³C, and 96 MHz for ¹¹B. ¹H and ¹³C NMR chemical shifts were referenced relative to Me₄Si as internal reference and ¹¹B NMR chemical shifts to external BF₃·OEt₂ (0.0 ppm). Deuterated chloroform CDCl₃, DMSO-*d*⁶ or *d*⁶-acetone were used for NMR spectra. NMR data are reported as chemical shift (ppm), multiplicity (s = singlet, d = doublet, t = triplet, q = quartet, dd = doublet of doublet, ddd = doublet of doublet of doublet, dt = doublet of triplet, m = multiplet, b = broad), coupling constant *J* (Hz), and integration.

Low resolution mass spectra (LRMS) and high-resolution mass spectra (HMRS) were obtained using a Waters (UK) TQD mass spectrometer (low resolution ESI+), Waters (UK) Xevo QTOF mass spectrometer (low and high resolution ASAP+), Shimadzu QP2010-Ultra (low resolution EI) or a Waters (UK) LCT premier XE (high resolution ESI+) in Durham University, or using a Bruker MicrO-Tof-Q 2 or a Waters Q-Tof 2 at the CRMPO (Centre Régional de Mesures Physiques de l'Ouest, Rennes, France) using ESI or EI techniques. Melting points were measured using a Gallenkamp Variable Heater and reported in °C and are uncorrected.

Infrared spectra were measured on a Perkin Elmer© Spectrum Two IR Spectrometers and reported in cm⁻¹.

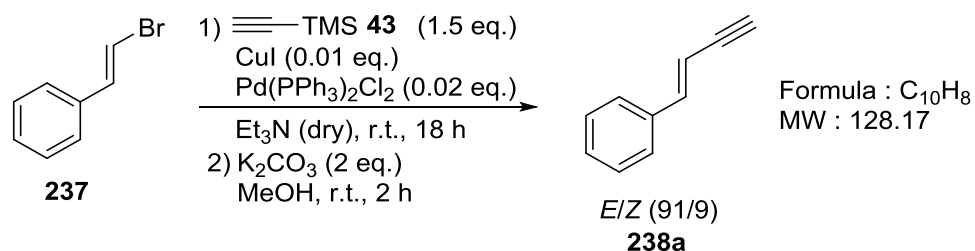
Products **252**, **259**, **264**, **276**, **277i**, **277j** and **277k** were synthesised and characterised by a previous PhD student (Dr Fabien Tripoteau). These reactions were not repeated.

All boronated MIDA ester oxazines were purified by solid phase silica gel chromatography. The crude mixture was dissolved in acetone and silica added. Acetone was cautiously evaporated to obtain a dry crude mixture adsorbed on silica. The sample was then dropped on the column.

Diene syntheses

A. Enyne hydroboration

Enyne 238a.



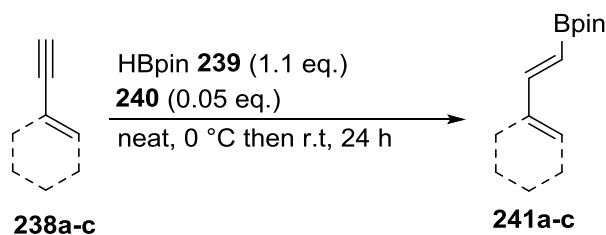
To a solution of **237** (1.6 g, 10.4 mmol) in dry Et₃N (25 mL) was added CuI (20.0 mg, 0.10 mmol) and Pd(PPh₃)₂Cl₂ (146.1 mg, 0.21 mmol). The reaction mixture was flushed with argon for 5 min. Trimethylsilylacetylene **43** (2.20 mL, 15.6 mmol) was added and the reaction mixture was stirred overnight (18 h) at room temperature. Aqueous HCl (1 M, 5 mL) was added and the crude mixture was extracted with Et₂O (3x). The organic layer was washed with water (2x), the organic layer was dried over MgSO₄, filtered and evaporated. The crude product was diluted with MeOH (5 mL) and K₂CO₃ (2.87 g, 20.8 mmol) was added and the reaction mixture was stirred for 2 h. The MeOH was evaporated and the crude mixture was diluted in Et₂O (20 mL). The organic layer was washed with brine (2x) and with H₂O (2x), dried over MgSO₄, filtered and evaporated. The crude product was purified by silica gel chromatography to afford compound **238a** in *E/Z* ratio of (91/9) as yellow oil (947.0 mg, 66%).

¹H NMR (400 MHz, Chloroform-*d*, δ ppm) 7.23 – 7.38 (m, 5H), 7.04 (d, *J* = 16.2 Hz, 1H), 6.11 (dd, *J* = 16.2, 2.4 Hz, 1H), 3.04 (d, *J* = 2.4 Hz, 1H).

¹³C NMR (101 MHz, Chloroform-*d*, δ ppm) 143.1, 135.9, 128.9, 128.7, 126.2, 107.1, 82.9, 79.2.

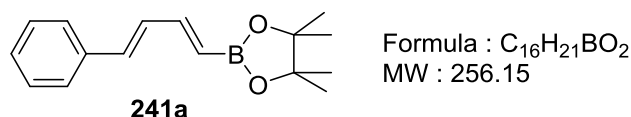
All analytical and spectroscopic properties were identical to those reported in the literature.¹⁷⁰

A.1. General procedure for the catalytic hydroboration:



To a mixture of diene **238** (1 eq.) and Schwartz catalyst **240** (0.05 eq.) at 0 °C under an inert atmosphere, was added HBpin **239** (1.1 eq.) dropwise. After addition, the reaction mixture was warmed and stirred at r.t. for 24 h. The reaction mixture was carefully diluted with Et₂O and H₂O, and stirred for 20 min. The mixture was stirred for 20 min. The aqueous layer was extracted with Et₂O (3x). The combined organic layer were then washed with brine (2x), then with H₂O (1x), and dried over MgSO₄, filtered and evaporated. The crude product was purified by either silica gel chromatography or bulb-to-bulb distillation.

Boronated pinacol ester diene **241a**.



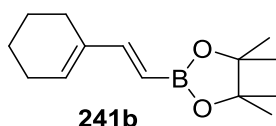
The general procedure for the catalytic hydroboration with a mixture of diene **238a** (500 mg, 3.90 mmol), Schwartz catalyst **240** (50.3 mg, 0.19 mmol) and HBpin **239** (622 μL, 4.29 mmol) afforded after silica gel chromatography, compound **241a** as a yellow oil (852.0 mg, 85%).

¹H NMR (300 MHz, Chloroform-*d*, δ ppm) 7.47 – 7.40 (m, 2H), 7.38 – 7.24 (m, 3H), 7.19 (dd, *J* = 17.6, 10.2 Hz, 1H), 6.92 – 6.80 (dd, *J* = 15.6, 10.2 Hz 1H), 6.70 (d, *J* = 15.6 Hz, 1H), 5.68 (d, *J* = 17.6 Hz, 1H), 1.30 (s, 12H).

^{13}C NMR (101 MHz, Chloroform-*d*, δ ppm) 149.8, 136.9, 136.2, 130.6, 128.7, 128.1, 126.8, 83.2, 24.8, C-B not visible.

All analytical and spectroscopic properties were identical to those reported in the literature.¹⁷¹

Boronated pinacol ester diene **241b**.



Formula : $\text{C}_{14}\text{H}_{23}\text{BO}_2$
MW : 234.15

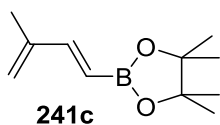
The general procedure for the catalytic hydroboration with a mixture of diene **238b** (500 mg, 4.71 mmol), Schwartz catalyst **240** (60.7 mg, 0.24 mmol) and HBpin **239** (752 μL , 5.18 mmol) afforded after silica gel chromatography, compound **241b** as a yellow oil (849.0 mg, 77%).

^1H NMR (400 MHz, Chloroform-*d*, δ ppm) 7.02 (d, $J = 18.3$ Hz, 1H), 5.98 – 5.95 (m, 1H), 5.42 (dd, $J = 18.3, 0.8$ Hz, 1H), 2.21 – 2.08 (m, 4H), 1.72 – 1.55 (m, 4H), 1.27 (s, 12H).

^{13}C NMR (101 MHz, Chloroform-*d*, δ ppm) 153.2, 137.1, 134.3, 134.2, 83.0, 26.2, 24.8, 23.7, 22.4, 22.3.

All analytical and spectroscopic properties were identical to those reported in the literature.¹⁷²

Boronated pinacol ester diene **241c**.



Formula : $\text{C}_{11}\text{H}_{19}\text{BO}_2$
MW : 194.08

The general procedure for the catalytic hydroboration with a mixture of diene **238c** (2 mL, 21.04 mmol), Schwartz catalyst **240** (271.0 mg, 1.05 mmol) and HBpin **239** (3.7 mL, 25.6 mmol) afforded after silica gel chromatography compound **241c** as a light yellow oil (3.59 g, 89%).

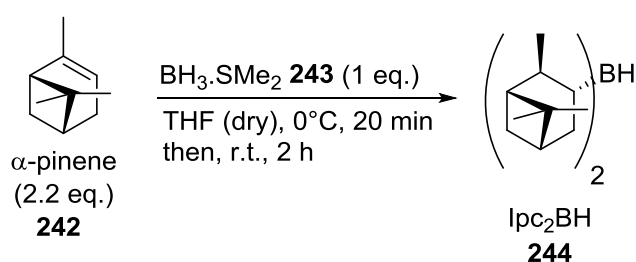
¹H NMR (400 MHz, Chloroform-*d*, δ ppm) 7.09 (d, *J* = 18.2 Hz, 1H), 5.54 (dt, *J* = 18.2, 0.6 Hz, 1H), 5.14 (tt, *J* = 1.1, 0.6 Hz, 2H), 1.83 (t, *J* = 1.1 Hz, 3H), 1.27 (s, 12H).

¹³C NMR (101 MHz, Chloroform-*d*, δ ppm) 152.3, 143.1, 120.2, 116.7, 83.3, 24.9, 17.8.

All analytical and spectroscopic properties were identical to those reported in the literature.¹⁷³

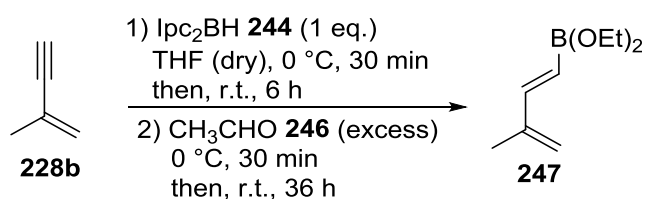
A.2. General procedure for the hydroboration using *Ipc*₂BH:

1st step: Preparation of *Ipc*₂BH **244**:



A solution of pinene **242** (2 eq.) in dry THF was cooled at 0 °C under an argon atmosphere. BH3.SMe2 **243** (1 eq.) was added and the reaction mixture was stirred at 0 °C for 15 min, then 2 h at r.t. Formation of *Ipc*₂BH **244** as a white precipitate was observed.

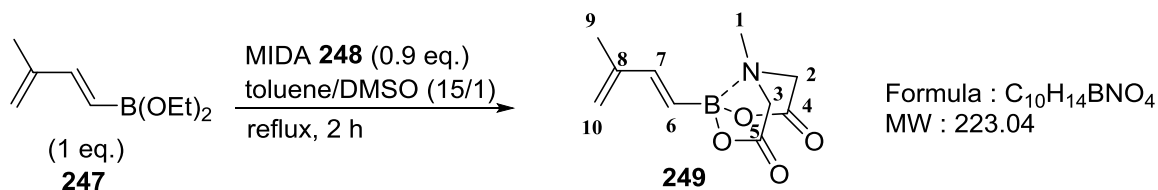
2nd step: Hydroboration:



The solution of *Ipc*₂BH **244** was cooled to 0 °C again, and 2-methyl-but-1-en-3-yne **238c** (1 eq.) was added. After stirring at 0 °C during 30 min, the solution was stirred 6 h at r.t. Freshly distilled acetaldehyde **246** (excess), was added to the solution at 0 °C, and the reaction mixture was stirred the time presented in the experimental procedure at r.t.. THF and excess of acetaldehyde were first distilled under inert atmosphere, then 1,3-dienylboronic ester intermediate **247** was distilled by bulb-to-bulb distillation. The 1,3-dienylboronic ester

intermediate **247** (1 eq.) was diluted in the solvent and at the temperature indicated in the experimental procedure.

Boronated MIDA ester diene **249**.



1st step: Pinene **242** (2.5 mL, 15.8 mmol) and $BH_3 \cdot SMe_2$ **243** (655 μ L, 7.0 mmol) in THF (2.5 mL) provided IPC_2BH **244**.

2nd step: Addition of 2-methyl-but-1-en-3-yne **238c** (655 μ L, 7.0 mmol) followed by freshly distilled acetaldehyde **246** (12 mL), afforded after bulb-to-bulb distillation intermediate **247** as a colourless oil (2.20 g, 13.1 mmol). The 1,3-dienylboronic ester intermediate **247** was diluted with a mixture of toluene/DMSO (15/1, 16 mL). MIDA **248** (1.73 g, 11.8 mmol) and phenothiazine (25 mg) as polymerisation inhibitor were added and the reaction mixture heated under an inert atmosphere at reflux for 2 h. The solution was cooled to r.t. and the white precipitate was filtered and washed with Et_2O to provide diene MIDA ester **249** as a white solid (2.40 g, 63%). ($Et_2O/MeCN$, 8/2 R_f = 0.45).

M.p. = 155 $^{\circ}C$.

1H NMR (400 MHz, Acetone- d_6 , δ ppm) 6.67 (d, J = 18.0, 1H, H_7), 5.70 (d, J = 18.0, 1H, H_6), 5.07 – 5.00 (m, 2H, H_{10}), 4.22 (d, J = 16.9 Hz, 2H, H_3 or H_2), 4.04 (d, J = 16.9 Hz, 2H, H_3 or H_2), 3.01 (s, 3H, H_1), 1.85 (dd, J = 1.4, 0.8 Hz, 3H, H_9).

^{13}C NMR (101 MHz, Acetone- d_6 , δ ppm) 169.1 (C_4 and C_5), 145.6 (C_7), 144.1 (C_8), 117.6 (C_{10}), 62.3 (C_2 and C_3), 47.4 (C_1), 18.4 (C_9), C-B not visible.

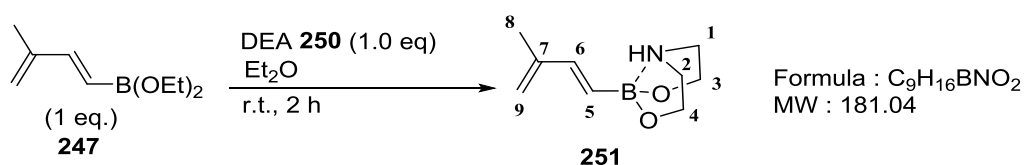
^{11}B NMR (400 MHz, Acetone- d_6 , δ ppm) 10.9.

IR (neat, ν) 1751, 1602, 1338, 1291, 1236, 1117, 1027, 999, 987, 951, 878 cm^{-1} .

LRMS (ESI+) 265.2 (26%) $[M+Na]^+$, 224.0 (100%) $[M+H]^+$.

HRMS (ESI+) calcd. for $[M+H]^+(C_{10}H_{15}NO_4^{10}B)$: 223.1130 found: 223.1114.

Boronated diethanolamine ester diene **251**.



1st step: Pinene **242** (2.2 mL, 13.9 mmol) and $BH_3 \cdot SMe_2$ **243** (650 μ L, 6.9 mmol) in THF (2.2 mL) provided IPC_2BH **244**.

2nd step: Addition of 2-methyl-but-1-en-3-yne **238c** (650 μ L, 6.9 mmol) followed by freshly distilled acetaldehyde **246** (5 mL), afforded after bulb-to-bulb distillation, intermediate **247** as colorless oil (900 mg, 5.3 mmol). The 1,3-dienylboronic ester intermediate **247** was diluted in Et_2O (8 mL). Diethanolamine **250** (875 mg, 8.3 mmol) was added and the reaction mixture was stirred until observing precipitation. The precipitate was filtered and washed with Et_2O and the solid was recrystallised from a mixture DCM/ Et_2O to provide diene DEA ester **251** as a white solid (213.3 mg, 22%).

M.p. = 166 °C.

1H NMR (400 MHz, Chloroform-*d*, δ ppm) 6.63 (d, $J = 18.0$ Hz, 1H, H_6), 5.73 (d, $J = 18.0$ Hz, 1H, H_5), 5.31 (bs, 1H, NH), 4.92 (s, 2H, H_9), 3.99 – 3.88 (m, 4H, H_4 and H_3), 3.32 – 3.21 (m, 2H, H_2 or H_1), 2.81 – 2.68 (m, 2H, H_2 or H_1), 1.83 (s, 3H, H_8).

^{13}C NMR (101 MHz, Chloroform-*d*, δ ppm) 144.0 (C_7), 142.0 (C_6), 115.2 (C_9), 63.3 (C_3 and C_4), 51.5 (C_1 and C_2), 18.6 (C_8), C-B not visible.

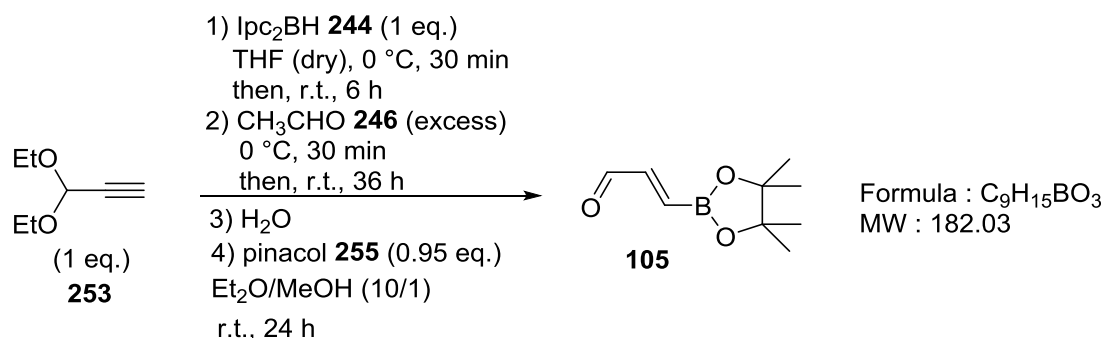
^{11}B NMR (400 MHz, Chloroform-*d*, δ ppm) 10.7.

IR (neat, ν) 3092, 1592, 1283, 1231, 1136, 1110, 1007, 995, 887, 870, 785 cm^{-1} .

LRMS (TOF ASAP+) 182.1 (100%) $[M+H]^+$, 114.1 (40%).

HRMS (TOF ASAP+) calcd. for $[M+H]^+(C_9H_{17}NO_2^{10}B)$: 181.1389 found: 181.1385.

Boronated pinacol ester acrolein **105**.



1st step: Pinene **242** (11.3 mL, 70.5 mmol) and BH₃SMe₂ **243** (3.3 mL, 35.5 mmol) in THF (11.5 mL) provided Ipc₂BH **244**.

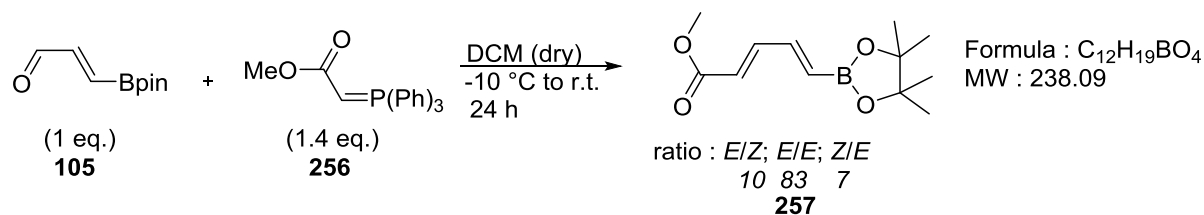
2nd step: Addition of alkyne **253** (5.1 mL, 35.5 mmol) was followed by freshly distilled acetaldehyde **246** (20 mL). After removing THF and excess of acetaldehyde, H₂O (5 mL) was added and the mixture stirred for 1.5 h at room temperature. Excess pinene was then removed using high vacuum and the crude mixture extracted with a mixture Et₂O/AcOEt (1/1, 3x). The organic layer was dried over MgSO₄, filtered and evaporated until precipitation started to be observed. Pentane (10 mL) was added and the mixture was stirred for 1 h. The solid was filtered and washed with pentane (2x) to afford boronic acid **254** as pale yellow powder (1.66 g, 47%). A solution of pinacol **255** (576.0 mg, 4.9 mmol) in a mixture of Et₂O/MeOH (9/1, 8 mL) was added to boronic acid **254** (500.0 mg, 5.0 mmol). The reaction mixture was stirred overnight (16 h) and cyclohexane (20 mL) was added to the mixture. The organic layer was washed with brine (2x), then dried over MgSO₄, filtered and evaporated. The crude product was purified by bulb-to-bulb distillation to afford compound **105** as a colorless oil (437.0 mg, 49%).

¹H NMR (400 MHz, Chloroform-*d*, δ ppm) 9.60 (d, *J* = 7.5 Hz, 1H), 6.81 (dd, *J* = 18.1, 7.5 Hz, 1H), 6.65 (d, *J* = 18.1 Hz, 1H), 1.30 (s, 12H).

¹³C NMR (75 MHz, Chloroform-*d*, δ ppm) 195.0, 147.7, 147.0, 84.4, 24.8.

All analytical and spectroscopic properties were identical to those reported in the literature.¹⁷⁴

Boronated pinacol ester diene **257**.



A solution of compound **105** (164.5 mg, 0.91 mmol) and ylide **256** (424.2 mg, 1.27 mmol) in dry DCM (6 mL) was stirred under an inert atmosphere at -10 °C for 30 min, then at r.t. for 24 h. Solvent was evaporated and the crude was purified by bulb-to-bulb distillation to afford compound **257** as a mixture of 3 isomers (*E,E,E,Z,Z,E* = 83:10:7) (175.0 mg, 81%).

¹H NMR (300 MHz, Chloroform-*d*, δ ppm) (*E,E* major isomer) 7.26 (ddd, *J* = 15.1, 10.9, 0.8 Hz, 1H), 7.03 (ddd, *J* = 17.5, 10.9, 0.4 Hz, 1H), 6.02 – 5.91 (m, 2H), 3.74 (s, 3H), 1.27 (s, 12H).

¹H NMR (300 MHz, Chloroform-*d*, δ ppm) (*E,Z* minor isomer) 8.11 (ddd, *J* = 17.7, 11.1, 1.1 Hz, 1H), 6.59 (td, *J* = 11.1, 0.9 Hz, 1H), 5.91 – 5.73 (m, 2H), 3.73 (s, 3H), 1.26 (s, 12H).

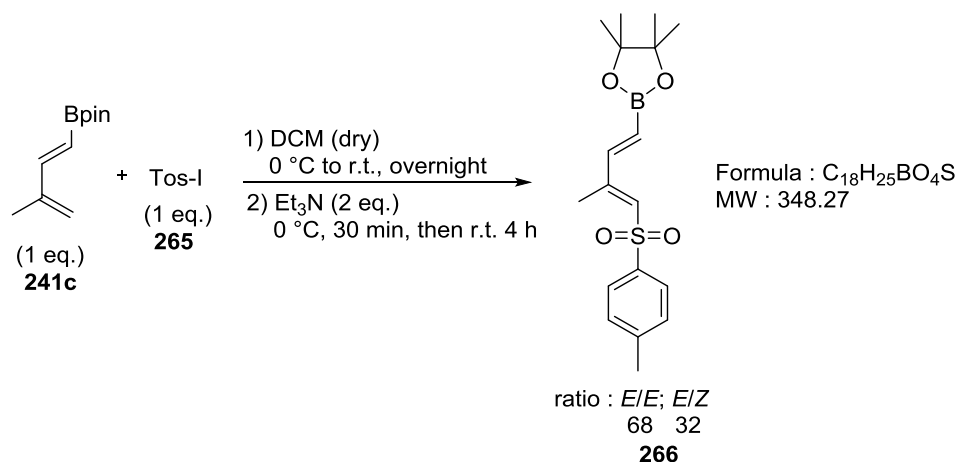
¹H NMR (300 MHz, Chloroform-*d*, δ ppm) (*Z,E* minor isomer) 8.02 (ddd, *J* = 15.4, 11.5, 0.9 Hz, 1H), 6.47 (dd, *J* = 17.9, 6.4 Hz, 1H), 6.00 – 5.91 (m, 1H), 5.31 (dd, *J* = 6.4, 0.9 Hz, 1H), 3.75 (s, 3H), 1.27 (s, 12H).

¹³C NMR (75 MHz, Chloroform-*d*, δ ppm) (*E,E* major isomer) 167.6, 146.2, 143.5, 122.8, 83.2, 51.8, 24.7, C-B not visible.

All analytical and spectroscopic properties were identical to those reported in the literature.¹¹⁹

B. Halosulfonylation of 1,3-dienylboronic ester **241c**

Boronated pinacol ester diene **266**.



A solution of diene **241c** (175.0 mg, 0.90 mmol) in dry DCM (12 mL) under an inert atmosphere was cooled to 0 °C. Tosyl iodide **265** (255.0 mg, 0.90 mmol) was added and the reaction mixture stirred at r.t. overnight (18 h). The reaction mixture was cooled to 0 °C and Et₃N (252 μL, 1.81 mmol) added dropwise. The reaction mixture was stirred for 4 h at r.t., the crude was washed with H₂O (2x). The organic layer was dried over MgSO₄, filtered and evaporated. The crude product was purified by silica gel chromatography to afford diene **266** as a mixture of 2 isomers (*E,E*:*E,Z* = 68:32) (125.2 mg, 43%).

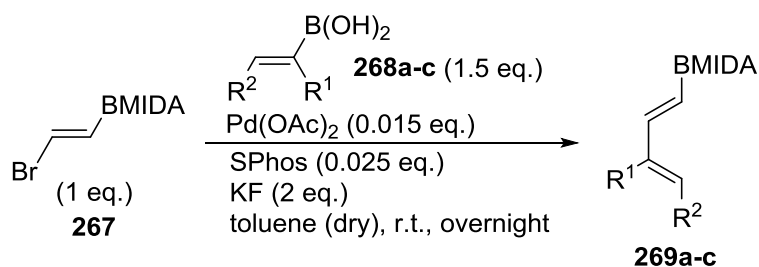
¹H NMR (300 MHz, Chloroform-*d*, δ ppm) (*E,E* major isomer) 7.73 – 7.68 (m, 2H), 7.29 – 7.21 (m, 2H), 6.81 (dd, *J* = 18.1, 0.7 Hz, 1H), 6.33 – 6.32 (m, 1H), 5.93 (dd, *J* = 18.1, 0.3 Hz, 1H), 2.35 (s, 3H), 2.14 (d, *J* = 1.2 Hz, 3H), 1.18 (s, 12H).

¹H NMR (300 MHz, Chloroform-*d*, δ ppm) (*E,Z* minor isomer) 8.15 (dd, *J* = 18.2, 0.9 Hz, 1H), 7.77 – 7.73 (m, 2H), 7.30 – 7.21 (m, 2H), 6.20 – 6.19 (m, 1H), 5.89 (dd, *J* = 18.2, 0.7 Hz, 1H), 2.35 (s, 3H), 1.88 (d, *J* = 1.3 Hz, 3H), 1.22 (s, 12H).

¹³C NMR (75 MHz, Chloroform-*d*, δ ppm) (*E,E* and *E,Z* isomers) 149.5, 148.9, 147.8, 144.3, 144.1, 142.1, 139.2, 139.1, 132.3, 129.9, 129.8, 129.7, 127.6, 127.3, 83.9, 83.8, 24.9, 24.8, 24.6, 21.6, 20.3, 12.5, C-B not visible.

All analytical and spectroscopic properties were identical to those reported in the literature.¹²¹

C. Coupling reaction of vinylboronic acid MIDA ester derivatives



C.1. General procedure for the Suzuki-Miyaura cross-coupling:

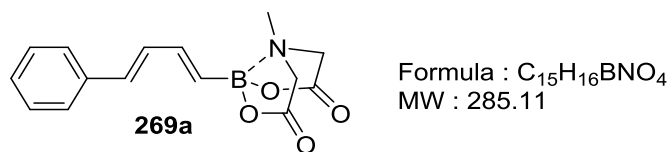
1st step: Catalyst preparation:

SPhos (0.025 eq.) and Pd(OAc)₂ (0.015 eq.) were stirred for 45 min at r.t. under an inert atmosphere in dry toluene.

2nd step: Cross-coupling reaction:

Trans-2-bromovinylboronic acid MIDA ester **267** (1 eq.), boronic acid **268a-c** (1.5 eq.) and KF (2 eq.) were suspended in dry toluene under an inert atmosphere. The catalyst solution was added to the mixture and the reaction was stirred at r.t. overnight (18 h). The solvent was evaporated and the crude product was solubilised in acetone and filtered through a pad of celite/silica. The filtrate was evaporated to give the product.

Boronated MIDA ester diene **269a**.



1st step: SPhos (12.0 mg, 0.029 mmol) and Pd(OAc)₂ (4.0 mg, 0.017 mmol) in dry toluene (2 mL) provided the catalyst solution.

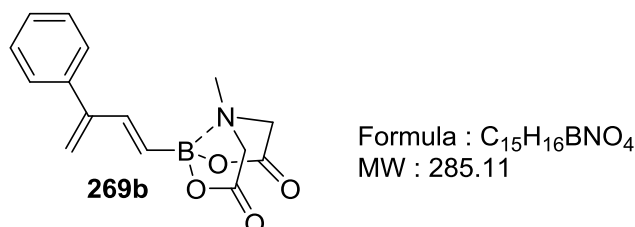
2nd step: *Trans*-2-Bromovinylboronic acid MIDA ester **267** (300.0 mg, 1.15 mmol), *trans*-2-phenylvinylboronic acid **268a** (255.0 mg, 1.72 mmol), KF (133.1 mg, 2.30 mmol) and the catalyst solution provided a full conversion of the starting material. The product **269a** was isolated as a yellow solid (248.3 mg, 76%).

¹H NMR (400 MHz, Acetone-*d*₆, δ ppm) 7.51 – 7.46 (m, 2H), 7.36 – 7.31 (m, 2H), 7.27 – 7.21 (m, 1H), 6.94 (ddd, *J* = 15.6, 10.3, 0.8 Hz, 1H), 6.75 (dd, *J* = 17.3, 10.3 Hz, 1H), 6.67 (d, *J* = 15.6 Hz, 1H), 5.84 (d, *J* = 17.3 Hz, 1H), 4.24 (d, *J* = 16.9 Hz, 2H), 4.06 (d, *J* = 16.9 Hz, 2H), 3.04 (s, 3H).

¹³C NMR (101 MHz, Acetone-*d*₆, δ ppm) 169.1, 143.5, 138.2, 134.0, 131.9, 129.5, 128.5, 127.3, 62.3, 47.4, C-B not visible.

All analytical and spectroscopic properties were identical to those reported in the literature.¹²²

Boronated MIDA ester diene **269b**.



1st step: SPhos (9.2 mg, 0.023 mmol) and Pd(OAc)₂ (3.0 mg, 0.014 mmol) in dry toluene (2 mL) provided the catalyst solution.

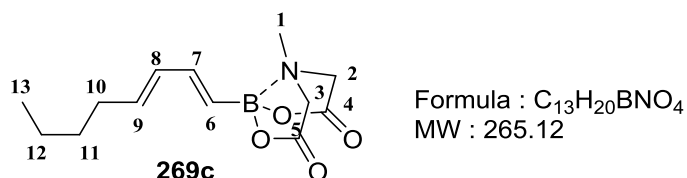
2nd step: *Trans*-2-bromovinylboronic acid MIDA ester **267** (236.0 mg, 0.90 mmol), 1-phenylvinylboronic acid **268b** (200.0 mg, 1.35 mmol), KF (105.1 mg, 1.80 mmol) and the catalyst solution provided a full conversion of the starting material. The product **269b** was isolated as yellow solid (168.2 mg, 68%).

¹H NMR (400 MHz, Acetone-*d*₆, δ ppm) 7.41 – 7.27 (m, 5H), 6.87 (d, *J* = 17.8 Hz, 1H), 5.68 (d, *J* = 17.8 Hz, 1H), 5.22 (d, *J* = 1.9 Hz, 1H), 4.22 (d, *J* = 16.9 Hz, 2H), 4.06 (d, *J* = 16.9 Hz, 2H), 3.01 (s, 3H).

¹³C NMR (101 MHz, Acetone-*d*₆, δ ppm) 169.0, 150.3, 144.2, 141.1, 129.1, 129.0, 128.3, 117.7, 62.5, 47.5, C-B not visible.

All analytical and spectroscopic properties were identical to those reported in the literature.¹²²

Boronated MIDA ester diene **269c**.



1st step: SPhos (9.2 mg, 0.023 mmol) and Pd(OAc)₂ (3.0 mg, 0.014 mmol) in dry toluene (2 mL) provided the catalyst solution.

2nd step: *Trans*-2-bromovinylboronic acid MIDA ester **267** (250.0 mg, 0.95 mmol), boronic acid **268c** (183.0 mg, 1.43 mmol), KF (111.4 mg, 1.91 mmol) and the catalyst solution provided after 48 h a 63% conversion of the starting *trans*-2-bromovinylboronic acid MIDA ester **267**. The crude was filtrated through celite and eluted with acetone (250 mL), evaporated and purified by silica gel chromatography using the solid sample method to afford two fractions. The first fraction was pure diene **269c** obtained as a white solid (48 mg) and the second was as a mixture of diene **269c** and starting material **367** (68/32, 115 mg). Total mass of desired diene **269c** (126.2 mg, 50%).

M.p. = 122 °C.

^1H NMR (400 MHz, Acetone- d_6 , δ ppm) 6.53 (dd, $J = 17.5, 10.2$ Hz, 1H, H₇), 6.18 – 6.07 (m, 1H, H₈), 5.81 – 5.72 (m, 1H, H₉), 5.54 (d, $J = 17.5$ Hz, 1H, H₆), 4.19 (d, $J = 16.8$ Hz, 2H, H₂ or H₃), 4.01 (d, $J = 16.8$ Hz, 2H, H₂ or H₃), 2.98 (s, 3H, H₁), 2.13 – 2.07 (m, 2H, H₁₀), 1.45 – 1.27 (m, 4H, H₁₂ and H₁₁), 0.89 (t, $J = 7.2$ Hz, 3H, H₁₃).

^{13}C NMR (101 MHz, Acetone- d_6 , δ ppm) 169.1 (C₅ and C₄), 143.7 (C₇), 136.4 (C₉), 133.6 (C₈), 62.2 (C₃ and C₂), 47.3 (C₁), 32.9 (C₁₀), 32.1 (C₁₁), 22.9 (C₁₂), 14.1 (C₁₃), C-B not visible.

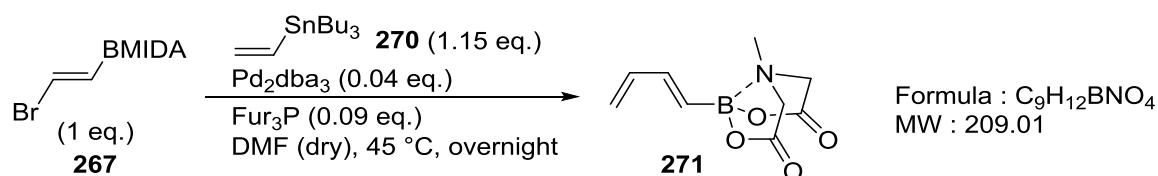
^{11}B NMR (96 MHz, Acetone- d_6 , δ ppm) 10.8.

LRMS (ESI+) 265.1 (100%) [M+H]⁺.

HRMS (ESI+) calcd. for C₁₃H₂₁¹⁰BNO₄ [M+H]⁺: 265.1485 found: 265.1484.

C.2. Stille cross-coupling:

Boronated MIDA ester diene 271.



Trans-2-bromovinylboronic acid MIDA ester **267** (262.0 mg, 1.00 mmol), Pd_2dba_3 (37.1 mg, 0.04 mmol), and Fur_3P (21.0 mg, 0.09 mmol) were dissolved under an inert atmosphere in dry DMF (8 mL). Tributylvinyltin **270** (346 μL , 1.15 mmol) was added and the reaction mixture stirred at 45 °C overnight (18 h). The DMF was removed by bulb-to-bulb distillation to afford a sticky black solid. The crude product was dissolved in AcOEt, filtered through a pad of Celite and rinsed with AcOEt several times. The filtrate was evaporated providing a biphasic (oil/liquid) mixture. The solvent liquid layer was separated by decanting and the residual oil was rinsed with Et₂O and separated again, by decanting until a colorless Et₂O washing solution was obtained. The remaining oil/solid was stirred overnight (16 h) in a mixture

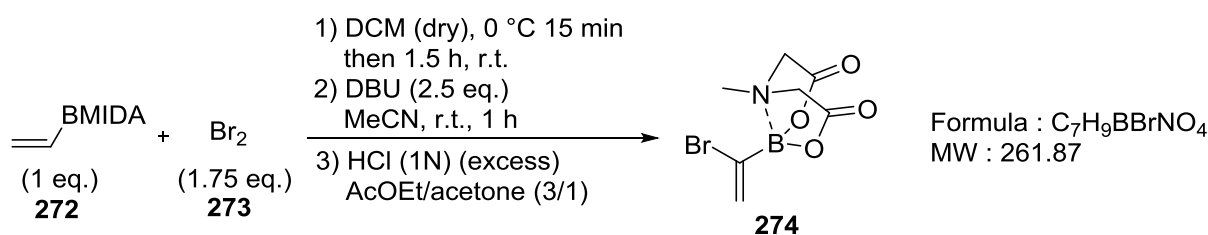
DCM/Et₂O (1/7, 24 mL). The resulting precipitate was filtered and washed with Et₂O (3x) to afford compound **271** as a light brown solid (140.2 mg, 67%).

¹H NMR (400 MHz, Acetonitrile-*d*₃, δ ppm) 6.56 (dd, *J* = 17.5, 10.5 Hz, 1H), 6.43 (dtd, *J* = 17.0, 10.0, 0.5 Hz, 1H), 5.66 (dd, *J* = 17.5, 0.5 Hz, 1H), 5.28 (ddt, *J* = 17.0, 2.0, 0.5 Hz, 1H), 5.14 (ddt, *J* = 10.0, 2.0, 0.5 Hz, 1H), 3.96 (d, *J* = 17.0 Hz, 2H), 3.79 (d, *J* = 17.0 Hz, 2H), 2.76 (s, 3H).

¹³C NMR (101 MHz, Acetonitrile-*d*₃, δ ppm) 169.5, 144.3, 119.0, 62.3, 47.6.

All analytical and spectroscopic properties were identical to those reported in the literature.¹²²

Vinyl boronated MIDA ester **274**.



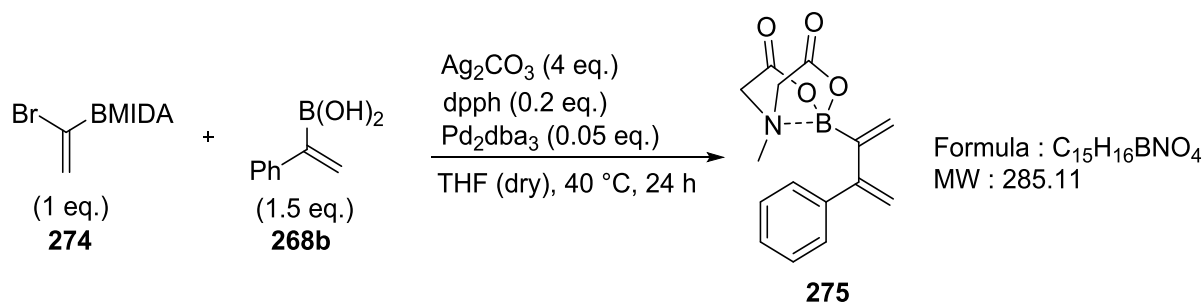
To a solution of vinylboronic MIDA ester **272** (2.0 g, 10.9 mmol) in dry DCM (10 mL) at 0 °C was added neat bromine **273** (1 mL, 19.1 mmol) drpwise. The reaction mixture was stirred at r.t. for 1.5 h. The excess of bromine and DCM were carefully removed by evaporation under a fume hood. DCM (10 mL) was added and re-evaporated (azeotropes bromine). The crude product was dissolved in MeCN (8 mL) and DBU (4.2 g, 27.3 mmol) was added in one portion at r.t. The reaction mixture was stirred for 1.5 h, aqueous HCl (1 M, 8 mL) was added and the mixture stirred for 15 min. The crude product was extracted with a mixture of AcOEt/acetone (3/1, 3x), and the organic layer was washed with a mixture of sodium metabisulfite/brine (3/2, 2x), then brine. The organic layer was dried over MgSO₄, filtered and evaporated until the formation of a precipitate was observed. Et₂O (80 mL) was added and the mixture was stirred overnight. The precipitate was filtered and washed with Et₂O (2x) to afford compound **274** as white powder (1.46 g, 51%).

¹H NMR (400 MHz, Acetone-*d*₆, δ ppm) 6.39 (d, *J* = 1.4 Hz, 1H), 6.19 (bs, 1H), 4.37 (d, *J* = 17.0 Hz, 2H), 4.16 (d, *J* = 17.0 Hz, 2H), 3.16 (s, 3H).

¹³C NMR (101 MHz, Acetone-*d*₆, δ ppm) 168.4, 129.6, 63.5, 47.3, C-B not visible.

All analytical and spectroscopic properties were identical to those reported in the literature.¹²³

Boronated MIDA ester diene **275**.



1st step: dpph (139.0 mg, 0.31 mmol) and Pd_2dba_3 (70.1 mg, 0.077 mmol) were stirred for 30 min at r.t. under an inert atmosphere in dry THF.

2nd step: Compound **274** (400.0 mg, 1.53 mmol), 1-phenylvinylboronic acid **268b** (340.2 mg, 2.29 mmol) and Ag_2CO_3 (1.69 g, 6.12 mmol) were suspended in dry THF (8 mL) under an inert atmosphere. The catalyst solution was added to the reaction and the mixture was stirred at 40 °C for 24 h. The crude product was purified filtered through a pad of Celite and washed with MeCN (200 mL). The filtrate was evaporated and purified by silica gel chromatography using the solid sample method to provide a mixture of diene **275** and starting material **274** (70/30, 343 mg). Mass total of desired diene **275** (240.1 mg, 55%).

¹H NMR (400 MHz, Acetone-*d*₆, δ ppm) 7.42 – 7.21 (m, 5H), 5.74 (d, *J* = 3.7 Hz, 1H), 5.64 – 5.61 (m, 1H), 5.27 (d, *J* = 1.8 Hz, 1H), 5.25 (d, *J* = 1.8 Hz, 1H), 4.21 – 4.15 (d, *J* = 16.9 Hz, 2H), 3.92 (d, *J* = 16.9 Hz, 2H), 3.08 (s, 3H).

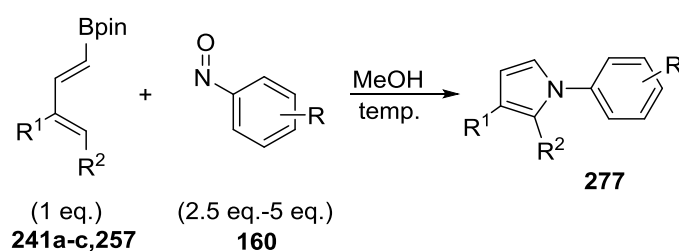
¹³C NMR (101 MHz, Acetone-*d*₆, δ ppm) 168.7, 154.6, 142.4, 129.1, 128.8, 128.3, 128.2, 114.0, 62.8, 47.5, C-B not visible.

All analytical and spectroscopic properties were identical to those reported in the literature.¹²³

Boronated dienes and aryl nitroso compounds

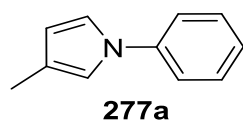
A. Reaction of 1-dienylboronate pinacolate esters with aryl nitroso compounds

General procedure:



To a solution of diene (1 eq) (pinacol boronate) in a solvent, was added aryl nitroso **160** (2.5 to 5 eq). The reaction mixture was stirred as indicated in the experimental procedure. The solvent was evaporated and the crude product was purified by silica gel chromatography.

Pyrrole **277a**.



Formula : C₁₁H₁₁N
MW : 157.22

Diene **241c** (21 mg, 0.11 mmol) and nitrosobenzene **160a** (29 mg, 0.27 mmol) were stirred in MeOH (1 mL) at r.t. for 5 h. The crude product was purified by silica gel chromatography (eluent, hexane/EtOAc, 9/1, R_f = 0.75) to afford compound **277a** (14.0 mg, 96%).

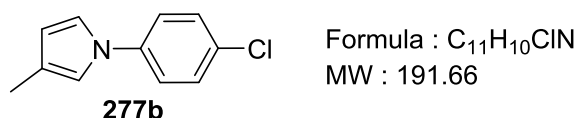
¹H NMR (400 MHz, Chloroform-*d*, δ ppm) 7.39 – 7.24 (m, 4H), 7.16-7.10 (m, 1H), 6.92 (t, *J* = 2.5 Hz, 1H), 6.81 – 6.79 (m, 1H), 6.11 (t, *J* = 2.5 Hz, 1H), 2.10 (s, 3H).

¹³C NMR (101 MHz, Chloroform-*d*, δ ppm) 140.8, 129.5, 125.1, 121.1, 120.0, 118.9, 117.1, 112.0, 12.0.

All analytical and spectroscopic properties were identical to those reported in the literature.¹³⁹

175

Pyrrole 277b.



Diene **241c** (21 mg, 0.11 mmol) and 4-chloronitrosobenzene **160b** (39 mg, 0.27 mmol) were stirred in MeOH (2 mL) at r.t. for 5 h. The crude product was purified by silica gel chromatography (eluent, hexane/EtOAc, 9/1, R_f = 0.9) to afford compound **277b** (15.1 mg, 68%).

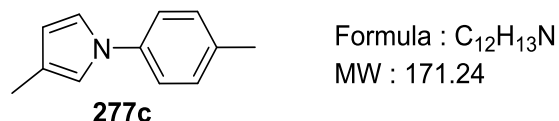
¹H NMR (400 MHz, Chloroform-*d*, δ ppm) 7.28 (d, *J* = 9.0 Hz, 2H), 7.19 (d, *J* = 9.0 Hz, 2H), 6.87 (t, *J* = 2.6 Hz, 1H), 6.74 – 6.73 (m, 1H), 6.11 (t, *J* = 2.4 Hz, 1H), 2.08 (s, 3H).

¹³C NMR (101 MHz, Chloroform-*d*, δ ppm) 139.3, 130.4, 129.5, 121.6, 121.0, 118.9, 117.0, 12.4, 11.9.

All analytical and spectroscopic properties were identical to those reported in the literature.¹³⁹

176

Pyrrole 277c.



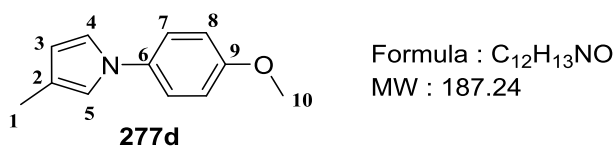
Diene **241c** (30 mg, 0.17 mmol) and 4-nitrosotoluene **160c** (52 mg, 0.43 mmol) were stirred in MeOH (1 mL) at r.t. for 5 h. The crude product was purified by silica gel chromatography (eluent, hexane/EtOAc, 9/1, R_f = 0.80) to afford compound **277c** (23.0 mg, 60%).

¹H NMR (400 MHz, Chloroform-*d*, δ ppm) 7.19 – 7.07 (m, 4H), 6.88 (t, *J* = 2.5 Hz, 1H), 6.78-6.76 (m, 1H), 6.08 (dd, *J* = 2.3, 2.1 Hz, 1H), 2.28 (s, 3H), 2.09 (s, 3H).

¹³C NMR (101 MHz, Chloroform-*d*, δ ppm) 138.5, 134.8, 130.0, 120.8, 120.0, 119.0, 117.3, 111.6, 20.8, 12.0.

All analytical and spectroscopic properties were identical to those reported in the literature.¹³⁹
177

Pyrrole **277d**.



Diene **241c** (28 mg, 0.16 mmol) and 4-methoxynitrosobenzene **160d** (55 mg, 0.4 mmol) were stirred in MeOH (1 mL) at r.t. for 5 h. The crude product was purified by silica gel chromatography (eluent, hexane/EtOAc, 9/1, R_f = 0.75) to afford compound **277d** as a white solid (23.0 mg, 77%).

M.p. = 86 °C.

¹H NMR (400 MHz, Chloroform-*d*, δ ppm) 7.19 (d, *J* = 9.0 Hz, 2H, H₇), 6.85 (d, *J* = 9.0 Hz, 2H, H₈), 6.82 (t, *J* = 2.4 Hz, 1H, H₄), 6.71 - 6.69 (m, 1H, H₅), 6.07 (t, *J* = 2.4 Hz, 1H, H₃), 3.75 (s, 3H, H₁₀), 2.09 (s, 3H, H₁).

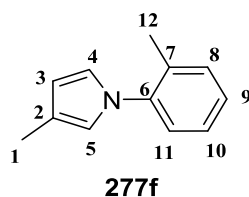
¹³C NMR (101 MHz, Chloroform-*d*, δ ppm) 157.3 (C₉), 134.6 (C₆), 121.7 (C₇), 120.6 (C₂), 119.3 (C₄), 117.6 (C₅), 114.6 (C₈), 111.3 (C₃), 55.6 (C₁₀), 12.0 (C₁).

IR (neat, ν) 1516, 1456, 1442, 1253, 1243, 1109, 1029, 822, 754, 606 cm⁻¹.

GCMS (EI) 187.1 (100%) [M]⁺, 172.1 (55%) [M-CH₄]⁺.

HRMS (ESI+) calcd. for C₁₂H₁₄NO [M+H]⁺: 188.1075 found: 188.1074.

Pyrrole 277f.



Formula : C₁₂H₁₃N
MW : 171.24

Diene **241c** (30 mg, 0.17 mmol) and 2-nitrosotoluene **160f** (52 mg, 0.43 mmol) were stirred in MeOH (1 mL) at r.t. for 5 h. The crude product was purified by silica gel chromatography (eluent, hexane/EtOAc, 9/1, R_f = 0.8) to afford compound **277f** as a yellow oil (20.2 mg, 69%).

¹H NMR (400 MHz, Chloroform-*d*, δ ppm) 7.25-7.09 (m, 4H, H₈, H₉, H₁₀ and H₁₁), 6.60 (t, *J* = 2.2 Hz, 1H, H₄), 6.50 - 6.47 (m, 1H, H₅), 6.06 (t, *J* = 2.2 Hz, 1H, H₃), 2.15 (s, 3H, H₁₂), 2.10 (s, 3H, H₁).

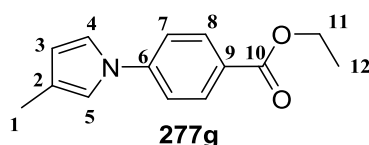
¹³C NMR (101 MHz, Chloroform-*d*, δ ppm) 140.8 (C₆), 133.6 (C₇), 131.1 (C₈), 127.1 (C₁₁), 126.5 (C₉ and C₁₀), 121.9 (C₄), 120.0 (C₅), 119.3 (C₂), 110.2 (C₃), 18.0 (C₁₂), 11.9 (C₁).

IR (neat, ν) 1503, 1461, 1384, 1116, 1069, 938, 760, 718, 620 cm⁻¹.

GCMS (EI) 171.0 (100%) [M]⁺, 156.1 (45%) [M-CH₃]⁺.

HRMS (ESI+) calcd. for C₁₂H₁₄N [M+H]⁺: 172.1126 found: 172.1126.

Pyrrole 277g.



Formula : C₁₄H₁₅NO₂
MW : 229.28

Diene **241c** (31 mg, 0.16 mmol) and ethyl 4-nitrosobenzoate **160g** (72 mg, 0.40 mmol) were stirred in MeOH (1 mL) at r.t. for 5 h. The crude product was purified by silica gel chromatography (eluent, hexane/EtOAc 9/1, R_f = 0.65) to afford compound **277g** as a white solid (21.1 mg, 57%).

M.p. = 88 °C.

¹H NMR (400 MHz, Chloroform-*d*, δ ppm) 8.09 (d, *J* = 8.9 Hz, 2H, H₈), 7.40 (d, *J* = 8.9 Hz, 2H, H₇), 7.07 (t, *J* = 2.4 Hz, 1H, H₄), 6.95 - 6.93 (m, 1H, H₅), 6.21 (dd, *J* = 2.4, 1.8, Hz, 1H, H₃), 4.36 (q, *J* = 7.1 Hz, 2H, H₁₁), 2.15 (s, 3H, H₁), 1.39 (t, *J* = 7.1 Hz, 3H, H₁₂).

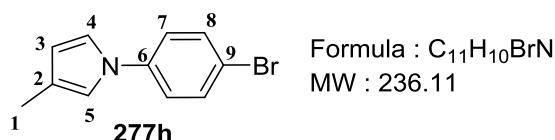
¹³C NMR (101 MHz, Chloroform-*d*, δ ppm) 166.0 (C₁₀), 143.9 (C₆), 131.2 (C₈), 126.7 (C₉), 122.3 (C₂), 118.6 (C₇), 116.7 (C₅), 113.1 (C₃), 61.0 (C₁₁), 14.3 (C₁₂), 12.0 (C₁).

IR (neat, ν) 1708, 1610, 1526, 1350, 1277, 1268, 1220, 1186, 1111, 1062, 842, 767, 751, 601 cm⁻¹.

GCMS (EI) 229.1 (100%) [M]⁺, 200.0 (30%) [M-C₂H₆].

HRMS (ESI+) calcd. for C₁₄H₁₅NO₂Na [M+Na]⁺: 252.1000 found: 252.1001.

Pyrrole **277h**.



Diene **241c** (20 mg, 0.1 mmol) and 4-bromonitrosobenzene **160h** (48 mg, 0.25 mmol) were stirred in MeOH (2 mL) at r.t. for 5 h. The crude product was purified by silica gel chromatography (eluent, hexane/EtOAc, 9/1, R_f = 0.9) to afford compound **277h** as a pale yellow solid (16.2 mg, 65%).

M.p. = 89 °C.

¹H NMR (400 MHz, Chloroform-*d*, δ ppm) 7.43 (d, *J* = 8.9 Hz, 2H, H₈), 7.14 (d, *J* = 8.9 Hz, 2H, H₇), 6.87 (t, *J* = 2.6 Hz, 1H, H₄), 6.76 - 6.73 (m, 1H, H₅), 6.11 (t, *J* = 2.2 Hz, 1H, H₃), 2.08 (s, 3H, H₁).

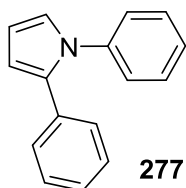
¹³C NMR (101 MHz, Chloroform-*d*, δ ppm) 139.8 (C₆), 132.5 (C₈), 121.7 (C₂), 121.4 (C₇), 118.8 (C₄), 118.1 (C₉), 117.0 (C₅), 112.5 (C₃), 11.9 (C₁).

IR (neat, ν) 1596, 1501, 1466, 1346, 1221, 1081, 1005, 930, 816, 756, 615, 509 cm⁻¹.

GCMS (EI) 237.0 (97%) [M+2], 235.0 (100%) [M]⁺, 155.1 (22%).

HRMS (ESI+) calcd. for C₁₁H₁₁N⁷⁹Br [M+H]⁺: 236.0075 found: 236.0074.

Pyrrole 277l.



Formula : C₁₆H₁₃N
MW : 219.29

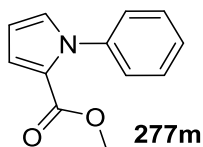
Diene **241a** (65 mg, 0.25 mmol) and nitrosobenzene **160a** (94.9 mg, 0.76 mmol) were stirred in MeOH (1 mL) under reflux for 22 h. The crude was purified by silica gel chromatography (eluent, cyclohexane/toluene, 98/2, R_f = 0.3) to afford pyrrole **277l** (19.7 mg, 36%).

¹H NMR (500 MHz, Chloroform-*d*, δ ppm) 7.35 – 7.25 (m, 4H), 7.24 – 7.13 (m, 6H), 6.97 – 6.94 (dd, *J* = 1.9, 2.8 Hz 1H), 6.45 (dd, *J* = 3.4, 1.9 Hz, 1H), 6.39 – 6.37 (dd, *J* = 3.4, 2.8 Hz 1H).

¹³C NMR (101 MHz, Chloroform-*d*, δ ppm) 140.7, 134.0, 133.1, 129.1, 128.4, 128.2, 126.7, 126.4, 125.9, 124.5, 110.8, 109.4.

All analytical and spectroscopic properties were identical to those reported in the literature.¹⁷⁸

Pyrrole 277m.



Formula : C₁₂H₁₁NO₂
MW : 201.22

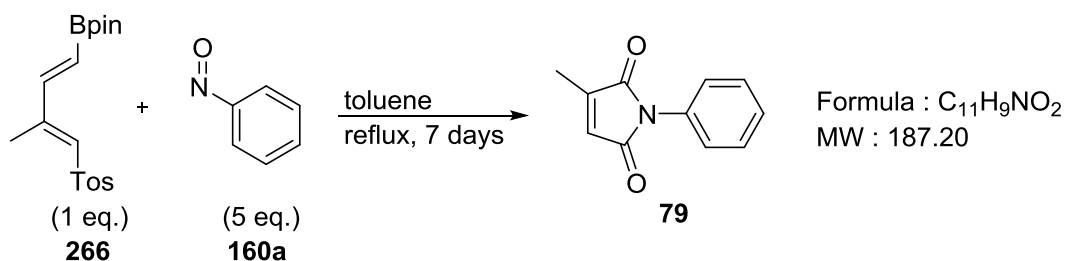
Diene **257** (65 mg, 0.25 mmol) and nitrosobenzene **160a** (133.9 mg, 1.25 mmol) were stirred in toluene (1 mL) under reflux for 128 h. The crude was purified by silica gel chromatography (eluent, cyclohexane/toluene, 98/2, R_f = 0.3) to afford pyrrole **277m** (15 mg, 26%).

¹H NMR (400 MHz, Chloroform-*d*, δ ppm) 7.47 – 7.37 (m, 3H), 7.35 – 7.29 (m, 2H), 7.10 (dd, *J* = 3.9, 1.8 Hz, 1H), 6.95 (dd, *J* = 2.6, 1.8 Hz, 1H), 6.29 (dd, *J* = 3.9, 2.6 Hz, 1H), 3.71 (s, 3H).

¹³C NMR (101 MHz, Chloroform-*d*, δ ppm) 161.1, 140.6, 130.0, 128.7, 128.0, 126.5, 123.4, 119.1, 109.3, 51.3.

All analytical and spectroscopic properties were identical to those reported in the literature.¹⁷⁹

Maleimide **79**.



Diene **266** (66 mg, 0.21 mmol) and nitrosobenzene **160a** (89.2 mg, 1.25 mmol) were stirred in toluene (2 mL) under reflux for 7 days. The crude was purified by silica gel chromatography (eluent, cyclohexane/AcOEt, 95/5, R_f = 0.4).to afford maleimide **79** (28.8 mg, 60%).

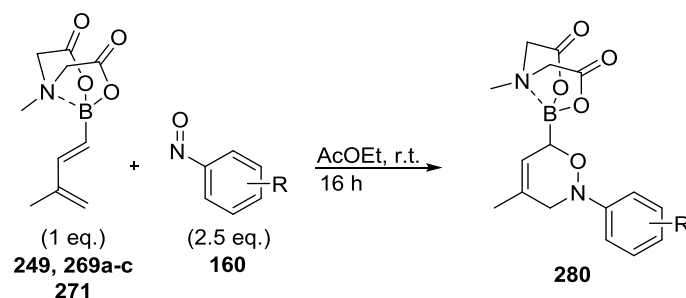
¹H NMR (300 MHz, DMSO-*d*₆, δ ppm) 7.63 – 7.61 (m, 2H), 7.30 – 7.28 (m, 2H), 7.06 – 7.04 (m, 1H), 6.05 (s, 1H), 2.06 (s, 3H).

¹³C NMR (101 MHz, DMSO-*d*₆, δ ppm) 166.4, 140.2, 139.1, 128.5, 122.8, 118.7, 9.3.

All analytical and spectroscopic properties were identical to those reported in the literature.¹⁸⁰

B. Reaction of tetracoordinated 1-borodienes with arylnitroso compounds

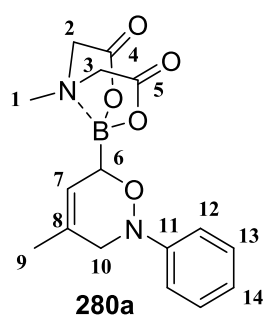
General procedure for the oxazine synthesis:



To a solution of diene (1 eq) (MIDA ester **249**, **269a-c** and **271**) in AcOEt was added the arylnitroso **160** (2.5 eq). The reaction mixture was stirred at room temperature or under reflux.

The solvent was evaporated and the crude product purified by silica gel chromatography.

Oxazine **280a**.



Formula : $C_{16}H_{19}BN_2O_5$
MW : 330.15

To a suspension of diene **249** (20 mg, 0.09 mmol) in AcOEt (1 mL) was added nitrosobenzene **160a** (15 mg, 0.13 mmol). The reaction mixture was stirred at r.t. overnight.

The solvent was evaporated and the residue was purified by silica gel chromatography (eluent, Et₂O/acetonitrile 8/2, R_f = 0.5) to afford oxazine **280a** as a white solid (19 mg, 64%).

M.p. = 211 °C.

¹H NMR (400 MHz, Acetone-*d*₆, δ ppm) 7.28 – 7.22 (m, 2H, H₁₃), 7.11 – 7.08 (m, 2H, H₁₂), 6.93 (tt, *J* = 7.3, 1.1 Hz, 1H, H₁₄), 5.75 – 5.72 (m, 1H, H₇), 4.52 (bs, 1H, H₆), 4.29 (dd, *J* = 16.9, 0.7 Hz, 2H, H₂ or H₃), 4.05 (dd, *J* = 16.9, 15.7 Hz, 2H, H₂ or H₃), 3.96 – 3.87 (m, 1H, H₁₀), 3.64 – 3.53 (m, 1H, H₁₀), 3.30 (s, 3H, H₁), 1.81 (s, 3H, H₉).

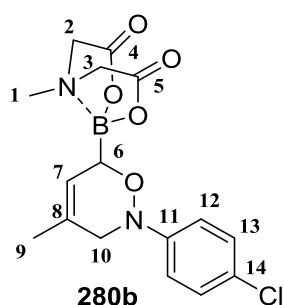
¹³C NMR (101 MHz, Acetone-*d*₆, δ ppm) 169.8 (C₄ or C₅), 167.6 (C₄ or C₅), 152.9 (C₁₁), 130.6 (C₁₃), 130.4 (C₈), 123.5 (C₁₄), 123.3 (C₇), 117.5 (C₁₂), 64.2 (C₂ and C₃), 57.1 (C₁₀), 47.9 (C₁), 21.5 (C₉), B-C not visible.

¹¹B NMR (96 MHz, Acetone-*d*₆, δ ppm) 10.1.

LRMS (ESI+) 353.1 (100%) [M+Na]⁺.

HRMS (ESI+) calcd. for [M+Na]⁺(C₁₆H₁₉N₂O₅¹¹BNa): 353.1284 found: 353.1285.

Oxazine 280b.



Formula : C₁₆H₁₈BClN₂O₅
MW : 364.59

To a suspension of diene **249** (50 mg, 0.22 mmol) in AcOEt (2 mL), was added 4-chloronitrosobenzene **160b** (47.6 mg, 0.34 mmol). The reaction mixture was stirred at r.t. overnight. The solvent was evaporated and the crude product purified by solid phase silica gel chromatography (eluent, Et₂O/MeCN, 8/2, R_f = 0.5) to afford oxazine **280b** as a white solid (61.0 mg, 77%).

M.p. = 224 °C.

¹H NMR (400 MHz, Acetone-*d*₆, δ ppm) 7.31 – 7.23 (m, 2H, H₁₃), 7.16 – 7.08 (m, 2H, H₁₂), 5.74 (s, 1H, H₇), 4.51 (bs, 1H, H₆), 4.29 (dd, *J* = 16.8, 0.7 Hz, 2H, H₂ or H₃), 4.05 (dd, *J* = 20.8, 16.8 Hz, 2H, H₂ or H₃), 3.94 – 3.89 (m, 1H, H₁₀), 3.62 – 3.54 (m, 1H, H₁₀), 3.29 (s, 3H, H₁), 1.81 (s, 3H, H₉).

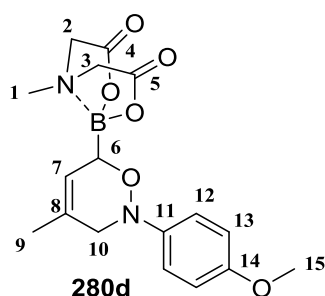
¹³C NMR (101 MHz, Acetone-*d*₆, δ ppm) 168.7 (C₄ or C₅), 168.5 (C₄ or C₅), 150.6 (C₁₁), 129.4 (C₁₃), 129.3 (C₈), 126.9 (C₁₄), 122.3 (C₇), 118.1 (C₁₂), 63.24 (C₂ or C₃), 63.23 (C₂ or C₃), 55.9 (C₁₀), 46.9 (C₁), 20.5 (C₉), B-C not visible.

¹¹B NMR (96 MHz, Acetone-*d*₆, δ ppm) 9.9.

LRMS (ESI+) 387.1 (100%) [M+Na]⁺.

HRMS (ESI+) calcd. for [M+Na]⁺(C₁₆H₁₈N₂O₅³⁵Cl¹¹BNa): 387.0889 found: 367.0888.

Oxazine 280d.



To a suspension of diene **249** (50.0 mg, 0.22 mmol) in AcOEt (2 mL), was added 4-methoxynitrosobenzene **160d** (61.5 mg, 0.45 mmol). The reaction mixture was stirred at r.t. overnight. The solvent was evaporated and the crude product purified by solid phase silica gel chromatography (eluent, Et₂O/MeCN, 8/2, R_f = 0.4) to afford oxazine **280d** as a white solid (37.2 mg, 47%).

M.p. = 164 °C.

¹H NMR (400 MHz, Acetone-*d*₆, δ ppm) 7.09 – 7.05 (m, 2H, H₁₃), 6.87 – 6.83 (m, 2H, H₁₂), 5.71 (s, 1H, H₇), 4.47 (bs, 1H, H₆), 4.26 (dd, *J* = 16.8, 6.8 Hz, 2H, H₂ or H₃), 4.01 (dd, *J* = 33.6, 16.8 Hz, 2H, H₂ or H₃), 3.75 (s, 3H, H₁₅), 3.74 – 3.69 (m, 1H, H₁₀), 3.57 – 3.51 (m, 1H, H₁₀), 3.27 (s, 3H, H₁), 1.79 (s, 3H, H₉).

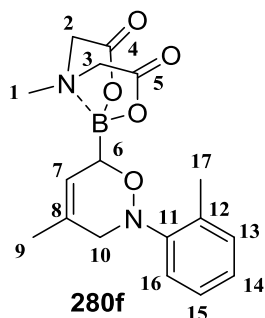
¹³C NMR (101 MHz, Acetone-*d*₆, δ ppm) 168.8 (C₄ or C₅), 168.5 (C₄ or C₅), 156.4 (C₁₄), 145.6 (C₁₁), 129.6 (C₈), 122.3 (C₇), 119.1 (C₁₂), 114.8 (C₁₃), 63.19 (C₂ or C₃), 63.17 (C₂ or C₃), 57.1 (C₁₅), 55.7 (C₁₀), 55.0, 46.8 (C₁), 20.6 (C₉), B-C not visible.

¹¹B NMR (96 MHz, Acetone-*d*₆, δ ppm) 9.9.

LRMS (ESI+) 383.1 (100%) [M+Na]⁺.

HRMS (ESI+) calcd. for [M+Na]⁺(C₁₇H₂₁N₂O₆¹¹BNa): 383.1385 found: 383.1382.

Oxazine 280f.



Formula : C₁₇H₂₁BN₂O₅
MW : 344.17

To a suspension of diene **249** (60 mg, 0.27 mmol) in AcOEt (2 mL), was added 2-nitrosotoluene **180f** (48.9 mg, 0.40 mmol). The reaction mixture was stirred at r.t. overnight. The solvent was evaporated and the crude product purified by solid phase silica gel chromatography (eluent, Et₂O/MeCN, 8/2, R_f = 0.5) to afford oxazine **280f** as a white solid (52.0 mg, 56%).

M.p. = 169 °C.

¹H NMR (400 MHz, Acetone-*d*₆, δ ppm) 7.24 – 7.22 (m, 1H, H₁₅), 7.18 – 7.14 (m, 2H, H₁₃ and H₁₄), 7.05 – 7.02 (m, 1H, H₁₆), 5.74 (s, 1H, H₇), 4.51 (bs, 1H, H₆), 4.21 (dd, *J* = 16.8, 11.1 Hz, 2H, H₂ or H₃), 3.94 (dd, *J* = 19.5, 16.8 Hz, 2H, H₂ or H₃), 3.69-3.65 (m, 1H, H₁₀) 3.45-3.41 (m, 1H, H₁₀), 3.17 (s, 3H, H₁), 2.30 (s, 3H, H₁₇), 1.80 (s, 3H, H₉).

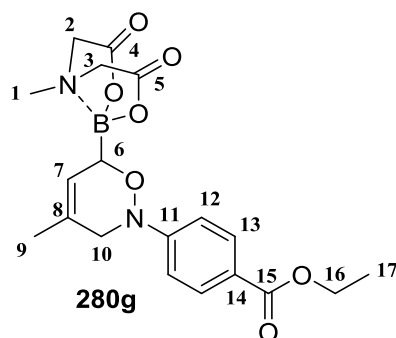
¹³C NMR (101 MHz, Acetone-*d*₆, δ ppm) 168.7 (C₄ or C₅), 168.6 (C₄ or C₅), 149.7 (C₁₁), 133.6 (C₁₂), 131.4 (C₁₄ or C₁₃), 130.2 (C₈), 127.1 (C₁₄ or C₁₃), 125.7 (C₁₅), 122.2 (C₇), 119.0 (C₁₆), 63.21 (C₂ or C₃), 63.16 (C₂ or C₃), 56.7 (C₁₀), 46.8 (C₁), 20.6 (C₉), 18.5 (C₁₇), , B-C not visible.

¹¹B NMR (96 MHz, Acetone-*d*₆, δ ppm) 9.9.

LRMS (ESI+) 367.1 (100%) [M+Na]⁺, 246.1 (9%) [M-C₇H₇NO+H+Na]⁺.

HRMS (ESI+) calcd. for [M+Na]⁺(C₁₇H₂₁N₂O₅¹¹BNa): 367.1436 found: 367.1439.

Oxazine **280g**.



Formula : C₁₉H₂₃BN₂O₇
MW : 402.21

To a suspension of diene **249** (100 mg, 0.45 mmol) in AcOEt (2 mL), was added 4-nitrosobenzoate **180g** (201.2 mg, 1.12 mmol). The reaction mixture was stirred at r.t. overnight. The solvent was evaporated and the crude product purified by solid phase silica gel chromatography (eluent, Et₂O/MeCN, 8/2, R_{f280g} = 0.45 and R_{f281g} = 0.2) to afford **280g** as a white solid (111.3 mg, 61%), and **281g** as pale yellow solid (31.9 mg, 18%).

M.p. = 210 °C.

¹H NMR (400 MHz, Acetone-*d*₆, δ ppm) 7.93 – 7.90 (m, 2H, H₁₃), 7.17 – 7.14 (m, 2H, H₁₂), 5.76 (s, 1H, H₇), 4.56 (bs, 1H, H₆), 4.32 (dd, *J* = 16.8, 0.8 Hz, 2H, H₂ or H₃), 4.29 (q, *J* = 7.1 Hz, 2H, H₁₆), 4.07 (ddd, *J* = 16.8, 10.1, 1.1 Hz, 2H, H₂ or H₃), 4.12 – 4.05 (m, 1H, H₁₀), 3.70 – 3.65 (m, 1H, H₁₀), 3.33 (s, 3H, H₁), 1.83 (s, 3H, H₉), 1.33 (t, *J* = 7.1 Hz, 3H, H₁₇).

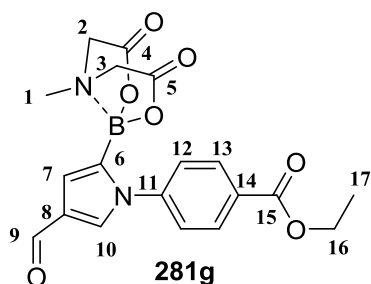
¹³C NMR (101 MHz, Acetone-*d*₆, δ ppm) 168.7 (C₄ or C₅), 168.5 (C₄ or C₅), 166.5 (C₁₅), 155.0 (C₁₁), 131.4 (C₁₃), 129.1 (C₈), 123.6 (C₁₄), 122.2 (C₇), 114.9 (C₁₂), 63.28 (C₂ or C₃), 63.25 (C₂ or C₃), 60.9 (C₁₆), 54.6 (C₁₀), 47.0 (C₁), 20.4 (C₉), 14.7 (C₁₇) B-C not visible.

¹¹B NMR (96 MHz, Acetone-*d*₆, δ ppm) 10.0.

LRMS (ESI+) 425.1 (100%) [M+Na]⁺, 447.1 (6%) [M-H+2Na]⁺.

HRMS (ESI+) calcd. for [M+Na]⁺(C₁₉H₂₃N₂O₇¹¹BNa): 425.1490 found: 425.1491.

Pyrrole 281g.



Formula : C₁₉H₁₉BN₂O₇
MW : 398.18

M.p. > 250 °C.

¹H NMR (400 MHz, DMSO-*d*₆, δ ppm) 9.76 (s, 1H, H₉), 8.03 – 7.98 (m, 2H, H₁₃), 7.89 (d, *J* = 1.7 Hz, 1H, H₁₀), 7.60 – 7.56 (m, 2H, H₁₂), 6.83 (d, *J* = 1.7 Hz, 1H, H₇), 4.33 (q, *J* = 7.1 Hz, 2H, H₁₆), 4.17 (d, *J* = 17.2 Hz, 2H, H₂ or H₃), 3.77 (d, *J* = 17.2 Hz, 2H, H₂ or H₃), 2.41 (s, 3H, H₁), 1.33 (t, *J* = 7.1 Hz, 3H, H₁₇).

¹³C NMR (101 MHz, DMSO-*d*₆, δ ppm) 185.4 (C₉), 168.4 (C₄ and C₅), 165.0 (C₁₅), 144.2 (C₁₁), 136.1 (C₁₀), 129.9 (C₁₃), 129.6 (C₁₄), 127.3 (C₁₂), 126.8 (C₇), 117.6 (C₈), 61.5 (C₂ and C₃), 61.1 (C₁₆), 47.3 (C₁), 14.1 (C₁₇), B-C not visible.

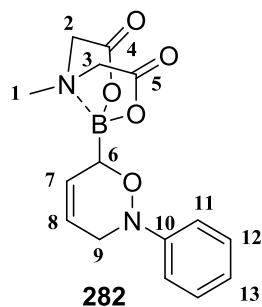
¹¹B NMR (96 MHz, DMSO-*d*₆, δ ppm) 10.3.

IR (neat, ν) 1762, 1743, 1694, 1668, 1601, 1545, 1406, 1328, 1287, 1269, 1150, 1132, 1025, 964, 833, 786, 762, 604 cm⁻¹.

LRMS (ESI+) 399.0 (100%) [M+H]⁺, 288.1 (2%) [M-C₅H₇NO₂+3H]⁺.

HRMS (ESI+) calcd. for [M+H]⁺(C₁₉H₂₀N₂O₇¹⁰B): 398.4000 found: 398.1395.

Oxazine 282.



Formula : C₁₅H₁₇BN₂O₅
MW : 360.17

To a suspension of diene **271** (40.0 mg, 2.21 mmol) in AcOEt (2 mL), was added nitrosobenzene **160a** (59.1 mg, 5.52 mmol). The reaction mixture was stirred at r.t. for 6 h. The solvent was evaporated and the crude product purified by solid phase silica gel chromatography (eluent, Et₂O/MeCN, 8/2, R_f = 0.4) to afford **282** as a white solid (28.0 mg, 43%).

M.p. = 161 °C.

¹H NMR (400 MHz, Acetone-*d*₆, δ ppm) 7.29-7.25 (m, 2H, H₁₂), 7.12-7.08 (m, 2H, H₁₁), 6.96-6.92 (m, 1H, H₁₃), 6.06 (dddd, *J* = 10.1, 2.4, 1.7, 1.6 Hz, 1H, H₈ or H₇), 5.93 (dddd, *J* = 10.1, 5.2, 2.8, 1.7 Hz, 1H, H₈ or H₇), 4.61 (bs, 1H, H₆), 4.29 (dd, *J* = 16.8, 0.7 Hz, 2H, H₂ or H₃), 4.10-4.04 (m, 1H, H₉), 4.06 (dd, *J* = 22.6, 16.8 Hz, 2H, H₂ or H₃), 3.70-3.64 (m, 1H, H₉), 3.32 (s, 3H, H₁).

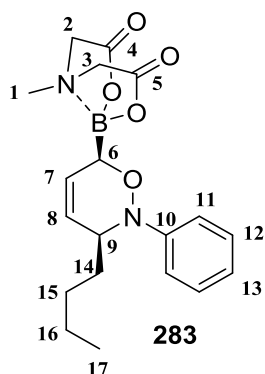
¹³C NMR (101 MHz, Acetone-*d*₆, δ ppm) 168.7 (C₄ or C₅), 168.5 (C₄ or C₅), 152.0 (C₁₀), 129.6 (C₁₂), 127.9 (C₇), 122.6 (C₈ or C₁₃), 122.2 (C₈ or C₁₃), 116.5 (C₁₁), 63.2 (C₂ and C₃), 52.6 (C₉), 46.9 (C₁), B-C not visible.

¹¹B NMR (96 MHz, Acetone-*d*₆, δ ppm) 9.9.

LRMS (ESI+) 339.1 (100%) [M+Na]⁺, 232.1 (24%) [M-C₆H₅NO+Na]⁺.

HRMS (ESI+) calcd. for [M+Na]⁺(C₁₅H₁₇N₂O₅¹¹BNa): 339.1128 found: 339.1125.

Oxazine 283.



Formula : C₁₉H₂₅BN₂O₅
MW : 372.23

To a suspension of diene **269c** (63.0 mg, 0.24 mmol) in AcOEt (3 mL), was added nitrosobenzene **160a** (64.0 mg, 0.60 mmol). The reaction mixture was stirred at r.t. for 6 h. The solvent was evaporated and the crude product purified by solid phase silica gel chromatography (eluent, Et₂O/MeCN, 8/2, R_f = 0.7) to afford **283** as a white solid (61.2 mg, 68%).

M.p. = 188 °C.

¹H NMR (400 MHz, Acetone-*d*₆, δ ppm) 7.28 – 7.21 (m, 2H, H₁₂), 7.02 (m, 2H, H₁₁), 6.86 (m, 1H, H₁₃), 6.06 (ddd, *J* = 10.3, 5.2, 2.8 Hz, 1H, H₈ or H₇), 5.91 (dt, *J* = 10.3, 1.4 Hz, 1H, H₈ or H₇), 4.37 (bs, 1H, H₆), 4.31 (dd, *J* = 19.2, 16.9 Hz, 2H, H₂ or H₃), 4.10 (dd, *J* = 16.9, 10.7 Hz, 2H, H₂ or H₃), 4.10 – 4.07 (m, 1H, H₉), 3.35 (s, 3H, H₁), 1.68 – 1.62 (m, 2H, H₁₄), 1.44 – 1.21 (m, 4H, H₁₅ and H₁₆), 0.85 (t, *J* = 7.2 Hz, 3H, H₁₇).

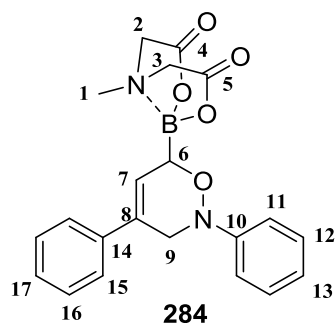
¹³C NMR (101 MHz, Acetone-*d*₆, δ ppm) 169.0 (C₄ or C₅), 168.1 (C₄ or C₅), 149.9 (C₁₀), 129.6 (C₁₂), 127.6 (C₇ or C₈), 126.3 (C₇ or C₈), 121.4 (C₁₃), 116.8 (C₁₁), 69.6 (C₆), 63.2 (C₂ and C₃), 58.1 (C₉), 46.8 (C₁), 31.9 (C₁₄), 28.4 (C₁₅), 23.4 (C₁₆), 14.3 (C₁₇).

¹¹B NMR (96 MHz, Acetone-*d*₆, δ ppm) 10.2.

LRMS (ESI+) 373.2 (16%) [M+H]⁺.

HRMS (ESI+) calcd. for [M+H]⁺(C₁₉H₂₅N₂O₅¹¹B): 373.1935 found: 373.1933.

Oxazine 284.



Formula : C₂₁H₂₁BN₂O₅
MW : 392.22

To a suspension of diene **269b** (30 mg, 0.11 mmol) in AcOEt (2 mL), was added nitrosobenzene **160a** (23 mg, 0.21 mmol). The reaction mixture was stirred at r.t. for 6 h. The solvent was evaporated and the crude product purified by silica gel chromatography (eluent, Et₂O/MeCN, 8/2, R_f = 0.4) to afford **284** as a white solid (32.2 mg, 78%).

M.p. = 207 °C.

¹H NMR (400 MHz, Acetone-*d*₆, δ ppm) 7.59-7.57 (m, 2H, H₁₂), 7.40-7.36 (m, 2H, H₁₁), 7.33-7.23 (m, 5H, H₁₅, H₁₆ and H₁₇), 7.00-6.96 (m, 1H, H₁₃), 6.51 (m, 1H, H₇), 4.74 (bs, 1H, H₆), 4.57 (ddd, *J* = 15.8, 2.8, 1.8 Hz, 1H, H₉), 4.33 (d, *J* = 16.8 Hz, H₂ or H₃), 4.10 (dd, *J* = 26.0, 16.8 Hz, H₂ or H₃), 4.01 (ddd, *J* = 15.8, 2.8, 1.1 Hz, 1H, H₉), 3.36 (s, 3H, H₁).

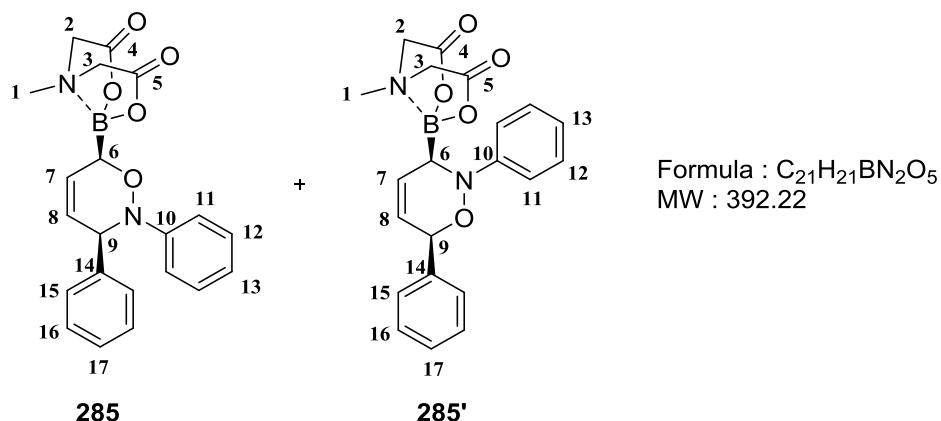
¹³C NMR (101 MHz, Acetone-*d*₆, δ ppm) 168.8 (C₄ or C₅), 168.6 (C₄ or C₅), 151.7 (C₁₀), 139.4 (C₈), 132.5 (C₁₄), 129.6 (C₁₂), 129.4 (C₁₆), 128.2 (C₁₇), 125.6 (C₁₅), 125.2 (C₇), 122.8 (C₁₃), 116.9 (C₁₁), 63.3 (C₂ and C₃), 53.8 (C₉), 47.0 (C₁), B-C not visible.

¹¹B NMR (96 MHz, Acetone-*d*₆, δ ppm) 10.2.

LRMS (ESI+) 393.2 (100%) [M+H]⁺, 308.1 (42%) [M-C₆H₅NO+Na]⁺.

HRMS (ESI+) calcd. for [M+H]⁺(C₂₁H₂₁N₂O₅¹¹B): 393.1622 found: 393.1618.

Oxazines **285** + **285'**.



To a suspension of diene **269a** (50 mg, 0.18 mmol) in AcOEt (2 mL), was added nitrosobenzene **160a** (38 mg, 0.35 mmol). The reaction mixture was stirred at reflux for 24 h. The solvent was evaporated and the crude product purified by solid phase silica gel chromatography (eluent, Et₂O/MeCN, 8/2, R_f = 0.4) to afford **285** + **285'** as a mixture (40/60, 62.8 mg, 89%). The mixture of isomers was dissolved in the minimum amount of CHCl₃, and left overnight in a fridge at + 5 °C to form a white precipitate. The precipitate was filtered, washed with Et₂O and recrystallized in MeOH to afford pure isomer **285'** as white crystals (29.3 mg, 42%). The filtrate was evaporated and diluted in CHCl₃ (1 mL). Aqueous HCl (1M) (0.5 mL) was added and heterogeneous mixture was vigorously stirred for 24 h to decompose the residual isomer **285'**. The organic phase was separated, dried over MgSO₄, filtered and concentrated under vacuum. After purification by silica gel chromatography (eluent, Et₂O/MeCN, 8/2, R_f = 0.4), isomer **285** was obtained as a pale yellow solid (21.3 mg, 30%).

285: M.p. = 174 °C.

¹H NMR (400 MHz, Acetone-*d*₆, δ ppm) 7.44-7.40 (m, 2H, H₁₂), 7.17-7.09 (m, 5H, H₁₅, H₁₆ and H₁₇), 7.00-6.95 (m, 2H, H₁₁), 6.81-6.75 (m, 1H, H₁₃), 6.17 (ddd, *J* = 10.0, 1.7, 1.6 Hz, 1H, H₈ or H₇), 6.04 (ddd, *J* = 10.0, 5.2, 2.9 Hz, 1H, H₈ or H₇) 5.24 (ddd, *J* = 4.8, 2.9, 1.7 Hz, 1H, H₉), 4.59 (bs, 1H, H₆), 4.36 (dd, *J* = 29.6, 16.9 Hz, 2H, H₂ or H₃), 4.10 (dd, *J* = 39.7, 16.9 Hz, 2H, H₂ or H₃), 3.33 (s, 3H, H₁).

¹³C NMR (101 MHz, Acetone-*d*₆, δ ppm) 169.1 (C₄ or C₅), 167.9 (C₄ or C₅), 150.1 (C₁₀), 139.1 (C₁₄), 130.5 (C₁₂, C₁₅ or C₁₆), 129.2 (C₁₂, C₁₅ or C₁₆), 128.4 (C₁₂, C₁₅ or C₁₆), 127.9 (C₁₇), 127.8 (C₈), 125.9 (C₇), 121.9 (C₁₃), 117.3 (C₁₁), 72.8 (C₆), 64.3 (C₉), 63.21 (C₂ or C₃), 63.16 (C₂ or C₃), 46.7 (C₁).

¹¹B NMR (96 MHz, Acetone-*d*₆, δ ppm) 10.3.

LRMS (ESI+) 393.2 (8%) [M+H]⁺, 115.1 (37%), 102.1 (100%).

HRMS (ESI+) calcd. for [M+H]⁺(C₂₁H₂₂N₂O₅¹¹B): 393.1622 found: 393.1624.

285': M.p. = 152 °C.

¹H NMR (400 MHz, Acetone-*d*₆, δ ppm) 7.60-7.58 (m, 2H, H₁₂), 7.37-7.31 (m, 5H, H₁₅, H₁₆ and H₁₇), 7.22-7.20 (m, 2H, H₁₁), 6.98-6.94 (m, 1H, H₁₃), 6.19 (ddd, *J* = 10.5, 4.8, 2.4 Hz, 1H, H₈ or H₇), 5.68 (ddd, *J* = 10.5, 1.7, 1.5 Hz, 1H, H₈ or H₇), 5.11 (m, 1H, H₆), 4.19 (dd, *J* = 88.8, 16.9 Hz, 2H, H₂ or H₃), 4.11 (dd, *J* = 54.0, 16.9 Hz, 2H, H₂ or H₃), 4.11-4.07 (m, 1H, H₉), 3.13 (s, 3H, H₁).

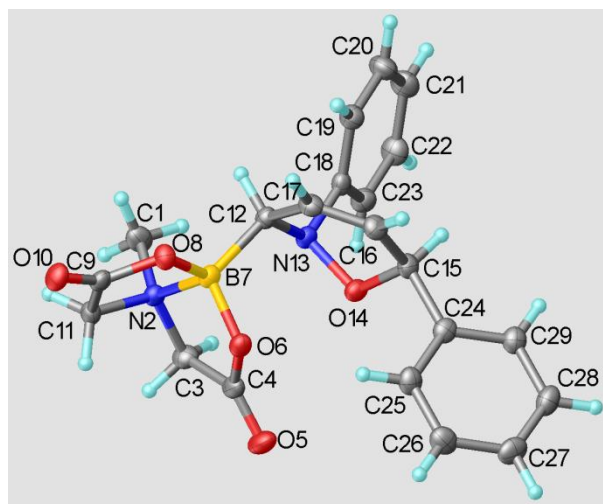
¹³C NMR (101 MHz, Acetone-*d*₆, δ ppm) 169.4 (C₄ or C₅), 167.8 (C₄ or C₅), 149.9 (C₁₀), 139.9 (C₁₄), 130.2 (C₁₂, C₁₅ or C₁₆), 129.6 (C₁₂, C₁₅ or C₁₆), 129.1 (C₁₂, C₁₅ or C₁₆), 129.0 (C₈), 127.0 (C₁₇), 125.1 (C₇), 122.1 (C₁₃), 117.1 (C₁₁), 72.8 (C₉), 63.08 (C₂ or C₃), 63.03 (C₂ or C₃), 47.3 (C₆), 45.4 (C₁).

¹¹B NMR (96 MHz, Acetone-*d*₆, δ ppm) 10.6.

LRMS (ESI+) 415.1 (100%) [M+Na]⁺, 145.0 (30%), 101.0 (41%).

HRMS (ESI+) calcd. for [M+H]⁺(C₂₁H₂₂N₂O₅¹¹B): 393.1622 found: 393.1632.

Crystal structure data for **285'**:



A suitable crystal was selected and measured on a APEXII, Bruker-AXS diffractometer. The crystal was kept at 120 K during data collection. The structure was solved by direct methods using the *SIR97* program,¹⁸¹ and then refined with full-matrix least-square methods based on F^2 (*SHELXL-97*)¹⁸² with the aid of the *WINGX* program.¹⁸³ All non-hydrogen atoms were refined with anisotropic atomic displacement parameters. H atoms were finally included in their calculated positions. A final refinement on F^2 with 4726 unique intensities and 284 parameters converged at $\omega R(F^2) = 0.0955$ ($R(F) = 0.0426$) for 3438 observed reflections with $I > 2\sigma(I)$.

Table I. Crystal data and structure refinement.

Empirical formula	$C_{21.67} H_{23.67} B N_2 O_{5.67}$
Extended formula	$C_{21} H_{19} B_1 N_2 O_4, 0.66667 (H_4O)$
Formula weight	413.59
Temperature	150(2) K
Wavelength	0.71073 Å
Crystal system, space group	monoclinic, $P 2_1/a$
Unit cell dimensions	$a = 13.4777(7)$ Å, $\alpha = 90^\circ$ $b = 9.3088(7)$ Å, $\beta = 106.022(3)^\circ$ $c = 17.2255(13)$ Å, $\gamma = 90^\circ$
Volume	$2077.2(2)$ Å ³
Z, Calculated density	4, 1.323 (g.cm ⁻³)
Absorption coefficient	0.095 mm ⁻¹
$F(000)$	872
Crystal size	0.31 x 0.3 x 0.08 mm
Crystal color	colourless
Theta range for data collection	3.04 to 27.44 °

h_min, h_max	-17 , 17
k_min, k_max	-12 , 12
l_min, l_max	-22 , 22
Reflections collected / unique	17579 / 4726 [R(int) ^a = 0.0411]
Reflections [I>2σ]	3438
Completeness to theta_max	0.998
Absorption correction type	multi-scan
Max. and min. transmission	0.992 , 0.869
Refinement method	Full-matrix least-squares on F ²
Data / restraints / parameters	4726 / 0 / 284
^b Goodness-of-fit	1.031
Final R indices [I>2σ]	R1 ^c = 0.0426, wR2 ^d = 0.0955
R indices (all data)	R1 ^c = 0.0661, wR2 ^d = 0.1068
Largest diff. peak and hole	0.482 and -0.208 e ⁻ .Å ⁻³

Table II. Fractional Atomic Coordinates ($\times 10^4$) and Equivalent Isotropic Displacement Parameters ($\text{\AA}^2 \times 10^3$).

U_{eq} is defined as 1/3 of the trace of the orthogonalised U_H tensor.

Atom	x	y	z	occ.	U(eq)
C1	0.09955(13)	0.41007(17)	0.37619(10)	1	0.0281(4)
H1A	0.0356	0.4456	0.3388	1	0.042
H1B	0.1531	0.4019	0.3478	1	0.042
H1C	0.1224	0.4772	0.4214	1	0.042
N2	0.08061(9)	0.26611(13)	0.40745(7)	1	0.0190(3)
C3	0.00434(11)	0.26881(18)	0.44743(10)	1	0.0257(4)
H3A	0.0546	0.3457	0.4243	1	0.031
H3B	0.0234	0.2852	0.5062	1	0.031
C4	0.05471(11)	0.12210(18)	0.43088(9)	1	0.0245(4)
O5	0.11923(8)	0.07740(14)	0.46162(7)	1	0.0344(3)
O6	0.01933(7)	0.05017(11)	0.37782(6)	1	0.0227(2)
B7	0.04516(12)	0.13949(19)	0.33938(10)	1	0.0199(4)
O8	0.14283(7)	0.06611(11)	0.34287(6)	1	0.0225(2)
C9	0.21508(11)	0.09313(17)	0.41167(9)	1	0.0211(3)
O10	0.29789(7)	0.03273(12)	0.43141(7)	1	0.0275(3)
C11	0.17955(11)	0.20550(17)	0.46113(9)	1	0.0216(3)
H11A	0.1674	0.1619	0.5101	1	0.026
H11B	0.2321	0.282	0.4779	1	0.026
C12	0.01466(10)	0.18918(17)	0.24874(8)	1	0.0197(3)
H12	0.0322	0.254	0.2289	1	0.024
N13	0.10849(9)	0.27168(14)	0.24912(7)	1	0.0197(3)
O14	0.18821(7)	0.17334(11)	0.25856(6)	1	0.0215(2)
C15	0.22300(11)	0.07501(17)	0.19020(9)	1	0.0221(3)
H15	0.267	0.1286	0.1428	1	0.027
C16	0.13314(11)	0.00890(18)	0.16749(9)	1	0.0241(3)
H16	0.1447	0.0729	0.1332	1	0.029
C17	0.03850(11)	0.06092(17)	0.19371(9)	1	0.0225(3)
H17	0.0158	0.0161	0.1774	1	0.027
C18	0.15201(11)	0.36720(17)	0.18231(9)	1	0.0203(3)
C19	0.12517(12)	0.36562(18)	0.10971(9)	1	0.0250(4)
H19	0.0779	0.296	0.1009	1	0.03
C20	0.16803(13)	0.4669(2)	0.04998(10)	1	0.0320(4)
H20	0.1494	0.4659	0.0007	1	0.038
C21	0.23714(13)	0.56820(19)	0.06177(10)	1	0.0327(4)
H21	0.2659	0.6367	0.0209	1	0.039
C22	0.26439(12)	0.56915(19)	0.13425(10)	1	0.0304(4)

H22	0.3121	0.6384	0.1427	1	0.037
C23	0.22216(12)	0.46949(17)	0.19410(10)	1	0.0257(4)
H23	0.2411	0.4709	0.2433	1	0.031
C24	0.28818(11)	0.03512(17)	0.21792(9)	1	0.0228(3)
C25	0.24372(12)	0.12723(17)	0.28181(10)	1	0.0264(4)
H25	0.1717	0.122	0.3073	1	0.032
C26	0.30342(13)	0.22613(18)	0.30844(10)	1	0.0299(4)
H26	0.2723	0.2887	0.3519	1	0.036
C27	0.40899(13)	0.23426(18)	0.27163(10)	1	0.0299(4)
H27	0.4502	0.3012	0.2906	1	0.036
C28	0.45400(12)	0.14473(18)	0.20733(10)	1	0.0288(4)
H28	0.526	0.1509	0.1817	1	0.035
C29	0.39347(11)	0.04539(17)	0.18029(9)	1	0.0254(4)
H29	0.4243	0.0155	0.136	1	0.03
O51	0.41267(15)	0.2772(2)	0.06600(12)	0.67	0.0483(5)
H51	0.3723	0.3453	0.0848	0.67	0.072
C52	0.4714(3)	0.3118(5)	0.00939(18)	0.67	0.0677(12)
H52A	0.5157	0.3938	0.0061	0.67	0.102
H52B	0.5145	0.2294	0.033	0.67	0.102
H52C	0.4265	0.337	0.0433	0.67	0.102

Table III. Anisotropic Displacement Parameters ($\text{\AA}^2 \times 10^3$). The Anisotropic displacement factor exponent takes the form: $-2\pi^2[h^2a^*U_{11}+2hka^*b^*U_{12}+\dots]$.

Atom	U11	U22	U33	U23	U13	U12
C1	0.0363(9)	0.0179(8)	0.0275(8)	0.0016(7)	0.0047(7)	-0.0047(7)
N2	0.0185(6)	0.0171(6)	0.0210(6)	0.0018(5)	0.0051(5)	0.0001(5)
C3	0.0227(8)	0.0294(9)	0.0276(8)	0.0007(7)	0.0112(6)	0.0041(7)
C4	0.0175(7)	0.0307(9)	0.0239(7)	0.0100(7)	0.0033(6)	0.0038(7)
O5	0.0242(6)	0.0439(8)	0.0375(6)	0.0152(6)	0.0125(5)	0.0006(5)
O6	0.0210(5)	0.0200(6)	0.0257(5)	0.0043(5)	0.0040(4)	-0.0021(4)
B7	0.0189(8)	0.0164(8)	0.0243(8)	0.0000(7)	0.0057(7)	0.0006(7)
O8	0.0197(5)	0.0226(6)	0.0237(5)	-0.0015(5)	0.0032(4)	0.0027(4)
C9	0.0184(7)	0.0202(8)	0.0249(7)	0.0044(6)	0.0062(6)	0.0031(6)
O10	0.0179(5)	0.0284(6)	0.0350(6)	0.0031(5)	0.0053(5)	0.0029(5)
C11	0.0191(7)	0.0228(8)	0.0206(7)	0.0015(6)	0.0019(6)	0.0009(6)
C12	0.0174(7)	0.0193(8)	0.0225(7)	0.0016(6)	0.0055(6)	0.0010(6)
N13	0.0177(6)	0.0180(7)	0.0233(6)	0.0012(5)	0.0053(5)	0.0009(5)
O14	0.0223(5)	0.0194(6)	0.0236(5)	-0.0009(4)	0.0077(4)	-0.0033(4)
C15	0.0217(7)	0.0206(8)	0.0224(7)	-0.0026(6)	0.0033(6)	-0.0005(6)
C16	0.0281(8)	0.0218(8)	0.0223(7)	-0.0045(7)	0.0066(6)	0.0004(7)
C17	0.0240(7)	0.0234(9)	0.0212(7)	0.0004(6)	0.0083(6)	0.0056(7)
C18	0.0184(7)	0.0174(8)	0.0227(7)	0.0010(6)	0.0015(6)	0.0017(6)
C19	0.0249(8)	0.0249(9)	0.0251(8)	0.0005(7)	0.0066(6)	0.0026(7)
C20	0.0341(9)	0.0374(10)	0.0237(8)	0.0062(7)	0.0069(7)	0.0038(8)
C21	0.0339(9)	0.0301(10)	0.0313(9)	0.0110(8)	0.0042(7)	0.0058(8)
C22	0.0273(8)	0.0265(9)	0.0360(9)	0.0034(8)	0.0062(7)	0.0079(7)
C23	0.0264(8)	0.0239(9)	0.0277(8)	0.0016(7)	0.0088(6)	0.0004(7)
C24	0.0244(8)	0.0180(8)	0.0265(8)	-0.0046(6)	0.0080(6)	-0.0006(6)
C25	0.0263(8)	0.0200(8)	0.0300(8)	-0.0020(7)	0.0031(6)	-0.0010(7)
C26	0.0384(9)	0.0198(8)	0.0294(8)	-0.0001(7)	0.0057(7)	-0.0025(7)
C27	0.0364(9)	0.0185(8)	0.0381(9)	-0.0054(7)	0.0154(7)	-0.0078(7)
C28	0.0229(8)	0.0239(9)	0.0393(9)	-0.0058(8)	0.0080(7)	-0.0026(7)
C29	0.0250(8)	0.0219(9)	0.0285(8)	-0.0030(7)	0.0059(6)	0.0010(7)

O51	0.0388(11)	0.0502(14)	0.0476(12)	0.0105(11)	-0.0020(9)	-0.0112(10)
C52	0.0500(19)	0.113(4)	0.0372(17)	0.019(2)	0.0074(15)	-0.015(2)

Table IV. Bond Lengths.

Atom	Atom	Length/Å	Atom	Atom	Length/Å
C1	N2	1.4922(19)	C16	H16	0.95
C1	H1A	0.98	C17	H17	0.95
C1	H1B	0.98	C18	C19	1.395(2)
C1	H1C	0.98	C18	C23	1.396(2)
N2	C3	1.4904(18)	C19	C20	1.397(2)
N2	C11	1.5070(18)	C19	H19	0.95
N2	B7	1.638(2)	C20	C21	1.380(2)
C3	C4	1.517(2)	C20	H20	0.95
C3	H3A	0.99	C21	C22	1.395(2)
C3	H3B	0.99	C21	H21	0.95
C4	O5	1.2099(18)	C22	C23	1.387(2)
C4	O6	1.3236(19)	C22	H22	0.95
O6	B7	1.484(2)	C23	H23	0.95
B7	O8	1.4694(19)	C24	C29	1.391(2)
B7	C12	1.614(2)	C24	C25	1.393(2)
O8	C9	1.3338(17)	C25	C26	1.382(2)
C9	O10	1.2116(17)	C25	H25	0.95
C9	C11	1.508(2)	C26	C27	1.391(2)
C11	H11A	0.99	C26	H26	0.95
C11	H11B	0.99	C27	C28	1.385(2)
C12	N13	1.4811(18)	C27	H27	0.95
C12	C17	1.503(2)	C28	C29	1.395(2)
C12	H12	1	C28	H28	0.95
N13	C18	1.4444(18)	C29	H29	0.95
N13	O14	1.4545(15)	O51	C52	1.360(3)
O14	C15	1.4627(17)	O51	H51	0.84
C15	C16	1.503(2)	C52	H52A	0.98
C15	C24	1.511(2)	C52	H52B	0.98
C15	H15	1	C52	H52C	0.98
C16	C17	1.322(2)			

Table V. Bond Angles.

Atom	Atom	Atom	Angle/°	Atom	Atom	Atom	Angle/°
N2	C1	H1A	109.5	C16	C15	H15	109.3
N2	C1	H1B	109.5	C24	C15	H15	109.3
H1A	C1	H1B	109.5	C17	C16	C15	122.13(14)
N2	C1	H1C	109.5	C17	C16	H16	118.9
H1A	C1	H1C	109.5	C15	C16	H16	118.9
H1B	C1	H1C	109.5	C16	C17	C12	121.64(14)
C3	N2	C1	112.42(12)	C16	C17	H17	119.2
C3	N2	C11	112.66(11)	C12	C17	H17	119.2
C1	N2	C11	110.31(11)	C19	C18	C23	119.44(14)
C3	N2	B7	103.50(11)	C19	C18	N13	124.00(13)
C1	N2	B7	115.66(11)	C23	C18	N13	116.52(13)
C11	N2	B7	101.75(11)	C18	C19	C20	119.76(15)

N2	C3	C4	105.01(13)	C18	C19	H19	120.1
N2	C3	H3A	110.7	C20	C19	H19	120.1
C4	C3	H3A	110.7	C21	C20	C19	120.77(15)
N2	C3	H3B	110.7	C21	C20	H20	119.6
C4	C3	H3B	110.7	C19	C20	H20	119.6
H3A	C3	H3B	108.8	C20	C21	C22	119.42(15)
O5	C4	O6	124.59(16)	C20	C21	H21	120.3
O5	C4	C3	124.46(15)	C22	C21	H21	120.3
O6	C4	C3	110.95(13)	C23	C22	C21	120.36(16)
C4	O6	B7	113.06(12)	C23	C22	H22	119.8
O8	B7	O6	110.46(12)	C21	C22	H22	119.8
O8	B7	C12	112.05(12)	C22	C23	C18	120.25(15)
O6	B7	C12	113.22(12)	C22	C23	H23	119.9
O8	B7	N2	102.95(11)	C18	C24	H23	119.9
O6	B7	N2	100.06(11)	C29	C24	C25	119.13(15)
C12	B7	N2	117.08(13)	C29	C24	C15	120.45(14)
C9	O8	B7	112.01(12)	C25	C24	C15	120.42(13)
O10	C9	O8	123.50(14)	C26	C25	C24	120.62(15)
O10	C9	C11	125.09(14)	C26	C25	H25	119.7
O8	C9	C11	111.41(12)	C24	C25	H25	119.7
N2	C11	C9	106.15(11)	C25	C26	C27	120.08(15)
N2	C11	H11A	110.5	C25	C26	H26	120
C9	C11	H11A	110.5	C27	C26	H26	120
N2	C11	H11B	110.5	C28	C27	C26	119.94(15)
C9	C11	H11B	110.5	C28	C27	H27	120
H11A	C11	H11B	108.7	C26	C27	H27	120
N13	C12	C17	112.37(11)	C27	C28	C29	119.88(15)
N13	C12	B7	110.09(11)	C27	C28	H28	120.1
C17	C12	B7	110.19(12)	C29	C28	H28	120.1
N13	C12	H12	108	C24	C29	C28	120.34(15)
C17	C12	H12	108	C24	C29	H29	119.8
B7	C12	H12	108	C28	C29	H29	119.8
C18	N13	O14	109.05(10)	C52	O51	H51	109.5
C18	N13	C12	118.37(11)	O51	C52	H52A	109.5
O14	N13	C12	109.40(11)	O51	C52	H52B	109.5
N13	O14	C15	112.73(10)	H52A	C52	H52B	109.5
O14	C15	C16	111.31(11)	O51	C52	H52C	109.5
O14	C15	C24	104.79(11)	H52A	C52	H52C	109.5
C16	C15	C24	112.64(13)	H52B	C52	H52C	109.5
O14	C15	H15	109.3				

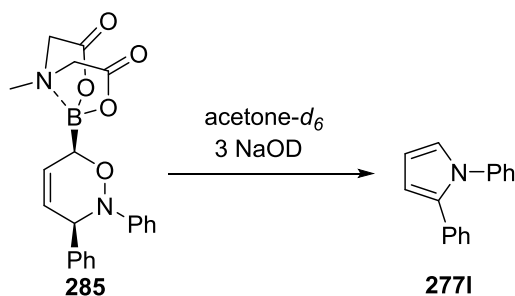
Table VI. Torsion angles.

Atom	Atom	Atom	Atom	Angle/°	Atom	Atom	Atom	Atom	Angle/°
C1	N2	C3	C4	147.64(12)	B7	C12	N13	C18	158.37(12)
C11	N2	C3	C4	-86.96(14)	C17	C12	N13	O14	47.29(14)
B7	N2	C3	C4	22.14(14)	B7	C12	N13	O14	-75.93(14)
N2	C3	C4	O5	170.96(14)	C18	N13	O14	C15	66.21(14)
N2	C3	C4	O6	-9.59(16)	C12	N13	O14	C15	-64.68(13)
O5	C4	O6	B7	169.88(14)	N13	O14	C15	C16	47.10(15)
C3	C4	O6	B7	-9.56(16)	N13	O14	C15	C24	169.13(10)
C4	O6	B7	O8	130.46(13)	O14	C15	C16	C17	-15.0(2)
C4	O6	B7	C12	-102.95(14)	C24	C15	C16	C17	-132.33(16)
C4	O6	B7	N2	22.45(14)	C15	C16	C17	C12	0.6(2)

C3	N2	B7	O8	-140.42(12)	N13	C12	C17	C16	-17.1(2)
C1	N2	B7	O8	96.18(14)	B7	C12	C17	C16	106.10(16)
C11	N2	B7	O8	-23.37(14)	O14	N13	C18	C19	-112.00(15)
C3	N2	B7	O6	-26.52(13)	C12	N13	C18	C19	13.9(2)
C1	N2	B7	O6	-149.91(12)	O14	N13	C18	C23	70.40(16)
C11	N2	B7	O6	90.53(12)	C12	N13	C18	C23	-163.73(13)
C3	N2	B7	C12	96.20(14)	C23	C18	C19	C20	0.5(2)
C1	N2	B7	C12	-27.20(17)	N13	C18	C19	C20	-177.02(14)
C11	N2	B7	C12	-146.76(12)	C18	C19	C20	C21	-0.3(3)
O6	B7	O8	C9	-86.83(14)	C19	C20	C21	C22	0.0(3)
C12	B7	O8	C9	145.93(13)	C20	C21	C22	C23	0.2(3)
N2	B7	O8	C9	19.26(15)	C21	C22	C23	C18	0.0(2)
B7	O8	C9	O10	172.10(14)	C19	C18	C23	C22	-0.3(2)
B7	O8	C9	C11	-7.07(17)	N13	C18	C23	C22	177.39(14)
C3	N2	C11	C9	130.00(13)	O14	C15	C24	C29	114.66(15)
C1	N2	C11	C9	-103.47(14)	C16	C15	C24	C29	-124.18(15)
B7	N2	C11	C9	19.80(14)	O14	C15	C24	C25	-64.99(17)
O10	C9	C11	N2	171.17(14)	C16	C15	C24	C25	56.17(19)
O8	C9	C11	N2	-9.68(16)	C29	C24	C25	C26	-1.0(2)
O8	B7	C12	N13	-175.89(12)	C15	C24	C25	C26	178.67(14)
O6	B7	C12	N13	58.36(17)	C24	C25	C26	C27	-0.2(2)
N2	B7	C12	N13	-57.29(16)	C25	C26	C27	C28	1.1(2)
O8	B7	C12	C17	59.63(16)	C26	C27	C28	C29	-0.8(2)
O6	B7	C12	C17	-66.12(16)	C25	C24	C29	C28	1.3(2)
N2	B7	C12	C17	178.23(12)	C15	C24	C29	C28	-178.37(14)
C17	C12	N13	C18	-78.41(16)	C27	C28	C29	C24	-0.4(2)

C. Mechanistic aspects of the reaction 1-borodienes with arylnitroso compounds

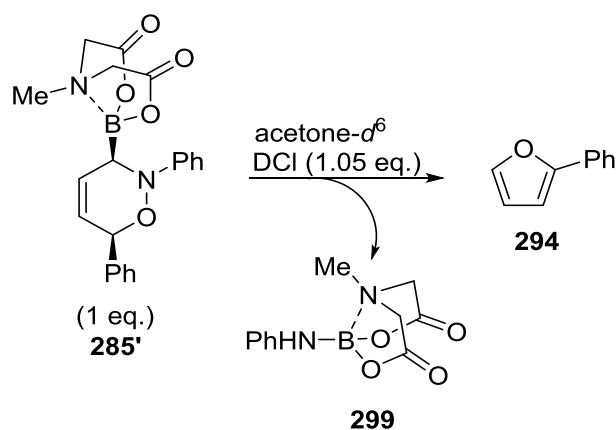
C.1. Conversion of **285** to pyrrole **277l** under basic conditions:



Oxazine **285** (6.0 mg, 0.015 mmol) was dissolved in acetone- d_6 (0.4 mL). NaOD (1 M in water, 15 μ L, 0.015 mmol) was then added and the reaction was directly followed by ^1H and

^{11}B NMR. After one night, a 32% conversion was observed with no further evolution if the reaction was left longer at r.t. NaOD (1 M, 30 μL , 0.030 mmol) was finally added to observe complete consumption of the starting oxazine **285**, followed by DCl (1 M in D_2O , 15 μL , 0.015 mmol). After 15 min, a full conversion into the corresponding pyrrole was observed. The reaction mixture was poured into DCM (2 mL), and H_2O (1 mL) was added. The aqueous layer was extracted with DCM (3 x) and the organic layer was dried over MgSO_4 , filtered over a pad of silica gel and eluted with DCM to give pyrrole **2771** (2.8 mg, 85%).

C.2. Conversion of **285'** to 2-phenylfuran **294** under acidic conditions:



Oxazine **285'** (6.8 mg, 0.017 mmol) was dissolved in acetone- d^6 (0.4 mL). DCl in D_2O (1 M, 18 μL , 0.018 mmol). After full conversion of the starting oxazine, reaction mixture was poured into DCM (1 mL). NaOH (1 M, 0.2 mL) was added. The aqueous layer was extracted with DCM (3 x), dried over MgSO_4 , filtered and purified over a pad of silica and eluted with DCM to give furan **294** (2.4 mg, quantitative).

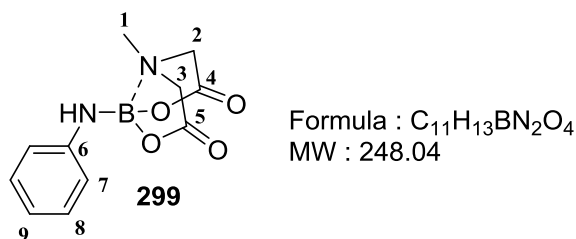
^1H NMR (400 MHz, Chloroform- d , δ ppm) 7.71 – 7.66 (m, 2H), 7.48 (dd, $J = 1.8, 0.7$ Hz, 1H), 7.42 – 7.36 (m, 2H), 7.30 – 7.24 (m, 1H), 6.66 (dd, $J = 3.4, 0.8$ Hz, 1H), 6.48 (dd, $J = 3.4, 1.8$ Hz, 1H).

^{13}C NMR (101 MHz, Chloroform- d , δ ppm) 154.1, 142.2, 131.0, 128.8, 127.5, 123.9, 111.8, 105.1.

All analytical and spectroscopic properties were identical to those reported in the literature.¹⁸⁴

C.3. Isolation of by-product boronated MIDA ester aniline **299**:

Oxazine **285'** (25.2 mg, 0.064 mmol) was dissolved in acetone-*d*₆ (0.7 mL). DCl (1 M in D₂O, 64 μL, 0.064 mmol) was then added and the reaction was followed by ¹H and ¹¹B NMR. After full conversion of the starting oxazine, the reaction mixture was extracted with DCM (3 x), dried over MgSO₄, filtered and concentrated. The crude yellow solid was suspended in CHCl₃ (0.5 mL) and filtered. The resulting solid was washed with CHCl₃ (3 x) to afford **299** as a white solid (4 mg, 25%).



¹H NMR (400 MHz, Acetone-*d*₆, δ ppm) 7.07 (m, 2H, H₈), 6.85 (m, 2H, H₇), 6.62 (m, 1H, H₉), 4.74 (bs, 1H, NH), 4.25 (d, *J* = 17.2 Hz, 2H, H₂ or H₃), 4.09 (d, *J* = 17.2 Hz, 2H, H₂ or H₃), 3.01 (s, 3H, H₁).

¹³C NMR (101 MHz, Acetone-*d*₆, δ ppm) 167.6 (C₄ and C₅), 147.2 (C₆), 129.0 (C₈), 117.4 (C₉), 116.2 (C₇), 62.1 (C₂ and C₃), 45.8 (C₁).

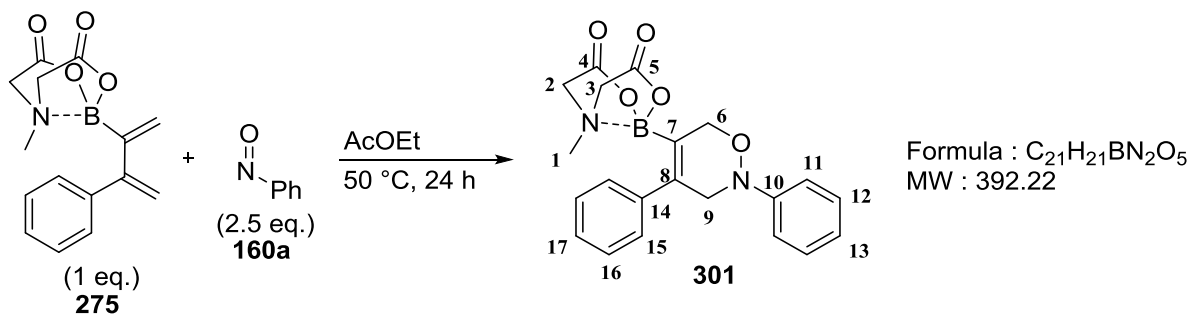
¹¹B NMR (96 MHz, Acetone-*d*₆, δ ppm) 9.9.

LRMS (ESI+) 271.1 (36%) [M+Na]⁺, 249.1 (100%) [M+H]⁺, 188.1 (11%), 156.0 (12%).

HRMS (ESI+) calcd. for [M+H]⁺(C₁₁H₁₄N₂O₄¹¹B): 249.1047 found: 249.1042.

D. Transformations of borono-1,6-dihydro-1,2-oxazine derivatives

Oxazine 301.



To a suspension of diene **277** (229 mg, 0.80 mmol) in AcOEt (10 mL), was added nitrosobenzene **160a** (221 mg, 2.06 mmol). The reaction mixture was stirred at 50 °C for 22 h. The solvent was evaporated and the crude product purified by solid phase silica gel chromatography (eluent, Et₂O/MeCN, 8/2, R_f = 0.4) to afford **301** as a white solid (229 mg, 73%).

M.p. = 153 °C.

¹H NMR (400 MHz, Acetone-*d*₆, δ ppm) 7.40 – 7.25 (m, 7H, H₁₅, H₁₆, H₁₇ and H₁₂), 7.17 (m, 2H, H₁₁), 6.94 (m, 1H, H₁₃), 4.67 (m, 2H, H₆), 3.97 (m, 2H, H₉), 3.94 (d, *J* = 16.8 Hz, 2H, H₂ or H₃), 3.43 (d, *J* = 16.8 Hz, 2H, H₂ or H₃), 3.07 (s, 3H, H₁).

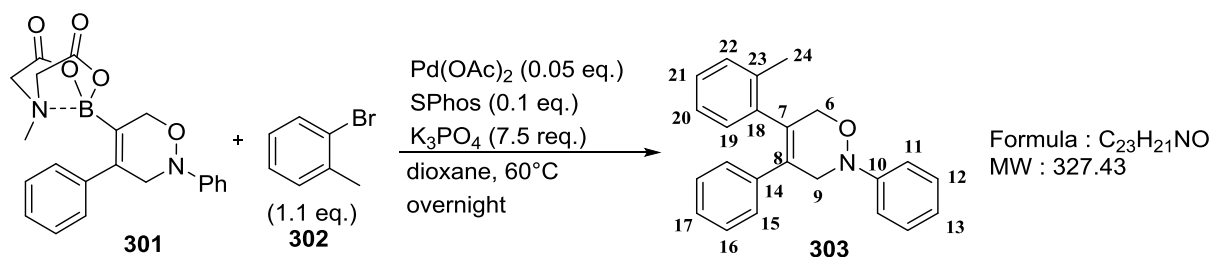
¹³C NMR (101 MHz, Acetone-*d*₆, δ ppm) 168.2 (C₄ and C₅), 151.5 (C₁₀), 144.4 (C₁₄), 141.9 (C₈), 129.7 (C₁₂, C₁₅ or C₁₆), 129.5 (C₁₂, C₁₅ or C₁₆), 129.4 (C₁₂, C₁₅ or C₁₆), 128.2 (C₁₇), 122.5 (C₁₃), 116.2 (C₁₁), 72.2 (C₆), 63.0 (C₂ and C₃), 58.3 (C₉), 47.3 (C₁), B-C not visible.

¹¹B NMR (96 MHz, Acetone-*d*₆, δ ppm) 10.4.

LRMS (ESI+) 393.1 (100%) [M+H]⁺, 281.7 (75%), 264.2 (52%), 220.1 (71%).

HRMS (ESI+) calcd. for [M+H]⁺(C₂₁H₂₂N₂O₅¹¹B): 393.1618 found: 393.1622.

Oxazine 303.



In a flask under an inert atmosphere was added oxazine **301** (41 mg, 0.10 mmol), Pd(OAc)₂ (1.2 mg, 0.0053 mmol), SPhos (4.3 mg, 0.010 mmol) and 2-bromotoluene **302** (14 μ L, 0.11 mmol) in dioxane (2 mL). An aqueous solution of K₃PO₄ (3 M, 190 mL, 0.57 mmol) previously degassed with argon for 15 min was then added. The orange reaction mixture was stirred at 60 °C overnight. Et₂O (5 mL) and NaOH (1 M, 5 mL) were added in the reaction mixture, then aqueous layer was extracted with Et₂O (3 x) and the organic layer was dried over MgSO₄, filtered and concentrated under vacuum. The crude compound was purified by silica gel chromatography (eluent, hexane/AcOEt 95/5, R_f = 0.4). to afford **303** as a white solid (27.1 mg, 71%).

M.p. = 161 °C.

¹H NMR (400 MHz, Chloroform-*d*, δ ppm) 7.40 – 6.83 (m, 14H, H_{Ar}), 4.58 (s, 2H, H₆), 4.12 (s, 2H, H₉), 2.00 (s, 3H, H₂₄).

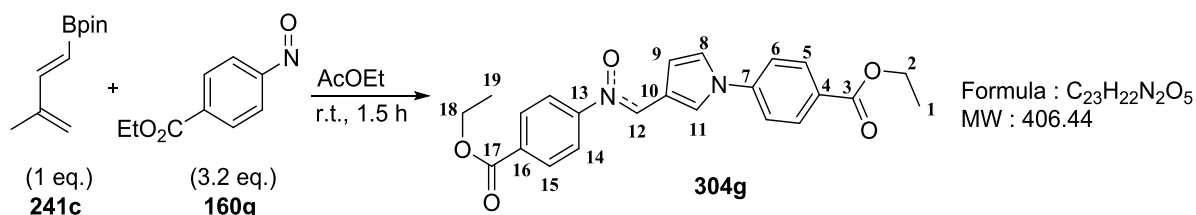
¹³C NMR (101 MHz, Chloroform-*d*, δ ppm) 150.2 (C₁₀), 138.9 (C), 137.1 (C), 136.1 (C), 134.1 (C₁₈), 131.0 (C₇), 130.3 (C), 130.0 (C), 129.1 (C₁₂, C₁₅ or C₁₆), 128.2 (C₁₂, C₁₅ or C₁₆), 128.1 (C₁₂, C₁₅ or C₁₆), 127.6 (C), 127.2 (C), 125.8 (C), 122.8 (C₁₃), 116.2 (C₁₁), 72.0 (C₆), 55.4 (C₉), 19.7 (C₂₄).

LRMS (ESI+) 328.2 (36%) [M+H]⁺.

HRMS (ESI+) calcd. for [M+H]⁺(C₂₃H₂₂NO): 328.1689 found: 328.1701.

E. The one-pot nitron formation/1,3-dipolar cycloaddition sequence

Nitron **304g**.



Diene **241c** (127.0 mg, 0.65 mmol) and 4-nitrosobenzoate **160g** (372.7 mg, 2.08 mmol) were dissolved in AcOEt (3 mL). The reaction mixture was stirred at r.t. for 1.5 h, then hexane (10 mL) was added to the crude mixture. The resulting solid was filtered and washed with hexane (2 x) to afford compound **304g** as an orange solid (142.7 mg, 54%).

M.p. = 165 °C.

¹H NMR (400 MHz, Chloroform-*d*, δ ppm) 8.99 (t, *J* = 1.9 Hz, 1H, H₁₂), 8.18 – 8.13 (m, 4H, H₅ and H₁₅), 8.08 (d, *J* = 0.6 Hz, 1H, H₁₁), 7.93 – 7.88 (m, 2H, H₁₄), 7.59 – 7.53 (m, 2H, H₆), 7.24 (dd, *J* = 3.2, 2.3 Hz, 1H, H₈), 6.70 (dd, *J* = 3.2, 1.5 Hz, 1H, H₉), 4.41 (q, *J* = 7.1 Hz, 2H, H₁₈ or H₂), 4.40 (q, *J* = 7.1 Hz, 2H, H₁₈ or H₂), 1.42 (t, *J* = 7.1, 3H, H₁ or H₁₉), 1.41 (t, *J* = 7.1, 3H, H₁ or H₁₉).

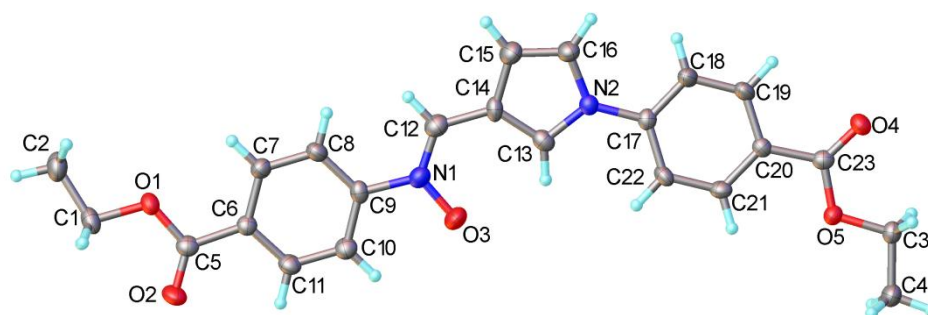
¹³C NMR (101 MHz, Chloroform-*d*, δ ppm) 165.8 (C₁₇ or C₃), 165.6 (C₁₇ or C₃), 150.7 (C₁₃), 143.1 (C₇), 131.5 (CH_{Ph}), 131.4 (C_{Ph}), 130.8 (CH_{Ph}), 130.4 (C₁₁), 128.6 (C_{Ph}), 124.0 (C₁₂), 121.2 (CH_{Ph}), 120.6 (C₈), 120.0 (CH_{Ph}), 117.9 (C₁₀), 112.9 (C₉), 61.5 (C₂ or C₁₈), 61.3 (C₂ or C₁₈), 14.5 (C₁ or C₁₉), 14.4 (C₁ or C₁₉).

IR (neat, ν) 2984, 1717, 1607, 1576, 1520, 1269, 1215, 1170, 1107, 1072, 1018, 840, 767, 691 cm⁻¹.

LRMS (ESI+) 407.0 (27%) [M+H]⁺, 391.3 (100%) [M-O]⁺.

HRMS (ESI+) calcd. for [M+H]⁺(C₂₃H₂₃N₂O₅): 407.1607 found: 407.1602.

Single crystal X-ray structure data for **304g**:



A suitable crystal was selected and measured on a D8V_Mo diffractometer. The crystal was kept at 120 K during data collection. Using Olex2,¹⁸⁵ the structure was solved with the ShelXS structure solution program¹⁸² using Direct Methods and refined with the ShelXL refinement package using Least Squares minimisation.¹⁸²

Table VII. Crystal data and structure refinement.

Empirical formula	C ₂₃ H ₂₂ N ₂ O ₆
Formula weight	422.42
Temperature/K	120
Crystal system	monoclinic
Space group	P2 ₁ /c
a/Å	9.8676(4)
b/Å	22.1740(9)
c/Å	9.4684(4)
α/°	90
β/°	105.0612(14)
γ/°	90
Volume/Å ³	2000.56(14)
Z	4
ρ _{calc} /cm ³	1.403
μ/mm ⁻¹	0.102
F(000)	888.0
Crystal size/mm ³	0.188 × 0.188 × 0.069
Radiation	MoKα (λ = 0.71073)
2θ range for data collection/°	4.652 to 49.994
Index ranges	-11 ≤ h ≤ 11, -26 ≤ k ≤ 26, -11 ≤ l ≤ 11
Reflections collected	65796
Independent reflections	3523 [R _{int} = 0.2185, R _{sigma} = 0.0726]
Data/restraints/parameters	3523/0/275
Goodness-of-fit on F ²	0.962
Final R indexes [I >= 2σ (I)]	R ₁ = 0.0490, wR ₂ = 0.0811
Final R indexes [all data]	R ₁ = 0.0941, wR ₂ = 0.0873
Largest diff. peak/hole / e Å ⁻³	0.23/-0.21

Table VIII. Fractional Atomic Coordinates ($\times 10^4$) and Equivalent Isotropic Displacement Parameters ($\text{\AA}^2 \times 10^3$). U_{eq} is defined as 1/3 of of the trace of the orthogonalised U_{ij} tensor.

Atom	x	y	z	U(eq)
O1	-913.7(12)	5626.9(5)	7148.9(11)	29.2(3)
O2	410.1(13)	4802.0(6)	7802.3(13)	41.2(4)
O3	4890.1(13)	5815.2(6)	3834.1(14)	46.7(4)
O4	11656.1(12)	7194.0(5)	-1447.8(13)	33.1(3)
O5	11982.0(11)	6304.8(5)	-270.4(11)	26.8(3)
N1	3860.7(15)	6175.3(7)	3875.4(15)	30.4(4)
N2	6468.3(14)	7106.0(6)	1490.5(14)	24.1(4)
C1	-1840.4(19)	5415.6(8)	8010.3(19)	34.6(5)
C2	-3048(2)	5846.0(9)	7730(2)	44.2(5)
C3	13245.2(17)	6208.7(8)	-747.9(17)	26.9(4)
C4	13806.4(18)	5607.8(8)	-154.5(18)	34.8(5)
C5	174.4(19)	5270.0(8)	7136.0(18)	27.7(5)
C6	1062.5(18)	5517.7(8)	6229.5(17)	23.7(4)
C7	827.2(18)	6083.2(8)	5566.1(17)	27.3(4)
C8	1721.7(18)	6303.9(8)	4789.8(17)	28.3(5)
C9	2861.9(17)	5961.1(8)	4666.5(16)	24.8(4)
C10	3103.2(19)	5399.8(8)	5312.5(18)	29.8(5)
C11	2201.9(18)	5184.4(8)	6086.8(17)	28.9(5)
C12	3740.4(19)	6703.1(8)	3264.9(18)	32.3(5)
C13	5889.0(18)	6687.1(8)	2234.6(16)	27.5(4)
C14	4717.1(18)	6943.6(8)	2531.1(17)	26.2(4)
C15	4592.3(19)	7537.9(8)	1965.9(18)	34.0(5)
C16	5669.9(19)	7626.0(8)	1340.9(19)	31.6(5)
C17	7678.8(17)	7028.2(8)	966.0(17)	23.1(4)
C18	7986.6(18)	7441.2(8)	4.0(18)	28.3(4)
C19	9162.9(18)	7366.6(8)	-505.7(18)	28.2(5)
C20	10056.9(17)	6880.3(7)	-79.0(16)	22.1(4)
C21	9745.5(19)	6467.9(8)	896.1(17)	25.9(4)
C22	8571.3(18)	6540.7(8)	1417.0(17)	25.8(4)
C23	11293.5(18)	6820.3(8)	-677.6(17)	25.0(4)

Table IX. Anisotropic Displacement Parameters ($\text{\AA}^2 \times 10^3$). The Anisotropic displacement factor exponent takes the form: $-2\pi^2[h^2a^2U_{11}+2hka*b*U_{12}+\dots]$.

Atom	U_{11}	U_{22}	U_{33}	U_{23}	U_{13}	U_{12}
O1	31.9(7)	25.6(7)	34.7(7)	1.8(6)	16.9(6)	-2.4(6)
O2	51.7(9)	25.4(8)	52.5(8)	13.0(7)	24.6(7)	5.9(7)
O3	40.1(9)	46.5(9)	61.3(9)	16.5(7)	27.0(7)	18.6(7)
O4	35.9(8)	28.8(8)	38.7(7)	8.6(6)	17.1(6)	0.3(6)
O5	24.2(7)	25.3(8)	32.8(7)	3.2(6)	11.1(6)	2.8(6)
N1	27.6(9)	32.4(10)	31.7(8)	1.5(8)	8.5(7)	5.0(8)
N2	24.5(9)	25.1(9)	23.2(8)	-0.2(7)	7.1(7)	-0.9(7)

C1	42.5(13)	32.3(12)	35.9(10)	-2.8(9)	22.4(10)	-9.1(10)
C2	41.1(13)	47.5(14)	52.0(12)	-2.2(11)	26.6(10)	-3.6(12)
C3	25.1(10)	29.9(11)	27.2(9)	-1.6(9)	9.6(8)	-0.6(9)
C4	32.5(12)	35.5(12)	40.6(11)	5.4(10)	17.3(9)	5.7(10)
C5	31.2(12)	21.7(12)	29.5(10)	-3.5(9)	6.6(9)	-1.9(10)
C6	25.2(11)	20.5(11)	25.2(9)	-3.2(8)	6.3(8)	-2.6(9)
C7	24.6(10)	27.5(11)	29.8(10)	1.1(9)	6.9(8)	1.9(9)
C8	30.5(11)	25.2(11)	29.4(10)	6.2(9)	8.1(9)	-0.5(9)
C9	23.7(10)	30.2(11)	21.1(9)	-2.9(8)	6.9(8)	-4.8(9)
C10	32.9(12)	25.6(11)	31.9(10)	-3.3(9)	10.2(9)	0.7(9)
C11	35.2(12)	20.8(11)	31.4(10)	0.2(9)	9.9(9)	-1.2(9)
C12	33.8(12)	28.8(12)	34(1)	-4.6(10)	8.6(9)	2.7(10)
C13	32.4(11)	25.5(11)	23.9(9)	-0.1(9)	6.2(9)	-5.1(10)
C14	23.6(11)	33.6(12)	23.9(9)	-5.0(8)	10.6(8)	-6.0(9)
C15	36.1(12)	32.4(12)	35.8(11)	-1.4(9)	13.8(10)	5.5(10)
C16	35.5(12)	27.0(12)	34.3(11)	2.2(9)	12.6(9)	4.9(10)
C17	22.4(10)	24.3(11)	23.0(9)	-4.1(8)	6.7(8)	-3.5(9)
C18	25.1(11)	28.6(11)	31.4(10)	7.4(9)	7.8(9)	1.8(9)
C19	29.6(11)	28.6(12)	26.4(10)	9.7(8)	7.4(9)	0.9(9)
C20	23.6(10)	22.4(11)	19.9(9)	-0.8(8)	4.8(8)	-2.3(9)
C21	31.9(11)	18.9(10)	26.6(9)	1.4(8)	6.9(9)	3.3(9)
C22	34.9(11)	22.4(11)	23.1(9)	2.0(8)	12.8(9)	-3.0(9)
C23	27.1(11)	21.8(11)	24.1(9)	-1.6(9)	3.2(8)	-0.2(9)

Table X. Bond Lengths.

Atom	Atom	Length/Å	Atom	Atom	Length/Å
O1	C1	1.4520(19)	C6	C11	1.381(2)
O1	C5	1.336(2)	C7	C8	1.377(2)
O2	C5	1.2053(19)	C8	C9	1.388(2)
O3	N1	1.3006(17)	C9	C10	1.380(2)
O4	C23	1.2175(19)	C10	C11	1.377(2)
O5	C3	1.4480(18)	C12	C14	1.430(2)
O5	C23	1.3344(19)	C13	C14	1.381(2)
N1	C9	1.463(2)	C14	C15	1.416(2)
N1	C12	1.297(2)	C15	C16	1.359(2)
N2	C13	1.377(2)	C17	C18	1.380(2)
N2	C16	1.383(2)	C17	C22	1.390(2)
N2	C17	1.418(2)	C18	C19	1.378(2)
C1	C2	1.495(2)	C19	C20	1.385(2)
C3	C4	1.495(2)	C20	C21	1.389(2)
C5	C6	1.482(2)	C20	C23	1.479(2)
C6	C7	1.395(2)	C21	C22	1.382(2)

Table XI. Bond Angles.

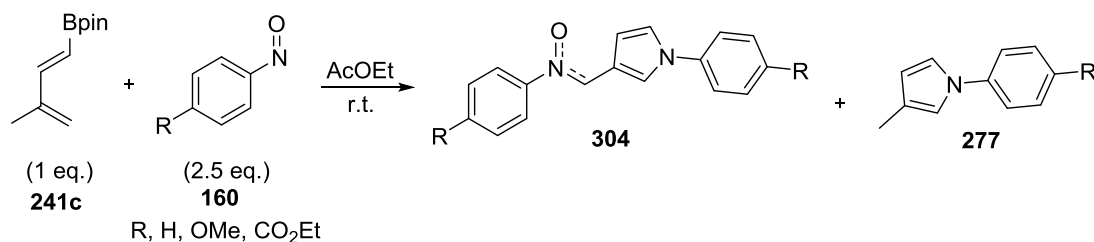
Atom	Atom	Atom	Angle/°	Atom	Atom	Atom	Angle/°
C5	O1	C1	116.03(13)	C10	C11	C6	121.42(17)
C23	O5	C3	116.79(13)	N1	C12	C14	123.92(17)
O3	N1	C9	116.82(14)	N2	C13	C14	107.88(16)
C12	N1	O3	121.49(15)	C13	C14	C12	130.60(17)
C12	N1	C9	121.68(16)	C13	C14	C15	107.56(16)
C13	N2	C16	108.29(14)	C15	C14	C12	121.84(17)
C13	N2	C17	126.63(15)	C16	C15	C14	107.30(17)
C16	N2	C17	125.08(15)	C15	C16	N2	108.96(16)
O1	C1	C2	106.45(14)	C18	C17	N2	120.02(16)
O5	C3	C4	106.18(13)	C18	C17	C22	119.24(16)
O1	C5	C6	112.54(16)	C22	C17	N2	120.74(15)
O2	C5	O1	123.45(17)	C19	C18	C17	120.10(16)
O2	C5	C6	124.01(17)	C18	C19	C20	121.45(16)
C7	C6	C5	122.65(16)	C19	C20	C21	118.17(16)
C11	C6	C5	118.50(16)	C19	C20	C23	118.98(15)
C11	C6	C7	118.80(16)	C21	C20	C23	122.85(16)
C8	C7	C6	120.34(16)	C22	C21	C20	120.74(16)
C7	C8	C9	119.77(16)	C21	C22	C17	120.29(16)
C8	C9	N1	122.27(16)	O4	C23	O5	123.33(16)
C10	C9	N1	117.26(16)	O4	C23	C20	124.64(16)
C10	C9	C8	120.46(16)	O5	C23	C20	112.03(15)
C11	C10	C9	119.21(17)				

Table XII. Hydrogen Atom Coordinates ($\text{\AA}\times 10^4$) and Isotropic Displacement Parameters ($\text{\AA}^2\times 10^3$).

Atom	x	y	z	U(eq)
H1A	-1343	5411	9063	42
H1B	-2175	5002	7711	42
H2A	-3514	5853	6681	53(3)
H2B	-2703	6251	8051	53(3)
H2C	-3717	5716	8273	53(3)
H3A	13940	6530	-365	32
H3B	13028	6210	-1829	32
H4A	13112	5295	-553	41(3)
H4B	14000	5612	914	41(3)
H4C	14675	5523	-436	41(3)
H7	46	6317	5650	33
H8	1559	6689	4340	34
H10	3882	5165	5224	36
H11	2367	4798	6533	35
H12	2956	6944	3308	39
H13	6234	6292	2498	33
H15	3886	7822	2015	41

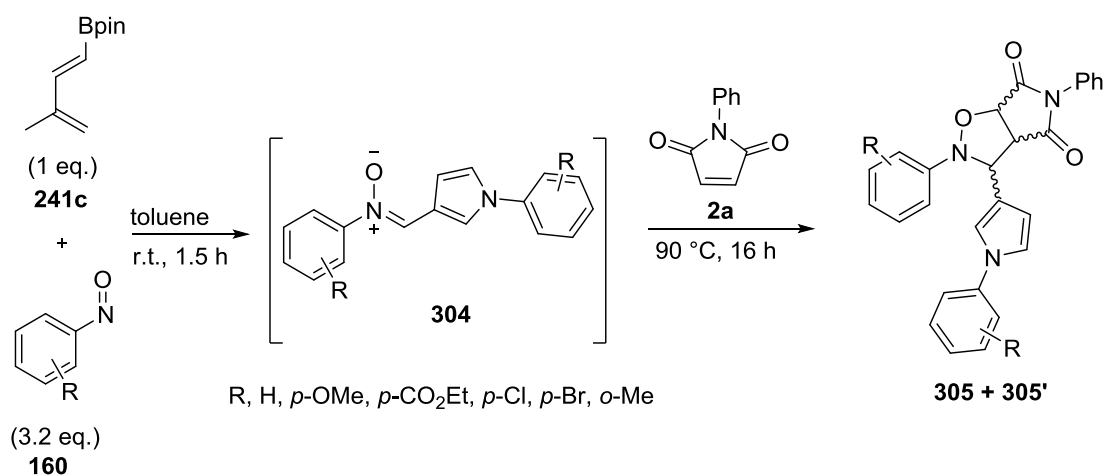
H16	5846	7987	876	38
H18	7387	7777	-307	34
H19	9365	7655	-1164	34
H21	10347	6132	1208	31
H22	8373	6256	2086	31

E.1. General procedure for the ^1H NMR monitoring:



Diene **241c** (1 eq.) and aryl nitroso **160** (2.5 eq.) were dissolved in AcOEt. The reaction mixture was stirred at r.t. and monitored by ^1H NMR analysis. A sample was taken by syringe after 24 h, and the reaction was stopped after 48 h.

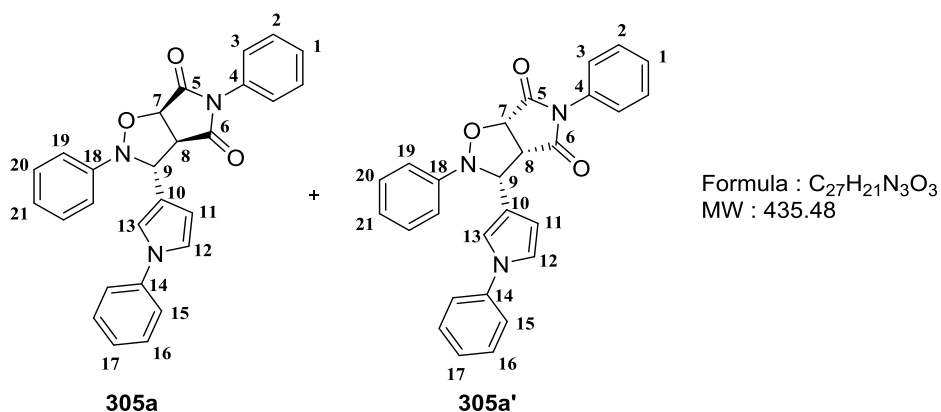
E.2 General procedure for the one-pot procedure nitron formation/1,3-dipolar cycloaddition:



To aryl nitroso compound **160** (3.2 eq) was added a solution of diene **241c** in dry toluene. The reaction mixture was stirred at r.t. for 1.5 h. *N*-phenyl maleimide **2a** (1.1 eq) was added and

the reaction mixture flushed with argon for 10 min. The reaction mixture was heated at 90 °C for 16 h under an inert atmosphere. The crude mixture was cooled to r.t., then toluene was evaporated and the crude product purified by silica gel chromatography.

Oxazolines **305a** and **305a'**.



To nitrosobenzene **160a** (153.6 mg, 1.43 mmol) was added a solution of diene **241c** (87.4 mg, 0.45 mmol) in dry toluene (1.5 mL). The reaction mixture was stirred at r.t. for 1.5 h. *N*-phenyl maleimide **2a** (85.8 mg, 0.49 mmol) was added and the reaction mixture was flushed with argon for 10 min. The reaction mixture was heated at 90 °C for 16 h under an inert atmosphere. The crude mixture was cooled to r.t., then toluene was evaporated and the crude product purified by silica gel chromatography (eluent, hexane/AcOEt, 1/1, R_{f305a} = 0.75, R_{f305a'} = 0.70) to afford isomer **305a** as a yellow-orange solid (29.0 mg, 15%), and isomer **305a'** as a yellow-orange solid (19.1 mg, 10%).

305a: M.p. = 87 °C.

¹H NMR (400 MHz, Chloroform-*d*, δ ppm) 7.45 – 7.41 (m, 2H, H_{Ph}), 7.38 – 7.32 (m, 5H, H_{Ph}), 7.29 – 7.22 (m, 3H, H_{Ph}), 7.19 – 7.14 (m, 3H, H_{Ph}), 7.06 (dd, *J* = 2.9, 2.3 Hz, 1H, H₁₂), 7.00 – 6.95 (m, 1H, H_{Ph}), 6.73 – 6.68 (m, 2H, H₁₃ and H_{Ph}), 6.39 (dd, *J* = 3.0, 1.8 Hz, 1H, H₁₁), 5.75 (s, 1H, H₇), 5.19 (dd, *J* = 7.5, 0.6 Hz, 1H, H₉), 4.04 (dd, *J* = 7.5, 0.9 Hz, 1H, H₈).

¹³C NMR (101 MHz, Chloroform-*d*, δ ppm) 174.5 (C₆), 173.1 (C₅), 148.7 (C₂₁), 140.4 (C₁₄), 131.5 (C₄), 129.8 (C_{Ph}), 129.4 (C_{Ph}), 129.1 (C_{Ph}), 129.0 (C_{Ph}), 126.3 (C_{Ph}), 126.1 (C_{Ph}),

123.8 (C₁₀), 122.9 (C_{Ph}), 120.6 (C_{Ph}), 120.3 (C₁₂), 117.7 (C₁₃), 115.0 (C_{Ph}), 109.3 (C₁₁), 77.2 (C₇), 65.0 (C₉), 56.9 (C₈).

IR (neat, ν) 1714, 1597, 1505, 1492, 1381, 1200, 1056, 860, 755, 689, 621, 609 cm⁻¹.

LRMS (ESI+) 436.2 (100%) [M+H]⁺, 152.0 (19%), 83.0 (66%).

HRMS (ESI+) calcd. for [M+H]⁺(C₂₇H₂₂N₃O₃): 436.1661 found: 436.1664.

305a': M.p. = 98 °C.

¹H NMR (400 MHz, Chloroform-*d*, δ ppm) 7.42 – 7.27 (m, 8H, H_{Ph}), 7.25 – 7.20 (m, 3H, H_{Ph}), 7.16 (t, *J* = 2.1 Hz, 1H, H₇), 7.12 – 7.01 (m, 4H, H₉ and H_{Ph}), 6.39 (dd, *J* = 2.9, 1.7 Hz, 1H, H₁₁), 5.34 (d, *J* = 8.1 Hz, 1H, H₇), 5.14 (d, *J* = 8.6 Hz, 1H, H₉), 3.99 (dd, *J* = 8.5, 8.3 Hz, 1H, H₈).

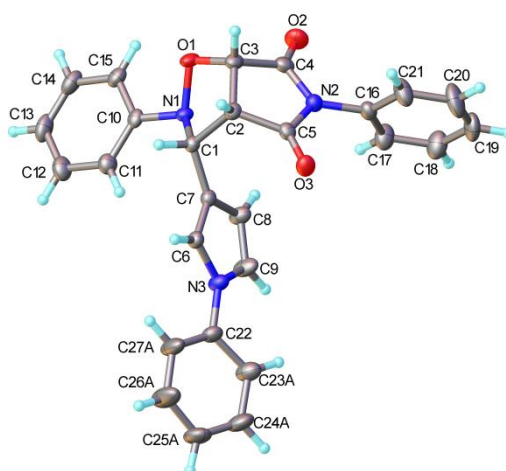
¹³C NMR (101 MHz, Chloroform-*d*, δ ppm) 173.4 (C₆), 171.9 (C₅), 162.5 (C_{Ph}), 159.1 (C_{Ph}), 148.4 (C₂₁), 140.3 (C₁₄), 131.4 (C₄), 129.9 (C_{Ph}), 129.7 (C_{Ph}), 129.3 (C_{Ph}), 129.2 (C_{Ph}), 129.0 (C_{Ph}), 128.9 (C_{Ph}), 126.2 (C_{Ph}), 126.1 (C_{Ph}), 125.4 (C), 120.5 (C), 120.2 (C), 120.1 (C), 119.5 (C), 119.0 (C), 118.5 (C), 117.9 (C), 108.8 (C₁₁), 75.2 (C₇), 64.1 (C₉), 55.9 (C₈), 18.4 (C₂₇), 17.6 (C₂₀).

IR (neat, ν) 1715, 1598, 1501, 1489, 1384, 1244, 1190, 1177, 1048, 861, 805, 753, 688, 590 cm⁻¹.

LRMS (ESI+) 436.2 (100%) [M+H]⁺, 263.2 (21%), 83.0 (53%).

HRMS (ESI+) calcd. for [M+H]⁺(C₂₇H₂₂N₃O₃): 436.1661 found: 436.1653.

Single crystal X-ray structure data for **305a'**:



A suitable crystal was selected and measured on a D8V_Mo diffractometer. The crystal was kept at 120 K during data collection. Using Olex2,¹⁸⁵ the structure was solved with the ShelXS structure solution program¹⁸² using Direct Methods and refined with the ShelXL refinement package using Least Squares minimisation.¹⁸²

Table XIII. Crystal data and structure refinement.

Empirical formula	C ₂₇ H ₂₁ N ₃ O ₃
Formula weight	435.47
Temperature/K	170
Crystal system	orthorhombic
Space group	Pna2 ₁
a/Å	11.2882(6)
b/Å	35.3470(19)
c/Å	5.3359(3)
α/°	90
β/°	90
γ/°	90
Volume/Å ³	2129.0(2)
Z	4
ρ _{calc} /g/cm ³	1.359
μ/mm ⁻¹	0.090
F(000)	912.0
Crystal size/mm ³	0.492 × 0.071 × 0.065
Radiation	MoKα (λ = 0.71073)
2θ range for data collection/°	4.282 to 54.996
Index ranges	-14 ≤ h ≤ 14, -45 ≤ k ≤ 45, -6 ≤ l ≤ 6
Reflections collected	32109
Independent reflections	4869 [R _{int} = 0.0570, R _{sigma} = 0.0429]
Data/restraints/parameters	4869/67/314
Goodness-of-fit on F ²	1.077
Final R indexes [I >= 2σ (I)]	R ₁ = 0.0433, wR ₂ = 0.0890
Final R indexes [all data]	R ₁ = 0.0597, wR ₂ = 0.0952
Largest diff. peak/hole / e Å ⁻³	0.17/-0.17
Flack parameter	-0.7(5)

Table XIV. Fractional Atomic Coordinates (×10⁴) and Equivalent Isotropic Displacement Parameters (Å²×10³).

U_{eq} is defined as 1/3 of the trace of the orthogonalised U_{ij} tensor.

Atom	x	y	z	U(eq)
O(1)	6089.5(14)	303.5(4)	3112(4)	27.3(4)
O(2)	3672.1(16)	506.2(5)	1358(4)	39.1(5)
O(3)	4614.2(15)	1296.8(5)	7803(4)	31.2(4)
N(1)	6716.0(17)	659.9(5)	2601(4)	20.8(5)
N(2)	3874.2(17)	945.4(6)	4536(4)	23.4(5)

N(3)	7562.2(19)	1856.5(6)	5573(4)	27.3(5)
C(1)	6814(2)	848.8(6)	5083(5)	19.7(5)
C(2)	5640(2)	730.4(6)	6394(5)	22.2(5)
C(3)	5156(2)	424.3(7)	4669(5)	24.9(5)
C(4)	4153(2)	617.0(7)	3234(5)	26.3(5)
C(5)	4687(2)	1029.8(7)	6427(5)	22.8(5)
C(6)	7625(2)	1487.3(6)	6375(5)	21.8(5)
C(7)	6985(2)	1266.8(6)	4788(5)	21.0(5)
C(8)	6507(2)	1505.7(7)	2914(5)	29.0(6)
C(9)	6871(3)	1863.8(8)	3445(6)	35.5(7)
C(10)	7795(2)	557.2(7)	1382(5)	21.7(5)
C(11)	8804(2)	777.1(8)	1644(5)	29.3(6)
C(12)	9815(2)	690.6(8)	261(6)	36.4(7)
C(13)	9821(3)	387.8(8)	-1383(6)	38.7(7)
C(14)	8823(3)	167.9(8)	-1602(6)	36.2(7)
C(15)	7809(2)	247.4(7)	-240(5)	28.2(6)
C(16)	2819(2)	1166.3(7)	4140(5)	25.3(6)
C(17)	2746(3)	1418.8(9)	2195(6)	38.1(7)
C(18)	1728(3)	1634.0(9)	1929(6)	44.6(8)
C(19)	807(3)	1594.8(9)	3567(6)	44.2(8)
C(20)	890(3)	1339.1(11)	5482(7)	54.6(9)
C(21)	1896(2)	1123.3(9)	5790(6)	43.7(8)
C(22)	8171(2)	2169.9(7)	6617(5)	28.8(6)
C(23A)	7770(5)	2538.2(12)	6129(10)	40.5(12)
C(24A)	8412(5)	2843.2(14)	7031(12)	46.6(14)
C(25A)	9420(20)	2785(6)	8450(30)	50.4(12)
C(26A)	9709(9)	2422(3)	9120(20)	68(4)
C(27A)	9101(6)	2115(2)	8188(16)	50(2)
C(23B)	8406(9)	2496(2)	5191(19)	40.5(12)
C(24B)	9030(10)	2793(3)	6250(20)	46.6(14)
C(25B)	9440(40)	2775(11)	8680(60)	50.4(12)
C(26B)	9321(17)	2445(6)	10030(50)	68(4)
C(27B)	8680(12)	2148(5)	8970(30)	50(2)

Table XV. Anisotropic Displacement Parameters ($\text{\AA}^2 \times 10^3$). The Anisotropic displacement factor exponent takes the form: $-2\pi^2[h^2a^*U_{11}+2hka^*b^*U_{12}+\dots]$.

Atom	U_{11}	U_{22}	U_{33}	U_{23}	U_{13}	U_{12}
O(1)	30.0(9)	14.1(8)	37.8(11)	-2.5(8)	7.3(9)	-3.3(7)
O(2)	38.2(11)	37.7(11)	41.3(12)	-14.4(9)	-8.5(10)	-4.4(9)
O(3)	28.8(10)	34.3(10)	30.6(11)	-10.7(9)	-0.8(8)	3.5(8)
N(1)	23.2(11)	15.3(9)	24.0(11)	-0.1(8)	1.5(9)	-2.2(8)
N(2)	21.2(10)	24.6(10)	24.5(11)	-1.7(9)	0.4(9)	-0.3(8)
N(3)	33.6(11)	19.5(10)	28.9(12)	-0.4(9)	-7.4(10)	-0.4(9)
C(1)	19.0(11)	19.9(11)	20.2(13)	1.3(9)	-1.7(10)	1.4(9)
C(2)	24.3(12)	21.1(11)	21.3(13)	3.3(10)	1.4(11)	1.4(10)
C(3)	24.3(12)	19.6(12)	30.8(13)	0.7(11)	6.4(11)	-3.4(10)
C(4)	24.0(12)	25.4(12)	29.5(14)	-2.0(12)	3.7(12)	-7(1)

C(5)	19.8(12)	26.1(12)	22.6(13)	1.8(11)	2.1(11)	-1.5(9)
C(6)	21.4(11)	21.3(12)	22.9(13)	1.1(10)	-3.1(10)	2.1(9)
C(7)	19.7(11)	21.4(12)	22.0(13)	0.8(10)	0.9(10)	2.1(9)
C(8)	38.0(14)	22.6(12)	26.5(14)	0.3(11)	-8.1(12)	-0.1(11)
C(9)	50.7(17)	22.1(13)	33.8(16)	5.3(12)	-16.2(14)	0.8(12)
C(10)	23.4(12)	22.2(12)	19.6(12)	5.7(10)	0.5(11)	6.5(9)
C(11)	27.5(13)	31.9(14)	28.6(14)	0.8(12)	4.4(12)	1.6(11)
C(12)	27.7(14)	44.5(16)	37.1(17)	6.8(14)	8.6(13)	3.5(12)
C(13)	38.0(16)	45.2(17)	33.1(16)	5.2(13)	13.3(13)	19.1(14)
C(14)	46.4(17)	29.9(14)	32.2(16)	-0.4(13)	7.9(13)	15.7(13)
C(15)	33.5(14)	21.7(12)	29.5(14)	1.2(11)	0.7(12)	7.1(11)
C(16)	20.2(12)	29.3(13)	26.4(14)	-4.2(10)	-2.5(10)	-0.2(10)
C(17)	33.8(15)	46.4(17)	34.0(17)	5.4(13)	7.4(12)	9.0(13)
C(18)	42.5(17)	50.2(18)	41.0(19)	8.8(15)	0.3(14)	15.1(15)
C(19)	26.2(14)	58(2)	48(2)	-2.5(17)	-8.7(14)	15.3(14)
C(20)	22.6(15)	92(3)	49(2)	14(2)	8.6(14)	8.3(16)
C(21)	24.1(14)	62(2)	45.5(19)	15.9(16)	2.1(13)	2.2(14)
C(22)	34.7(14)	19.5(12)	32.2(15)	-4.2(11)	-1.3(13)	-1.5(11)
C(23A)	51(3)	26.9(18)	44(3)	0(2)	-13(2)	-2(2)
C(24A)	61(4)	18.8(19)	60(4)	-2(2)	-11(3)	0(3)
C(25A)	56(2)	25.1(18)	70(4)	-10(2)	-15(3)	-10.0(16)
C(26A)	67(7)	33(2)	105(10)	-11(4)	-54(6)	0(4)
C(27A)	49(5)	20(2)	80(6)	-3(3)	-32(4)	1(3)
C(23B)	51(3)	26.9(18)	44(3)	0(2)	-13(2)	-2(2)
C(24B)	61(4)	18.8(19)	60(4)	-2(2)	-11(3)	0(3)
C(25B)	56(2)	25.1(18)	70(4)	-10(2)	-15(3)	-10.0(16)
C(26B)	67(7)	33(2)	105(10)	-11(4)	-54(6)	0(4)
C(27B)	49(5)	20(2)	80(6)	-3(3)	-32(4)	1(3)

Table XVI. Bond Lengths.

Atom	Atom	Length/Å	Atom	Atom	Length/Å
O(1)	N(1)	1.470(2)	C(11)	C(12)	1.392(4)
O(1)	C(3)	1.408(3)	C(12)	C(13)	1.384(4)
O(2)	C(4)	1.205(3)	C(13)	C(14)	1.374(4)
O(3)	C(5)	1.199(3)	C(14)	C(15)	1.385(4)
N(1)	C(1)	1.487(3)	C(16)	C(17)	1.371(4)
N(1)	C(10)	1.428(3)	C(16)	C(21)	1.373(4)
N(2)	C(4)	1.389(3)	C(17)	C(18)	1.386(4)
N(2)	C(5)	1.396(3)	C(18)	C(19)	1.364(4)
N(2)	C(16)	1.440(3)	C(19)	C(20)	1.368(5)
N(3)	C(6)	1.375(3)	C(20)	C(21)	1.377(4)
N(3)	C(9)	1.378(3)	C(22)	C(23A)	1.403(5)
N(3)	C(22)	1.418(3)	C(22)	C(27A)	1.357(7)
C(1)	C(2)	1.556(3)	C(22)	C(23B)	1.406(9)
C(1)	C(7)	1.498(3)	C(22)	C(27B)	1.383(14)
C(2)	C(3)	1.522(4)	C(23A)	C(24A)	1.385(6)

C(2)	C(5)	1.509(3)	C(24A)	C(25A)	1.383(17)
C(3)	C(4)	1.527(4)	C(25A)	C(26A)	1.372(14)
C(6)	C(7)	1.359(3)	C(26A)	C(27A)	1.377(9)
C(7)	C(8)	1.416(3)	C(23B)	C(24B)	1.386(11)
C(8)	C(9)	1.361(4)	C(24B)	C(25B)	1.380(19)
C(10)	C(11)	1.386(3)	C(25B)	C(26B)	1.375(19)
C(10)	C(15)	1.396(4)	C(26B)	C(27B)	1.396(16)

Table XVII. Bond Angles.

Atom	Atom	Atom	Angle/°	Atom	Atom	Atom	Angle/°
C(3)	O(1)	N(1)	102.09(16)	C(11)	C(10)	C(15)	119.6(2)
O(1)	N(1)	C(1)	104.80(16)	C(15)	C(10)	N(1)	119.4(2)
C(10)	N(1)	O(1)	106.08(16)	C(10)	C(11)	C(12)	119.8(3)
C(10)	N(1)	C(1)	117.15(18)	C(13)	C(12)	C(11)	120.7(3)
C(4)	N(2)	C(5)	113.0(2)	C(14)	C(13)	C(12)	119.2(3)
C(4)	N(2)	C(16)	124.6(2)	C(13)	C(14)	C(15)	121.2(3)
C(5)	N(2)	C(16)	122.3(2)	C(14)	C(15)	C(10)	119.6(2)
C(6)	N(3)	C(9)	107.7(2)	C(17)	C(16)	N(2)	120.9(2)
C(6)	N(3)	C(22)	126.4(2)	C(17)	C(16)	C(21)	120.8(3)
C(9)	N(3)	C(22)	125.7(2)	C(21)	C(16)	N(2)	118.3(2)
N(1)	C(1)	C(2)	102.50(18)	C(16)	C(17)	C(18)	119.0(3)
N(1)	C(1)	C(7)	111.0(2)	C(19)	C(18)	C(17)	120.7(3)
C(7)	C(1)	C(2)	114.97(19)	C(18)	C(19)	C(20)	119.6(3)
C(3)	C(2)	C(1)	103.0(2)	C(19)	C(20)	C(21)	120.8(3)
C(5)	C(2)	C(1)	115.05(19)	C(16)	C(21)	C(20)	119.2(3)
C(5)	C(2)	C(3)	104.5(2)	C(23A)	C(22)	N(3)	119.7(3)
O(1)	C(3)	C(2)	107.72(19)	C(27A)	C(22)	N(3)	120.3(4)
O(1)	C(3)	C(4)	113.2(2)	C(27A)	C(22)	C(23A)	119.8(4)
C(2)	C(3)	C(4)	104.59(19)	C(23B)	C(22)	N(3)	121.3(4)
O(2)	C(4)	N(2)	125.8(2)	C(27B)	C(22)	N(3)	120.9(7)
O(2)	C(4)	C(3)	127.3(2)	C(27B)	C(22)	C(23B)	117.3(8)
N(2)	C(4)	C(3)	106.9(2)	C(24A)	C(23A)	C(22)	119.3(4)
O(3)	C(5)	N(2)	124.4(2)	C(25A)	C(24A)	C(23A)	120.3(10)
O(3)	C(5)	C(2)	127.5(2)	C(26A)	C(25A)	C(24A)	118.6(16)
N(2)	C(5)	C(2)	108.1(2)	C(25A)	C(26A)	C(27A)	121.6(14)
C(7)	C(6)	N(3)	108.8(2)	C(22)	C(27A)	C(26A)	119.7(8)
C(6)	C(7)	C(1)	124.7(2)	C(24B)	C(23B)	C(22)	119.9(9)
C(6)	C(7)	C(8)	107.5(2)	C(25B)	C(24B)	C(23B)	121.2(19)
C(8)	C(7)	C(1)	127.8(2)	C(26B)	C(25B)	C(24B)	120(3)
C(9)	C(8)	C(7)	107.0(2)	C(25B)	C(26B)	C(27B)	119(3)
C(8)	C(9)	N(3)	109.0(2)	C(22)	C(27B)	C(26B)	122.7(18)
C(11)	C(10)	N(1)	120.8(2)				

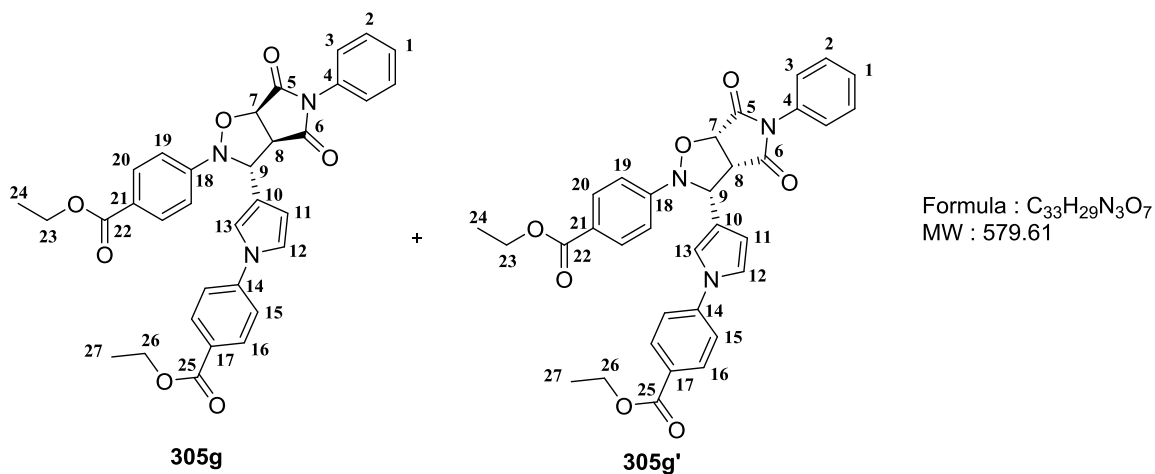
Table XVIII. Hydrogen Atom Coordinates ($\text{\AA}\times 10^4$) and Isotropic Displacement Parameters ($\text{\AA}^2\times 10^3$).

Atom	<i>x</i>	<i>y</i>	<i>z</i>	U(eq)
H(1)	7501	740	6022	24
H(2)	5792	629	8115	27
H(3)	4843	207	5673	30
H(6)	8047	1401	7805	26
H(8)	6023	1430	1545	35
H(9)	6680	2083	2502	43
H(11)	8807	986	2763	35
H(12)	10507	841	447	44
H(13)	10507	333	-2348	46
H(14)	8829	-43	-2708	43
H(15)	7127	92	-408	34
H(17)	3384	1446	1048	46
H(18)	1669	1811	593	53
H(19)	114	1744	3378	53
H(20)	247	1310	6613	65
H(21)	1950	947	7128	52
H(23A)	7066	2578	5191	49
H(24A)	8157	3094	6676	56
H(25A)	9906	2991	8941	60
H(26A)	10343	2381	10261	82
H(27A)	9330	1865	8642	60
H(23B)	8138	2512	3507	49
H(24B)	9175	3014	5281	56
H(25B)	9812	2989	9419	60
H(26B)	9665	2421	11644	82
H(27B)	8589	1921	9905	60

Table XIX. Atomic Occupancy.

Atom	Occupancy	Atom	Occupancy	Atom	Occupancy
C(23A)	0.643(5)	H(23A)	0.643(5)	C(24A)	0.643(5)
H(24A)	0.643(5)	C(25A)	0.643(5)	H(25A)	0.643(5)
C(26A)	0.643(5)	H(26A)	0.643(5)	C(27A)	0.643(5)
H(27A)	0.643(5)	C(23B)	0.357(5)	H(23B)	0.357(5)
C(24B)	0.357(5)	H(24B)	0.357(5)	C(25B)	0.357(5)
H(25B)	0.357(5)	C(26B)	0.357(5)	H(26B)	0.357(5)
C(27B)	0.357(5)	H(27B)	0.357(5)		

Oxazolines **305g** and **305g'**.



To ethyl 4-nitrosobenzoate **160g** (262.4 mg, 1.46 mmol) was added a solution of diene **241c** (91.7 mg, 0.472 mmol) in dry toluene (1.6 mL). The reaction mixture was stirred at r.t. for 1.5 h. *N*-phenyl maleimide **2a** (90,0 mg, 0.520 mmol) was added and the reaction mixture was flushed with argon for 10 min. The reaction mixture was heated at 90 °C for 16 h under an inert atmosphere. The crude mixture was cooled to r.t., then toluene was evaporated and the crude product purified by silica gel chromatography (eluent, hexane/AcOEt, 1/1, $R_{f305g} = 0.65$, $R_{f305g'} = 0.60$) to afford isomer **305g** as an orange solid (38.3 mg, 14%) and isomer **305g'** as a pale orange solid (70,0 mg, 26%).

305g: M.p. = 97 °C.

¹H NMR (700 MHz, Chloroform-*d*, δ ppm) 8.12 – 8.08 (m, 2H, H₁₆), 7.95 – 7.91 (m, 2H, H_{Ph}), 7.42 – 7.38 (m, 2H, H_{Ph}), 7.38 – 7.33 (m, 3H, H_{Ph}), 7.22 (t, $J = 2.1$ Hz, 1H, H₁₂), 7.16 – 7.12 (m, 2H, H_{Ph}), 7.10 (t, $J = 2.6$ Hz, 1H, H₁₃), 6.84 – 6.82 (m, 2H, H_{Ph}), 6.39 (dd, $J = 3.0$, 1.7 Hz, 1H, H₁₁), 5.72 (s, 1H, H₉), 5.22 (d, $J = 7.4$ Hz, 1H, H₇), 4.39 (q, $J = 7.1$ Hz, 2H, H₂₃ or H₂₆), 4.32 (qd, $J = 7.1$, 1.3 Hz, 2H, H₂₃ or H₂₆), 4.04 (dd, $J = 7.4$, 0.9 Hz, 1H, H₈), 1.41 (t, $J = 7.1$ Hz, 3H, H₂₄ or H₂₇), 1.35 (t, $J = 7.1$ Hz, 3H, H₂₄ or H₂₇).

¹³C NMR (101 MHz, Chloroform-*d*, δ ppm) 174.0 (C₆), 172.7 (C₅), 166.2 (C₂₂ or C₂₅), 165.9 (C₂₂ or C₂₅), 151.8 (C₂₁), 143.4 (C₁₄), 131.4 (C_{Ph}), 131.1 (C_{Ph}), 131.0 (C_{Ph}), 129.3 (C_{Ph}), 129.2 (C_{Ph}), 128.0 (C_{Ph}), 126.1 (C_{Ph}), 124.7 (C₁₀), 123.8 (C_{Ph}), 120.3 (C₁₃), 119.5 (C_{Ph}), 117.5

(C₁₂), 114.6 (C_{Ph}), 110.2 (C₁₁), 76.9 (C₇), 64.7 (C₉), 61.3 (C₂₃ or C₂₆), 60.9 (C₂₃ or C₂₆), 56.7 (C₈), 14.50 (C₂₄ or C₂₇), 14.48 (C₂₄ or C₂₇).

IR (neat, ν) 1714, 1700, 1603, 1520, 1367, 1274, 1177, 1104, 1017, 851, 768, 691, 611, 511 cm⁻¹.

LRMS (ESI+) 580.0 (100%) [M+H]⁺, 83.0 (58%).

HRMS (ESI+) calcd. for [M+H]⁺(C₃₃H₃₀N₃O₇): 580.2084 found: 580.2088.

305g': M.p. = 97 °C.

¹H NMR (400 MHz, Chloroform-*d*, δ ppm) 8.10 – 8.05 (m, 2H, H_{Ph}), 7.99 – 7.95 (m, 2H, H_{Ph}), 7.39 – 7.32 (m, 5H, H_{Ph}), 7.23 – 7.19 (m, 3H, H_{Ph}), 7.14 (dd, *J* = 3.0, 2.3 Hz, 1H, H₁₂), 7.04 – 6.99 (m, 2H, H₁₃ and H_{Ph}), 6.43 (dd, *J* = 3.0, 1.7 Hz, 1H, H₁₁), 5.37 (d, *J* = 8.1 Hz, 1H, H₇), 5.18 (d, *J* = 8.7 Hz, 1H, H₉), 4.39 (q, *J* = 7.1 Hz, 2H, H₂₃ or H₂₆), 4.39 (q, *J* = 7.1 Hz, 2H, H₂₃ or H₂₆), 4.04 (dd, *J* = 8.8, 8.1 Hz, 1H, H₈), 1.42 (t, *J* = 7.1 Hz, 3H, H₂₄ or H₂₇), 1.37 (t, *J* = 7.1 Hz, 3H, H₂₄ or H₂₇).

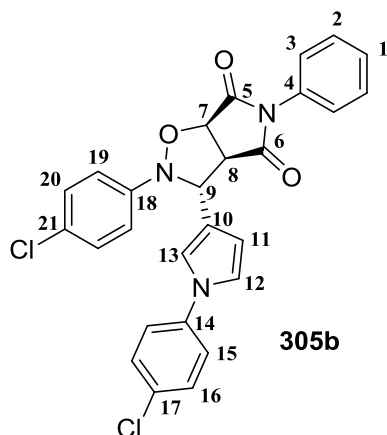
¹³C NMR (101 MHz, Chloroform-*d*, δ ppm) 172.8 (C₆), 171.3 (C₅), 166.2 (C₂₂ or C₂₅), 165.9 (C₂₂ or C₂₅), 152.0 (C₂₁), 143.4 (C₁₄), 131.4 (C_{Ph}), 131.2 (C_{Ph}), 130.8 (C_{Ph}), 129.3 (C_{Ph}), 129.0 (C_{Ph}), 128.1 (C_{Ph}), 126.1 (C_{Ph}), 126.0 (C₁₃), 120.33 (C₁₀), 120.3 (C₁₂), 119.5 (C_{Ph}), 118.2 (C_{Ph}), 116.6 (C_{Ph}), 111.2 (C₁₁), 77.4 (C₇), 66.1 (C₉), 61.3 (C₂₃ or C₂₆), 61.0 (C₂₃ or C₂₆), 54.3 (C₈), 14.49 (C₂₄ or C₂₇), 14.48 (C₂₄ or C₂₇).

IR (neat, ν) 1710, 1704, 1605, 1521, 1367, 1274, 1178, 1103, 1018, 854, 769, 692, 514 cm⁻¹.

LRMS (ESI+) 580.7 (100%) [M+H]⁺, 83.0 (27%).

HRMS (ESI+) calcd. for [M+H]⁺(C₃₃H₃₀N₃O₇): 580.2084 found: 580.2090.

Oxazoline 305b.



Formula : C₂₇H₁₉Cl₂N₃O₃
MW : 504.37

To ethyl 4-chloronitrosobenzene **160b** (195.1 mg, 1.38 mmol) was added a solution of diene **241c** (83.6 mg, 0.43 mmol) in dry toluene (1.5 mL). The reaction mixture was stirred r.t. for 1.5 h. *N*-phenyl maleimide **2a** (82.0 mg, 0.47 mmol) was added and the reaction mixture was flushed with argon for 10 min. The reaction mixture was heated at 90 °C for 16 h under an inert atmosphere. The crude mixture was cooled to r.t., then toluene was evaporated and the crude product purified by silica gel chromatography (eluent, hexane/AcOEt, 1/1, R_f = 0.75) to afford isomer **305b** as an orange solid (57.2 mg, 26%).

M.p. = 98 °C

¹H NMR (400 MHz, Chloroform-*d*, δ ppm) 7.42 – 7.36 (m, 5H, H_{Ph}), 7.30 – 7.24 (m, 2H, H_{Ph}), 7.21 – 7.16 (m, 2H, H_{Ph}), 7.09 – 7.07 (m, 1H, H₁₂), 7.07 – 7.02 (m, 2H, H_{Ph}), 6.99 (dd, *J* = 3.0, 2.4 Hz, 1H, H₁₃), 6.83 – 6.78 (m, 2H, H_{Ph}), 6.35 (dd, *J* = 3.0, 1.7 Hz, 1H, H₁₁), 5.61 (s, 1H, H₉), 5.18 (d, *J* = 7.4 Hz, 1H, H₇), 4.01 (dd, *J* = 7.4, 0.9 Hz, 1H, H₈).

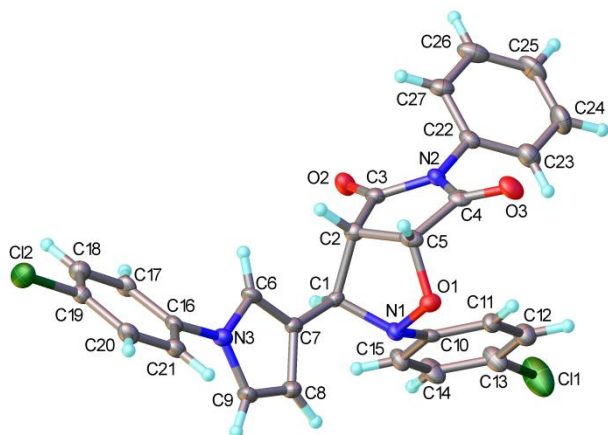
¹³C NMR (101 MHz, Chloroform-*d*, δ ppm) 174.3 (C₆), 172.9 (C₅), 146.9 (C₂₁), 138.9 (C₁₄), 131.7 (C_{Ph}), 131.1 (C_{Ph}), 129.9 (C_{Ph}), 129.3 (C_{Ph}), 129.2 (C_{Ph}), 128.2 (C_{Ph}), 126.2 (C_{Ph}), 123.4 (C₁₀), 121.7 (C_{Ph}), 120.5 (C₁₃), 117.7 (C₁₂), 116.8 (C_{Ph}), 109.7 (C₁₁), 77.0 (C₇), 65.1 (C₉), 56.8 (C₈).

IR (neat, ν) 1717, 1700, 1596, 1505, 1487, 1380, 1318, 1197, 1095, 826, 760, 690, 612, 518 cm⁻¹.

LRMS (ESI+) 391.2 (100%), 152.0 (52%).

HRMS (ESI+) calcd. for [M+H]⁺(C₂₇H₂₀Cl₂N₃O₃): 504.0882 found: 504.0883.

Single crystal X-ray structure data for **305b**:



A suitable crystal was selected and measured on a D8V_Mo diffractometer. The crystal was kept at 120 K during data collection. Using Olex2,¹⁸⁵ the structure was solved with the ShelXS structure solution program¹⁸² using Direct Methods and refined with the ShelXL refinement package using Least Squares minimisation.¹⁸²

Table XX. Crystal data and structure refinement.

Empirical formula	C ₂₉ H ₂₃ Cl ₂ N ₃ O ₄
Formula weight	548.40
Temperature/K	120
Crystal system	monoclinic
Space group	P2 ₁ /c
a/Å	14.6746(8)
b/Å	6.4961(4)
c/Å	26.7054(14)
α/°	90
β/°	91.634(3)
γ/°	90
Volume/Å ³	2544.7(2)
Z	4
ρ _{calc} /cm ³	1.431
μ/mm ⁻¹	2.647
F(000)	1136.0
Crystal size/mm ³	0.3 × 0.04 × 0.03
Radiation	CuKα (λ = 1.54184)
2θ range for data collection/°	6.026 to 136.312
Index ranges	-17 ≤ h ≤ 16, -7 ≤ k ≤ 7, -30 ≤ l ≤ 32
Reflections collected	17303
Independent reflections	4446 [R _{int} = 0.0443, R _{sigma} = 0.0483]
Data/restraints/parameters	4446/0/317
Goodness-of-fit on F ²	1.058

Final R indexes [$I >= 2\sigma(I)$]	$R_1 = 0.0655$, $wR_2 = 0.1344$
Final R indexes [all data]	$R_1 = 0.0818$, $wR_2 = 0.1412$
Largest diff. peak/hole / $e \text{ \AA}^{-3}$	0.80/-0.66

Table XXI. Fractional Atomic Coordinates ($\times 10^4$) and Equivalent Isotropic Displacement Parameters ($\text{\AA}^2 \times 10^3$).

U_{eq} is defined as 1/3 of the trace of the orthogonalised U_{ij} tensor.

Atom	<i>x</i>	<i>y</i>	<i>z</i>	$U(eq)$
Cl(1)	9382.5(7)	-3943(2)	917.3(5)	56.5(4)
Cl(2)	678.5(6)	11194.5(16)	528.9(4)	28.8(2)
O(0AA)	5091.9(16)	-1006(4)	1230.3(9)	20.5(6)
O(1AA)	6896.5(18)	3318(4)	1991.1(9)	26.6(6)
O(3)	5293.5(18)	-2556(5)	2306.9(9)	28.8(7)
N(1)	5745.8(19)	60(5)	933.9(10)	17.9(7)
N(2)	6258.8(19)	239(5)	2237.4(10)	17.6(7)
N(3)	3638(2)	5011(5)	497.4(11)	20.1(7)
C(0AA)	5624(2)	2248(6)	1059.1(12)	16.4(7)
C(1AA)	5439(2)	2202(6)	1623.7(13)	18.8(8)
C(2AA)	6286(2)	2068(6)	1959.0(13)	19.8(8)
C(3AA)	5495(2)	-926(6)	2117.5(13)	20.4(8)
C(4AA)	4971(2)	145(6)	1690.9(13)	21.1(8)
C(5AA)	4236(2)	4615(6)	893.6(13)	19.0(8)
C(7)	4840(2)	3144(6)	752.5(13)	17.2(8)
C(8)	4602(3)	2593(6)	246.9(13)	22.5(8)
C(9)	3867(3)	3756(6)	104.5(13)	23.5(8)
C(10)	6638(2)	-822(6)	982.1(12)	19.3(8)
C(11)	6791(2)	-2698(6)	1218.0(13)	21.0(8)
C(12)	7639(3)	-3635(7)	1204.0(14)	26.8(9)
C(13)	8328(3)	-2698(7)	954.9(15)	31.1(10)
C(14)	8196(3)	-806(7)	726.4(15)	31.7(10)
C(15)	7352(2)	116(6)	735.6(14)	24.4(9)
C(16)	2932(2)	6504(6)	493.0(12)	18.3(8)
C(17)	3105(2)	8446(6)	685.0(13)	20.6(8)
C(18)	2408(2)	9883(6)	698.5(14)	24.1(9)
C(19)	1551(2)	9381(6)	512.7(13)	20.0(8)
C(20)	1379(3)	7458(6)	305.7(13)	23.0(8)
C(21)	2074(2)	6000(6)	298.0(13)	22.6(8)
C(22)	6935(2)	-304(6)	2611.0(13)	20.8(8)
C(23)	7293(3)	-2271(7)	2613.6(15)	29.6(9)
C(24)	7966(3)	-2795(7)	2970.9(16)	36.6(11)
C(25)	8279(3)	-1338(8)	3309.3(15)	36.4(11)
C(26)	7911(3)	627(8)	3305.8(14)	34.4(11)
C(27)	7229(3)	1149(7)	2957.3(13)	26.2(9)

Table XXII. Anisotropic Displacement Parameters ($\text{\AA}^2 \times 10^3$). The Anisotropic displacement factor exponent takes the form: $-2\pi^2[h^2a^{*2}U_{11}+2hka^*b^*U_{12}+\dots]$.

Atom	U_{11}	U_{22}	U_{33}	U_{23}	U_{13}	U_{12}
Cl(1)	29.5(6)	73.5(10)	67.6(8)	29.9(7)	18.6(6)	19.5(6)
Cl(2)	20.4(4)	32.2(6)	33.3(5)	-2.2(4)	-6.8(4)	5.5(4)
O(0AA)	19.8(12)	22.1(14)	19.8(13)	-2.5(11)	2.7(10)	-3.1(11)
O(1AA)	31.2(15)	24.4(15)	23.9(14)	5.4(12)	-4.8(12)	-6.9(12)
O(3)	28.8(14)	34.4(17)	23.4(14)	8.3(13)	3.8(12)	-8.4(13)
N(1)	19.4(15)	18.6(17)	15.9(14)	2.5(13)	2.0(12)	0.9(13)
N(2)	19.6(15)	19.2(17)	14.0(14)	2.7(13)	0.5(12)	0.1(13)
N(3)	20.9(15)	22.5(18)	16.7(15)	-0.2(13)	-2.1(12)	1.9(13)
C(0AA)	20.0(18)	14.9(19)	14.4(17)	-2.7(14)	-0.2(14)	-0.2(15)
C(1AA)	17.6(17)	21(2)	17.7(18)	-0.3(15)	-0.3(15)	1.9(15)
C(2AA)	24.1(19)	21(2)	13.8(17)	-1.6(15)	0.3(15)	1.2(16)
C(3AA)	18.3(17)	28(2)	15.1(17)	-1.2(16)	7.0(15)	-1.8(16)
C(4AA)	16.0(17)	31(2)	15.9(18)	0.1(16)	2.0(14)	0.5(16)
C(5AA)	21.6(18)	24(2)	11.3(16)	-0.1(15)	-4.2(14)	-2.5(16)
C(7)	20.6(18)	16.1(19)	14.9(17)	-0.6(14)	1.5(14)	-3.4(15)
C(8)	29(2)	22(2)	16.4(18)	-1.6(16)	1.0(16)	3.0(17)
C(9)	34(2)	23(2)	13.4(17)	-0.5(16)	-5.0(16)	1.7(17)
C(10)	20.4(18)	28(2)	9.8(16)	-3.1(15)	0.0(14)	0.7(16)
C(11)	24.4(19)	19(2)	19.3(18)	1.8(16)	3.8(15)	-1.5(16)
C(12)	26(2)	30(2)	25(2)	3.0(18)	3.9(16)	1.7(18)
C(13)	25(2)	41(3)	28(2)	11(2)	5.9(17)	8.9(19)
C(14)	26(2)	42(3)	28(2)	12.6(19)	8.1(17)	-0.1(19)
C(15)	25.3(19)	26(2)	21.6(19)	8.0(17)	2.9(16)	4.3(17)
C(16)	21.1(18)	20(2)	13.2(17)	3.7(15)	-1.4(14)	1.2(15)
C(17)	16.7(17)	25(2)	20.0(18)	2.4(16)	-7.9(15)	1.3(15)
C(18)	25(2)	25(2)	22.4(19)	-0.6(17)	-3.2(16)	-1.1(17)
C(19)	20.5(18)	23(2)	16.7(17)	3.0(15)	-0.7(15)	0.2(16)
C(20)	21.8(19)	26(2)	20.9(19)	3.7(17)	-5.7(15)	-4.3(16)
C(21)	26.0(19)	25(2)	16.6(18)	2.9(16)	-2.7(15)	-1.4(17)
C(22)	20.6(18)	27(2)	15.3(17)	4.3(16)	1.6(15)	2.6(16)
C(23)	31(2)	32(2)	26(2)	5.8(18)	-2.3(17)	-2.4(18)
C(24)	39(2)	33(3)	38(2)	13(2)	-6(2)	7(2)
C(25)	31(2)	51(3)	26(2)	14(2)	-9.6(18)	4(2)
C(26)	29(2)	55(3)	18(2)	0(2)	-2.6(17)	-8(2)
C(27)	28(2)	34(2)	16.0(18)	-1.2(17)	2.5(16)	-1.3(18)

Table XXIII. Bond Lengths.

Atom	Atom	Length/ \AA	Atom	Atom	Length/ \AA
Cl(1)	C(13)	1.751(4)	C(7)	C(8)	1.431(5)
Cl(2)	C(19)	1.742(4)	C(8)	C(9)	1.362(5)
O(0AA)	N(1)	1.439(4)	C(10)	C(11)	1.387(5)
O(0AA)	C(4AA)	1.455(4)	C(10)	C(15)	1.394(5)
O(1AA)	C(2AA)	1.210(4)	C(11)	C(12)	1.387(5)

O(3) C(3AA)	1.214(5)	C(12) C(13)	1.369(6)
N(1) C(0AA)	1.472(5)	C(13) C(14)	1.383(6)
N(1) C(10)	1.431(4)	C(14) C(15)	1.376(5)
N(2) C(2AA)	1.403(5)	C(16) C(17)	1.382(5)
N(2) C(3AA)	1.382(5)	C(16) C(21)	1.387(5)
N(2) C(22)	1.431(4)	C(17) C(18)	1.386(5)
N(3) C(5AA)	1.380(4)	C(18) C(19)	1.378(5)
N(3) C(9)	1.378(5)	C(19) C(20)	1.386(5)
N(3) C(16)	1.419(5)	C(20) C(21)	1.393(5)
C(0AA) C(1AA)	1.540(5)	C(22) C(23)	1.382(6)
C(0AA) C(7)	1.510(5)	C(22) C(27)	1.382(5)
C(1AA) C(2AA)	1.513(5)	C(23) C(24)	1.396(6)
C(1AA) C(4AA)	1.516(5)	C(24) C(25)	1.378(6)
C(3AA) C(4AA)	1.525(5)	C(25) C(26)	1.385(7)
C(5AA) C(7)	1.363(5)	C(26) C(27)	1.389(5)

Table XXIV. Bond Angles.

Atom	Atom	Atom	Angle/°	Atom	Atom	Atom	Angle/°
N(1)	O(0AA)	C(4AA)	108.5(2)	C(8)	C(9)	N(3)	108.9(3)
O(0AA)	N(1)	C(0AA)	104.6(2)	C(11)	C(10)	N(1)	121.9(3)
C(10)	N(1)	O(0AA)	112.4(3)	C(11)	C(10)	C(15)	118.9(3)
C(10)	N(1)	C(0AA)	118.8(3)	C(15)	C(10)	N(1)	118.8(3)
C(2AA)	N(2)	C(22)	123.3(3)	C(12)	C(11)	C(10)	120.5(3)
C(3AA)	N(2)	C(2AA)	112.1(3)	C(13)	C(12)	C(11)	119.6(4)
C(3AA)	N(2)	C(22)	124.6(3)	C(12)	C(13)	Cl(1)	119.2(3)
C(5AA)	N(3)	C(16)	125.7(3)	C(12)	C(13)	C(14)	120.8(4)
C(9)	N(3)	C(5AA)	108.0(3)	C(14)	C(13)	Cl(1)	119.9(3)
C(9)	N(3)	C(16)	126.3(3)	C(15)	C(14)	C(13)	119.6(4)
N(1)	C(0AA)	C(1AA)	103.3(3)	C(14)	C(15)	C(10)	120.5(4)
N(1)	C(0AA)	C(7)	110.2(3)	C(17)	C(16)	N(3)	119.6(3)
C(7)	C(0AA)	C(1AA)	112.7(3)	C(17)	C(16)	C(21)	120.7(3)
C(2AA)	C(1AA)	C(0AA)	114.6(3)	C(21)	C(16)	N(3)	119.7(3)
C(2AA)	C(1AA)	C(4AA)	104.3(3)	C(16)	C(17)	C(18)	119.8(3)
C(4AA)	C(1AA)	C(0AA)	103.1(3)	C(19)	C(18)	C(17)	119.8(4)
O(1AA)	C(2AA)	N(2)	124.2(3)	C(18)	C(19)	Cl(2)	119.7(3)
O(1AA)	C(2AA)	C(1AA)	126.7(3)	C(18)	C(19)	C(20)	120.8(4)
N(2)	C(2AA)	C(1AA)	109.1(3)	C(20)	C(19)	Cl(2)	119.5(3)
O(3)	C(3AA)	N(2)	125.9(3)	C(19)	C(20)	C(21)	119.6(3)
O(3)	C(3AA)	C(4AA)	125.8(3)	C(16)	C(21)	C(20)	119.4(4)
N(2)	C(3AA)	C(4AA)	108.2(3)	C(23)	C(22)	N(2)	119.2(3)
O(0AA)	C(4AA)	C(1AA)	106.6(3)	C(27)	C(22)	N(2)	119.7(3)
O(0AA)	C(4AA)	C(3AA)	109.0(3)	C(27)	C(22)	C(23)	121.1(4)
C(1AA)	C(4AA)	C(3AA)	105.6(3)	C(22)	C(23)	C(24)	119.4(4)
C(7)	C(5AA)	N(3)	108.9(3)	C(25)	C(24)	C(23)	119.8(4)

C(5AA)	C(7)	C(0AA)	127.7(3)	C(24)	C(25)	C(26)	120.4(4)
C(5AA)	C(7)	C(8)	107.0(3)	C(25)	C(26)	C(27)	120.1(4)
C(8)	C(7)	C(0AA)	125.3(3)	C(22)	C(27)	C(26)	119.2(4)
C(9)	C(8)	C(7)	107.1(3)				

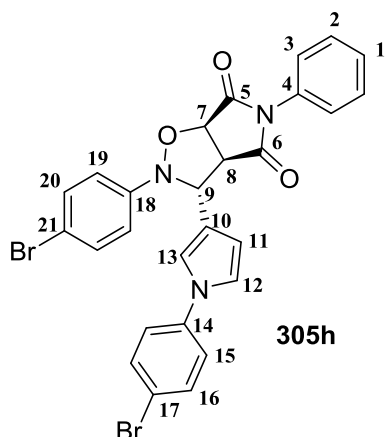
Table XXV. Hydrogen Atom Coordinates ($\text{\AA}\times 10^4$) and Isotropic Displacement Parameters ($\text{\AA}^2\times 10^3$).

Atom	x	y	z	U(eq)
H(0AA)	6197	3030	997	20
H(1AA)	5039	3370	1723	23
H(4AA)	4311	316	1767	25
H(5AA)	4229	5261	1213	23
H(8)	4900	1601	48	27
H(9)	3562	3710	-214	28
H(11)	6312	-3345	1390	25
H(12)	7741	-4919	1366	32
H(14)	8684	-148	564	38
H(15)	7256	1401	573	29
H(17)	3699	8793	807	25
H(18)	2522	11212	835	29
H(20)	791	7138	170	28
H(21)	1962	4672	161	27
H(23)	7083	-3258	2375	35
H(24)	8209	-4151	2981	44
H(25)	8748	-1683	3547	44
H(26)	8127	1620	3542	41
H(27)	6968	2487	2957	31

Table XXVI. Solvent masks information.

Number	X	Y	Z	Volume	Electron count	Content
1	0.000	-0.822	0.250	193.8	52.3	?
2	0.000	-0.607	0.750	193.8	52.3	?

Oxazoline 305h.



Formula : C₂₇H₁₉Br₂N₃O₃
MW : 593.27

To ethyl 4-bromonitrosobenzene **160h** (255.1 mg, 1.37 mmol) was added a solution of diene **241c** (83.2 mg, 0.43 mmol) in dry toluene (1.5 mL). The reaction mixture was stirred at r.t. for 1.5 h. *N*-phenyl maleimide **2a** (81.7 mg, 0.47 mmol) was added and the reaction mixture was flushed with argon for 10 min. The reaction mixture was heated at 90 °C for 16 h under an inert atmosphere. The crude mixture was cooled to r.t., then toluene was evaporated and the crude product purified by silica gel chromatography (eluent, hexane/AcOEt, 1/1, R_f = 0.75) to afford isomer **305h** as an orange solid (59.1 mg, 23%).

M.p. = 109 °C.

¹H NMR (400 MHz, Chloroform-*d*, δ ppm) 7.56 – 7.52 (m, 2H, H_{Ph}), 7.44 – 7.36 (m, 3H, H_{Ph}), 7.36 – 7.31 (m, 2H, H_{Ph}), 7.25 – 7.20 (m, 2H, H_{Ph}), 7.09 (ddd, *J* = 2.4, 1.7, 0.6 Hz, 1H, H₁₂), 7.04 – 6.98 (m, 3H, H₁₃ and H_{Ph}), 6.82 – 6.76 (m, 2H, H_{Ph}), 6.36 (dd, *J* = 3.0, 1.8 Hz, 1H, H₁₁), 5.62 (s, 1H, H₉), 5.18 (dd, *J* = 7.5, 0.6 Hz, 1H, H₇), 4.02 (dd, *J* = 7.5, 0.9 Hz, 1H, H₈).

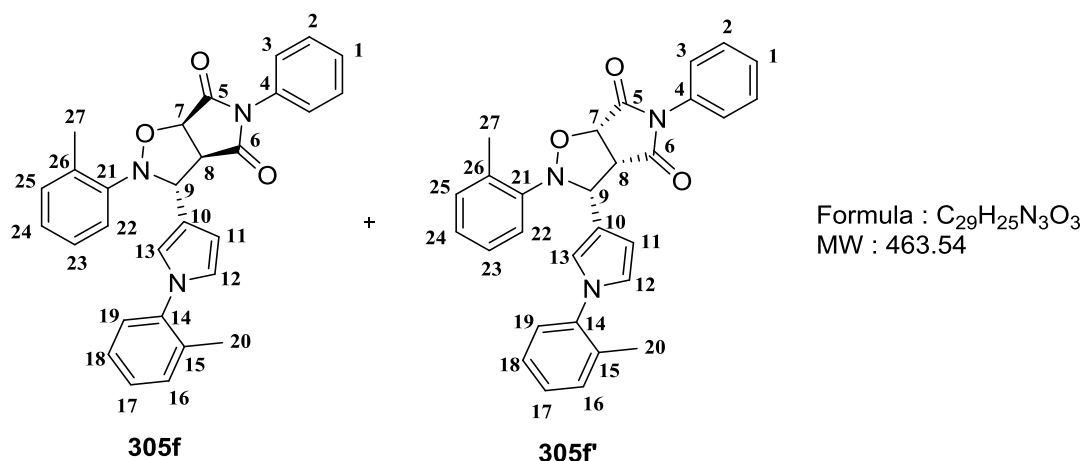
¹³C NMR (101 MHz, Chloroform-*d*, δ ppm) 174.2 (C₆), 172.9 (C₅), 147.5 (C₂₁), 139.3 (C₁₄), 132.8 (C_{Ph}), 132.1 (C_{Ph}), 131.0 (C_{Ph}), 129.3 (C_{Ph}), 129.2 (C_{Ph}), 126.2 (C_{Ph}), 123.5 (C₁₀), 122.1 (C_{Ph}), 120.4 (C₁₃), 119.4 (C_{Ph}), 117.7 (C₁₂), 117.1 (C_{Ph}), 115.7 (C_{Ph}), 109.7 (C₁₁), 77.0 (C₇), 65.0 (C₉), 56.8 (C₈).

IR (neat, ν) 1715, 1591, 1501, 1483, 1382, 1197, 1075, 1008, 821, 758, 690, 614 cm⁻¹.

LRMS (ESI+) 391.2 (69%), 152.1 (100%).

HRMS (ESI+) calcd. for [M+H]⁺(C₂₇H₂₀Br₂N₃O₃): 591.9871 found: 591.9861.

Oxazolines **305f** and **305f'**.



To 2-nitrosotoluene **160f** (156.6 mg, 1.25 mmol) was added a solution of diene **241c** (78.4 mg, 0.40 mmol) in dry toluene (1.5 mL). The reaction mixture was stirred at r.t. for 1.5 h. *N*-phenyl maleimide **2a** (76.9 mg, 0.44 mmol) was added and the reaction mixture was flushed with argon for 10 min. The reaction mixture was heated at 90 °C for 16 h under an inert atmosphere. The crude mixture was cooled to r.t., then toluene was evaporated and the crude product purified by silica gel chromatography (eluent, hexane/AcOEt, 1/1, R_{f305f} = 0.75, $R_{f305f'}$ = 0.70) to afford isomer **305f** as a white solid (23.1 mg, 12%). The isomer **305f'** was not isolated.

305f: M.p. = 179 °C.

¹H NMR (700 MHz, Chloroform-*d*, δ ppm) 7.52 – 7.49 (m, 2H, H_{Ph}), 7.45 – 7.42 (m, 1H, H_{Ph}), 7.35 – 7.32 (m, 2H, H_{Ph}), 7.26 – 7.18 (m, 3H, H_{Ph}), 7.09 – 7.05 (m, 3H, H_{Ph}), 6.98 – 6.92 (m, 2H, H_{Ph}), 6.61 (t, J = 2.5 Hz, 1H, H₁₂), 6.36 (t, J = 2.0 Hz, 1H, H₁₃), 6.10 (dd, J = 2.8, 1.8 Hz, 1H, H₁₁), 5.25 (d, J = 7.4 Hz, 1H, H₇), 5.18 (s, 1H, H₉), 4.11 (dd, J = 7.4, 1.1 Hz, 1H, H₈), 2.26 (s, 3H, H₂₇), 1.92 (s, 3H, H₂₀).

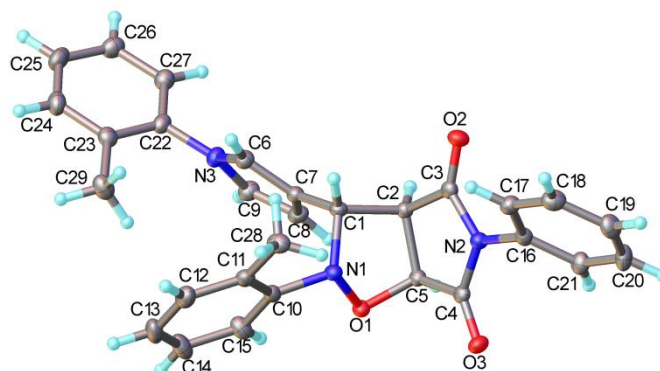
¹³C NMR (101 MHz, Chloroform-*d*, δ ppm) 175.4 (C₆), 173.9 (C₅), 144.1 (C₂₁), 140.1 (C₁₄), 134.2 (C), 131.7 (C), 131.1 (C), 130.2 (C), 129.4 (C), 129.1 (C), 128.8 (C), 128.0 (C), 126.63 (C), 126.60 (C), 126.5 (C), 125.9 (C), 124.9 (C), 122.5 (C₁₂), 121.3 (C₁₃), 119.9 (C), 118.8 (C₁₀), 108.8 (C₁₁), 75.2 (C₇), 64.1 (C₉), 55.9 (C₈), 18.4 (C₂₇), 17.6 (C₂₀).

IR (neat, ν) 1710, 1700, 1597, 1505, 1391, 1328, 1195, 1185, 1065, 851, 749, 688, 625, 612 cm⁻¹.

LRMS (ESI+) 464.2 (100%) $[M+H]^+$, 83.0 (30%).

HRMS (ESI+) calcd. for $[M+H]^+(C_{29}H_{26}N_3O_3)$: 464.1974 found: 464.1971.

Single crystal X-ray structure data for **305f**:



A suitable crystal was selected and measured on a D8V_Mo diffractometer. The crystal was kept at 120 K during data collection. Using Olex2,¹⁸⁵ the structure was solved with the ShelXS structure solution program¹⁸² using Direct Methods and refined with the ShelXL refinement package using Least Squares minimisation.¹⁸²

Table XXVII. Crystal data and structure refinement.

Empirical formula	$C_{29}H_{25}N_3O_3$
Formula weight	463.52
Temperature/K	120
Crystal system	orthorhombic
Space group	Pbca
$a/\text{\AA}$	5.9334(2)
$b/\text{\AA}$	20.7173(6)
$c/\text{\AA}$	38.0315(12)
$\alpha/^\circ$	90
$\beta/^\circ$	90
$\gamma/^\circ$	90
Volume/ \AA^3	4675.0(3)
Z	8
$\rho_{\text{calc}}/\text{cm}^3$	1.317
μ/mm^{-1}	0.694
F(000)	1952.0
Crystal size/ mm^3	$0.568 \times 0.079 \times 0.075$
Radiation	$\text{CuK}\alpha$ ($\lambda = 1.54184$)
2θ range for data collection/ $^\circ$	4.646 to 151.09
Index ranges	$-7 \leq h \leq 6, -26 \leq k \leq 25, -46 \leq l \leq 36$
Reflections collected	25628

Independent reflections	4622 [R _{int} = 0.0545, R _{sigma} = 0.0365]
Data/restraints/parameters	4622/0/321
Goodness-of-fit on F ²	1.039
Final R indexes [I >= 2σ (I)]	R ₁ = 0.0365, wR ₂ = 0.0804
Final R indexes [all data]	R ₁ = 0.0519, wR ₂ = 0.0899
Largest diff. peak/hole / e Å ⁻³	0.29/-0.21

Table XXVIII. Fractional Atomic Coordinates ($\times 10^4$) and Equivalent Isotropic Displacement Parameters ($\text{\AA}^2 \times 10^3$). U_{eq} is defined as 1/3 of the trace of the orthogonalised U_{ij} tensor.

Atom	<i>x</i>	<i>y</i>	<i>z</i>	U(eq)
O(1)	12076.8(16)	2969.3(5)	999.3(3)	18.2(2)
O(2)	7159.1(17)	2867.9(5)	78.3(3)	22.1(2)
O(3)	13764.1(17)	3815.7(5)	422.4(3)	22.6(2)
N(1)	9772.3(19)	3221.0(5)	1047.0(3)	17.0(3)
N(2)	10384(2)	3460.3(5)	186.0(3)	17.3(3)
N(3)	6877(2)	1345.2(6)	1486.7(4)	20.0(3)
C(1)	8383(2)	2679.3(6)	894.1(4)	16.8(3)
C(2)	9686(2)	2557.7(6)	551.4(4)	16.2(3)
C(3)	8861(2)	2958.7(6)	245.4(4)	17.5(3)
C(4)	12252(2)	3429.6(7)	408.6(4)	17.6(3)
C(5)	12039(2)	2820.5(7)	634.0(4)	17.0(3)
C(6)	6387(2)	1908.1(7)	1311.1(4)	19.2(3)
C(7)	8223(2)	2085.6(7)	1117.1(4)	17.4(3)
C(8)	9915(2)	1606.9(7)	1174.8(4)	20.9(3)
C(9)	9043(2)	1161.8(7)	1402.0(4)	21.5(3)
C(10)	9408(2)	3344.2(6)	1415.1(4)	18.4(3)
C(11)	7614(3)	3757.7(7)	1500.3(4)	20.7(3)
C(12)	7203(3)	3871.6(8)	1856.7(5)	27.6(4)
C(13)	8531(3)	3601.5(8)	2118.0(5)	31.1(4)
C(14)	10305(3)	3204.0(8)	2028.0(5)	30.4(4)
C(15)	10742(3)	3073.9(7)	1676.6(4)	25.4(3)
C(16)	10061(2)	3933.2(6)	-86.2(4)	18.3(3)
C(17)	8020(3)	4258.8(7)	-104.9(4)	21.8(3)
C(18)	7692(3)	4706.6(7)	-370.9(5)	26.4(4)
C(19)	9385(3)	4828.7(8)	-615.0(5)	27.9(4)
C(20)	11409(3)	4500.0(8)	-592.8(4)	27.7(4)
C(21)	11765(3)	4051.6(7)	-325.9(4)	22.7(3)
C(22)	5382(2)	991.0(7)	1709.3(4)	19.8(3)
C(23)	4520(3)	1276.3(7)	2014.3(4)	21.7(3)
C(24)	3094(3)	903.2(8)	2222.1(4)	27.0(4)
C(25)	2564(3)	268.7(8)	2135.6(5)	28.7(4)
C(26)	3473(3)	-6.7(7)	1835.6(5)	26.2(4)
C(27)	4875(3)	355.8(7)	1622.1(4)	23.0(3)
C(28)	6198(3)	4076.8(7)	1222.6(5)	25.0(3)
C(29)	5162(3)	1953.4(7)	2123.6(5)	28.6(4)

Table XXIX. Anisotropic Displacement Parameters ($\text{\AA}^2 \times 10^3$). The Anisotropic displacement factor exponent takes the form: $-2\pi^2[h^2a^{*2}U_{11}+2hka^*b^*U_{12}+\dots]$.

Atom	U_{11}	U_{22}	U_{33}	U_{23}	U_{13}	U_{12}
O(1)	14.1(5)	24.2(5)	16.4(5)	-1.1(4)	-0.1(4)	-0.3(4)
O(2)	20.2(5)	24.6(5)	21.6(6)	-1.3(4)	-5.4(5)	-3.3(4)
O(3)	17.5(5)	26.2(5)	24.2(6)	1.8(5)	0.7(5)	-5.7(4)
N(1)	13.7(5)	19.5(5)	17.7(7)	-2.0(5)	-0.3(5)	-0.5(4)
N(2)	16.2(5)	18.8(5)	16.8(6)	-0.4(5)	-0.5(5)	-1.0(5)
N(3)	18.0(6)	21.0(6)	21.0(7)	2.8(5)	2.4(6)	0.8(5)
C(1)	14.4(6)	18.5(6)	17.5(7)	-1.0(6)	-1.6(6)	-1.3(5)
C(2)	16.1(6)	17.3(6)	15.2(7)	-1.0(6)	0.7(6)	-1.2(5)
C(3)	18.3(7)	17.8(6)	16.4(8)	-4.0(6)	2.5(6)	-0.3(5)
C(4)	15.2(6)	20.3(6)	17.2(7)	-3.3(6)	2.9(6)	1.1(5)
C(5)	14.6(6)	19.7(6)	16.7(7)	-2.1(6)	1.1(6)	-0.1(5)
C(6)	17.7(6)	19.4(7)	20.5(8)	1.2(6)	-0.5(6)	1.0(5)
C(7)	15.8(6)	19.8(6)	16.6(7)	-1.6(6)	-0.2(6)	-1.5(5)
C(8)	15.0(6)	23.0(7)	24.9(9)	-0.8(6)	0.3(7)	-0.1(5)
C(9)	18.5(7)	20.1(7)	25.8(9)	0.8(6)	0.0(7)	2.5(5)
C(10)	21.3(7)	18.0(6)	16.0(8)	-1.4(6)	0.4(7)	-4.3(5)
C(11)	20.6(7)	20.2(7)	21.4(8)	-3.0(6)	0.8(7)	-5.0(6)
C(12)	27.7(8)	28.6(8)	26.4(9)	-6.8(7)	7.3(8)	-3.8(6)
C(13)	43.2(10)	32.3(8)	17.6(8)	-3.9(7)	6.0(8)	-8.6(7)
C(14)	45.1(10)	28.4(8)	17.7(8)	0.0(7)	-4.0(8)	-0.5(7)
C(15)	31.7(8)	23.3(7)	21.1(8)	-1.5(6)	-3.4(7)	3.4(6)
C(16)	21.9(7)	16.8(6)	16.3(7)	-0.6(6)	-0.6(7)	-1.3(5)
C(17)	19.7(7)	22.6(7)	23.0(8)	0.3(6)	0.5(7)	-1.7(6)
C(18)	24.7(8)	23.9(7)	30.7(9)	1.6(7)	-4.8(7)	1.7(6)
C(19)	36.4(9)	25.5(7)	21.9(8)	4.7(7)	-1.9(8)	0.9(7)
C(20)	34.4(9)	28.4(8)	20.3(8)	2.8(7)	7.9(8)	1.8(7)
C(21)	24.4(7)	22.4(7)	21.3(8)	-1.8(6)	4.9(7)	3.1(6)
C(22)	16.7(6)	22.6(7)	20.1(8)	5.2(6)	0.2(7)	0.6(6)
C(23)	21.7(7)	23.9(7)	19.4(8)	1.6(6)	-2.1(7)	2.0(6)
C(24)	25.9(8)	34.8(8)	20.5(8)	1.5(7)	4.1(7)	2.2(7)
C(25)	24.4(7)	32.8(8)	28.8(9)	9.8(7)	3.6(8)	-4.5(6)
C(26)	24.5(7)	22.9(7)	31.1(9)	4.4(7)	-1.0(7)	-2.2(6)
C(27)	22.1(7)	23.3(7)	23.7(8)	0.7(6)	1.1(7)	0.6(6)
C(28)	20.9(7)	25.8(7)	28.4(9)	-5.4(7)	-1.6(7)	2.7(6)
C(29)	38.5(9)	24.7(7)	22.7(9)	-1.7(7)	-0.8(8)	1.6(7)

Table XXX. Bond Lengths.

Atom	Atom	Length/ \AA	Atom	Atom	Length/ \AA
O(1)	N(1)	1.4746(14)	C(10)	C(11)	1.404(2)
O(1)	C(5)	1.4232(17)	C(10)	C(15)	1.389(2)
O(2)	C(3)	1.2078(18)	C(11)	C(12)	1.397(2)
O(3)	C(4)	1.2033(17)	C(11)	C(28)	1.503(2)
N(1)	C(1)	1.5090(17)	C(12)	C(13)	1.386(3)

N(1)	C(10)	1.4393(19)	C(13)	C(14)	1.380(3)
N(2)	C(3)	1.3955(18)	C(14)	C(15)	1.388(2)
N(2)	C(4)	1.3958(19)	C(16)	C(17)	1.388(2)
N(2)	C(16)	1.4382(18)	C(16)	C(21)	1.383(2)
N(3)	C(6)	1.3751(18)	C(17)	C(18)	1.386(2)
N(3)	C(9)	1.3783(19)	C(18)	C(19)	1.391(2)
N(3)	C(22)	1.4290(19)	C(19)	C(20)	1.383(2)
C(1)	C(2)	1.536(2)	C(20)	C(21)	1.392(2)
C(1)	C(7)	1.4972(19)	C(22)	C(23)	1.399(2)
C(2)	C(3)	1.511(2)	C(22)	C(27)	1.390(2)
C(2)	C(5)	1.5316(18)	C(23)	C(24)	1.392(2)
C(4)	C(5)	1.531(2)	C(23)	C(29)	1.512(2)
C(6)	C(7)	1.366(2)	C(24)	C(25)	1.391(2)
C(7)	C(8)	1.4280(19)	C(25)	C(26)	1.385(2)
C(8)	C(9)	1.365(2)	C(26)	C(27)	1.384(2)

Table XXXI. Bond Angles.

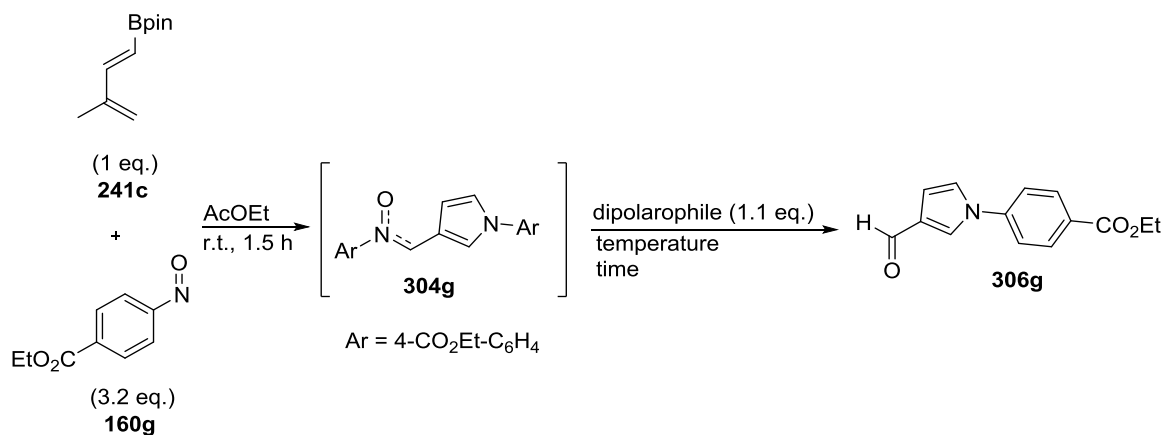
Atom	Atom	Atom	Angle/°	Atom	Atom	Atom	Angle/°
C(5)	O(1)	N(1)	100.50(10)	C(8)	C(9)	N(3)	108.36(13)
O(1)	N(1)	C(1)	101.32(9)	C(11)	C(10)	N(1)	116.54(13)
C(10)	N(1)	O(1)	108.77(11)	C(15)	C(10)	N(1)	122.64(13)
C(10)	N(1)	C(1)	115.12(11)	C(15)	C(10)	C(11)	120.82(14)
C(3)	N(2)	C(4)	112.46(12)	C(10)	C(11)	C(28)	121.99(14)
C(3)	N(2)	C(16)	122.51(12)	C(12)	C(11)	C(10)	117.36(15)
C(4)	N(2)	C(16)	124.98(12)	C(12)	C(11)	C(28)	120.64(14)
C(6)	N(3)	C(9)	108.51(12)	C(13)	C(12)	C(11)	121.87(16)
C(6)	N(3)	C(22)	126.29(12)	C(14)	C(13)	C(12)	119.77(16)
C(9)	N(3)	C(22)	125.16(12)	C(13)	C(14)	C(15)	119.82(17)
N(1)	C(1)	C(2)	100.01(11)	C(14)	C(15)	C(10)	120.33(15)
C(7)	C(1)	N(1)	115.30(12)	C(17)	C(16)	N(2)	118.95(13)
C(7)	C(1)	C(2)	112.20(11)	C(21)	C(16)	N(2)	119.86(13)
C(3)	C(2)	C(1)	113.60(11)	C(21)	C(16)	C(17)	121.19(14)
C(3)	C(2)	C(5)	104.94(11)	C(18)	C(17)	C(16)	119.01(15)
C(5)	C(2)	C(1)	103.09(11)	C(17)	C(18)	C(19)	120.50(15)
O(2)	C(3)	N(2)	124.91(14)	C(20)	C(19)	C(18)	119.78(15)
O(2)	C(3)	C(2)	126.17(13)	C(19)	C(20)	C(21)	120.32(15)
N(2)	C(3)	C(2)	108.92(12)	C(16)	C(21)	C(20)	119.20(14)
O(3)	C(4)	N(2)	126.03(14)	C(23)	C(22)	N(3)	120.09(13)
O(3)	C(4)	C(5)	125.80(14)	C(27)	C(22)	N(3)	118.62(14)
N(2)	C(4)	C(5)	108.17(11)	C(27)	C(22)	C(23)	121.26(14)
O(1)	C(5)	C(2)	106.95(11)	C(22)	C(23)	C(29)	121.87(14)
O(1)	C(5)	C(4)	111.51(11)	C(24)	C(23)	C(22)	117.28(14)
C(4)	C(5)	C(2)	104.67(11)	C(24)	C(23)	C(29)	120.81(15)
C(7)	C(6)	N(3)	108.78(12)	C(25)	C(24)	C(23)	121.86(16)

C(6)	C(7)	C(1)	125.29(13)	C(26)	C(25)	C(24)	119.75(15)
C(6)	C(7)	C(8)	106.90(13)	C(27)	C(26)	C(25)	119.58(15)
C(8)	C(7)	C(1)	127.81(13)	C(26)	C(27)	C(22)	120.25(15)
C(9)	C(8)	C(7)	107.46(13)				

Table XXXII. Hydrogen Atom Coordinates ($\text{\AA}\times 10^4$) and Isotropic Displacement Parameters ($\text{\AA}^2\times 10^3$).

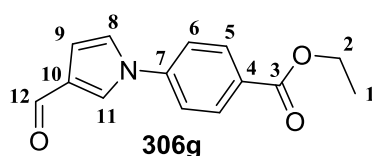
Atom	x	y	z	U(eq)
H(1)	6835	2840	838	20
H(2)	9732	2088	491	19
H(5)	13233	2499	573	20
H(6)	4999	2136	1323	23
H(8)	11378	1600	1074	25
H(9)	9800	789	1487	26
H(12)	5978	4142	1922	33
H(13)	8220	3690	2358	37
H(14)	11225	3020	2206	36
H(15)	11959	2799	1615	30
H(17)	6865	4176	62	26
H(18)	6301	4932	-387	32
H(19)	9151	5137	-796	33
H(20)	12562	4581	-761	33
H(21)	13162	3830	-309	27
H(24)	2464	1087	2429	32
H(25)	1583	25	2282	34
H(26)	3135	-442	1777	31
H(27)	5494	170	1415	28
H(28A)	7141	4180	1019	35(3)
H(28B)	5544	4475	1317	35(3)
H(28C)	4986	3783	1151	35(3)
H(29A)	6771	2022	2079	47(4)
H(29B)	4850	2011	2375	47(4)
H(29C)	4281	2266	1988	47(4)

E.3. General procedure for the screening of the dipolarophile for the [3+2]-cycloaddition:



Diene **241c** (1 eq.) and 4-nitrosobenzoate **160g** (3.2 eq.) were dissolved in AcOEt. The reaction mixture was stirred at r.t. for 1.5 h. The dipolarophile (1.1 eq.) was added and the reaction mixture stirred under reflux for 22 h. The crude reaction mixture was evaporated and purified by silica gel chromatography.

Pyrrole 306g.



Formula : C₁₄H₁₃NO₃
MW : 243.26

Diene **241c** (50.0 mg, 0.24 mmol) and 4-nitrosobenzoate **160g** (138.3 mg, 0.76 mmol) were dissolved in AcOEt (1.2 mL). The reaction mixture was stirred at r.t. for 1.5 h. Diethyl azodicarboxylate **307** (45 μ L, 0.28 mmol) was added and the reaction mixture stirred under reflux for 22 h. The crude reaction mixture was evaporated and purified by silica gel chromatography (eluent, hexane/AcOEt, 1/1, R_f = 0.65) to afford **306g** as a yellow-orange solid (19.2 mg, 33%).

M.p. = 94 - 95 °C.

¹H NMR (400 MHz, Chloroform-*d*, δ ppm) 9.88 (d, *J* = 0.7 Hz, 1H, H₁₂), 8.20 – 8.14 (m, 2H, H₅), 7.74 (dd, *J* = 2.2, 1.6 Hz, 1H, H₁₁), 7.52 – 7.47 (m, 2H, H₆), 7.17 (ddd, *J* = 3.0, 2.1, 0.7 Hz, 1H), 6.84 (dd, *J* = 3.1, 1.6 Hz, 1H), 4.41 (q, *J* = 7.1 Hz, 2H, H₂), 1.42 (t, *J* = 7.1 Hz, 3H, H₁).

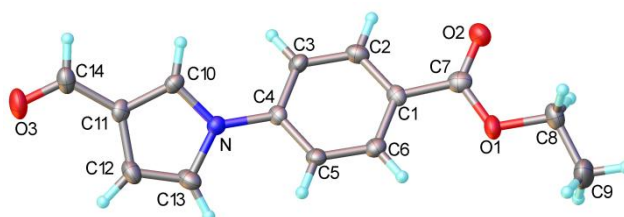
¹³C NMR (101 MHz, Chloroform-*d*, δ ppm) 185.5 (C₁₂), 165.7 (C₃), 142.9 (C₇), 131.6 (C₅), 129.4 (C), 128.9 (C), 126.8 (CH), 122.1 (CH), 120.4 (C₆), 110.5 (C₉), 61.5 (C₂), 14.5 (C₁).

IR (neat, ν) 2973, 1714, 1671, 1614, 1538, 1476, 1286, 1236, 1209, 1100, 1047, 787, 766, 722, 692 cm⁻¹.

LRMS (ESI+) 245.5 (90%) [M+2H]⁺.

HRMS (ESI+) calcd. for [M+H]⁺(C₁₃H₁₄NO₂): 244.0974 found: 244.0983.

Single crystal X-ray structure data for **306g**:



A suitable crystal was selected and measured on a D8V_Mo diffractometer. The crystal was kept at 120 K during data collection. Using Olex2,¹⁸⁵ the structure was solved with the ShelXS structure solution program¹⁸² using Direct Methods and refined with the ShelXL refinement package using Least Squares minimisation.¹⁸²

Table XXXIII. Crystal data and structure refinement.

Empirical formula	C ₁₄ H ₁₃ NO ₃
Formula weight	243.25
Temperature/K	120
Crystal system	orthorhombic
Space group	P2 ₁ 2 ₁ 2 ₁
<i>a</i> /Å	7.092(2)
<i>b</i> /Å	10.597(3)
<i>c</i> /Å	15.834(5)
α /°	90
β /°	90
γ /°	90

Volume/Å ³	1190.0(6)
Z	4
ρ _{calc} /cm ³	1.358
μ/mm ⁻¹	0.791
F(000)	512.0
Crystal size/mm ³	0.156 × 0.043 × 0.04
Radiation	CuKα (λ = 1.54184)
2θ range for data collection/°	10.044 to 131.582
Index ranges	-6 ≤ h ≤ 8, -11 ≤ k ≤ 12, -18 ≤ l ≤ 17
Reflections collected	7950
Independent reflections	2011 [R _{int} = 0.0911, R _{sigma} = 0.0897]
Data/restraints/parameters	2011/0/164
Goodness-of-fit on F ²	1.006
Final R indexes [I >= 2σ (I)]	R ₁ = 0.0552, wR ₂ = 0.1020
Final R indexes [all data]	R ₁ = 0.0994, wR ₂ = 0.1172
Largest diff. peak/hole / e Å ⁻³	0.22/-0.23
Flack parameter	0.5(3)

Table XXXIV. Fractional Atomic Coordinates (×10⁴) and Equivalent Isotropic Displacement Parameters (Å²×10³). U_{eq} is defined as 1/3 of of the trace of the orthogonalised U_{ij} tensor.

Atom	x	y	z	U(eq)
O(1)	1446(4)	3288(3)	2081.2(17)	29.5(9)
O(2)	1255(4)	5240(3)	2620.4(18)	34.3(9)
O(3)	1721(5)	1038(3)	8787.9(19)	40.9(10)
N	1149(5)	1798(3)	5950(2)	20.7(9)
C(1)	1180(6)	3467(4)	3551(3)	21.6(11)
C(2)	841(6)	4194(4)	4266(3)	25.4(11)
C(3)	801(6)	3653(4)	5052(3)	22.7(11)
C(4)	1140(6)	2371(4)	5136(3)	19.5(11)
C(5)	1445(6)	1638(4)	4427(3)	21.8(11)
C(6)	1450(6)	2180(4)	3637(3)	23.6(11)
C(7)	1280(6)	4105(4)	2721(3)	27.8(12)
C(8)	1724(7)	3826(4)	1249(3)	32.5(13)
C(9)	1612(8)	2787(4)	623(3)	46.9(16)
C(10)	1583(6)	2385(4)	6692(2)	21.5(11)
C(11)	1458(6)	1516(4)	7335(3)	22.7(11)
C(12)	949(6)	343(4)	6958(3)	29.0(12)
C(13)	762(7)	540(4)	6126(3)	29.3(12)
C(14)	1842(7)	1798(5)	8207(3)	31.0(13)

Table XXXV. Anisotropic Displacement Parameters (Å²×10³). The Anisotropic displacement factor exponent takes the form: -2π²[h²a*²U₁₁+2hka*b*U₁₂+...].

Atom	U ₁₁	U ₂₂	U ₃₃	U ₂₃	U ₁₃	U ₁₂
O(1)	36(2)	32.8(18)	19.5(17)	7.5(15)	-0.6(17)	-4.1(16)
O(2)	45(2)	27.3(17)	30.8(19)	5.8(15)	-4.3(17)	-0.3(17)

O(3)	52(3)	46(2)	24(2)	13.5(17)	1.9(18)	5.9(18)
N	20(2)	21.7(19)	20(2)	-1.3(17)	0.7(19)	0.2(17)
C(1)	14(3)	26(2)	26(3)	5(2)	-4(2)	-1(2)
C(2)	22(3)	20(2)	34(3)	0(2)	-2(2)	1(2)
C(3)	24(3)	24(2)	20(3)	-4(2)	-4(2)	1(2)
C(4)	15(3)	22(2)	21(3)	2(2)	-5(2)	0(2)
C(5)	21(3)	19(2)	25(3)	-1(2)	-3(2)	-3(2)
C(6)	21(3)	25(2)	25(3)	-4(2)	-3(2)	-2(2)
C(7)	19(3)	29(3)	35(3)	-2(2)	-5(3)	0(2)
C(8)	35(3)	34(3)	28(3)	11(2)	0(2)	4(2)
C(9)	69(5)	46(3)	26(3)	5(3)	6(3)	0(3)
C(10)	19(3)	24(2)	21(3)	-5(2)	0(2)	3(2)
C(11)	16(3)	32(2)	19(3)	0(2)	4(2)	1(2)
C(12)	28(3)	31(3)	28(3)	11(2)	-1(2)	-4(2)
C(13)	28(3)	24(3)	37(3)	5(2)	-4(2)	-5(2)
C(14)	34(3)	35(3)	24(3)	6(2)	4(2)	8(2)

Table XXXVI. Bond Lengths.

Atom Atom	Length/Å	Atom Atom	Length/Å
O(1) C(7)	1.338(5)	C(2) C(3)	1.371(6)
O(1) C(8)	1.449(5)	C(3) C(4)	1.386(5)
O(2) C(7)	1.213(5)	C(4) C(5)	1.382(6)
O(3) C(14)	1.225(5)	C(5) C(6)	1.376(6)
N C(4)	1.425(5)	C(8) C(9)	1.483(6)
N C(10)	1.364(5)	C(10) C(11)	1.376(5)
N C(13)	1.390(5)	C(11) C(12)	1.425(6)
C(1) C(2)	1.391(6)	C(11) C(14)	1.439(6)
C(1) C(6)	1.384(5)	C(12) C(13)	1.340(6)
C(1) C(7)	1.479(6)		

Table XXXVII. Bond Angles.

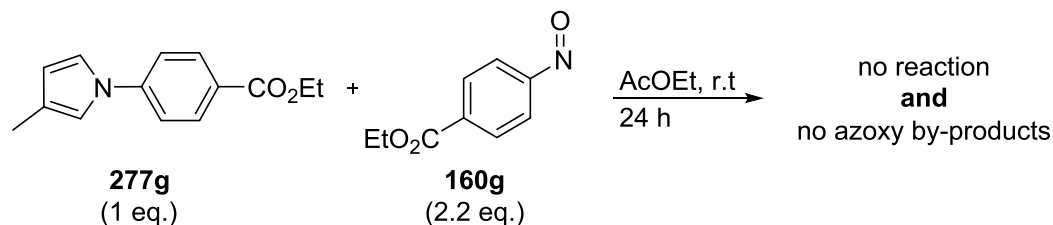
Atom Atom Atom	Angle/°	Atom Atom Atom	Angle/°
C(7) O(1) C(8)	116.4(3)	C(5) C(6) C(1)	120.1(4)
C(10) N C(4)	125.8(3)	O(1) C(7) C(1)	112.4(4)
C(10) N C(13)	108.0(3)	O(2) C(7) O(1)	122.9(4)
C(13) N C(4)	126.1(3)	O(2) C(7) C(1)	124.7(4)
C(2) C(1) C(7)	118.6(4)	O(1) C(8) C(9)	107.9(3)
C(6) C(1) C(2)	119.3(4)	N C(10) C(11)	108.5(3)
C(6) C(1) C(7)	122.1(4)	C(10) C(11) C(12)	106.8(4)
C(3) C(2) C(1)	120.7(4)	C(10) C(11) C(14)	124.0(4)
C(2) C(3) C(4)	119.6(4)	C(12) C(11) C(14)	129.1(4)
C(3) C(4) N	120.3(4)	C(13) C(12) C(11)	107.5(4)
C(5) C(4) N	119.7(3)	C(12) C(13) N	109.1(4)

C(5)	C(4)	C(3)	120.0(4)	O(3)	C(14)	C(11)	124.8(4)
C(6)	C(5)	C(4)	120.3(4)				

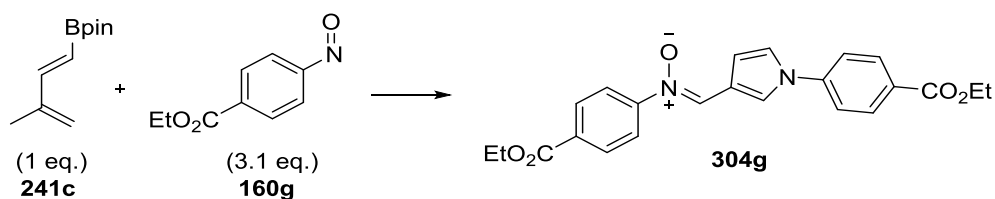
Table XXXVIII. Hydrogen Atom Coordinates ($\text{\AA}\times 10^4$) and Isotropic Displacement Parameters ($\text{\AA}^2\times 10^3$).

Atom	x	y	z	U(eq)
H(2)	635	5076	4210	30
H(3)	542	4153	5536	27
H(5)	1652	757	4484	26
H(6)	1640	1671	3151	28
H(8A)	2972	4242	1217	39
H(8B)	740	4465	1132	39
H(9A)	1880	3119	58	70
H(9B)	343	2422	632	70
H(9C)	2538	2135	766	70
H(10)	1916	3248	6754	26
H(12)	774	-436	7244	35
H(13)	420	-82	5722	35
H(14)	2216	2635	8343	37

E.4. Procedures for the study of the mechanistic aspects:

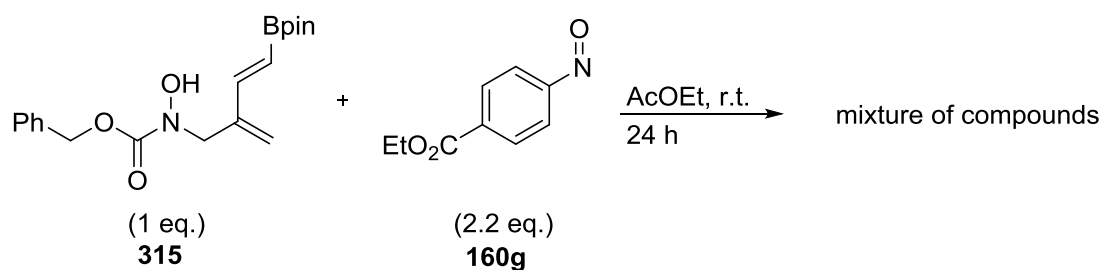


Pyrrole **277g** (47.0 mg, 0.20 mmol) and 4-nitrosobenzoate **160g** (77.2 mg, 0.45 mmol) were dissolved in AcOEt (1 mL). The reaction mixture was stirred at r.t. A sample was taken by syringe after 1.5 h and the reaction stopped after 24 h. The crude reaction mixture was evaporated, and no purification was performed.



Diene **241c** (1 eq.), 4-nitrosobenzoate **160g** (3.2 eq.) and TEMPO **314** (0.1 or 1 eq.) were dissolved in AcOEt. The reaction mixture was stirred at r.t. for 1.5 h. The solvent was evaporated and the crude reaction mixture analysed by ^1H NMR. No purification was performed.

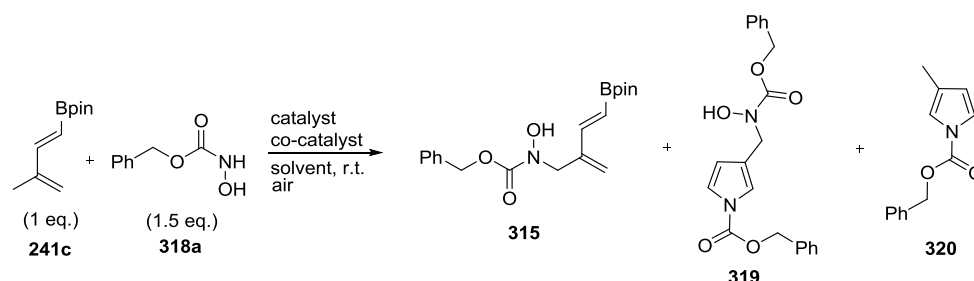
To a solution of 4-nitrosobenzoate **160g** (3.2 eq.) in AcOEt under an inert atmosphere was added a solution of diene **241c** (1 eq.) in AcOEt. The reaction was stirred at r.t. for 1.5 h under an inert atmosphere. The solvent was evaporated and the crude reaction mixture analysed by ^1H NMR. No purification was performed.



Compound **315** (50.0 mg, 0.14 mmol) and 4-nitrosobenzoate **160g** (55.0 mg, 0.31 mmol) were dissolved in AcOEt (0.7 mL). The reaction mixture was stirred r.t. A sample was taken by syringe after 1.5 h and the reaction stopped after 24 h. The crude reaction mixture was evaporated, and no purification was performed.

Boronated dienes and carbonylnitroso compounds

A. Reaction of 1-dienylboronate pinacolate esters with carbonylnitroso compounds



Procedure using Bu₄NIO₄:

A solution of diene **241c** (37.5 mg, 0.19 mmol) and nitroso precursor **318a** (32.3 mg, 0.19 mmol) in DCM (0.5 mL) was cooled to -5 °C. A DCM solution (2 mL) of Bu₄NIO₄ (83.8 mg, 0.19 mmol) was added dropwise. The reaction mixture was stirred at -5 °C for 2 h. The crude mixture was washed with a saturated solution of Na₂S₂O₅ (2 x), saturated solution of NaHCO₃ (2 x), water (1 x) and finally brine (1 x). The organic layer was dried over MgSO₄, filtered and evaporated. The crude product was analysed by ¹H NMR, (no purification was performed).

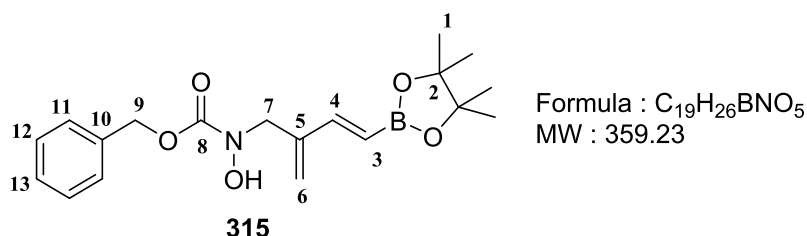
Procedure using Rose Bengal:

To a solution of Rose Bengal (4.6 mg, 0.0045 mmol) in MeCN (1 mL), was added pyridine (26 μL, 6.20x10⁻⁴ mol.L⁻¹ in MeCN). Nitroso precursor **318a** and diene **241c** (87.0 mg, 0.45 mmol) were then added successively. The reaction mixture was stirred at 35 °C (heating from the light) for 22 h under irradiation from a light bulb (40W).

Procedure using aerobic copper method:

A solution of copper source (0.2 eq.) and pyridine (0.05 eq.) was stirred at r.t. in THF for 5 min. To the solution was added diene **241c** (1 eq.) and carbonylnitroso precursor **318a** (1.5 eq.) and THF. The reaction mixture was stirred at r.t. until TLC showed full completion of the diene. The solvent was evaporated and the crude reaction product was purified by silica gel chromatography.

Carbonylnitroso ene-product 315.



A solution of CuCl (4.2 mg, 0.043 mmol) and pyridine (18 μ L, 6.19x10⁻⁴ mol.L⁻¹ in THF) was prepared in THF (1 mL). After 5 min, diene **241c** (82.0 mg, 0.42 mmol), carbonyl nitroso precursor **318a** (106.0 mg, 0.63 mmol) and THF (1 mL) were added. The reaction mixture was stirred between 10 and 17 °C (cryostat) for 28 h. The solvent was evaporated, and the crude reaction product was purified by silica gel chromatography (eluent, hexane/AcOEt, 7/3, R_f = 0.55) to afford compound **315** as a white solid (100.0 mg, 66%).

M.p. = 98 °C.

¹H NMR (400 MHz, Chloroform-*d*, δ ppm) 7.36 (m, 5H, H₁₁, H₁₂ and H₁₃), 7.06 (d, *J* = 18.6 Hz, 1H, H₄), 5.66 (d, *J* = 18.6 Hz, 1H, H₃), 5.39 (s, 1H, H₆), 5.34 (d, *J* = 1.0 Hz, 1H, H₆), 5.20 (s, 2H, H₉), 4.36 (s, 2H, H₇), 1.28 (s, 12H, H₁).

¹³C NMR (101 MHz Chloroform-*d*, δ ppm) 157.4 (C₈), 149.2 (C₄), 140.7 (C₅), 135.9 (C₁₀), 128.7 (C₁₂), 128.4 (C₁₃), 128.3 (C₁₁), 121.0 (C₆), 117.6 (C₃), 83.5 (C₂), 68.3 (C₉), 51.6 (C₇), 24.9 (C₁).

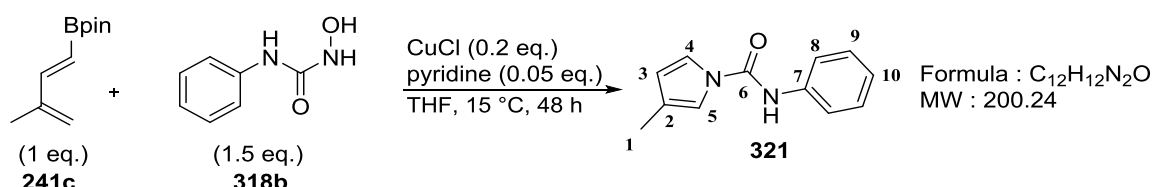
¹¹B NMR (96 MHz, Chloroform-*d*, δ ppm) 30.1.

IR (neat, ν) 3263, 1700, 1605, 1353, 1244, 1101, 1001, 907, 846, 756, 700, 590 cm^{-1} .

LRMS (ESI+) 360.2 $[\text{M}+\text{H}]^+$, 315.6 (59%), 283.3 (22%).

HRMS (ESI) calcd. for $[\text{M}+\text{H}]^+(\text{C}_{19}\text{H}_{27}\text{NO}_5^{11}\text{B})$: 360.1982 found: 360.1992.

Pyrrole **321**.



Oxidation using aerobic copper method was followed using CuCl (9.1 mg, 0.092 mmol) and pyridine (39 μL , $6.19 \times 10^{-4} \text{ mol} \cdot \text{L}^{-1}$ in THF) in THF (1 mL). After 5 min, diene **241c** (80.0 mg, 0.46 mmol), carbonyl nitroso precursor **318b** (105.5 mg, 0.69 mmol) and THF (1 mL) were added. The reaction mixture was stirred at r.t. for 48 h. The crude reaction mixture was filtered over a pad of celite and washed with acetone (150 mL). The solvent was evaporated and the crude product was purified by silica gel chromatography (eluent, hexane/AcOEt, 7/3, $R_f = 0.60$). to afford pyrrole **321** as a yellow solid (14.8 mg, 16%).

M.p. = 120 °C.

^1H NMR (400 MHz, Chloroform-*d*, δ ppm) 7.53 – 7.47 (m, 2H, H_8), 7.40 – 7.35 (m, 2H, H_9), 7.23 (dd, $J = 3.0, 1.6 \text{ Hz}$, 1H, H_4), 7.18 – 7.14 (m, 1H, H_{10}), 7.13 (bs, 1H, NH), 7.03 – 7.02 (m, 1H, H_5), 6.18 (dd, $J = 3.4, 1.6 \text{ Hz}$, 1H, H_3), 2.12 (d, $J = 1.1 \text{ Hz}$, 3H, H_1).

^{13}C NMR (101 MHz, Chloroform-*d*, δ ppm) 137.1 (C_7), 129.4 (C_9), 124.9 (C_{10}), 123.6 (C_2), 120.4 (C_8), 118.9 (C_4), 115.8 (C_5), 114.6 (C_3), 12.1 (C_1).

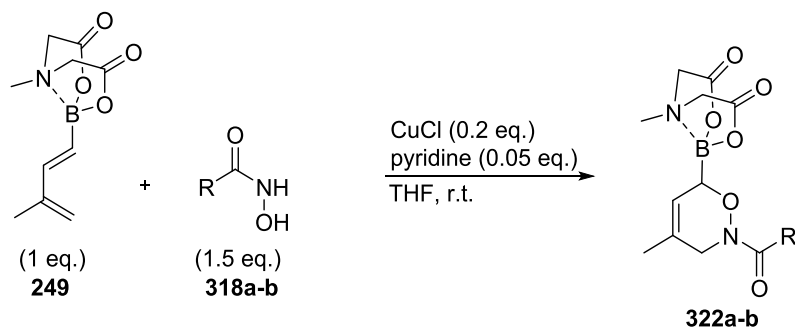
IR (neat, ν) 3354, 1680, 1600, 1533, 1444, 1339, 1313, 1253, 1085, 781, 744, 688, 599, 575 cm^{-1} .

LRMS (ESI+) 201.5 $[\text{M}+\text{H}]^+$.

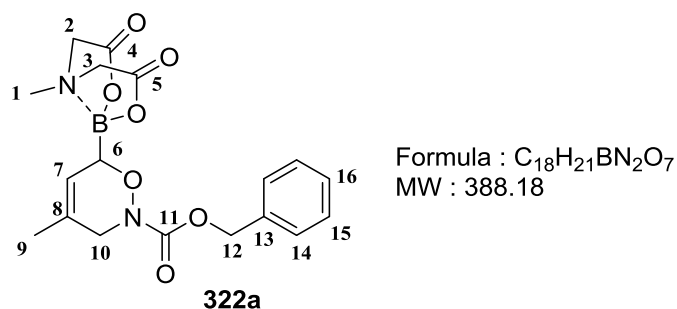
HRMS (ESI+) calcd. for $[\text{M}+\text{H}]^+(\text{C}_{12}\text{H}_{13}\text{N}_2\text{O})$: 201.1028 found: 201.1034.

B. Reaction of tetracoordinated 1-borodienes with carbonylnitroso compounds

B.1. Reaction using BMIDA diene **249**:



Oxazine **322a**.



Procedure using aerobic copper method:

CuCl (8.9 mg, 0.090 mmol) and pyridine (36 μL , $6.19 \times 10^{-4} \text{ mol.L}^{-1}$ in THF) in THF (1 mL). After 5 min, diene **249** (100.0 mg, 0.45 mmol), carbonyl nitroso precursor **318a** (113.5 mg, 0.67 mmol) and THF (1 mL) were added. The reaction mixture was stirred at r.t. for 9 days. The solvent was evaporated and the crude product was purified by solid phase silica gel chromatography (eluent, Et₂O/MeCN, 8/2, R_f = 0.55) to afford oxazine **322a** as a white solid (125.4 mg, 72%).

Procedure using Bu₄NIO₄:

A solution of diene **249** (40 mg, 0.18 mmol) and nitroso precursor **318a** (37.4 mg, 0.22 mmol) in DCM (0.5 mL) was cooled to -5 °C. A DCM solution (2 mL) of Bu₄NIO₄ (97.1 mg 0.22 mmol) was added dropwise. The reaction mixture was stirred at -5 °C for 2 h. The crude was washed with a saturated solution of Na₂S₂O₅ (2 x), a saturated solution of NaHCO₃ (2 x), water (1 x) and finally brine (1 x). The organic layer was dried over MgSO₄, filtered and evaporated. The crude product was purified by solid phase silica gel chromatography (eluent, Et₂O/MeCN, 8/2, R_f = 0.55) to afford oxazine **322a** as a white solid (26.0 mg, 37%).

M.p. = 185 °C.

¹H NMR (400 MHz, Acetone-*d*₆, δ ppm) 7.45 – 7.31 (m, 5H, H₁₄, H₁₅ and H₁₆), 5.64 (m, 1H, H₇), 5.21 – 5.11 (m, 2H, H₁₂), 4.40 (bs, 1H, H₆), 4.30 (d, *J* = 17.2, 1H, H₂ or H₃), 4.17 (d, *J* = 16.4, 1H, H₂ or H₃), 4.16 – 4.11 (m, 1H, H₁₀), 4.03 (d, *J* = 17.2, 1H, H₂ or H₃) 3.86 (d, *J* = 16.4, 1H, H₂ or H₃), 3.87 – 3.80 (m, 2H, H₁₀), 3.20 (s, 3H, H₁), 1.74 (dq, *J* = 2.4, 1.1 Hz, 3H, H₉).

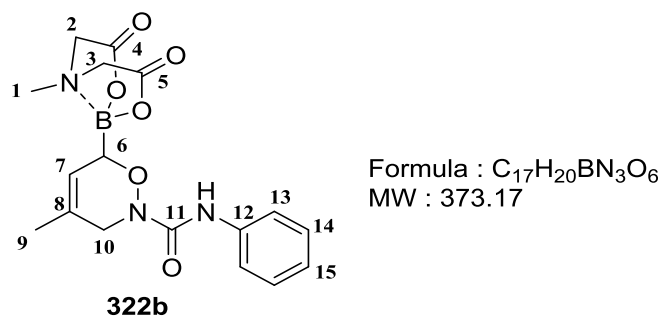
¹³C NMR (101 MHz, Acetone-*d*₆, δ ppm) 169.1 (C₄ or C₅), 168.0 (C₄ or C₅), 156.3 (C₁₁), 137.4 (C₁₃), 129.4 (C₁₅), 129.2 (C₁₆), 129.1 (C₁₄), 128.8 (C₈), 120.9 (C₇), 68.2 (C₁₂), 63.1 (C₂ or C₃), 63.0 (C₂ or C₃), 49.1 (C₁₀), 46.5 (C₁), 20.1 (C₉), B-C not visible.

¹¹B NMR (96 MHz, Acetone-*d*₆, δ ppm) 9.7.

LRMS (ESI+) 389.1 [M+H]⁺, 345.1 (43%), 172.1 (75%).

HRMS (ESI+) calcd. for [M+H]⁺(C₁₈H₂₂N₂O₇¹⁰B): 388.1155 found: 388.1535.

Oxazine 322b.



Oxidation using aerobic copper method was followed using CuCl (8.9 mg, 0.090 mmol) and pyridine (36 μ L, 6.19×10^{-4} mol.L⁻¹ in THF) in THF (1 mL). After 5 min, diene **249** (100.0 mg, 0.45 mmol), carbonyl nitroso precursor **318b** (103.2 mg, 0.67 mmol) and THF (1 mL) were added. The reaction mixture was stirred at r.t. for 7 days. The solvent was evaporated and the crude product was purified by solid phase silica gel chromatography (eluent Et₂O/MeCN, 8/2, R_f = 0.6) to afford oxazine **322b** as a white solid (37.2 mg, 58%).

M.p. = 145 °C.

¹H NMR (400 MHz, Acetone-*d*₆, δ ppm) 7.95 (s, 1H, NH), 7.56 – 7.50 (m, 2H, H₁₃), 7.32 – 7.24 (m, 2H, H₁₂), 7.06 – 6.99 (m, 1H, H₁₅), 5.75 (m, 1H, H₇), 4.60 (bs, 1H, H₆), 4.38 (d, *J* = 8.2 Hz, 1H, H₂ or H₃), 4.31 (d, *J* = 8.2 Hz, 1H, H₂ or H₃), 4.26 – 4.20 (m, 1H, H₁₀), 4.18 (d, *J* = 16.9 Hz, 1H, H₂ or H₃), 4.14 (d, *J* = 16.9 Hz, 1H, H₂ or H₃), 3.76 – 3.70 (m, 1H, H₁₀), 3.32 (s, 3H, H₁), 1.80 (dt, *J* = 2.4, 1.2 Hz, 3H, H₉).

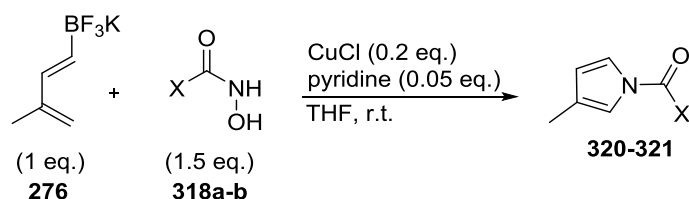
¹³C NMR (101 MHz, Acetone-*d*₆, δ ppm) 168.8 (C₄ or C₅), 168.7 (C₄ or C₅), 156.4 (C₁₁), 139.9 (C₁₂), 129.7 (C₈), 129.6 (C₁₄), 123.6 (C₁₅), 120.7 (C₇), 119.6 (C₁₃), 63.5 (C₂ or C₃), 63.4 (C₂ or C₃), 48.1 (C₁₀), 47.1 (C₁), 20.3 (C₉), B-C not visible.

¹¹B NMR (96 MHz, Acetone-*d*₆, δ ppm) 9.7.

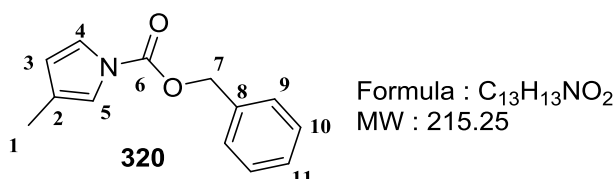
LRMS (ESI+) 412.1 (39%) [M+K]⁺, 396.1 (100%) [M+Na]⁺, 264.1, 246.2.

HRMS (ESI+) calcd. for [M+Na]⁺(C₁₇H₂₀N₃O₆¹¹BNa): 396.1343 found: 396.1346.

B.2. Reaction using BF_3K diene **276**:



Pyrrole **320**.



Oxidation using aerobic copper method was followed using CuCl (9.1 mg, 0.092 mmol) and pyridine (39 μL , $6.19 \times 10^{-4} \text{ mol.L}^{-1}$ in THF) in THF (1 mL). After 5 min, diene **276** (80.0 mg, 0.46 mmol), carbonyl nitroso precursor **318a** (115.3 mg, 0.69 mmol) and THF (1 mL) were added. The reaction mixture was stirred at r.t. for 22 h. The crude reaction mixture was filtered over a pad of celite and washed with acetone (150 mL). The solvent was evaporated and the crude product was purified by silica gel chromatography (eluent hexane/AcOEt, 7/3, $R_f = 0.85$) to afford pyrrole **320** as a yellow oil (48.2 mg, 48%).

^1H NMR (400 MHz, Chloroform-*d*, δ ppm) 7.45 – 7.35 (m, 5H, H_9 , H_{10} and H_{11}), 7.21 (t, $J = 2.8$ Hz, 1H, H_4), 7.06 – 7.02 (m, 1H, H_5), 6.09 (ddd, $J = 3.2, 1.7, 0.6$ Hz, 1H, H_3), 5.35 (s, 2H, H_7), 2.06 (dd, $J = 1.2, 0.6$ Hz, 3H, H_1).

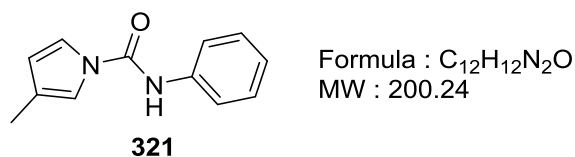
^{13}C NMR (101 MHz, Chloroform-*d*, δ ppm) 150.4 (C_6), 135.2 (C_8), 128.8 (C_9 or C_{10}), 128.5 (C_9 or C_{10}), 123.4 (C_2), 120.3 (C_4), 117.4 (C_5), 114.9 (C_3), 68.8 (C_7), 12.0 (C_1).

IR (neat, ν) 1739, 1491, 1456, 1406, 1338, 1241, 1222, 1117, 1068, 971, 767, 696, 616 cm^{-1} .

LRMS (ESI+) 216.1 (71%) [$M+H$] $^+$, 172.4 (100%).

HRMS (ESI+) calcd. for [$M+H$] $^+$ ($C_{13}H_{14}NO_2$): 216.1025 found: 216.1021.

Pyrrole **321**.



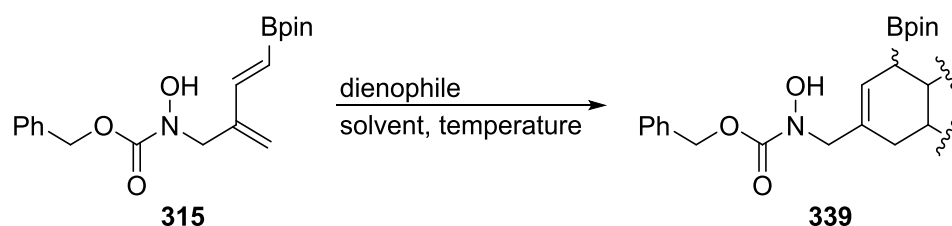
Oxidation using aerobic copper method was followed using CuCl (9.1 mg, 0.092 mmol) and pyridine (39 μ L, 6.19×10^{-4} mol.L⁻¹ in THF) in THF (1 mL). After 5 min, diene **250** (80.0 mg, 0.46 mmol), carbonyl nitroso precursor **318b** (105.5 mg, 0.69 mmol) and THF (1 mL) were added. The reaction mixture was stirred at r.t. for 20 h. The crude reaction mixture was filtered over a pad of celite and washed with acetone (150 mL). The solvent was evaporated and the crude product was purified by silica gel chromatography (eluent, hexane/AcOEt, 7/3, R_f = 0.60). to afford pyrrole **321** as a yellow solid (49.1 mg, 53%).

For characterisation, refer to section A.

The ene-adduct as key intermediate in cascade reactions

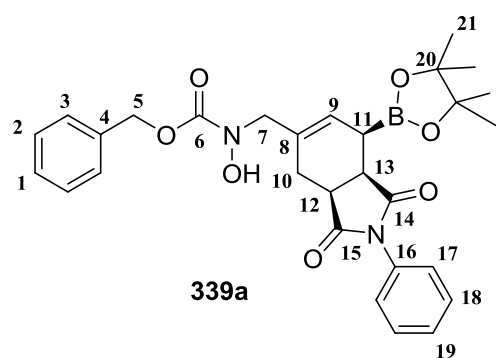
A. The Diels-Alder/allylboration sequence

A.1. General procedure for the Diels-Alder step:



To a solution of **315** in the solvent (DCM or toluene) was added the dienophile (1.1 eq). The reaction mixture was stirred at the temperature indicated in the work procedure. The crude reaction mixture was evaporated and the crude product purified by silica gel chromatography.

Diels-Alder cycloadduct **339a**.



Formula : C₂₉H₃₃BN₂O₇
MW : 532.40

Compound **315** (54.0 mg, 0.15 mmol) and *N*-phenyl maleimide **2a** (28.6 mg, 0.17 mmol) were stirred in DCM (2 mL) at r.t. for 18 h. The crude was purified by silica gel chromatography (eluent, hexane/EtOAc, 1/1, R_f = 0.60) to afford compound **339a** as a white solid (67.1 mg, 84%).

M.p. = 89 - 90°C.

¹H NMR (600 MHz, Chloroform-*d*, δ ppm) 7.41– 7.37 (m, 2H, H₁₈), 7.36 – 7.28 (m, 6H, H₁, H₂, H₃ and H₁₉), 7.23 – 7.19 (m, 2H, H₁₇), 6.82 (bs, 1H, OH), 6.07 (dt, *J* = 4.9, 1.6 Hz, 1H, H₉), 5.15 (s, 2H, H₅), 4.22 (d, *J* = 15.4 Hz, 1H, H₇), 4.07 (d, *J* = 15.4 Hz, 1H, H₇), 3.42 (ddt, *J* = 9.6, 6.5, 1.7 Hz, 1H, H₁₃), 3.25 (ddt, *J* = 11.7, 6.5, 3.0 Hz, 1H, H₁₂), 2.71 – 2.65 (m, 1H, H₁₀), 2.30 (dd, *J* = 15.4, 7.7 Hz, 1H, H₁₀), 2.11 – 2.07 (m, 1H, H₁₁), 1.28 – 1.24 (m, 12H, H₂₁).

¹³C NMR (101 MHz, Chloroform-*d*, δ ppm) 180.1 (C₁₄), 179.0 (C₁₅), 157.4 (C₆), 136.0 (C₄), 135.3 (C₈), 132.1 (C₁₆), 129.1 (C₁₈), 128.6 (C₃ or C₂), 128.3 (C₁₉ or C₁), 128.2 (C₃ or C₂), 127.0 (C₁₉ or C₁), 126.7 (C₁₇), 84.2 (C₂₀), 68.2 (C₅), 55.2 (C₇), 42.0 (C₁₃), 40.4 (C₁₂), 25.9 (C₁₀), 25.0 (C₂₁), 24.8 (C₂₁), 21.8 (C₁₁).

¹¹B NMR (96 MHz, Chloroform-*d*, δ ppm) 32.7.

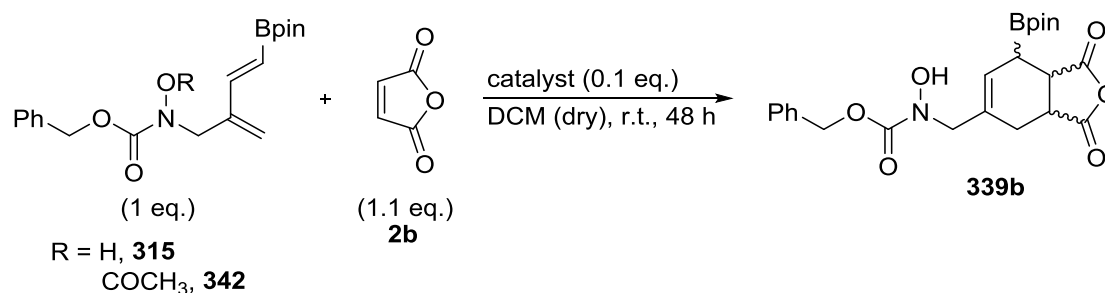
IR (neat, ν) 3316, 1706, 1704, 1700, 1381, 1329, 1167, 1140, 1098, 853, 738, 693, 623 cm⁻¹.

LRMS (ESI+) 533.1 (100%) [M+H]⁺, 489.2 (98%).

HRMS (ESI+) calcd. for [M+H]⁺(C₂₉H₃₄¹⁰BN₂O₇): 532.2495 found: 532.2505.

Reaction using **2b**, **23**, **12** and **341** were performed at r.t. in DCM or at 90°C in toluene following the general procedure. No products were isolated.

A.2. General procedure for the Lewis acid catalysed Diels-Alder reaction:



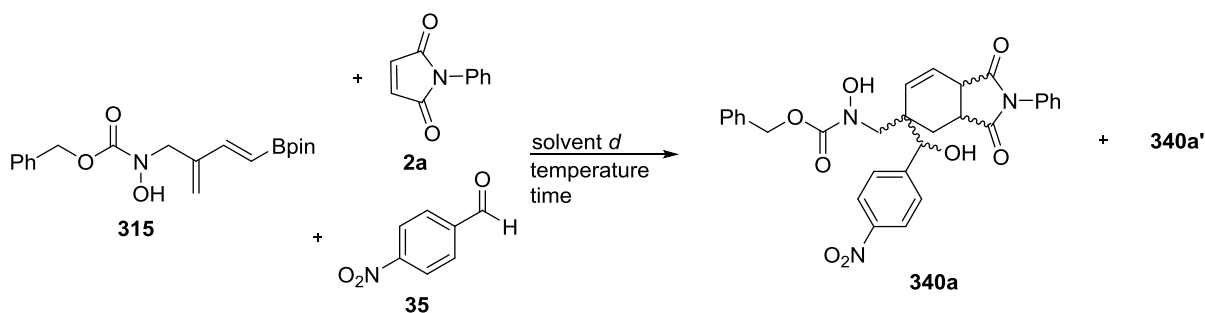
In a oven-dried flask were solubilised compound **315** or compound **342** (1 eq.), freshly ground maleic anhydride (1.1 eq.) and the catalyst (0.1 eq.) in dry DCM under inert atmosphere. The reaction mixture was stirred at r.t. for 48 h. The crude reaction mixture was

washed with H₂O (3 x). The aqueous layer was extracted with DCM (2 x). The organic layer was dried over MgSO₄, filtered and evaporated.

A.3. Calculations for the determination of the stereochemistry of 339a:

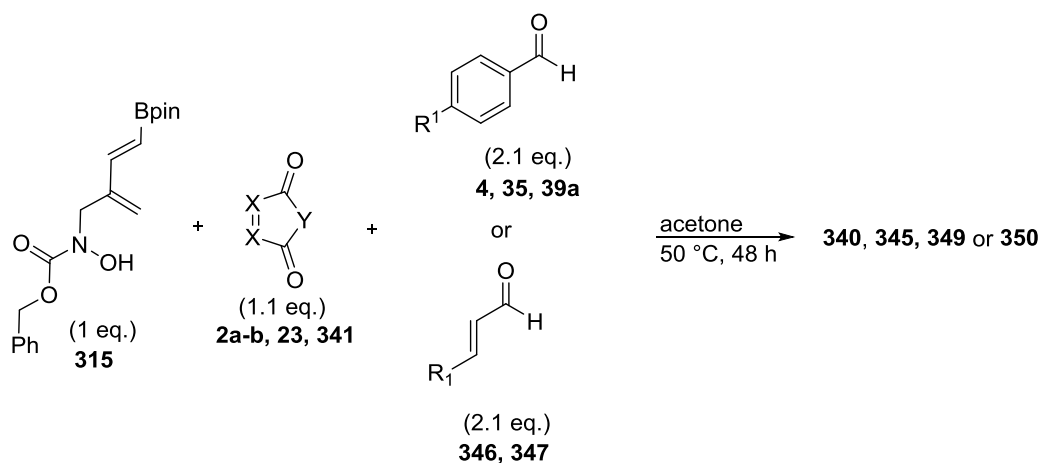
Conformational searches were carried out using Spartan '10.¹⁸⁶ Each structure was drawn and subjected to a full conformational search, using the Monte-Carlo algorithm with 500 conformations examined, and semi-empirical (AM1) energy minimisations to give the predictions of the 10 lowest energy conformations. Dihedral angles generated from the conformational searches were used to calculate coupling constants, using the MestReJ software.¹⁸⁷

A.4. General procedure for the optimisation of the one-pot Diels-Alder/allylboration sequence:



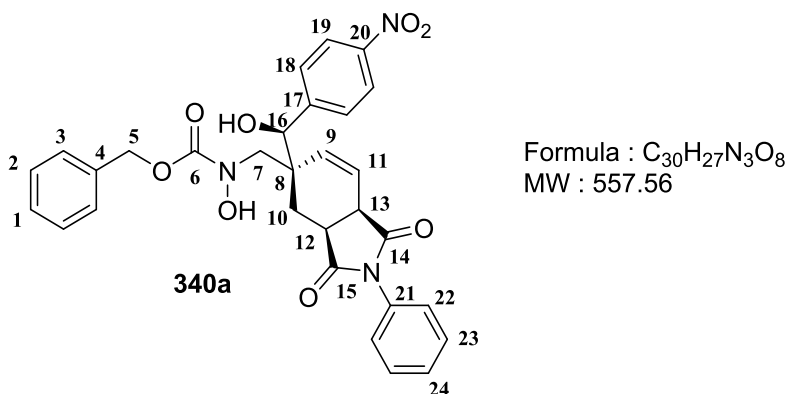
To a solution of **315** [X] in the solvent, were added *N*-phenyl maleimide **2a** (x eq) and *p*-nitrobenzaldehyde **35** (x eq). The reaction mixture was stirred at the temperature presented in Table 20. The reaction was stirred from 48 hours to 1 week and monitored by ¹H NMR analysis. Reaction with [**315**] = 0.17 and 0.1 M were directly performed in NMR tube. Reaction with [**315**] = 1.00 M were performed in a hemolysis tube and sample were taken and diluted for NMR measurement.

A.5. General procedure using the optimised reaction conditions with substituted arylaldehydes and α,β unsaturated aldehydes:



To a solution of **315** [1 M] in acetone, were added the dienophile (1.1 eq) and the aldehyde (2.1 eq). The reaction mixture was stirred at 50 °C for 48 h. The solvent was evaporated and the crude product was purified by silica gel chromatography.

Polycyclic product 340a.



Compound **315** (61.8 mg, 0.17 mmol), *N*-phenyl maleimide **2a** (32.8 mg, 0.19 mmol) and 4-nitrobenzaldehyde **35** (54.6 mg, 0.36 mmol) were stirred in acetone (170 μ L) at 50 °C for 48 h. The crude was purified by silica gel chromatography (eluent, hexane/EtOAc, 1/1, R_f = 0.40) to afford compound **340a** as a pale yellow solid (46.0 mg, 48%).

M.p. = 127 °C (changed in state but not liquid), 158 °C.

¹H NMR (400 MHz, Chloroform-*d*, δ ppm) 8.19 (bs, 1H, N-OH), 8.09 – 8.07 (m, 2H, H₁₉) 7.44 – 7.31 (m, 10H, H_{Ar}), 7.14 – 7.09 (m, 2H, H₁₈), 6.19 (d, *J* = 10.3 Hz, 1H, H₁₁), 6.07 (dd, *J* = 10.3, 2.6 Hz, 1H, H₉), 5.23 – 5.19 (m, 2H, H₅), 4.66 (s, 1H, H₁₆), 4.08 – 4.06 (m, 1H, H₇), 3.45 (m, 2H, H₁₂ and H₁₃), 3.34 (d, *J* = 15.5 Hz, 1H, H₇), 2.37 – 2.26 (m, 2H, H₁₀).

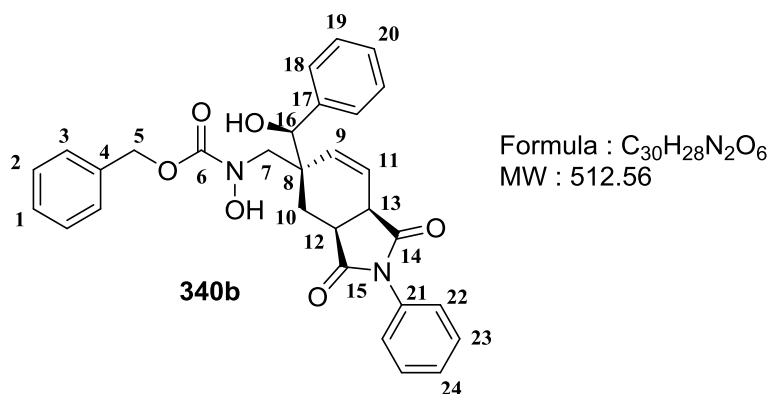
¹³C NMR (101 MHz, Chloroform-*d*, δ ppm) 175.0 (C₁₄), 171.4 (C₁₅), 158.5 (C₆), 147.6 (C₂₀), 146.7 (C₁₇) 135.4 (C₄), 131.5 (C₂₁), 131.4 (C₁₁), 129.4 (CH), 129.0 (CH), 128.89 (CH), 128.86 (CH), 128.8 (CH), 128.5 (CH), 126.3 (C₁₈), 124.1 (C₉), 123.2 (C₁₉), 75.4 (C₁₆), 69.0 (C₅), 53.6 (C₇), 45.0 (C₈), 40.8 (C₁₃), 36.6 (C₁₂), 24.9 (C₁₀).

IR (neat, ν) 3370, 2943, 1704, 1700, 1696, 1519, 1499, 1346, 1180, 755, 731, 693 cm⁻¹.

LRMS (ESI+) 558.0 (27%) [M+H]⁺, 514.1 (100%).

HRMS (ESI+) calcd. for [M+H]⁺(C₃₀H₂₈N₃O₈): 558.1876 found: 558.900.

Polycyclic product **340b**.



Compound **315** (82.2 mg, 0.23 mmol), *N*-phenyl maleimide **2a** (43.6 mg, 0.25 mmol) and benzaldehyde **4** (26 μL, 0.25 mmol) were stirred in acetone (230 μL) at 50 °C for 48 h. The crude was purified by silica gel chromatography (eluent, hexane/EtOAc, 1/1, R_f = 0.40) to afford compound **340b** as a white solid (46.0 mg, 39%).

M.p. = 107 °C (changed in state but not liquid), 116 °C.

¹H NMR (400 MHz, Chloroform-*d*, δ ppm) 7.46 – 7.25 (m, 14H, H_{Ar} and N-OH), 7.18 – 7.14 (m, 2H, H_{Ar}), 6.08 – 5.99 (m, 2H, H₉ and H₁₁), 5.22 (s, 2H, H₅), 4.55 (d, *J* = 3.7 Hz, 1H,

H₁₆), 3.92 (d, *J* = 15.5 Hz, 1H, H₇), 3.51 – 3.41 (m, 3H, H₁₂, H₁₃ and OH), 3.49 (d, *J* = 15.5 Hz, 1H, H₇), 2.18 (dd, *J* = 13.9, 6.5 Hz, 1H, H₁₀), 1.69 (dd, *J* = 13.9, 8.9 Hz, 1H, H₁₀)

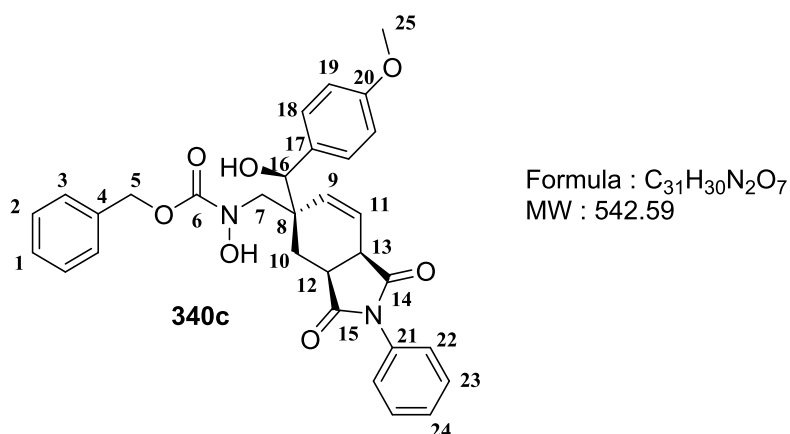
¹³C NMR (101 MHz, Chloroform-*d*, δ ppm) 179.6 (C₁₄), 175.5 (C₁₅), 157.8 (C₆), 139.0 (C₁₇), 135.7 (C₄), 132.7 (C₁₁), 131.7 (C₂₁), 129.3 (CH), 128.9 (CH), 128.8 (CH), 128.7 (CH), 128.5 (CH), 128.2 (CH), 128.16 (CH), 128.0 (CH), 126.4 (CH), 123.2 (C₉), 76.9 (C₁₆), 68.7 (C₅), 53.9 (C₇), 44.7 (C₈), 40.9 (C₁₃), 36.8 (C₁₂), 28.0 (C₁₀)

IR (neat, ν) 3352, 2948, 1704, 1700, 1696, 1497, 1455, 1378, 1178, 1075, 755, 731, 691 cm⁻¹.

LRMS (ESI+) 513.6 (100%) [M+H]⁺.

HRMS (ESI+) calcd. for [M+H]⁺(C₃₀H₂₉N₂O₆): 513.2026 found: 513.2028.

Polycyclic product 340c.



Compound **315** (85.5 mg, 0.24 mmol), *N*-phenylmaleimide **2a** (45.4 mg, 0.26 mmol) and 4-anisaldehyde **39a** (61 μL, 0.50 mmol) were stirred in acetone (240 μL) at 50 °C for 48 h. The crude was purified by silica gel chromatography (eluent, hexane/EtOAc, 1/1, R_f = 0.30) to afford compound **340c** as a white solid (21.1 mg, 16%).

M.p. = 110 °C (changed in state but not liquid), 132 °C.

¹H NMR (400 MHz, Chloroform-*d*, δ ppm) 7.52 (bs, 1H, N-OH), 7.48 – 7.30 (m, 8H, H_{Ar}), 7.22 – 7.15 (m, 4H, H_{Ar}), 6.85 – 6.79 (m, 2H, H₁₉), 6.11 – 5.98 (m, 2H, H₉ and H₁₁), 5.22 (s, 2H, H₅), 4.51 (d, *J* = 3.8 Hz, 1H, H₁₆), 3.90 (d, *J* = 15.5 Hz, 1H, H₇), 3.79 (s, 3H, H₂₅), 3.49 (d, *J* = 15.5 Hz, 1H, H₇), 3.49 – 3.39 (m, 2H, H₁₂, H₁₃ and OH), 2.17 (dd, *J* = 13.8, 6.5 Hz, 1H, H₁₀), 1.65 (dd, *J* = 13.8, 9.1 Hz, 1H, H₁₀).

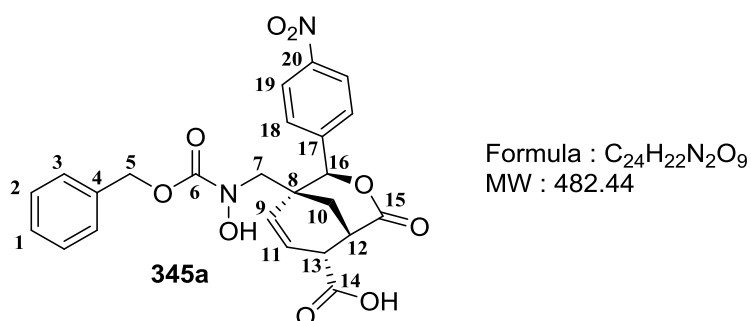
^{13}C NMR (101 MHz, Chloroform-*d*, δ ppm) 179.5 (C₁₄), 175.5 (C₁₅), 159.4 (C₂₀), 157.7 (C₆), 135.7 (C₄), 132.8 (C₁₁), 131.7 (C₂₁), 131.0 (C₁₇), 129.4 (CH), 129.1 (CH), 128.9 (CH), 128.8 (CH), 128.7 (CH), 128.5 (CH), 126.4 (CH), 123.2 (C₉), 113.6 (C₁₉), 76.6 (C₁₆), 68.7 (C₅), 55.4 (C₂₅), 53.9 (C₇), 44.7 (C₈), 40.9 (C₁₃), 36.8 (C₁₂), 28.1 (C₁₀).

IR (neat, ν) 3326, 2936, 1704, 1699, 1499, 1380, 1249, 1177, 1141, 1029, 752, 693 cm^{-1} .

LRMS (ESI+) 542.6 (100%) [M+H]⁺.

HRMS (ESI+) calcd. for [M+H]⁺(C₃₁H₃₁N₂O₇): 543.2131 found: 543.2109.

Polycyclic product 345a.



Compound **315** (83.7 mg, 0.23 mmol), maleic anhydride **2b** (25.1 mg, 0.25 mmol) and 4-nitrobenzaldehyde **35** (73.0 mg, 0.48 mmol) were stirred in acetone (240 μL) at 50 °C for 48 h. Acetone was evaporated and the crude product was dissolved in a minimum of CHCl₃ and stored 24 h at + 4 °C. The precipitate was filtered and washed with Et₂O (2x) to afford compound **345a** as a white solid (64.1 mg, 75%).

M.p. = 147 °C (changed in state but not liquid), 189 °C.

^1H NMR (400 MHz, Acetone-*d*⁶, δ ppm) 8.68 (bs, 1H, N-OH), 8.32 – 8.27 (m, 2H, H₁₉), 7.77 – 7.72 (m, 2H, H₁₈), 7.47 – 7.26 (m, 5H, H₁, H₂ and H₃), 6.18 – 6.06 (m, 2H, H₉ and H₁₁), 5.61 (d, J = 1.5 Hz, 1H, H₁₆), 5.11 – 5.02 (m, 2H, H₅), 3.90 (d, J = 14.5 Hz, 1H, H₇), 3.60 – 3.55 (m, 2H, H₁₂ and H₁₃), 2.95 (d, J = 14.5 Hz, 1H, H₇), 2.39 – 2.33 (m, 1H, H₁₀), 2.13 – 2.08 (m, 1H, H₁₀).

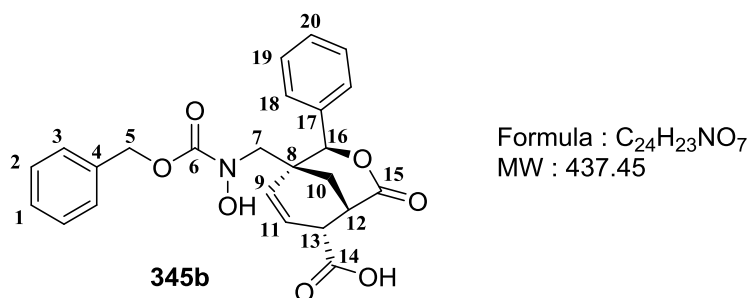
^{13}C NMR (101 MHz, Acetone-*d*⁶, δ ppm) 172.2 (C₁₄), 169.8 (C₁₅), 158.2 (C₆), 148.9 (C₂₀), 145.2 (C₁₇), 135.7 (C₄), 133.5 (C₁₁), 130.0 (CH), 129.2 (CH), 128.9 (C₁), 128.8 (CH), 124.2 (C₁₉), 85.2 (C₁₆), 68.0 (C₅), 57.1 (C₇), 46.5 (C₈), 40.2 (C₁₃), 39.9 (C₁₂), 26.7 (C₁₀).

IR (neat, ν) 3194, 2982, 1717, 1688, 1520, 1349, 1266, 1221, 1170, 1094, 1058, 852, 746, 698 cm^{-1} .

LRMS (ESI+) 483.4 (100%) $[\text{M}+\text{H}]^+$, 439.1 (79%).

HRMS (ESI+) calcd. for $[\text{M}+\text{H}]^+(\text{C}_{24}\text{H}_{23}\text{N}_2\text{O}_9)$: 483.1404 found: 483.1414.

Polycyclic product **345b**.



Compound **315** (82.5 mg, 0.23 mmol), maleic anhydride **2b** (24.8 mg, 0.25 mmol) and benzaldehyde **4** (50 μL , 0.48 mmol) were stirred in acetone (230 μL) at 50 $^\circ\text{C}$ for 48 h. Acetone was evaporated and the crude product was dissolved in a minimum of CHCl_3 and stored 24 h at + 4 $^\circ\text{C}$. The precipitate was filtered and washed with Et_2O (2x) to afford compound **345b** as a white solid (64.0 mg, 64%).

M.p. = 121 $^\circ\text{C}$.

^1H NMR (400 MHz, Acetone- d_6 , δ ppm) 8.61 (bs, 1H, N-OH), 7.49 – 7.28 (m, 10H, H_{Ar}), 6.13 – 6.02 (m, 2H, H_9 and H_{11}), 5.39 (d, $J = 1.7$ Hz, 1H, H_{16}), 5.07 (d, $J = 2.4$ Hz, 2H, H_5), 3.86 (d, $J = 14.5$ Hz, 1H, H_7), 3.56 – 3.50 (m, 2H, H_{12} and H_{13}), 2.90 (d, $J = 14.5$ Hz, 1H, H_7), 2.43 – 2.36 (m, 1H, H_{10}), 2.08 – 2.04 (m, 1H, H_{10}).

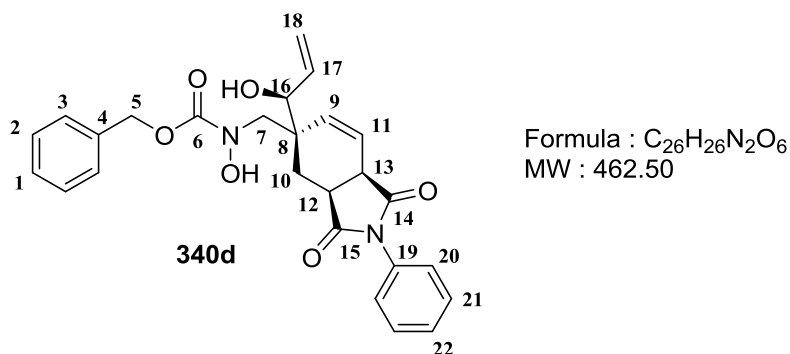
^{13}C NMR (101 MHz, Acetone- d_6 , δ ppm) 172.3 (C_{15}), 170.1 (C_{14}), 159.3 (C_6), 137.9 (C), 137.6 (C), 134.0 (C_9), 129.4 (CH), 129.3 (CH), 129.2 (CH), 128.8 (CH), 128.7 (CH), 128.6 (CH), 128.3 (CH), 86.2 (C_{16}), 67.9 (C_5), 57.4 (C_7), 46.6 (C_{13}), 40.3 (C_8), 40.0 (C_{12}), 26.7 (C_{10}).

IR (neat, ν) 3184, 2943, 1729, 1717, 1706, 1424, 1374, 1355, 1265, 1221, 1174, 1099, 1054, 747, 735, 696 cm^{-1} .

LRMS (ESI+) 438.0 (100%) $[\text{M}+\text{H}]^+$, 394.1 (46%), 331.1 (26%), 136.1 (27%).

HRMS (ESI+) calcd. for $[\text{M}+\text{H}]^+(\text{C}_{24}\text{H}_{24}\text{NO}_7)$: 438.1553 found: 438.1544.

Polycyclic product **340d**.



Compound **315** (80.0 mg, 0.22 mmol), *N*-phenyl maleimide **2a** (42.4 mg, 0.24 mmol) and acrolein **346** (32 μ L, 0.47 mmol) were stirred in acetone (225 μ L) at 50 °C for 48 h. The crude was purified by silica gel chromatography (eluent hexane/EtOAc, 1/1, R_f = 0.35) to afford compound **340d** as a white solid (38.1 mg, 37%).

M.p. = 105 °C.

¹H NMR (400 MHz, Chloroform-*d*, δ ppm) 8.02 (bs, 1H, N-OH), 7.50 – 7.30 (m, 8H, H_{Ar}), 7.25 – 7.21 (m, 2H, H_{Ar}), 6.09 (dd, *J* = 10.2, 3.8 Hz, 1H, H₁₁), 5.96 (dd, *J* = 10.2, 2.6 Hz, 1H, H₉), 5.82 (ddd, *J* = 16.5, 10.9, 7.1 Hz, 1H, H₁₇), 5.29 – 5.19 (m, 5H, H₁₈, H₁₆ and H₅), 3.90 – 3.84 (m, 1H, H₁₃), 3.80 (d, *J* = 15.5 Hz, 1H, H₇), 3.51 (d, *J* = 15.5 Hz, 2H, H₇ and OH), 3.45 – 3.34 (m, 1H, H₁₂), 2.14 (dd, *J* = 14.0, 6.6 Hz, 1H, H₁₀), 1.75 (dd, *J* = 14.0, 9.4 Hz, 1H, H₁₀).

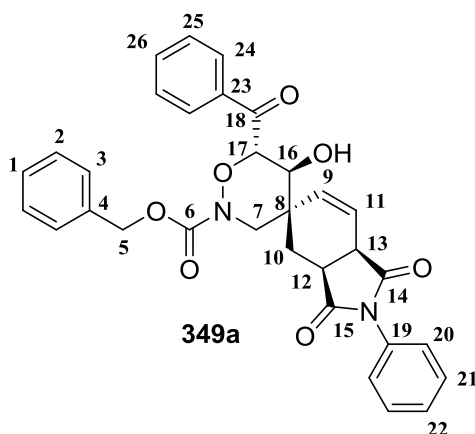
¹³C NMR (101 MHz, Chloroform-*d*, δ ppm) 179.6 (C₁₃), 175.5 (C₁₂), 157.6 (C₆), 135.8 (C), 135.0 (CH), 132.5 (C₉), 131.7 (C), 129.4 (CH), 128.9 (CH), 128.8 (CH), 128.6 (CH), 128.5 (CH), 126.4 (CH), 123.4 (CH), 119.4 (C₁₈), 76.3 (C₁₆), 68.5 (C₅), 53.6 (C₇), 43.7 (C₁₃), 41.0 (C₈), 36.7 (C₁₂), 22.8 (C₁₀).

IR (neat, ν) 3358, 2923, 1704, 1700, 1498, 1378, 1261, 1179, 1074, 988, 752, 693 cm⁻¹.

LRMS (ESI+) 463.1.0 (32%) [M+H]⁺, 445.0 (100%), 419.1 (84%), 401.1 (61%), 356.1 (22%).

HRMS (ESI+) calcd. for [M+H]⁺(C₂₆H₂₇N₂O₆): 463.1869 found: 463.1874.

Polycyclic product 349a.



Formula : C₃₂H₂₈N₂O₇
MW : 552.58

Compound **315** (85.4 mg, 0.24 mmol), *N*-phenyl maleimide **2a** (45.4 mg, 0.26 mmol) and *trans*-cinnamaldehyde **347** (63 μ L, 0.50 mmol) were stirred in acetone (240 μ L) at 50 °C for 48 h. The crude was purified by silica gel chromatography (eluent, hexane/EtOAc, 1/1, R_f = 0.60) to afford compound **349a** (62.3 mg, 47%).

M.p. = 205 °C.

¹H NMR (700 MHz, Chloroform-*d*, δ ppm) 8.21 (bs, 2H, H₂₄), 7.55 – 7.53 (m, 1H, H_{Af}), 7.49 – 7.36 (m, 8H, H_{Af}), 7.28 – 7.23 (m, 4H, H_{Af}), 6.28 (dd, *J* = 10.0, 4.0 Hz, 1H, H₁₁), 5.83 (dd, *J* = 10.1, 2.7 Hz, 1H, H₉), 5.41 (d, *J* = 11.8 Hz, 1H, H₅), 5.25 (d, *J* = 11.8 Hz, 1H, H₅), 5.02 (d, *J* = 9.3 Hz, 1H, H₁₇), 4.21 (dd, *J* = 9.3, 3.5 Hz, 1H, H₁₆), 4.05 (d, *J* = 14.3 Hz, 1H, H₇), 3.59 (d, *J* = 8.9 Hz, 1H, H₁₃), 3.40 – 3.30 (m, 1H, H₁₂), 3.28 (d, *J* = 14.3 Hz, 1H, H₇), 3.11 (d, *J* = 3.6 Hz, 1H, OH), 2.25 (dd, *J* = 14.4, 9.5 Hz, 1H, H₁₀), 2.19 (dd, *J* = 14.4, 7.8 Hz, 1H, H₁₀).

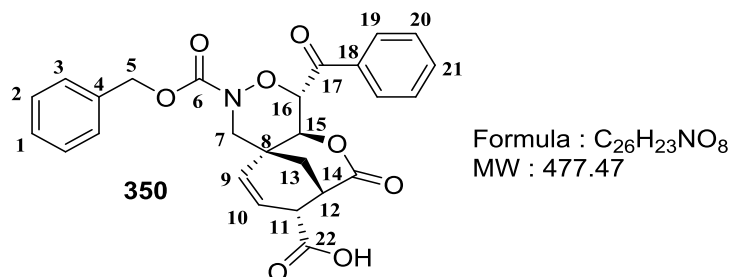
¹³C NMR (101 MHz, Chloroform-*d*, δ ppm) 195.4 (C₁₈), 178.2 (C₁₃), 175.3 (C₁₂), 155.4 (C₆), 135.3 (C), 134.6 (C), 134.5 (CH), 133.5 (C₉), 132.0 (C₁₉), 130.2 (C₂₄), 129.3 (CH), 129.2 (2 CH), 129.04 (2 CH), 128.98 (CH), 128.71 (CH), 128.68 (2 CH), 126.5 (2 CH), 125.4 (C₁₁), 79.2 (C₁₇), 72.0 (C₁₆), 69.1 (C₅), 51.9 (C₇), 40.5 (C₁₃), 39.6 (C₈), 36.3 (C₁₂), 24.5 (C₁₀).

IR (neat, ν) 3527, 2917, 1704, 1683, 1675, 1447, 1387, 1228, 1187, 1103, 887, 751, 693, 682 cm⁻¹.

LRMS (ESI⁺) 553.0 (100%) [M+H]⁺, 505.1 (27%), 354.2 (19%).

HRMS (ESI+) calcd. for $[M+H]^+(C_{32}H_{29}N_2O_7)$: 553.1975 found: 553.1965.

Polycyclic product **350**.



Compound **315** (81.0 mg, 0.23 mmol), maleic anhydride **2b** (24.3 mg, 0.25 mmol) and *trans*-cinnamaldehyde **347** (60 μ L, 0.47 mmol) were stirred in acetone (230 μ L) at 50 $^{\circ}$ C for 48 h. The crude was purified by silica gel chromatography (eluent, hexane/EtOAc, 1/1, R_f = 0.60) to afford compound **350** (62.3 mg, 47%).

M.p. = 195 $^{\circ}$ C

1H NMR (700 MHz, Acetone- d_6 , δ ppm) 11.02 (bs, 1H, COOH), 8.27 – 8.26 (m, 2H, H₁₉), 7.65 – 7.63 (m, 1H, H₂₁), 7.53 – 7.50 (m, 2H, H₁₉), 7.44 – 7.38 (m, 5H, H₁, H₂ and H₃), 6.21 (ddd, J = 10.1, 1.9, 0.9 Hz, 1H, H₁₀), 5.80 (dt, J = 10.1, 2.4 Hz, 1H, H₉), 5.65 (d, J = 9.7 Hz, 1H, H₁₆), 5.36 – 5.29 (m, 2H, H₅), 4.84 (dd, J = 9.7, 1.7 Hz, 1H, H₁₅), 4.19 (d, J = 14.3 Hz, 1H, H₇), 3.74 (d, J = 14.3 Hz, 1H, H₇), 3.63 (ddd, J = 4.9, 2.8, 1.9 Hz, 1H, H₁₁), 3.35 (td, J = 4.6, 2.4 Hz, 1H, H₁₂), 2.82 (ddd, J = 13.4, 5.2, 1.9 Hz, 1H, H₁₃), 1.87 (dt, J = 13.4, 1.7 Hz, 1H, H₁₃)

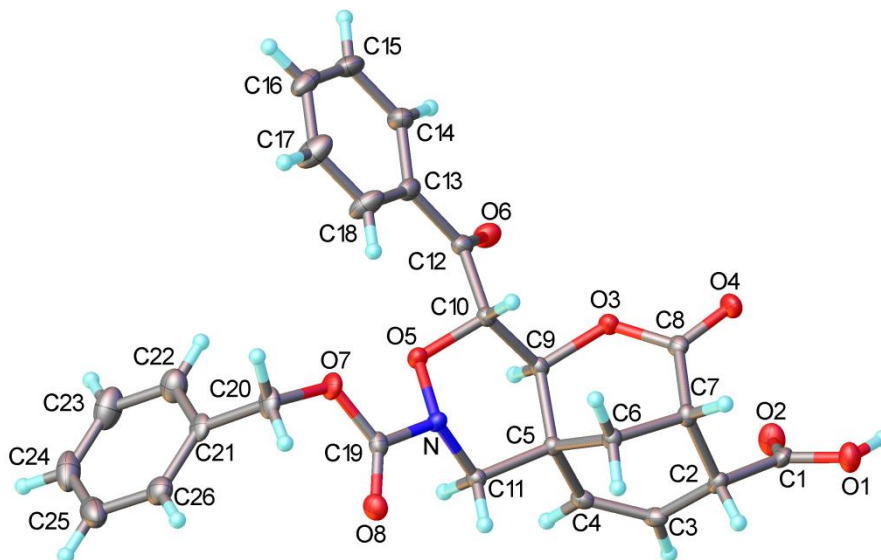
^{13}C NMR (101 MHz, Acetone- d_6 , δ ppm) 191.1 (C₁₇), 171.9 (C₁₃), 168.7 (C₁₂), 156.2 (C₆), 136.8 (C₄ or C₁₈), 136.4 (C₄ or C₁₈), 135.0 (C₂₁), 130.5 (C₉), 130.3 (C₁₉), 130.2 (C₁₀), 129.6 (2x C_{Ar}), 129.5 (C_{Ar}), 129.4 (C_{Ar}), 77.0 (C₁₅), 76.9 (C₁₆), 69.1 (C₅), 53.7 (C₇), 46.6 (C₁₁), 39.6 (C₁₂), 34.6 (C₈), 28.3 (C₁₃).

IR (neat, ν) 3069, 2957, 1734, 1690, 1665, 1450, 1361, 1203, 1120, 1089, 757, 694, 650 cm^{-1} .

LRMS (ESI+) 478.0 (100%) $[M+H]^+$, 434.1 (15%).

HRMS (ESI+) calcd. for $[M+H]^+(C_{26}H_{24}NO_8)$: 478.1502 found: 478.1497.

Single crystal X-ray structure for **350**:



A suitable crystal obtained in DCM was selected and measured on a D8V_Mo diffractometer. The crystal was kept at 120 K during data collection. Using Olex2,¹⁸⁵ the structure was solved with the ShelXS structure solution program,¹⁸² using Direct Methods and refined with the ShelXL refinement package using Least Squares minimisation.¹⁸²

Table XXXIX. Crystal data and structure refinement

Empirical formula	C ₂₆ H ₂₃ NO ₈
Formula weight	477.45
Temperature/K	120
Crystal system	triclinic
Space group	P-1
a/Å	5.4952(2)
b/Å	14.8829(6)
c/Å	15.0258(6)
α/°	62.4438(14)
β/°	85.7136(15)
γ/°	89.0614(15)
Volume/Å ³	1086.19(7)
Z	2
ρ _{calc} /cm ³	1.460
μ/mm ⁻¹	0.109
F(000)	500.0
Crystal size/mm ³	0.154 × 0.103 × 0.049
Radiation	MoKα (λ = 0.71073)

2 θ range for data collection/ $^{\circ}$	5.264 to 59.996
Index ranges	$-7 \leq h \leq 7, -20 \leq k \leq 20, -21 \leq l \leq 21$
Reflections collected	24112
Independent reflections	6336 [$R_{\text{int}} = 0.0370, R_{\text{sigma}} = 0.0419$]
Data/restraints/parameters	6336/0/320
Goodness-of-fit on F^2	1.029
Final R indexes [$I \geq 2\sigma(I)$]	$R_1 = 0.0465, wR_2 = 0.1048$
Final R indexes [all data]	$R_1 = 0.0727, wR_2 = 0.1166$
Largest diff. peak/hole / $e \text{ \AA}^{-3}$	0.42/-0.27

Table XL. Fractional Atomic Coordinates ($\times 10^4$) and Equivalent Isotropic Displacement Parameters ($\text{\AA}^2 \times 10^3$).

U_{eq} is defined as 1/3 of the trace of the orthogonalised U_{ij} tensor.

Atom	x	y	z	$U(\text{eq})$
O(1)	2389(2)	6123.7(9)	9156.8(9)	24.5(2)
O(2)	-492.3(19)	5658.0(9)	8476.0(9)	26.8(3)
O(3)	2079.4(17)	3160.4(7)	8638.6(7)	16.6(2)
O(4)	1676(2)	3642.3(8)	9802.5(8)	23.2(2)
O(5)	5366.9(17)	2292.1(7)	6989.7(7)	16.6(2)
O(6)	355.2(19)	1495.9(8)	8484.4(8)	22.8(2)
O(7)	9312(2)	1900.1(8)	6315.2(8)	23.2(2)
O(8)	10465.7(18)	3559.7(8)	5432.5(8)	20.8(2)
N	7228(2)	3062.4(8)	6599.6(9)	15.1(2)
C(1)	1618(3)	5797.3(10)	8539.4(11)	18.1(3)
C(2)	3698(2)	5617.3(10)	7914.8(10)	16.0(3)
C(3)	2755(3)	5751.4(10)	6949.3(10)	17.6(3)
C(4)	3141(2)	5097.4(10)	6586.1(10)	15.4(3)
C(5)	4711(2)	4175.6(10)	7063.2(10)	12.2(2)
C(6)	6388(2)	4304.1(10)	7765.3(10)	14.1(3)
C(7)	4779(2)	4545.2(10)	8497.1(10)	14.6(3)
C(8)	2748(2)	3764.8(10)	9020.8(10)	15.4(3)
C(9)	3060(2)	3233.1(10)	7685(1)	13.5(2)
C(10)	4337(2)	2234.2(10)	7919.7(10)	14.4(3)
C(11)	6105(2)	4049.7(10)	6202.9(10)	14.6(3)
C(12)	2492(3)	1337.3(10)	8354.5(10)	16.8(3)
C(13)	3355(3)	297.2(11)	8610.0(11)	19.2(3)
C(14)	1727(3)	-508.0(12)	9174.2(12)	26.3(3)
C(15)	2354(3)	-1489.7(12)	9396.8(13)	30.8(4)
C(16)	4582(3)	-1675.3(12)	9045.4(13)	28.8(4)
C(17)	6223(3)	-885.7(13)	8498.9(16)	36.2(4)
C(18)	5640(3)	100.2(12)	8288.1(15)	31.5(4)
C(19)	9116(2)	2889.2(11)	6037.4(10)	16.3(3)
C(20)	11286(3)	1625.8(12)	5791.2(12)	23.9(3)
C(21)	10423(3)	1601.0(11)	4878.4(11)	20.1(3)
C(22)	8280(3)	1082.0(13)	4946.4(14)	30.1(4)
C(23)	7543(3)	1041.5(15)	4103.6(16)	38.5(4)
C(24)	8931(4)	1502.5(15)	3202.2(15)	37.7(4)
C(25)	11059(4)	2011.2(14)	3132.5(13)	35.2(4)

Table XLI. Anisotropic Displacement Parameters ($\text{\AA}^2 \times 10^3$). The Anisotropic displacement factor exponent takes the form: $-2\pi^2[h^2a^2U_{11}+2hka*b*U_{12}+\dots]$.

Atom	U_{11}	U_{22}	U_{33}	U_{23}	U_{13}	U_{12}
O(1)	24.0(6)	29.8(6)	26.7(6)	-19.7(5)	4.0(5)	-2.3(4)
O(2)	16.8(5)	35.9(6)	33.8(6)	-22.3(5)	4.6(4)	-2.4(4)
O(3)	17.6(5)	16.4(5)	15.9(5)	-8.3(4)	5.3(4)	-3.6(4)
O(4)	28.7(6)	21.8(5)	19.2(5)	-11.1(4)	9.2(4)	-1.4(4)
O(5)	18.7(5)	15.2(5)	17.3(5)	-9.2(4)	4.0(4)	-4.4(4)
O(6)	19.7(5)	19.4(5)	27.9(6)	-10.1(5)	2.3(4)	-3.4(4)
O(7)	28.1(6)	20.2(5)	25.1(6)	-14.7(5)	4.1(4)	4.6(4)
O(8)	17.4(5)	24.2(5)	21.9(5)	-12.2(4)	2.9(4)	0.5(4)
N	16.6(5)	12.2(5)	16.6(5)	-7.3(4)	2.7(4)	-1.3(4)
C(1)	23.5(7)	11.8(6)	19.3(7)	-8.0(5)	2.9(5)	-0.5(5)
C(2)	16.0(6)	13.3(6)	19.8(7)	-9.4(5)	4.5(5)	-2.2(5)
C(3)	17.8(6)	14.3(6)	16.5(6)	-4.1(5)	2.0(5)	1.7(5)
C(4)	13.9(6)	15.8(6)	13.2(6)	-4.2(5)	0.5(5)	0.2(5)
C(5)	12.1(6)	12.2(6)	12.1(6)	-5.8(5)	0.5(5)	0.3(4)
C(6)	12.1(6)	15.5(6)	16.4(6)	-8.9(5)	0.5(5)	0.0(5)
C(7)	13.6(6)	17.1(6)	15.4(6)	-9.6(5)	0.6(5)	-0.1(5)
C(8)	16.1(6)	13.3(6)	15.8(6)	-6.1(5)	0.0(5)	3.5(5)
C(9)	13.3(6)	14.5(6)	13.2(6)	-7.0(5)	0.8(5)	-0.8(5)
C(10)	15.9(6)	13.4(6)	13.4(6)	-6.2(5)	0.9(5)	-1.0(5)
C(11)	16.0(6)	13.8(6)	13.5(6)	-6.2(5)	1.6(5)	0.4(5)
C(12)	19.6(7)	15.2(6)	14.9(6)	-6.2(5)	-0.6(5)	-2.4(5)
C(13)	24.0(7)	14.7(7)	19.1(7)	-7.9(6)	-3.0(6)	-1.8(5)
C(14)	34.3(9)	18.9(7)	23.3(8)	-8.6(6)	6.1(6)	-5.4(6)
C(15)	44.4(10)	15.4(7)	26.8(8)	-5.4(6)	2.2(7)	-7.6(7)
C(16)	38.4(9)	15.8(7)	33.2(9)	-10.7(7)	-12.8(7)	2.9(6)
C(17)	26.5(8)	22.3(8)	60.8(13)	-20.1(8)	-2.9(8)	4.0(6)
C(18)	24.0(8)	17.9(7)	50.4(11)	-14.1(7)	-0.3(7)	-3.1(6)
C(19)	16.4(6)	20.4(7)	15.9(6)	-11.4(6)	-3.7(5)	4.4(5)
C(20)	22.6(7)	28.0(8)	28.7(8)	-19.7(7)	-3.4(6)	10.6(6)
C(21)	20.4(7)	19.4(7)	25.5(7)	-14.8(6)	-3.3(6)	8.8(5)
C(22)	23.9(8)	35.5(9)	37.6(9)	-23.0(8)	0.9(7)	1.5(7)
C(23)	29.1(9)	46.3(11)	58.0(12)	-38(1)	-13.2(8)	7.6(8)
C(24)	48.4(11)	42.3(11)	37.1(10)	-29.1(9)	-20.4(9)	20.7(9)
C(25)	51.0(11)	30.7(9)	24.8(8)	-14.0(7)	-2.6(8)	11.4(8)
C(26)	28.4(8)	23.7(8)	30.5(8)	-15.0(7)	0.7(7)	2.8(6)

Table XLII. Bond Lengths.

Atom Atom	Length/ \AA	Atom Atom	Length/ \AA
O(1) C(1)	1.3259(17)	C(5) C(11)	1.5377(18)
O(2) C(1)	1.2000(18)	C(6) C(7)	1.5262(18)

O(3)	C(8)	1.3395(16)	C(7)	C(8)	1.5096(19)
O(3)	C(9)	1.4485(15)	C(9)	C(10)	1.5314(18)
O(4)	C(8)	1.2089(16)	C(10)	C(12)	1.5413(18)
O(5)	N	1.4252(14)	C(12)	C(13)	1.491(2)
O(5)	C(10)	1.4326(16)	C(13)	C(14)	1.392(2)
O(6)	C(12)	1.2130(17)	C(13)	C(18)	1.387(2)
O(7)	C(19)	1.3363(17)	C(14)	C(15)	1.383(2)
O(7)	C(20)	1.4553(17)	C(15)	C(16)	1.371(3)
O(8)	C(19)	1.2066(17)	C(16)	C(17)	1.378(2)
N	C(11)	1.4525(17)	C(17)	C(18)	1.388(2)
N	C(19)	1.3851(17)	C(20)	C(21)	1.501(2)
C(1)	C(2)	1.5236(19)	C(21)	C(22)	1.390(2)
C(2)	C(3)	1.501(2)	C(21)	C(26)	1.379(2)
C(2)	C(7)	1.5552(19)	C(22)	C(23)	1.385(2)
C(3)	C(4)	1.3258(19)	C(23)	C(24)	1.375(3)
C(4)	C(5)	1.5114(18)	C(24)	C(25)	1.375(3)
C(5)	C(6)	1.5285(18)	C(25)	C(26)	1.386(2)
C(5)	C(9)	1.5383(18)			

Table XLIII. Bond Angles.

Atom Atom Atom	Angle/°	Atom Atom Atom	Angle/°
C(8) O(3) C(9)	124.63(10)	C(10) C(9) C(5)	113.45(10)
N O(5) C(10)	107.46(9)	O(5) C(10) C(9)	108.06(10)
C(19) O(7) C(20)	115.82(12)	O(5) C(10) C(12)	105.59(10)
O(5) N C(11)	109.26(10)	C(9) C(10) C(12)	111.18(11)
C(19) N O(5)	113.52(10)	N C(11) C(5)	109.85(11)
C(19) N C(11)	119.75(11)	O(6) C(12) C(10)	118.90(12)
O(1) C(1) C(2)	112.89(12)	O(6) C(12) C(13)	121.35(13)
O(2) C(1) O(1)	123.78(13)	C(13) C(12) C(10)	119.75(12)
O(2) C(1) C(2)	123.33(13)	C(14) C(13) C(12)	117.36(13)
C(1) C(2) C(7)	111.53(11)	C(18) C(13) C(12)	123.56(13)
C(3) C(2) C(1)	108.53(12)	C(18) C(13) C(14)	119.04(14)
C(3) C(2) C(7)	110.73(11)	C(15) C(14) C(13)	120.65(16)
C(4) C(3) C(2)	123.45(13)	C(16) C(15) C(14)	120.02(15)
C(3) C(4) C(5)	123.59(13)	C(15) C(16) C(17)	119.80(15)
C(4) C(5) C(6)	109.79(11)	C(16) C(17) C(18)	120.83(17)
C(4) C(5) C(9)	109.22(10)	C(13) C(18) C(17)	119.59(16)
C(4) C(5) C(11)	107.20(11)	O(7) C(19) N	111.03(12)
C(6) C(5) C(9)	108.65(10)	O(8) C(19) O(7)	126.41(13)
C(6) C(5) C(11)	113.27(10)	O(8) C(19) N	122.37(13)
C(11) C(5) C(9)	108.64(10)	O(7) C(20) C(21)	110.70(12)
C(7) C(6) C(5)	107.32(10)	C(22) C(21) C(20)	120.51(15)
C(6) C(7) C(2)	109.30(11)	C(26) C(21) C(20)	120.21(14)
C(8) C(7) C(2)	110.14(11)	C(26) C(21) C(22)	119.25(15)

C(8)	C(7)	C(6)	111.43(11)	C(23)	C(22)	C(21)	119.84(17)
O(3)	C(8)	C(7)	120.74(11)	C(24)	C(23)	C(22)	120.43(18)
O(4)	C(8)	O(3)	116.86(12)	C(25)	C(24)	C(23)	119.96(17)
O(4)	C(8)	C(7)	122.39(12)	C(24)	C(25)	C(26)	119.96(17)
O(3)	C(9)	C(5)	113.32(10)	C(21)	C(26)	C(25)	120.54(16)
O(3)	C(9)	C(10)	106.83(10)				

Table XLIV. Hydrogen Bonds

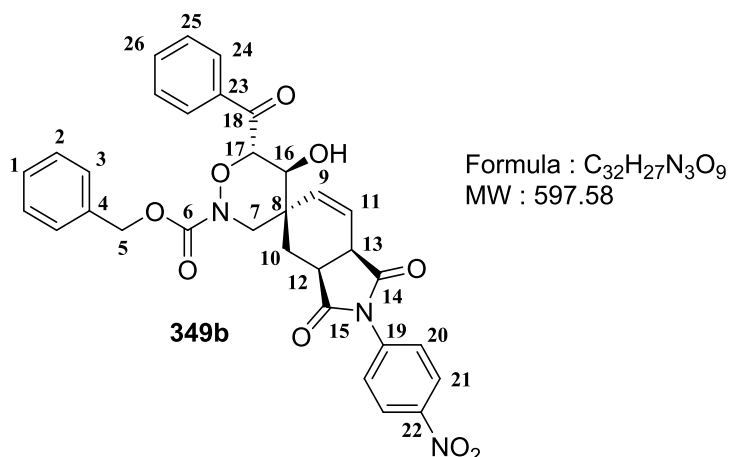
D	H	A	d(D-H)/Å	d(H-A)/Å	d(D-A)/Å	D-H-A/°
O(1)	H(1)	O(4) ¹	0.88(2)	1.86(2)	2.7410(15)	175(2)

¹-X,1-Y,2-Z

Table XLV. Hydrogen Atom Coordinates (Å×10⁴) and Isotropic Displacement Parameters (Å²×10³).

Atom	x	y	z	U(eq)
H(1)	1070(40)	6161(18)	9512(18)	56(7)
H(2)	5019	6136	7751	19
H(3)	1832	6336	6579	21
H(4)	2390	5215	5993	18
H(6A)	7289	3673	8138	17
H(6B)	7587	4863	7373	17
H(7)	5810	4547	9017	18
H(9)	1651	3279	7282	16
H(10)	5636	2112	8393	17
H(11A)	4966	4114	5697	18
H(11B)	7380	4589	5867	18
H(14)	169	-382	9409	32
H(15)	1241	-2035	9793	37
H(16)	4993	-2346	9178	35
H(17)	7772	-1018	8264	43
H(18)	6799	637	7925	38
H(20A)	11897	951	6251	29
H(20B)	12651	2125	5585	29
H(22)	7323	756	5569	36
H(23)	6069	693	4149	46
H(24)	8419	1470	2628	45
H(25)	12028	2324	2512	42
H(26)	13246	2431	3914	32

Polycyclic product **349b**.



Compound **315** (65.0 mg, 0.18 mmol), 4-nitro-*N*-phenylmaleimide **348** (43.5 mg, 0.20 mmol) and *trans*-cinnamaldehyde **347** (48 μ L, 0.38 mmol) were stirred in acetone (180 μ L) at 50 °C for 70 h. The crude was purified by silica gel chromatography (eluent, hexane/EtOAc, 1/1, R_f = 0.55) to afford compound **349b** (16.2 mg, 15%).

M.p. = 173 °C.

¹H NMR (400 MHz, Chloroform-*d*, δ ppm) 8.35 – 8.27 (m, 2H, H₂₁), 8.22 – 8.20 (m, 2H, H₂₄), 7.60 – 7.52 (m, 3H, H₂₀ and H₂₆), 7.50 – 7.22 (m, 7H, H_{Ar}), 6.28 (dd, *J* = 10.1, 4.2 Hz, 1H, H₁₁), 5.83 (dd, *J* = 10.1, 2.6 Hz, 1H, H₉), 5.40 (d, *J* = 11.7 Hz, 1H, H₅), 5.26 (d, *J* = 11.7 Hz, 1H, H₅), 5.00 (d, *J* = 9.2 Hz, 1H, H₁₇), 4.18 (dd, *J* = 9.2, 1.8 Hz, 1H, H₁₆), 4.06 (d, *J* = 14.3 Hz, 1H, H₇), 3.64 (ddd, *J* = 9.2, 3.9, 2.6 Hz, 1H, H₁₃), 3.40 – 3.34 (m, 1H, H₁₂), 3.31 (d, *J* = 14.3 Hz, 1H, H₇), 3.16 (s, 1H, OH), 2.33 (dd, *J* = 14.3, 8.4 Hz, 1H, H₁₀), 2.15 (dd, *J* = 14.3, 7.8 Hz, 1H, H₁₀)

¹³C NMR (101 MHz, Chloroform-*d*, δ ppm) 195.4 (C₁₈), 177.4 (C₁₃), 174.6 (C₁₂), 155.3 (C₆), 147.0 (C₂₂), 137.6 (C₁₉), 135.2 (C), 134.7 (C), 134.4 (C₂₆), 133.4 (C₉), 130.2 (C₂₄), 129.2 (CH), 129.1 (CH), 129.0 (CH), 128.7 (CH), 126.9 (C₂₀), 125.0 (C₁₁), 124.5 (C₂₁), 79.1 (C₁₇), 71.8 (C₁₆), 69.2 (C₅), 52.5 (C₇), 40.3 (C₁₃), 39.5 (C₈), 36.6 (C₁₂), 24.6 (C₁₀)

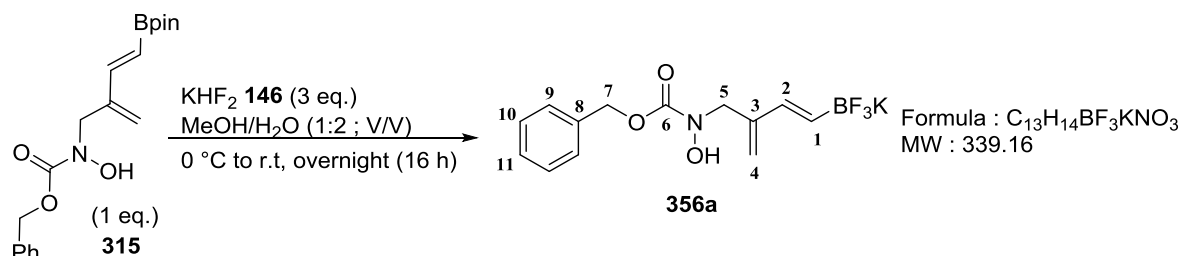
IR (neat, ν) 3487, 2947, 1700, 1676, 1525, 1499, 1384, 1346, 1229, 1176, 1098, 854, 813, 751, 695, 683 cm⁻¹.

LRMS (ESI+) 598.2 (100%) [M+H]⁺, 554.1 (20%).

HRMS (ESI+) calcd. for [M+H]⁺(C₃₂H₂₉N₃O₉): 598.1826 found: 598.1844.

B. Modification of the boron substituent

B.1. Trifluoroboronated salt **356a** synthesis:



A solution of diene **315** (209 mg, 0.58 mmol) in MeOH (2 mL) was cooled to $0\text{ }^\circ\text{C}$. An aqueous solution of KHF_2 **146** (137 mg, 1.75 mmol, in 4 mL) was added to the reaction mixture. The reaction was allowed to reach r.t., and stirred overnight. The crude was evaporated to dryness. The residue was dissolved in acetone and the remaining salt was filtered. The salt was washed with acetone and the filtrate was evaporated. The white solid was resolubilised in the minimum amount of acetone. The solution was stirred vigorously and Et_2O was added to precipitate the afford compound **356a** as a white solid (170.0 mg, 86%).

M.p. = $123\text{ }^\circ\text{C}$ (decomposition).

^1H NMR (400 MHz, Acetone- d_6 , δ ppm) 8.47 (bs, 1H, NH), 7.43 – 7.27 (m, 5H, H_9 , H_{10} and H_{11}), 6.38 (d, $J = 18.5\text{ Hz}$, 1H, H_2), 5.80 (dq, $J = 18.5, 3.5\text{ Hz}$, 1H, H_1), 5.15 (s, 2H, H_4), 4.89 (s, 2H, H_7), 4.31 (t, $J = 1.3\text{ Hz}$, 2H, H_5).

^{13}C NMR (101 MHz Acetone- d_6 , δ ppm) 157.9 (C_6), 143.9 (C_3), 138.1 (C_8), 135.0 (q, $J = 4.7\text{ Hz}$, C_2), 129.2 (C_{10}), 128.65 (C_9), 128.64 (C_{11}) 111.1 (C_4), 67.5 (C_7), 53.2 (C_5), B-C not visible.

^{11}B NMR (96 MHz, Acetone- d_6 , δ ppm) 2.6.

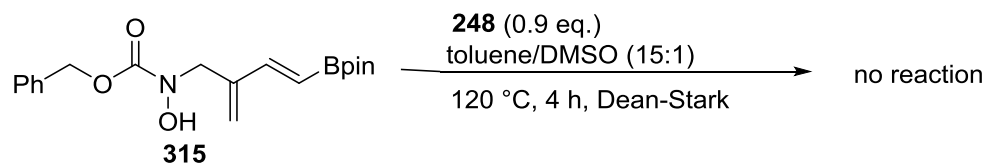
^{19}F NMR (376 MHz, Acetone- d_6 , δ ppm) -141.8.

IR (neat, ν) 3234, 1655, 1600, 1457, 1414, 1358, 1275, 1253, 1106, 1088, 999, 971, 942, 893, 761, 694, 596 cm^{-1} .

LRMS (ESI+) 300.3 (23%) $[\text{M}-\text{K}]^+$, 278.3 (49%), 234.2 (100%).

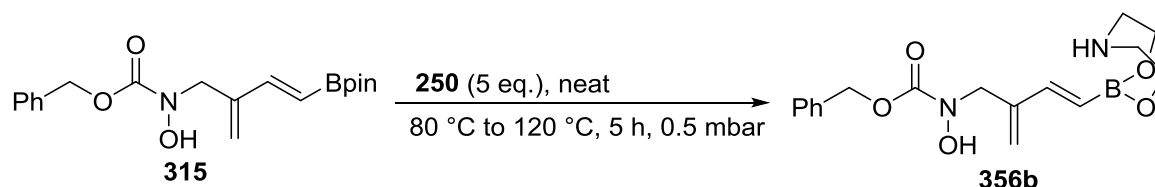
HRMS (ESI+) calcd. for $(\text{C}_{13}\text{H}_{14}^{10}\text{BNO}_3\text{F}_3)$: 299.1055 found: 299.1046.

B.2. Boronated MIDA ester derivative synthesis:



To a solution of **315** (50.0 mg, 0.14 mmol) in a mixture of toluene/DMSO (15/1 : 3 mL), were added MIDA **248** (18.4 mg, 0.12 mmol) and phenothiazine (2 mg) as polymerisation inhibitor. The reaction mixture was heated under inert atmosphere in reflux conditions for 4 h. The solution was cooled to r.t. and Et₂O (10 mL) was added. The reaction mixture was stirred overnight. The white precipitate was filtered and washed with Et₂O to provide starting MIDA ester **248** as a white solid (quantitative). The filtrate was evaporated and a mixture of starting **315**, pinacol **255**, and another boron species were obtained.

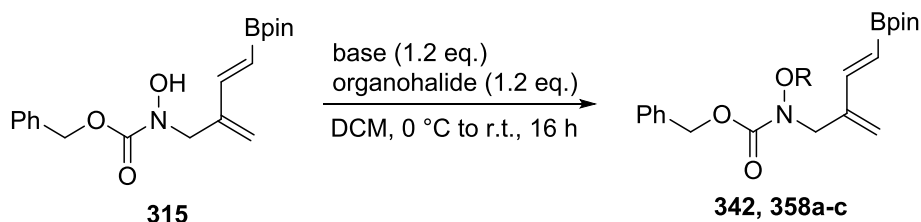
B.3. Boronated DEA ester derivative synthesis:



A solution of diethanolamine **250** (80.2 mg, 0.76 mmol) and **315** (54.8 mg, 0.15 mmol) in DCM (1 mL) was evaporated to dryness. The crude reaction mixture was then distilled by bulb to bulb distillation at 80 °C for 2 h, then at 120 °C for 3 h. The crude reaction mixture was cooled to r.t., then Et₂O (10 mL) was added and the reaction mixture was stirred overnight. The white precipitate was filtered and washed with Et₂O (2 x). ¹H and ¹¹B NMR showed a mixture of two species.

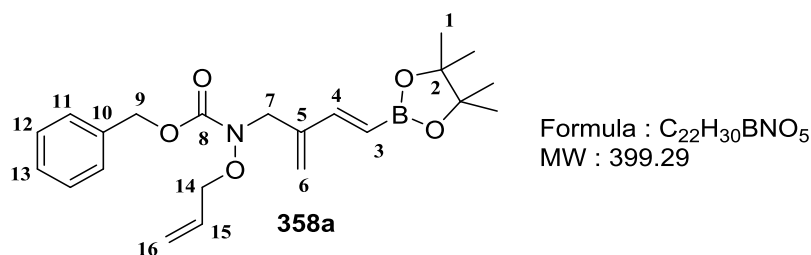
C. The metathesis/arylnitroso Diels-Alder/ring contraction sequence

C.1. General procedure for the Synthesis of the O-substituted hydroxycarbamates:



A solution of diene **315** (1 eq) in DCM was cooled to 0 °C. Organohalide **357** (1.2 eq.) and base (1.2 eq.) were added successively at 0 °C. The mixture was stirred at 0 °C for 10 min, then at r.t. for 16 h. BHT was added and the crude mixture was evaporated. The crude was diluted in the minimum amount of DCM. The crude was filtered over a pad of silica and eluted with a mixture hexane/AcOEt (9/1) containing BHT. The filtrate was evaporated.

Allyl-protected ene-product **358a**.



General procedure was followed using diene **315** (719 mg, 2.00 mmol), allylbromide **357a** (208 μ L, 2.40 mmol) and DBU (359 μ L, 2.40 mmol) in DCM (17 mL). The crude was filtered over a pad of silica (hexane/AcOEt, 7/3, R_f = 0.80) and eluted with a mixture hexane/AcOEt (9/1, 555 mL) containing BHT (18 mg). The filtrate was evaporated to afford a mixture of compound **358a**/BHT (88/12, ¹H NMR measurement, 768 mg, 85%).

¹H NMR (400 MHz, Chloroform-*d*, δ ppm) 7.42 – 7.29 (m, 5H, H₁₁, H₁₂ and H₁₃), 7.07 (d, *J* = 18.6 Hz, 1H, H₄), 5.90 (ddt, *J* = 16.9, 10.3, 6.4 Hz, 1H, H₁₅), 5.66 (d, *J* = 18.6 Hz, 1H, H₃), 5.39 (s, 1H, H₆), 5.34 (d, *J* = 1.1 Hz, 1H, H₆), 5.30 – 5.21 (m, 2H, H₁₆), 5.23 (s, 2H, H₉), 4.33 – 4.30 (m, 2H, H₁₄), 4.32 (s, 2H, H₇), 1.28 (s, 12H, H₁).

¹³C NMR (101 MHz Chloroform-*d*, δ ppm) 157.2 (C₈), 149.3 (C₄), 141.0 (C₅), 136.2 (C₁₀), 132.4 (C₁₅), 128.6 (C₁₂), 128.3 (C₁₃), 128.1 (C₁₁), 121.5 (C₆), 120.0 (C₁₆), 117.6 (C₃), 83.5 (C₂), 76.6 (C₁₄), 67.4 (C₉), 51.2 (C₇), 24.9 (C₁).

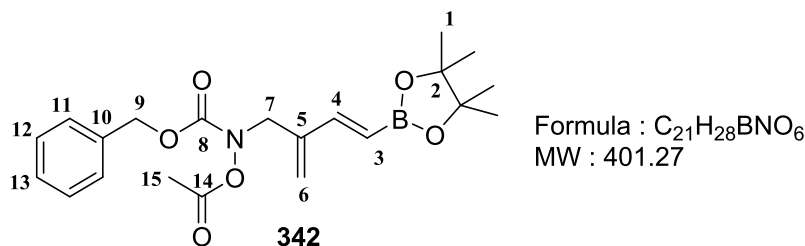
¹¹B NMR (96 MHz, Chloroform-*d*, δ ppm) 30.1.

IR (neat, ν) 2978, 1706, 1630, 1600, 1380, 1338, 1217, 1143, 1090, 971, 929, 849, 754, 697 cm⁻¹.

LRMS (ESI+) 422.0 (37%) [M+Na]⁺, 400.7 (74%) [M+H]⁺, 356.9 (100%).

HRMS (ESI+) calcd. for [M+H]⁺(C₂₂H₃₁NO₅¹⁰B): 399.2333 found: 399.2332.

Acetyl-protected ene-product **342**.



General procedure was followed using diene **315** (59.6 mg, 0.17 mmol), acetylchloride **357b** (18 μL, 0.20 mmol) and Et₃N (15 μL, 0.20 mmol) in DCM (2 mL). The crude was filtered over a pad of silica (hexane/AcOEt, 7/1, R_f = 0.20) and eluted with a mixture hexane/AcOEt (9/1, 335 mL) containing BHT (10 mg). The filtrate was evaporated to afford a mixture of compound **342**/BHT (87/13, ¹H NMR measurement, 37.1 mg, 56%).

¹H NMR (400 MHz, Chloroform-*d*, δ ppm) 7.45 – 7.26 (m, 5H, H₁₁, H₁₂ and H₁₃), 7.05 (d, *J* = 18.7 Hz, 1H, H₄), 5.64 (d, *J* = 18.7 Hz, 1H, H₃), 5.36 – 5.33 (m, 2H, H₆), 5.19 (s, 2H, H₉), 4.45 (s, 2H, H₇), 2.09 (s, 3H, H₁₅), 1.27 (s, 12H, H₁).

¹³C NMR (101 MHz Chloroform-*d*, δ ppm) 168.5 (C₁₄), 155.5 (C₈), 148.5 (C₄), 140.3 (C₅), 135.7 (C₁₀), 128.7 (C₁₂), 128.4 (C₁₃), 128.1 (C₁₁), 121.5 (C₆), 117.9 (C₃), 83.5 (C₂), 68.5 (C₉), 51.5 (C₇), 24.9 (C₁), 18.4 (C₁₅).

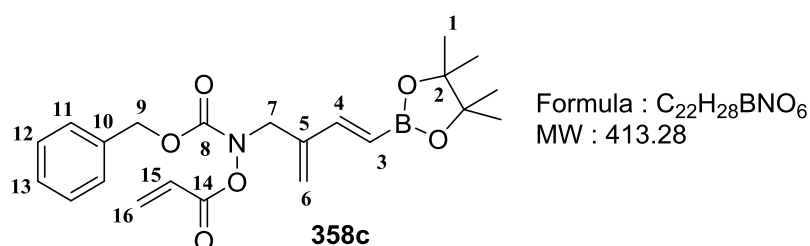
¹¹B NMR (96 MHz, Chloroform-*d*, δ ppm) 29.8.

IR (neat, ν) 2976, 1792, 1717, 1456, 1330, 1260, 1169, 1142, 1089, 1008, 850, 697, 673, 593 cm⁻¹.

LRMS (ESI+) 402.1 (36%) [M+H]⁺, 359.0 (78%), 298.1 (100%).

HRMS (ESI+) calcd. for [M+H]⁺(C₂₁H₂₉NO₆¹⁰B): 399.2124 found: 401.2138.

Acryloyl-protected ene-product **358c**.



General procedure was followed using diene **315** (202.0 mg, 0.56 mmol), acryloylchloride **357c** (55 μL, 0.68 mmol) and DBU (101 μL, 0.68 mmol) in DCM (5 mL). The crude was filtered over a pad of silica (hexane/AcOEt, 7/1, R_f = 0.20) and eluted with a mixture hexane/AcOEt (9/1, 335 mL) containing BHT (11 mg). The filtrate was evaporated to afford a mixture of compound **358c**/BHT (82/18, ¹H NMR measurement, 198.4 mg, 70%).

¹H NMR (400 MHz, Chloroform-*d*, δ ppm) 7.43 – 7.29 (m, 5H, H₁₁, H₁₂ and H₁₃), 7.05 (d, *J* = 18.6 Hz, 1H, H₄), 6.53 (dd, *J* = 17.4, 1.2 Hz, 1H, H₁₆), 6.15 (dd, *J* = 17.4, 10.6 Hz, 1H, H₁₅), 5.96 (dd, *J* = 10.6, 1.2 Hz, 1H, H₁₆), 5.65 (d, *J* = 18.6 Hz, 1H, H₃), 5.37 - 5.35 (m, 2H, H₆), 5.20 (s, 2H, H₉), 4.49 (s, 2H, H₇), 1.27 (s, 12H, H₁).

¹³C NMR (101 MHz Chloroform-*d*, δ ppm) 163.9 (C₁₄), 155.5 (C₈), 148.9 (C₄), 140.3 (C₅), 135.7 (C₁₀), 134.0 (C₁₆), 128.7 (C₁₂), 128.4 (C₁₃), 128.1 (C₁₁), 124.9 (C₁₅), 121.5 (C₆), 83.5 (C₂), 68.5 (C₉), 51.6 (C₇), 24.9 (C₁), B-C not visible.

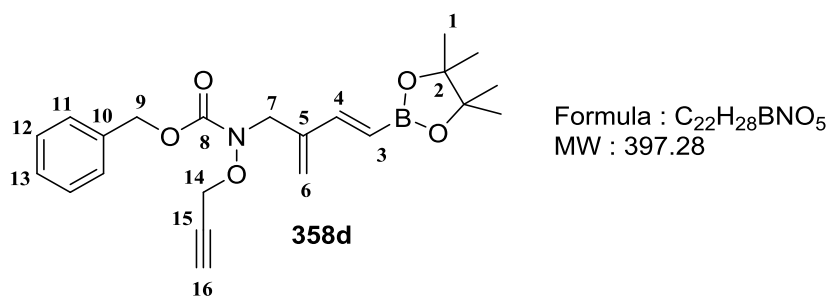
¹¹B NMR (96 MHz, Chloroform-*d*, δ ppm) 29.8.

IR (neat, ν) 2983, 1795, 1708, 1442, 1335, 1255, 1171, 1153, 1090, 1002, 847, 703, 653, 586 cm⁻¹.

LRMS (ESI+) 414.0 (100%) [M+H]⁺, 368.8 (58%), 297.4 (72%), 172.0 (57%).

HRMS (ESI+) calcd. for [M+H]⁺(C₂₂H₂₉NO₆¹⁰B): 413.2124 found: 413.2140.

Propargyl-protected ene-product **358d**.



General procedure was followed using diene **315** (92.0 mg, 0.26 mmol), propargylbromide **357d** (35 μ L, 0.31 mmol) and DBU (46 μ L, 0.31 mmol) in DCM (2.5 mL). The crude was filtered over a pad of silica (hexane/AcOEt, 7/1, R_f = 0.25) and eluted with a mixture hexane/AcOEt (9/1, 270 mL) containing BHT (6 mg). The filtrate was evaporated to afford a mixture of compound **358d**/BHT (80/20, ¹H NMR measurement, 77.3 mg, 60%).

¹H NMR (400 MHz, Chloroform-*d*, δ ppm) 7.39 – 7.29 (m, 5H, H₁₁, H₁₂ and H₁₃), 7.07 (d, *J* = 18.6 Hz, 1H, H₄), 5.64 (d, *J* = 18.6 Hz, 1H, H₃), 5.37 (s, 1H, H₆), 5.31 (d, *J* = 1.4 Hz, 1H, H₆), 5.20 (s, 2H, H₉), 4.46 (d, *J* = 2.4 Hz, 2H, H₁₄), 4.42 (s, 2H, H₇), 2.45 (t, *J* = 2.4 Hz, 1H, H₁₆), 1.28 (s, 12H, H₁).

¹³C NMR (101 MHz Chloroform-*d*, δ ppm) 157.1 (C₈), 149.3 (C₄), 140.7 (C₅), 135.9 (C₁₀), 128.6 (C₁₂), 128.3 (C₁₃), 128.2 (C₁₁), 121.2 (C₆), 117.5 (C₃), 83.5 (C₂), 78.2 (C₁₅), 76.0 (C₁₆), 68.1 (C₉), 62.9 (C₁₄), 51.6 (C₇), 24.9 (C₁).

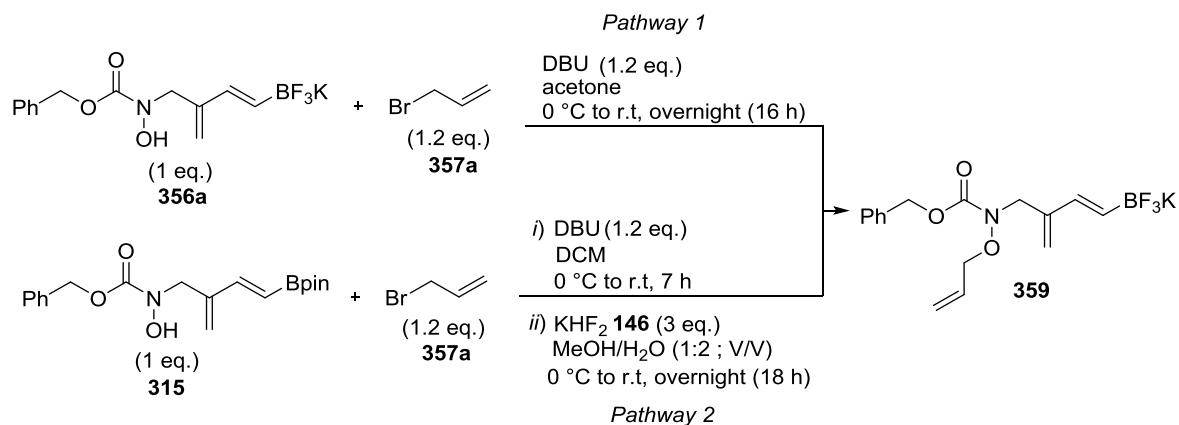
¹¹B NMR (96 MHz, Chloroform-*d*, δ ppm) 30.1.

IR (neat, ν) 2977, 1712, 1600, 1338, 1217, 1143, 1089, 997, 970, 848, 754, 696, 633 cm⁻¹.

LRMS (ESI+) 398.7 (83%) [M+H]⁺, 355.0 (100%), 298.1 (49%), 283.2 (34%), 172.0 (53%).

HRMS (ESI+) calcd. for [M+H]⁺(C₂₂H₂₉NO₅¹⁰B): 397.2175 found: 397.2188.

C.2. Protection of the hydroxycarbamate with the BF_3K variant:



Pathway 1:

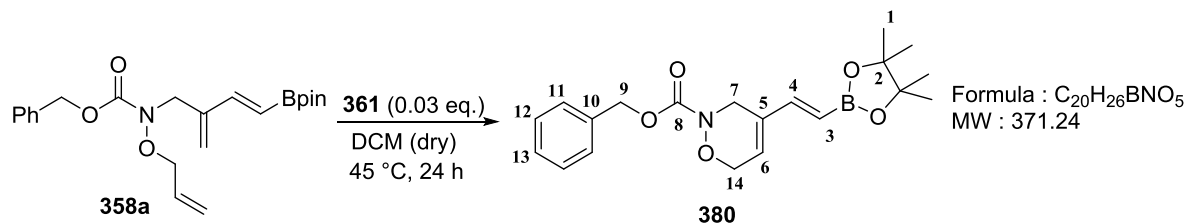
A solution of diene **356a** (0.30 mg, 0.074 mmol) in acetone (1 mL) was cooled to 0 °C. Allylbromide **357a** (8 μ L, 0.089 mmol) and DBU (14 μ L, 0.089 mmol) were added successively at 0 °C. The mixture was stirred at 0 °C for 10 min, then at r.t. for 16 h. The reaction mixture was evaporated.

Pathway 2:

A solution of diene **315** (57.5 mg, 0.16 mmol) in DCM (0.5 mL) was cooled to 0 °C. Allylbromide **357a** (17 μ L, 0.19 mmol) and DBU (48 μ L, 0.32 mmol) were added successively at 0 °C. The mixture was stirred at 0 °C for 10 min, then at r.t. for 7 h. DCM was evaporated and the crude reaction mixture was diluted in MeOH (1 mL), then cooled to 0 °C. An aqueous solution of KHF_2 **146** (37.5 mg in 0.5 mL) was added to the crude at 0 °C and the reaction mixture was stirred at r.t. overnight (18 h). The mixture was evaporated.

C.3. The ring closure metathesis (RCM) of hydroxamates 358a-c

Metathesis product 380.



Compound **358a** (170 mg, 0.43 mmol) and Grubbs catalyst 2nd generation **361** (18.1 mg, 0.021 mmol) were solubilised in dry DCM (13 mL) under inert atmosphere. The reaction mixture was stirred at 45 °C for 24 h. The reaction mixture was cooled to r.t. and H₂O (5 mL) was added and the aqueous phase extracted with DCM (3 x). The organic phase was dried over MgSO₄, filtered and evaporated. The crude product was purified by silica gel chromatography (eluent, hexane/AcOEt, 8/1, R_f = 0.05) to afford **380** as a white solid (98.0 mg, 70%).

M.p. = 124 °C.

¹H NMR (400 MHz, Chloroform-*d*, δ ppm) 7.42 – 7.29 (m, 5H, H₁₁, H₁₂ and H₁₃), 6.97 (d, *J* = 18.5 Hz, 1H, H₄), 5.98 (bs, 1H, H₆), 5.48 (d, *J* = 18.5 Hz, 1H, H₃), 5.21 (s, 2H, H₉), 4.53 (d, *J* = 2.7 Hz, 2H, H₁₄), 4.31 (d, *J* = 2.1 Hz, 2H, H₇), 1.27 (s, 12H, H₁).

¹³C NMR (101 MHz Chloroform-*d*, δ ppm) 155.5 (C₈), 147.0 (C₄), 136.0 (C₁₀), 133.0 (C₅), 128.7 (C₁₂), 128.4 (C₁₃), 128.3 (C₁₁), 127.2 (C₆), 115.8 (C₃), 83.6 (C₂), 68.7 (C₁₄), 67.9 (C₉), 44.8 (C₇), 24.9 (C₁).

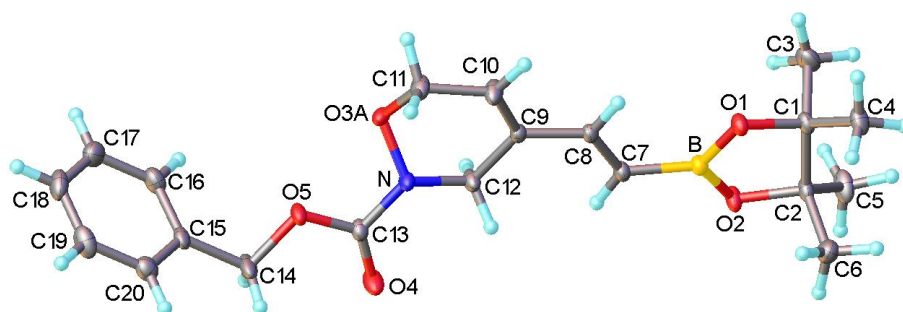
¹¹B NMR (96 MHz, Chloroform-*d*, δ ppm) 30.0.

IR (neat, ν) 2977, 1704, 1608, 1343, 1319, 1217, 1200, 1129, 1093, 1010, 965, 846, 790, 747, 694, 651 cm⁻¹.

LRMS (ESI+) 372.0 (81%) [M+H]⁺, 329.6 (100%), 234.1 (34%).

HRMS (ESI+) calcd. for [M+H]⁺(C₂₀H₂₇NO₅¹⁰B): 371.2015 found: 371.2019.

Single crystal X-ray structure data for **380**:



A suitable crystal obtained in DCM was selected and measured on a D8V_Mo diffractometer. The crystal was kept at 120 K during data collection. Using Olex2,¹⁸⁵ the structure was solved with the ShelXS structure solution program,¹⁸² using Direct Methods and refined with the ShelXL refinement package using Least Squares minimisation.¹⁸²

Table XLVI. Crystal data and structure refinement.

Empirical formula	C ₂₀ H ₂₆ BNO ₅
Formula weight	371.23
Temperature/K	120
Crystal system	monoclinic
Space group	P2 ₁ /n
a/Å	12.8072(10)
b/Å	10.7432(9)
c/Å	14.2090(11)
α/°	90
β/°	98.573(3)
γ/°	90
Volume/Å ³	1933.2(3)
Z	4
ρ _{calc} /cm ³	1.275
μ/mm ⁻¹	0.090
F(000)	792.0
Crystal size/mm ³	0.316 × 0.311 × 0.257
Radiation	MoKα (λ = 0.71073)
2θ range for data collection/°	4.64 to 61.886
Index ranges	-18 ≤ h ≤ 18, -15 ≤ k ≤ 15, -20 ≤ l ≤ 20
Reflections collected	44140
Independent reflections	6129 [R _{int} = 0.0325, R _{sigma} = 0.0206]
Data/restraints/parameters	6129/2/256
Goodness-of-fit on F ²	1.038
Final R indexes [I ≥ 2σ (I)]	R ₁ = 0.0455, wR ₂ = 0.1184
Final R indexes [all data]	R ₁ = 0.0543, wR ₂ = 0.1247
Largest diff. peak/hole / e Å ⁻³	0.56/-0.34

Table XLVII. Fractional Atomic Coordinates ($\times 10^4$) and Equivalent Isotropic Displacement Parameters ($\text{\AA}^2 \times 10^3$). U_{eq} is defined as 1/3 of the trace of the orthogonalised U_{ij} tensor.

Atom	x	y	z	U(eq)
O(1)	5357.6(6)	9295.8(7)	8423.5(5)	17.86(15)
O(2)	6237.4(7)	9548.3(7)	7146.1(5)	21.09(16)
O(4)	4818.2(8)	3145.7(9)	5356.0(7)	31.6(2)
O(5)	3405.0(6)	2024.0(7)	5658.2(5)	19.71(16)
N	3731.6(7)	3889.0(8)	6348.0(6)	17.84(17)
C(1)	5788.6(8)	10556.9(9)	8502.0(7)	17.14(18)
C(2)	6655.5(9)	10502.7(9)	7838.3(7)	18.79(19)
C(3)	4878.7(10)	11427.3(11)	8143.6(10)	29.1(2)
C(4)	6207.5(10)	10813.0(11)	9539.3(8)	24.2(2)
C(5)	6816.5(12)	11697.6(11)	7312.5(9)	29.2(3)
C(6)	7710.0(9)	10013.3(12)	8331.8(10)	28.3(2)
C(7)	5106.3(8)	7572.3(9)	7159.8(7)	16.88(18)
C(8)	4401.3(8)	6941.4(9)	7582.4(7)	15.38(18)
C(9)	3891.3(8)	5770.0(9)	7270.8(7)	14.74(17)
C(10)	3197.2(10)	5249.2(11)	7765.5(8)	25.2(2)
C(11)	2612.4(9)	4086.7(11)	7450.7(8)	24.7(2)
C(12)	4163.6(9)	5134.2(10)	6393.8(8)	20.8(2)
C(13)	4038.0(8)	3026.8(9)	5735.2(7)	17.95(19)
C(14)	3744.9(11)	1027.5(12)	5082.4(10)	31.1(3)
C(15)	2890.6(9)	62.2(10)	4968.8(7)	20.1(2)
C(16)	1871(1)	359.2(11)	4538.2(9)	26.3(2)
C(17)	1083.5(10)	-531.9(13)	4433.8(9)	30.3(3)
C(18)	1308.4(11)	-1736.4(12)	4752.9(9)	30.7(3)
C(19)	2317.8(12)	-2038.4(11)	5169.3(9)	29.9(3)
C(20)	3111.7(10)	-1141.6(11)	5276.6(8)	24.7(2)
B	5576.4(9)	8815(1)	7579.5(8)	16.2(2)
O(3A)	2665.4(6)	3838.9(8)	6472.7(6)	18.82(17)
O(3B)	3233(5)	3366(6)	7060(4)	20.5(13)

Table XLVIII. Anisotropic Displacement Parameters ($\text{\AA}^2 \times 10^3$). The Anisotropic displacement factor exponent takes the form: $-2\pi^2[h^2a^2U_{11}+2hka*b*U_{12}+\dots]$.

Atom	U_{11}	U_{22}	U_{33}	U_{23}	U_{13}	U_{12}
O(1)	23.4(4)	13.1(3)	18.1(3)	-2.6(3)	6.5(3)	-4.1(3)
O(2)	30.1(4)	16.8(3)	17.9(3)	-5.7(3)	8.7(3)	-8.9(3)
O(4)	35.4(5)	27.6(4)	37.4(5)	-14.4(4)	23.5(4)	-13.5(4)
O(5)	23.5(4)	16.7(3)	20.9(4)	-8.0(3)	9.6(3)	-6.7(3)
N	16.7(4)	16.4(4)	22.0(4)	-6.2(3)	8.1(3)	-5.6(3)
C(1)	23.4(5)	11.1(4)	17.3(4)	-1.8(3)	4.2(3)	-1.9(3)
C(2)	26.2(5)	13.7(4)	17.2(4)	-3.4(3)	5.5(4)	-6.5(4)
C(3)	31.8(6)	20.0(5)	34.7(6)	-3.0(4)	2.2(5)	7.2(4)
C(4)	36.4(6)	19.7(5)	16.6(4)	-4.0(4)	4.9(4)	-6.0(4)

C(5)	47.2(7)	18.8(5)	23.2(5)	0.1(4)	10.0(5)	-12.7(5)
C(6)	22.7(5)	26.0(5)	36.2(6)	-6.1(5)	4.7(4)	-3.5(4)
C(7)	19.3(4)	13.7(4)	18.0(4)	-3.1(3)	3.8(3)	-1.7(3)
C(8)	16.4(4)	13.8(4)	15.6(4)	-2.9(3)	1.4(3)	-0.4(3)
C(9)	15.1(4)	14.4(4)	14.5(4)	-1.5(3)	1.4(3)	-1.1(3)
C(10)	28.3(5)	28.1(5)	21.3(5)	-9.7(4)	11.0(4)	-12.1(4)
C(11)	25.9(5)	27.7(5)	22.9(5)	-7.7(4)	11.8(4)	-12.6(4)
C(12)	22.8(5)	16.4(4)	25.4(5)	-6.6(4)	11.0(4)	-6.2(4)
C(13)	21.8(5)	16.7(4)	15.9(4)	-3.6(3)	5.0(3)	-4.2(4)
C(14)	35.1(6)	26.0(5)	37.2(6)	-19.4(5)	22.1(5)	-12.9(5)
C(15)	26.1(5)	17.3(4)	18.7(4)	-8.2(4)	9.2(4)	-5.3(4)
C(16)	34.1(6)	18.0(5)	26.4(5)	-3.1(4)	3.4(4)	1.5(4)
C(17)	25.4(5)	33.5(6)	30.5(6)	-9.6(5)	-0.7(5)	-1.6(5)
C(18)	37.3(7)	28.3(6)	27.9(6)	-8.8(5)	9.5(5)	-16.2(5)
C(19)	49.4(8)	17.4(5)	23.5(5)	1.0(4)	7.3(5)	-4.1(5)
C(20)	28.7(5)	24.5(5)	20.3(5)	-3.2(4)	2.0(4)	2.1(4)
B	18.2(5)	13.8(4)	16.6(5)	-1.3(4)	2.8(4)	-1.1(4)
O(3A)	12.9(3)	23.5(4)	20.7(4)	-7.2(3)	4.5(3)	-4.6(3)

Table XLIX. Bond Lengths.

Atom	Atom	Length/Å	Atom	Atom	Length/Å
O(1)	C(1)	1.4609(12)	C(7)	C(8)	1.3404(14)
O(1)	B	1.3724(13)	C(7)	B	1.5471(14)
O(2)	C(2)	1.4657(12)	C(8)	C(9)	1.4560(13)
O(2)	B	1.3682(13)	C(9)	C(10)	1.3357(14)
O(4)	C(13)	1.2105(13)	C(9)	C(12)	1.5068(14)
O(5)	C(13)	1.3430(12)	C(10)	C(11)	1.4903(15)
O(5)	C(14)	1.4530(13)	C(11)	O(3A)	1.4264(14)
N	C(12)	1.4454(13)	C(11)	O(3B)	1.293(6)
N	C(13)	1.3682(13)	C(14)	C(15)	1.4987(15)
N	O(3A)	1.4039(11)	C(15)	C(16)	1.3940(17)
N	O(3B)	1.393(6)	C(15)	C(20)	1.3809(16)
C(1)	C(2)	1.5612(15)	C(16)	C(17)	1.3824(18)
C(1)	C(3)	1.5215(16)	C(17)	C(18)	1.387(2)
C(1)	C(4)	1.5166(15)	C(18)	C(19)	1.378(2)
C(2)	C(5)	1.5148(15)	C(19)	C(20)	1.3925(17)
C(2)	C(6)	1.5198(17)			

Table L. Bond Angles.

Atom	Atom	Atom	Angle/°	Atom	Atom	Atom	Angle/°
B	O(1)	C(1)	106.96(8)	C(10)	C(9)	C(8)	120.37(9)
B	O(2)	C(2)	106.83(8)	C(10)	C(9)	C(12)	119.97(9)
C(13)	O(5)	C(14)	114.14(8)	C(9)	C(10)	C(11)	122.50(10)
C(13)	N	C(12)	120.73(8)	O(3A)	C(11)	C(10)	110.73(9)

C(13)	N	O(3A)	115.53(8)	O(3B)	C(11)	C(10)	108.5(3)
C(13)	N	O(3B)	113.3(3)	N	C(12)	C(9)	108.82(8)
O(3A)	N	C(12)	113.75(8)	O(4)	C(13)	O(5)	125.21(9)
O(3B)	N	C(12)	123.7(3)	O(4)	C(13)	N	123.09(9)
O(1)	C(1)	C(2)	102.36(7)	O(5)	C(13)	N	111.59(9)
O(1)	C(1)	C(3)	106.41(9)	O(5)	C(14)	C(15)	107.17(9)
O(1)	C(1)	C(4)	108.50(8)	C(16)	C(15)	C(14)	120.66(11)
C(3)	C(1)	C(2)	113.51(9)	C(20)	C(15)	C(14)	120.13(11)
C(4)	C(1)	C(2)	114.42(9)	C(20)	C(15)	C(16)	119.20(10)
C(4)	C(1)	C(3)	110.86(9)	C(17)	C(16)	C(15)	120.61(11)
O(2)	C(2)	C(1)	102.11(8)	C(16)	C(17)	C(18)	119.89(12)
O(2)	C(2)	C(5)	108.96(9)	C(19)	C(18)	C(17)	119.73(11)
O(2)	C(2)	C(6)	106.15(9)	C(18)	C(19)	C(20)	120.47(11)
C(5)	C(2)	C(1)	115.32(9)	C(15)	C(20)	C(19)	120.09(11)
C(5)	C(2)	C(6)	110.11(10)	O(1)	B	C(7)	122.90(9)
C(6)	C(2)	C(1)	113.41(9)	O(2)	B	O(1)	113.40(9)
C(8)	C(7)	B	120.87(9)	O(2)	B	C(7)	123.69(9)
C(7)	C(8)	C(9)	127.04(9)	N	O(3A)	C(11)	107.71(8)
C(8)	C(9)	C(12)	119.65(8)	C(11)	O(3B)	N	116.6(5)

Table LI. Hydrogen Atom Coordinates ($\text{\AA}\times 10^4$) and Isotropic Displacement Parameters ($\text{\AA}^2\times 10^3$).

Atom	x	y	z	U(eq)
H(3A)	4630	11258	7470	38(3)
H(3B)	5120	12292	8218	38(3)
H(3C)	4300	11292	8512	38(3)
H(4A)	5617	10851	9905	32(2)
H(4B)	6586	11609	9593	32(2)
H(4C)	6691	10144	9790	32(2)
H(5A)	7366	11572	6910	39(3)
H(5B)	7033	12362	7773	39(3)
H(5C)	6154	11932	6914	39(3)
H(6A)	7599	9236	8663	34(2)
H(6B)	8035	10631	8793	34(2)
H(6C)	8177	9858	7857	34(2)
H(7)	5320	7252	6595	20
H(8)	4214	7297	8146	18
H(10)	3071	5634	8340	30
H(11A)	2921	3379	7844	30
H(11B)	1865	4174	7543	30
H(11C)	2382	3664	8004	30
H(11D)	1978	4288	6988	30
H(12A)	3865	5608	5819	25
H(12B)	4940	5098	6421	25
H(14A)	4416	664	5400	37
H(14B)	3856	1350	4452	37
H(16)	1716	1182	4314	32

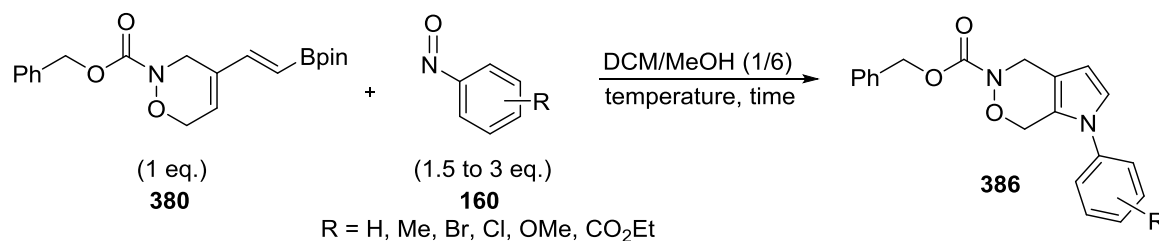
H(17)	389	-320	4144	36
H(18)	769	-2351	4685	37
H(19)	2473	-2864	5385	36
H(20)	3806	-1358	5562	30

Table LII. Atomic Occupancy.

Atom	Occupancy	Atom	Occupancy	Atom	Occupancy
H(11A)	0.875	H(11B)	0.875	H(11C)	0.125
H(11D)	0.125	O(3A)	0.89	O(3B)	0.11

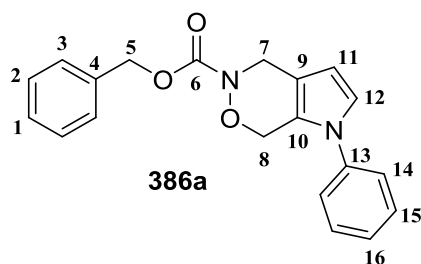
Reactions using **358b** and **358c** were performed using the same procedure as for **358a**. No products were isolated.

C.4. General procedure for the arylnitroso Diels-Alder/ring contraction sequence:



To a solution of **380** (1 eq) in a mixture of MeOH/DCM (6/1) was added aryl nitroso compounds **160** (1.5 to 3 eq). The reaction mixture was stirred at the indicated temperature in the experimental procedure. The solvent was evaporated and the crude product was purified by silica gel chromatography.

Fused oxazine-pyrrole **386a**.



Formula : C₂₀H₁₈N₂O₃
MW : 334.37

Compound **380** (51.3 mg, 0.14 mmol) and nitrosobenzene **160a** (37.5 mg, 0.35 mmol) were stirred in DCM/MeOH (6/1) (2 mL) at r.t. for 24 h. The crude product was purified by silica gel chromatography (eluent, hexane/EtOAc, 6/1, R_f = 0.30) to afford compound **386a** as an orange oil (39.0 mg, 96%).

¹H NMR (400 MHz, Chloroform-*d*, δ ppm) 7.47 – 7.29 (m, 8H), 7.22 – 7.17 (m, 2H, H₁₄), 6.87 (d, *J* = 2.9 Hz, 1H, H₁₂), 6.19 (d, *J* = 2.9 Hz, 1H, H₁₁), 5.26 (s, 2H, H₅), 5.00 (s, 2H, H₈), 4.76 (s, 2H, H₇)

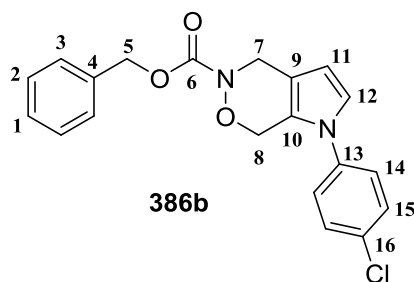
¹³C NMR (101 MHz, Chloroform-*d*, δ ppm) 155.6 (C₆), 139.1 (C₁₃), 136.1 (C₄), 129.8 (C₁₅), 128.7 (C₂), 128.4 (C₁), 128.3 (C₃), 126.9 (C₁₆), 123.4 (C₁₀), 123.1 (C₁₄), 121.0 (C₁₂), 114.7 (C₉), 106.3 (C₁₁), 68.0 (C₅), 67.9 (C₈), 45.1 (C₇)

IR (neat, ν) 1704, 1503, 1454, 1390, 1338, 1312, 1202, 1072, 1115, 787, 753 cm⁻¹.

LRMS (ESI+) 336.4 (100%) [M+H]⁺, 291.2 (20%), 246.1 (84%), 170.0 (77%), 156.0 (65%).

HRMS (ESI+) calcd. for [M+H]⁺(C₂₀H₁₉N₂O₃): 335.1396 found: 335.1391.

Fused oxazine-pyrrole **386b**.



Formula : C₂₀H₁₇ClN₂O₃
MW : 368.82

Compound **380** (54.0 mg, 0.14 mmol) and 4-chloronitrosobenzene **160b** (30.9 mg, 0.22 mmol) were stirred in DCM/MeOH (6/1) (2.4 mL) at r.t. for 24 h. The crude product was purified by silica gel chromatography (eluent, hexane/EtOAc, 6/1, R_f = 0.35) to afford compound **386b** as an orange oil (41.1 mg, 77%).

¹H NMR (400 MHz, Chloroform-*d*, δ ppm) 7.44 – 7.31 (m, 7H, H₁, H₂, H₃ and H₁₅), 7.14 – 7.09 (m, 2H, H₁₄), 6.82 (d, *J* = 2.9 Hz, 1H, H₁₂), 6.19 (d, *J* = 2.9 Hz, 1H, H₁₁), 5.26 (s, 2H, H₅), 4.96 (s, 2H, H₈), 4.74 (s, 2H, H₇)

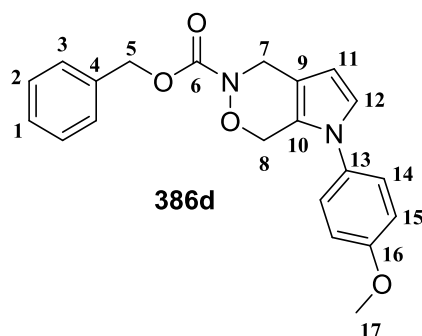
¹³C NMR (101 MHz, Chloroform-*d*, δ ppm) 155.6 (C₆), 137.7 (C₁₃), 136.1 (C₄), 132.6 (C₁₆), 130.0 (C₁₅), 128.7 (C₂), 128.4 (C₁), 128.3 (C₃), 124.3 (C₁₄), 123.4 (C₁₀), 121.0 (C₁₂), 115.1 (C₉), 106.7 (C₁₁), 68.0 (C₅), 67.7 (C₈), 55.7 (C₁₇), 45.1 (C₇)

IR (neat, ν) 1723, 1501, 1401, 1340, 1308, 1203, 1169, 1069, 838, 752, 695, 659, 515 cm⁻¹.

LRMS (ESI+) 369.5 (100%) [M+H]⁺, 280.0 (22%), 204.0 (17%).

HRMS (ESI+) calcd. for [M+H]⁺(C₂₀H₁₈ClN₂O₃): 369.1006 found: 369.1013.

Fused oxazine-pyrrole **386d**.



Formula : C₂₁H₂₀N₂O₄
MW : 364.40

Compound **380** (51.5 mg, 0.14 mmol) and 4-methoxynitrosobenzene **160d** (57.2 mg, 0.42 mmol) were stirred in DCM/MeOH (6/1) (2.4 mL) at r.t. for 72 h. The crude product was purified by silica gel chromatography (eluent, hexane/EtOAc, 6/1, R_f = 0.15) to afford compound **386d** as an orange oil (37.1 mg, 73%).

¹H NMR (400 MHz, Chloroform-*d*, δ ppm) 7.43 – 7.31 (m, 5H, H₁, H₂ and H₃), 7.15 – 7.09 (m, 2H, H₁₄), 6.97 – 6.91 (m, 2H, H₁₅), 6.78 (d, *J* = 2.9 Hz, 1H, H₁₂), 6.15 (d, *J* = 2.9 Hz, 1H, H₁₁), 5.25 (s, 2H, H₅), 4.94 (s, 2H, H₈), 4.75 (s, 2H, H₇), 3.84 (s, 3H, H₁₇).

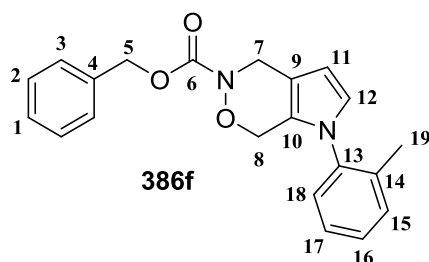
¹³C NMR (101 MHz, Chloroform-*d*, δ ppm) 158.6 (C₁₆), 155.6 (C₆), 136.1 (C₄), 132.2 (C₁₃), 128.7 (C₂), 128.4 (C₁), 128.3 (C₃), 124.8 (C₁₄), 123.6 (C₁₀), 121.3 (C₁₂), 114.9 (C₁₅), 114.0 (C₉), 105.7 (C₁₁), 67.9 (C₅), 67.8 (C₈), 55.7 (C₁₇), 45.1 (C₇).

IR (neat, ν) 1703, 1515, 1390, 1248, 1202, 1169, 1107, 1071, 1030, 834, 697, 604 cm⁻¹.

LRMS (ESI+) 366.5 (100%) [M+H]⁺, 276.1 (20%), 186.1 (46%).

HRMS (ESI+) calcd. for [M+H]⁺(C₂₁H₂₁N₂O₄): 365.1501 found: 365.1500.

Fused oxazine-pyrrole 386f.



Formula : C₂₁H₂₀N₂O₃
MW : 348.40

Compound **380** (61.0 mg, 0.16 mmol) and 2-nitrosotoluene **160f** (58.2 mg, 0.48 mmol) were stirred in DCM/MeOH (6/1) (2.4 mL) in reflux condition for 72 h. The crude product was purified by silica gel chromatography (eluent, hexane/EtOAc, 6/1, R_f = 0.25) to afford compound **386f** as a yellow oil (38.2 mg, 67%).

¹H NMR (400 MHz, Chloroform-*d*, δ ppm) 7.41 – 7.29 (m, 7H, H₁, H₂, H₃ and H₁₈), 7.24 (m, 1H, H₁₆), 7.14 (m, 1H, H₁₇), 6.63 (d, *J* = 2.8 Hz, 1H, H₁₂), 6.16 (d, *J* = 2.8 Hz, 1H, H₁₁), 5.24 (s, 2H, H₅), 4.76 (s, 2H, H₈), 4.70 (s, 2H, H₇), 2.08 (s, 3H, H₁₉).

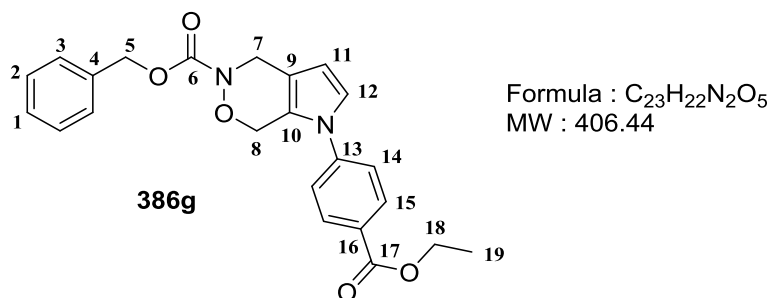
¹³C NMR (101 MHz, Chloroform-*d*, δ ppm) 155.7 (C₆), 137.9 (C₁₃), 136.2 (C₄), 135.3 (C₁₄), 131.3 (C₁₅), 128.7 (C₁₈), 128.6 (C₂), 128.3 (C₁), 128.2 (C₃), 127.4 (C₁₇), 126.8 (C₁₆), 124.3 (C₁₀), 122.0 (C₁₂), 113.0 (C₉), 105.2 (C₁₁), 67.8 (C₅), 67.5 (C₈), 45.0 (C₇), 17.4 (C₁₉).

IR (neat, ν) 1702, 1501, 1455, 1405, 1340, 1308, 1204, 1171, 1130, 1070, 752, 718, 696 cm⁻¹.

LRMS (ESI⁺) 350.1 (100%) [M+H]⁺, 260.3 (17%), 184.1 (26%).

HRMS (ESI⁺) calcd. for [M+H]⁺(C₂₁H₂₁N₂O₃): 349.1552 found: 349.1548.

Fused oxazine-pyrrole **386g**.



Compound **380** (51.3 mg, 0.14 mmol) and ethyl 4-nitrosobenzoate **160g** (37.1 mg, 0.21 mmol) were stirred in DCM/MeOH (6/1) (2.4 mL) at r.t. for 24 h. The crude product was purified by silica gel chromatography (eluent, hexane/EtOAc, 6/1, $R_f = 0.25$) to afford compound **386g** as an orange oil (46.1 mg, 82%).

¹H NMR (400 MHz, Chloroform-*d*, δ ppm) 8.13 – 8.10 (m, 2H, H₁₅), 7.43 – 7.32 (m, 5H, H₁, H₂ and H₃), 7.23 – 7.19 (m, 2H, H₁₄), 6.91 (d, $J_{12-11} = 3.0$ Hz, 1H, H₁₂), 6.22 (d, $J_{11-12} = 3.0$ Hz, 1H, H₁₁), 5.26 (s, 2H, H₁₂), 5.02 (s, 2H, H₁₀), 4.74 (s, 2H, H₉), 4.40 (q, $J = 7.1$ Hz, 2H, H₁₈), 1.41 (t, $J = 7.1$ Hz, 3H, H₁₉).

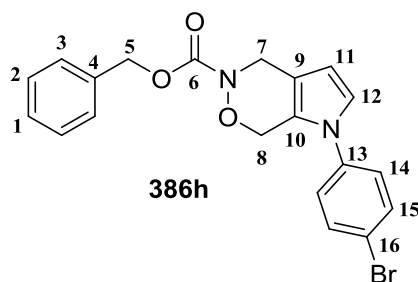
¹³C NMR (101 MHz, Chloroform-*d*, δ ppm) 165.8 (C₁₇), 155.7 (C₆), 142.7 (C₁₃), 136.1 (C₄), 131.4 (C₁₅), 128.7 (C₂), 128.6 (C₁₆), 128.4 (C₁), 128.3 (C₃), 123.5 (C₁₀), 122.1 (C₁₄), 120.8 (C₁₂), 115.9 (C₉), 107.3 (C₁₁), 68.0 (C₅), 67.9 (C₈), 61.4 (C₁₈), 45.1 (C₇), 14.5 (C₁₉).

IR (neat, ν) 1709, 1608, 1516, 1271, 1202, 1168, 1100, 1072, 1017, 772, 732, 696 cm⁻¹.

LRMS (ESI+) 307.0 (100%) [M+H]⁺.

HRMS (ESI+) calcd. for [M+H]⁺(C₂₃H₂₃N₂O₅): 707.1607 found: 407.1603.

Fused oxazine-pyrrole **386h**.



Formula : C₂₀H₁₇BrN₂O₃
MW : 413.27

Compound **380** (61.0 mg, 0.16 mmol) and 4-bromonitrosobenzene **160h** (45.9 mg, 0.25 mmol) were stirred in DCM/MeOH (6/1) (2.4 mL) at r.t. for 24 h. The crude product was purified by silica gel chromatography (eluent, hexane/EtOAc, 6/1, R_f = 0.35) to afford compound **386h** as a yellow/orange solid (58.0 mg, 66%).

M.p. = 92-95 °C

¹H NMR (400 MHz, Chloroform-*d*, δ ppm) 7.59 – 7.52 (m, 2H, H₁₅), 7.44 – 7.31 (m, 5H, H₁, H₂ and H₃), 7.08 – 7.02 (m, 2H, H₁₄), 6.82 (d, *J*₆₋₅ = 2.9 Hz, 1H, H₁₂), 6.19 (d, *J*₅₋₆ = 2.9 Hz, 1H, H₁₁), 5.25 (s, 2H, H₅), 4.97 (s, 2H, H₈), 4.74 (s, 2H, H₇)

¹³C NMR (101 MHz, Chloroform-*d*, δ ppm) 155.6 (C₆), 138.2 (C₁₃), 136.1 (C₄), 132.9 (C₁₅), 128.7 (C₂), 128.4 (C₁), 128.3 (C₃), 124.6 (C₁₄), 123.4 (C₁₀), 120.9 (C₁₂), 120.4 (C₁₆), 115.2 (C₉), 106.8 (C₁₁), 68.0 (C₅), 67.7 (C₈), 45.1 (C₇)

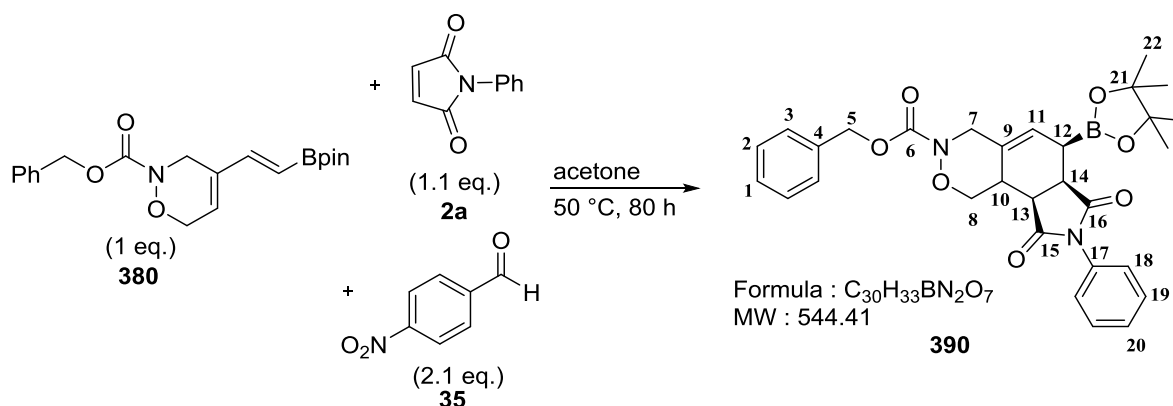
IR (neat, ν) 1723, 1498, 1401, 1340, 1308, 1203, 1169, 1070, 836, 751, 694, 508 cm⁻¹.

LRMS (ESI+) 414.9 (100%) [M+H]⁺, 368.1 (12%).

HRMS (ESI+) calcd. for [M+H]⁺(C₂₀H₁₈BrN₂O₃): 413.0501 found: 413.0507.

D. The Diels-Alder/allylboration sequence

Polycyclic product **390**.



To a solution of **380** (50.0 mg, 0.14 mmol) [1 M] in acetone (140 μ l), were added *N*-phenyl maleimide **2a** (25.7 mg, 0.15 mmol) and 4-nitrobenzaldehyde **35** (42.8 mg, 0.28 mmol). The reaction mixture was stirred at 50 °C for 48 h. The solvent was evaporated and the crude product was purified by silica gel chromatography (eluent, hexane/EtOAc, 1/1, R_f = 0.50) to afford compound **390** (28.1 mg, 38%).

M.p. = 79 - 81 °C

1H NMR (700 MHz, Chloroform-*d*, δ ppm) 7.44 – 7.29 (m, 8H, H_{Ar}), 7.20 – 7.18 (m, 2H, H_{Ar}), 6.05 (s, 1H, H_{11}), 5.17 (s, 2H, H_5), 4.47 (d, J = 14.2, Hz, 1H, H_7), 4.45 (dd, J = 12.0, 7.1 Hz, 1H, H_8), 4.36 (dd, J = 12.0, 8.8 Hz, 1H, H_8), 4.21 (ddt, J = 15.7, 3.7, 1.9 Hz, 1H, H_7), 3.58 (dd, J = 8.9, 5.3 Hz, 1H, H_{14}), 3.35 (t, J = 8.9 Hz, 1H, H_{13}), 2.90 (d, J = 8.9 Hz, 1H, H_{10}), 1.92 (dt, J = 5.9, 2.8 Hz, 1H, H_{12}), 1.30 (d, J = 2.1 Hz, 12H, H_{22}).

^{13}C NMR (101 MHz, Chloroform-*d*, δ ppm) 178.1 (C_{16}), 176.2 (C_{15}), 155.4 (C_6), 136.0 (C_4), 131.8 (C_{17}), 130.7 (C_9), 129.2 (CH), 128.70 (CH), 128.68 (CH), 128.4 (CH), 128.2 (CH), 126.5 (CH), 124.6 (C_{11}), 84.4 (C_{21}), 71.4 (C_8), 68.0 (C_5), 49.5 (C_7), 43.0 (C_{14}), 41.7 (C_{13}), 33.0 (C_{10}), 25.1 (C_{22}), 24.9 (C_{22}), 20.2 (C_{12}).

^{11}B NMR (96 MHz, Chloroform-*d*, δ ppm) 32.4.

IR (neat, ν) 2964, 1706, 1700, 1372, 1344, 1259, 1139, 1087, 1016, 795, 752, 693 cm^{-1} .

LRMS (ESI+) 545.1 (67%) [$M+H$] $^+$, 501.1 (100%).

HRMS (ESI+) calcd. for [$M+H$] $^+$ ($C_{30}H_{34}^{10}BN_2O_7$): 544.2495 found: 544.2513.

References

-
- ¹ Zhu, J.; Bienaymé, H. Eds. *Multicomponent Reactions* Wiley-VCH, Weinheim, Germany, 2005.
- ² Dömling, A. *Chem. Rev.*, **2006**, *106*, 17-89.
- ³ Eckert, H. *Heterocycles*, **2007**, *73*, 149-158.
- ⁴ Sunderhaus, J. D.; Martin, S. F. *Chem. Eur. J.*, **2009**, *15*, 1300-1308.
- ⁵ Coquerel, Y.; Boddaert, T.; Presset, M.; Mailhol, D.; Rodriguez, J. *Ideas in Chemistry and Molecular Sciences: Advances in Synthetic Chemistry*; Pignataro, B., Eds. Wiley-VCH: Weinheim, Germany, 2010; pp. 187-202.
- ⁶ Orru, R. V. A.; Ruijter, E. Eds. *Synthesis of Heterocycles via Multicomponent Reactions I*; Topics in Heterocyclic Chemistry; Springer Verlag: New York, NY, USA, 2010; Volume 23.
- ⁷ Orru, R. V. A.; Ruijter, E., Eds. *Synthesis of Heterocycles via Multicomponent Reactions II*; Topics in Heterocyclic Chemistry; Springer Verlag: New York, NY, USA, 2010; Volume 25.
- ⁸ Ruijter, E.; Scheffelaar, R.; Orru, R. V. A. *Angew. Chem. Int. Ed.*, **2011**, *50*, 6234-6246.
- ⁹ Van der Heijden, G.; Ruijter, E.; Orru, R. V. A. *Synlett*, **2013**, *24*, 666-685.
- ¹⁰ Matteson, D. S.; Kaufmann, D. Eds. *Boron compounds* In Science of Synthesis, Houben–Weyl, Methods of Molecular Transformations, George Thieme Verlag. Stuttgart, Germany, 2004, vol. 6.
- ¹¹ Hall, D. G. Ed. *Boronic acids: Preparation, Applications in Organic Synthesis and Medicine*, 2nd Edition, Wiley-VCH: Weinheim, Germany, 2011.
- ¹² Petasis, N. A.; Akritopoulou, I. *Tetrahedron Lett.*, **1993**, *34*, 583-586.
- ¹³ Candeias, N. R.; Montalbano, F.; Cal, P. M.; Gois, P. M. *Chem. Rev.*, **2010**, *110*, 6169-6193.
- ¹⁴ Batey, R. A. In *Boronic acids: Preparation, Applications in Organic Synthesis and Medicine*, Hall, D. G. Ed.; 2nd Edition, Wiley-VCH: Weinheim, Germany, 2011, pp 427-477.
- ¹⁵ Carboni, B.; Berrée, F. In *Science of Synthesis: Multicomponent Reactions*, Müller, T. J. J., Ed; Thieme: New York, 2013, vol 5.
- ¹⁶ Luan, Y.; Schaus, S. E. *Org. Lett.*, **2011**, *13*, 2510-2513.

-
- ¹⁷ Kielland, N.; Catti, F.; Bello, D.; Isambert, N.; Soteras, I.; Luque, F. J.; Lavilla, R. *Chem. Eur. J.*, **2010**, *16*, 7904-7915.
- ¹⁸ Yang, C. M.; Jeganmohan, M.; Parthasarathy, K.; Cheng, C. H. *Org. Lett.*, **2010**, *12*, 3610-3613.
- ¹⁹ Berree, F.; Gernigon, N.; Hercouet, A.; Lin, C. H.; Carboni, B. *Eur. J. Org. Chem.*, **2009**, 329-333.
- ²⁰ Liao, L.; Jana, R.; Urkalan, K. B.; Sigman, M. S. *J. Am. Chem. Soc.*, **2011**, *133*, 5784-5787.
- ²¹ Melhado, A. S.; Brenzovich, W. E.; Lackner, A.D.; Toste, F. D. *J. Am. Chem. Soc.*, **2010**, *132*, 8885-8887.
- ²² Sieber, J. D.; Morken, J. P. *J. Am. Chem. Soc.*, **2006**, *128*, 74-75.
- ²³ Tonogaki, K.; Itami, K.; Yoshida, J. *J. Am. Chem. Soc.*, **2006**, *128*, 1464-1465.
- ²⁴ Yamamoto, Y.; Ishii, J.; Nishiyama, H.; Itoh, K. *J. Am. Chem. Soc.*, **2004**, *126*, 3712-3713.
- ²⁵ Yamamoto, Y.; Ishii, J.; Nishiyama, H.; Itoh, K. *J. Am. Chem. Soc.*, **2005**, *127*, 9625-9631.
- ²⁶ Nishiyabu, R.; Kubo, Y.; James, T. D.; Fossey, J. S. *Chem. Comm.*, **2011**, *47*, 1124-1150.
- ²⁷ For previous reviews of this topic, see: Hilt, G.; Bolze, P. *Synthesis*, **2005**, *13*, 2091-2114.
- ²⁸ Welker, M. A. *Tetrahedron*, **2008**, *64*, 11529-11539.
- ²⁹ Mikhailov, B. M.; Cherkasova, K. L. *Zhu. Obsh. Khim.*, **1972**, *42*, 138-146.
- ³⁰ Vaultier, M.; Truchet, F.; Carboni, B.; Hoffmann, R. W.; Denne, I. *Tetrahedron Lett.*, **1987**, *28*, 4169-4172.
- ³¹ Renard, P. Y.; Lallemand, J-Y. *Bull. Soc. Chem. Fr.*, **1996**, *133*, 143-149.
- ³² Renard, P. Y.; Six, Y.; Lallemand, J-Y. *Tetrahedron Lett.*, **1997**, *38*, 6589-6590.
- ³³ Six, Y.; Lallemand, J-Y. *Tetrahedron Lett.*, **1999**, *40*, 1295-1296.
- ³⁴ Lallemand, J-Y.; Six, Y.; Ricard, L. *Eur. J. Org. Chem.*, **2002**, *3*, 503-513.
- ³⁵ Vaultier, M.; Lorvelec, G.; Plunian, B.; Paulus, O.; Bouju, P.; Mortier, J. In *Contemporary Boron Chemistry*, Davidson, M. G.; Hughes, A. K.; Marder, T. B.; Wade, K., Eds, The Royal Society of Chemistry, Cambridge, 2000, pp 464-471.

-
- ³⁶ Wang, X. *Chem. Commun.*, **1991**, *21*, 1515-1517.
- ³⁷ Garnier, L.; Plunian, B.; Mortier, J.; Vaultier, M. *Tetrahedron Lett.*, **1996**, *37*, 6699-6700.
- ³⁸ Mortier, J.; Vaultier, M.; Plunian, B.; Toupet, L. *Heterocycles*, **1999**, *50*, 703-711.
- ³⁹ Zhang, A.; Kan, Y.; Jiang, B. *Tetrahedron.*, **2001**, *57*, 2305-2309.
- ⁴⁰ Renard, P. Y.; Lallemand, J-Y. *Tetrahedron: Asymmetry*, **1996**, *7*, 2523-2524.
- ⁴¹ Gao, X.; Hall, D. G. *Tetrahedron Lett.*, **2003**, *44*, 2231-2235.
- ⁴² Hercouet, A.; Berrée, F.; Lin, C. H.; Toupet, L.; Carboni, B. *Org. Lett.*, **2007**, *9*, 1717-1720.
- ⁴³ Hilt, G.; Hess, W.; Harms, K. *Org. Lett.*, **2006**, *8*, 3287-3290.
- ⁴⁴ Linker, T.; Krüger, T.; Hess, W.; Hilt, G. *Arkivoc*, **2007**, *8*, 85-96.
- ⁴⁵ Hilt, G.; Lüers, S.; Smolko, K. I. *Org. Lett.*, **2005**, *7*, 251-253.
- ⁴⁶ Cannillo, A.; Norsikian, S.; Retailleau, P.; Tran Huu Dau, M. E.; Iorga, B. I.; Beau, J. M. *Chem. Eur. J.*, **2014**, *20*, 9127-9131.
- ⁴⁷ Cannillo, A.; Norsikian, S.; Tran Huu Dau, M. E.; Retailleau P.; Iorga, B. I.; Beau, J. M. *Chem. Eur. J.*, **2013**, *19*, 12133-12143.
- ⁴⁸ Zhao, T. S. N.; Zhao, J.; Szabo, K. J. *Org. Lett.*, **2015**, *17*, 2290-2293.
- ⁴⁹ Guennouni, N.; Rasset-Deloge, C.; Carboni, B.; Vaultier, M. *Synlett*, **1992**, 581-584.
- ⁵⁰ Kamabuchi, A.; Moriya, T.; Miyaura, N.; Suzuki, A. *Tetrahedron Lett.*, **1993**, *34*, 4827-4828.
- ⁵¹ Carreaux, F.; Possémé, F.; Carboni, B.; Arrieta, A.; Lecea, B.; Cossio, F. P. *J. Org. Chem.*, **2002**, *67*, 9153-9161.
- ⁵² De, S.; Welker, M. E. *Org. Lett.*, **2005**, *7*, 2481-2484.
- ⁵³ De, S.; Day, C.; Welker, M. E. *Tetrahedron*, **2007**, *63*, 10939-10948.
- ⁵⁴ Wang, L.; Day, C. S.; Wright, M. W.; Welker, M. E. *Beilstein J. Org. Chem.*, **2009**, *5*, 1-9.

-
- ⁵⁵ Wang, L.; Welker, M. E. *J. Org. Chem.*, **2012**, *77*, 8280-8286.
- ⁵⁶ De, E.; Solano, J. M.; Wang, L.; Welker, M. E. *J. Organomet. Chem.*, **2009**, *694*, 2295-2298.
- ⁵⁷ Wang, L.; Welker, M. E. *J. Organomet. Chem.*, **2013**, *723*, 15-18.
- ⁵⁸ Shimizu, M.; Kurahashi, T.; Hiyama, T. *Synlett*, **2001**, 1006-1008.
- ⁵⁹ Kurahashi, T.; Hata, T.; Masai, H.; Kitagawa, H.; Shimizu, M.; Hiyama, T. *Tetrahedron*, **2002**, *58*, 6381-6395.
- ⁶⁰ Shimizu, M.; Shimino, K.; Hiyama, T. *Chem. Asian J.*, **2007**, *2*, 1142-1149.
- ⁶¹ Gonzalez, J. R.; Soderquist, J. A. *Org. Lett.*, **2014**, *16*, 3840-3843.
- ⁶² Semba, K.; Fujihara, T.; Terao, J.; Tsuji, Y. *Angew. Chem. Int. Ed.*, **2013**, *52*, 12400-12403.
- ⁶³ Gao, X.; Hall, D. G. *J. Am. Chem. Soc.*, **2003**, *125*, 9308-9309.
- ⁶⁴ Deligny, M.; Carreaux, F.; Carboni, B.; Toupet, L.; Dujardin, G. *Chem. Commun.*, **2003**, *24*, 276-277.
- ⁶⁵ Deligny, M.; Carreaux, F.; Toupet, L.; Carboni, B. *Adv. Synth. Catal.*, **2003**, *345*, 1215-1219.
- ⁶⁶ Deligny, M.; Carreaux, F.; Carboni, B. *Synlett*, **2005**, *9*, 1462-1464.
- ⁶⁷ Carreaux, F.; Favre, A.; Carboni, B.; Rouaud, I.; Boustie, J. *Tetrahedron Lett.*, **2006**, *47*, 4545-4548.
- ⁶⁸ Favre, A.; Carreaux, F.; Deligny, M.; Carboni, B. *Eur. J. Org. Chem.*, **2008**, *29*, 4900-4907.
- ⁶⁹ Bouziane, A.; Régnier, T.; Carreaux, F.; Carboni, B.; Bruneau, C.; Renaud, J. L. *Synlett*, **2010**, *2*, 207-210.
- ⁷⁰ Gao, X.; Hall, D. G. *J. Am. Chem. Soc.*, **2005**, *127*, 1628-1629.
- ⁷¹ Marion, O.; Gao, X.; Marcus, S.; Hall, D. G. *Bioorg. Med. Chem.*, **2009**, *17*, 1006-1017.
- ⁷² Penner, M.; Rauniyar, V.; Kaspar, L. T.; Hall, D. G. *J. Am. Chem. Soc.*, **2009**, *131*, 14216-14217.
- ⁷³ Tailor, J.; Hall, D. G. *Org. Lett.*, **2000**, *2*, 3715-3718.
- ⁷⁴ Touré, B. B.; Hoveyda, H. R.; Tailor, J.; Ulaczyk-Lesanko, A.; Hall, D. G. *Chem. Eur. J.*, **2003**, *9*, 466-474.

-
- ⁷⁵ Ułaczyk-Lesanko, A.; Pelletier, E.; Lee, M.; Prinz, H.; Waldmann, H.; Hall, D. G. *J. Comb. Chem.*, **2007**, *9*, 695-703.
- ⁷⁶ Touré, B. B.; Hall, D. G. *Angew. Chem. Int. Ed.*, **2004**, *43*, 2001-2004.
- ⁷⁷ Touré, B. B.; Hall, D. G. *J. Org. Chem.*, **2004**, *69*, 8429-8436.
- ⁷⁸ Mackay, E. G.; Sherburn, M. S. *Pure Appl. Chem.*, **2013**, *85*, 1227-1239.
- ⁷⁹ Tripoteau, F.; Verdelet, T.; Hercouet, A.; Carreaux, F.; Carboni, B. *Chemistry, Eur. J.*, **2011**, *17*, 13670-13675.
- ⁸⁰ Wichterle, O. *Collec. Czech. Chem. Comm.*, **1947**, *12*, 292-304.
- ⁸¹ Arbuzov, Y. A. *Doklady Akad. Nauk S.S.S.R.*, **1948**, *60*, 993.
- ⁸² a) Streith, J.; Defoin, A. *Synthesis*, **1994**, 1107-1117, b) Yamamoto, Y.; Yamamoto, H. *Eur. J. Org. Chem.*, **2006**, 2031-2043, c) Bodnar, B. S.; Miller, M. J. *Angew. Chem. Int. Ed.*, **2011**, *50*, 5630-5647, d) Carosso, S.; Miller, M. J. *Org. Biomol. Chem.*, **2014**, *12*, 7445-7468.
- ⁸³ Cohen, A. D.; Zeng, B. B.; King, S. B.; Toscano, J. P. *J. Am. Chem. Soc.*, **2003**, *125*, 1444-1445.
- ⁸⁴ a) Ridd, Q. Q. *Chem. Soc. Rev.*, **1961**, *15*, 418-441, b) Challis, B. C.; Lawson, A. J. *J. Chem. Soc. B*, **1971**, 770-775, c) Bosch, E.; Kochi, J. K. *J. Org. Chem.*, **1994**, *59*, 5573-5586, d) Atherton, J. H.; Moodie R. B.; Noble, D. R. *J. Chem. Soc., Perkin Trans. 2*, **2000**, 229-234, e) Kauffman, J. M.; Green, J.; Cohen, M. S.; Fein, M. M.; Cottrill, E. L. *J. Am. Chem. Soc.*, **1964**, *86*, 4210-4211, f) Eaborn, C.; Jenkinsand, I. D.; Walton, D. R. M. *J. Chem. Soc., Perkin Trans. 1*, **1974**, 870-871, g) Taylor, E. C.; Danforth, R. H.; McKillop, A. *J. Org. Chem.*, **1973**, *38*, 2088-2089.
- ⁸⁵ a) Streith, J.; Defoin, A. *Synthesis*, **1994**, 1107-1117, b) Yamamoto, Y.; Yamamoto, H. *Eur. J. Org. Chem.*, **2006**, 2031-2043, c) Bodnar, B. S.; Miller, M. J. *Angew. Chem. Int. Ed.*, **2011**, *50*, 5630-5647, d) Carosso, S.; Miller, M. J. *Org. Biomol. Chem.*, **2014**, *12*, 7445-7468.
- ⁸⁶ Martin, S. F.; Hatmann, M.; Josey, J. A. *Tetrahedron Lett.*, **1992**, *33*, 3583-3586.
- ⁸⁷ Jenkins, N. E.; Ware, Jr., R. W.; Atkinson, R. N.; King, S. B. *Synth. Commun.*, **2000**, *30*, 947-953.

-
- ⁸⁸ Dao, L. H.; Dust, J. M.; Mackay, D.; Watson, K. N. *Can. J. Chem.*, **1979**, *57*, 1712-1719.
- ⁸⁹ a) Flower, K. R.; Lightfoot, A. P.; Wan, H.; Whiting, A. *Chem. Commun.*, **2001**, *18*, 1812-1813, b) Iwasa, S.; Tajima, K.; Tsushima, S.; Nishiyama, H. *Tetrahedron Lett.*, **2001**, *42*, 5897-5899, c) Flower, K. R.; Lightfoot, A. P.; Wan, H.; Whiting, A. *J. Chem. Soc., Perkin Trans 1*, **2002**, *18*, 2058-2064, d) Iwasa, S.; Fakhruddin, A.; Tsukamoto, Y.; Kameyama, M.; Nishiyama, H. *Tetrahedron Lett.*, **2002**, *43*, 6159-6161, e) Fakhruddin, A.; Iwasa, S.; Nishiyama, H.; Tsutsumi, K. *Tetrahedron Lett.*, **2004**, *45*, 9323-9326, f) Kalita, B.; Nicholas, K. M. *Tetrahedron Lett.*, **2005**, *46*, 1451-1453, g) Adamo, M. F. A.; Bruschi, S. *J. Org. Chem.*, **2007**, *72*, 2666-2669, h) Atkinson, D.; Kabeshov, M. A.; Edgar, M.; Malkov, M. V. *Adv. Synth. Catal.*, **2011**, *353*, 3347-3351, i) Hoshino, Y.; Suzuki, K.; Honda, K. *Synlett*, **2012**, *23*, 2375-2380.
- ⁹⁰ a) Chaiyaveij, D.; Cleary, L.; Batsanov, A.; Marder, T. B.; Shea, K. J.; Whiting, A. *Org. Lett.*, **2011**, *13*, 3442-3445, b) Frazier, C. P.; Engelkind, J. R.; Read de Alaniz, J. *J. Am. Chem. Soc.*, **2011**, *133*, 10430-10433.
- ⁹¹ Baidya, M.; Griffin, K. A.; Yamamoto, H. *J. Am. Chem. Soc.*, **2012**, *134*, 18566-18569.
- ⁹² a) Teo, Y. C.; Pan, Y.; Tan, C. H. *ChemCatChem.*, **2013**, *5*, 235-240, b) Frazier, C. P.; Palmer, L. I.; Samoshin, A. V.; Read de Alaniz, J. *Tetrahedron Lett.*, **2015**, *56*, 3353-3357.
- ⁹³ Quadrelli, P.; Mella, M.; Invernizzi, A. G.; Caramella, P. *Tetrahedron*, **1999**, *55*, 10497-10510.
- ⁹⁴ O'Bannon, P. E.; William, D. P. *Tetrahedron Lett.*, **1988**, *29*, 5719-5722.
- ⁹⁵ Corrie, J. E. T.; Kirby, G. W.; Mackinnon, J. W. M. *J. Chem. Soc., Perkin Trans. 1*, **1985**, *4*, 883-886.
- ⁹⁶ Quadrelli, P.; Mella, M.; Caramella, P. *Tetrahedron Lett.*, **1999**, *40*, 797-800.
- ⁹⁷ a) Srivastava, R. S.; Nicholas, K. M. *Chem. Commun.*, **1996**, *20*, 2335-2336, b) Ho, C.-M.; Lau, T.-C. *New J. Chem.*, **2000**, *24*, 859-863, c) Srivastava, R. S.; Khan, M. A.; Nicholas, K. M. *J. Am. Chem. Soc.*, **2005**, *127*, 7278-7279.
- ⁹⁸ a) Kresze, G.; Saitner, H.; Firl, J.; Kosbahn, W. *Tetrahedron*, **1971**, *27*, 1941-1950, b) Kresze, G.; Kosbahn, W. *Tetrahedron*, **1971**, *27*, 1931-1939.
- ⁹⁹ a) Weinreb, S. M.; Staib, R. R. *Tetrahedron*, **1982**, *38*, 3087-3128, b) Boger, D. L.; Patel, M.; Takusagawa, F. *J. Org. Chem.*, **1985**, *50*, 1911-1916.

-
- ¹⁰⁰ Defoin, A.; Fritz, H.; Geffroy G.; Streith, J. *Tetrahedron Lett.*, **1986**, 27, 3135-3138.
- ¹⁰¹ McClure, K. F.; Danishefsky, S. J. *J. Am. Chem. Soc.*, **1993**, 42, 6094-6100.
- ¹⁰² Benbow, J. W.; McClure, K. F.; Danishefsky, S. J. *J. Am. Chem. Soc.*, **1993**, 115, 12305-12314.
- ¹⁰³ Monbaliu, J-C.; Tinant, B.; Marchand-Brynaert, M. *J. org. Chem.*, **2010**, 75, 547-5486.
- ¹⁰⁴ Berti, F.; Di Bussolo, V.; Pineschi, M. *J. Org. Chem.*, **2013**, 78, 7324-7329.
- ¹⁰⁵ Kirby, G. W.; Bentley, K. W.; Horsewood, P.; Singh S. *J. Chem. Soc., Perkin Trans. 1*, **1979**, 12, 3064-3066.
- ¹⁰⁶ a) Aoyagi S.; Tanaka, R.; Naruse, M.; Kibayashi, C. *Tetrahedron Lett.*, **1998**, 39, 4513-4516, b) Aoyagi S.; Tanaka, R.; Naruse, M.; Kibayashi, C. *J. Org. Chem.*, **1998**, 63, 8397-8406.
- ¹⁰⁷ Hudlicky, T.; Rinner, U.; Gonzalez, D.; Akgun, H.; Schilling, S.; Siengalewicz, P.; Martinot, T. A.; Pettit, G. *R. J. Org. Chem.*, **2002**, 67, 8726-8743.
- ¹⁰⁸ Ozawa, T.; Aoyagi S.; Kibayashi, C. *J. Org. Chem.*, **2001**, 66, 3338-3347.
- ¹⁰⁹ Blakemore, P. R.; Kim, S-K.; Schulze, V. K.; White, J. D.; Yokochi, A. F. T. *J. Chem. Soc., Perkin Trans 1*, **2001**, 15, 1831-1847.
- ¹¹⁰ a) Ghosh, A.; Ritter, A. R.; Miller, M. J. *J. Org. Chem.*, **1995**, 60, 5803-5813, b) Zhang, D.; Ghosh, A.; Stiling C.; Miller, M. J. *Tetrahedron Lett.*, **1996**, 37, 3799-3802, c) Vogt P. F.; Hansel, J-G.; Miller, M. J. *Tetrahedron Lett.*, **1997**, 38, 2803-2804, d) Mulvihill, M. J.; Miller, M. J. *Tetrahedron*, **1998**, 54, 6605-6626, d) Shireman, B. T.; Miller M. J. *Tetrahedron Lett.*, **2000**, 41, 9537-9540, e) Jiang, M. X. W.; Jin, B.; Gage, J. L.; Priour, A.; Savela, G.; Miller, M. J. *J. Org. Chem.*, **2006**, 71, 4164-4169.
- ¹¹¹ Behr, J-B.; Chevrier, C.; Defoin, A.; Tarnus, C.; Streith J. *Tetrahedron*, **2003**, 59, 543-553.
- ¹¹² Yang, B.; Miller, P. A.; Möllmann, U.; Miller, M. J. *Org. Lett.*, **2009**, 11, 2828-2831.
- ¹¹³ Pereira, S.; Srebnik, M. *Organomet.*, **1995**, 14, 3127-3128.
- ¹¹⁴ Schabel, T.; Plietker B. *Chem. Eur. J.*, **2013**, 19, 6938-6941.
- ¹¹⁵ Brown, H. C.; Naik, R. G.; Bakshi, R. K.; Pyun, C.; Singaram, B. *J. Org. Chem.*, **1985**, 50, 5586-5592.

-
- ¹¹⁶ Martinez-Fresneda, P., Vaultier, M. *Tetrahedron Lett.*, **1989**, *30*, 2929-2932.
- ¹¹⁷ Woerly, E. M., Cherney, A. H., Davis, E. K.; Burke, M. D. *J. Am. Chem. Soc.*, **2010**, *132*, 6941-6943.
- ¹¹⁸ Sun, J.; Perfetti, M. T.; Santos, W. L. *J. Org. Chem.*, **2011**, *76*, 3571-3575.
- ¹¹⁹ Rasset-Deloge, C.; Vaultier M. *Bull. Soc. Chim. Fr.*, **1994**, *131*, 919-925.
- ¹²⁰ Wang, C.; Tobrman, T.; Xu, Z.; Negishi E.-I. *Org. Lett.*, **2009**, *11*, 4092-4095.
- ¹²¹ Guennouni, N.; Rasset-Deloge, C.; Carboni, B.; Vaultier, M. *Synlett*, **1992**, *7*, 581-584.
- ¹²² Lee, S. J.; Gray, K. C.; Paek, J. S.; Burke, M. D. *J. Am. Chem. Soc.*, **2008**, *130*, 466-468.
- ¹²³ Woerly E. W.; Miller, J. E.; Burke, M. D. *Tetrahedron*, **2013**, *69*, 7732-7740.
- ¹²⁴ Molander, G. A.; Bernardi, C. R. *J. Org. Chem.*, **2002**, *67*, 8424-8429.
- ¹²⁵ a) Al-Harrasi, A.; Bouché L.; Zimmer, R.; Reissig, H.-U. *Synthesis*, **2011**, 109-118, b) Bressel, B.; Reissig, H.-U. *Org. Lett.*, **2009**, *11*, 527-530, c) Krchnak, V.; Waring, K. R.; Noll, B. C.; Moellmann, U.; Dahse, H.-M.; Miller, M. J. *J. Org. Chem.*, **2008**, *73*, 4559-4567, d) Pulz, R.; Schade, W.; Reissig, H.-U. *Synlett*, **2003**, 405-407, e) Blakemore, P. R.; Kim, S.-K.; Schulze, V. K.; White, J. D.; Yokochi, A. F. *J. Chem. Soc., Perkin Trans. I*, **2001**, 1831-1847, f) Hart, H.; Ramaswami, S.K.; Willer, R. *J. Org. Chem.* **1979**, *44*, 1-7.
- ¹²⁶ Kefalas, P.; Grierson, D. S. *Tetrahedron Lett.*, **1993**, *34*, 3555-3558.
- ¹²⁷ a) Givens, R. S.; Choo, D. J.; Merchant, S. N.; Stitt, R. P.; Matuszewski, B. *Tetrahedron Lett.*, **1982**, *23*, 1327-1330, b) Scheiner, P.; Chapman, O. L.; Lassila, J. D. *J. Org. Chem.*, **1969**, *34*, 813-816.
- ¹²⁸ Ragaini, F.; Cenini, S.; Brignoli, D.; Gasperini, M.; Gallo, E. *J. Org. Chem.*, **2003**, *68*, 460-466.
- ¹²⁹ Jasiński, M.; Watanabe, T.; Reissig, H.-U. *Eur. J. Org. Chem.*, **2013**, 605-610.
- ¹³⁰ Calvet, G.; Blanchard, N.; Kouklovsky, C. *Synthesis*, **2005**, 3346-3354.
- ¹³¹ a) Humenny, W. J.; Kyriacou, P.; Sapeta, K.; Karadeolian, A.; Kerr, M. A. *Angew. Chem. Int. Ed.*, **2012**, *51*, 1-5, b) Shi, G.-Q.; Schlosser M. *Tetrahedron*, **1993**, *49*, 1445-1456, c) Firl, J. *Chem. Ber.*, **1968**, *101*, 218-225.

¹³² a) Cha, J. S.; Brown, H. C. *Bull. Korean Chem. Soc.*, **2005**, *26*, 292-296, b) Bonin, H.; Delacroix, T.; Gras, E. *Org. Biomol. Chem.*, **2011**, *9*, 4714-4724.

¹³³ a) Gillis, E. P.; Burke, M. D. *Aldrichim. Acta*, **2009**, *42*, 17-27 and references therein, b) Knapp, D.M.; Gillis, E. P.; Burke, M. D. *J. Am. Chem. Soc.*, **2009**, *131*, 6961-6963, c) He, Z.; Zajdlik, A.; Yudin, A. K. *Acc. Chem. Res.*, **2014**, *47*, 1029-1040, d) Li, J.; Ballmer, S. G.; Gillis, E. P.; Fujii, S.; Schmidt, M. J.; Palazzolo, A. M. E.; Lehmann, J. W.; Morehouse, G. F.; Burke, M. D. *Science*, **2015**, *347*, 1221-1226.

¹³⁴ Tran, A. T.; Liu, P.; Houk, K. N.; Nicholas, K. M. *J. Org. Chem.*, **2014**, *79*, 5617-5626.

¹³⁵ Berionni, G.; Maji, B.; Knochel, P.; Mayr, H. *Chem. Sci.*, **2012**, *3*, 878-882.

¹³⁶ Frisch, M. J.; Trucks, G. W.; Schlegel, H. B.; Scuseria, G. E.; Robb, M. A.; Cheeseman, J. R.; Scalmani G.; Barone, V.; Mennucci, B.; G. Petersson, A.; Nakatsuji, H.; Caricato, M.; Li, X.; Hratchian, H. P.; Izmaylov, A. F.; Bloino, J.; Zheng G.; Sonnenberg J. L.; Hada M.; Ehara M.; Toyota K.; Fukuda, R.; Hasegawa J.; Ishida M.; Nakajima T.; Honda Y.; Kitao, O.; Nakai, H.; Vreven, T.; Montgomery, Jr. J. A.; Peralta, J. E.; Ogliaro, F.; Bearpark, M.; Heyd, J. J.; Brothers, E.; Kudin, K. N.; Staroverov, V. N.; Kobayashi, R.; Normand J.; Raghavachari K.; Rendell, A.; Burant, J. C.; Iyengar, S. S.; Tomasi, J.; Cossi, M.; Rega, N.; Millam J. M.; Klene, M.; Knox, J. E.; Cross, J. B.; Bakken, V.; Adamo, C.; Jaramillo, J.; Gomperts, R.; Stratmann, R. E.; Yazyev, O.; Austin, A. J.; Cammi, R.; Pomelli, C.; Ochterski, J. W.; Martin R. L.; Morokuma, K.; Zakrzewski, V. G.; Voth, G. A.; Salvador, P.; Dannenberg, J. J.; Dapprich, S.; Daniels, A. D.; Farkas, O.; Foresman, J. B.; Ortiz, J. V.; Cioslowski, J.; Fox, D. J. *Gaussian 09, Revision A.02*, Gaussian, Inc., Wallingford CT, 2009.

¹³⁷ a) Becke, A. D. *J. Chem. Phys.*, **1993**, *98*, 5648-5652, b) Lee, C.; Yang, W.; Parr, R. G. *Phys. Rev. B*, **1988**, *37*, 785-789, c) Petersson, G. A.; Al-Laham, M. A. *J. Chem. Phys.*, **1991**, *94*, 6081-6090, d) Petersson, G. A.; Bennett, A.; Tensfeldt, T. G.; Al-Laham, M. A.; Shirley, W. A.; Mantzaris, J. *J. Chem. Phys.*, **1988**, *89*, 2193-2218.

¹³⁸ Leach, A. G.; Houk, K. N. *J. Org. Chem.*, **2001**, *66*, 5192-5200.

¹³⁹ Tripoteau, F.; Eberlin, L.; Fox, M. A.; Carboni, B.; Whiting, A. *Chem. Commun.*, **2013**, *49*, 5414-5416.

¹⁴⁰ a) Herrera, R.; Nagarajan, A.; Morales, M. A.; Mendez, F.; Jimenez-Vazquez, H. A.; Zepeda, L. G.; Tamariz. *J. J. Org. Chem.*, **2001**, *66*, 1252-1263, b) Kliegel, W.; Metge, J.; Rettig, S. J.; Trotter, J. *Can. J. Chem.*, **1998**, *76*, 389-399.

-
- ¹⁴¹ Padwa, A.; Pearson, W. H. *The Chemistry of Heterocyclic Compounds, Vol 59: Synthetic Applications of 1,3-Dipolar Cycloaddition Chemistry Toward Heterocycles and Natural Products*, 2002, pp 1-81.
- ¹⁴² Knight, G. T.; Pepper, B. *Tetrahedron*, **1971**, *27*, 6201-6208, and references therein.
- ¹⁴³ Sullivan, A. B. *J. Org. Chem.*, **1966**, *31*, 2811-2817.
- ¹⁴⁴ Kang, J. Y.; Bugarin, A.; Connell, B. T. *Chem. Commun.*, **2008**, *30*, 3522–3524.
- ¹⁴⁵ Sasaki, T.; Eguchi, S.; Ishii, T.; Yamada, H. *J. Org. Chem.*, **1970**, *35*, 4273-4275.
- ¹⁴⁶ Chachignon, H.; Scalacci, N.; Petricci, E.; Castagnolo, D. *J. Org. Chem.*, **2015**, *80*, 5287-5295.
- ¹⁴⁷ Palmer, L.; Frazier, C.P.; Read de Alaniz, J. *Synthesis*, **2014**, *46*, 269-280.
- ¹⁴⁸ Mirica, L. M.; Ottenwaelder, X.; Stack, T. D. P. *Chem. Rev.*, **2004**, *104*, 1013-1045.
- ¹⁴⁹ Fukuzumi, S.; Karlin, K. D. *Coordination Chemistry Reviews*, **2013**, *257*, 187-195.
- ¹⁵⁰ Deng, Y.; Zhang, G.; Qi, X.; Liu, C.; Miller, J. T.; Kropf, A. J.; Bunel, E. E.; Lan, Y.; Lei, A. *Chem. Commun.*, **2015**, *51*, 318-321.
- ¹⁵¹ Susnik, P.; Hilt, G. *Organometallics*, **2014**, *33*, 5907-5910.
- ¹⁵² Alessandri, L.; Angeli, A.; Pegna, R. *Chem. Abs.*, **1910**, *4*, 2457.
- ¹⁵³ Woodward, R. B.; Hoffmann, R. *Ang. Chem. Int. Ed. Engl.*, **1969**, *8*, 781-853.
- ¹⁵⁴ a) Davies, A. G.; Schiesser, C. H. *Tetrahedron*, **1991**, *47*, 1707-1726, b) Adam, W.; Bottke, N.; Krebs, O. *J. Am. Chem. Soc.*, **2000**, *122*, 6791-6792, c) Adam, W.; Bottke, N.; Engels, B.; Krebs, O. *J. Am. Chem. Soc.*, **2001**, *123*, 5542-5543.
- ¹⁵⁵ a) Leach, A. G.; Houk, K. N. *J. Am. Chem. Soc.*, **2002**, *124*, 14820-14821, b) Leach, A. G.; Houk, K. N. *Org. Biomol. Chem.*, **2003**, *1*, 1389-1403.
- ¹⁵⁶ Hamer, J.; Macaluso, A. *Tetrahedron. Lett.*, **1963**, *4*, 381-384.
- ¹⁵⁷ For a review on nitroso ene reaction : Adam, W.; Krebs, O. *Chem. Res.*, **2003**, *103*, 4131-4146.
- ¹⁵⁸ Eberlin, L.; Tripoteau, F.; Carreaux, F.; Whiting, A.; Carboni, B. *Beilstein J. Org. Chem.*, **2014**, *10*, 237-250.

-
- ¹⁵⁹ a) Kennedy, J. W.; Hall, D. G. in *Boronic Acids*, Hall, D. G. Ed. Wiley-VCH, Weinheim, 2005, 241-277, b) Lachance, H.; Hall, D. G. *Org. React.* **2008**, *73*, 1-573, c) Hall, D. G. *Pure Appl. Chem.*, **2008**, *80*, 913-927.
- ¹⁶⁰ Mo, J.; Kim, S. H.; Lee, P. H.; *Org. Lett.*, **2010**, *12*, 424-427.
- ¹⁶¹ Schmidt, V. A.; Alexanian, E. J. *Chem. Sci.*, **2012**, *3*, 1672-1674.
- ¹⁶² a) Schmidt, B.; Hanke, S.; Krehl, S.; Kunz, O. *Comprehensive Organic Synthesis II*, 2nd edition, Elsevier B. V., Amsterdam, 2014, Vol 5, 1400-1482, b) Zukowska, K.; Grela, K. *Comprehensive Organic Synthesis II*, 2nd edition, Elsevier B. V., Amsterdam, 2014, Vol 5, 1257-1301, c) Zukowska, K.; Szadkowska, A.; Grela, K. *Comprehensive Inorganic Chemistry II*, Elsevier B. V., Amsterdam, 2013, Vol 6, 105-126, d) Herndon, J. W. *Comprehensive Organometallic Chemistry III*, Elsevier Ltd, Oxford, 2007, Vol 1, 167-195, e) Grubbs, R. H.; Wenzel, A. G.; Chatterjee, A. K. *Comprehensive Organometallic Chemistry III*, Elsevier Ltd, Oxford, 2007, Vol 11, 179-205, f) Li, J.; Lee, D. *Eur. J. Org. Chem.*, **2011**, *23*, 4269-4287, g) Van Otterlo, W. A. L.; de Koning, C. B. *Chem. Rev.*, **2009**, *109*, 3743-3782, h) Kurteva, V. B.; Afonso, C. A. M. *Chem. Rev.*, **2009**, *109*, 6809-6857, i) Gradillas, A.; Pérez-Castells, J. *Ang. Chem. Int. Ed.*, **2006**, *45*, 6086-6101, j) Deiters, A.; Martin, S. F. *Chem. Rev.*, **2004**, *104*, 2199-2238, k) Armstrong, S. K. *J. Chem. Soc., Perkin Trans. 1*, **1998**, 371-388, l) Grubbs, R. H.; Chang, S. *Tetrahedron*, **1998**, *54*, 4413-4450
- ¹⁶³ Yang, Y.-K.; Tae, J. *Synlett*, **2003**, *7*, 1043-1045.
- ¹⁶⁴ Le Flohic, A.; Meyer, C.; Cossy, J.; Desmurs J.-R. *Tetrahedron Lett.*, **2003**, *44*, 8577-8580.
- ¹⁶⁵ Watson, K. D.; Carosso, S.; Miller, M. *J. Org. Lett.*, **2013**, *15*, 358-361.
- ¹⁶⁶ a) Koide, K.; Finkelstein, J. M.; Ball, Z.; Verdine, G. L. *J. Am. Chem. Soc.*, **2001**, *123*, 398-408, b) Miyabe, H.; Moriyama, K.; Takemoto, Y. *Chem. Pharm. Bull.*, **2011**, *59*, 714-720.
- ¹⁶⁷ Yang, Y.-K.; Lee, S.; Tae, J. *Bull. Korean Chem. Soc.*, **2004**, *25*, 1307-1308.
- ¹⁶⁸ Thadani, A. N.; Batey, R. A.; Lough, A. J. *Acta Cryst.*, **2001**, *E57*, 1010-1011.
- ¹⁶⁹ Williams, D. B. G.; Lawton, M. *J. Org. Chem.*, **2010**, *75*, 8351-8354.
- ¹⁷⁰ Hoshi, M.; Kawamura, N.; Shirakawa, K. *Synthesis*, **2006**, *12*, 1961-1970.
- ¹⁷¹ Coombs, J. R.; Zhang, L.; Morken, J. P. *Org. Lett.*, **2015**, *17*, 1708-1711.

-
- ¹⁷² Shade R. E.; Hyde, A. M.; Olsen, J-C.; Merlic, C. A. *J. Am. Chem. Soc.*; **2010**, *132*, 1202-1203.
- ¹⁷³ Vaultier, M.; Truchet, F.; Carboni, B. *Tetrahedron Lett.*, **1987**, *36*, 4169-4172.
- ¹⁷⁴ Jin, B.; Liu, Q.; Sulikowski, G.A. *Tetrahedron*, **2005**, *61*, 401-408.
- ¹⁷⁵ Brinker, U. H.; Boxberger, M. *J. Chem. Res.*, **1983**, 100-101.
- ¹⁷⁶ Schmidt, B.; Krehl, S.; Jablowski, E. *Org. Biomol. Chem.*, **2012**, *10*, 5119-5130.
- ¹⁷⁷ Meng, J.; Li, Y-J.; Zhao, Y-L.; Bu, X-B.; Liu, Q. *Chem. Commun.*, **2014**, *50*, 12490-12492.
- ¹⁷⁸ Kel'in, A. V.; Sromek, A. W.; Gevorgyan, V. *J. Am. Chem. Soc.*, **2001**, *123*, 2074-2075.
- ¹⁷⁹ Bilodeau, F.; Brochu, M-C.; Guimond, N.; Thesen, K. H.; Forgione, P. *J. Org. Chem.* **2010**, *75*, 1550-1560.
- ¹⁸⁰ Matuszak, N.; Muccioli, G. G.; Labar, G.; Lamber D. M. *J. Med. Chem.*, **2009**, *52*, 7410-7420.
- ¹⁸¹ Altomare, A.; Burla, M. C.; Camalli, M.; Cascarano, G.; Giacovazzo, C.; Guagliardi, A.; Moliterni, A. G. G.; Polidori, G.; Spagna, R. *J. Appl. Cryst.*, **1999**, *32*, 115-119.
- ¹⁸² Sheldrick G. M. *Acta Cryst. A64*, **2008**, *64*, 112-122.
- ¹⁸³ Farrugia, L. J. *J. Appl. Cryst.*, **1999**, *32*, 837-838.
- ¹⁸⁴ Egi, M.; Azechi, K.; Akai, S. *Org. Lett.* **2009**, *11*, 5002-5005.
- ¹⁸⁵ Dolomanov, O. V.; Bourhis, L. J.; Gildea, R. J.; Howard, J. A. K.; Puschmann, H. *J. Appl. Cryst.*, **2009**, *42*, 339-341.
- ¹⁸⁶ Spartan '10, Wavefunction, Inc., 18401 Von Karman Avenue, Suite 370, Irvine, CA 92612 U.S.A.
- ¹⁸⁷ MestReJ, Mestrelab Research, S.L., 9B Bajo, 15706 Santiago de Compostela, Spain.